DOCTOR OF PHILOSOPHY

Optimisation of the Design and Operation of Chemically Dosed Activated Sludge Plants

Ojo, Peter

Award date:
2019

Awarding institution:
Coventry University

Optimisation of the Design and Operation of Chemically Dosed Activated Sludge Plants

by

Ojo Peter

A thesis submitted in partial fulfilment of the requirement of Coventry University for the degree of Doctor of Philosophy (PhD)

August 2019

Declaration

I hereby affirm that all the effort in this PHD thesis is my own and no component of this thesis has been presented for any degree requirement. The contribution to knowledge and information from previous research authors during the path of this current research study have been properly referenced and recognised.

Dedication

This thesis is dedicated to the Ancient of Days who defended me from commencement and extended his love towards me.

To My Dear Parents: Mr J.K. Ojo (late) and Mrs Victoria T. Ojo, My Sister Iyabo Ojo, My Brother Akinola Ojo, for their tireless effort to ensure that I have the best of quality education.

To My Daughter: Miss Ayomide V. Ojo for the joy of her gift from God during my PhD research.

To My Life Mentors: Dr. Enoch Adejare Adeboye; Dr. David Olaniyi Oyedepo; Dr. David Olatunji Abioye and Prof. Augustine Osamor Ifelebuegbu.

Acknowledgements

Predominantly, I give my weighty appreciation to the Almighty God for his grace that sustained me all through the completion of my course of study. I am deeply grateful to my Director of Studies Prof. Augustine Ifelebuegu, a father I hold in high esteem whose guidance, advice, constructive criticism, untiring supervision, patience and careful reading of the work that made the thesis a success. I am also grateful to my supervisors: Dr. Mark Bateman and Prof. Alan Newman who always listens to my question about the research work and always give adequate direction to the work and Dr. Les Duckers for his constant guidance in the beginning period of this PhD research study. I would like to demonstrate my gratitude to Dr. Iyabo Adamu, Dr. Mark Hodds and Prof. Tim Sparks for their highly valuable mathematical and statistical contribution during the PhD research. I would like to show my gratitude to Dr. Mark Buttree and Charles Chan for their guidiance on Adobe Illustrator software during the PhD research.

Thanks, as well, to the Coventry University for providing the laboratory support for this research. I am also very thankful to Dr. Adebanwo and Dr. Enobong Bassey for his constructive criticism of my research ideas and on-time attendance to my questions during the PhD study and Prof. Anne James for constructive criticism during the progress review panel session.

Intense gratefulness to my Best Mother Mrs Victoria Ojo and sister Iyabo Ojo, for their un-defatiqueable support and back-up during the entire PhD study. I also appreciate profoundly best aunties Mrs Bunmi Harriot, Comfort Alemoru, Mrs Everlyn Garuba, Mrs Lucia Ifelebuegu, and best uncles (Mr Ola Garuba; Abayomi Alemoru and Daniel Harriot), Michelle Allden and Pastor Cletus Onwenonye.

Special thanks to my fathers in the faith; Pastor Enoch Adejare Adeboye, Bishop David Olaniyi Oyedepo, Bishop David Olatunji Abioye, Pastor (Mrs) Mary Abioye, Pastor Wisdom Obaisi and Pastor Olarewaju Adetoyi.

Table of Contents

List of Supporting Papers (LSP)

Ojo, P., and Ifelebuegu, A.O. (2019a) ‘Effect of Aluminium Salt Dosing on Activated Sludge Settleability Indicators: A New Settleability Model Development’. *Water* 11, 179.

Ojo, P., and Ifelebuegu, A.O. (2019b) ‘The Effects of Aluminium- and Ferric Based Chemical Phosphorus Removal on Activated Sludge Digestibility and Dewaterability’. *Journal of Processes* 7, 228.

Ojo, P., and Ifelebuegu, A.O. (2019c) ‘Modelling the effects of ferric salt dosing on the Settleability of activated sludge’. *Journal of Environmental Chemical Engineering* 7(5), 103256.

Ojo, P., and Ifelebuegu, A.O. (2018) ‘The Impact of Aluminium Salt for Chemical Phosphorus Removal on the Settleability of Activated Sludge’. *Environments 5*, 1–13.

Ojo, P., and Ifelebuegu, A.O. (2016) ‘The Impact of Alum on the Bulking of a Full scale Activated Sludge Plant ’. *Environmental Engineering* 3(2374-1724) 6-10

Ojo, P., and Ifelebuegu, A.O (2015) ‘Optimising final clarifier design and performance of an activated sludge plant using mathematical modelling’. *International Journal of Environmental Engineering*, 2(1) 2374-1724

List of Appendices

Appendix A- Determination of discrete settling velocity for a spherical discrete particle

Appendix B- Activated Sludge Sampling Schedule (sampling phase and testing) for Settleability, Digestibility and Dewaterability test

Appendix C-Tables of the factors that influence precision of laboratory Iron dosed sludge and its past research Evaluation

Appendix D-Tables of the Cummulative Biogas Volume Production for Aluminium (Al^{3+}) and Ferric (Fe^{3+}) Dosed and Undosed surplus activated sludge (SAS) for (12days)

List of Tables (LOT) – Appendices

LOT A -Tables of the urban wastewater treatment directive, Main component of and Unit processes of Activated sludge plant

LOT B -Tables of settling batch test results for un-dosed and Aluminium dosed sludge

LOT C-Tables of settling batch test results for un-dosed and Ferric dosed sludge

LOT D-Tables of settling batch test results for un-dosed and Calcium dosed sludge

List of Figures (LOF) – Appendices

List of Abbreviations

Abbreviation	Meaning
AT	Aeration Tank
ASP	Activated Sludge Process
AS	Activated Sludge
ADP	Anaerobic Digestion Process
AD	Anaerobic Digester
ASM	Algebraic Slip Model
ATP	Adenosine triphosphate
BOD	Biochemical Oxygen Demand
BSC	Batch Settling Curve
BSE	Batch Settling Experiment
BPR	Biological P-Removal
BMP	Biochemical Methane Potential
CAL	Calculated
CST	Capillary Suction Test
COSHH	Control of Substance Hazardous to Health
CPR	Chemical P-Removal
COD	Chemical Oxygen Demand
CFD	Computational Fluid Dynamics
CAS	Conventional Activated Sludge
C/N ratio	Carbon-nitrogen ratio

CS	Compression settling
CHP	Combined heat and power
DSVI	Diluted Sludge Volume Index
1D	One Dimensional
2D	Two Dimensional
3D	Three Dimensional
2D	Two Dimensional
DO	Dissolved Oxygen
DVLO	Derjaguin Landau Verwey Overbeek
DCB	Divalent Cation Bridging
EXP	Experimental
ESS	Effluent Suspended Solids
EDI's	Energy Dissipating Inlets
EP	Effluent Phosphorus
EN	Effluent Nitrate
EPS	Extracellular Polymeric Substances
EBPR	Enhanced Biological Nutrient Removal
FFT	Full Flow to Treatment
FST	Final Sedimentation Tank
FITs)	Feed-In-Tariffs
FDH)	Formate Dehydrogenase
GAO	Glycogen Accumulating Organism
GHG	Green House Gas
HRT	Hydraulic Retention Time
HP	Hydrogen Peroxide
IEP	Isoelectric point
LOF	List of Figures
LOT	List of Tables
LB	Loosely Bound
MLSS	Mixed Liquor Suspended Solids
MSDS	Material Safety Data Sheet
ML	Mixed liquor
meq	milli-equivalent
MSP	MSP
NO_3	Nitrate
$NADH_2$	Nicotinamide adenine dinucleotide dehydrogenase
NVSS	Non-Volatile Suspended Solids
OM	Organic Matter

ODEs	Ordinary Differential Equations
OLR	Organic Loading Rate
PhD	Doctor of philosophy
PST	Primary Treatment Tank
PHB	Polyhydroxybutyrate
PVC	Polyvinyl chloride
PDEs	Partial Differential Equations
P	Phosphorus
PS	Primary sludge
RAS	Return activated sludge
RT	Retention Time
rb	Readily Biodegradable Material
RHS	Right Hand Side
RHI	Renewable Heat Incentive
SV	Sludge Volume
SSV	Settled Sludge Volume
SVI	Sludge Volume Index
SSVI	Stirred Sludge Volume Index
SD	Standard Deviation
SSD	Sum of Square Deviation
SEM	Scanning Electronic Microscope
SAS	Surplus activated sludge
SRF	Specific Resistance of cake to Filtration
SS	Suspended Solids
SLR	Solids Loading Rate
SOR	Surface Overflow Rate
SA	Sludge Age
SBH	Sludge Blanket Height
SRT	Sludge Residence Time
SC	Surface Charge
sp	State Point Analysis
SCOD	Soluble Chemical Oxygen Demand
TSS	Total Suspended Solids
TS	Total Solids
TB	Tightly Bound
TKN	Total Kjeldahl Nitrogen
TS	Transition Settling
UWWTD	Urban Wastewater Treatment Directive

UK	United Kingdom
UCT	University of Cape Town
UASB	Upflow anaerobic sludge blanket
VFA	Volatile Fatty Acid
VSS	Volatile Suspended Solids
VSCs	Volatile Sulphur Compounds
VS	Volatile Solids
WWTP	Waste Water Treatment Plant
WRc	Water Research Council
WAS	Wasted Activated Sludge
WWF	Wet Weather Flow
WWT	Waste Water Treatment
ZSV	Zone Settling Velocity
ZVI	Zero Valent Iron
ZS	Zone Settling
ZVSI	Zero Valent Scrap Iron
ZSC	Zone Settling Curve

List of Symbols

Symbols	Meaning
e	Exponential
X	Activated Sludge (Solids) Concentration
>	Greater Than
<	Less Than
%	Percentage
℃	Degree Celsius
w/w	weight by weight
Rev/min	revolutions per minutes
ML/D	Mega Litres per Day
Hrs	Hours
d	days

cm	centimetres
m^3	Cubic metres
mm	millimetres
mL	millilitres
mL/L	millilitre per litre
m/s	metres per seconds
g/L	grams per litres
m/h	metre per hours
k	sludge settleability constant
L	Litres
mg/L	milligram per litres
ppm	Part per million
Al	Aluminium
Fe	Ferric
Ca	Calcium
$\mathrm{Fe\ Cl_3\ 6H_2O}$	Ferric chloride hexahydrate
$\mathrm{Al_2(SO_4)\ 16H_2\ O}$	Aluminium sulphate Hexadecahydrate
$\mathrm{Ca(OH)_2}$	Calcium hydroxide
$\mathrm{W_2}$	Weight of Filter Paper and Dried Sludge Cake
$\mathrm{W_1}$	Weight of Empty Filter Paper
$R_{1\%}$	Reduction percentage CST
CSTo	Initial Sludge CST(s)
CSTd	Sludge CST after chemical dosing (s)
R^2	Coefficient of Determination

v_0	Sludge settleability constant
ρ_P	Density of particle
ρ_w	Density of water
g	Gravitational constant
∅	Diameter of Particle
μ	Dynamic viscosity of solid particle
H	Depth
Re	Reynolds number
$\mathrm{X_{min}}$	Minimum suspended solids concentration
$\mathrm{C_P}$	Proportionality Constant with an average value = 2/3
$\mathrm{f_s}$	Active fraction of the volatile sludge
V_S	Settling Velocity
ln	Natural Logarithm
V_c	Compression settling velocity
σ	Effective Solid Stress
$\mathrm{NH_3}^+$	Amino functional group
COO^-	Carboxyl groups
μ_p	Plastic Viscosity
A	Surface Area
Sg	Specific gravity of dried sludge
$\mathrm{K_1}$	Settling parameter characteristics of the zone settling regime
$\mathrm{K_2}$	Settling parameter characteristics of the low solids concentration
$\mathrm{X_{min}}$	Minimum suspended solids concentration
V_c	Compression settling velocity

ρ_s	Density of sludge
σ	Effective solid stress
$\mathrm{COO^-}$	Carboxyl Groups
Mm	millimoles
$\mathrm{D_C}$	Chemical Dosing Parameter
A	Activity (the number of unstable nuclei remaining), Bq
$\mathrm{A_o}$	Original number of unstable nuclei, Bq
e	Constant =2.718
λ	Decay constant, s^{-1}
t	Time, s
ZSV	Actual settling velocity (m/h)
$\mathrm{ZSV_O}$	Maximum settling velocity (m/h) for aluminium dosed sludge
$\mathrm{K_d}$	Empirical dosed sludge settling parameter relating to sludge compaction
$\mathrm{C_O}$	Empirical dosing constant related to stokes settling velocity
$\mathrm{C_K}$	Empirical dosing constant related sludge compaction

Abstract

The use of metal salts such as aluminium (Al^{3+}), ferric (Fe^{3+}) and calcium (Ca^{2+}) in the precipitation of phosphorus in activated sludge plants has increased considerably in recent years to achieve tighter discharge consents for phosphorus in treated wastewater effluent. Despite this, the modelling of the settleability of the resultant metal salt dosed sludge in current engineering practice for design and optimisation are still based on conventional sludge settleability models. Also, the full impacts of the metal dosing on other downstream processes including dewaterability and digestibility of the chemical dosed sludge are not fully understood. In this research, the impact of aluminium (Al^{3+}), ferric (Fe^{3+}) and calcium (Ca^{2+}) salt dosing on the settleability of activated sludge as a function of zone settling velocity (ZSV) and stirred sludge volume index (SSVI) were investigated in batch settleability tests over a three years' period. The effect of chemical phosphorus removal (CPR) on sludge dewaterability and digestibility were investigated in a laboratory-scale experiments using sludge samples from a full-scale wastewater treatment plant.

The results of the settleability tests showed that ZSV increased with increasing dose of aluminium, ferric and calcium salt as SSVI decreased. This trend was observed for dosing concentrations of less than 100mg/L. At a dose concentration >100mg/L the trend was reversed as ZSV decreased and SSVI increased. At dose concentrations of <100mg/L, Al^{3+}, Fe^{3+} and Ca^{2+} helped in the bioaggregation of dispersed activated sludge flocs thereby improving settleability. At >100mg/L of Al^{3+}, Fe^{3+} and Ca^{2+} the sludge settleability started to disintegrate due mainly to surface charge reversal linked to the formation of aluminium, ferric and calcium hydroxides and the resultant disintegration of the activated sludge floc structure. Revised activated sludge settleability models which is designed to predict the effects to Al^{3+}, Fe^{3+} and Ca^{2+} salts dosing on activated sludge settleability indicators; zone settling velocity (ZSV) and stirred specific volume index (SSVI) were described. The exponential form of the Vesilind equation was optimised and validated to include aluminium, ferric and calcium chemical dosing parameters. The proposed model equation which is an extended exponential relationship was found to effectively describe the settleability of aluminium, ferric and calcium sludge for dosing concentrations of 0 to <100mg/L of Al^{3+}, Fe^{3+} and Ca^{2+} respectively.

The results of the digestibility tests showed that there was a 21.3% and 35.7% reduction in the biogas volume during anaerobic digestion of surplus activated sludge (SAS) at 100mg/L doses of $Al^{3+}$and Fe^{3+} salts respectively. This demonstrates that Al^{3+} has less of a reduction effect compared with Fe^{3+} salts on biogas generation during anaerobic digestion of sludge. The dewaterability tests showed that primary sludge (PS) dewaterability was improved by up to 16.25% by Al^{3+}, 25.10% by Fe^{3+} and 26.77 % by Ca^{2+}, while that of surplus activated sludge (SAS) was reduced by 72.96%, 63.82% and 52.56% respectively, at a metal salt (Al^{3+}, Fe^{3+} and Ca^{2+}) dose of 50mg/L. Consequently, a pre-precipitation process during CPR where

phosphorus is removed in the primary tank would, therefore, enhance sludge dewaterability. The reason for capillary suction time (CST) reduction in primary sludge may be due to surface chemistry and disruption of extacellular polymeric substances (EPS) structure, causing the release of interstitial water into surrounding sludge matrix through the interaction between multivalent and divalent ions (Al^{3+}, Fe^{3+} and Ca^{2+}) and sludge particles. Therefore, the CST increase in secondary sludge may be due to the interaction of multivalent coagulant (Al^{3+} and Fe^{3+}) and divalent ion (Ca^{2+}) with higher EPS content limiting the outflow of interstitial water from the sludge floc pore spaces.

Chapter One

Introduction

1.0 Background

Due to the increasingly stringent requirements for effluent quality, particularly the removal of nutrients (phosphates and nitrates), the activated sludge process (ASP) has become widely used in Europe for the treatment of wastewater. Old biofilters are being replaced by ASPs to help meet <1mg/L phosphorus consents (Ojo and Ifelebuegu 2016**).** Phosphorus removal is achieved by either enhanced biological phosphorus removal (EBPR) or chemical phosphorus removal (CPR). The use of EBPR is limited by the requirement for strong wastewater with high readily biodegradable biological oxygen demand (BOD). Hence, CPR is the most widely used for phosphorus removal in wastewater treatment. In the United Kingdom (UK), over 80 per cent of WWTPs remove phosphorus by CPR (Haandel and Lubbe 2012). The ASP involves the removal of both the biological and non-biological particulate from its biological reactors by settling. The suspension is well mixed and aerated to provide the required oxygen level for microbial metabolism and reduce potential settling of the suspension. The bacteria (heterotrophic, nitrifying, denitrifying, poly-phosphate and glycogen-accumulating) accounts for most pollutant removal from wastewater, but some other bacteria called filamentous bacteria negatively impacts activated sludge settling and affects the operational capacity of wastewater treatment plants through sludge bulking and foaming (Leven *et al.* 2016; Jenkins *et al.* 2003; Martins *et al.* 2004)**.** Increasing economic development and continuous rise in the human population are adding to the burden of phosphorus (P) discharges into our receiving waters leading to eutrophication problems and leading to environmental pollution and adverse human health issues (Zou *et al.* 2017; Wilfert *et al.* 2015; Ojo and Ifelebuegu 2016). To achieve the increasingly stringent effluent P consents of 1mg/L or less as a result of the EU Water Framework Directive, the activated sludge plants (ASP) are predominantly used by water companies in the EU (Li *et al.* 2014a; Li *et al.* 2014b; Ojo and Ifelebuegu 2019a).

The activated sludge process (ASP) is a well-known suspended growth system for wastewater treatment where suspended solids (SS) are separated from clarified water by downward gravitational settling to produce a clear supernatant low in effluent suspended solid (ESS), effluent nitrogen (EN), and effluent phosphorus (EP) concentration (Xu *et al.* 2017; Li and Stenstrom 2014a; François *et al.* 2016**).** The efficiency of the ASP depends on effective liquid-solids separation within a quiescent environment of the final sedimentation tank (FST) (Kartashevsky *et al.* 2015)**.** In order to remove suspended solids (SS) at the lowest possible cost, the solid removal process during the ASP should be done speedily and efficiently by increasing the SS removal from the sedimentation tank. This will not just increase the treatment efficiency in the tank, but also reduce the size of wastewater treatment facilities located downstream of the clarifiers since the investment costs of settling facilities accounts for a third to a quarter of the total cost of treatment plant construction (Heikal *et al.* 2017**).** Therefore, increasing the SS removal efficiency in sedimentation tanks to optimise activated sludge settleability is vital. The three main factors that affect activated sludge settleability in wastewater treatment include particle size, particle structure, and particle densification. Particle densification is affected by microbial storage product content (MSP), polyhydroxyl butyrate (PHB), non-volatile suspended solids (NVSS), and chemical coagulants added in the reactors (Rittmann and McCarty 2001**).** Other factors affecting settleability include extracellular polymeric substances (EPS) and flocculating capability (Wilén *et al.* 2003; Li and Yang 2007; Liao *et al.* 2006). The EPS contains proteins, deoxyribonucleic acids (DNA) and polysaccharides (Neyens *et al.* 2004).The EPS also impacts activated sludge settling processes and physicochemical properties of activated sludge flocs due to the ability of its internal layer to bind tightly and adhere closely with strong stability to the cellular surface (Rittmann and Laspidou 2002; Sheng *et al.* 2010)**.** Earlier studies have also shown that the activated sludge flocs are embedded in the EPS structure (Biggs and Lant 2000; Jin *et al.* 2003) and the amount of EPS extractable from the activated sludge is positively related to stirred sludge volume index (SSVI). Wang *et al.* (2013a) also reported a similar linear relationship between loosely and tightly bound EPS and SSVI. The EPS also comprises of high negative charge density, which makes cations to play a significant role in activated sludge flocculability and settleability (Wilén *et al.* 2008). Sobeck and Higgins (2002) reported the theories that explain the role of cations in activated sludge flocculation and these include; Divalent Cation Bridging (DCB) and Derjaguin-Landau-Verwey-Overbeek (DVLO) theory. The DCB theory explains the interaction between the divalent cations in the wastewater and negatively charged functional groups within the EPS produced by the microorganisms in an ASP. The DCB theory helps to promote activated sludge flocculation. The DVLO theory explains colloidal suspensions stability and takes into consideration the Van der Waals force of attraction and electric double layer repulsive energy. Literature has also found that the multivalent and DVLO theory are related to cations because multivalent cations can bridge EPS and neutralise the negative charges on the activated sludge surface (Kara *et al.* 2008). Subramanian *et al.* (2010) reported aluminium (Al^{3+}) and ferric (Fe^{3+}) as multivalent coagulants used in WWTP because of their ability in promoting activated sludge flocculation and settleability. Divalent cations such as calcium (Ca^{2+}) and magnesium (Mg^{2+}) was added to play a notable impact in activated sludge flocculation and settleability positively (Sobeck and Higgins 2002; Nguyen *et al.* 2008a,b; Park *et al.* 2010). While sludge particle size and structure have received substantial consideration in the literature, there are limited studies addressing the impact of multivalent cations (Al^{3+}, Fe^{3+} and Ca^{2+}) on activated sludge settleability.

To achieve effluent phosphorus removal in ASPs, chemical phosphorus removal with aluminium and ferric salts is predominantly used (Ojo and Ifelebuegu 2019c**)**. Coagulants such as aluminium salts (Al^{3+}) and ferric salts (Fe^{3+}) are increasingly being used for the precipitation of phosphates from wastewater (Wilfert *et al.* 2015; Haandel and Lubbe 2012). Aluminium and calcium alongside ferric salts are the most widely used chemicals for the chemical precipitation of phosphorus and their use is more common in activated sludge plants (ASP) (Ge *et al.* 2018; Zou *et al.* 2017). Urbain *et al.* (1993) reported that the overall activated sludge floc structures are negatively charged due to the physical and chemical interactions between sludge flocs, EPS and multivalent cations. This explains why aluminium salts (Al^{3+}) have the potential to be strongly absorbed by the surface of sludge flocs since they produce positively charged metal hydroxides, which are responsible for the charge neutralization and reversal process during periods of aluminium overdosing. The impact of aluminium, ferric and calcium coagulants on activated sludge has been explained through charge neutralisation of negatively charged colloids by cationic hydrolysis products (Duan and Gregory 2003). According to Higgins *et al.* (2004a) multivalent cations such as aluminium (III) ion (Al^{3+}) are an effective way to optimise activated sludge settleability. In support of this claim, Higgins and Novak (1997b) and Subramanian *et al.* (2010) have also explained that aluminium (Al^{3+}) will promote activated sludge settleability performance due to its ability to neutralise the sludge surface charge. Nevertheless, Jin *et al.* (2003) demonstrated that dense, strong, and large flocs are required for good activated sludge settleability and compaction. Li *et al.* (2012) equally reported that aluminium supplements promote larger flocs. Also, aluminium has been used in wastewater treatment due to its higher valency and low solubility (Kakii *et al.* 1985; Abu-orf *et al.* 2004). Besides, it has been reported that**,** the addition of calcium salt (Ca^{2+}) to influent wastewater has the capacity to improve the sludge settling characteristics by neutralising the negative charge on the surface of the bacteria (Liu *et al.* 2010). Researchers added that chemical precipitation of calcium particles embedded in the sludge floc structure such as phosphate and carbonate salt out of the wastewater due to low solubility of its salts in water is another approach of describing improving activated sludge settleability in the ASP (Peeters *et al.* 2011; Sobeck and Higgins 2002).

Ferric salts have merit over other coagulants used in phosphorus removal and are effective in the removal of P from wastewater and also are a low-cost product (Li *et al.* 2018; Kelly and He 2014; Luo *et al.* 2017). The most obvious impact of ferric salt on wastewater treatment plant (WWTP) is the hydrolysis reactions of the ferric salts during phosphorus (P) removal process (Wang *et al.* 2016a) and the potential surface charge neutralisation of negatively charged colloids by cationic hydrolysis products (Wang *et al.* 2016b; Azam and Finneran 2014). The presence of a high concentration of iron resulting from the CPR process alters the overall sludge characteristics and is likely to impact the activated sludge settleability. Liu *et al.* (2017) reported the effect of different multivalent cations on settleability of sludge and it was found that ferric salts (Fe^{3+}) showed the best sludge settleability for all treated sludge samples (sodium, potassium, magnesium, calcium and magnesium). The sludge settleability rate of calcium (Ca^{2+}) and magnesium (Mg^{2+}) was slower. Also, settling rates of trivalent (Fe^{3+}) and bivalent (Mg^{2+}, Ca^{2+}) cations compared to the settling rate of monovalent cations (potassium- K^+ and sodium- Na^+) was slowest, and the reason for the observed trend in sludge settleability rate using multivalent cations was attributed to the different charge densities of the different multivalent cations. Liu *et al.*'s (2017) findings showed the importance of investigating the impact of chemical dosing coagulant on activated sludge settleability. The variation of the supernatant volume during the sludge settling process was noticed and it was observed that settleability of the raw sludge did not improve until multivalent cations (NaCl, $MgCl_2$, $CaCl_2$, KCl and $FeCl_3$) were added to the sludge sample. The settling interface of the treated sludge sample became clearer with rising volumes of the supernatant to validate sludge settleability performance. Despite these studies, there is no data available on how varying concentrations of aluminium, ferric and calcium used in CPR impact on the settleability parameters of ZSV and SSVI. The purpose of this recent study is to evaluate the impact of varying aluminium, ferric and calcium dosing concentrations on the settleability of activated sludge as a function of ZSV and SSVI.

The FST produces a full clarified effluent overflow and determines the level of effluent quality in ASP (Haandel and Lubbe 2012*;* Wilfert *et al.* 2015; Agridiotis *et al.* 2007). The description of the complete settling process in FST is not yet fully understood. Also, the increasing use of ferric and aluminium salts for CPR has changed the traditional sludge characteristics. Therefore, an adequate understanding of the effect of CPR on activated sludge settleability characteristics is vital for proper design and operation of the FST (Metcalf and Eddy 2014). Final sedimentation tanks (FST's) are critical component of the activated sludge treatment processes and contributes greatly to the overall efficiency of an ASP and determines the final effluent quality of the activated sludge (Xu *et al.* 2017; Zhang *et al.* 2006). The functions of FST includes; thickening which maintains a continuous underflow of concentrated sludge for recirculation to the biological reactors, clarification which ensures a clarified effluent is produced and sludge storage tank which ensures storage of sludge (under peak wet weather flow-PWWF) to prevent loss of SS and maintain the effluent quality (Mancell-Egala *et al.* 2016; Ramin *et al.* 2014; Ekama *et al.* 1997).

Activated sludge settleability is a very complex process which has made the description of the complete settling process in the FST difficult (Li and Stenstrom 2014a; Li and Stenstrom 2014b). The characterisation of the complete settling process in FST is not yet fully understood and this has created challenges in the optimisation of activated sludge settling in WWTPs. Several factors affect the efficiency of FSTs ranging from hydraulic and loading factors to external factors such as tank configuration, surface area, depth, flow distribution, and turbulence in conveyance structures (Ghawi and Kris 2012; Ghawi and Kris 2011; WEF 2005; Ekama *et al.* 1997). Also, several other factors affecting sludge settleability including; particle size, sludge particle shape, sludge floc porosity, flocculability tendency and extracellular polymeric substances (EPS) have been extensively investigated by various researchers (WEF 2005; Ojo and Ifelebuegu 2018; Wilén *et al.* 2003). However, the effects of chemical dosing on activated sludge settleability have been largely neglected.

The evaluation of zone settling velocity (ZSV) is vital in both the design and modelling of FSTs. The settling classifications are typically reliant on the nature and concentration of the sludge particulates and the interaction between the activated sludge particulates (Tchobanoglous 2003). Based on the flocculation, sedimentation propensity, and concentration of sludge flocs, the settling in FST can be classified into four major types including; free, flocculent, zone, and compression settling (Ekama *et al.* 1997). While the free settling classification is attributed to both very low concentrations and flocculation propensity and occurs in the upper region of the FST (Jung *et al.* 2015). Flocculent settling occurs in the upper mid stream region of the FST where though low solids concentration exists, the floc particles show a resilient flocculating ability and the settling velocity will equally depend on individual sludge floc properties since there is no interaction between sludge particulates. Zone settling occurs in the middle section of FST and this takes place when the concentration of particles increases, and sludge particles settle as one mass with the same velocity and in the same direction. Compression settling occurs at the bottom area of the FST and at a much higher concentration as sludge particulates come in close interaction with each other and form a compression layer.

Since the mass flux theory was developed by Kynch (1952) various studies have been conducted (Xu *et al.* 2017; Li and Stenstrom 2014a; Torfs *et al.* 2017), to examine the relationship between zone settling velocity (ZSV) and activated sludge concentration (X) and to also evaluate the efficiency of FSTs in an ASP, by a number of empirical models (Dupont and Dahl 1995; Cho *et al.* 1993; Takács *et al.* 1991; Dick and Young 1972; Vesilind 1968). Other empirical settling velocity models were proposed due to different activated sludge settling zones and they find application in forecasting the flow field and velocity of flow and estimating the sludge blanket height (Zhang *et al.* 2015a; Ramin *et al.* 2014). They include; one-dimensional (1-D) and two-dimensional (2-D) settling models (Guyonvarch *et al.* 2015; Bürger *et al.* 2013; De Clercq *et al.* 2008; De Clercq 2003). Among the empirical models proposed to relate the initial settling velocity to the sludge concentration is the Vesilind equation (Vesilind 1968). It is the most acceptable empirical model for predicting the sludge settleability behaviour within the FST. The model is expressed in Equation (1.1).

$$\mathrm{ZSV} = \mathrm{v_0}\ \mathrm{e}^{-\mathrm{kX}} \tag{1.1}$$

Where,

ZSV =zone settling velocity (m/h)

X = activated sludge concentration (g/L)

$\mathrm{v_0}$= sludge settleability constant (m/h)

k = sludge settleability constant (L/g)

The Vesilind parameters k and vo from Equation (1.1), can be obtained from the slopes of batch test settling curves. Likewise, the correlations between ZSV (Vesilind 1968 equation) and sludge volume index (SVI), diluted sludge volume index (DSVI), and stirred sludge volume index (SSVI) are derived from empirical equations described in Haandel and Lubbe (2012). Other reviews addressing reasons for variable sludge density and its effects on activated settleability in a full-scale secondary wastewater treatment system have been conducted (De Clercq 2003). In addition, further studies were reported on the effect of settling velocity within various sludge concentration and thicknesses (Schuler and Jang 2007a). The findings showed agreement with Vesilind's (1968) assertion that as biomass concentration was increased in zone settling test, settling velocities decreased but a non-linear correlation between the settling velocity and the range of buoyant density was observed but investigations have not considered the impact of chemical dosing on activated sludge settleability. A new model that included a buoyant density parameter in the Vesilind settling velocity model$(V = (m\rho^{/} + V_0{}^{/})e^{-k^{/}\mathrm{x}})$, was proposed, but again, this did not include a chemical dosing parameter. Further details on the proposed model are provided in Schuler and Jang (2007a).

The modelling of the design and optimisation of activated sludge settleability to date is based on Pitman and White settleability models. The Pitman (1980) and White (1975) models are based on Vesilind's (1968) equation. The Pitman (1980) and White (1975) models are expressed in Equation (1.2). The SSVI is the volume of a unit mass of suspended solids after 30 min of settling in a measuring cylinder with the application of a gentle stirring (mL/g) and the Small $\mathrm{v_0}$ and k are sludge settleability constants for Vesilind (1968). The $\mathrm{v_0}$ explains the effect of sludge settleability on the actual settling velocity in Vesilind's equation (Equation 1.1) and k explains the effect of sludge settleability on sludge compaction (SSVI).

$$\frac{\mathrm{V_0}}{\mathrm{k}} = 68\mathrm{e}^{(-0.016\times\mathrm{SSVI})} \qquad (1.2)$$

Where,

SSVI = Stirred sludge volume index (mL/g)

The model was designed mainly on the settling characteristics of conventional activated sludge (CAS) but with the increasing usage of metal salts such as aluminium, ferric and calcium in the precipitation of phosphates today, the overall characteristics of sludge are different from the conventional sludges on which the existing models were based. Therefore, there is a need to develop a new model that describes the settling properties of chemically dosed activated sludge (CDAS). This recent study is an attempt to develop a new CDAS model that describes the effects of the varying concentration of Al^{3+}, Fe^{3+} and Ca^{2+} dosing on activated sludge settleability indicators. The proposed new model equation will address the limitation of Pitman (1980) and White (1975) models for the modelling of the settleability of CDAS.

CPR has been reported to cause an increased volume of sludge between 37 % and 97 % (Yeoman *et al.* 1988). This is due to most WWTPs in Europe using CPR to achieve their effluent P- consents using mainly aluminium (Al^{3+}), ferric (Fe^{3+}) and calcium (Ca^{2+}) salts for precipitation of phosphorus (Ojo and Ifelebuegu 2016; Ge *et al.* 2018; Ojo and Ifelebuegu 2019a; Wilfert *et al.* 2015). Sun *et al.* (2014; 2015) reported the importance of multivalent and divalent cations in evaluating sludge settleability and dewaterability. This shows that multivalent and divalent cations (Na^{+}, Mg^{2+}, Ca^{2+}, K^{+}, Fe^{3+}) were effective in making available positive charge to neutralise the negative charge on surface of sludge particles and creating larger sludge flocs. This also confirms the importance of investigating the impact of varying chemical coagulant dosing concentrations on activated sludge dewaterability. Therefore, the CPR processes are likely to impact downstream processes due to the heavier load of metal salts (Al^{3+}, Fe^{3+} and Ca^{2+}) used in the processes. The vital downstream processes include the anaerobic digestion (AD) and sludge dewatering processes (Sawatdeenarunat *et al.* 2015). The former is a well-known technology that biologically treats and degrades organic substrates in the absence of oxygen, the impact of which has been progressively increasing over the last decade (Zhang *et al.* 2016; Romero-Güiza *et al.* 2016), while the latter is known to reduce the sludge volume by separating the water from the activated sludge (AS) solids (Niu *et al.* 2013). The addition of coagulants (Al^{3+} and Fe^{3+}) can adversely impact the AD process and the dewaterability of the resultant sludges due to increased sludge production. Sludge treatment and disposal accounts for nearly 60% of the entire running cost of WWTPs (Zhou *et al.* 2014). Therefore, the sludge treatment and disposal process needs further comprehension for the purpose of process optimisation and cost savings. There have been various reports on the use of metal salts for the conditioning of sludge and their effects on sludge treatment processes (Zhang *et al.* 2016; Romero-Güiza *et al.* 2016; Niu *et al.* 2013; Zhou *et al.* 2014; Haandel and Lubbe 2012). Also, previous studies by Smith and Carliell-Marquet (2008; 2009) have reported on the digestibility of Fe-dosed sludge, with a reduced biogas production rate as a result of Fe dosing. Besides, the effect of calcium on the anaerobic digestion treating swine wastewater has been reported (Ahn *et al.* 2006). The result showed the digestibility of Ca-dosed sludge, with total biogas production been maximum at calcium dosing concentration of 3g/L. Also, other researchers have reported the impact of calcium salts on digestibility of activated sludge (Kumar *et al.* 2016;

Ahn *et al.* 2006; Lar *et al.* 2010; Junoh *et al.* 2016; Ji *et al.* 2017). Research on the effects of Al^{3+} salt on the digestibility of activated sludge is limited in the literature. This recent study provides a comparative assessment of the effects of Fe^{3+} and Al^{3+} on the digestibility of surplus activated sludge (SAS).

Several factors have been reported to affect the dewaterability of activated sludge, including surface chemistry (zeta potential) (Lee *et al.* 2000); yield stress, which explains the sludge rheological characteristics (Lotito *et al.* 1997); bound water content (Keiding *et al.* 2001) and extracellular polymeric substances (EPS) content (Mowla *et al.* 2013). Several chemicals have been researched as conditioners for the improvement of sludge dewaterability including chemical coagulants such as aluminium sulphate, ferric chloride, calcium hydroxide, polyelectrolyte, surfactants and enzymes (Ruiz-Hernando *et al.* 2013), acids and surfactants (Chen *et al.* 2001), Fenton's reagent pretreatment (Tony *et al.* 2008), calcined aluminium salt and potassium ferrate (Ye *et al.* 2012). While most of these studies focused on the effects of the use of these conditioners when used for conditioning during sludge treatment processes, there has been limited research on the effects of the chemicals used in the upstream activated sludge process for the precipitation of phosphorus on the downstream dewatering process. This recent study will further investigate the effects of CPR (Al^{3+}, Fe^{3+} and Ca^{2+}) on the dewaterability of WWTP primary sludge and SAS.

1.2 Aim of Research

The overall aim of this study is to investigate the impact of chemical dosing (Al^{3+}, Fe^{3+} and Ca^{2+}) on Activated sludge settleability, digestibility and dewaterability with a view to develop a novel numerical model to describe activated sludge settleability (ZSV and SSVI) as a function of chemical dosing and predict the impact of varying chemical dosing concentration on experimental ZSV and SSVI.

1.3 Objectives of Research

The objectives of this research study were to:

1. Evaluate the impact of chemical dosing (Al^{3+}, Fe^{3+} and Ca^{2+}) on activated sludge settleability parameter (ZSV and SSVI) data.
2. Develop models to predict ZSV and SSVI as a function of chemical dosing (Al, Fe and Ca) concentrations using estimated laboratory ZSV and SSVI data.
3. Investigate the impact of chemical dosing on experimental biogas production in a laboratory scale anaerobic digester.
4. Investigate the impact of chemical dosing (Al^{3+}, Fe^{3+} and Ca^{2+}) concentrations on dewaterability of activated sludge.

1.4 Research Motivation

This current research originates from the necessity to understand the impact of chemical dosing on settleability of activated sludge and develop a new numerical model to describe activated sludge settleability (ZSV and SSVI) as a function of chemical dosing and predict the impact of varying chemical dosing concentration on experimental ZSV and SSVI data. This will give better insight into the impact of chemical dosing (Al^{3+}, Fe^{3+} and Ca^{2+}) on activated sludge settleability operating curves, estimated experimental activated sludge settleability parameter (ZSV and SSVI) data. It also helps to understand and predict the impacts on activated sludge dewaterability and digestibility.

In summary, Chapter One presented the background information on why the current study investigates the impact of chemical dosing (Al^{3+}, Fe^{3+} and Ca^{2+}) on activated sludge settleability, digestibility and dewaterability. The aim and objective of research was addressed, and the research motivation was presented. Chapter Two will review related literature on activated sludge setttleability, digestibility and dewaterability.

Chapter Two

Literature Review

2.0 Introduction

This chapter reviews relevant literatures on the optimisation of the design and operation of chemically dosed activated sludge plants and is presented in three sections. The first section (2.1) is a review of relevant literatures on activated sludge settleability, the second section (2.2) is on activated sludge digestibility and the third section (2.3) is on activated sludge dewaterability respectively. In this section, the acronym LOT (list of tables) and LOF (List of figures) will be used often and is provided just after the appendices section of this thesis.

2.1 Activated Sludge Settleability

A critical process in activated sludge plant is the separation of suspended solid particles from treated water by means of gravity sedimentation which rely on effective sludge flocculation and sedimentation. Therefore, section 2.1.1 will review relevant literatures on activated sludge processes to give understanding on how settling and compressionability of activated sludge impacts settleability efficiency and effluent quality of receiving water.

2.1.1 Activated Sludge Process

Water has been identified as the most important resource in the world. This has placed municipal water systems under rising pressure due to huge wastewater production requiring treatment based on increasing population size (Burt *et al.* 2013). Thus, water and wastewater engineers are left with the task of providing good water quality and public health by ensuring efficient and economical treatment of final wastewater effluent to meet the urban wastewater treatment discharge guidelines. Although there are clear international and national guidelines and regulation in wastewater treatment legislation, the most relevant to this study is the urban wastewater treatment directive (UWTD 91/271/EEC) (List of tables, LOT-A1). It stipulates mandatory secondary treatment requirement for all sewered domestic wastewaters and all biodegradable industrial wastewaters. The minimum effluent standards were provided by the UWTD and include; 25mg/L biochemical oxygen demand (BOD), 125mg/L chemical oxygen demand (COD) and 35mg/L suspended solids (SS). Additionally, because eutrophication of water bodies in the UK as mentioned in section 1.1 may have adverse impact on biodiversity, the urban wastewater treatment directive has also proposed a more stringent regulation requiring reductions of 10-15mg/L total nitrate (TN) and 1-2mg/L total phosphorus (TP) concentration in outlets of wastewater treatment plant (WWTP) (European Commission 1991, 2016; Smith and Carliell-Marquet, 2008, 2009; Kroiss *et al.* 2011) before disposal to natural waters.

Most impurities in a wastewater final sedimentation tank occur as suspended solids which are suspended in the dispersion liquid and flow downwards under the force of gravity (the suspended matter was reported to be larger than the neighbouring liquid so that sedimentation can take place) (Metcalf and Eddy 2014; Bajcar *et al.* 2011; Zhang *et al.* 2010a; Metcalf and Eddy 2004; Metcalf and Eddy Inc. 1991; Gray 2010; Tebbutt 1998; Hammer 2008). The sedimentation processes in wastewater treatment includes; preliminary (separation of heavy particles at the wastewater treatment plant (WWTP) inlet by screening, fat removal, degreasing and grit removal), primary (removal of light organic matter from the influent wastewater, secondary (separation of biodegradable organic matter, suspended solids and nutrients using combination of an aeration tank and final sedimentation tank to enhance treatment and disposal) and tertiary sedimentation (final polishing unit process for further removal of residual suspended solids like the slow and rapid filtration process) (Tchobanoglous *et al.* 2014; Gray 2010; Metcalf and Eddy 2014).

Largely known globally to treat industrial and domestic wastewaters is the conventional activated sludge process (CAS) plant (Figure 2.1) that treats industrial and domestic wastewaters, and this was first initiated in 1913 in Manchester, United Kingdom (UK) in the Davyhulme treatment works built by Ardern and Lockett 1914 and 1923 (Tchobanoglous *et al.* 2003). The Davyhulme treatment works involved designs that consisted of a fill and draw batch process where both aeration and sedimentation takes place. This is followed by a continuous process in which settled wastewater enters the aeration tank and the flocculated microbial population in the mixed liquor settles out of the suspension in a settlement tank and forms a layer of sludge void of suspended solids and clarified effluent discharged as final effluent.

Figure 2.1. Schematic diagram of conventional activated sludge (CAS) Plant (Kroiss *et al.* 2011)

The ASP (Figure 2.2) is a calm environment for treatment of wastewater sludge and comprises mostly of a biological reactor called aeration tank and final sedimentation tank (FST). The treated effluent from the primary treatment tank (PST) after the preliminary wastewater processes (screening, grit removal etc.) has been completed is conveyed to the aeration tank (AT). The essence of supplying aeration in the activated sludge plant is to transfer oxygen to the mixed liquor (activated sludge) content and organic matter (OM) so that degradation takes place to form activated sludge flocs. The mixed liquor (ML) in AT is transferred to the FST where the clarified clear supernatant liquid is produced through gravity while the thickened sludge is conveyed to the bottommost part of the tank as a little thickened underflow or return activated sludge (RAS). This process is called sludge thickening. The RAS is used to maintain mixed liquor suspended solid (MLSS) concentration in the AT and the remaining sludge is wasted as wasted activated sludge (WAS). The aeration can be supplied either through surface aeration (mechanical aeration) or diffused aeration.

Figure 2.2. Activated sludge process (Metcalf and Eddy 2004)

The surface aeration involves air bubbles that are released into the liquid phase and instantaneous drops of mixed liquor are suspended into the air phase (Gray 2004; Gray 2010) while in the diffused system, air bubbles are introduced from the bottom of the aeration tank and the oxygen transfer occurs during the up-flow movement of these air bubbles within the aeration system (Tchobanoglous 2003). The elimination of biochemical oxygen demand (BOD) and ammonium (nitrification) requires an AT while nitrate removal (de-nitrification) requires another tank called anoxic tank (Tchobanoglous *et al.* 2014;2003). It can be concluded that the activated sludge treatment system comprises of five (5) main unit treatment processes addressed already; preliminary, primary, secondary, tertiary and advanced (LOT A3).

The surface aerators can either use a vertical or horizontal shaft but the vertical shaft type is more common to a conventional activated sludge system while the horizontal shaft system is identified for extended aeration in biological treatment processes such as oxidation ditches. Literature has reported 250 activated sludge plants in the UK serving a population equivalence of over 10,000 persons but about 40 have been identified as diffused aeration systems (Figure 2.3) while over 50 %

of surface aeration treatment plants treat wastewater for < 40,000 persons (Gray 2004; Gray 2010). The FST essentially are designed to reduce the velocity of water to allow the final effluent to be clarified and thickened to decrease the effluent suspended solids (ESS). The main component of an ASP (LOT-A2) includes the reactor, activated sludge, aeration and mixing, sedimentation tank and return sludge.

Figure 2.3. Mixing cycle setup by diffusers within the aeration tank (Gray 2004)

2.1.2 Final Sedimentation Tank (FST)

In wastewater treatment processes, there is an increasing need of disposal of final effluent to meet wastewater treatment consent. The FST is known to enhance the biomass-liquid separation within the ASP to produce a clear final effluent supernatant which will increase demand in disposal of final effluent meeting discharge consent (Li and Stenstrom 2014a). The need for effective and economic use of FST becomes vital since it contributes to increased treatment performance in ASP. FST is one of the most vital water and wastewater processing reactors used for removal of settleable solids by gravitational sedimentation (Tarpagkou *et al.* 2014). FSTs have two main functions which include the removal of settleable solids to produce clarified final effluent and the concentration of solids to a handleable sludge (Gray 2004). Since the FST is the last stage before discharging the effluent to the water bodies in the wastewater treatment works (WWTP), FST's efficiency becomes vital in meeting the stringent effluent quality standard and is the most critical unit process in ASP (Burt *et al.* 2013; Matko *et al.* 1996).

2.1.2.1 Principle of operation of FST

The functional zone of FST is vital and according to a previous review in WEF (2005), the identified four functional zones (Figure 2.4) include; Inlet region where the influent flow homogeneously enters the influent well (J in Figure 2.4), settling region in which settling occurs under calm environments, sludge region where the sludge is received below settling zone and Outlet Zone where the effluent (D in Figure 2.4) from tank is received (C in Figure 2.4) and released through the effluent weir (B in Figure 2.4).

Figure 2.4. A circular centre-feed FST with a scraper sludge removal system (WEF 2005)

2.1.2.2 Function of FST

The secondary treatment processes are globally used in activated sludge plants (ASP) to remove OM, SS and to reduce nutrients such as nitrogen and phosphorus. The ASP efficient operation demands that the sludge removed from the influent wastewater should pass through a solid and liquid separation process called sedimentation. However, for the sedimentation process to be termed effective, the activated sludge must be made up of large flocs with sufficient velocity for the removal process in a settling tank of reasonable volume called FST (Parker *et al.* 2004). The treated influent wastewater from the aeration tank needs to be separated from the biomass in the FST to produce a clarified final effluent (Ekama *et al.* 1997). Although there are many solid separation processes such as filtration etc., the most commonly used in wastewater treatment processes are the FSTs where the solid is separated from the liquid by downward gravitational force. Moreover, FSTs have been identified as one of the most vital unit operations in ASPs since it determines the efficiency of the wastewater treatment process (Bajcar *et al.* 2011; Ekama and Marias 2002) and loss of solids can result in low RAS in the AT which impacts negatively on the performance of ASP. This makes investigating the function of FSTs vital in the optimisation of the design and operation of FST'S in ASP. Li and Stenstrom (2014a, b) and Ojo and Ifelebuegu (2015) reported two related but dissimilar functions namely clarification (occurs at upper part of FST) and thickening (occurs at the bottom of FST). Clarification is the separation of suspended particles from the liquid stream to produce a clear effluent with reduced ESS, low effluent phosphorus (EP) and low effluent nitrate (EN) while thickening is the conveyance of suspended solids (> 98 %) to the bottom of the FST resulting in a slightly concentrated underflow or returned activated sludge (RAS). Other functions exhibited by FST during high peak flow include FST acting as a sludge storage tank. Known in ASP is the wet weather flow (WWF) condition which has a negative impact on wastewater treatment plant performance due to increased solids loading rate (SLR) and surface overflow rate (SOR) causing the conveyance of sludge from the aeration tank to the FST. The FST storage function is to cut down the loss of suspended solids (SS) through storing the extra sludge generated during WWF conditions. Researchers have identified different design options to accommodate the increased flow rate of sludge into the FST and these include; designing for additional FST volume for storage (De Clercq 2003), and aeration tank settling during peak flow period to cut down sludge intake in the FST (Reardon 2005).

Failure in both clarification and thickening leads to increased concentration of ESS and resultant loss in SS and reduction in mixed liquor suspended solids (MLSS) level within the aeration tank and the necessary sludge age (SA) reduces below the acceptable limit for effective ASP performance, resulting in the issue of effluent permit violation. Hence, two commonly used parameters, overflow rate and solids flux, have been developed for FST design and evaluation. Numerous factors affect the clarification function and therefore the efficiency of the FST. However, Ghawi and Kris (2012; 2011); WEF (2005) and Guola *et al.* (2008), identified some factors that limits the clarification efficiency of FST and these include external FST design parameters such as surface area (A) and depth (H), internal factors such as inlet structure, outlet structure, sludge collection, McKinney baffle arrangement, hydraulic instability (hydraulic short-circuiting and re-suspension of sludge particles based on the high velocity currents), thickening excesses because of high sludge blankets, denitrification processes in the FST and the flocculation propensity of the activated sludge (capacity to form large settleable flocs with decreased concentration of discrete solids that lack required weight to settle in the FST). Nevertheless, Nopens (2005) also added some factors that limit the degree of thickening in the FST such as the flow rates, tank's geometry, settleability and compactability of the activated sludge and the amount of the SS present within the aeration tank (AT). A well compacted activated sludge is known to reduce the cost of sludge disposal and dewatering processes. Therefore, should the FST fail in thickening efficiency, the treatment efficiency in the ASP will reduce because of decreased RAS transfer to the AT. The condition of an over-aerated sludge will cause poor flocculation and formation of pin-point floc while under-aerated sludge can lead to creation of an anaerobic or anoxic zone with excessive growth of filamentous bacteria (bulking activated sludge) which also affects activated sludge settleability. This is the reason why the flocculation well has been incorporated into the FST designs more recently. The presence of high shear zone during aeration can cause sludge floc breakup and variations that impacts clarification capacity negatively. The two basic conditions for FST operation reported are MLSS and RAS (Jenanayagam 2006). In section 2.1.6, more insight into flocculation will be explored.

2.1.2.3 Types of FST

Although, the type of FST has been identified to vary based on some key parameters, the earlier designs were to reduce velocity of flow so that particles settle during their retention time (RT), and were called Fill and Draw type of tanks (batch process) or the Continuous flow tanks

(Tchobanoglous *et al.* 2003). Some FST are also classified based on the flow diversion which can be horizontal or vertical. The horizontal flow inclined tank includes; longitudinal and radial flow tanks while the vertical flow inclined tanks include circular (upward) flow tank (Gray 2004). In wastewater practice, the most common types of tanks include; continuous circular or rectangular, horizontal flow type tanks (WEF 2005; Cassey 1992). The rectangular horizontal flow tanks (Figure 2.5) are suitable for large coastal sites where primary treatment alone is required before discharge to sea. The length varies from 2.5 to 4.0 times its width and depths vary from 2.5 - 3.5m.

Figure 2.5. Section through a horizontal-flow rectangular sedimentation tank (Gray 2004)

There are also baffle (B and E in Figure 2.5) installations whose primary function is to deflect the incoming wastewater to attain a uniform flow and avoids high velocity flows within the body of liquid which could cause hydraulic short circuiting of the liquid (Metcalf and Eddy 2014). Other types includes; the radial-flow sedimentation tanks which are circular in plan with diameter ranging from 15-30m (Gray 2004). Although there may be much smaller ones of 5m and larger diameter ones of 50m, their depths are the same as that of rectangular tanks ranging from 2.5 to 3.5m. The upward flow sedimentation tank has found usage in small treatment plants. The settling in this tank occurs by upward movement of the influent wastewater that initiates flocculation leading to increased particle size that makes the particle move through a sludge blanket where particles settle under a slow regime (Gray 2004). These tanks are deep and have a slope of 45 degrees when in conical form and a 60-degree slope when in pyramid side view. The distinction of these tanks with other rectangular and circular types is the absence of scraper (sludge collection mechanism) and sludge withdrawal taking place by hydrostatic pressure at the base of the tank. The conical-shaped circular FST is designed with a revolving scraper to distribute the activated sludge from the settling points to the sludge hopper (WEF 2005). However, the most common type of FSTs found in wastewater treatment are the circular and rectangular.

2.1.2.4 Efficiency of FST

The thickening and clarification efficiency of a FST is impacted by the activated sludge properties as well as internal and external hydrodynamic features in the FST (Nopens *et al.* 2005). Although the activated sludge settling, and flocculation properties correlates with the secondary treatment processes within the ASP (Wilén *et al.* 2008, 2010) these are related with the hydrodynamics in the FST. As mentioned in section 2.1.2.2, the sludge floc breakage and variation in FST is a function of the degree of turbulence experienced within the high shear zone during aeration in the aeration tank before transfer to the FST. The variation noticed in the FST is to increase the sludge floc production by increasing the weight of the floc formed (Biomass) and reducing the concentration of the dispersed SS in the sludge flow.

The activated sludge settleability can impact the return activated sludge (RAS) flow rate by limiting the maximum permissible flow rate entering the FST. This is called the solid loading rate (SLR) criteria (Ojo and Ifelebuegu 2015; Ekama *et al.* 1997). The FST must not be overloaded in thickening but, if this must occur, there must exist a limiting rate of solid flux (F) reaching the bottom of the FST (SLR must not be greater than limiting rate of solid flux). Figure 2.6 shows elements of state point analysis on good settleability which have been reviewed in Ojo and Ifelebuegu (2015) as mentioned. Martins *et al*. (2004) commented on poor settling of activated sludge linked to excessive filamentous bacteria growth. Therefore, inadequate thickening of the activated sludge will affect the efficiency of the FST because the sludge retention time will be altered. Burt and Ganeshalingam (2005) stated that the hydrodynamic flow path of FST influences the settling efficiency of the FSTs and the effluent quality of the ASP. Also, Anderson (1945) reported the impact of internal flows within a FST on the observed billowing suspended solids below the effluent weir. This reveals that flows in the circular FST is beyond one dimensional (1D) but are regard as two dimensional (2D) with axis regularity. The installed conventional stilling well was utilised in the circular FST to reduce the force of turbulent inlet flow and produce density driven current as reported in Burt and Ganeshalingam (2005).

Figure 2.6. Elements of state point analysis (Jeyanayagam n.d.)

The review in Burt and Ganeshalingam (2005), further reported that MLSS entering the FST under investigation by Anderson (1945) formed a radial underflow in the FST ranging from 2000 to 6000mg/L, which is far above the density of water. This explains why observed sludge blankets lift at the side wall of FST below the effluent weir. The momentum of the horizontal density current (density jetting developed at the bottom of the FST due to the falling ability of high density solid influent within the solid-liquid matrix) generated at the underflow was balanced by a counter density current of return flow at the upper portion of the tank. Since the strong density current is greater than the water density, a control become necessary and this can be achieved through optimising the internal structure of the FST by obstructing the sludge blanket and moving the SS to the effluent flow. The introduction of modified inlet structures such as baffles can reduce the bio-kinetic energy of flow and buoyant potential energy (Larsen 1977; Krebs 1991; Bretscher *et al.* 1992; Krebs *et al.*1995) and this will improve the solid removal efficiency of the FST. Increased depth of the tank can also decrease the dwindling impact of strong density currents on the effluent quality in ASP (Krebs *et al.* 1998) and various FST designs has been evaluated using numerical tools with recommended large radius for FST with strong density current (Zhou and McCorquodale 1992). Other internal feature modifications were investigated to including energy dissipating inlets (EDI), varying the centre feed basin diameter, providing an inlet floor baffle (McKinney) underneath the centre feed basin (reviewed in Burt and Ganeshalingam 2005). This shows that hydrodynamics of the FST impacts the sludge distribution within the FST due to the density classification in the FST. According to Ghawi and Kris (2011; 2012), to account for the limiting factors to efficiency of FST (section 2.1.2.2), designers are over-designing and oversizing the FSTs within the biological treatment processes (ASP). The need for optimisation of the design and operational efficiency of FSTs in ASP has led to exploring numerical computational fluid dynamic (CFD) analysis in the last decade. The following section 2.1.2.5 (Modelling FST) will review literature on linkages between efficiency of FST and numerical modelling. This current study will not assess the impact of applying internal hydrodynamic tank configuration on both solid removal efficiency and settling velocity within the FST using CFD modelling but will focus on investigating the impact of extra weight of chemical dosing on conventional settling velocity model as a tool to predict the efficiency of FSTs regarding ESS concentration.

2.1.2.5 Modelling of FST

Based on section 1.1, the scope of current study is limited to the most common settling velocity model provided by Vesilind (1968). It was stated that conventional activated sludge rheology has changed due to chemical dosing with aluminium, ferric and calcium salt and it becomes paramount to investigate the extra weight of chemical dosing on the existing empirical equation (Vesilind 1968; Pitman 1980; 1984; White 1975) used in final sedimentation tank design. This shows that chemical dosing varies between wastewater treatment systems and determination of the impact of chemical dosing (Al, Fe and Ca) on zone settling velocities (Vesilind 1968) will help provide important understanding about the effect of chemical dosing on activated sedimentation processes. Furthermore, better improved prediction of the impact of chemical dosing (Al, Fe and Ca) on FST performance by including a chemical dosing protocol as a variable in conventional settling velocity model (Vesilind 1968) can be realised. The process data from ZSV and SSVI tests can be utilised to predict ZSV as a function of chemical dosing parameters. In this vein, reviewing relevant literature on numerical models available in wastewater treatment becomes important in modelling the impact of chemical dosing (Al, Fe and Ca) on conventional settling velocity equation (Vesilind 1968). This mathematical modelling will not just provide information about the physical, biological and chemical phenomena happening in the FST but will further impact the overall prediction of the performance of the entire ASP. It is vital to mention that mathematical modelling can only provide approximate process results or simplification of a real process in wastewater treatment plant.

Mathematical modelling has already been established in terms of its theoretical, economic and practical relevance in the water and wastewater industry (Ghawi and Kris 2011). Modelling FST using mathematical modelling equations will not just provide understanding about the fundamental mechanism and processes impacting the efficiency of FST but will serve as a process optimisation tool. The process data obtained from batch settling experiments (ZSV test) can be used to optimise the process of settling in FST without conducting ZSV test. The one dimensional (1D), two dimensional (2D), three dimensional (3D) and the state point analysis (sp) has been reported in review by WEF (2005). However, mathematical modelling in its modest form has been reported as mathematical functions that are statistical built-in to known input and output data (black box or empirical model) (Ekama *et al.* 1997). These black box models are bound to the calibration condition employed in the setting up process and example is the one dimensional (1D) model. The 1D model also evaluates the flow field and concentration profile in the vertical direction of the FST. They are used mainly for operational control and are based on flux theory of Kynch (1952). The 1D model has drawbacks which include the impacts of key features and internal configurations in the tank hydrodynamics which considerably affect the FST efficiency. The models identified included; Glass box or deterministic models that can predict almost any fluid flow and heat transfer process as a solution of a set of partial differential equations that describe the fundamental physical processes (continuity, momentum, energy, transport of solids and biological reactions) (Zikanov 2010). The computational fluid dynamics (CFD) models are that category that solves both 2D and 3D momentum and continuity equations are examples of the glass models but have a limitation of high computational power requirement (Wicklein and Samstag 2009). The Grey models are yet another category of numerical model based on grossly simplified physical laws and they find relevance in the solid flux theory, diffusion reactor models and models of simple velocity profile in fluid mechanics (plug-flow models) (WEF 2005). Past studies on the merit of 3D and 2D CFD modelling has been reviewed in Ghawi and Kris (2011 and 2012) and governing equations for CFD modelling (Equation 2.1-2.26) are provided below.

Continuity and density

The conservation of mass or continuity equation is given in Equation 2.1

$$\frac{\partial \rho}{\partial t} + \nabla . \rho U = 0 \tag{2.1}$$

In the drift flux the fluid mixture density varies throughout the domain as a function of concentration.

$$\rho = \rho_{mixture} \tag{2.2}$$

According to Zhou and McCorquodale (1992), the relation for density mixture can be expressed as Equation 2.3

$$\rho = \rho_w + C\ (1 - \frac{1}{Sg}) \quad ‘ \tag{2.3}$$

Where,

ρ_w = density of water

C = Solid concentration expressed in the same unit as density (Kg/m^3).

However,

Sg = specific gravity of dried sludge = 1.45 (2.4)

Besides, Sg with a value of 1.45 as indicated in Equation 2.4 was subject to the research studies of Larsen (1977).

But,

C= ρY (2.5)

Where,

Y = solid mass fraction

Substituting Equation 2.5 into Equation 2.3, another expression Equation 2.6 will be realised.

$$\rho = \rho_w + \rho Y(1 - \frac{1}{Sg}) \tag{2.6}$$

But, Equation 2.6 in terms of volume fraction (r_s) can be modified as Equation 2.7

$$\rho = r_s Sg\rho_w + (1 - r_s)\, \rho_w \tag{2.7}$$

Momentum and Effective Viscosity

The conservation of momentum is expressed as:

$$\frac{\partial}{\partial t}(\rho U) + \nabla.(\rho U(X)\mathrm{U}) - \nabla.\left(\mu_{eff}\left(\nabla U + (\nabla U)^T\right)\right) = -\nabla P + \mathrm{g}\,(\rho - \rho_w) \tag{2.8}$$

The effective viscosity in the diffusive term is a function of the fluid rheology and is equally impacted by the local turbulence. More so, the buoyancy force is included as a source on the right-hand side (RHS) of Equation 2.8 but added is a modified pressure incorporating the hydrostatic component as shown in Equation 2.9

$$\mathrm{P} = \mathrm{p} - \rho_0(\mathrm{g}^*\mathrm{x}) \tag{2.9}$$

Rheology

The modelling of activated sludge properties with the drift flux model allows a prediction of the sludge blanket height and the influence of scouring from the top of the sludge blanket. However, to effectively describe the sludge blanket dynamics a suitable rheology model will be required for the sludge. Thus, viscosity may be thought of as having two components namely; molecular component which is essentially a definitive physical property while the other is a turbulence component which is a constructed model that allows the influence of turbulence on the diffusion of various fluid fields.

$$\mu_{eff} = \mu_p + \mu_T \tag{2.10}$$

Where,

μ_p = plastic viscosity

Moreover, Bokil and Bewtra (1972) model described the plastic viscosity (μ_p) as a function of the concentration and hence it can be expressed as Equation 2.11

$$\mu_p = 0.00327 \times 10^{0.132C} \tag{2.11}$$

Another complex model was proposed by Lakehal *et al.* (1999) that treat the sludge as a Bingham plastic and this further modifies the molecular viscosity expression as Equation 2.12

$$\mu_m = \frac{\tau_b}{\gamma} + \mu_p \tag{2.12}$$

Where,

γ = The rate of shear strain

However, Dick and Ewing (1967) defined the plastic yield stress (τ_b) in Equation 2.13

$$\tau_b = \beta_1 e^{C\times\beta_2} \qquad (2.13)$$

But, Dahl (1994), defined (μ_p) as plastic viscosity in an expression given in Equation 2.14

$$\mu_p = \mu_w + C_{Pa} \times C_{Pl} \times (C - C_{Ps})^K \qquad (2.14)$$

Nonetheless, Armbruster (2003) proposed various coefficients for Dahl (1994) plastic viscosity expression stated in Equation 2.14, to derive a power law relationship for sludge. Still, De Clercq (2003) further modified Lakehal *et al.* (1999) expression in Equation 2.12, Dick and Ewing (1967) Equation 2.13 and a new hertschel bulky like relationship was realised in Equation 2.15 and Equation 2.16

$$\tau_b = \beta_1 \times C^{\beta_2} \qquad (2.15)$$

$$\mu_m = \frac{\tau_b}{\gamma}(1 - e^{(-m\gamma)}) + \mu_p\, \gamma^{n-1} \qquad (2.16)$$

Although, μ_p can be computed from Equation 2.14 but according to Burt and Ganeshalingam (2005) β_1, C_{Pa}, C_{Pl}, m and k are identified as model constants.

Turbulence

Research studies, Gray (2010) and Gray (2004) have shown that the flow in FST in operation is more quiescent in nature when progressing from the influent but becomes agitating within the stilling well. Thoughit is possible to compute the global and localised Reynolds numbers but it will be limited if some local areas have a huge velocity but no velocity of flow in other regions. However, the standard k-ε model which adopts a logarithmic wall function accommodates this limitation by could adjust for the turbulence realised in the near wall region. The correct use of the wall functions depends on the quality of grids adopted for the modelling. Thus, for this research a low Reynolds number version of the k-ε Turbulence model will be investigated.

Importantly, turbulence has been related back to momentum equations through the effective viscosity covered in Equation (2.10-2.12) given by Bokil and Bewtra (1972) and Lakehal *et al.* (1999).

Thus, the turbulent contribution to effective viscosity is given in Equation 2.17

$$\mu_T = \rho \times \frac{k}{\omega} \qquad (2.17)$$

Transport equations can be calculated for turbulence kinetic energy (k) and turbulence dissipation rate (ω) using Equation 2.18 and Equation 2.19

$$\frac{\partial}{\partial t}(\rho k) + \nabla.(\rho U k) - \nabla.((\mu_m + \frac{\mu_T}{\sigma_K})\nabla k) = P + G - \rho\omega k \qquad (2.18)$$

$$\frac{\partial}{\partial t}(\rho\omega) + \nabla.(\rho U\omega) - \nabla.((\mu_m + \frac{\mu_T}{\sigma_\omega})\nabla\omega) = C_1 \frac{\omega}{k}(P + C_3 \max(G, 0)) - C_2\rho\omega^2 + D \qquad (2.19)$$

Where,

P= shear production term

G = Buoyancy Production term

1C_1, C_2, C_3 = Empirical constants with defined defaults but C_3 is unknown for stratified flows.

D = complex expression used to force the turbulence model into the regions outside of the fluid boundary layer.

Drift flux scalars and settling relationships

The conservation of solid species equation has been given in Equation 2.20

$$\frac{\partial}{\partial t}(\rho\, Y_i) + \nabla.(\rho(\mu + \mu_{si})\, Y_i - \nabla.((\mu_m + \frac{\mu_T}{\sigma_C})\, \nabla\, Y_i = 0 \qquad (2.20)$$

Where,

Y_i = mass fraction used as the marker for the drift flux or algebraic slip scalar

i = subscript that denotes the possibility of having multiple mass fractions representing multiple solid size group

μ_{si} = slip velocity component that represents the difference between the solid and fluid velocities

However, solid size group has its own fixed slip velocity or single slip scalar is used with μ_{si} some functions of local concentrations.

In contrast, Takács *et al*. (1991) reported an empirical hindered settling velocity that may be beneficial in combining with the slip scalar equation. This expression takes the form of a double exponential given in Equation 2.21

$$V = v_0 \times \exp[-r_h(C - C_{ns})] - v_0 \times \exp[-r_p(C - C_{ns})] \qquad (2.21)$$

Where,

v_0 = the free settling velocity or stokes velocity for a single floc in infinite fluid

C_{ns} = concentration of non-settleables taken to be 0.2% of the MLSS concentration

r_h and r_p = free settling and colloids settling parameters

Although, the settling models covered earlier in the literature review chapter can be used in one dimensional solid flux theory for the design of FST was based on the Vesilind equation which followed the research studies of Kynch (1952) expressed in Equation 2.22

$$\mathrm{V} = \mathrm{v}_0 \times \exp\,(-\,\mathrm{r_h}\mathrm{C}) \tag{2.22}$$

Although, the single exponential form of Equation 2.22 is known to be appropriate only for the zone or sludge line settling phase but, in the case of sludge settleability column test using the settlometer, a discrete interface is seen between the solids and a clear supernatant. Thus, the need to extend the vesilind equation to the Takács *et al.* (1991) form of a double exponential to model the four regions of sedimentation namely; lag, hindered, transition and compression (Ekama *et al.* 1997). Nevertheless, there are many empirical correlations that relates v_0 and r_h to measurable indices such as SVI, SSVI and DSVI. However, the standard UK Water Research Council (WRc) method for designing FST uses the Pitman (1980) and White (1975) correlation (Equation 2.23) for linking $SSVI_{3.5}$ to the Vesilind coefficients.

$$\frac{v_0}{r_h} = 6.79 \,*\, \exp\,(-0.016\mathrm{SSVI}_{3.5}) \tag{2.23}$$

$$r_h = 0.88 \,-\, 0.393\log\,(\frac{v_0}{r_h}) \tag{2.24}$$

The omitted factor (r_p) can be computed experimentally between 3 and 10 to obtain the best tangent to fit to the Takács operational curve. On the other hand, the Vesilind coefficients can be related to SSVI the Wahlberg and Keinath (1968) which is valid but for American sludges. This can be expressed in Equation (2.25 and 2.26)

$$v_0 = 15.3 - 0.0615\mathrm{SSVI}_{3.5} \tag{2.25}$$

$$r_h = .436 - 0.00384\mathrm{SSVI}_{3.5} + 0.0000543(\mathrm{SSVI}_{3.5})^2 \tag{2.26}$$

The internal hydrodynamic issues in FST may be resolved through achieving optimised final effluent quality and underflow solid concentration by utilising numerical experimental result in filling the gap of wearisome and time-consuming field experimental results (Huggins *et al.* 2005).

However, this current study will focus on the empirical model and not the CFD modelling procedure in developing a mathematical model that describes the impact of chemical dosing (Al, Fe and Ca) on the activated sludge settling behaviour in FSTs. The reason for selecting the empirical model approach is because mathematical settling velocity equations can be used to fit experimental settling velocity data for chemically dosed activated sludge. It makes it easier to evaluate ZSV as a function of a new chemical dosing parameter.

2.1.3 Settling Characteristics of the Activated Sludge

As mentioned in section 2.1.2.4, the capacity of sludge particles to flocculate and form large flocs, that can settle speedily and be separated in the FST, describes the efficiency of the ASP. The settling regime of activated sludge differs among various areas in the FST and it is monitored by the activated sludge concentration and flocculation propensity. The sludge settling characteristics (sludge concentration and flocculation of sludge particles) investigation in this current study will provide understanding of the different sludge settling behavior that can be observed in the FST during the batch settling experiment. Wilén *et al.* (2008) stated that a typical activated sludge matrix will show particle size distribution ranging from free cells (≤ 5μm) to aggregate flocs (25-100μm). The batch settling experiment in this current study will involve measuring the descending liquid/solid interface level called the sludge blanket height (SBH). Therefore, during the batch settling test, four dissimilar settling regimes (Figure 2.7) will be expected as reported in review by Ekama *et al.* (1997). The dissimilar settling regimes includes lag, hindered/zone, transient, and compression settling. The lag regime noticed at the beginning of the SBH measurements explains the spread of the kinetic energy added with uneven air bubbles used to unify the activated sludge in the batch settling reactor before the estimation of SBH commences. The consequent constant descending rate of SBH corresponds to the zone settling velocity of the mixture settling with concentration equal to the initial value.

Figure 2.7. Different settling regimes of activated sludge during (a) sludge blanket height measurement (b) batch column settling tests (Ekama *et al.* 1997)

The transition phase between the zone (hindered) to compression settling regimes can be observed in the SBH measurements when the thickened sludge beneath moves up until it meets the liquid-biomass interface. However, Figure 2.8 further shows four settling categories based on both the sludge concentration (vertical axis) and flocculating characteristics (horizontal axis).

Figure 2.8. Four classes of activated sludge settling regimes and clarification, compression and zone settling regions (Ekama *et al.* 1997)

In the upper part, at low concentrations, discrete settling (Class I-top left of Figure 2.8) and flocculation settling (Class II-Top right of Figure 2.8) occurs. This discrete particle will settle individually since the concentration is too low for interaction between particles making the settling velocity a function of individual particle properties such as porosity, density and size (Vesilind 2003). Therefore, this class of discrete settling is called clarification. However, flocculent settling will also take place at low solids concentrations, but when the particles show a strong flocculating tendency with dense individual flocs they finally settle faster. This process occurs in the upper middle region of the FST. This type of settling is also known as clarification. In contrast, increasing concentration in the lower part will cause the distance between the flocs to reduce and hence they no longer settle as individuals but result in hindered or zone settling (Class III- Lower middle region of Figure 2.8). The claim for the occurrence of zone settling is based on the fact that, as the particles settle, an upward movement of water is created which increases the particle drag, and as a result decreases the relative settling velocity of mixture (Probstein 2003). This phenomenon was further commented in Kynch (1952) that the particles settle with the velocity that is only a function of local concentration (sludge concentration) despite the size or density of individual particles. At the bottom region, where the concentration further increases, the particles, in addition to gravity and drag forces, are exposed to the inter-particle compressive stress and settle slower than in zone settling (Class IV-Bottom region of Figure 2.8). This class IV is called compression settling.

2.1.4 Settling Velocity Models

The modelling of FSTs requires an appropriate mathematical explanation of the settling characteristics of activated sludge. This section 2.1.4 is vital in this current study because of the limitation of characterising the entire settling process in the FST due to the co-existence of different settling regimes in the FST. Therefore, this section will review related up-to-date literature on settling velocity model or equation used to describe the settling behaviour in the different regions within the FST.

The efficiency of activated sludge plants depends essentially on the settling and thickening characteristics within the FST (Li and Stenstrom 2014a, b; Burt and Ganeshalingam 2005). This is partly due to the diversity and complexity of the mechanisms involved in the separation of liquid and solid phases (Lee *et al.* 1999). The development of settling velocity of activated sludge has been designed on both mathematical and experimental basis. These consist of fitting mathematical formula to experimental data (black box model) and this forms the fundamentals in modelling and designing of FSTs. The typical example is empirical settling velocity equation called Vesilind (1968) expression [ZSV = v_o * exp (-k.X)], used for explaining the activated sludge settling characteristics for municipal and industrial wastewater treatment, where, ZSV =zone settling velocity (m/h); X = activated sludge concentration (g/l); v_0 = sludge settleability constant (m/h) and k = sludge settleability constant (l/g). The empirical description of activated sludge settleability characteristics for modelling and designing FSTs is vital because of the challenge of characterising the entire settling process in ASPs. This challenge has been attributed to the distinction observed in sedimentation regimes in FSTs ranging from discrete, zone, flocculent-discrete and compression settling (section 2.1.3) (Ekama *et al.* 1997). The various settling regimes within the FST (2.1.3) will be used in explaining the various developed settling velocity models used in the modelling and design of FST. Also, justification of the reason for utilising the conventional Vesilind (1968) settling velocity model will be explored. As earlier reported in section 2.1.3, at the upper part of FST, at low concentrations, discrete and flocculation settling does exist. However, since particles settle individually because of low sludge concentration with absence of interaction between particles, determination of an accepted sludge settling velocity model becomes difficult. Therefore, settling velocity has been investigated as a function of individual particle properties such as porosity, density and size (Vesilind 2003), and the sludge water interaction (Kinnear 2002; Vanderhasselt and Vanrolleghem 2000). Also, Figure 2.9 shows the forces acting on activated sludge floc and among the four forces identified in the discrete spherical particles, three principal forces impacting on sludge particles are gravity (F_G) buoyancy (F_B) and drag(F_D) (Figure 2.10)

Figure 2.9. Force acting on activated sludge floc settleability

Figure 2.10. Force on a discrete particle (Wu and He 2010)

Tchobanoglous *et al.* (2003), reported that the terminal settling velocity of discrete spherical particles (V_s) falling in a quiescent fluid obeys Stokes law and it can be used to determine the settling velocity of discrete particles in Equation 2.27 for laminar condition and Equation 2.28 for turbulent condition (Tebbutt 1998; Carlsson 1998; Cassey 1992). Stokes law suffers from certain limitations which include; shapes of particle not always spherical in real practice, liquid may not be at rest, all particles may not be discrete, Stokes law is valid only when Re≤ 1.0 and fluid temperature may not be consistent However, more detailed evaluation of Stokes law can be found in Appendix-A**).**

$$V_S = (\rho_P - \rho_W)\ gd^2 \backslash\ 18\mu \qquad (2.\ 27)$$

$$V_S = \sqrt{3.3\mathrm{g}\ (\rho_P - \rho_W)/\ \rho_w} \qquad (2.\ 28)$$

Where:

ρ_P = Density of particle (kg/m^3)

ρ_w = density of water (kg/m^3)

g = Gravitational constant (m/s^2)

d= diameter of Particle

μ = dynamic viscosity of solid particle and water mixture (kg/ms).

Moreover, under quiescent conditions, discrete particles settle out at their terminal velocity, which will remain constant provided the fluid temperature does not alter. The knowledge of this velocity is fundamental in the design of sedimentation tanks and in evaluation of their performance. Thus, *a sedimentation tank is designed to remove all particles that have a terminal velocity (V_S) equal to or greater than (>) V_S*. The selection of V_S depends on the specific function of the tank and on the physical characteristics of the particle to be removed (Gray 2010). In contrast, sludge particles may not always be spherical in shape and as such the sludge floc structure is irregular and not regular as expected and, as mentioned earlier, sludge particle porosity depends on the sedimentation velocity of discrete solid particles and the density of sludge particles is not easy to estimate. Kinnear (2002) has made the determination of settling velocity for discrete particle using Stokes law debateable (Jorand *et al.* 1995).

Although, discrete settling regime in FSTs has been explained in literature by direct modification of the classical zone settling velocity models (Takács *et al.* 1991; Dupont and Dahl 1995) but suffered from some drawbacks as the Takács *et al.* (1991) empirical model could not model discrete settling of different floc sizes. In solving this challenge, different discrete settling velocities of each floc size particles was investigated (Dupont and Henze 1992; Lyn *et al.* 1992; Otterpohl and Freund 1992; Mazzolani *et al.* 1998; Zhang *et al.* 2006), but result was limited because the individual floc size particles with different discrete settling velocities still have capacity to change in size because of the flocculation and capacity of the sludge floc to break up during settling. Existing research studies assessed the development of empirical models to explain discrete velocity settling of different sludge particles such as the work of Kinnear (2002); De Clercq (2003); Griborio (2004); McCorquodale *et al.* (2004) but Mahdavi Mazdeh (2014) used an innovative sludge settling column to evaluate discrete settling rates of different sludge particle sizes.

As stated earlier in section 2.1.3, in the zone settling regime sludge particles settles as a zone of blanket and the interface between the sludge and the clear water supernatant can be separated within the settling column (Figure 2.11). This makes evaluation of zone settling velocity (ZSV) in a settling column feasible using the experimental batch settling test for different initial sludge concentrations (Ekama *et al.* 1997). The sludge sample is collected over a range of diluted concentrations (X, mg/L) and allowed to settle under a quiescent condition in the settling column. The sludge height is deduced at a defined time interval and the slope of the linear tangent to the settling curve gives an approximate value of the settling velocity.

Figure 2.11. Settling column Interface between sludge subsiding and clear supernatant (Alrawi *et al.* 2011)

Although, since the mass flux theory was developed by Kynch (1952), various studies have been conducted to examine the relationship between zone settling velocity and activated sludge concentration using many empirical and theoretical model (Vesilind 1968, Dick and Young 1972; Vearenbergh 1980, Vanderhasselt and Vanrolleghem 2000; Giokas *et al.* 2003; Zhang *et al.* 2006; De Clercq *et al.* 2008; Watts *et al.* 1996, Lakehal *et al.* 1999; Takács *et al.* 1991;Cho *et al.* 1993). These models postulate that the ZSV is only a function of the sludge concentration and it is valid for zone settling regime in FSTs (Vanderhasselt and Vanrolleghem 2000).

However, the most acceptable models are those suggested by Vesilind (1968) and Dick and Young (1972). The Actual ZSV is expressed as Equation 1.1 (ZSV = $\mathrm{v_0\ e^{-kX}}$) (Vesilind 1968) and Equation 2.29 (Dick and Young 1972). The X is the solids concentration, Vesilind parameters (k and $\mathrm{v_0}$) and Dick and Young parameters (K and $\mathrm{V_0}$) can be obtained from the slopes of batch test settling curves for Vesilind and Dick and Young experiment. The Capital V_0 and K are sludge settleability constants expression for Dick and Young (1972) expression in Equation 2.30. The $\mathrm{V_0}$ explains the effect of sludge settleability on the actual settling velocity while K explains the effect of sludge settleability on sludge compaction (sludge volume index—SVI). Furthermore, the Vesilind’s and Dick and Young 1972 model equations have been reported to be the most accepted worldwide for predicting the sludge settleability behaviour within the FSTs (Haandel and Lubbe 2012).

$$\mathrm{ZSV} = \mathrm{V_0}\,(\mathrm{X})^{\mathrm{K}} \qquad (2.29)$$

Activated sludge (AS) usually shows a strong flocculating ability even at low concentrations (below 1kg/m³) which results in a zone settling behaviour in FSTs. It is equally challenging to investigate settling behaviour of activated sludge at low concentrations specifically below 1 kg/m³ due to the limit of evaluation (there is no interaction with the sludge particles and the settling velocity will be a function of individual floc properties and, also, since no clear relationship with the concentration of the activated sludge particle exists at low sludge concentration). This is because the zone settling velocity ($\mathrm{v_O}$) predicted by Vesilind exceeds the actual settling velocity of the particles (ZSV) within the upper region of FSTs at a lower concentration. Therefore, the Vesilind equation was optimised to accommodate zone settling of particles at lower concentrations in Takács *et al.* (1991). The improved zone settling velocity by Takács *et al.* (1991) is expressed as Equation 2.30:

$$\mathrm{ZSV} = \mathrm{V_O}\,\mathrm{e}^{-\mathrm{K_1 X_a}} - \mathrm{V_O}\,\mathrm{e}^{-\mathrm{K_2 X_a}} \qquad (2.30)$$

The initial part of Equation 2.30 shows Takács' deduction of zone settling velocity of the large and well flocculated particles while the second component of Equation 2.30 shows a zone settling velocity correction for smaller and slow settling particles. The $\mathrm{V_O}$ is the maximum settling velocity (m/h); $\mathrm{K_1}$ is the settling parameter characteristics of the zone settling regime (m³/g); $\mathrm{K_2}$ is the settling variable that explains the behaviour of the low solids concentration (m³/g); $\mathrm{X_a}$ is X-$\mathrm{X_{min}}$ and $\mathrm{X_{min}}$ is the minimum suspended solids concentration (g/m³). The settleability parameters can be obtained by fitting Equation 2.30 to experimentally determined batch settling data. Figure 2.12 shows experimental batch settling curve for Vesilind (1968) and Takács *et al.* (1991). Despite the empirical model selected in FST design and operation, the settling velocity measurements are used for calibration (Schuler and Jang 2007a, b and c).

On the contrary, some drawbacks were spotted with the Takács *et al.* (1991) empirical model which was linked to its calibration. The issue was that the parameter related to discrete settling regime cannot be determined using the batch settling test since at a lower concentration discrete particles settle individually without interaction and the settling velocity will be a function of individual particle properties such as porosity, density and size (Torfs *et al.* 2013b). Hence it is challenging to monitor the sludge water interface in the settling column.

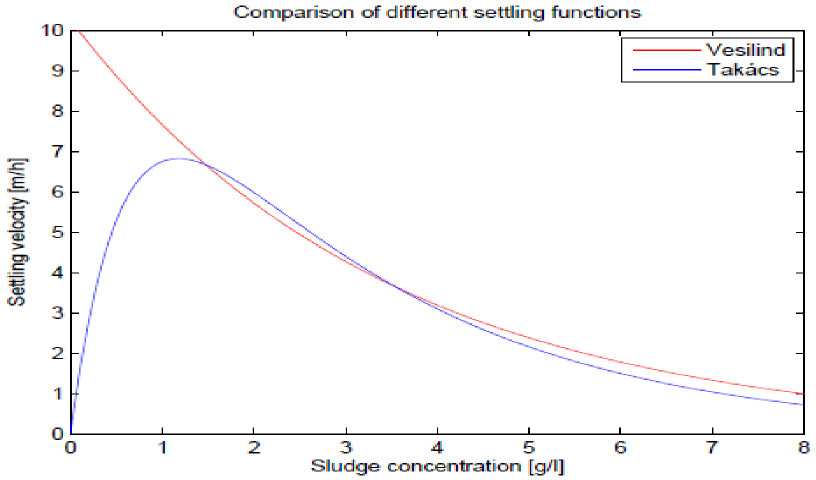

Figure 2.12. Experimental batch settling curves for Vesilind 1968 and Takács *et al.* (1991) model.

Although, so far, the Takács *et al.* (1991) equation is still relevant to predict the ESS concentration during solid flux analysis but cannot be satisfactory outside its boundary of calibration due to the limitation of providing only an insight into the basic mechanism (Figure 2.12). As a black box model (Takács model) it cannot provide any physical meaning compared to other models that can investigate the internal flow pattern of the solid and liquid within the FST (glass box model).

Amongst the limitations in the use of the zone settling velocity mathematical model (Equation 1.1) is the laborious standardization technique comprising of a series of laboratory batch settling tests (section 2.1.5). This calibration procedure is enabled using a device called a settlometer (Vanrolleghem *et al.* 1996) to spontaneously record batch settling curves. However, Vanderhasselt and Vanrolleghem (2000) further examined the effectiveness of single batch settling curve (BSC) techniques compared to the conventional dilution experiments in determination of settling velocity models. The settling velocity models of Vesilind (1968), Takács *et al.* (1991), and Cho *et al.* (1993), had sludge blanket height data obtained from a single BSC which was a limitation to batch settling test and improvement was made with the batch settling test by accommodating more high settling rates data points for identifying the sludge blanket height (SBH) during the batch settling test. Nonetheless, Vanderhasselt and Vanrolleghem (2000) added that continuous column settling tests will provide a better result with studying the hindered and transient settling regime within FST. The investigation of settling velocity under turbulence boundary conditions in the review of Rasmussen and Larsen (1996) utilised the continuous column settling test.

As mentioned earlier that since the advent of mass flux theory by Kynch (1952) the most acceptable models are those suggested by Vesilind (1968) and the Vesilind parameters k and

v_0 are obtained using batch settling tests. On the contrary, other procedures relating empirical functions with the sludge settleability indicators such as SVI, DSVI and SSVI have been reported by researchers (Pitman 1984; Ekama and Marias 1986; Wahlberg and Keinath 1988; Giokas *et al.* 2003; Diagger 1995). However, sludge concentration has been an added issue linked to activated sludge settleability and to eradicate the challenge, the diluted sludge volume index (DSVI) was developed (Stobbe 1964). This test was achieved from a simple settling test in a 1 Litre settling column with a diluted sludge sample (to eradicate impact of sludge concentration), where the volume of the settled sludge per gram of solids is measured after 30 minutes. It was observed that when the sludge volume after settling was less than about 25% of the original volume, the calculated SVI value was almost constant and was not dependent on the initial sludge concentration. Therefore, it was recommended that sludge batches be diluted until the volume of the diluted suspension after settling assumed a volume of 200ml or less per litre of initial volume used. The stirred sludge volume index (SSVI) was also investigated as a more competent approach and it was defined as the volume of a unit mass of suspended solids after 30 min of settling in a measuring cylinder with the application of a gentle stirring in Equation 2.31 (White 1975). According to White (1975), the SSVI was virtually free of the initial sludge concentration unless for occasions where the ZSV is very low (1< m/h). Importantly, in resolving the issue of poor settling sludges, White (1975) advised the use of a standard concentration of 3.5 g/l thus re-defining it as $SSVI_{3.5}$ against the previous expression of SSVI. Nevertheless, further research was conducted on 25 activated sludge processes in the Netherlands and another value of $SSVI_{3.5}$ and DSVI was determined which led to discovery of another proportional link between these two process parameters as shown in Equation 2.32 (Stofkoper and Trentelman 1982).

$$\mathrm{SSVI\ (ml/g)} = \frac{\mathrm{Volume\ of\ Settled\ Sludge\ after\ 30\ mins}\ ,\frac{\mathrm{mL}}{\mathrm{L}}(\frac{1000\mathrm{mg}}{\mathrm{g}})}{\mathrm{MLSS\ Concentration,mg/L}} \quad (2.31)$$

The Relation between $\mathrm{SSVI}_{3.5}$ and DSVI can be computed from Equation 2.32.

$$\mathrm{SSVI}_{3.5} = \mathrm{C_P} \times \mathrm{DSVI} \quad (2.32)$$

Where,

$\mathrm{C_P}$ = Proportionality Constant with an average value = 2/3

Additionally, further investigation was made which involved the use of sludge with varying fractions of active sludge and result revealed that the value of the proportionality constant ($\mathrm{C_P}$) was reliant on the active fraction of the volatile sludge ($\mathrm{f_s}$) as calculated from Equation 2.33 (Catunda *et al.* 1989)

$$\mathrm{C_P} = 1 - 0.35 \times \mathrm{f_s} \quad (2.33)$$

The relationship between different sludge settleability parameters reported in literature ranging from the research conducted by Pitman (1984) involving analysis of six years full-scale study which resulted to developed empirical relationship between the constants of Vesilind's equation and SSVI. The correlation obtained was earlier given in Equation 1.2 ($\frac{v_0}{k} = 68 \; * \; \exp\left(- 0.016 \times \mathrm{SSVI}_{3.5}\right)$).

The data of Ekama and Marias (1986) was analysed along with that of other researchers (Rachwal *et al.* 1982; White 1975; Koopman and Cadee 1983) and came up with the findings that Pitman's empirical expression in Equation 1.2 resulted in a good description for all and that a relationship exists between $\frac{v_0}{K}$ and k . This is expressed as Equation 2.34

$$k = 0.88 - 0.393 \times \log\left(v_0 \; \times \; k\right) \tag{2.34}$$

However, since the value of k is known then the value of v_0 (Equation 2.35) can be computed using Equations 1.2 and 2.34.

$$v_0 = \left(\frac{v_0}{K}\right) \times k \tag{2.35}$$

According to suggestions from Catunda *et al.* (1989), rearranging Equations 2.34 to 2.35 will make it possible to express k and v_0 as a function of $SSVI_{3.5}$ which can be expressed in Equation 2.36.

$$k = 0.16 + 2.7 \times 10^{-3} \times \mathrm{SSVI}_{3.5} \tag{2.36}$$

Upon substituting Equations 2.35 and 2.36 into Equation 2.34 the following expression in Equation 2.37 would be realised:

$$v_0 = \left(10.9 + 0.18 \; \times \mathrm{SSVI}_{3.5}\right) \; \times \; \exp\left(- 0.016 \times \mathrm{SSVI}_{3.5}\right) \tag{2.37}$$

The $SSVI_{3.5}$values are of great importance for activated sludge process and hence Equation 2.37 can be further expressed in Equation 2.38 as follows:

$$v_0 = \left(11.2 \; - \; 0.06 \; \times \mathrm{SSVI}_{3.5}\right) \tag{2.38}$$

It was observed that Equations 2.37 and 2.38 can be utilised to compute the constants k and v_0 directly from the $SSVI_{3.5}$ values without conducting a ZSV test.

Other settling velocity models reported in literature and reviewed in Li and Stenstrom (2014b) includ; Foster (1982) who developed a model which considered SSVI and revealed that parameter n varied smoothly with the SSVI and the settling velocity V_S (m/h) was calculated from the SSVI (ml/g) and concentration X (mg/L) using Equation 2.39.

$$V_S = 5e^{-[0.2498 \exp(0.0046\mathrm{SSVI})]\,\mathrm{X}} \tag{2.39}$$

The Diagger and Roper model (1985) design of an experiential relationship between SVI of an activated sludge and its settling characteristics were represented by the correlation between v_O and X (Equation 2.40).

$$\ln \mathrm{v} = 1.871 - (0.1646 + 0.00158\,\mathrm{SVI})\,\mathrm{X} \qquad (2.40)$$

The outcome of Diagger and Roper (1985) model as reported in WEF (2005), was a realistic model for estimating activated sludge settling characteristics on 46 separate activated sludge samples with SVI ranging from 36 to 402 ml/g but did not give an outcome for the SSVI measurement as given by the Pitman (1980) and White (1975) model discussed earlier. Therefore, care must be taken when using Diagger and Roper (1985) model in operating activated sludge systems without chemical phosphorus removal (CPR) because of the limitation of SVI which is due to absence of a stirring regime in the treatment process. Another reason is due to the tighter phosphorus consent of < 1mg/L which makes the CPR a better option for most wastewater treatment works than biological phosphorus removal (BPR). The BPR limitation is because most treatment works struggle to meet the required sewage strength with high readily biodegradable biological oxygen demand (BOD).

Wahlberg and Keinath's (1988) model discovered a functional relationship between the SVI measured according to four different techniques for determining SVI and the two adjustable parameters namely v_O and n of the Vesilind formulas that defines the interface settling velocities as a function of concentration X (WEF 2005). However, the research was based on the outcome obtained from 21 full- scale activated sludge plants that varied significantly with size, geographic location, mode of operation, method of aeration and amount of industrial input. The outcome of the research showed that none of the sludge tested was chemically amended and due to this Wahlberg and Keinath developed the experimental model for predicting settling flux from SSVI data and this was expressed as Equation 2.41 in which 35ml/g < stirred SVI < 220ml/g. Therefore, the Keinath model accommodated a better settleability measurement approach using the SSVI data rather than the SVI data.

$$\mathrm{V_S} = (153 - 0.615\,\mathrm{SVI})\,\exp - 80.426 - 3.84 \times 10 - 3\,\mathrm{SVI} + 5.43 \times 10 - 5\,(\mathrm{SVI})\,2\mathrm{X} \qquad (2.41)$$

The Cho *et al.* (1993) model was used to investigate settleability within the FSTs, but it relied on the Carmen - Kozeny equation which was developed into new models (Equation 2.42-44) by adding the slurry viscosity term and X= solid concentrations, v_O, n, n1 and n2 - constants

$$V_S = \mathrm{v_0 e^{-nX/X}} \qquad (2.42)$$

$$V_S = {}^{v_0(\,n_1 X)^4}\!/_X \qquad (2.43)$$

$$V_S = \mathrm{v}_0(1 - \mathrm{n}_1\mathrm{X})^4 \, \mathrm{e}^{-\mathrm{n}_2\mathrm{X}}/\mathrm{X} \qquad (2.44)$$

The power model, the exponential model and the new model $\mathrm{v} = \mathrm{k} \times \exp(-\mathrm{nX}/\mathrm{C})$ fitted well with the experimental data and the last fit was the best. The new model is suggested to be used for modelling FST instead of the power model which is not viable in the dilute concentration range. The new model is also used instead of the exponential model because the latter is complicated with the permissible flux theory (Stypka 1998). The Cho model was more realistic in evaluating the batch settling curves than the Vesilind function due to the poor ability of the latter in describing the transition stage (Zhang *et al.* 2006). The comparison of the reviewed settling velocity models was summarised by Ozinsky and Ekama (1995) (Table 2.1).

It was discovered from other studies that because SVI test was empirical, it has the tendency of suffering from some significant errors linked to absence of unstirred condition and lack of true representation of wastewater samples and, as such, Jenkins *et al.* (1993), in a bid of avoiding inaccurate results and to allow for a meaningful evaluation of SVI results for dissimilar sludges, the diluted SVI (DSVI) has been investigated. In Jenkins' examination, the sludge sample was diluted with process effluent until the settled volume after 30 min is 250ml/l or less and afterwards, the standard SVI test was monitored with this sample. Several wastewater treatment plants conduct SVI tests using a 2L settlometer that has a larger diameter than 1L or 2L graduated measuring cylinders. Wahlberg and Keinath (1988) in their research to eradicate wall effects on solids settling in a small diameter test apparatus proposed the use of a slow speed stirring device. This test was called a stirred SVI (SSVI) when a stirring device is installed (APHA 1998; SMEW 1995). The stirred SVI test has now been used frequently in Europe.

The compression settling regime as earlier mentioned in section 2.1.3, controls the FST thickening function and occurs at high sludge concentration region in the bottom of the FST where existing settled sludge particles undergo thickening due to the load of the overlying sludge in the FST. The compression sludge settling characteristics is a function of the measured sludge blanket height (SBH) and underflow concentration.

Table 2.1. Comparison of the settling velocity models (Ozinsky and Ekama 1995)

Settling Velocity Model	**Model Integration Year**	**Parameter explored**	**Settling Velocity Model equation**	**Observations**
Foster	1982	SVI and SSVI	$V_S = 5e^{-[0.2498 \exp(0.0046SSVI)]\,X}$	Parameter n varies smoothly with SSVI, and suitable in evaluating settling velocity

Pitman, White and Ekama	1984	SVI and SSVI	$V_0/n= 37.63$ exp (-o.00388*SVI) $V_0/n= 67.9$ exp (-0.0016*SSVI$_{3.5}$) (r^2=1.968) n=0.88-0.393 log (V_0/n) (r^2= 0.976)	Small sludge diversity and limited database was noticed but there was Relationship between SVI, V_0 and r^2 but should not be used because of its dependence on concentration at a high 30 min settled volume interval of >400ml
Daigger and Roper	1985	SVI	ln v =1.871 – (0.1646 +0.00158 SVI) X	Data exhibited considerable scatter
Wahlberg and Keinath	1988	SVI and SSVI	V_S = (153 - 0.615 SVI) exp -80.426 - 3.84*10-3 SVI + 5.43*10-5 (SVI) 2X	SVI was found to be an imprecise measurement while SSVI was recommended as a good measurement parameter
Cho	1993	SSVI	V_S = v_O (1-n 1 X) 4 e-n 2 X/X	Exponential model is complicated to be used with permissible flux theory (limiting mass flux theory provided by Kynch (1952). This is the limiting rate of the solids flux reaching the bottom of the tank per hour (hr). it is measured as KgSS/m^2.h (Mass in Kg (kilogram), SS – suspended solids, Area (m^2)
Takács	1991	hindered settling parameter and flocculent settling parameter	V_s = v_0 (e^{-k1} (X-X_{min}) – e^{-k2}(X-X_{min}))	SVI not considered but can be integrated altering settling velocity parameters

Li and Stenstrom (2014a) stated that settling velocity as a function of particle concentration assumes a uniform particle size and density following a Stoke regime with Reynolds number (RE) < 1 and added settling velocity as a function of voids and hydraulic radius (R) and, nevertheless, commented that settling velocity in a column equal to average velocity in a porous bed based on Carman-Kozeny equation that thickening process can be compared to the transport of fluid in a non-rigid saturated porous medium. However, Cho *et al.* (1993) also added a slurry viscosity term to the Carman-Korenzy equation**.** The Cho *et al.* (1993) study showed improved correlation with the inclusion of the slurry viscosity term compared with models reported by Li and Stenstrom (2014a). However, Kinnear (2002) and De Clercq *et al.* (2008) used the theory of mixture of classical continuum mechanics (Bustos 1999; Bürger 2000) and developed settling functions to define compression settling velocity in Equation 2.45.

$$V_c = V_h\left(1 - \frac{\rho_s}{(\rho_s - \rho_W)gX}\frac{d_\sigma}{dX}\frac{dX}{dZ}\right) \qquad (2.45)$$

In which, V_c = compression settling velocity; ρ_s = density of sludge; ρ_W= density of water; σ = effective solid stress; X = sludge concentration; Z= depth and g= gravity. The uniqueness of this compression model compared to other theoretical model is provision of a relationship between the hindered settling velocity, effective solid stress and the compression settling velocity. The standardisation approach of the compression models involving un broken monitoring of the dynamic settling characteristics during batch experiments like radiotracer tests (De Clercq *et al.* 2005) which are not easily carried out in wastewater treatment processes. Therefore, compression settling models is only applicable to limited cases of 1-D FST modelling (De Clercq *et al.* 2008; Bürger *et al.* 2011).

In contrast, the empirical functions proposed for investigating settling velocity functions in FST design are based on the Kynch (1952) solid flux theory. This allows solid flux operating curves to be developed near with batch settling experimental data (Zeidan *et al.* 2004). The empirical functions are more unique in engineering application due to their simplicity and practicality compared to other theoretical functions that utilise particle size, sludge density, shape, slurry viscosity and porosity to predict the settling velocity (Li and Stenstrom 2014a).

In summary, settling velocity models are integrated in FST models and in solid flux theory and state point analysis for design and operation of FST. However, in the last decade, numerous studies on developing a suitable empirical model to evaluate discrete settling, compression settling and zone settling velocities has been reported in literature provided in this section 2.1.4 but mathematical models to evaluate the zone settling characteristics of a chemically dosed (Al, Fe and Ca) activated sludge (AS) have not been extensively provided. This makes this study on the impact of chemical dosing on activated sludge settleability insightful. Additionally, this current research will not investigate compression settling characteristics of activated sludge nor discrete settling but focus on the zone settling regime.

2.1.5 Zone Settling Velocity (ZSV) Model Standardisation

The precision of the settling velocity models in section 2.1.4 is dependent on the quality of their standardisation to experimental batch test data. Although, one of the main limitations in the use of the zone settling velocity mathematical model (Equation 1.1) as earlier mentioned in section 2.1.4 is the laborious standardization technique comprising of a series of laboratory batch settling tests. The calibration procedure as reported in review by Vanrolleghem *et al.* (1996) will enable the spontaneous recording of batch settling curves using settlometer equipment (Figure 2.13 and 2.14).

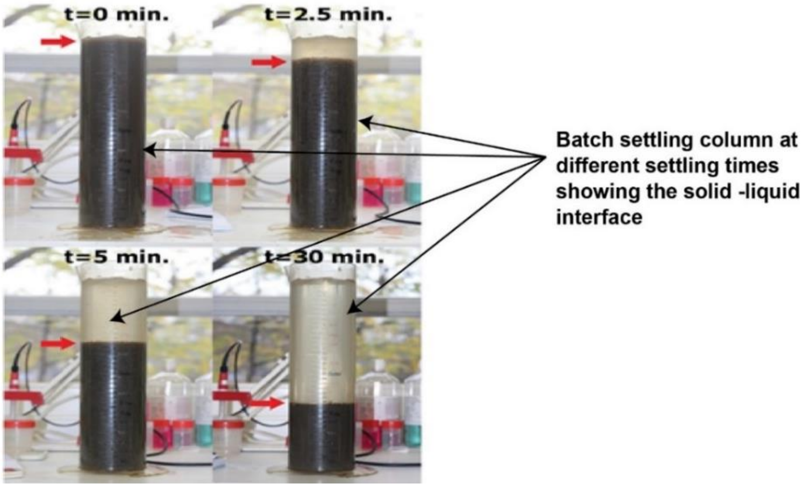

Figure 2.13. Batch settling tests (Vanderhasselt and Vanrolleghem 2000; Torfs *et al.* 2016)

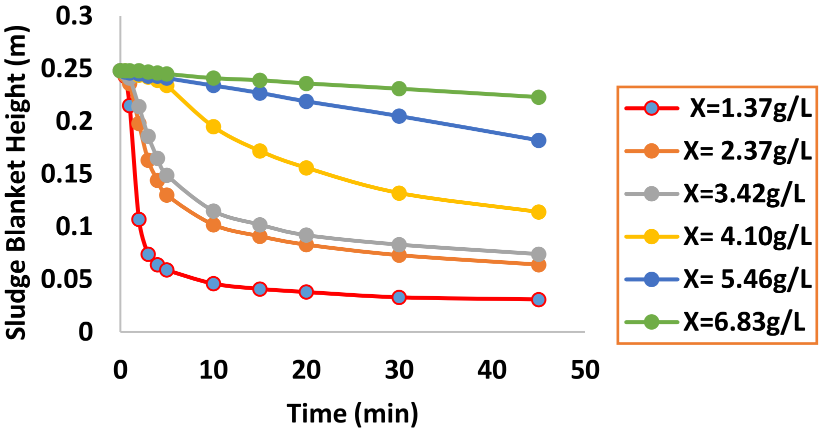

Figure 2.14. Batch settling curves obtained from batch settling tests (Vanderhasselt and Vanrolleghem 2000; Torfs *et al.* 2016)

However, in this current research, the more updated type 305 settlometer device (Triton Electronic Limited 2018b) was used to investigate the impact of chemical dosing (Al, Fe and Ca) on activated sludge settleability. According to Ekama *et al.* (1997), the settling velocity in the zone settling regime is a function of the local sludge concentration (beyond 600-700mg/L) instead of individual particle characteristics in the free settling regime. The settling velocity of each particle slows down the velocity of other non-stokian zone settling particles and the sludge blanket height is estimated as a function of the time during the batch settling test (Vanderhasselt and Vanrolleghem 2000). The initial mixed liquor sample of known solids concentration is poured into the settlometer column and the sludge interface position is recorded at the end of a specific time (30 minutes) duration. The method is repeated at a smaller sludge concentration and a new batch settling curve (BSC) is recorded. This experiment is repeated until several settling curves at different sludge concentrations are achieved. The ratio of the final settled sludge volume to the initial volume is used to indicate the SSVI as ml of settled bed containing 1g of solids while the linear slope of each curve gives data on the zone settling velocity at that sludge concentration. Conversely, after the initial MLSS concentration and an initial time zero, the sludge interface is recorded at regular time intervals, initially when the interface is fast settling (1 minute) and then at 5 minute intervals. Plots of the interfacial position with time are recorded and the slopes of the BSC are evaluated to give the ZSV for the zone settling regime. The procedure can be repeated for up to six to seven different sludge concentrations and graphs of ZSV against concentration are plotted on a natural log to linear scale. The slope and intercept of this BSC provides the Vesilind coefficients (Equation 1.1). Moreover, in wastewater treatment practice, once the Vesilind coefficients are utilised for validating a numerical model it is desirable to obtain the Vesilind coefficients (vo and k) in Equation 1.1, directly from SBC instead of utilising the decisive estimated SSVI value related as $SSVI_{3.5}$ measured by conducting numerous SSVI tests at different sludge concentrations and interpolating for the 3500mg/L value. This is because the $SSVI_{3.5}$values are required to back estimate for the Vesilind coefficients in the Vesilind settling velocity model. In order to calibrate models of sedimentation in FSTs, laboratory determined ZSVs are universally used but the conventional empirical model for sedimentation in FSTs expressed as a function of solid concentration, termed Vesilind equation is provided in Equation 1.1 (Vesilind 1968). The empirical coefficient Vo and K are obtained by performing ZSV test over a range of mixed liquor suspended solids (MLSS) concentration. Schuler and Jang (2007b) result of effect of settling velocity within various sludge concentration and thicknesses agreed with Vesilind (1968) assertion that as biomass concentration was increased in zone settling test, settling velocities decreased as shown in Figure 2.15.

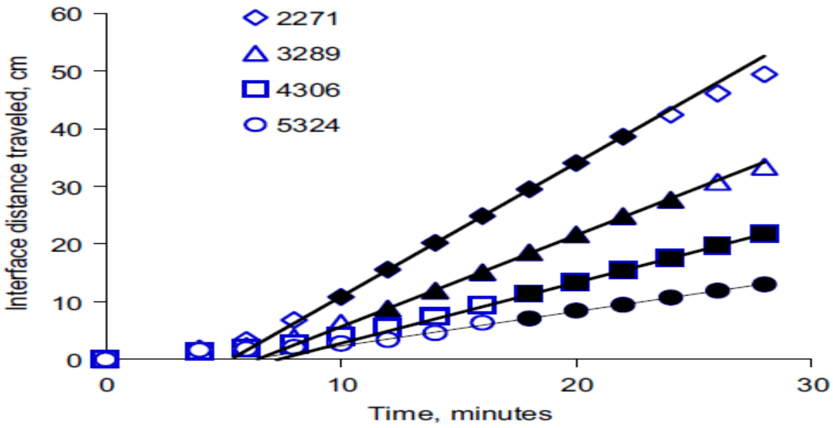

Figure 2.15. Typical zone settling velocity test results, North Durham sample. Filled symbols indicate linear portion of data used for calculation of settling velocities (slopes of linear regression lines). The legend shows the four biomass concentrations evaluated in this test in mg TSS/L

However, in Figure 2.16 and 2.17 a non-linear correlation between the settling velocity and the range of buoyant density was reported. Furthermore, to investigate the effect of sludge thickening on activated sludge zone settling velocities, regression analysis was applied to a linearized form of Vesilind equation (in ZSV = -kX + ln v_O). It was observed that there exists a non-linear correlation between the settling velocity and the density and sludge concentration which is contrary to the linear correlation in Vesilind settling velocity models.

This led to a new model that included a buoyant density parameter in the vesilind settling velocity model (V = $(m\rho^{/}+Vo^{1})e^{-k^{/}/x}$)), in which m is linear buoyant density coefficient (slope of the linear portion of the Vo against buoyant density curve, $k^{/}$ is the average vesilind k and Vo^{1} is the intercept of the linear portion of the Vo against buoyant density curve. Further details are provided in a review by Schuler and Jang (2007b). This new model explains the effect of density on the activated sludge zone settling velocity (ZSV) but did not provide insight into the impact of chemical dosing on the ZSV and SSVI as indicators of activated sludge settleability.

The hypothesis arises as to whether dosing mixed liquor sample with chemicals (Al, Fe and Ca) at different dosing concentrations (20, 50, 100, 150, 200 and 250mg/L) in a simple settling batch test (BSC) will provide adequate SSVI and ZSV data at the end of 30 minutes that can be used in validating a new numerical model and describes activated sludge settleability (ZSV and SSVI) as a function of chemical dosing. This will assist in evaluating whether the numerical activated sludge settling velocity equations fit to experimental settling velocity data for chemically dosed activated sludge (black box model).

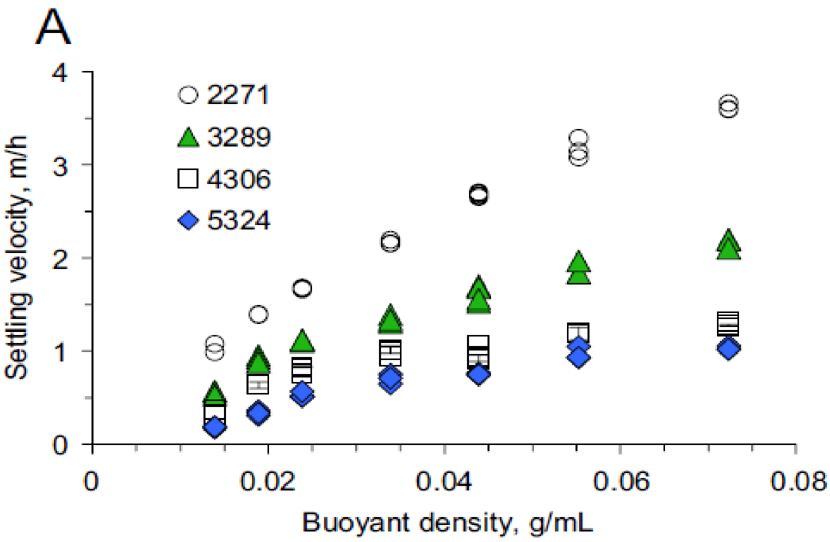

Figure 2.16. Settling velocities as a function of buoyant density determined at four concentrations for the North Durham plants (A). The legend shows biomass concentrations in mg TSS/L with three more settling experiments performed for condition A

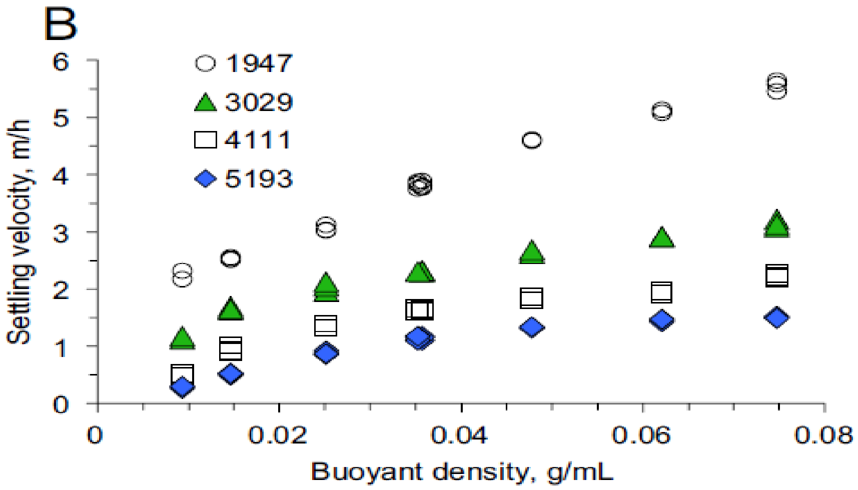

Figure 2.17. Settling velocities as a function of buoyant density determined at four concentrations for the North Cary plants (B). The legend shows biomass concentrations in mg TSS/L with three more settling experiments performed for condition (B)

To provide an answer to the claim on whether or not chemically dosed (Aluminium-Al^{3+}, Ferric-Fe^{3+} and Calcium-Ca^{2+}) activated sludge impacts activated sludge settleability, in Chapter three of this thesis, an experimental methodology using a simple batch settling experiment (BSE) called a settlometer test (section 3.3.1) where the ZSV and SSVI was measured from a chemically dosed sludge sample at different dosing concentrations (Figure 3.3-3.4) and model validation was conducted (Chapters Four, Five and Six) to evaluate whether or not the proposed revised mathematical model describes properly the settling characteristics of Al^{3+}, Fe^{3+} and Ca^{2+} dosed sludge. The approach is used to check whether the revised model fits the experimental batch test results. The revised model was designed to analyse the effects of Al^{3+}, Fe^{3+} and Ca^{2+} dosing concentration on activated sludge settleability indicators (Zone settling velocity-ZSV and Stirred sludge volume index-SSVI) using linear transformation of polynomial and exponential functions to achieve replication of a non-linear correlation between the Al^{3+}, Fe^{3+} and Ca^{2+} dosing concentration and activated sludge settleability indicators (ZSV and SSVI).

2.1.6 Flocculation

2.1.6.1 Activated sludge flocs

Activated sludge flocs are known to be the most important aspect of the activated sludge unit operation in wastewater treatment (Gray 2004). Activated sludge flocs comprise discrete clumps of microorganisms which differ mutually in shape and sizes. Whether a FST acts successfully as a sedimentation tank is highly dependent on the ability of the microorganisms to form a flocculent biomass which settles and compacts well, producing a clear effluent (Das *et al.* 1993). The aim of the flocculation process is to combine individual flocs into large and dense flocs that settle rapidly. In case of failure of the flocculation process or break-up of flocs during the activated sludge process, a fraction of the particles are not incorporated into flocs. This usually distresses a small part of the activated sludge solids, also referred to as non-settleable particles. They remain in the supernatant (supernatant turbidity) at the upper layer of the FST due to lack of sufficient mass and are carried over the effluent weir deteriorating the effluent quality (Ekama *et al.* 1997). This fraction can only be removed from the FST when they adhere to large and dense flocs with sufficient mass to settle. From this point of view, flocculation and break-up processes of AS are of crucial consideration in clarification function of the FST (Biggs 2000). While flocculation process is vital in activated sludge settleability, it has not been well comprehended but bio-flocculation accounts for numerous variations in activated sludge floc's characteristics, especially cationic impact on bio-flocculation process in activated sludge settling, dewatering and digestibility (Eriksson and Alm 1991; Bruus *et al.* 1992; Higgins and Novak 1997b, c). However, in realising the aim of the current study on the impact of chemical dosing on the design and operation of activated sludge plants, including evaluation of the impact of chemical dosing (Al, Fe and Ca) on activated sludge settleability, digestibility and dewaterability, a clear insight into the composition (nature), characteristics of activated sludge flocs and the role of chemical coagulant in activated sludge settling, dewatering and digestion process becomes vital. Bio-flocculation will provide better explanation of the two most vital daily requirements in an activated sludge plant (ASP) as reported in Chen *et al.* (2007) namely; efficient settling of organics in the FST after organic breakdown of pollutants from the influent wastewater in the aeration tank has been achieved and the downstream running cost for wasted activated sludge (WAS) treatment evaluated by the efficiency of dewaterability process.

Various studies have been conducted to examine activated sludge flocs and aggregates of suspended solids (Nopens 2005); microbial aggregates, filamentous organisms, organic and inorganic particles and exocellular polymeric substance (Tezuka 1969; Novak and Haugan 1980; Eriksson and Alm 1991; Bruus *et al.* 1992; Higgins and Novak 1997a); polymeric network of extracellular polymeric substances (EPS) which have the capacity to combine different floc components together in one structure or floc (Wilén *et al.* 2003); cation bridging phenomena of multivalent cations (Mg and Ca) which have ability to stabilize sludge flocs and facilitate flocculation (Cousin and Ganczarczyk 1999); a mixture of different microorganisms such as bacteria, fungi, protozoa and metazoa which are found in AS flocs due to the availability of a large variety of substrates in wastewaters (Jenkins *et al.* 1993). This group of microorganisms were classified as floc formers (*Escherichia, flavobacterium, nocardia and pseudomonas zoogloe*a), non-floc formers and filamentous microorganisms (algae, bacteria and fungi) (Figure 2.18). Though, floc formers and filamentous bacteria are necessary in the activated sludge process (ASP) their speedy growth is needless since it causes increased floatability of activated sludge floc which leads to recurrent activated sludge settleability issues and losses in effluent suspended solid (ESS).

Figure 2.18. Bacteria involved in Activated Sludge Floc Structure (Gerardi 2002)

The floc formers stick together with increasing sludge age and begin floc formation through cellular fibrils, sticky polysaccharides, and granular starches like polyhydroxybutyrate (PHB) (Figure 2.19), by promoting degradation of carbonaceous BOD (biological and chemical oxygen demand) and removal of fine solids and heavy metals while the non-floc formers equally degrade carbonaceous BOD and removes both fine solid and heavy metals. Conversely, the filamentous bacteria does not just degrade carbonaceous BOD and removes fine solids and heavy metals as well but provides the required strength to sludge floc particles that enables their resistance to shearing action within the aeration zone and increase in size (Gerardi 2002). The extent to which these different groups (floc formers, filamentous organism and non-floc formers) occur has a large impact on the settleability and flocculation behaviour of the activated sludge and with a good balance between them the filamentous microorganisms will provide a network to which floc formers can attach (backbone structure) resulting in large and strong flocs which are more resistant to shear stresses (Parker *et al.* 1970; Sezgin *et al.* 1980).

Figure 2.19. Floc formation cellular components in activated sludge process (Gerardi 2002)

The heterogeneous nature of biological flocs and their complex structure makes both the floc size and the floc morphology change significantly in a FST since floc sizes may differ from a few to a thousand µm (Li and Ganczarczyk 1991). Floc sizes and floc size distribution is a function of the active equilibrium existing between flocculation and break-up of the microbial aggregates (Lu and Spielman 1985; Spicer *et al.* 1996; Mikkelsen 2001). Wastewater systems are active unit processes and as such various changes occur ranging from temperature, substrate loading, shear forces, sludge age, ionic strength and dissolved oxygen concentration affecting the composition, sizes and structural stability of activated sludge which has an overall impact on flocculation mechanism (Mikkelsen *et al.* 1996; Wilén and Nielsen 2000; Mikkelsen and Nielsen 2001; Mikkelsen 2001) and this flocculation mechanism accounts for both breakage of activated sludge and bio-flocculation (Govoreanu *et al.* 2004). Gray (2004), reported that particle magnitudes in the activated sludge process vary from individual bacteria of between 0.5 and 5.0µm to large flocs with greater than 1mm in diameter. Furthermore, the content of dry sludge floc ranges from 60 to 90% organic matter and, 40 to 10% inorganic depending on the composition of the wastewater (Gray 2004; Wilén *et al.* 2003). Sanin *et al.* (2006) reported that peak growth in bacteria depends on the availability of potassium (K^+) and magnesium (Mg^{2+}) where, potassium (K^+) and magnesium (Mg^{2+}) are mainly intracellular ions and controlled amount of extracellular ion like Ca^{2+} and Na^+, but Conn *et al.* (1987); Gray (2004) supported these findings that a small amount of these cations is necessary to facilitate the enzymatic reaction process. However, Figure 2.20 shows a pictorial view of activated sludge flocs and their nature.

Figure 2.20. Activated sludge floc and itsnature (Govoreanu *et al.* 2004)

Some studies have concluded that different floc formation processes occur before a steady state between flocculation and breakage of activated sludge is assumed in a wastewater treatment process (Spicer *et al.* 1996). There are two main separate phases in a flocculation mechanism namely suspended particle transportation and attachment (Thomas *et al.* 1999). The initial floc formation process enables sludge flocs to gain the required weight to settle and this is achieved when suspended particles interact in the presence of biopolymers. The biopolymers in activated sludge comprise of proteins, polysaccharides, lipids, nucleic acids, biopolymers and cations. However, excessive filamentous bacteria (filamentous bulking) has not been concluded as always responsible for poorly activated sludge settleability and dewaterability efficiency in FSTs (Urbain *et al.* 1993; Frolund *et al.* 1996). Activated sludge bulking will be discussed in more detail in Section 2.1.6.2. Also, various researchers, Higgins (1995), Bruus *et al*. (1992), Eriksson and Alm (1991), Morgan *et al.* (1990), Novak and Haugan (1979), Tezuka (1969), have observed that variation in activated sludge floc is equally linked to the collaboration between cations with negatively charged biopolymers in activated sludge floc. While divalent cations were noticed to optimise activated sludge settleability and dewaterability, the monovalent cations declined settleability and dewaterability efficiency of activated sludge (Higgins 1995). This will be covered in detail in section 2.1.6.3.2 (Impact of cation on activated sludge floc characteristics). Additionally, the earlier identified transport flocculation mechanism depends on variation in the sludge and liquid velocities.

De Clercq (2003) reported three transport mechanisms (Figure 2.21) that include perikinetic (micro-flocculation) flocculation which is a stochastic process driven by differences in temperature and particles within this phase sense each other by random Brownian motions. Tchobanoglous *et al.* (2003) further added that only very small particles with less than 1µm are satisfactory within the micro-flocculation phase, but the differential settling flocculation mechanism on the other hand is driven by differences in settling velocity between dissimilar large particle sizes with particle size range of 1-2µm. Large particles which settle swiftly can collide and integrate with small, slowly settling particles during the settling process which would have escaped from the supernatant and settle poorly by decreasing the effluent quality efficiency. The orthokinetic flocculation mechanism comprises of aggregation through forcing of velocity gradients by mixing. During this process, when swift-moving particles surpass the gentler moving particles in end-to-end regions with a lesser velocity, they may collide and form a larger floc that settles more quickly (Tchobanoglous *et al.* 2003).

Figure 2.21. Different flocculation mechanisms that induce particle collisions (Tchobanoglous *et al.* 2003)

2.1.6.2 Activated sludge bulking

The concept of bulking has been used over many decades to define the problem associated with the separation of activated sludge. However, there are still some uncertainties on how bulking applies to an activated sludge plant, but research defines bulking as a phenomenon that occurs in an activated sludge plant when the sludge occupies an excessive volume that does not settle readily and in extreme cases results in effluent that contains excessive amounts of suspended solids (Jenkins *et al.* 2003; Bitton 2005; Richard 1989; Tomlinson and Chambers 1979). Bulking sludge was described as the excessive growth of filamentous bacteria but the volume fraction of filamentous bacteria that could result in bulking sludge was estimated to range between 1-20 % (Palm *et al.* 1980; Kappeler and Gujer 1994). Also, the filamentous bacteria are not just vital in the floc formation process but its filaments act as a backbone for the floc's development and as an attachment for the fingered zoogloeal ramigera bacterium (Wanner 1994). This filamentous bacterium and zoogleal organism is both vital in achieving a satisfactory sludge quality and clean water leaving the final sedimentation tank (FST) and back to receiving waters. In addition, flocculation is vital for effective solid's separation to take place in a sedimentation tank. This is a phenomenon in which particles aggregate into larger particles ranging from a diameter of 2mm, settling readily. However, when this flocculation occurs in a biological system it is called bio-flocculation (Jeyanayagam n.d.). According to Jenkins *et al.* (2003), bio-flocculation is made up of two mechanisms, the first one is a floc former producing exocellular polymers that allows them to stick to each other to form smaller flocs which are prone to shearing, while the other mechanism is a filamentous bacterium forming a reinforcing network that strengthens the floc and creates room for them to grow into larger flocs. Consequently, there are some commonly associated problems linked to the variation in the degree of flocculation (Table 2.2) but if there be a good settleability then a balance must be reached between the floc formers and the filamentous organism.

Consequently, research has identified operational problems with activated sludge process specifically with the split-up of the sludge from the treated wastewater in the FST and some of this sludge settleability problems discussed in this research includes bulking, deflocculation, pin-point flocs, foaming or denitrification. The bacteria, for instance, account for a particle size of 0.5 to 5 micrometre in larger activated sludge flocs in the range of > 1mm diameter but according to Parker *et al.* (1971), bimodal particle distribution of flocs in activated sludge does exist and this shows that smaller particles in form of single microorganism might have been sheared off by larger activated sludge flocs. Parker *et al.* (1972) concluded that the determining factor for variation in the size of flocs are either their cohesive strength or the effect of shearing due to the turbulence within the aeration process. Sezgin *et al.* (1978, 1980) further investigated floc's structure and discovered that two main classes exist namely; micro-structure and macro-structure (Figure 2.22).

While, the micro-structure consists of flocs that are spherical in shape, weak, compact, smaller below 75 micrometer in diameter and are mostly made up of floc forming bacteria formed by bioflocculation when the smaller unit particulate combines to form larger ones (Gray 2004). However, the issue with the smaller flocs is that, after forming larger flocs, the smaller remnant that do not settle adds to the treatment process as they escape with the final effluent making the effluent suspended solid (ESS) high and this causes turbidity level to increase in the treated effluent. In contrast, macro-structure occurs when a filamentous microorganism is available in the activated sludge flocs. These microorganisms tend to move around these filament strands which makes them have irregularities in their shapes and creates capacity to withstand the turbulent effect of the aeration system.

Lau *et al.* (1984) conducted a laboratory study on difference between a micro-structured floc and a macro-structured floc and found that floc forming bacteria called *Citromonas* sp, when grown on its own, formed a compact spherical floc which was a typical micro-structural floc, but filamentous bacterium *sphaerotilus natans* when grown together in almost the same ratios with *citromonas* sp, an irregular shaped floc was realised which defined a macro-structured flocs.

Table 2.2. The causes and impact of activated sludge process (ASP) separation issues (Jenkins *et al.* 1984; WEF 2005; Jeyanayagam n.d.)

Nature of Issues	Causes of Issues	Impact of Issues
Dispersed growth or deflocculation	Microorganisms do not form flocs but are dispersed. Foaming only small clumps	Turbid effluent. No zone settling of sludge

Viscous or non-filamentous bulking	Microorganisms are present in large amounts of exocellular slime. In severe cases the slime imparts a jelly-like consistency to the activated sludge	Reduced settling and compaction rates, virtually no solids separation in severe cases resulting in overflow of sludge blanket from secondary sedimentation tank. In less severe cases, viscous foam is often present.
Pin-Point Floc	Small, compact, weak roughly spherical flocs are formed, the larger of which settle rapidly. Smaller aggregates settle slowly	Low sludge volume index (SVI) and cloudy and turbid effluent
Bulking	Filamentous organisms extend from flocs into the bulk solution and Interfere with compaction and settling of activated sludge	High SVI- very clear supernatant. Low return activated sludge (RAS) and wasted activated sludge (WAS) solids concentration. In severe cases overflow of sludge blanket occurs. Solids handling processes become hydraulically overloaded
Blanket Rising or denitrification	Denitrification in secondary sedimentation tank releases poorly soluble N_2 gas which attaches to activated sludge flocs and floats them to the secondary sedimentation tank surface	A scum of activated sludge foam on the surface of secondary sedimentation tank
Foaming or Scum Formation	The first cause is non-degradable surfactants. Secondly, by the presence of Nocardia sp. And other foam associated species	Foams float large amounts of activated sludge solids to surface of treatment units. Nocardia and Microthrix foams are persistent and difficult to break mechanically. Foams accumulate and can putrify. Solids can overflow into secondary effluent or even overflow out of the tank free-board onto walkways

Figure 2.22. Structure of micro and macro flocs (Gray 2004)

2.1.6.2.1 Dispersed Growth (Deflocculation)

According to Gray (2004), deflocculation can be traced to the micro-structure of flocs having a reduction in stability or breaking up due to turbulence from over-aeration within the aeration tank. It was also linked to bacteria not aggregating into flocs. As mentioned in section 2.1.6.1**,** the effluent suspended solid content will be higher and rise in turbidity level of the treated effluent because of micro-structural problem of the flocs. If this issue persists and is not controlled, then bulking will result in the variation of MLSS concentration in the aeration basin as most of the microbial flocs will be lost with increased sludge loading rate (F/M ratio). Other impacts of deflocculation include low dissolved oxygen (DO) levels, low pH and shock loads. However, Pipes (1979), based on his investigation, proposed that > 0.4 kg/kg/d solid loadings will cause dispersed growth. Thus, a sludge with micro-structural flocs which has a high level of SLR (sludge loading rate) will result in bulking. Moreover, to correct this process fluctuation it is necessary to reduce the SLR to < 0.4 kg/kg/d.

2.1.6.2.2 Pin-Point Floc

Contrary to the deflocculation problem as mentioned earlier in section 2.1.6.2.1 which was traced to absence of filamentous microorganism in the activated sludge flocs (micro-structure flocs) making their structure weak, small, compact and spherical in shape, caused them to easily break up into smaller flocs in the aeration tank under a turbulent environment. This is not the case with the pin floc issue involving high magnitudes of flocs with small particle size that takes longer period for settleability to occur than larger flocs in deflocculation. Moreover, in the case of deflocculation the high ESS caused advanced turbidity in the final effluent but for pin flocs there is no high turbidity since the particles are far bigger and noticeable to the naked eye as discrete flocs in the final effluent (Gray 2004). Consequently, Pipes (1979) identified some process boundary to deduce a pin-point floc situation during sludge settleability. This includes long sludge age (SA) >5 to 6 days and low organic loadings < 0.2 kg/m³/d. Moreover, Forster (1971), concluded that if the pin floc is justified to be associated with long SA and low organic loading of < 5 to 6 days then the small flocs are presumably non-biodegradable portion of aerobically broken down mixed liquor.

2.1.6.2.3 Foaming Floc

According to Gray (2004), initially, the formation of frothy foam was mainly encountered at activated sludge plants and was linked to the now banned use of non-degradable detergents. However, Jenkins *et al. (*1984) described foam as a dispersion of gas bubbles in a liquid or solid by identifying different air-water-foam interface. Al-Diwamy and Cross (1978), Pipes (1978b) and Dhaliwal (1979) reported activated sludge foam to be dense foam that can be likened to the colour and texture of chocolate mousse. This foaming was traced to a hydrophobic filamentous microorganism called Nocardia. Chun *et al.* (1996) and Stratton *et al.* (1998), added that Norcardia was a potential hydrophobic filamentous microorganism causing activated sludge foaming because of the available long chain mycolic acid on the Norcadia cell wall. This nature makes flocs adhere to bubbles in the aeration tank which are transferred to the FST and afterwards escape with the final effluent adding to the effluent suspended solid level (ESS). Additionally, it was stated that if aeration takes place in a closed tank then foaming will reduce the hydraulic head for gravity flow to happen via the aeration tank. Lechevalier (1975) estimated the bulk density of foam to be 0.7g/ml. Vega-Rodriquez (1983) used a laboratory scale plant and estimated that 90% of Norcadia filaments are released from the mixed liquor into the foam. This is an indication that the mixed liquor suspended solids (MLSS) becomes stuck in the foam with a resulting dark brown colour which makes 30 to 50 % of the activated sludge content to be entrained in the foam.

2.1.6.2.4 Filamentous Bulking

In research studies conducted by Pipes (1967) and Anon (1979), bulking has been described to occur where filamentous organisms impede the settleability of an activated sludge by spreading from the flocs into the bulk solution. Consequently, it was identified as the compaction of activated sludge with a SVI > 150ml/g. When bulking becomes more pronounced, an indication of clear supernatant is noticed due to the abundant extended filaments filtering out the small particle which can potentially cause turbidity. However, poor sludge settleability will extend the sludge blanket and the bigger flocs will be discharged from the FST with an increased SS and BOD of the final effluent. Thus, bulking is an indication of poor compaction of the activated sludge (Metcalf and Eddy 2004; Gray 2004). Importantly, bulking has been investigated from its structural perspective (Gray 2004). Bulking was also attributed to strong macro-structural flocs which possess higher numbers of filamentous organisms. It was emphasized that when the SVI lies between 80 to 120ml/g and final effluent is void of SS and turbidity then the filamentous microorganism and floc-forming bacteria are in good ratio within the unit operation. Although, the filamentous organism, as earlier mentioned, provides strength against the effect of turbulence during the aeration period, but there are still some filamentous organisms that have their filaments extending out from the flocs. When this situation persists with more of filaments extending from the flocs then sludge bulking occurs. Still, long filaments extending out of the floc and joining together separate flocs resulting in a network of filaments have been identified as bridging flocs (Figure 2.23) while when the flocs are formed along the length of the filaments are called spindly flocs (Figure 2.24). According to Anon (1979), the type of compaction and settleability problems and type of flocs in activated sludge depends on the type of filamentous organism available in the sludge. Literature has identified bacterial species causing bridging bulking to include; type 021N, *Sphaerotilus natans*, type 0961, type 0803, *Thiothrix* sp., type 0041 and *Haliscomenobacter hydrosis*, while those causing spindly bulking was type 1701, type 0041, type 0675, *Nostocoida limicola*, and *Microthrix parvicella* (Farquhar and Boyle 1971a; Eikelboom and Van Buijsen 1981; Jenkins *et al.* 1984).

Figure 2.23. Bridging bulking in activated sludge (Gray 2004)

Figure 2.24. Spindly bulking in activated sludge (Gray 2004)

2.1.6.2.5 Non-filamentous Bulking

Although bulking rarely occurs without filaments, it has been traced to deflocculation which resulted in a dispersed bacterium producing a viscous bulking. Still, it is linked to the alteration in the micro-structure of flocs which causes excess extra-cellular polymer (ECP) to generate with a jelly-like consistency noticed in the mixed liquor (Gray 2004).

2.1.6.2.6 Denitrification

Haandel and Lubbe (2012) and Gray (2004) identified that dissolved oxygen is usually used up faster than expected by activated sludge flocs during separation from the treated effluent and as such an anoxic environment should be maintained. On the contrary, when the sludge residence time (SRT) becomes lengthier and the treated effluent becomes fully nitrified within the aeration basin for the denitrifying bacteria to reduce the nitrate to nitrogen gas, it was observed that the nitrogen gas released in the process was entrained in the flocs causing them to float to the surface of the tank and escape with the final effluent. This process was termed rising sludge and it is paramount in final sedimentation tanks (FST) (Metcalf and Eddy 2004). However, control for rising sludge issues was investigated by Chambers and Tomlinson (1981) and suggestions were made that the sludge recycle rate from the FST should be increased. In addition, the mixed liquor should be well aerated before entering the FST.

2.1.6.3 Factors Impacting Activated Sludge Floc Characteristics

The biopolymers in activated sludge flocs (proteins, polysaccharides, humic acid and lipids) tend to impact both the physical and chemical characteristics related to activated sludge flocs namely; bound water, hydrophobicity, microorganisms, extracellular polymeric substances (EPS), floc particle size, and floc density, surface charge density, and surface area that explains activated sludge settling and dewaterability (Jeyanayagam 2005). Moreover, for gravity sedimentation process to be effective, bioflocculation must take place in the FSTs. This is a biological phenomenon in which particles agglomerate into larger particles ranging from diameter of 2mm and settle readily within the tank (Jeyanayagam 2006). Bioflocculation is made up of two mechanisms (Figure 2.25), floc formers producing exocellular polymers that allows them to stick to each other to form smaller flocs which are prone to shearing, while the other mechanism is a filamentous bacterium forming a reinforcing network that strengthens the floc and makes room for them to grow into larger flocs (Jenkins *et al.* 2003).

Figure 2.25. Bio-flocculation mechanism (Jeyanayagam 2006)

Increased specific surface area of sludge flocs can cause a decline in the settleability and dewaterability characteristics (Sorensen and Wakeman 1996; Andreadakis 1993). Kolda (1995) has added that an increase in activated sludge floc density will enhance dewatering characteristics through a decrease in bound water content of the sludge flocs and Forster (1983) has further added that the impact of calcium (Ca) on sludge floc may result in a denser sludge floc because of a drop in the bound water content of activated sludge floc. Jorand *et al.* (1995) contributed that improvement in bioflocculation and activated sludge settleability was observed, as activated sludge floc hydrophobicity increased.

2.1.6.3.1 Extracellular polymeric substances (EPS)

Although extracellular proteins in activated sludge flocs can occur in the exterior of the cells and classed as bound proteins, some exist as unbound proteins since they are free in the liquid. While the former is responsible for enhancing both activated sludge settleability and dewaterability efficiency, the latter accounts for poor effluent quality (activated sludge settleability) and poor dewaterability efficiency (Wilén *et al.* 2003). The latter settleability and dewaterability problems has been linked to shearing action within the aeration tank due to mixing regimes that causes the sheared activate sludge flocs (Gerardi 2002) to release metabolic products such as proteins and polysaccharides into the free liquid (Figure 2.26).

Figure 2.26. Shearing action within the aeration tank of an activated sludge process (Gerardi 2002)

The floc-forming bacteria converts organic materials into extracellular substances (EPS) and these EPS materials form an EPS environment for encapsulating bacteria and microorganisms (Raszka *et al.* 2006). EPS are negatively charged polymers that interact with water molecules as a gel (Figure 2.27) which has capacity to absorb large quantities of water and swell but not dissolve in water (bound EPS) (Keiding *et al.* 2001), but the EPS bound to cells and are soluble in water are called soluble EPS (Laspidou and Rittmann 2002). Nielson and Jahn (1999), classed EPS as tightly bound (TB) EPS and loosely bound (LB) EPS (Figure 2.28). Therefore, EPS in activated sludge floc can cause dewatering problems (Nelson *et al.* 1998). Higgins and Novak (1997a) added that some proteins that constitute activated sludge components exhibit lectin-like action which enables extracellular proteins attachment to polysaccharides to facilitate bioflocculation process. Wahlberg (1992) further contributed on the impact of extracellular polysaccharides on activated sludge settleability and dewaterability efficiency and reported sludge flocs that agglutinated and broke up with time and that the rate of sludge floc break up increased with increasing polysaccharides but a decrease in supernatant turbidity was observed with increasing polysaccharides. Other research contributions included sugar acids (Uronic acids) in polysaccharides impacting agglutination positively in activated sludge flocs, and the negatively charged uronic acids collaborate via charge bridging process with divalent cations to enhance bioflocculation in activated sludge flocs (Takeda *et al.* 1994; Bender *et al.* 1994; Steiner *et al.*1976; Frolund *et al*. 1996; Higgins and Novak, 1997b; Jin *et al.* 2003; Jin *et al.* 2004; Sanin *et al.* 2006).

Figure 2.27. Gel-like activated sludge floc structure (Keiding *et al.* 2001)

Figure 2.28. Two-layer model for EPS (TB and LB EPS) (Nielson and Jahn 1999)

Sanin *et al.* (2011) observed that extracellular polymeric substances (EPS) originated from biological synthesis, metabolic excretion, disintegration of cell wall or cell membrane of microbes and shedding of cell surface components and consist of biopolymers present in activated sludge such as carbohydrates (polysaccharides), proteins, nucleic acids, and lipids. Sanin *et al.* (2011) further added that the percentage availability of the EPS components ranged from 40-95% polysaccharides, 1-60% proteins, 1-10% nucleic acids and 1-40% lipids based on the microbial system and wastewater treatment operational factors (for example the protein-to-carbohydrate ratio in the EPS increased with sludge retention time (SRT) and decreased with carbon-to-nitrogen ratio in the influent wastewater). Wilén *et al.* 2003 stated that about 50-60 % of the activated sludge floc organic constituent accounts for the total mass of EPS in an activated sludge floc. Moreover, Li and Yang (2007); Sanin *et al.* (2011) stated that biopolymers have the capacity to tightly bound to the cell wall and can exist as a slimy, gelatinous material that can be loosely stick to the cell surface resulting in a 3-D gel-like and highly hydrated environment outside the cell surfaces which encloses the microorganism and supports agglutination to form sludge flocs, but Le-Clech *et al.* (2006) defined EPS as glue or cement to hold together microbial aggregates in biofilms and activated sludge flocs. Mikkelsen *et al.* (2002) further explained EPS as a tangled linkage of cross-related extracellular polymers that can stick together individual microorganisms in a certain shape and size and Sanin and Vesilind (2000) reported a floc model (Figure 2.29) that explains the bio-flocculation mechanism.

Figure 2.29. Proposed activated sludge floc model (Sanin and Vesilind 2000)

Sobeck and Higgins (2002) and Wilén *et al.* (2003) explained that ionisation of the functional group such as the carboxyl, sulphate and phosphate present in the EPS contributes to the negative charge in activated sludge flocs at an ideal wastewater pH of 6.5-8.5. Also, extracellular proteins may have both a positive and negative charge, because of ionized amino functional group ($\mathrm{NH_3}^+$) and ionized carboxyl groups (COO^-), but at neutral pH, most extracellular proteins are overall negatively charged which validates the negative charge of activated sludge flocs (Conn *et al.* 1987). The total negative surface charge (SC) of flocs ranges from -0.1 to -0.7 milli-equivalent (meq)/ g volatile suspended solids (VSS) depending on the composition of the EPS present (Shin *et al.* 2000; Liao *et al.* 2001; Sponza 2002, 2003; Jin *et al.* 2003; Mikkelsen 2003). Wilén *et al.* (2003), further added that proteins have the largest influence on the surface properties and the isoelectric point (IEP) of most bacteria ranges from pH 2 to 3 (VanLoon and Duffy 2011).

Though, Vesilind and Martel (1990) and Colin and Gazbar (1995) has reported different forms of water available in activated sludge structure namely; free water (water not attached to solid particle), vicinal water (water physically bound to solid particles but cannot be separated mechanically), interstitial water (water trapped within the floc and can be released by breaking up the floc) and hydration water (water which are chemically bound to solid particles but can be released only at temperatures > 105℃). However, the water in the activated sludge floc is classed as bound water and free water (Mowla *et al.* 2013), where, the foremost is physically and chemically held to the floc while the latter is easily separated. In addition, the sum of interstitial, vicinal and hydration water (Bound water) has been reported as the key limiting issue in optimising the efficiency of activated sludge dewaterability process due to the excessive energy requirement in cell disruption. However, Wingender *et al.* (1999) stated that EPS whether in the exterior neither of the cell nor inside the microbial aggregates has capacity to bind with cells to form vast net-like structure with plenty of water locked up against dewatering. The author further stated that activated sludge faces challenges in dewatering processes and this has been linked to not just the presence of colloidal particulates but EPS within them. It is vital to mention that many functional groups in EPS mentioned earlier (carboxyl, sulphate, phosphate group) impacts surface charge (SC) of activated sludge flocs (Wilén *et al.* 2003; Wang *et al.* 2005a). Also, total EPS content has a negative impact on flocculation (Morgan *et al.* 1990; Liu *et al.* 2007; Liu *et al.* 2010). As mentioned earlier EPS are negatively charged and this leads to an increase in the surface charge of microbial aggregates causing an increase in the repulsive forces between the microbial cells. Liao *et al.* (2002); Jin *et al.* (2003); Yang and Li (2009) identified that these repulsive forces will constitute a decrease in both flocculability and settleability of microbial clusters and an increased EPS content causes activated sludge dewaterability problems because repulsive forces between cells which diminish capacity of flocculation and settleability of microbial clusters, increase much water retention ability causing an increase in the quantity of interstitial water in activated sludge flocs, creation of a stable gel-like material which prevents water seepage from the pores of flocs and increased sludge viscosity. Therefore, EPS removal from activated sludge floc will enhance dewatering characteristics (Houghton *et al.* 2001). The EPS is responsible for binding the water molecules to the surface and locking them up inside the sludge floc which makes high water content a major limiting factor when considering dewaterability of activated sludge. (This is explained in detail in section 2.3).

2.1.6.3.2 Cations

Cations play a vital role in optimisation of activated sludge settleability and dewaterability efficiency in activated sludge plants (ASP). Smith and Carliell-Marquet (2008) stated that UWWTD has proposed reduction of 80% phosphorus concentrations in eutrophic sensitive areas. Moreover, two methods of P-removal from wastewater are biological P-removal (BPR) and Chemical P-removal (CPR). The CPR process comprise of the addition of either aluminium (Al), Iron (Fe) or Lime (Ca) respectively (Ofverstrom *et al.* 2011a). The investigation of impact of chemical dosing ranging from monovalent, divalent and multivalent coagulants is vital in this current studies because most wastewater treatment plants (WWTP) struggles to meet the conventional biological phosphorus removal (BPR) approach because of most wastewater company struggles to meet the requirement of a strong sewage of which are, BOD: P 20mg/L, COD: P 50mg/L and adequate readily biodegradable material (rb) COD: P 25mg/L for a biological P- removal (BPR) process (Siebritz *et al.* 1982). Consequently, most P-removal are conducted using chemical phosphorus removal (CPR) in most wastewater treatment plants (WWTP) in the UK. The use of ferric chloride, aluminium sulphate and lime as a CPR approach to precipitate complex metal phosphorus like ferric phosphate, calcium sulphate amongst others from wastewater has been reported (Haandel and Lubbe 2012). The CPR and BPR are covered in more detail in Section 2.1.7.2 and 2.1.7.3

It has been stated in section 2.1.6.3.1 that EPS are composed of negatively charged biopolymers and numerous research studies show that cations interaction with negatively charged biopolymers causes a variation in the structural component of activated sludge floc (Higgins and Novak 1997b). In actualising bio-flocculation mechanism in activated sludge flocs, cations have been reported to play the role of binding between negatively charged biopolymers where microbial aggregates are entangled (Bruus *et al.* 1992; Urbain *et al.* 1993; Higgins and Novak 1997a). Higgins and Novak (1997b) and Higgins (1995) further added that monovalent cations have the propensity to decline the activated sludge settleability and dewaterability efficiency, but divalent cations have the capacity to enhance activated sludge settleability and dewaterability efficiency. This charge bridging between the biopolymers and divalent cations impacts the sludge floc positively by increasing the size of the sludge floc and the density, which results in an increased sludge floc resistance against shearing forces within the turbulence matrix in the aeration zone during mixing (Higgins and Novak 1997b). On the other hand, charge bridging between monovalent cations and the biopolymers impacts the sludge floc negatively by reducing the strength of the bond between them causing a loosed activated sludge floc structure which results in an overall reduction in the sludge floc size, density and resistance to shear forces within the aeration zone (Higgins and Novak 1997b; Higgins 1995). In exploring the relevance of cations in activated sludge floc structure, the study of models that describes activated sludge flocculation (bio-flocculation mechanism) becomes vital. As earlier stated section 2.1.6.3.1, proteins and polysaccharides are major constituents of EPS and their interactions with divalent cations (calcium and magnesium) will give a better insight into the comprehension of bio-flocculation mechanism. These models include; alginate model, divalent cation bridging (DCB) model, Derjaguin, Landau, Verwey, Overbeek (DVLO) model and hydrophobic interactions model. The alginate model (egg-box model) for investigating the responsibility of cations in bio-flocculation of activated sludge flocs was postulated by Bruus *et al.* (1992) and explained that polysaccharide in biopolymers produced by bacteria are alginates and these biopolymers consist of repeating mannuronic and glucuronic acids which have capacity to adsorb to divalent cations to form alginate sludge floc structure. However, a further claim was made that these biopolymers also bind to magnesium because enhanced bio-flocculation was also noticed when magnesium ions were included (Sobeck and Higgins 2002).

Although this claim was proposed, the alginate model does not agree since the affinity of the alginate towards magnesium ions was lower compared with the calcium ions. Urbain *et al.* (1993) and Dignac *et al.* (1998), on the contrary, further commented that protein has higher affinity for calcium while deoxyribonucleic acid (DNA) has higher affinity for magnesium. Another floc model where proteins with lectin activity (extracellular proteins) are cross-interrelated with polysaccharides and both magnesium and calcium ion provided bridging to this biopolymer was reported and the conclusion was that polysaccharide was released when pronase (isolated protease from extracellular fluid) was added to sludge and the bound protein increased when sludge was fed with magnesium and calcium (Higgins and Novak 1997a). The divalent cation bridging (DCB) model (Figure 2.30) also reinforces the role of divalent cations in bioflocculation and this model proposes that divalent cations have the capacity to bridge negatively charged functional groups present in the EPS environment. The aggregation mechanism and stability of the matrix of the biopolymer and individual microbes are sustained to optimise activated sludge settleability and dewaterability (Busch and Stumm 1968; Sobeck and Higgins 2002). Additionally, calcium ion bridging, negatively charged functional group present in EPS is also reported in literature as EPS-Ca^{2+}-EPS cross-association (Liu and Sun 2011). Conversely, Higgins and Novak 1997b; Higgins *et al.* 2004a, 2004b, identified the fragmentation of sludge floc matrix and linked this to dislocation of the divalent cation from the sludge flocs during the ion exchange process. This led to a loss of both the divalent cations and bridging functional groups, because of increased concentration of monovalent cations such as potassium and sodium in the sludge flocs.

Figure 2.30. Divalent cation bridging within floc matrix (Sobeck and Higgins 2002)

As stated in section 2.1.6.3.1 in the review by Sobeck and Higgins (2002); Wilén *et al.* (2003) that ionisation of the functional group like such as the carboxyl, sulphate and phosphate present in the EPS contributes to the net negative charge in activated sludge flocs at an ideal wastewater pH of 6.5-8.5, makes activated sludge floc possess a high adsorption power for cations and forms a good medium for cationic ion exchange polymer. However, several studies have been conducted to explain the positive impact of divalent cations in bio-flocculation mechanism which includes; calcium and magnesium divalent cations contributed to good flocculent growth in activated sludge, *Flavobacterium* (Tezuka 1969), calcium ion was responsible for the structural integrity of biofilm (Turakhia *et al.* 1983), experimental studies involving removal of calcium ion from activated sludge flocs on lab-scale, pilot-scale and full-scale industrial basis, through ion exchange process showed a weakened activated sludge floc structure causing decrease in the activated sludge settleability and dewaterability efficiency (Bruus *et al.* 1992; Chang *et al.* 1997; Higgins and Novak 1997b, 1997c; Keiding and Nielsen 1997; Murthy *et al.* 1998; Novak *et al.* 1998; Sobeck and Higgins 2002; Higgins *et al.* 2004a, 2004b; Peeters and Herman 2007; Kara *et al.* 2008; Nguyen *et al.* 2008a,b; Peeters *et al.* 2011). A surplus of monovalent cations like Na+ and K+ in the wastewater revealed deteriorated sludge floc structures which impacts the bioflocculation process negatively (Nguyen *et al.* 2008a,b; Peeters *et al.* 2011). Polymer bridging model can be estimated as monovalent cations (M^{+}) divided by the sum of divalent cations (D^{2+}) present in the wastewater. The $(\mathrm{M}^{+}/\mathrm{D}^{2+})$ (meq/L) as an activated settleability indicator can either enhance or lead to a deteriorated biofloculation. It was found that $\mathrm{M}^{+}/\mathrm{D}^{2+}$ value of greater than two shows poor activated sludge settleability and dewaterability characteristics and hence, to avoid sludge floc characteristic deterioration, a value less than two was proposed (Higgins and Novak 1997b).

Sanin *et al.* (2006) reported that among the various physical properties of activated sludge that adversely impacts bio-flocculation, dewaterability is the most pronounced due to its link to sludge floc-forming capability. Murthy *et al.* 1998; Sobeck and Higgins 2002; Higgins *et al.* 2004a; Peeters and Herman 2007; Sanin *et al.* 2011) commented that creation of stronger sludge flocs with more shear resistance by means of calcium polymer bridging can optimise activated sludge dewaterability efficiency. Liu and Sun 2011 observed yet another impact of calcium on the optimisation of activated sludge dewaterability is linked to its charge neutralising impact on sludge surface charge by decreasing the repulsive forces of the sludge flocs and Higgins and Novak (1997b) and Jin *et al.* (2004) stated that impact of calcium dosing on enhanced dewaterability depends on the lower quantity of the bound water content in the activated sludge. This polymer bridging model in comparison with the alginate model has been reported to propose a non-specific binding of divalent cations rather than specific divalent cation as in the case of alginate model and equally agree with the assertion of deflocculation from introducing monovalent cation (sodium ion) (Sobeck and Higgins 2002).

The double layer model (Derjaguin, Landau, Verwey, Overbeek or DLVO model) also known as the colloidal interaction model (Zita and Hermansson 1994) has been proposed to explain interactions between colloidal particles (Hiemenz and Rajagopalan 1997; Verwey and

Overbeek 1948). Colloids are impacted by Brownian movement because the colloidal particles are non-settleable and have size range of between 1nm to 1µm. Sobeck and Higgins (2002); Higgins *et al.* (2004b) define charged particles as having a double layer of counter ions surrounding the particle. The observed association between the particles depends on their surface potentials and thickness of the electrical double layer with negative charged ions surrounded by oppositely charged ions. Some charges accumulate on the stern surface layer while majority are found on the diffused layer (Figure 2.31).

Figure 2.31. Formation of an electrical double layer (Sobeck and Higgins 2002)

If two equally charged particles approach one another, they experience repulsive electrostatic forces. The electrostatic repulsion depends on the thickness of the double layer, which varies in reverse to the ionic strength. Thus, the electrostatic repulsion declines if the electrolyte concentration is high. Large amounts of divalent and trivalent ions also lead to an increase of the ion strength and a reduction of the particles surface potential. The addition of cations compresses the double layer near the negatively charged sludge flocs which causes the repulsive forces between the sludge floc to decrease and facilitate aggregation (Zita and Hermansson 1994).The Van der Waals force is a function of the separation distance, the geometry of the system and the Hamaker constant, which depends on the hydrophobicity of the concerned particles. The DLVO model further describes Gibbs interaction energy, summing the Van der Waals attraction and electrostatic repulsion forces (Higgins *et al.* 2004b). This total interaction energy is a function of the separation distance of two particles (Figure 2.32). When repulsion surpasses attraction, there is a potential energy barrier, which obstructs interaction between particles. For two particles to aggregate, this energy barrier must be overcome via kinetic energy exhibited by the discharge or otherwise decreased by the addition of coagulant.

Figure 2.32. Interaction energy between two particles as a function of separation distance according to the DLVO theory (Sobeck and Higgins 2002)

Once the barrier has been overcome, the particles are strongly held in the deep primary minimum. It is assumed that flocculation of activated sludge is due to attraction forces of the secondary minimum, since sludge aggregates tend to deflocculate under turbulent conditions and at relatively low shear rates. Sobeck and Higgins (2002) debate the rationality of this theory due to an enhancement of bioflocculation by addition of monovalent cations. This causes a rise in the ionic strength but decrease in the thickness of the double layer which might not be applicable in practice. A further comparison was made by Sobeck and Higgins (2002) between the alginate theory, DLVO theory and DCBT, which concluded that the DCB model best explains bio-flocculation with cations playing an imperative part.

The last model investigated is called the hydrophobic interaction model which is based on hydrophobic molecules which are non-polar or non-charged molecules. Meanwhile, these hydrophobic molecules lack the electrostatic interactive capability and does not form hydrogen bonds with water which limits its ability to mix with water and hence plays a major role in binding together of the activated sludge flocs (Liao *et al.* 2001; Jin *et al.* 2003). Nevertheless, internal hydrophobic interactions of sludge particles especially with lipids have been reported to be vital in the bio-flocculation at a cell surface level (Wilén *et al.* 2003).

Moreover, in explaining the role of cation influencing the activated sludge floc properties, there have been arguments that multivalent (divalent and trivalent) cations offer better flocculating tendencies than monovalent cation. Murthy *et al.* (1998) also added that WWTPs using sodium hydroxide for pH control generates sludge with poor settling and dewatering efficiency. Novak *et al. (*2001) further commented on another monovalent cation, ammonium ion that deteriorating sludge floc characteristics in the same capacity as sodium monovalent cation. Higgins and Novak (1997b) recommended that the ratio of monovalent to divalent cations is an indicator of activated sludge floc characteristics and ratio beyond two caused a huge reduction in the sludge filtering rate and hence it is used as an optimal ratio of M/D, where M is monovalent, and D is divalent. Murthy (1998) supported this assertion and added that the M/D ratio was equally effective for explaining the activated sludge effluent quality. On the other hand, trivalent cations' (iron and aluminium) role in affecting activated sludge floc characteristics has not been extensively researched compared with numerous research contributions on the monovalent and divalent cations. Kakii *et al.* (1985) reported their availability at high concentrations in activated sludge because of greater charge valence and lower solubility than divalent cations and monovalent cations, makes studying their impact on activated sludge floc stability vital in this current research. Experimental results based on Kakii *et al.* (1985) findings showed that iron and aluminium were not affected by the acid treatment of activated sludge at pH3 whilst most of the calcium and magnesium were extracted, demonstrating that iron and aluminium are more strongly connected with activated sludge floc matrix than divalent cations. Other studies that explain the role of trivalent cation include Caccavo *et al.* (1996) and Nielsen and Keiding (1998) investigating the role of iron in activated sludge, iron (III) reduction to iron (II) by iron reducing bacteria and sulphate reduction to sulphide showed that turbidity increases in bulk water of sludge, which suggested that oxidized iron plays a vital role in floc stabilization. Rasmussen and Nielsen (1996) reported that about 70 to 90% of iron was present as ferric iron in the fresh activated sludges they investigated. However, they also admitted difficulties in identifying the species or chemical forms of iron; whether they are present in floc as crystalline, amorphous or organically bound iron. Nielsen and Keiding (1998) equally proposed that either the reaction of ferric ion with EPS or the precipitation as ferric hydroxides or both are involved in flocculation but both species were demonstrated as stronger flocculants than calcium ion.

2.1.6.3.3 Bound water

The key limiting rate factor that impact activated sludge dewaterability and settleability performance is the bound water as stated in section 2.1.6.3.1 (Vesilind and Martel 1990; Colin and Gazbar 1995; Liao *et al.* 2000). The sum of interstitial, vicinal and hydration water was termed as bound water (Mowla *et al.* 2013). The bound water was also reported to correlate with the EPS but no relationship between bound water and sludge residence time and surface charge of sludge floc (Liss *et al.* 1996). Bound water and EPS is further discussed in section 2.3.1.3 and 2.3.1.4 on dewatering of activated sludge.

2.1.6.3.4 Floc size and strength

Researchers commented on bimodal size distribution with floc size range of 25µm – 300µm, showing that smaller flocs in form of single microorganism might have been sheared off by larger activated sludge flocs (Parker *et al.* 1970; Li and Ganczarczyk 1991). However, Parker *et al.* (1971) attributed the determining factor for variation in the size of flocs to include either their cohesive strength or effect of shearing due to the turbulence within the aeration process. Li and Ganczarczyk 1991 added that bacteria for instance accounted for a particle size of 0.5 to 5 micrometre in larger activated sludge flocs in the range of > 1mm diameter. Mikkelsen (2001) further added that the upper margin for flocs to be around 1000µm. Other studies observed higher floc strength particularly with activated sludge having a low EPS content (Wilén *et al.* 2003). Section 2.1.6.2 (activated sludge bulking) explored some more details on floc sizes and strength.

2.6.3.5 Floc structure and density

Researchers have reported that activated sludge flocs microphotographs revealed that microbes, water and EPS in the activated sludge matrix are haphazardly distributed within the floc (Li and Ganczarczyk 1990; Jorand *et al.* 1995; Liss *et al.* 1996). Li and Ganczarczyk (1990) and Gregory (1997) experimented on activated sludge flocs and the investigation by Gregory (1997) showed on one hand that the effective density of sludge particles reduced as the sizes increased while on the contrary, large and low-density sludge particles settle with lower velocity than compact dense particles due to the lower density of sludge particulate and experience more floc breakage. However, it was added that if the sludge floc was permeable, the settling velocity will rise because of the lower drag force compared to an impermeable activated sludge floc. This shows that floc size and density determine the efficiency of FST.

2.1.7 Phosphorus and Nitrogen removal

2.1.7.1 Nitrogen removal

Amongst the most vital components considered in the activated sludge plant is nutrient removal. Over the years nutrient removal has drawn so much attention in activated sludge processes because of its contribution to eutrophication in the water bodies receiving untreated wastewater and effluent from diverse wastewater treatment works (Hammer 2008 and Tebbutt 1998). The challenge of optimum nutrient removal has made tertiary treatment an important polishing stage in the wastewater clarification process. Yet another challenge in ASPs is the floating sludge due to denitrification taking place within the anoxic zone of the tank with presence of nitrate and absence of dissolved oxygen as key indicators of anoxic processes (Kim *et al.* 2008; Knowles 1982). This issues was averted through occurrence of nitrification and denitrification under a controlled condition before the mixed liquor enters the final sedimentation tank (FST) (Kelley and He 2014).

2.1.7.1.1 The Impact of Nitrogen removal

Nitrogenous organic matters like protein are essential for living organisms and waste from industrial processes are usually tested for nitrogen and phosphorus content to predict the right quantity required for biological treatment. The identified form of nitrogen includes organic, ammonia, nitrite, nitrate and gaseous nitrogen (Hammer 2008). Organic nitrogen has been reported as domestic waste, animal slurry from farm lands and high protein waste from industries like meat industry (Gray 2004). Urea is another important source of nitrogen in wastewater which can be converted to peptides and amino acid by extracellular proteolytic enzymes. The resulting amino acid is further reduced or oxidised to produce ammonia but it was noted by Culp *et al.* (1978) that once the raw wastewater enters the treatment works, 90 % of the nitrogen will either be present as ammonia or unstable organic compounds which over time are converted into ammonia. Inorganic nitrogen in the form of ammonia ($\mathrm{NH_3}$) and nitrate ($\mathrm{NO_3}$) are useful for green plants during photosynthesis. Although, natural waters are limited in nitrogen, but nitrogen has an impact of water pollution since nitrogen wastes can support the growth of algae causing a green colouration in water (Eutrophication) and the inorganic nitrogen like ammonia poses a threat on fish because of its toxic effect (Tebbutt 1998).

Although the test for ammonia nitrogen ($\mathrm{NH_4}^+$) involves a distillation process with a chemical equation in Equation 2.46 while organic nitrogen in wastewater can be obtained by digestion of organic matter with ammonia (Equation 2.47) but if both ammonia and organic nitrogen is required then the sample can be tested first for ammonia and afterwards digested and tested for organic nitrogen. The outcome is the sum of Equations 2.46 and 2.47 called total kjeldahl nitrogen (TKN).

$$\mathrm{NH_4}^+ \leftrightarrow \mathrm{NH_3} + \mathrm{H}^+ \tag{2.46}$$

$$\text{Organic nitrogen} \rightarrow \mathrm{NH_4}^+ \tag{2.47}$$

Though, the main organisms relevant in wastewater treatment includes bacteria, virus, algae, protozoa and crustacean, the identified major group of microorganisms relevant to the secondary treatment processes are bacteria and protozoan. Bacteria are colourless and single cell plants that use soluble food and are capable of self-reproduction without sunlight effect, but protozoa are single celled animals that multiplies by binary fission. Furthermore, protozoa unlike bacteria have complex digestive systems and thus make use of mainly bacteria as food. Bacteria has been known to constitute settleability issues due to filamentous growth that produces more buoyant activated sludge flocs. This bacterium has been classified based on their source of nutrient as heterotrophic and autotrophic. The heterotrophs have been identified to use organic matter as an energy for respiration, motility and carbon source for synthesis (Equation 2.48) but classification includes aerobes (Equation 2.49) which use available oxygen

(O_2) to breakdown organics and the anaerobes (Equation 2.50-2.53) which metabolise organic matter in the absence of available oxygen by utilising oxygen bound in either nitrate (NO_3) or sulphate (SO_4)compounds. The last classification is called facultative bacteria which has both attributes of aerobes and anaerobes in place.

Microbial Synthesis (Anabolism)

$$\text{Energy} + \text{Organics} \rightarrow \text{New Cell Growth} \quad (2.48)$$

Aerobic Reaction (Catabolism)

$$\text{Organics} + O_2 \rightarrow CO_2 + H_2O + \text{Energy} \quad (2.49)$$

Anaerobic Reaction

$$\text{Organics} + NO_3 \rightarrow CO_2 + N_2 + \text{Energy} \quad (2.50)$$

$$\text{Organics} + SO_4 \rightarrow CO_2 + H_2S + \text{Energy} \quad (2.51)$$

$$\text{Organics} \rightarrow \text{Organic acids} + CO_2 + H_2O + \text{Energy} \quad (2.52)$$

$$\text{Organics} \rightarrow CH_4 + CO_2 + H_2O + \text{Energy} \quad (2.53)$$

The main aim of heterotrophic bacteria metabolising organics includes ability to gain energy for synthesis of new cells by binary fission, respiration and motility. Although, a small percentage of the used energy is lost as heat, but the amount of energy is a function of the available oxygen for metabolism. The aerobic digestion process will offer the largest energy yield because of the available dissolved oxygen level compared to the anaerobic processes. In Equations 2.50 and 2.51 it was noticed that anaerobically operating organisms within the biological system could obtain oxygen from a nitrate and sulphate compound to release nitrogen and hydrogen sulphide which has a rotten egg smell.

Crown Corrosion in sewers

$$H_2S + O_2 \rightarrow H_2SO_4 + \text{Energy} \quad (2.54)$$

It is vital to mention that when wastewater flowing through a sewer becomes septic over time, it is known to release H_2S gas and if allowed to stay around the crown of the pipe which contains some condensate of water, the sulphur bacteria which feeds on wastewater and tolerates a pH of 1.0 will oxidize this weak acid (H_2S) and produce sulphuric acid (H_2SO_4) (Equation 2.54). The impact of sulphuric acid on the concrete will reduce its structural strength and places the pipe under corrosion. This process has been termed crown corrosion in sewers. Thus, most material make up of sewers are recommended to be polyvinyl chloride (PVC) plastics. Consequently, if methane forming bacteria are used in metabolism, then Equation 2.52 holds, and hence organic acids will be converted to methane (CH_4) and carbondioxide (CO_2).

Conversely, the autotrophic bacteria oxidise inorganic compounds for energy and use carbondioxide as a source of carbon. The examples of these bacteria are nitrifying, sulphur and iron bacteria. On the other hand, researchers have reported that the conventional nitrogen removal process can efficiently remove reactive nitrogen from wastewater as reflective in the two-stage equation of nitrification in Equation 2.56 to 2.58 (Nancharaiah *et al.* 2016). In Equation 2.55, Nitrosamines converts ammonium nitrogen (NH_3) to nitrite (NO_2)and Equation 2.56, Nitrobacter autotrophic bacteria convert nitrite (NO_2) to nitrate (NO_3). Although, nitrification is unavoidable in biological treatment processes in tropical regions once it reaches a temperature of 22 to 24 degree Celsius under a low organic loading (Haandel *et al.* 2012) but to achieve a more stable effluent, nitrification is avoided to decrease the consumption rate of oxygen in the metabolism of organics in wastewater treatment units. Nevertheless, nitrification is avoided in final sedimentation tanks (FST) to prevent floating sludge on the FST. This floating sludge is formed on the liquid surface of the FST due to microscopic nitrogen gas bubbles developed inside the sludge flocs because of denitrifying bacteria in an anoxic environment, causing a reduction in the nitrate level and converting the nitrate to nitrogen gas (Equation 2.57). The nitrification of wastewater has the potential to destroy alkalinity which results in a low pH when treating wastewater with a fair hardness or better still alum destroying alkalinity which causes wastewater to behave absurdly. This further impacts results in the cement on concrete surface and FST metallic mechanisms to corrode, but this was being dealt with using lime or soda ash additions (Hammer 2008). Nonetheless, it was reported that the pH in activated sludge processes was set based on carbonic system (Equation 2.58) and since the organics present in the wastewater was at higher concentration than the acid-base systems. In addition, the equilibrium of the weak acid and base like ammonium nitrogen was not considered when the pH was 7.0 as in the case of the mixed liquor since they are in ionic form (Haandel and Lubbe 2012). The nitrogen removal through nitrification and denitrification process is an energy demanding process as literature has identified it as a major cost factor in wastewater treatment as the oxygen requirement for nitrification equates 60% of the operation cost of treating wastewater (Ledezma *et al.* 2015).

Impact of Nitrosomonas

$$\mathrm{NH_3 + O_2 \rightarrow NO_2 + Energy} \qquad (2.55)$$

Impact of Nitrobacter

$$\mathrm{NO_2 + O_2 \rightarrow NO_3 + Energy} \qquad (2.56)$$

Impact of Denitrifying Bacteria (Anoxic Reaction)

$$\mathrm{NO_3} \rightarrow \mathrm{N_2} + \mathrm{O_2} \tag{2.57}$$

The Carbonic System

$$\mathrm{CO_2} \leftrightarrow \mathrm{HCO_3}^{-1} \leftrightarrow \mathrm{CO_3}^{2-} \tag{2.58}$$

2.1.7.2 Phosphorus removal and enhanced biological phosphorus removal

According to studies by Hammer (2008), phosphorus exists in different forms in wastewater and it includes orthophosphate ($\mathrm{PO_4}^{2-}$), polyphosphate and originally bound phosphate. The bacterial metabolism of organics produces orthophosphate. All polyphosphates or phosphoric acid easily hydrolyses in water to form orthophosphate but the challenge of phosphorus in wastewater is ensuring the required amount of phosphorus for growth of microorganisms. Though, there are two-point sources of phosphorus discharge into surface water namely runoff from cultivated farm land with chemical phosphorus fertiliser and discharge from untreated wastewater from treatment works, Polyphosphate washing powder was a point source but with the advent of washing powders void of phosphate this has been addressed. Additionally, with majority of the organic phosphorus been converted into inorganic materials, effluent in an activated sludge process is made up of ortho-phosphate. The bulk of compounds in wastewater have been identified to be in a soluble state hence phosphorus removal will be minor just sedimentation. Thus, a conventional treatment system removes 20 to 40% influent phosphorus. The biological phosphorus is integrated into the activated sludge flocs and as such they can be removed partly by biological and chemical processes. Following this further, to control phosphorus direct discharge to rivers each country has a customised permissible concentration which ranges from 1 to 2mg/L P by Hammer (2008) but Haandel and Lubbe (2012) accounted that a developed country the ratio between phosphorus and COD (chemical oxygen demand) value in wastewater lies from 0.02 to 0.03 mg P/mg COD and a reduced value of less than 1mg/L P removal was agreed. Further still, Gray (2004) identified a stricter consent of below 2mg/L P removal before discharge into sensitive waters. Therefore, phosphate will be required in a controlled measure to avoid activated sludge plant operational issues like sludge bulking since this ortho-phosphate is integrated into the activated sludge biomass. Fowler *et al.* (2013) added a new limit of 1-3mgN/L and < 0.1mgP/L and nutrient recovery and conversion into a reusable form has been reported (Ledezma *et al.* 2015)

A study by Haandel and Lubbe (2012) concluded that the estimated proportion of phosphorus mass in volatile activated sludge was 2.5% of the concentration of the volatile suspended solid (VSS) concentration. This is an indication that the part of proportion phosphorus content will be removed with the excess activated sludge. Furthermore, the authors stated that assuming an activated sludge plant operating at a sludge age (SA) of 8 to 12 days the effluent concentration realised will be in the range of 0.004 to 0.014mg P/mg COD. However, when the SA becomes higher then supplementary means will be required. The traditional approach involving application of coagulants like ferric (Iron), aluminium and lime was earlier adopted for phosphorus removal in the final activated sludge effluent. This could precipitate complex metal phosphorus like calcium phosphate, ferric phosphate, apatite and struvite. Some limitations were identified by Haandel and Lubbe (2012) which included a high cost of chemicals and increased excess sludge generation attributed to overdosed quantity of coagulants (ferric and aluminium) required to achieve a low effluent phosphorus (EP) result. Additionally, another limitation was reduction in the recycling potential of the effluent due to an increased salt content realised in the effluent (Gray 2004; Hammer 2008). The limitations attributed to the use of coagulant for phosphorus removal has made this study on optimisation of phosphorus removal vital.

On the contrary, enhanced biological phosphorus removal (EBPR) is also known as the luxury phosphorus uptake. As mentioned earlier the proportion of phosphorus mass content is 2.5% of the volatile suspended solid concentration but the luxury phosphorus uptake approach accounts for additional 38% biological sludge mass using an artificial substrate called Ethanoate (acetate). Thus, the mean phosphorus mass fraction ranges from 80 to 100mg P/gVSS based on the composition of organic matter in the influent flow. Various process conditions were identified for the excess biological phosphorus removal to take place (Figure 2.33). Firstly, was introduction of an anaerobic zone into the process configuration of the enhanced biological phosphorus removal. This caused an increased mass fraction of phosphorus in the activated sludge flocs and this agreed with the findings by Barnard (1975), Comeau *et al*. (1985) and Wentzel *et al.* (1988), reviewed in Haandel and Lubbe (2012), that the sludge in the anaerobic zone will discharge phosphate to the liquid phase of the activated sludge and in the other anoxic and aerobic zones, phosphorus uptake was such that the phosphorus in the biomass contained in the anaerobic zone was higher than that realised in a conventional activated sludge system. Secondly, it was to design an anaerobic zone in the activated sludge system and this agreed with the findings of Barnard (1975) on modification of the bardenpho system (an activated sludge process provided to achieve biological phosphorus (P) and nitrogen (N) removal by designing an anaerobic and aerobic zone) (Emara *et al.* 2014). The anaerobic zone was designed immediately after the nitrate removal in the Bardenpho process because if the nitrate is first released to the anaerobic zone, they will all be removed by denitrification process. It was also investigated by Siebritz *et al.* (1982) which was reviewed in Haandel and Lubbe (2012) that both the nature and concentration of organic materials contribute largely to the phosphorus release and absorption. Nevertheless, the presence of nitrate in anaerobic zone of the bardenpho process contributed to the partial or complete removal of the decomposable matter. Consequently, Yuan *et al.* 2012; Oehmen *et al.* 2007; Wentzel *et al*. (1986) reported the use of a synthetic feed called phosphorus accumulating organism (PAO) (Figure 2.33) along with acetate to generate sludge mass with a phosphorus mass fraction of 38%.

Figure 2.33. Metabolism of biological –P organism (PAO) under anaerobic and aerobic/anoxic condition (Smolders *et a*l. 1994a).

The research studies by Van Haandel and Lettinga (1994) on a detailed metabolic model on cell microbiology, in the first discovery biological phosphorus organisms was made up of three internal cell storage products relevant for excess phosphorus removal; polyphosphate, polyhydroxyl-alkanoate (PHB) and glycogen. Also, under anaerobic conditions, volatile fatty acid are taken up from the liquid phase and stored as PHB. Relevant to this process is an energy carrier released during the formation of PHB from glycogen is known as Nicotinamide adenine dinucleotide dehydrogenase ($\mathrm{NADH_2}$). More so the required energy for $\mathrm{NADH_2}$ comes from hydrolysis of polyphosphate and formation of Adenosine triphosphate (ATP). The research by Filipe *et al.* (2001a) identified other groups of microorganisms which depend on glycogen as a source of energy and carbon storage called glycogen accumulating organism (GAO). It was realised that they have capacity to store low molecular organic compounds for example volatile fatty acid (VFA) under anaerobic conditions and growth under aerobic condition. However, it was discovered that GAO lacked the behaviour for a biological-P organism which release phosphorus under anaerobic condition and taking it up under aerobic condition.

2.1.7.2.1 Biological Phosphorus Removal System Configuration

2.1.7.2.1.1 Phoredox and A/O (Anaerobic /Oxic) Configuration

It was reported from studies conducted by Barnard (1976) that this configuration as shown in **Figure 2.34** was made up of two reactors in series with the influent going into the first reactor which has an anaerobic zone and the second aerobic. The anaerobic reactor helps to ensure contact between the activated sludge and the influent wastewater flow before the aerobic degradation to accomplish the biological phosphorus removal (BPR). The detention time for the anaerobic process in the anaerobic reactor is (Between 30 minutes to 120 minutes).

Figure 2.34. Phoredox and A/O configuration (Haandel and Lubbe 2012)

However, phosphorus and carbon removal takes place with no nitrification and a low operating sludge residence time (SRT) (between 2 to 4days) to avoid the commencement of nitrification. Furthermore, the system volume is compact and no requirement of anoxic reactor. Nevertheless, if nitrification process occurs there will be issues of reduction of the BPR treatment efficiency due to the nitrate entering the anaerobic zone through the return activated sludge (RAS) recirculation and heterotrophic bacteria using the available nitrate to consume readily biodegradable (rb) chemical oxidation demand (COD) and resulting in less rbCOD available for phosphorus storing bacteria (Figure 2.34). The limitation of decreased BPR efficiency was averted using the A^2/O process (Anaerobic/Anoxic/Oxic) that provided an anoxic zone that contained recycled aerobic nitrate (Figure 2.35).

On the other hand, the A/O (anaerobic/Oxic) Configuration designed by Timmerman (1979) has been accounted to mirror the phoredox system but because of the compartment within the anaerobic zone, it was able to initiate a plug flow system that allows the biodegradable material to be converted to acetate which increases the phosphorus removal efficiency. Additionally, it was discovered that the application of Phoredox system is mostly used in Europe and the United States of America (USA). Although, application was limited to temperate region with hotter climate, but nitrification was still experienced at low sludge ages (SA) but the release of nitrate into the anaerobic reactor was unavoidable and hence the phosphorus removal ability decreased.

2.1.7.2.1.2 Modified pre-denitrification (D), A^2/O (Anearobic/Anoxic/Oxic) and Bardenpho Configuration

The A^2/O process (Figure 2.35) is a modification of the A/O process (Figure 2.46) and provides an anoxic zone for denitrification.

Figure 2.35. Modified pre-D, A^2/O and bardenpho configuration (Haandel and Lubbe 2012)

The detention time in the anoxic zone is approximately 60minutes. The anoxic reactor is limited in oxygen but chemically bound oxygen in the form of nitrate is introduced from the aerobic reactor as recycled nitrified mixed liquor as shown in Figure 2.35. The merit of introducing the anoxic reactor, is to reduce the amount of nitrate fed to the anaerobic reactor through the RAS recycling. This configuration in Figure 2.35 had an anaerobic zone introduced upstream of the pre-D (denitrification) anoxic reactor. The influent and return sludge flow was reported to be received by the anaerobic reactor. Following this further, the nitrate removal could be completed first before transferring it to the anaerobic zone because if this was not the case then the nitrate will be conveyed into the anaerobic zone and when this occurs, the biological phosphorus organism will be restricted from access to the easily biodegradable organic material. Thus, the phosphorus removal ability will be reduced. Additionally, it is equivalent to the A^2/O configuration and is be popular globally but has been replaced by the University Cape Town (UCT) or modified UCT system (Figure 2.36 and 2.37).

2.1.7.2.1.3 UCT System and Modified UCT Configuration

Following the research development by Rabinowitz and Marias (1980) of the UCT system (Figure 2.36); it was designed to reduce the impact of nitrate in weaker wastewaters entering the anaerobic reactor. The UCT system is vital as the concentration of nitrate in the anaerobic reactor determines the BPR efficiency.

Figure 2.36. UCT system configuration (Haandel and Lubbe 2012**)**

The UCT system achieved its treatment efficiency by maintaining the RAS recycle to anoxic reactor, mixed liquor recycle to anaerobic reactor drawn following to anoxic reactor (minimising amount of nitrate entering to anaerobic reactor). This process is similar to the A²/O system with two main exceptions as shown earlier in Figure 2.35; The RAS is recycled to anoxic zone instead of aerobic zone, the internal recycle is from the anoxic zone to the anaerobic zone. Therefore, introduction of the activated sludge to the anoxic zone shows that the concentration of nitrate in the anaerobic zone will be removed and hence the uptake of phosphorus in the anaerobic zone will be enhanced. Furthermore, while the anoxic recycle zone will ensure increased organic consumption in the anaerobic reactor, the anoxic mixed liquor (soluble BOD with minimum nitrate concentration) recycle will provide the required optimal condition for fermentation uptake in the anaerobic zone.

On the other hand, the modified UCT configuration (Figure 2.37) was designed to ensure that the RAS is directed to an anoxic reactor without an internal nitrate recycle flow. This will reduce the nitrate concentration in the tank and ensure a recirculation of the mixed liquor from the anoxic zone to the anaerobic zone. The second anoxic reactor following the first anoxic reactor (Figure 2.37) is to receive the internal nitrate recycle from the aerobic reactor to provide the major portion of nitrate removal for the UCT modified process. However, In this case the anoxic zone that is divided into two parts with the recycled sludge being introduced into the first anoxic while the second anoxic is used to achieve denitrification of the nitrate recycle with recirculation. This is an indication that denitrification will be completed in the first anoxic zone but there will be no nitrate returned to the anaerobic zone.

Figure 2.37. Modified UCT configuration (Haandel and Lubbe 2012)

The limitation of this configuration compared to the modified bardenpho process is that the anoxic zone will be under loaded with the required nitrate and it will have a larger volume capacity anoxic zone. If this is not checked then there is a potential issue of floating sludge in the FST. This issues was addressed in the Johannesburg configuration (Figure 2.38).

2.1.7.2.1.4 The Johannesburg configuration

According to Osborn and Nicholls (1978), the Johannesburg Configuration (Figure 2.38) was designed to address the limitation of the modified UCT (Figure 2.37) processes by minimising the nitrate feeding concentration to the anaerobic reactor to maximise the efficiency of BPR for weaker wastewaters.

Figure 2.38. Johannesburg configuration (Haandel and Lubbe 2012)

In actualising this design, the RAS was directed to an anoxic reactor that possess sufficient detention time to decrease the nitrate level in the mixed liquor prior to its feeding to the anaerobic reactor. However, compared to the modified UCT system, the Johannesburg configuration can maintain a higher MLSS concentration in the anaerobic reactor with a detention time of about 60 minutes. It was discovered that once the sludge concentration in the FST which is a function of the recirculation factor, increased above the mixed liquor entering the FST, the denitrification in the post denitrification zone increased. Thus, it is possible to produce mixed liquor in the post denitrification zone to the anaerobic zone when nitrate was found in the effluent.

Besides the **Table 2.3**, shows the summary comparison of various biological phosphorus removal configurations.

Table 2.3. Comparison of Various Biological Phosphorus Removal Configurations (Haandel and Lubbe 2012)

Configurations	Merits	Demerits
Phoredox and A/O	Small and simple system with short residence time	No nitrogen removal and in hot climate system will not be reliable
Modified Pre-D, A^2/O	High denitrification rate and short sludge age	Might not function properly due to recirculation of nitrate and has incomplete denitrification with tendency of inducing sludge bulking
Modified Bardenpho	Excellent configuration for nitrogen removal	If denitrification is incomplete, then nitrate will be recycled to anaerobic zone which adversely affect P-removal
UCT	prevents recirculation of nitrate	Utilisation of denitrification capacity is inefficient
Modified UCT	Ensures absence of nitrate in the anaerobic zone	Utilisation of denitrification capacity is inefficient to greater extent than UCT.
Johannesburg	Efficient use of denitrification zone	Incomplete denitrification

2.1.7.3 Chemical Phosphorus Removal (CPR)

This has been defined as the process used to form and precipitate insoluble metal phosphate salts by the addition of coagulants which range from lime, iron or aluminium salts (Haandel and Lubbe 2012; Gray 2004; Hammer 2008). According to Wilfert *et al.* (2015) and Hammer (2008), chemical precipitation using aluminium or iron coagulants which involved combining of orthophosphate with metal cations was effective in phosphate removal, but it was stated that the reactions are complex. On the other hand, polyphosphate and organic phosphorus compound were removed by being entrapped or adsorbed in the activated sludge flocs.

2.1.7.3.1 Stoichiometry of Chemical Coagulants (Metal Salt) for CPR

The hydrated aluminum sulphate ($Al_2(SO_4)_3 \cdot 14.3H_2O$) was used globally to precipitate phosphates as aluminum phosphate ($AlPO_4$) and the outcome was a reduced pH value with sulphate ion discharge into the wastewater. Additionally, it was identified that 80-90% phosphorus removal was achieved at Aluminum coagulant dosing concentration of 50-200mg/L but a dosage concentration of 150mg/L aluminum will pose threats to the microbial population. Nevertheless, if a desired phosphorus removal percentage ranging from 75% to 95% then a dosage ratio of aluminum to phosphorus ranging 13:1, 16:1 and 22:1 was recommended (Gray 2004; Hammer 2008). This is due to the finding from Equation 2.59, that the molar ration for aluminum salt to phosphorus was 1:1 and the weight of commercial aluminum salt to phosphorus was 9.7 to 1.0 (Hammer 2008).

$$Al_2(SO_4)_3 \cdot 14.3H_2O + 2PO_4^{3-} \rightarrow 2AlPO_4 + 3SO_4^{2-} + 14.3\ H_2O \qquad (2.59)$$

Furthermore, the research studies by Anderson and Hammer (1973) on strategic modifications to activated sludge system legitimated the use of coagulants for phosphorus removal based on observed removal efficiency trend during the dosing of settled sewage (six synthetic wastewaters comprising of glucose and glumatic acid) with 10mg/lLconcentration of phosphorus with aluminium salt. The impact of ferric chloride ($FeCl_3$), although accepted worldwide for phosphorus removal, the reactions are sometimes unclear. This was because ferric chloride reactions are sometimes slow and will require additional assistance of coagulant aid like lime (Hammer 2008; Gray 2004). The aid from lime was to raise the pH level to increase the hydroxyl concentration and speed up the coagulation process. Equation 2.60 shows how the ferric ions combine with both the lime and natural alkalinity to precipitate ferric hydroxide ($Fe(OH)^3$) (Equation 2.61).

$$FeCl_3 + PO4^{3-} \rightarrow FePO4 + 3Cl^- \qquad (2.60)$$

$$FeCl_3.6H_2O + 3HCO_3^- \rightarrow Fe(OH)^3 + 3CO_2 + 3Cl^- + 6H_20 \qquad (2.61)$$

However, lime addition removes calcium ions as well as phosphorus from wastewater together with the suspended solids. It was discovered that the lime reacts with the natural alkalinity initially in the wastewater to form calcium carbonate ($CaCO_3$) in Equation 2.62. This helps to increase the suspended solids (SS) removal.

$$Ca\ (HCO3)2 + Ca\ (OH)\ 2 \rightarrow 2CaCO3 + 2H2O \qquad (2.62)$$

Subsequently, the resulting calcium ions react with the orthophosphate under a basic condition of pH of 10.5 to form insoluble and gelatinous calcium hydroxyapatite ($Ca_5\ (OH)\ (PO_4)_3$ (Equation 2.63)

$$5Ca^{2+} + 4OH^{-} + 3HPO_4{}^{2-} \rightarrow Ca_5(OH)(PO_4)_3 + 3H_2O \tag{2.63}$$

In view of preserving the life of the microbial biomass in the aeration tank, neutralisation was noted as an option through infusing carbondoxide into the tank to control the 10.5 pH as the lime dosed equals 1.5 times the CaCO3 alkalinity. It was further added (Gray 2004; Haandel and Lubbe 2012; Hammer 2008) that the use of coagulant has an impact on the pH because in precipitation processes alkalinity was removed and acidity released. It was observed by Hammer (2008) that almost half of the coagulant salt like ferric and aluminium etc. combine with phosphate and the remaining precipitate as hydroxide (Equation 2.62 and 2.63). Following this further, another impact of pH can be evaluated from the amount of coagulant present in the final effluent.

2.1.7.3.2 Configuration of Chemical Phosphorus Removal (CPR)

The configuration of a CPR (Haandel and Lubbe 2012) comprises of pre-precipitation where chemicals are added to the raw influent or in the primary sedimentation tank (PST). In this process, the coagulant takes out the metal phosphate with the primary sludge from the PST. The next configuration is the simultaneous precipitation which entails adding the chemical to the mixed liquor in the aeration tank. In this case there is removal of the metal phosphate with the excess biological activated sludge. Another configuration is post precipitation where chemicals are added to the effluent of the FST. Lastly, the side-stream precipitation is a configuration which acts as a supplement to the biological phosphorus removal. This is achieved by concentrating phosphorus into a small volume side stream with high phosphorus content and the side stream placed under CPR process.

2.1.7.3.2.1 Pre-precipitation

Figure 2.39 depicts a flow scheme of phosphorus removal by pre-precipitation. This coagulation process is rather dual as it achieves both the aim of the coagulation and takes out the phosphorus. The organic load entering the biological treatment unit was found to be reduced due to the metallic complex salt hydroxide ($Fe(OH)_3$) component flocculation was enhanced and suspended solid (SS) removal rate increased. This finding agrees with the result of De Jong *et al.* (1993) where the primary sedimentation tank (PST) of a Dutch municipal wastewater treatment plant was investigated and the mean BOD removal in the PST was observed to increase form an initial level of 20-40% to 50-75% after the addition of a metallic salt (coagulant).

Figure 2.39. Chemical phosphorus removal (CPR): Pre-precipitation (Haandel and Lubbe 2012 and Zhou 2009)

In addition, it was noted by De Jong *et al.* (1993) that if denitrification is required, then the pre-precipitation approach will not be applicable due to the increased nitrate level in the pre-clarified influent. This process will also, remove all sulphides responsible for odour through precipitating the metal sulphides.

2.1.7.3.2.2 Simultaneous precipitation

This process of precipitation as shown in Figure 2.40 can be applicable as the primary approach to phosphorus removal or an added means of biological phosphorus removal. In the case where the simultaneous precipitation is the main mechanism, the major removal obtained will be nitrogen and organic matter with some phosphorus. This phosphorus at the end will be removed with the excess sludge generated which makes this process designed to remove excess phosphorus and not to enhance biological growth. Therefore, it is not applicable to develop an enhanced phosphorus removal process called the luxury uptake.

It was further found in the research studies by De Jong *et al.* (1993), that when 1mole of influent P was dosed with one mole of Fe, there was not adequate in reducing the effluent PO4-P concentration to a consent value below 1mg/L but when it was increased to 1.7 mole of Fe/ mol of P, the effluent concentration reduced to a lower consent value of < 1mg/L. On the other hand, it was discovered from further investigation by De Jong *et al.* (1993), but in this case lime was examined and it was found that the influent phosphorus concentration was not a function of the influent phosphorus concentration but a function of the pH of the reactor.

Figure 2.40. Chemical phosphorus removal (CPR): Simultaneous precipitation (Haandel and Lubbe 2012)

The suggested pH boundary for reduction of effluent phosphorus concentration to a consent value of < 2mg/L will be achieved at a pH between 8.5 to 8.7, however if the target effluent phosphorus concentration is < 1mg/L then the required pH of the reactor should be 9.0. Further still, De Jong *et al.* (1993) commented that a lime dosing rate of 150-350g Ca $(\mathrm{OH})_2$ will account for 20-50% excess sludge generation. Subsequently, Table 2.4 showed the impact of simultaneous precipitation on sludge behaviour.

Table 2.4: showed the impact of simultaneous precipitation on sludge behaviour (Haandel and Lubbe 2012)

Behaviour	Impact of simultaneous precipitation on sludge behaviour
Settling	➢ Improved sludge settleability, DSVI decreases ➢ Al salt settleability better than Fe salt: reduction levels of 120-140ml/g TSS< 100ml/g TSS was observed in Dutch wastewater plant ➢ Lime result in a SVI < 50%
Thickening	➢ Metal salt has no significant impact ➢ Lime has a significant impact in an increasing range of 5-7% dry solids
Dewatering	➢ Metal salt has no significant impact ➢ Lime has a significant impact in an increasing range of 2-7% dry solids

2.1.7.3.2.3 Post-precipitation

According to Haandel and Lubbe (2012), this approach (Figure 2.41) is feasible for a situation where the required effluent phosphorus values are low and an effluent polishing stage is required. The challenge with this option of precipitation was that the additional capital cost incurred compared to other options would be higher as an additional unit operation for example a mixing tank will be required.

Figure 2.41. Chemical phosphorus removal (CPR)-Post precipitation (Haandel and Lubbe 2012)

This is not relevant at present but has potential when the effluent discharge consent becomes stricter. Further research comment from Gray (2004); saw it as an effective means of phosphorus removal as the coagulant are added after the secondary treatment. In this secondary stage, virtually all the phosphorus present must have been hydrolysed to orthophosphate which makes removal quite easy. However, a part of the chemical floc was reported to be returned to the aeration tank along with the return activated sludge which causes the mixed liquor to increase in its inorganic content. This will mean an additional increase in the MLSS to maintain the BOD removal process. The issue of the chemical flocs returning with the RAS can be avoided but will mean dosing after the FST. However, additional capital cost will be required because an additional mixing tank for coagulant will be necessary. This further confirms post –precipitation as a complex process.

2.1.7.3.2.4 Side-stream precipitation

As stated earlier, that the configuration for side stream phosphorus precipitation can be viewed from two perspectives namely; precipitation of phosphorus in return streams from sludge treatment and variation of the biological phosphorus removal process by concentrating phosphorus into a side stream system where chemical precipitation occurs.

(i) Precipitation of phosphorus in return stream from sludge treatment

It was reported by Haandel and Lubbe 2012 that though biological phosphorus removal has some merits above the chemical phosphorus removal (CPR), one of the key demerits was the identified discharge of the accumulated poly-P Phosphate from the biological phosphorus activated sludge flocs during sludge treatment and the recirculation of phosphate (V) $(PO4^{3-})$ back to the activated sludge process. In contrast, the release of phosphate does not happen with chemical precipitated phosphate. However, during dewatering, thickening and anaerobic digestion process (sludge treatment), phosphates are released to the liquid surface of the process. Consequently, it was reported that gravitational thickening of sludge with a hydraulic retention time of 1day has the capacity to account for about 50% of all the phosphate. More so due to the presence of easily biodegradable COD within the primary sludge, thickening of surplus activated sludge will achieve an increased phosphate release. The sludge digestion process on the contrary will cause all the polyphosphate in the digested sludge to be degraded to orthophosphate but the precipitated phosphate using chemicals like coagulants will not be released in the liquid phase during digestion. Also, when both the thickened and digested sludge is dewatered, it was observed that all the phosphate in the liquid phase was recovered back and returned to the ASP. Furthermore, during digestion, the Mg^{2+}will be precipitated with the $PO4^{3-}$ as $Mg_2(PO4)_3$ while if ammonium is present it will be precipitated as struvite.

(ii) Supplementary Side-stream phosphorus removal

This requires the use of the luxury phosphorus uptake approach where the phosphorus realised from the main biological excess phosphorus removal (BEPR) is removed and concentrated in a small side stream and removed by chemical coagulant treatment (Haandel and Lubbe 2012). In Figure 2.42, mixed liquor was taken from the aerobic zone and directed to an anaerobic phosphate stripper where a carbon source ethanoate was added to release the stored polyphosphate.

Figure 2.42. Chemical phosphorus removal (CPR): Side-stream precipitation (Haandel and Lubbe 2012)

Immediately the solid and liquid separation was completed the sludge was then returned to the first anoxic or anaerobic zone since a low nitrate level was noticed because of the added carbon source. The supernatant was equally transferred to a thickener to be thickened. It was observed that in both cases the unit operations were dosed with coagulant like lime, ferric and alum respectively. This was to precipitate the phosphate. The merit of this process of supplementary side stream was that chemical phosphorus removal did not affect the biological phosphorus removal process. In contrast, the demerit was that extra running cost would be incurred because of an external carbon source. This process can accommodate all the process used for post – precipitation approach.

2.2 Activated Sludge Digestibility

Over the twentieth and into the twenty first century, fossil fuel has contributed to the economic, social and political trends in the world. Although, energy crisis was reported due to increasing population demand for this non-renewable resource and some political impact linked to the exploitation of the fossil fuel in the energy exporting countries of the world (Fehrenbach *et al.* 2008; BP Statistical Review of World Energy 2014). There is a need to explore sustainable cleaner energy resource due to the dwindling trend of the fossil fuel as the fossil fuel already contributes to issues of greenhouse gas (GHG) emission resulting in enhanced global warming issues (Zhang *et al.* 2015b). Bioenergy has been reported as the fourth largest energy resource available globally and a GHG replacement for fossil fuel due to its renewable energy capabilities (Chen and Lee 2014; Haberl *et al.* 2012). Methane production from anaerobic digestion process (ADP) as an attractive and potential method to obtain renewable biofuel due to its great environmental, societal, and economic merits (Chynoweth *et al.* 2011). Europe has been reported to convert a range of feedstocks into biogas and ultimately bioelectricity, bioheat or transport fuel. This has risen largely in reaction to energy-related subsidies paid to anaerobic digester operators, such as feed-in-tariffs (FITs) paid for bioelectricity and the Renewable Heat Incentive (RHI) paid for bioheat (Styles *et al.* 2016; OFGEM 2014). The need to meet the 2020 bioenergy renewable target becomes a necessity in this research on the impact of chemical dosing (Al and Fe) on biogas production from digested activated sludge. On the contrary, untreated organic content from different origins ranging from agriculture, industrial and urban sources accounts for environmental degradation due to decomposition of untreated organic waste compounds resulting in land, water and air pollution issues. This has led to legislative enforcement towards the cut down in the concentration of organic waste material infiltrating into the landfills. However, the huge generation of waste activated sludge (WAS) is fast becoming one of the most serious environmental challenges facing our world (Feng *et al.* 2014). WAS anaerobic digestion (AD) has gathered much responsiveness lately (Jang *et al.* 2014; Zhen *et al.* 2013; Zhen *et al.* 2014a) due to sludge stabilization, odour control (Appels *et al.* 2008) and bioenergy recovery (Luostarinen *et al.* 2009) achievable in WWTP. The biological degradation of organic substrates in wastewater has been achieved through anaerobic digestion (AD) process (Zhang *et al.* 2014; Forster 2003).

Anaerobic and aerobic digestion process has been globally used to digest and stabilise the activated sludge before final solid disposal in waste water treatment plant (Metcalf and Eddy 2003; Metcalf and Eddy 1991). Both digestion processes have a major common goal of biologically degrading a significant part of the volatile solids (VS) in the sludge and to reduce the putrescibility of the sludge (Gerardi 2003). Although, aerobic and anaerobic digestion undergo dissimilar microbiological and biochemical reactions, the main distinction is that the latter occur in the absence of molecular oxygen while the former occur in the presence of molecular oxygen and degrades organics into carbon dioxide, water, nitrate and sulphates. Huang *et al.* (2017) and Zheng *et al.* (2017) commented that digested microorganisms in sludge can be consumed during aerobic and anaerobic digestion processes. This will result reduction in the pathogenic infection and sludge stabilization. Whilst, the aerobic digestion finds relevant in small scale pilot WWTPs because of its merits like simplicity of digestion mechanism and low capital cost, there are still some limitations which includes; reduced pathogen inactivation and increased energy cost (Grady *et al.* 1999). Other limitations of the aerobic digestion that makes the AD a more attractive option includes; accelerated sludge production due to increased aerobic growth rate because of the presence of sufficient aeration within the treatment reactors, and the insolubility of some organic matter is another drawback of the aerobic digestion (Christy *et al.* 2014).

In this current study anaerobic digestion is of interest as wide spread of this technology has been provided as an answer to treating organic waste streams (Lettinga 2014; Mata-Alvarez 2003). Also, literatures has provided digester designs, operation and efficiency in addition to limiting factors affecting digestion process have been traced to the nature and origin of the organic waste under investigation (Batstone and Jenson 2011). Ariunbaatar *et al.* (2014), added that the effectiveness of pretreatment methods during anaerobic digestion process depends on the substrate characteristics. The nature and origin of organic waste has been classified into different segments, ranging from sewage sludge, animal manure, energy crops, food industry waste and organic waste from municipal solid waste (Carlsson *et al.* 2012; Mata-Alvarez *et al.* 2014). Although, another key aspect that informs digestion processes is the digester design configuration, but literature has made it clear that this not an issue because anaerobic digestion plants are more streamlined to both continuous stirred tank (CSTR) reactors and up flow anaerobic sludge blanket (UASB) reactors (Girault *et al.* 2012; Chong *et al.* 2012; Mahmoud *et al.* 2003). In this current study, the nature and origin of the organic waste will focus on sewage sludge (activated sludge). Conventional activated sludge process produces a huge quantity of waste sludge (Vorkamp *et al.* 2001; Kayser 2005; Liang *et al.* 2006; Seo *et al.* 2017). The disposal of sludge during treatment of wastewater has been reported as a growing challenge as it accounts for up to 50% of the present running costs of a wastewater treatment plant (WWTP) (Fenxia *et al.* 2014; Appels *et al.* 2008; Baeyens *et al.* 1997). The AD has been identified as a waste to energy technique that will treat solid waste and waste water but activated sludge from WWTP has been reported to contribute to global environmental problem due to huge waste sludge produced and increasing organic and pathogenic content of activated sludge (Ahring 2003). This problem will accelerate if the wasted sludge is not properly treated. Anaerobic digesters (AD) which perform majority of the digestion of organic compounds at the WWTP has been installed and pre-treatment processes have been explored as options to overcome the issue of about 60% of the total operational cost of a WWTP required for sludge treatment and disposal (Seo *et al.* 2017; Zhao and Kugel 1996; Ge *et al.* 2013; Wan *et al.* 2016). The cut down in the carbon dioxide emission and carbon taxes and carbon subsidies on bioenergy makes the AD a more robust technology for waste to energy compared to other bioenergy options (Parawira 2004). Foladori *et al.* (2010) has reported other alternative technologies which entails degrading activated sludge using physico-chemical, thermal and biological methods. It was added that this method degraded the sludge and increased solubility by heat application (Neyens and Baeyens 2003), ozone (Seo *et al.* 2017; Sakai *et al.* 1997; Zhang *et al.* 2009), ultra-sound (Wang *et al.* 2005b; Yang *et al.* 2015), and microwave (Park *et al.* 2004). Other reviews have commented on the importance of optimising the economic viability, of anaerobic digestion plants (biogas yields) and the potential approach of biogas generation namely; pre-treatments, co-digestion, digester configuration and inorganic and organic additive dosing (Carlsson *et al.* 2012; Hii *et al.* 2014; bayane and Guiot 2010; Tyagi and Lo 2011; Montalvo *et al.* 2012; Tada *et al.* 2005; Hendriks and Zeeman 2009, Carrèrea *et al.* 2010).

The purpose of the current study is to optimize the anaerobic digestion process using mesophilic anaerobic and chemical coagulant pre-treatment. It is anticipated that these pre-treatment strategies will improve the hydrolysis of the organic matter in the sludge and increase the efficiency of the organic matter conversion to methane. Also, pathogens in the digested sludge can be totally eradicated during this pre-treatment and digested effluent can meet the legislation obligation on reuse of the digested sludge in agriculture (Vesilind 2000) and production of energy from waste sludge to cut down reliance on energy from fossil fuel and boost environmental benefits of bioenergy globally (Chynoweth *et al.* 2001).

Table 2.5 shows research contribution on benefits of cleaner energy resource- biogas over conventional fossil fuel resources. Appendix C (Table C2) further reveals past research assessment of the impact of CPR (chemical phosphorus removal) on AD and factors that impact on the precision of Iron dosed sludge in laboratory bench scale.

Table 2.5. Biogas Environmental Merit Evaluation

Biogas	Benefits	References
GHG emission reduction	Neutral replacement for fossil fuel	Cuéllar and Webber 2008
Environmental protection	Pathogen reduction through sanitation, air and water pollution reduction and eutrophication and acidification reduction.	Cuéllar and Webber 2008
Green energy production	Electricity, heat and transport fuel	Rehl and Muller 2011
Organic waste disposal	Municipal, industrial, residential waste and agricultural residues	
Biogas linked agrosystem	Livestock biogas fruit system and pig biogas vegetable system	Qi *et al.* 2005; Jiang *et al.* 2011

2.2.1 Environmental and Operational Factors required for Anaerobic Digestion

Anaerobic digestion is known to be a complex process because of the links between different microorganisms which enhance the organic degradation to methane. Therefore, there is a need to maintain anaerobes with a high metabolic action during anaerobic digestion processes in digesters. This makes investigation of specific properties of activated sludge and environmental conditions and operational factors that can limit the anaerobes metabolic activity of paramount interest in this current study. The facultative anaerobes and anaerobes (methane-forming bacteria) are required in an anaerobic digester for hydrolysis of complex organics and metabolic breakdown of volatile fatty acids and methane gas production. Secondary sludge consists of many facultative anaerobes and several particulate and colloidal organics, but primary sludge is made up of merely a lesser quantity of facultative anaerobes that would not adequately replace the bacteria wasted from the digester during routine solids pumping and dewatering operations. The specific properties of activated sludge include; the nature of sludge, composition of complex organics and size distribution; while the environmental conditions include; temperature, alkalinity and pH, and toxicity, nutrient and nutrient concentration, and the operational factors includes; retention time (RT), organic loading rate (OLR), mixing, volatile fatty acid (VFA) and carbon-nitrogen ratio (C/N ratio).

2.2.2 Properties of activated sludge

The specific properties of activated sludge include the primary and secondary sludges or the mixtures of both, for provision of the required substrate for an anaerobic digester. They also provide the anaerobes required for the hydrolysis and metabolic activity of the complex organic compounds and the biochemical methane potential (BMP). As stated in section 2.2.1, that anaerobic digesters need both facultative anaerobes and anaerobes, but literature has reported that methanogenic bacteria are strict anaerobes and experience a faster rate of extinction in the activated sludge process (Mao *et al.* 2015). This makes seeding secondary sludge with primary sludge to enhance the availability of not just facultative anaerobes but methanogenic bacteria in the AD. Gerardi (2003), has suggested ratio of 1:10 of secondary sludge to primary sludge during seeding process in AD. Whilst, primary sludge comprises merely a lower concentration of facultative anaerobes that would not sufficiently interchange the bacteria wasted from the digester during daily solids pumping and dewatering operations. On the other hand, secondary sludge comprises various facultative anaerobes and many particulate and colloidal organics. The seeding process is completed effectively in AD, then the secondary sludge can be fed into the digester without a mixture with the primary sludge.

2.2.2.1 Organic loading rate (OLR)

Known over the decades are anaerobic digesters for degradation of particulate and colloidal waste materials, and hence organic loads (sludge feed) to digesters are typically stated as volatile solids (VS). The number of volatile solids fed into a digester per day under continuous feeding pattern is called OLR (Kondusamy and Kalamdhad 2014). The Designed and recommended loadings for anaerobic digesters that are mixed and heated range from 3.2–7.2kgVS/m^3/day. However, loading rates of 0.5 to 0.6kgVS/m^3/day are typical in WWTP (Gerardi 2003). On the contrary, higher loading rates could be treated once a better concentrated activated sludge could be fed to the digester.

The VS loadings to AD are regulated in the majority of WWTP by the performance of the primary and final sedimentation tanks (PST and FST) in removal and concentrating of primary and secondary sludge. Hence, the thickening capacity of this sludge becomes a vital AD operational factor. Moreover, raw sludges or feed sludges having low solids content (dilute feed sludge) are sometimes transported to municipal anaerobic digesters. They compose of 3–6% solids and constitute a negative impact on AD performance by decreasing hydraulic retention time (HRT), decrease volatile solids destruction, and overall decreasing the methane production.

With higher OLR, the biogas production rises to a degree, but the stability and productivity of the anaerobic digestion process can also be greatly upset. The Addition of a huge volume of new biomass daily may result in variations in the digester's environment and temporarily limits bacterial degradation during the initial fermentation reaction. This bacterial inhibition occurs because excessively high OLR cause a higher hydrolysis/ acidogenesis bacterial metabolism than methanogenesis bacterial activity and hence a much higher VFA production rate, which causes a permanent acidification. If this persists, the pH of the digester reduces, and the hydrolysis process becomes obstructed and restricted methanogenic bacteria are cannot convert as much VFA to methane production. Therefore, literature has provided maximum allowable OLR of 5gVS/L/d in WAS (wasted activated sludge), 9.2kgVS/m3/d in FW (food waste) co-digestion, 10.5kgVS/m3/d in sludge and 9.2gCOD/L/d in OMSR (olive mill sludge residue) (Gou *et al.* 2014; Rincón *et al.* 2008; Kougias *et al.* 2013; Nagao *et al.* 2012). Other reported allowable OLR in the investigation on the step wise increase in OLR and SRT (solid retention time) on integrated two stage process is 22.65 kg VS/m3 d (160 hours) for hydrogen fermentation and 4.61(26.67days) for methane fermentation digester (Nagao *et al.* 2012).

2.2.2.2 Retention time (RT)

The retention time (RT) is the time required to complete the degradation of organic matter. It is linked with the microbial growth rate and a function of the process temperature, OLR and substrate composition (Mao *et al.* 2015). However, two major types of retention time (RT) have been provided in literature namely; SRT (solid retention time), which is the average time that bacteria (solids) occupy in a digester, and HRT (hydraulic retention time) is the time that the wastewater or sludge is in the anaerobic digester and is expressed in Equation 2.64 (Ekama and Wentzel 2008).

$$\mathrm{HRT} = \frac{\mathrm{V}}{\mathrm{Q}} \tag{2.64}$$

Where, V is the biological reactor volume and Q the influent flow rate in time.

The SRT and the HRT are the same for a suspended-growth anaerobic digester that has no recycling. If recycling of solids is integrated in the operation of the digester, then the SRT and HRT may vary significantly. On the contrary anaerobic digesters that uses fixed-film media for bacteria growth favour the formation of concentrated mass (biomass) of bacteria that are attached to the media. The biomass formed inhibits the washout of huge numbers of bacteria and allows high SRT values. An average retention time of 15–30 days is required to treat waste under mesophilic digestion conditions but as earlier mentioned attaining an efficient HRT is subject to substrate composition and OLR (Mao *et al.* 2015). Also, reduction in HRT ordinarily causes VFA accumulation, however, an extended than optimal HRT results in inadequate use of digester contents. Besides, in an algal biomass, an HRT lower than 10 days accounts for the low methane productivity (Kwietniewska and Tys 2014). Therefore, a low OLR and a long HRT are the most benign approach for realising constant and maximum methane production. Figure 2.43 shows how changes in the SRT can disrupt and reduce the performance of anaerobic digester (Nges and Liu 2010).

Figure 2.43. Impact of SRT on AD progress stability and performance (Nges and Liu 2010)

It was reported that an increase in the SRT from 10 to 20 days resulted in a 25% reduction in specific methane gas production during agricultural waste (AWS) digestion (Bolzonella *et al.* 2005). The biogas production obtained at a 12-day SRT was tripled relative to that perceived for a 35-day SRT. Process imbalance occurred because of foaming, VFAs accumulation and increased alkalinity at a 9-day SRT during the digestion of dewatered wastewater sludge (Nges and Liu 2010). Since the time required for a population of methanogenic bacteria to double in size of is reasonably lengthy compared with aerobic bacteria and facultative anaerobic bacteria (Table 2.6), typical SRTs for anaerobic digesters are >12 days. Detention times <10 days are not suggested because substantial washout of methanogenic bacteria happens. This shows that SRT and not HRT is the more important retention time. The SRT is not seriously affected by the type of the wastewater or biomass sludge under treatment unless the wastewater or biomass sludge is toxic to the bacteria (Gerardi 2003).

The research studies on the investigation of the effects of stepwise increase in OLR and SRT on integrated two-stage process reported that at steady state, the optimal SRT was found to be 160 hours for hydrogen fermentation reactor and 26.67 days for methane fermentation reactor (Nagao *et al.* 2012; Gerardi 2003). High SRT values are beneficial for anaerobic digesters. High SRT values maximize removal capacity, reduce required digester volume, and provide buffering capacity for protection against the effects of shock loadings and toxic compounds in wastewaters and sludges.

Table 2.6. Estimated SRT for vital groups of wastewater bacteria (Geradi 2003)

2.2.2.3 Temperature

Romero-Güiza *et al.* (2016) commented that temperature remains one of the most vital process parameters that impacts on both the efficiency and stability of the anaerobic digestion process. Lettinga *et al.* (1999) added that AD can occur at all temperatures ranging from mesophilic, thermophilic and cryophilic conditions. Angelidaki *et al.* (1999); Angelidaki and Ahring (1994); Buhr and Andrew (1977) mentioned that in thermophilic boundary condition with greater than 45 °C, optimisation of the performance of AD occurred due to higher solubility of organic compounds, higher chemical and biochemical reaction rates, lower gas solubility in the liquid, lower liquid viscosity, higher pathogen deactivation and less odour emission. The impact of temperature can be studied from the microbial metabolic processes, gas transfer rate and settling behaviour within the anaerobic digesters. Angelidaki and Ahring (1993; 1992) on the other hand added that rises in temperature will increase the inhibitory impact of ammonia and VFA by increasing and reducing their negative base-10 logarithm of the acid dissociation constant (K_a) of the solution (pka). However, less sensitivity to inhibitors and stable process performance in AD was also considered as an advantage of mesophilic AD over thermophilic (Kim *et al.* 2006). Metcalf and Eddy (2003) further added that temperature fluctuation can affect hydrolytic bacteria required to promote degradation of complex organics into simple soluble substances, but hydrolytic bacteria are not as sensitive to temperature change as the acetate-forming bacteria and methane-forming bacteria. The methanogenic bacteria is not an exception in terms of temperature variations as they cannot thrive outside a temperature range of 1^{O}C/d but was also reported that acidogenesis depends on optimum temperature and any variation will result in VFA accumulation which affects the stability of the AD process. Temperature impacts not only methane-forming bacteria but also volatile acid-forming bacteria. Thus, variations in temperature may be a merit to some groups and demerit to other groups. For example, a 10°C temperature rise can hinder methane production or methane-forming bacterial metabolism within 12 hours, whereas the volatile acid production increases (Gerardi 2003). These variations in the activity of different groups of volatile acid-forming bacteria result in fluctuations in the relative concentrations of organic acids and alcohols generated during fermentation process which impacts on the overall digester efficiency. This is attributed to the fact that methanogenic bacteria will utilise these organic acids and alcohols concentrations as substrate during methane production within the anaerobic digesters.

Westerholm *et al.* (2012) reported on the effect of temperature in co-digestion of whole stillage and cattle manure and discovered a high methane production in both mesophilic and thermophilic temperature boundaries; Sanchez *et al.* (2005) also affirmed that AD processes investigated under mesophilic condition were more stable compared to that observed under an ambient temperature condition. The general frequent challenges connected with AD are loss of heating ability and maintenance of optimum anaerobic digester temperature. An acceptable and uniform temperature must be sustained throughout the AD to avoid confined compartments of decreasing temperature and unwanted bacterial degradation. Adequate mixing of the digester content prevents the development of restricted temperature variation. Variations in temperature of even a few degrees affect almost all biological activity including the inhibition of some anaerobic bacteria, especially methane-forming bacteria. The environmental temperature has a major effect on the anaerobic microbial reactor, which impacts the metabolic rate, ionization equilibrium, substrate solubility and fats and bioavailability of iron (Speece 1996).

Most methane-forming bacteria are active in two temperature ranges. These ranges are the mesophilic range from 30 to 35°C and the thermophilic range from 50 to 60°C (Ahn and Forster 2002). At temperatures between 40°C and 50°C, methane-forming bacteria are inhibited (Mao *et al.* 2015). Digester performance abates somewhere near 42°C, as this represents the transition from mesophilic to thermophilic organisms (Gerardi 2003). Although methane production can occur over a wide range of temperatures (Figure 2.44), anaerobic digestion of sludge and methane production at municipal wastewater treatment plants is performed in the mesophilic range, with an optimum temperature of approximately 35°C (Table 2.7).

Figure 2.44. Methane production over relatively large temperature values (most AD in WWTP operates in mesophilic range of temperature) (Gerardi 2003)

Table 2.7. Temperature range for methane production for municipal anaerobic digesters (Gerardi 2003)

Temperature, ℃	**Methane Production**
35	Optimum
32-34	Minimum
21-31	Little, “digester going sour”
< 21	Nil, “digester is sour”

Whenever digester temperature falls below 32°C, attention should be given to the volatile acid-to-alkalinity ratio. Volatile acid formation continues at decreased temperatures, but methane production proceeds slowly. The sludge retention time (SRT) is usually long, often greater than 12 weeks because of the observed depressed temperatures. Volatile acid production can continue at a rapid rate as low as 21°C, whereas methane production is essentially non-existent. Therefore, 32°C is the minimum temperature that should be maintained, and 35°C is the preferred temperature (Kondusamy and Kalamdhad 2014). While methanogenic bacteria are dynamic and grow in numerous temperature ranges (Table 2.8), most methane-forming bacteria are mesophiles and others are psychrophiles, thermophiles, and hyperthermophiles. The thermophilic range is usually performed at industrial wastewater treatment plants that can heat wastewaters or sludges.

Table 2.8. Optimum Temperature Ranges for the Growth of Methane –Forming Bacteria (Gerardi 2003)

Bacterial Group	**Temperature Range, ℃**
Psychrophiles	5-25
Mesophiles	30-35
Thermophiles	50-60
Hyperthermophiles	>65

An evaluation of advantages and disadvantages of mesophilic and thermophilic digesters is presented in Table 2.9

Table 2.9. Comparison of Mesophilic and Thermophilic Digesters (Mao *et al.* 2015; Gerardi 2003)

Parameters	**Mesophilic Digester**	**Thermophilic Digester**
Loading rates	Lower	Higher
Destruction of pathogens	Lower	Higher
Sensitivity to toxicants	Lower	Higher
Operational cost	Lower	Higher
Temperature control	Less difficult	More difficult
Load bearing capacity	Lower	Higher
Productivity	Lower	Higher

Nonetheless, the increased destruction of pathogens by thermophilic digesters has been linked to their relevance in meeting the present and future regulations for the disposal and reuse of municipal sludges. The rate of anaerobic digestion of activated sludge and methane production is proportional to digester temperature (Gerardi 2003). This implies that increased temperature will result in a higher rate of volatile solids destruction and methane generation. The rate of anaerobic digestion of sludge and methane production is considerably faster in thermophilic digesters than in mesophilic digesters (Mao *et al.* 2015). Therefore, variations in digester temperature should be as small as possible, that is, <1°C per day for thermophiles and 2–3°C per day for mesophiles.

The Equation 2.65 and 2.66 shows the reaction rate dependency of biological processes to temperature and Arrhenius expression on the temperature dependency of the reaction (Riffat 2012; Kadlec and Wallace 2008).

$$K_{T} = K_{20}\theta^{(T-20)} \tag{2.65}$$

$$K = Ae\frac{-E_a}{RT} \tag{2.66}$$

Where, K_T = reaction rate constant at temperature (T) in Molarity(M) per unit time (seconds) (i.e M/s), K_{20} = reaction rate constant at 20^{O}C (M/s), θ = temperature activity coefficient **(**a factor used in thermodynamics to account for deviations from ideal behaviour in a mixture of chemical substances and it is a unitless thermodynamic function), A = pre-exponential factor (identical to those of the rate constant and will vary depending on the order of the reaction but, for first order it has the unit: s^{-1}), E_a = activation energy in Kilojoules (KJ) per mole (mol) of reactant (i.e KJ/mol), R = universal gas constant in Joules (J) per unit moles(mol) per unit kelvin (K) (i.e J/molK) and T = temperature (degree celcius- ^{O}C or Kelvin-K).

Typical values for universal gas constant(R) is 8.3145 J/molK. The rate of a reaction is measured in terms of how fast the concentration of one of the reactants is falling (mol dm^{-3} s^{-1}). The typical values for rate constant (k) is 5 x 10^{9} when the reaction is very fast and k = 1 x 10^{-10} when it is very slow. The Arrhenius function is known to explain the impact of temperature to the optimum growth rate of bacteria on substrates during wastewater treatment process. Aisami et al. (2017), has reported range of Arrhenius activated energy (E_a) values of between 57.9 to 67.5 KJmol/L. However, the pseudo first-order pre-exponential factors for various rate limiting steps reaction has been reported to include adsorption (10^{2} –10^{4} sec^{-1}), diffusion (10^{7}–10^{11} sec^{-1}), surface reaction (10-10^{13} sec^{-1}) and desorption (10^{13}–10^{16} sec^{-1}) (Baetzold and Somorjai 1976). Temperature affects most biological activities (Gerardi 2003). This effect is due mostly to the impact of temperature on enzymatic activity or reactions. Therefore, increases in temperature result in more enzymatic activity whereas reductions in temperature result in a reduced amount of enzymatic activity. Because of the impact of temperature on enzymatic activity, SRT within digesters should increase with reducing temperatures.

Although anaerobic bacteria can be acclimated to operating temperatures outside their optimum range, biomass activity and digester efficiency may be negatively affected. Because methanogenic bacteria grow slowly and are very sensitive to small changes in temperature, acclimation must advance very slowly (Kondusamy and Kalamdhad 2014; Gerardi 2003). Elevated temperature affects the activity of hydrogenotropic methanogens in the anaerobic process and enriches hydrogen producing bacteria and spore forming bacteria. The optimum temperature for anaerobic digestion is represented in Table 2.10.

Table 2.10. Optimum Conditions required for anaerobes metabolic activity (Kondusamy and Kalamdhad 2014)

Features	**Optimum conditions**	**References**
Temperature	Mesophilic range (35-40℃) and Thermophilic range (50-55℃)	Van Haandel and Lettinga (1994); Arsova (2010)
pH	6.3-7.8	Wang *et al.* (2012)
Carbon-nitrogen ratio	23-30	Ghosh and Pohland (1974)
Volatile fatty acid	2000-3000mg/L	Eastman and Ferguson (1981)
Organic loading rate (OLR) and nutrient concentration	Varies according to the substrate and inoculum	Kondusamy and Kalamdhad 2014

2.2.2.4 Nutrients

Nutrients are required for bacterial growth in aerobic and anaerobic biological treatment processes. These nutrients are classed as macronutrients and micronutrients. There exist differences in the nutrient requirement in the aerobic and anaerobic treatment processes. This is because of the peculiar nutrient demand in methanogenic bacteria and fermentative bacteria during the anaerobic digestion process as compared to aerobic bacteria in aerobic biological treatment process like the activated sludge process. Example of these macronutrients required in large quantities by bacteria includes; nitrogen and phosphorus (Gerardi 2003). Merchant and Helmann (2012), also added that metal nutrients can be categorised according to their various amount in the bacterial cells as major cations namely; K, Mg and Ca and micronutrients which includes manganese (Mn), iron (Fe), cobalt (Co), copper (Cu), molybdenum (Mo), nickel (Ni), selenium (Se) and tungsten (W). Other researchers contributed that trace metals required in smaller quantity (micronutrients) by most bacteria especially during the conversion of acetic acid to methane (rate limiting factor in anaerobic digestion process) are iron, cobalt, and nickel (Oleszkiewicz and Sharma 1990; Fermoso *et al.* 2009; Demirel and Scherer 2011; Schattauer *et al.* 2011; Zhang *et al.* 2012). Williams and Fraústo da Silva (2000) reported Metal concentration in the cells range from 10^{-7} to 10^{-3} molar in major cations (K, Mg and Ca) while 10^{-6} to 10^{-15} molar was mentioned in micronutrients like Mn, Fe, Co, Cu, Mo, Ni, Se and W. Romero-Güiza *et al.* (2016) also added that not only does nutrient supplement dosing impacts methane production but improves process stability. Nges and Björnsson (2012); Gerardi (2003); Zhang and Jahng (2011) stated that process stability in AD can ensure that pH is kept at required optimum values through reduction in volatile fatty acid accumulation and alkalinity levels. Macro nutrients (P, N and S) have been reported as a vital buffering agent to ensure process stability by avoiding rapid change in the pH level (Schattauer *et al.* 2011; Lo *et al.* 2012). Moreover, micro nutrients serve the purpose of co-factors in enzymatic reactions responsible for methane production as explained in review by Schattauer *et al.* (2011) and Lo *et al.* (2012), but Lo *et al.* (2012) reported that excessive concentrations of macro and micro nutrient will result in inhibition of the AD process.

The importance of some of the micro and macronutrients has been mentioned in literature ranging from Fe used in the transport system of the methane forming bacteria for the conversion of carbondioxde to methane and as a binding factor in sulphide precipitation in anaerobic digesters which helps in controlling the concentration of hydrogen sulphide in biogas production in the AD (Vintiloiu *et al.* 2013; Gustavsson *et al.* 2013a); Cobalt (Co) also serve as a binding agent to sensitive coenzyme required in speeding up the methane production in both acetoclastic methanogenic and hydrogenotrophic bacteria during methanogenesis and hydrolytic anaerobic digestion stages (Schonheit *et al.* 1979; Kida *et al.* 2001); Mn serve as electron acceptor in anaerobic respiration processes (Langenhoff *et al.* 1997); Zn acts as activator of enzymes involved in methanogenesis such as coenzyme M methyltransferase (Sauer and Thauer 2000) and Zn, Cu, and Ni have all been equally present in a single hydrogenase (Jarrell and Kalmokoff 1988); also, the F430 enzyme in methane-forming bacteria contains nickel and the addition of nickel can increase acetate consumption rate of methane-forming bacteria; while trace metal like W and Mo are were present in enzymes such as formate dehydrogenase (FDH), which catalyses formate production by propionate oxidizers (Dong *et al.* 1994; Fermoso *et al.* 2009; Banks *et al.* 2012). Literature has also provided that the concentration of N and P in the digester can be estimated from the COD of the feed sludge in the anaerobic digester and COD: N: P of 1000:7:1 and 350:7:1 have been reported for high-strength wastes and low loadings and C/N value of at least 25:1 has been proposed for optimal gas production (Gerardi 2003). Raposo *et al.* (2011) stated that trace inorganic elements such as iron, nickel, cobalt, and zinc must be in desired concentrations to initiate the digestion process. Also, because wastes generated vary in their nutrient content concentration, therefore effective operation of AD will require not just correct concentration of inorganic elements present as supplements but also the AD design capacity and the nature of the wasted activated sludge (WAS).

Experimental study revealed that a shortage in nutrient (< 0.1mg Ni^{2+}/kg and < Co^{2+}/kg in wet basis) at an organic loading rate (OLR) of greater than 2.6g total solids per litre per day, did not optimise methane production from digested maize silage under a mesophilic condition. However, an increase in the Ni and Co content between 0.6 and 0.05mg/kg, at an OLR of about 4.3gTS/l/d was found to optimise the methane production by stabilising the digester efficiency (Pobeheim *et al.* 2011). The impact of Fe, Co and Ni, on methanol Upflow anaerobic sludge blanket (UASB) reactor was evaluated (Zandvoort *et al.* 2003) and methane production rate increased from 156mg/CH_4CODg/VSS/d to 1291156mg/CH_4 CODg/VSS/d. Further studies, on the impact of Fe powder on rusty scrap in wasted activated sludge (WAS) was conducted and result revealed improved methane production with all Fe added (Zhang *et al.* 2014). Appendix C (Table C1) further reveals past research assessment of the impact of stimulatory and inhibitory concentrations of metals on anaerobic biomass and their role in methanogenesis.

2.2.2.5 Volatile fatty acid (VFA)

The various amount of VFA within an anaerobic digestion process have demonstrated significant impact on different stages of anaerobic digestion (AD); the hydrolysis, acidogenesis and biogas production (Schamber *et al.* 2005). Siegert and Bank (2005) stated that apart from pH, VFA of the reactor hinders the cellulolytic activity at concentrations ≥2 g/L. It was further added that the rate of cellulose hydrolysis and the glucose fermentation is also affected above 4 g/L thereby having inhibitory effects on the production of biogas. It was observed from this investigation that CH_4 to CO_2 ratio gives much difference above 6 g/L VFA if cellulose and glucose is used as major source. Komisar *et al.* (1998), added that co-digestion of cellulose waste material with paper as primary substrate, biogas production was reduced more than a half due to 1 g/L initial VFA, showing inhibition of the hydrolysis process. It was further concluded that glucose as primary substrate biogas production was more than halved when VFA was above 8 g/L which indicated that the digestion process was less sensitive to inhibition by VFA. The build-up of VFA caused in unstable microbial groups, which led to collapse of the anaerobic digestion in the anaerobic digestion reactor (Vijayaghavan *et al.* 2012; Labatut *et al.* 2011).

2.2.2.6 Carbon-Nitrogen (C/N) Ratio

Nitrogen is the foremost nutrient for the development of microorganisms and the concentration of nitrogen uptake by the aerobic and anaerobic bacteria differs in relation to their nature. The C/N ratio explains the nutrient levels of a digestion substrate in ADP and as such digestion systems are sensitive to C/N ratio. A high C/N ratio causes a low protein solubilisation rate and leads to low total ammonia nitrogen and free ammonia concentrations within AD (Zhang *et al.* 2013). Thus, ammonia hindrances may be avoided by optimizing the C/N ratio in the AD process. However, an excessively high C/N ratio provides inadequate nitrogen to sustain cell biomass and leads to fast nitrogen degradation by microorganism, resulting in lower biogas production but for solid wastes with a high C/N ratio, the ammonia inhibition effect can be controlled by dilution with water, because of its reductions in the concentration of ammonia toxicity (Punal *et al.* 2000). Substrates with an extremely low C/N ratio increase the risk of ammonia obstruction, which is toxic to methanogenic bacteria responsible for biogas production and causes inadequate use of carbon sources. Microorganisms in anaerobic digestion use the carbon 25–35 times higher than nitrogen and hence optimal digestion, the ratio of the carbon to nitrogen should be about 25–30:1 in the substrate (Kondusamy and Kalamdhad 2014; Yen and Brune 2007). The concentrations of carbon and nitrogen indicate the performance of the anaerobic digestion process (Yen and Brune 2007). Whereas carbon acts as the energy source of the micro- organisms and nitrogen plays a role in enhancing the microbial population. Nitrogen can be used in two ways by the microorganisms in anaerobic digestion such as absorption where nitrate as an electron acceptor is converted to nitrogen gas (denitrification) and reduction reactions where nitrate has been converted to ammonia (ammonification) (Mao *et al.* 2015). Therefore, increased nitrate leads to ammonification while reduced nitrate leads to nitrogen deficiency. This makes nitrogen a key controlling factor for microbial population in AD and major limiting nutrient in treatment of municipal solid waste, since low nitrogen content will mean less microbial population which increases the duration to degrade the available organics.

2.2.2.7 Mixing

Mixing increases the efficiency of the digestion process by ensuring a good spread of bacteria, substrate, and nutrients with proper temperature equalization in the anaerobic digestion unit. The degradation activities of acetogenic bacteria and methanogenic bacteria in the anaerobic digester usually depends on the proximity of the bacteria. The slow and gentle mixing provides for efficient hydrolysis of wastes and production of organic acids and alcohols by acidogenic bacteria (Gerardi 2003). The Mixing action can be achieved either through mechanical means or gas recirculation. These methods comprise of external pumps, gas injection or recirculation from the floor or roof of the digester, propellers or turbines, and draft tubes. On one hand, the mechanical mixers are more effective than gas recirculation, but on the other hand can become blocked or polluted with digester solids. The Figure 2.45 and 2.46 shows two mixing styles with the former involving heating with limited mixing through the recycling of sludge in a heat exchanger called an intermediate style and the latter as a rapid style involving heating and complete mixing with significant volatile solids destruction achieved.

Figure 2.45. Intermediate style of mixing (Gerardi 2003)

Figure 2.46. Rapid (high rate) mixing style (Gerardi 2003)

The mixing regime must equally be continuous to achieve significant volatile solid destruction but is cost challenging and potential washout of methanogenic bacteria during rapid mixing is pertinent and affects the desired retention time in the digesters. However, Gerardi (2003) reported a better approach of a routine mixing of digester content with three to six periods of mixing per day of 1 to 3-hour duration for each mixing period.

2.2.2.8 Alkalinity and pH

The pH of the digester affects the ADP and the performance of the anaerobic digestion mechanism. It has been stated in literature that methanogenic bacteria thrive within pH range of 6.5–8.2 and optimum pH 7.0 which ensures that satisfactory buffering capacity (alkalinity) is present to neutralize the organic acids within the AD (Lee *et al.* 2009; Eastman and Ferguson 1981; Sosnowski *et al.* 2002). Also confirmed is the optimal range of pH for attaining maximal biogas production in AD within the range of 6.5–7.5. It was added that the pH range is relatively comprehensive in activated sludge plants and the optimal value of pH varies with substrate and digestion procedure (Liu 2008). The growth rate of methanogenic bacteria significantly reduced at pH below 6.6, and the metabolic activity of methanogenic bacteria decreased at a greater or lesser pH (Zhang *et al.* 2009). Fang and Liu (2002), added that significant abundance of microbial species has been noticed to increase from 6 at pH 4.0 to 14 at pH 7.0. The optimum pH of acidogenesis was between pH 5.5 and 6.5 (Kim *et al.* 2003) and this explain why the two-stage AD process separating the hydrolysis/acidification and acetogenesis/methanogenesis processes is the preferred mode of operation. The pH changes due to process parameters for example volatile fatty acid (VFA), bicarbonate concentration, and alkalinity of the AD and by fraction of carbondioxide (CO_2) produced during the AD process. In sustaining a constant pH value, it is essential to control the association between the VFA and bicarbonate concentrations (Zhang *et al.* 2011). But in regulating the pH, sodium bicarbonate (NaHCO3) and sodium hydroxide (NaOH) were added in the continuous reactor during initial anaerobic digestion period and suggested as a potential strategy (Goel *et al.* 2003). In Figure 2.47, the pH has been reported as a limiting factor in the VFA composition (Fang and Liu 2002). Subsequent studies were conducted and pH level of 6.0 was provided and a resultant hydrolytic enzyme degradation was the highest with a corresponding highest VFA concentration, soluble chemical oxygen demand (SCOD) concentration and VFA/SCOD ratio and the lowest VS levels (Jiang *et al.* 2011). Further research studies showed a positive correlation (P = 0.01) between hydrolysis and pH (Zhang *et al.* 2009).

Figure 2.47. Volatile fatty acid composition based on carbon basis affected by pH (Fang and Liu 2002).

Numerous chemicals (Anhydrous ammonia, hydrated lime, quick lime, caustic soda, sodium ash and sodium bicarbonate) can be added to an AD to maintain adequate pH and alkalinity. The selection of choice of chemical is a function of some factors like handling, cost, safety, storage, and requirements for feeding the chemical to the digester. However, if the pH within the AD is greater than the optimum range, ammonia toxicity may happen. Ammonia in the digester may be in the form of ammonium ions (ionized ammonia-NH_4+) or dissolved ammonia gas (non-ionized ammonia-NH_3). As soon as, AD pH is 7.2 or less, the existence of NH_4+ is preferred. When the digester pH is greater than 7.2, the presence of NH_3 is favoured. However, the dissolved ammonia gas is toxic to bacteria, especially methane forming bacteria responsible for production of biogas. Ammonia toxicity can be reduced if the digester pH is maintained within the optimum range of 6.8 to 7.2 and the ammonia-nitrogen concentration does not rise into the range of 1500 to 3000 mg/l (Gerardi 2003). Another challenge attributed to increased ammonia-nitrogen or alkalinity is foam and scum production which is usually observed at the initial stage of anaerobic digestion process. In an anaerobic digester, if the feed sludge to the anaerobic digester does not contain alkali compounds or precursors of alkali compounds, alkalinity must be added to the digester to maintain stable and acceptable values for alkalinity and pH. The amount of alkalinity to be added may be dependent on organic acid production volume of the sludge feed (1 g of volatile acids per gram of volatile solids). Examples of chemicals used for addition of alkalinity include; sodium carbonate, potassium carbonate, sodium carbonate (soda ash), calcium carbonate (lime), calcium hydroxide (quick lime) and anhydrous ammonia gas.

Other impact of pH can be explored from its effect on trace metal speciation in AD. Researchers have concluded that medium pH can impact solution phase metal concentration. Trace metals with high pH have the capacity to form insoluble metal phosphates and carbonates (Rensing and Maier 2003), but on the contrary Zandvoort *et al.* (2005) and Gonzalez-Gil *et al.* (2012) has further added that at low pH the initial discharge of metals takes place with increased solubility for metal bioavailability.

2.2.3 Anaerobic Digestion Stages

The anaerobic digestion process and production of biogas is divided into three stages. The stages are used to show the categorization of microbial process that occur during the anaerobic digestion process (ADP) and the production of methane and carbodioxide called biogas for continuous power generation (Mao *et al.* 2015; Christy *et al.* 2014; Lyberatos and Skiadas 1999; Gerardi 2003). Figure 2.48 shows typical ideal anaerobic digestion process in a WWTP.

Figure 2.48. Three stages in anaerobic digestion process (Gerardi 2003)

Step 1-Hydrolysis

In the Anaerobic digester complex, insoluble organic compounds such as proteins, polysaccharides and fats that compose the cellular mass of the microorganisms are converted into simplistic organic and inorganic compounds (peptides, saccharides and fatty acids) that are soluble in water by hydrolytic microorganisms like clostridia, fusobacterium, selenomonas and streptococcus) (Kondusamy and Kalamdhad 2014; Noike *et al.* 1985). The slow hydrolysis and solubilisation reaction is conducted by exo-enzymes secreted by obligate or facultative fermentative bacteria, which is a key limiting factor in the rate of anaerobic digestion process (Mata-Alvarez *et al.* 2000; Kaseng *et al.* 1992). The exo-enzymes (cellulase, lipase, amylase, protease, glycosidase and esterase) during the hydrolytic reaction converts polymers into soluble monomers by breaking the chemical bonds joining the large insoluble molecules consisting of many small molecules called polymeric substances. The lipases hydrolyse the ester bonds of lipids to produce fatty acid and glycerol, while protease hydrolyses the protein to amino acids and amylase converts carbohydrate to simple sugar (Cirne *et al.* 2007; Lai *et al.* 2001). Cellulose is an insoluble starch that is usually present in primary and secondary urban wastewater sludges. Cellulose may make up approximately 15% of the dry weight of the sludges (Gerardi 2003). Cellulose consists of many sugar units of glucose ($C_6 H_{12} O_6$) joined together by chemical bonds. However, glucose is soluble in water, but the linkages of many units of glucose together by chemical bonds cause the formation of insoluble polymer cellulose. The Equation 2.67 shows the hydrolytic reaction in which exo-enzymes catalyses the complex organic molecules into simplistic organic and inorganic compound, while Equation 2.68 shows many molecules of glucose formed when cellulose is hydrolysed (Mata-Alvarez *et al.* 2003; Gerardi 2003). Hydrolysis of cellulose by the enzyme complex cellulase yield glucose, hemicellulose degradation results in monosaccharide- ides such as xylose, glucose, galactose, arabinose and mannose.

$$\mathrm{C_6H_{10}O_4 + 2H_2O \rightarrow C_6H_{12}O_6 + 2H_2} \tag{2.67}$$

$$\mathrm{(C_6H_{12}O_6 + 2H_2O)_n \rightarrow nC_6H_{12}O_6} \tag{2.68}$$

Step 2- Acid forming (Acidogenesis)

In the acid-forming step, Hydrolytic and acidogenic microorganisms are growing about ten times faster than methanogens. The soluble compounds generated through hydrolysis and released to the anaerobic digester are degraded by numerous facultative anaerobes and anaerobes through many fermentative reactions. Acidification is known to be the quickest reaction in the anaerobic conversion of complex organic matter in liquid phase digestion (Christy *et al.* 2014; Mosey and Fernandes 1989). The degradation of these compounds during acidogenesis results in the production of carbon dioxide, hydrogen gas, alcohols (butanol, ethanol, propanol, and methanol), organic acids (acetic, propionic and butyric), some organic-nitrogen compounds, and some organic-sulphur compounds (Kalyuzhhnyi *et al.* 2000; Gujer and Zehnder 1983). However, the most vital reported in literature of the organic acids is acetate (Gerardi 2003). Equation 2.69-2.71 shows the typical acidification reactions. However, in Equation 2.69, glucose is transformed to ethanol and further conversion produced propionate (Equation 2.70) and finally in Equation 2.71, acetic acid was produced.

$$C_6H_{12}O_6 \xleftrightarrow{\text{Acid Forming Bacteria}} CH_3CH_2OH + 2CO_2 \tag{2.69}$$

$$C_6H_{12}O_6 + 2H_2 \xleftrightarrow{\text{Acid Forming Bacteria}} CH_3CHOOH + 2H_2O \tag{2.70}$$

$$C_6H_{12}O_6 \xleftrightarrow{\text{Acid Forming Bacteria}} CH_3COOH \tag{2.71}$$

The pH of 4.5 to 5.5 is beneficial environment for acidogenic and acetogenic bacteria to thrive during anaerobic digestion (Christy *et al.* 2014). The Acetate produced during acidification is the principal organic acid (volatile acid) used as source of food by methane-forming bacteria and Carbon dioxide and hydrogen can be transformed directly to acetate or methane in the methanogenic stage of ADP. Other alcohol, organic –nitrogen compounds and organic acids used as substrate directly by methanogenic bacteria includes; formate, methanol and methylamine while the ones used indirectly when degraded to acetate by fermentative anaerobes are ethanol, butyrate and propionate (Demirel and Yenigun 2002). The presence of organic-nitrogen compounds and organo-sulphur compounds is attributed to the degradation of amino acids and proteins. Also, some of the organic compounds are converted to organic acids and alcohols, and some are converted to new bacterial cells (Geradi 2003). It is only in methane formation or the methanogenic stage that degradable organic compound is transformed into methane and carbon dioxide.

Step 3- Acetogenesis

Acetogenic bacteria in the acetogenic step of ADP are strict anaerobes with a slow growth rate and sensitive to both fluctuation in organic loading and environmental variations. They have an optimum pH of about 6 and are restrained from anoxic environment and utilize a pathway termed acetyl coenzyme A pathway which consist of enzymes exceptionally sensitive to oxygen (Wood and Ljungahl 1991). They require long lag periods for adjustment to new environmental conditions (Xing *et al.* 1997). The accumulative hydrogen concentration in the liquid will lead to accumulation of electron sinks (lactate ethanol, propionate, butyrate and higher volatile acids) which methanogenic bacteria struggle to absorb directly and hence further degradation is required by obligate hydrogen producing acetogenic bacteria (Bjornsson *et al.* 2000). The obligate hydrogen producing acetogenic bacteria degrade the electron sinks to acetate, carbon dioxide and hydrogen and this process is termed acetogenesis and must occur for efficient biogas generation. Acetogens make syntrophic relationships with hydrogen-consuming methanogens since they rely on low hydrogen partial pressure for their degradation (Salminen *et al.* 2000; Schink 1997).

The methane required in the acetogenic process can be produced first through fermentation of acetic acid to methane and carbon dioxide by acetoclastic methanogens in Equation 2.72 and using CO_2 as a source of carbon and hydrogen as a reducing agent by hydrogen trophic methanogens as given in Equation 2.73. The same approach can be used in hydrolysing CO_2 to carbonic acid and to methane as given in Equation 2.74-2.75. The two most common methanogenic bacteria found in biogas digesters reported in literature are methanobacterium and methanothermobacter. On the contrary, CO_2 in the biogas is unwanted and is usually eradicated for best efficiency of biogas as biofuel. Kondusamy and Kalamdhad (2014) as added that the CO_2 is eradicated by passing the gas into lime water which turns milky due to formation of calcium carbonate. H_2S is also another unwanted in the biogas due to presence of sulphate in the substrate during ADP. However, percentage of H_2S present in biogas varies as a function of the sulphate percentage.

$$\mathrm{CH_3COOH} \xleftrightarrow{\text{Acetoclastic Methanogens Bacteria}} \mathrm{CH_4} + \mathrm{CO_2} \tag{2.72}$$

$$\mathrm{CO_2} \ + 4\mathrm{H_2} \xrightarrow{\text{Reduction}} \mathrm{CH_4} + 3\mathrm{H_2O} \tag{2.73}$$

$$\mathrm{CO_2} \ + \mathrm{H_2O} \xrightarrow{\text{Hydrolysis}} \mathrm{H_3CO_3} \tag{2.74}$$

$$4\mathrm{H_2} + \mathrm{H_2CO_3} \xrightarrow{\text{Reduction}} \mathrm{CH_4} + 3\mathrm{H_2O} \tag{2.75}$$

Step 4- Methanogenesis

In the methanogenic step of ADP as given in Equation 2.76, methane (CH_4) is formed normally from acetate and carbon dioxide and hydrogen gas. The products of the acid fermentation (acetic acid) reaction are converted into CO_2 and CH_4 by acetoclastic methanogens and the resultant methane is mainly desorbed in the liquid phase (Ostrem 2004). The Acids, alcohols, and organic-nitrogen substances that are not degraded by methanogenic bacteria accumulate in the anaerobic digester supernatant. The accumulation of these substances is responsible for the relatively high organic strength (carbonaceous biochemical oxygen demand- cBOD) of the supernatant.

$$\mathrm{CH_3COOH} \xrightarrow{\text{Methane Forming Bacteria}} \mathrm{CH_4} + \mathrm{CO_2} \tag{2.76}$$

Methanogens are very sensitive to changes and prefer slightly alkaline environment between pH 6.8 and 7.2 (Gas Technology 2003; Gerardi 2003). In contrast, If the pH falls below 6 methanogenic bacteria activities is hindered in the digester. Therefore, Methanogenesis becomes the rate controlling factor of the anaerobic digestion process (Davis and Cornwell 1998). Provided that the working velocity of acid-forming bacteria and methanogenic bacteria are approximately the same, the degradation activity of the methanogenic step is secured. If the methanogenic step is secured, the acids are degraded and a slightly alkaline medium is achieved due to the formation of ammonia (NH_2) from amino groups (–NH2) that are released through the degradation of proteins and amino acids (Gerardi 2003). Ammonia released in the sludge often reacts with carbon dioxide and water, resulting in the production of ammonium carbonate that provides alkalinity to the system (Equation 2.77). The ammonium carbonate is available to react with the volatile acids that are present in the sludge. This reaction results in the production of volatile acid salts (Equation 2.78).

$$NH_3 + CO_2 + H_2O \rightarrow NH_3HCO_3 \tag{2.77}$$

$$NH_3HCO_3 + RCOOH^* \rightarrow RCOONH_4 + H^+ + HCO_3^- \tag{2.78}$$

Where,

R = non-carboxyl (-COOH) part of the volatile acid

The degradation of complex organic compounds to methane will be rapid if the compounds can be converted to substrates usable by methane-forming bacteria. Within the anaerobic conversions and degradations of organic compounds, the production of acetate is the rate-limiting step or “bottle neck” in the final degradation of complex organic compounds. For organic compounds that are poorly biodegradable, the hydrolysis stage may become the rate-limiting step.

2.2.4 The Impact of chemical dosing on Activated Sludge digestibility

Surplus activated sludge (SAS) generated from municipal wastewater treatment plant (WWTP) is a challenge with growing significance because of its enormous production, associated environmental pollution, high cost for sludge treatment and disposal (Feng *et al.* 2014). Anaerobic digestion (AD) process as stated in section 1.1 is the most energy saving option for sludge (SAS) reduction and stabilisation, and biogas waste product as a potential biofuel may decease sludge treatment cost (Wang *et al.* 2013b). The anaerobic digestion stages has been earlier covered in section 2.2.3. As earlier stated in section 1.1 CPR has been reported to cause an increased volume of sludge between 37% and 97% (Yeoman *et al.* 1988). This is due to most WWTPs in Europe using CPR to achieve their effluent P consents using mainly aluminium (Al^{3+}), ferric (Fe^{3+}) and calcium (Ca^{2+}) salts for precipitation of phosphorus (Ojo and Ifelebuegu 2016; Ge *et al.* 2018; Ojo and Ifelebuegu 2019a; Wilfert *et al. 2015*). Therefore, the CPR processes are likely to impact downstream processes due to the increased weight of metal salts (Al^{3+}, Fe^{3+} and Ca^{2+}) used in the processes. Supportive evidence on the direct impact of coagulants (Al^{3+}, Fe^{3+} and Ca^{2+}) on anaerobic digestibility will be investigated in this section 2.2.4.

Phosphorus is one of the nutrients in WWTP responsible for eutrophication and its discharge to receiving waters is strictly regulated globally (less than 1mgP/l) by urban wastewater treatment directive 1991 (Ojo and Ifelebuegu 2016; Kroiss 2011; European Commission 2000; Smith and Carliell-Marquet 2008, 2009). The generation of sulphide in conveyance systems like sewers has been known to cause concern in wastewater treatment process due to odour, corrosion and health hazard challenges (Thistlethwayte 1972; USEPA 1974; Boon 1995; Hvitved-Jacobsen

2002; Zhang *et al.* 2008). Iron salts (ferric or ferrous ion) are frequently added to sewers as chloride salt (Jameel 1989; Nielsen *et al.* 2005), sulphate salts (USEPA 1974) or nitrate salt (Padival *et al.* 1995) for reducing hydrogen sulphide (H_2S) discharge to sewer air (Nielsen *et al.* 2005). Iron (II) (Fe^{2+}) salt removes sulphide by precipitating it as ferrous sulphide (FeS), while Fe^{3+} salt oxidizes sulphide to sulphur with Fe^{3+} being reduced to Fe^{2+}, which then precipitates sulphide to produce FeS (Nielsen *et al.* 2005). Iron salts are often added to wastewater treatment plants (WWTP) to precipitate phosphate as insoluble ferric hydroxyl-phosphate complexes and ferric chloride is most commonly used for P precipitation in activated sludge plants (Rasmussen and Nielsen 1996; Nielsen *et al.* 2005) but ferrous salts may also be used (Singer 1972; Jameel 1989). Ferric Iron as ferric hydroxide is assumed to be active compound for phosphorus precipitation (Leudecke *et al.* 1989) and hence it is vital to keep Fe in the oxidised form in wastewater treatment plants (WWTP) to avoid Iron reduction. Simultaneous dosing of ferrous and ferric salts has been shown as a more effective method for P removal than the dosing of a single iron form (Tomar and Abdullah 1994; De Haas *et al.* 2000a). The anaerobic degradation process in WWTP involving Iron and Sulphate reduction can cause disintegration of the activated sludge flocs resulting in deteriorated dewaterability characteristics during the storage of activated sludge before the dewatering process (Rasmussen *et al.* 1994). Rasmussen and Nielsens (1996) study observed that iron reduction in activated sludge after extraction with HCL, oxalate or ferrozine showed a significant release of phosphate into bulk water in an anaerobic biological-P tank and anaerobic storage of sludge before dewatering due to EPS more affinity for Fe (III) than Fe (II) which makes them bound in the sludge floc matrix. Clark *et al.* (2000) reported that the little reduction in efficiency of BOD_5. COD removal and suspended solids (SS) observed when doses of 2:1 (molar ratio Fe: P) for Fe (II) and 1.75:1 (molar ratio Fe: P) for Fe (III) was added to the pre-mixing zone consisting of settled sewage, return activated sludge (RAS) and final effluent is due to the excess growth of filamentous bacteria. Iron salts are used to enhance activated sludge settling characteristics (Bowen and Dempsey 1992) and optimisation of activated sludge plant performance, by the removal of organic compounds (humic substances) (Lefebvre and Legube 1990) and other nutrients (Crozes *et al.* 1995).

Scott (1973) added that iron salts benefit over other precipitants as low cost and sludges that are easy to dewater. Nielsen and Keiding (1998) further commented that Fe (III) has better flocculating properties than Fe (II), owing to the lower solubility and the higher valence of Fe (III), since overall the trivalent cations will flocculate better than divalent cations. Philips *et al.* (2003) reported the impact of iron salts on activated sludge and its interaction with nitrite or nitrate and findings showed that continuous dosing of ferrous or ferric iron salts to activated sludge produces a progressive inhibition of total nitrifying activity. The observed toxicity could be partly attributed to the drop in pH caused by the formation of iron hydroxides or the negative effect of ferric iron on the floc structure. However, Nitrate was reported to neutralize the negative effects of the iron salts which influenced activated sludge performance. Lees *et al.* (2001) investigations revealed that the presence of Fe (III) resulted in formation of denser flocs which were smaller than the control. Conversely, Caccavo *et al.* (1996) reported that 1–2.5 millimoles (Mm) Fe (III) flocculated autoclaved activated sludge better than Fe (II).

It has been reported that ferric iron has a high affinity for protein (Murthy *et al.* 2000; Muller 2001; Novak *et al.* 2003). Murthy *et al.* (2000) demonstrated that iron (III) salts selectively coagulated protein in solution produced from auto thermal thermophilic aerobic digesters. Muller (2001) compared the efficiencies of iron (III) and iron (II) salts for coagulation of solution protein and found that the former worked more effectively than the latter. There is limited information present for the specific role of aluminium in activated sludge floc. Some investigations about aluminium were found in the field of water treatment and aluminium salts are often used as coagulants for removing natural organic matters in water treatment plants. The addition of iron (Fe) has shown to be a popular option for chemical P removal (CPR) in water and wastewater treatment plants(WWTP) for evaluating the impact of iron on anaerobic digestibility but negative impact on the downstream process of anaerobic digestion (AD) in wastewater treatment (WWTP) through reduction of the volume and/or quality of biogas produced has been reported (Dentel and Gossett 1982; Gossett *et al.* 1978; Johnson *et al.* 2003; Kindzierski and Hrudey 1986; Rudolfs and Setter 1931; Rudolfs *et al.* 1932; Smith 2006; Smith and Carliell-Marquet 2008; Van Fleet *et al.* 1974; Yeoman *et al.* 1990). A volume reduction by 12-20% (biogas) and 10-22% ($\mathrm{CH_4}$) during the anaerobic digestion process (ADP) has been attributed to lower concentrations of bioavailable Fe and P in Fe dosed sludge which was found to hinder ability of microbes to breakdown organics substrate especially proteins (Smith and Carliell-Marquet 2008, 2009).

Ofverstrom *et al.* (2010), reported a comparative investigation involving the relative digestibility of Iron-dosed and Aluminium-Iron-dosed sludge with un-dosed sludge. The experiments were conducted in triplicates and the findings showed that Iron and Aluminium negatively impacted anaerobic digestion process by reducing the volume of biogas produced. Iron-dosed sludge produced 20-50% less biogas and Aluminium-Iron-dosed sludge produced 30-40% less biogas in comparison to the same un-dosed sludge. VS destruction decreased during dosing of Iron and Aluminium salt. The addition of Aluminium salt into Iron-dosed sludge mixture increased biogas production up to 10-20% compared to biogas production from Iron-dosed sludge.

The addition of zero valent iron (ZVI) was shown to improve production of volatile fatty acids (VFAs) by 37.3% during the hydrolysis and acidification stage of anaerobic digestion (Feng *et al.* 2014). Additional result of 43.5% methane production with 20g ZVI/L gave further description to anaerobic degradation and concluded that this was due to the activities of major enzymes related to hydrolysis and acidification were enhanced after adding ZVI. Iron salt added to high rates activated sludge was described to stabilise the digestion of kitchen waste and this improvement was attributed to a high content of Fe in high rate activated sludge (Vrieze *et al.* 2013). The Fe-rich activated sludge (1350 mg Fe/L) was argued to be an effective co-substrate which enhanced methane generation by 32.6% compared to a mono-digestion reactor fed with kitchen waste under a mesophilic state (Choong *et al.* 2016; Vrieze *et al.* 2013). Iron salt (ferric) has been added directly into wastewater digestion system and 65% removal of hydrogen sulphide (H_2S) known for difficult odour causing products was achieved (Choong *et al.* 2016; Park and Novak 2013). This removal of H_2S was attributed to the consumption of the bisulphide (HS^-) metabolic substance produced by the sulphate reducing bacteria through the precipitation of ferric sulphide (FeS), which will cut down on the cost implication involved in the processing H_2S removed to obtain biogas. Zero valent scrap iron (ZVSI) is used to stimulate the anaerobic digestion of sludge and highest methane yield of 174.9 ± 1.5mL/g VSS_{fed} with ZVSI 1.0 g/g VSS, increasing by 38.3% has been reported to improve the methanogenesis by acting as electron donors and creating favourable environment (pH environment and low hydrogen concentration) that further optimises the hydrolysis, acidogenesis rate and overall methane production (Zhen *et al.* 2015).

Novak (2010) reported that Iron and aluminum were added to waste activated sludge (WAS) to simulate the dosing of iron (Fe^{3+}) and aluminium (Al^{3+}) for chemical phosphorus removal in the activated sludge system. Iron was also added directly to the combined primary and secondary sludge prior to anaerobic digestion. Result revealed that the volatile solids destruction by anaerobic digestion (AD) reduced by approximately 2% when aluminum was added to the WAS for phosphorus control. However, the volatile solids destruction by anaerobic digestion was unaffected or increased slightly when iron was added to the WAS for phosphorus control. Other findings was that the total volatile organic sulphur concentration (TVOSC) generally reduced for both iron and aluminum dosed sludge, but iron resulted in the highest reduction.

Ofverstrom *et al.* (2011a,b), reported the effects of adding iron salt on the digested primary-waste activated sludge mixture through experimental studies and result showed that the anaerobic digestion of Fe-dosed sludge with minimum dose (Fe concentration of 0.84gFe/L) resulted similar biogas production as from un-dosed sludge mixture. The average biogas production was 1.20 L/g volatile solid (VS) fed. In contrast, Fe-dosed sludge with maximum dose produced 30% less biogas in comparison with biogas production from un-dosed sludge. The average phosphate content in digested sludge liquor from un-dosed sludge increased by 38% due to the solubilization of phosphate during anaerobic digestion. It is essential not to overdose Fe salt during sludge digestion because higher Fe salt doses could negatively impact biogas production.

Liu *et al.* (2012) proposed an innovative approach for improving anaerobic wastewater treatment by adding ferric powder (Fe^0) in an acidogenic reactor. The hydrolysis stage was speeded and extent of volatile fatty acid (VFA) (1170-1340mg/L), COD removal (45-56%), and the acetogenesis and methanogenesis process were improved. This improvement was attributed to the dosed Fe powder in the wastewater content in the acidogenic reactor which increased the abundance of acidogenic and methanogenic bacteria in the reactor.

Zhang *et al.* (2015b) showed that after heat and alkali pre-treatment, the dosed waste sludge with zero-valent iron (ZVI) was used to enhance the methanogenic activity in an anaerobic sludge digester under two methanogens-suppressing conditions, i.e. heat-pre-treatment and alkali condition respectively. The result indicates that ZVI shortened the lag time of methane production and increased the methane yield by 91.5% and volatile suspended solid (VSS) removal increased from 44.4% to 60.06% after the digestion at pH 10 and degradation rate of acetate and hydrogen were increased by ZVI, and both the acetogenesis and methanogenesis stage of anaerobic digestion were optimised.

Abbott and Eskicioglu (2015) explained that highly odorous and toxic volatile sulphur compounds (VSCs) in AD biogas can limit wider implementation and the impact of metal salt (ferric chloride, alum and magnesium hydroxide) on anaerobic digestion stability and odour were investigated. It was reported that Ferric chloride was very effective (87%) in reducing odorous VSCs produced during AD, Alum was reported with a negative impact as alum increased VSC levels by 920% (negative effect) but magnesium hydroxide dosing showed no appreciable impact on biogas VSC concentration. Abdelsalam et al. (2016) reported the optimisation of biogas production and reduction of lag phase of anaerobic digestion by adding nanoparticles. Result showed that by adding 1-20mg/L cobalt (Co), nickel (Ni), iron (Fe), iron II, III oxide (Fe_3O_4) nanoparticles the biogas produced could be improved by 1.5 to 1.8 times.

Kumar *et al.* 2016 reported the effect of calcium chloride on abating inhibition due to volatile fatty acids during the start-up period in anaerobic digestion of municipal solid waste (MSW) and result showed that the addition of calcium chloride ($CaCl_2$) during anaerobic digestion (AD) of MSW is crucial to improve its efficiency. Within an optimum concentration of 2.5g/L $CaCl_2$, the AD process performance was enhanced but at higher concentration of $CaCl_2$ (>5g/L), the hydrolysis process seems to have been inhibited thus affecting the performance of AD process. The effect of calcium on the anaerobic digestion treating swine wastewater has been reported (Ahn *et al.* 2006). The result showed the digestibility of Ca-dosed sludge, with total biogas production been maximum at calcium dosing concentration of 3g/L.

Lar *et al.* (2010), investigated the influence of calcium and iron supplementationson the yield of methane in batch anaerobic digester treating dairy manure under mesophilic conditions. Result showed that both calcium and iron have a positive impact on methane production. The increase in biodegradation during calcium dosing was attributed to the ability of calcium to enhance the initial adhesion of the cells through exo-cellular polymers, which bind to divalent metals. This will further result in calcium getting embedded into the dairy manure sludge extracellular polysaccharides (EPS) and proteins, leading to an increased mass transfer. Calcium likewise has the ability to bridge between the electronegative carboxyl and phosphate groups associated with bacterial surfaces which is responsible for the increase in the biodegradation rate. However, excess calcium may lead to cementation due to precipitation causing a mass transfer limitation (Tiwari *et al.* 2006), which is due to formation of calcium carbonate precipitates blocking the inter-granular ores (Yu *et al.* 2001) which result in a decrease in the biodegradation process.

The concentration of calcium with organic loading rate (OLR) of 60g/L up to 200mg/L and with OLR 80g/L up to 2,500mg/L was effective to increase the ultimate biogas production. On the contrary, the concentration of iron with OLR 60 g/L up to 300 mg/L and with OLR 80g/L up to 400mg/L was effective to increase the ultimate biogas production. Iron dosing may promote the excretion of extracellular polymers and also have a positive influence on granulation, which results in an increase in mass transfer and ultimately increases methane contents (Tiwari *et al.* 2006). Junoh *et al.* (2016) investigated the effect of chemical pretreatment ($Ca(OH)_2$) pretreatment on the enhanced biogas production of organic food waste. Result revealed that COD solubilisation was optimized at 166.98 milliequivalent per litres (mEq/L) which is equivalent to 6.1 g $Ca(OH)_2$/L for 1 hour. The Calcium hydroxide enhanced up to 20.0% of specific methane production compared to untreated food waste. Ji *et al.* (2017) reported the efficiency of co-pretreatment of $Ca(OH)_2$ and steam explosion (SE) on the cumulative methane production of corn stover (CS). Result showed that Co-treated CS of 1.0% $Ca(OH)_2$ and SE at 1.5 megapascal (MPa) provided the highest experimental methane yield (EMY) of 275.58mL/g vs, which improved 61.54% compared to that of untreated CS. The highest EMY indicates that the mild pretreatment condition of 1.0% $Ca(OH)_2$ and SE at 1.5 MPa might be optimum. Nevertheless, further comparison on the impact of CPR on AD and the Factors that influence precision of laboratory Iron dosed sludge have been provided in Table C1 and C2 (Appendix C).

2.3 Activated Sludge Dewaterability

Activated sludge processes (ASP) have been extensively used for wastewater treatment in the wastewater industry globally; however, the economic impact associated with the resultant huge amount of surplus activated sludge (SAS) requiring both further unit process treatment and disposal makes optimising dewaterability of activated sludge of great necessity (Neyens *et al.* 2004; Stickland *et al.* 2008; Feng *et al.* 2009; Curvers *et al.* 2009; Zhang *et al.* 2010b; Wang *et al.* 2013a). ASP do not just generate SAS but SAS with over 90% water accounting for severe environmental pollution (Niu *et al.* 2013). This makes the current study on the impact of chemical dosing (Al, Fe and Ca) on activated sludge dewaterability of utmost importance in wastewater treatment, since reduction in cost of further treatment, sludge disposal and transportation can be achieved through dewatering in the dewatering unit. The dewatering process also have the benefit of improved sludge structure and agricultural benefit as a soil conditioner. The impact of more stringent legislation (The Disposal of Sewage Sludge to Agricultural Land Directive-86/278/EEC) necessitating sludges from wastewater treatment plants to be re-used wherever possible and disposal routes to cut down on the concentration of heavy metals in sludges which has adverse impact on the environment (Christensen and Dick, 1985). A proper dewatering mechanism will reduce the effect of environmental pollution globally.

Moreover, increased industrialisation and population growth amounts to increased volume of sludge flow requiring treatment and the resultant wasted activated sludge (WAS) otherwise called surplus activated sludge (SAS) equally requires disposal. The cost of both treatment and disposal has been reported to be equivalent to 60% of the total running cost of a WWTP (Canales *et al.* 1994). Although, conventional approaches for sludge disposal (composting, incineration and landfill) has been reported in literature (Mowla *et al.* 2013) but due to their economic and environmental limitations, a more robust approach that deals with the issue of SAS treatment and disposal becomes an interest in this current research. Also, overdosing of coagulants may result in environmental and cost related issues in the wastewater treatment supernatant generated during the sludge dewatering process. The residual coagulant in the dewatered sludge cakes may pose a lasting risk to the environment particularly when the sludge cakes are disposed through landfill option and landfill transportation cost apply (Van der Roest *et al.* 1999). Furthermore, approximately 80% of water content of activated sludge is bound water which is difficult to remove by conventional dewatering equipment namely; centrifuge and filter press mechanism because of strong intermolecular forces between liquid-solid surfaces. Hence, any dewatering optimisation strategy that reduces the volume of SAS bulk water in surplus of 98% becomes profitable from both environmental and economic perspective. Wang *et al.* (2010) stated that dewatering the sludge to 60% water portion will account for the cost efficiency reduction in the amount of SAS produced. The general activated sludge floc structure depends on both physical and chemical interaction between inorganic matter, extracellular polymeric substances (EPS), multivalent cations and bacteria colony (Govoreanu 2004). Thus, filamentous bacteria form the back bone for firm attachment of floc forming bacteria (Wanner 1994) and floc forming bacteria converts organic matter to extracellular materials (EPS) that houses various bacteria and microbes (Keiding *et al.* 2001; Biggs and Lant 2000; Jin *et al*. 2003; Wilén *et al.* 2003). EPS can exist as either tightly bound or loosely bound (Laspidou and Rittman 2002; Nelson *et al*. 1998). It is vital to mention that there exists a negative impact of filamentous bacteria and EPS, the former has a protruding nature from the floc resulting in poor settleability while the later binds the floc constituents together and water molecules strongly to solid surfaces and detains them inside the floc (Urbain *et al.* 1993; Snidaro *et al.* 2006). EPS also accounts for the maintenance of activated floc structure and functionability (Higgins and Sobeck 2002; Sheng *et al.* 2006).

Literature has reported three key limiting elements in dewaterability of activated sludge; low settleability of colloidal substances, high attraction of EPS for trapping water molecules (bound water) and high compressibility of sludge solids (Mowla *et al.* 2013). EPS has the potential to impact dewatering of activated sludge negatively (Yu *et al.* 2008; Nelson *et al.* 1998) but diverse methods have been reported for optimising activated sludge dewaterability quality in previous studies, including chemical coagulants like aluminium sulphate, ferric chloride, calcium hydroxide, polyelectrolyte, surfactants and enzymes (Neyens *et al.* 2004 ; Van der Roest *et al.* 1999, Abu-Orf *et al.* 2007 and Ruiz- Hernando *et al.* 2013), Acids and surfactants (Chen *et al.* 2001), Fenton's reagent pre-treatment (Lu *et al.* 2003; Tony *et al.* 2008), Microwave conditioning (Wojciechowska 2005), mechanical pretreatment (Hwang *et al.* 1997); Ultrasonication (Bien 1991; Bien and Wolny 1997; Neis 2000; Na *et al.* 2007; Feng *et al.* 2009; Gallipoli *et al.* 2014; Gianico *et al.* 2013), Fry-drying technology (Ohm *et al.* 2009),calcined aluminium salt (Zhen *et al.* 2011; Devlin *et al.* 2011),ultra-rapid freezing (Parker and Collins 1999), bio-acidification (Shi *et al.* 2013; Song and Zhou 2008**;** Wong *et al.* 2004,2014); Ferrous activated persulfate oxidation (Zhen *et al.* 2014b) and potassium ferrate (Ye *et al.* 2012). The neutralisation of negative charge on the sludge floc and reduction of repulsive forces between sludge particles has capacity to cause both bio-flocculation and release of bound water to the surrounding to occur (Song *et al.* 2010). Also, without an enhanced comprehension of major sludge dewatering pathway (energy and structural binding between water molecules and binding materials) it becomes difficult to suggest the best strategy for optimising sludge dewatering process (Houghton *et al.* 2001). The water in the activated sludge floc is classed as bound water and free water (Hsu and Lee 1995). The boundwater is physically and chemically held to the floc while the freewater is easily separated. Vesilind and Martel (1990);Colin and Gazbar (1995); has reported different forms of water available in activated sludge structure namely; free water (water not attached to solid particle), vicinal water (water physically bound to solid particles but cannot be separated mechanically), interstitial water (water trapped within the floc and can be released by breaking up the floc) and hydration water (water which are chemically bound to solid particles but can be released only at temperatures > 105℃). On the other hand, the sum of interstitial, vicinal and hydration water (Bound water) is the key limiting issue in optimisation of the efficiency of activated sludge dewaterability process due to the excessive energy required to break the capillary force and chemical bond in bound water.

Although, earlier studies; Dentel (2001), Mowla (1996) and Zhao *et al.* (2002) reported on different methods of optimising activated sludge dewaterability process; sludge thickening (using rotary drum and gravity belt to increase solid content from 2% to >15%), sludge dewatering (increasing solid content of up to 50% through application of pressure) and sludge drying (increasing solid content of up to >90% based on application of heat to destroy water molecular bonding).

In the current study, although, as mentioned earlier that there are three limiting factors in activated sludge dewatering (low settleability, high compressibility of sludge and bound water) and activated sludge dewatering is achieved using mechanically driven device that utilises pressure to compel water from the activated sludge flocs. In order to improve the dewatering performance, sludge pre-treatment is crucial. The impact of coagulant (Aluminium-Al, Ferric–Fe and Calcium-Ca) salt on activated sludge dewaterability as a pre-treatment option will enhance the activated sludge flocs for water withdrawal. This will optimise the limiting factor in activated sludge dewatering. However, there are two indexes for the evaluation of activated sludge dewaterability and filterability namely capillary suction time (CST) test and the specific resistance of cake to filtration (SRF) test (Scholz 2005; Gale 1967) but in this study capillary suction time (CST) test is of interest.

2.3.1 The Impact of Sludge properties on activated sludge dewaterability

Although, literature has provided some properties that affect activated sludge dewaterability such as surface chemistry (zeta potential) which defines the surface attributes of sludge and colloidal particulate stability (Lee and Liu 2000; Velegol *et al.* 2000), yield stress that explains the sludge rheological characteristics (Lotito *et al.* 1997), bound water content (Keiding *et al.* 2001) and EPS content (Mowla *et al.* 2013). The two most vital sludge properties that are key limiting factors in activated sludge dewaterability are EPS content and bound water content. Also, the two-key sludge dewaterability indicators used for evaluating the efficiency of sludge dewaterability are CST (capillary suction time) and SRF (specific resistance to filtration).

2.3.1.1 The Capillary Suction Time (CST) Test

The CST estimation used for quick determination of sludge filterability and conditionability in wastewater treatment plant (WWTP) was first discovered by Gale and Baskerville (1967). CST, which is inversely proportional to activated sludge dewaterability, is used as a benchmark of sludge dewaterability (To *et al.* 2016a,b; Gharibi *et al.* 2013; Xiao *et al.* 2019). This is an indication of how fast an activated sludge releases its water during the dewaterability process. The advantages of usability of the equipment are limited cost, simplicity, reliability, quick operation, no requirement for external pressure, automation and less training required for operators. The type 304B CST device utilized in wastewater treatment for measuring sludge dewaterability functions is based on the operational principle of sludge filterability and this will be adapted in this study. The CST device components includes; CST Meter, perspex block assembly, stainless steel funnel (18mm and 10mm diameter reservoir) and filter papers (Whatman 20). The CST is assessed by pouring the primary and secondary test samples into the 18mm and 10mm diameter reservoir placed on Whatman 20 filter paper. The filtrate is drained from the reservoir through the capillary suction effect of the filter paper so that a filter cake is formed on the filter paper. This reveals that CST test value is not influenced by the mass of liquid in the reservoirs, provided that the liquid capacity can generate the required suction pressure (Smeulders and Meeten 1995). The fluid soaks the paper and disseminate outwards in a circular shape based on the viscosity of the filtrate and filterability of the sludge. The sludge cake resistance (m/s) is measured based on the distance the filtrate travels along the paper as function of time. The filter resistance is taken as negligible while the CST value is calculated as the time taken for the filtrate to travel between two (2) concentric and adjustable circles on the filter paper. Although, CST test suffers from limitations tied to incomparability of test data using different types of sludge's and the potentials of replicated test producing variable result, and Scholz (2005 and 2006) reported the need for more concentration on the precision of CST result and this study by building it into the CST test assessment. More details on the CST device operation and protocol are reported in Baskerville and Gale (1968).

2.3.1.2 The Specific Resistance to Filtration (SRF) Test

The SRF test is alternative measurement for sludge dewaterability in WWTP. Although, Baskerville and Gale (1968) reported that sludge samples with high CST data similarly possessed high SRF results. In contrast, Smeulders and Meeten (1995) commented on estimating SRF from mathematical modelling through estimating SRF as the slope of regression analysis of CST test results against the successive distances to power four (d^4) of the multiple electrodes of the CST equipment. Although, SRF can be calculated using the standard Buchner funnel apparatus with a filter paper (Whatman 15.0 cm). The well mixed primary and secondary sludge sample was poured into the Buchner funnel and vacuum pressure was applied through a filter paper and the filtrate volume (V) was measured at stable time intervals until the fluid drainage ends. Hypothetically, the graph of t/V (s/m³m^{-2}) versus V (m³m^{-2}), where t = a given time and V = cumulative volume filtered, is a linear relationship. The slope of this straight line gives the mean SRF that defines sludge dewaterability (filterability). This slope can be used to justify dewaterability improvement (steep slope = poor filterability and flat slope = good filterability). The SRF can be calculated based on two deductions which includes; Carman (1938) incorporating Darcy's Law into the filtration theory and Gale (1967) assumptions that the filter sludge cake is incompressible, and the filter media resistance is negligible. The following Equations 2.79 to 2.80 were realized to define the volume of filtrate and subsequently determine the SRF value (r, m/kg):

$$\frac{\mathrm{AdV}}{\mathrm{dt}} = \frac{\mathrm{PA}}{\mathrm{\mu rcV}} \qquad (2.79)$$

Where,

V = cumulative filtration volume per unit area (m³/m²) or (m)

P= applied vacuum pressure (Pa)

A= Filter Area (m^2)

c = concentration of slurry (kg/m^3)

r = specific resistance of cake to filtration (SRF) (m/kg)

μ = Filtrate viscosity (Ns/m^2)

t = given time(s)

$c = \frac{\text{weigth of dry solids}}{\text{Volume of filtrate}}$ = concentration of slurrry (kg/m^3)

Considering a batch filtration test the equation 2.79 becomes:

$$t = (\frac{\mu rc}{2PA^2})V^2 \tag{2.80}$$

However, if μ, r, c, P and A are constant then equation 2.81 holds

$$b = (\frac{\mu rc}{2PA^2}) \tag{2.81}$$

If equation 2.81 is substituted into equation 2.80 then the following holds

$$t = bV^2 \tag{2.82}$$

Plotting t/V against V and taking the slope of straight line as b the specific resistance to filtration (r) can be calculated using equation 2.83 below.

$$r = SRF = (\frac{2A^2P}{\mu c})b \tag{2.83}$$

Therefore, SRF can be estimated from Equation 2.83 and typical value of SRF for raw sludge is 7.3 x 10^{12} m/kg. If the value of t given in Equation 2.82 stays constant irrespective of the slurry concentration then standardizing the applied vacuum pressure makes direct evaluation of all sludge's possible. Just as mentioned earlier the CST drawbacks, likewise Ayol and Dentel (2005) and Yukseler *et al.* (2007) identified some limitation of SRF to include; time constraint, more demanding compared to CST and no specific device to measure SRF and variation in material and procedure (type of filter medium and specific vacuum pressure employed) reported in literature by Smollen, (1986a; 1986b).

2.3.1.2.1 The Relationship between Specific Resistance to Filtration (SRF) and Capillary Suction Time (CST) Test

As mentioned earlier, CST was developed as a substitute for SRF to measure dewatering rate. However, Scholz (2005), reported that there is a relationship between the SRF and CST for a wide range of different types of sludges. Notwithstanding, various studies have tried to investigate and model the correlation between CST and SRF with the aim of finding the mean SRF from the CST experimental data. Lee and Hsu (1994) proposed a method that allowed SRF to be calculated without the liquid invasion volume measurement using capillary suction apparatus. A related research study by Herwijn *et al.* (1995) reported a newly developed model of CST apparatus able to estimate the specific cake resistances of both unflocculated and flocculated sludges. Although, the relationship between CST and SRF was not earlier measured and modelled using appropriate empirical data, but investigation made by Sawalha (2010) and

Sawalha and Scholz (2010) on modelling the relationship between CST and SRF has filled this research gap. The mathematical model predicted the result of SRF using the results of CST and two other parameters namely; temperature (15, 20, 25 degree celcius) and sludge concentrations (8.8, 12.1, 15.3 and 31.6g/L). The mathematical models required the use of logarithmic transformations and polynomial terms to simulate non-linear characteristic and the best fitting empirical model to predict the results of CST tests from temperature, paper type, and funnel geometry, excluding anomalies was provided (Equation 2.84).

$$\mathrm{Log\ CST} = 3.645 + 0.303\mathrm{TSS} - 0.005\mathrm{TSS}^2 - 0.197\ \mathrm{T} + 0.006\ \mathrm{T}^2 + 0.274\mathrm{P} - 0.226\ \mathrm{F} \quad (2.84)$$

Where,

CST = capillary suction time (s)

TSS = total suspended solids (g/l)

Temperature = ^{o}C

P = Fisher 200 Chr paper = 0

P = Whatman 17 Chr paper = 1

F= Circular funnel = 0

F= Rectangular funnel = 1

In addition, it was suggested that SRF experimental results can be predicted from the results of CST tests using the model (Equation 2.85).

$$\mathrm{Log\ SRF} = 46.128 - 1.346\mathrm{T} + 0.035\mathrm{T}^2 + ({}^{13.760\mathrm{F}}/_{\mathrm{TSS}}) \quad (2.85)$$

Where,

SRF = Specific Resistance to Filtration (m/kg)

T= Temperature (^{o}C)

F = Filterability (log s/m^2)

TSS= Total Suspended Solids Concentration (g/l).

This mathematical model (Equation 2.85) that predicts the SRF for suspended solid concentrations (8.8, 12.1, 15.3 and 31.6g/L) within the solid content of experimentation. The practical relevance of this model is that, if SRF values are required but only the data of CST tests are known, the model can estimate the required SRF values. The key aim of conducting CST and SRF test at wastewater treatment plants (WWTP) is to reduce running costs by evaluating the optimal dose of the sludge conditioner, defined as the dose of coagulant that yields the minimal capillary suction time or resistance to filtration (Wu *et al.* 2000). Therefore, WWTP can make economic and energy cost savings along with decrease in the environmental damage if the dosing system for the sludge conditioners are kept at or near optimum efficiency by plant operators. This can be achieved by using the model for interpreting the SRF and CST test results (Equation 2.84 and 2.85), to re-estimate the proper use of sludge conditioners and save operational cost.

Furthermore, Peng *et al.* (2011) obtained a relatively good correlation between normalized CST and SRF ($R^2 = 0.9450$). They concluded that it is not necessary to use both these parameters simultaneously to evaluate the dewatering rate. Most recently, Arimieari and Ademiluyi (2018), reported the relationship between Sludge Filtration Resistance (SFR) and Capillary Suction Time (CST) using the result realised from different concentrations of calcium chloride ($CaCl_2$) for SFR and CST empirically using the Equation 2.86 proposed by Christensen *et al*. 1993).

$$\mathrm{CST} = \mathrm{C}_1 \times \mathrm{SRF} \times \mu_f \times \mathrm{w} + \mathrm{C}_2 \times \mu_f \tag{2.86}$$

Where,

C_1 and C2 = Coefficients related to CST

μ_f = Viscosity of the filtrate (Pascal seconds)

w = Solid content in unit volume of filtrate (g/L)

The results revealed that the values of CST decreased with increasing $CaCl_2$ concentration, and that a good dewaterability could be obtained at the $CaCl_2$ dosage of 18 g with the resultant CST of 5.52 s for 20 mm internal cylinder and 30.84 s for 14.5 mm internal cylinder. The results of SFR tests revealed decreased with an increase in $CaCl_2$ dosage. The optimal $CaCl_2$ dosage was 18 g and the resultant SFR was 2.65 x 10^8 N·s/m^5. The results for CST recommend larger diameter cylinder to be used to test heavy sludge since the larger cylinder considerably reduces the changeability and the time taken to conduct the CST tests.

Other studies reported that compared CST and SRF includes; Wong *et al.* (2015), that investigated the impact of different concentration of Fe^{2+} on sludge dewaterability after 24 h in terms of CST and SRF. The result showed that the control sludge without any supplement of Fe^{2+}, had high CST (356 s) and SRF (4.56×10^{12} m/kg) values. The sludge CST and SRF were significantly reduced after addition of Fe^{2+} at the end of 24 hour treatment. It was observed that for an efficient sludge dewaterability, the addition of 2g/L of Fe^{2+} concentration was found to be optimum. At this optimum concentration, sludge CST and SRF were 15.5 s and 5.4×10^{11}m/kg with 96% and 88% reduction, respectively. Dewatering characteristics of sludge treated with potassium ferrate under different pH conditions was investigated by Zhang *et al.* (2012). The result showed that the SRF value and the moisture of sludge cake for the control sludge were, 7.08×10^9m/kg and 86.13%, and decreased to 4.92×10^9m/kg and 75.35% treated with potassium ferrate (1200mg/L sludge) at pH3, this indictated that potassium ferrate had a positive impact on the dewaterability of sludge at pH3. Yuan *et al.* (2011), investigated the impact of electrolysis conditioning on sludge dewaterability, and the results showed that when electrolysis time was at 15 min, the CST and SRF values decreased from 60.8 s and 8.67×10^{11}m/kg for the control sludge to 45.5 s and 4.56×10^{11} m/kg for the treated sludge with an electrolysis voltage of 20 V. When the electrolysis voltage was increased to 50 V, both the CST and SRF values quickly extended to 79.4 s and 1.33×10^{12}m/kg, increases of 30.59% and 53.4% were reported, as compared to that of the control sludge. However, with electrolysis time reaching over 20 min, both the CST and SRF values swiftly increased and even surpassed that of the control sludge. When the electrolysis time increased to 60 min, both of the CST and SRF values speedily reached 143.8 s and 2.54×10^{12}m/kg, increases of 54.71% and 23.3%, were observed, and compared to the control sludge. Therefore, a relationship exists between electrolysis voltage/time and CST/SRF since enhanced dewaterability of sludge was realised at electrolysis time of between 15min and 20min with electrolysis voltage set as 20V and 50V respectively. Zhou *et al.* (2014) investigated on the improvement of dewaterability of waste activated sludge (WAS) by combined conditioning with zero-valent iron (ZVI) and hydrogen peroxide(HP). The results showed that significant improvement of WAS dewaterability was attained in the presence of ZVI and HP at pH 2.0. The CST reduction rate increased from 31.4 to 50.7% ($p < 0.05$) while the ZVI concentration increased from 0 to 500mg/L. At the same time, the dissolved iron from ZVI, which played an important role in the ZVI activated Fenton reactions, increased from 0 to 192 mg/L when the ZVI con-centration increased from 0 to 500mg/L. Table 2.11 showed additional comparison between SRF and CST.

Table 2.11. Comparison between Specific Resistance to Filtration (SRF) and Capillary Suction Time (CST)

SRF	**References**	**CST**	**References**
SRF is essentially used to evaluate the filtration quality of sludge when exposed to a constant pressure difference	Mowla *et al.* 2013	The theory of CST was first as a substitute for SRF test and it has easiness of operation and removal of moisture from sludge since no pressure is applied	Baskerville and Gale 1968; Sawalha and Scholz 2007
The basic measure of SRF uses Buchner funnel apparatus and It measures the resistance of sludge to the removal of water through a porous media either by vacuum or pressure	Christensen and Dick 1985; Graham 1999	CST is essentially the time required for a certain volume of filtrate drawn out of the sludge and sucked into the blotter paper by capillary force	Vesilind 1988
The higher the SRF, the more challenging to dewater sludge but the lower the SRF to more easier to dewater sludge	To *et al.* 2014	CST has been extensively used for evaluating the impacts of conditioning on sludge filterability in addition to investigating the	Novak 2006

		optimal dose of conditioners for dewatering processes	
High SRF is a function of decreasing sludge permeability with increasing solid pressure	Olivier *et al.* 2007; Sorensen and Sorensen 1997	CST has been extensively used for evaluating the impacts of conditioning on sludge filterability in addition to investigating the optimal dose of conditioners for dewatering processes	Graham 1999
Sludge with typical SRF value as low as 10^{10} – 10^{11}m/kg is categorised as easy to dewater, while whereas, sludge with SRF value as high as 10^{14} – 10^{15} m/kg is classified as challenging to withdraw water	To *et al.* 2014	Sludge with short CST, which is less than 20s, shows a readily dewaterable sludge, while a long CST is illustrative of a poorly dewatering sludge. CST of autothermal thermophilic aerobic digested sludge was found to exceed 50,000s	To *et al.* 2014; Agarwal *et al.* 2005
Describes the filtration rate of sludge by utilising the plot of the inverse flux (Filtration time divided by filtrate volume i.e t/V) versus filtrate volume (V) to calculate the filtration rate of sludge. The linear slope depicts the SRF	Olivier *et al.* 2007	CST is also a function of various parameters such as filter paper properties, instrumental properties and sludge–related properties	Vesilind 1988
Specific resistance varies with applied pressure, filter area and pore size and liquid viscosity, making it more complex to compare and estimate it	Marinetti *et al.* 2009	It was reported that using CST and SRF tests to determine optimum polymer dose (OPD) could lead to overdosing, specifically regarding polymer conditioning. This was attributed to the too fast escape of water from the floc	Scholz 2005; Sanin *et al.* 2011
The bottle necks with SRF is that the time required for estimations was reached when a cake was formed and eventually cracked with a resultant drop in pressure.	Vesilind1988; Notebaert *et al.* 1975	CST is limited by the concentration of solids, and thus it is not significant to compare CST of different sludge types from different plants. In addressing this shortcoming, a normalised value of CST was	Vesilind 1988; Yu *et al.* 2008

Measurement time depends on sample volumes, applied pressure, filter area, pore size and initial solid content of sludge, causing challenges in directly comparing results obtained from different research studies		proposed and used for the purpose of comparison. The normalised value was determined by dividing CST value by the initial total suspended solids (TSS) concentration of sludge and expressed in unit of seconds per litre per gram TSS	
The SRF units frequently used by previous researches includes; the square seconds per gram (s^2/g), centimetres per gram (cm/g) and meters per kilogram (m/kg) or tetrameters per kilogram (Tm/kg). The s^2/g was reported incorrect and cm/g was agreed as suitable. However, m/kg was reported as a more reliable choice for specific resistance in the SI system. The Tm/kg was consequently suggested to remove the use of bulky scientific representation	Gale 1967; Christensen 1983	An additional shortcoming in the CST measurement concerns the use of standard filter paper, especially the Whatman No. 17 chromatographic paper. Though this paper has been used globally, some limitations were reported which includes, anisotropic properties, relatively oversized pores and economic concerns. However, less expensive filters such as the Fisher 200 chromatographic papers can be used without considerably altering the range of estimated CST values	Sawalha and Scholz 2007

2.3.1.3 Extracellular Polymeric Substance (EPS) Content

In wastewater biological treatment process the microbes exist as activated sludge flocs and the sludge flocs consist of 50-60% polymeric substances as organic complex substances that serve as Gluing and cementing agent for holding firm together the sludge floc called extracellular polymeric substances (Wingender *et al.* 1999; Frolund *et al.* 1996). In addition, 20% of the total sludge particulate consists of humic substances like nucleic acids, uronic acids (Sheng *et al.* 2010; Dignac *et al.* 1998; Frolund *et al.* 1996; Mowla *et al.* 2013; D'Abzac *et al.* 2010). EPS does not just impact zeta potential where the EPS content demonstrate a positive impact on the net negative surface charge of sludge (Wang *et al.* 2005a; Wilén *et al.* 2003; Liao *et al.* 2002), activated sludge settleability and bio-flocculation (Yang and Li 2009; Jin *et al.* 2003; Liu *et al.* 2007; Morgan *et al.* 1990) but also impact activated sludge dewaterability which is of particular interest in this current study (Neyens *et al.* 2004; Houghton *et al.* 2001; Comte *et al.* 2007; Raszka *et al.* 2006). The relevance of EPS content in dewaterability of sludge can be understood from the characteristics of EPS capacity to adsorb to both internally and externally to microbial cells forming sturdy gel like and net like structure with huge water molecules that restrain the microbial cells pores from being easily dewatered (Mowla *et al.* 2013; Wingender *et al.* 1999).

EPS content has a negative impact on both settleability of activated sludge and bio-flocculation because EPS are negative charges and their adsorption to microbial cells will accelerate the surface negative charge of the microorganism causing an increased repulsive force between the microbial cells (Liu *et al.* 2007; Morgan *et al.* 1990). These increased repulsive forces will reduce the flocculent and settleability capacity of microbial aggregates and will further increase water retention in activated sludge flocs because of increased EPS content. This increased EPS content explains poor activated sludge dewaterability (Jin *et al.* 2003; Liao *et al.* 2002). Houghton *et al.* (2001) added that removal of the EPS gel-like structure from activated sludge will accelerate the optimisation of activated sludge dewaterability by releasing the trapped bound water. Although, the impact of EPS on sludge dewatering lies on the content of the EPS in activated sludge (Houghton *et al.* 2001), literature has provided further insights into EPS content called EPS threshold limit. The activated sludge dewaterability was enhanced with increasing EPS content and decreased beyond certain EPS content boundary. This may be attributed to the ability of low EPS content to be impacted by multivalent cations which makes them bind more tightly to microbial cells and optimised bio-flocculation and activated sludge settleability but on the contrary at accelerated EPS content the bound water by EPS structure will increase reasonably and decrease activated sludge dewaterability (Houghton and Stephenson 2002; Mowla *et al.* 2013).

2.3.1.4 Bound water Content

The bound water content is one of the key limiting rate factors that impacts activated sludge dewaterability performance. Wang *et al.* (2010); Lee and Hsu (1995) research findings on the correlation between dewatering energy requirement and activated sludge water content shows that the dewatering energy requirement decreased with increasing activated sludge water content. The result from Chu and Lee (1999) experiment on variation of bound water energy with residual water content of control and flocculated activated sludge agreed with the same assertion. As mentioned earlier based on Vesilind and Martel (1990); Colin and Gazbar (1995) research findings on categories of water in activated sludge, explains that bound water carries the capillary force and chemical bond that requires excessive energy to break it for trapped water to be released compared to the free water removable by gravity because it does not attach to solid particulate of biosludge (Wang *et al.* 2010; Chu and Lee 1999; Lee and Hsu 1995; Coumans and Kerkhof 1992).

Bound water measurement has been investigated and literature has provided previous numerous approaches namely; differential thermal analysis (Katsiris and Kouzeli-Katsiri 1987), water vapour sorption isotherms (Coumans and Kerkhof 1992), differential scanning calorimetry (Lee and Lee 1995; Lee *et al.* 1975), nuclear magnetic resonance (Mowla *et al.* 2013; Haschemeyer et al. 1977), suction pressure (Lewicki *et al.* 1978). But because of the absence of standard reference sludge for measurement, three main approaches have been provided for bound water content measurement namely; drying test (Vesilind and Hsu 1997; Lee and Hsu 1995; Robinson and Knocke 1992), constant pressure expression test (Chu and Lee 1999; Lee and Hsu 1995), dilatometry (Smith and Vesilind 1995; Robinson and Knocke 1992) and centrifugal settling test (Lee and Hsu 1995; Lee 1994a). In the constant pressure expression test, the bound water was estimated as the residual water content when it is in equilibrium with a constant applied pressure in the order of 20.7 mega pascal (Chu and Lee 1999; Lee and Hsu 1995). On the other hand, bound water was determined as the water content of sludge sediment using centrifugal settling test by subjecting test sludge to centrifugation under very high rotational speeds of 3500 to 4000 revolution per minute (rpm) (Lee and Hsu 1995; Lee 1994a). The bound water was estimated in the dry test on the claim that the resistance of bound water to evaporation should be larger than the free water (Vesilind and Hsu 1997; Lee and Hsu 1995; Robinson and Knocke 1992). The rate of drying of test sludge is plotted versus its moisture content at constant temperature so that water content equivalent to the shift points between drying periods can be recorded. As well, the Dilatometry method utilises equipment called a dilatometer. The experiment involve firstly including a measured concentration of sludge to some volume of measuring fluid xylene and hydraulic oil, which followed placing the dilatometer in a freezer at 20^0C for at least one night and standard cooling and freezing curves of distilled water and measuring fluid was used to estimate the concentration of contraction and expansion of each fluid and the corresponding freezable water was recorded and dry analysis was utilised to estimate the total water content (Smith and Vesilind 1995; Robinson and Knocke 1992). The bound water was obtained from the difference between the total water content and freezable water (Lee and Hsu 1995).

2.3.2 The Impact of Chemical Dosing on Activated Sludge Dewaterability

Over the years the capillary suction time (CST) and specific resistance to filtration (SRF) has been accepted as both an experimental and practical approach estimating activated sludge dewaterability globally (Xiao *et al.* 2019; Wang *et al.* 2019; Olivier *et al.* 2018). However, SRF relevance is based on its potentials in formulating a key dependent factor within the theoretical model for sludge filtration analysis Sawalha and Scholz (2010). The correlation between Carman 1938 supporting the claim of Darcy's law and Gale (1967) assuming the assertion of the incompressibility of the sludge cake nature and the negligibility of the filter media resistance has made the estimation of the volume of sludge that deposits its solid component on the filter cake practicable in calculating the SRF. It has served the purpose of sludge dewaterability indicator whilst account is taken for both the sludge concentration and mean SRF values within the experimental work station (Chen *et al*. 1996). Although, Kempa and Fukas-Plonka (1982) reported variability in the experimental protocol between various experimental setup as a key impact on SRF test results. However, filtration is a key aspect of the sludge dewatering process but the resistance to filtration is dependent on the hydraulic resistance of fluid in the sludge floc pores of the filter solid cake. Whilst, Neyens and Baeyens (2003) has identified causes for higher SRF of sludge dewaterability to be associated with rise in resistance from the filter cake solids and improved binding but Extensive CST and greater SRF value are indicators of poor sludge dewaterability (Feng *et al.* 2009; Wakeman 2007). On the contrary Scholz (2005) comments that CST values does not accommodate the solids content and experimental deduction of the solid content of the sludge becomes vital. In addition, claim was made that dewatering becomes effective when activated sludge with a reduced CST test value and high solids content is realised. The ultimate application of the CST and SRF test is to indicate the efficiency of sludge dewaterability during activated sludge dewatering process (ASDP) within wastewater treatment industries which is vital in this present study. In actualising the research demand of efficient activated sludge dewaterability, decreasing the sludge volume becomes a key option, since sludge water content of between 60 to 85% volume represents the activated sludge matrix (Lu *et al.* 2003). Vesilind and Martel (1990) reported that the free water component in the activated sludge structure can be released through gravity separation, but the bound water separation requires greater energy (Yu *et al.* 2008). The disruption of the gelatinous structure of activated sludge to activate the removal of the trapped bound water known as a limiting factor for sludge dewaterability has been reported achievable through chemical conditioning (Vaxelaire and Cezac 2004; Wu *et al.* 1998) and bio-flocculation has also been identified as a global industrial approach for solid-liquid separation during wastewater treatment processes (Letterman *et al.* 1999). Past research studies have identified destabilisation of colloidal particles through charge neutralisation and polymer bridging as key in sludge conditioning and the amount of coagulant utilised in achieving charge neutralisation defines the peak coagulant supplement in the sludge matrix (Higgins *et al*. 2006). Therefore, In order to realise the aim and objectives of this study, optimisation of the activated sludge dewaterability, appropriate sludge conditioning (increasing solid content of sludge through floc separation from liquid) option becomes vital. Sludge conditioning is the pre-treatment offered to sludge content before bio-sludge dewatering takes place. The sludge conditioning approach ranges from physical; non-chemical supplements which involves reduction in the sludge compressibility and increasing the solid content like fly ash (Chen *et al.* 2010; Wang and Viraraghavan 1997), rice shell (Lee *et al.* 2001), Coal (Hirota *et al.* 1975), lignite (Thapa *et al.* 2009), gypsum (Zhao 2006 and Zhao 2002) and acoustic and hydrodynamic cavitation (Huan *et al.* 2009; Khanal *et al.* 2006;Gogate and Kabadi 2009) which involves reduction of the pressure in the aqueous portion of sludge below equilibrium vapour pressure with microbubbles formation and collapses over an unstable diameter generating high temperature(500-15000K) and pressure (10-500MPa) in microseconds, thermal pre-treatment (Wang *et al.* 2010; Tuncal 2011 and Rai *et al.* 2001) involving the application of heat (60-80℃)to liquid sludge for cell wall destruction and protein release for bio-degradation process, and Freeze/Thaw pre-treatment (Franceschini 2010; Ormeci 2004; Vesilind *et al.* 1991;Martel 1993) involving changing the floc structure and lowering the bound water in the sludge structure based on water freezing point (-15℃) and thawing at room temperature to optimise the sludge dewatering characteristics, and chemical sludge conditioning; organic polymers like cationic, anionic, and non-ionic polymers (Dieude-Fauvel and Dental 2011; Bache *et al.* 2003; Dentel 2001) and inorganic polymers like conventional chemical additives including aluminium sulphate, ferric chloride and lime (Ruiz-Hernando *et al.* 2013; Higgins and Novak 1997b; Novak and Park 2004; Park *et al.* 2006; Nguyen *et al.* 2008a,b; Neyens *et al.* 2004); electrolysis process conditioning (Yuan *et al.* 2011); thermochemical conditioning (Ruiz-Hernando *et al.* 2013) and biological conditioning (Dursun *et al.* 2006; Ayol and Dental 2005; Thomas *et al.* 1993; Wawrzynczk *et al.* 2007; Sarkar 2004; Parmer *et al.* 2001) involving enzyme pre-treatment application to deteriorate the gelatinous sludge floc structure through the hydrolysis of EPS present in the sludge to optimise dewaterability of the sludge. Also, surfactants have been reported as a dewatering agent due to its ability to lower the surface tension between liquid and solid interfaces (Rosen 2004; Chen *et al.* 2001) and has the potentials to disrupt bacterial cell structure by separating cell materials from the bacterial cell structure and reducing the water content of the sludge flocs (Chen *et al.* 2004; Ruiz-Hernando *et al.* 2013; Neyens *et al.* 2004). Besides, some further investigation on the impact of sludge conditioning on CST and SRF was conducted and a minimum CST was reported at optimal dosage of acrylamide-based Zetag cationic polymer (Dieude-Fauvel and Dental 2011). This shows the importance of controlling polymer dosing regime because of potential impact of overdosing on increasing operational cost of WWTP. The negative impact of decreased sludge dewaterability was identified with too high polymer dosage and its presence in both treated and wastewater will have negative effect on human and biodiversity (Bohm and

Kulicke 1997). Wang *et al.* (2019), added that conventional coagulants such as ferric salts and polyaluminium chloride (PAC) can promote the release of bound water inside sludge particulates caused by hydrolysis and surface surface charge neutralisation.

Previous studies have reported that the efficiency of sludge pretreatment can be evaluated by the variations in CST (Ning *et al.* 2015). The optimum coagulant and flocculant dose required to condition the activated sludge corresponds to the lowest CST and SRF value (Olivier *et al.* 2018; Wu 2013). Many researches have been conducted to investigate the impact of different sludge conditioners on CST and SRF test result. The most typical multivalent cations used are trivalent ions. These have the capacity to change the sludge surface charge, particle size and floc strength, when added to sludge sample (Liu *et al.* 2017). Turchiuli and Fargues (2004) noticed that ferric chloride conditioning improves synthetic sludge dewatering rate as shown by the decrease of the capillary suction time (CST). Simultaneously, ferric sludge flocs adhere to water and increased the bound water content. Zhou *et al.* (2014) research findings on the impact of zero-valent iron (ZVI) and hydrogen peroxide (HP) on sludge dewaterability properties revealed substantial improvement with CST reduction rate increment from 31.4 to 50.7% at 500mgZVI/L and 33.2 to 48.7% at 250mgHP/L of sludge. The result of CST reduction rate increment using HP followed similar CST reduction rate (47 to 48.6%) using classical Fenton oxidation process (Tony *et al.* 2009; Buyukkamaci 2004). However, it was observed that increase in ZVI concentration from 500 to 750mg/L with continuous increase in Fe^{2+} from 192.5 to 256mgFe/L and HP with increase from 250 to 750mg/L showed no additional increase in the CST reduction rate. Martins *et al.* (2012), linked the reason for this contrary result for ZVI to be due to excess Fe^{2+} utilising the hydroxyl radical required for the oxidation reaction with the sludge flocs, while that of HP was reported to be associated with formation of hydroperoxyl a result of reaction between hydroxyl radical and HP which does not support its reaction with the sludge flocs. Wong *et al.* (2015), investigated the impact of pre-treated activated sludge with sulphuric acid and bioleaching using Acidithiobacillus ferrooxidans along with addition of Fe^{2+} on sludge dewaterability and reported improved sludge dewaterability from a control sludge void of Fe^{2+} (high CST of 356 s and SRF of 4.56×10^{12}m/kg) to a 2gFe/L treated sludge (CST of 15.5s and SRF of 5.4×10^{11}m/kg) after 24h of sludge treatment. As well, at optimum pH of 2.5 at 2gFe/L a 96% and 88% reduction in CST and SRF was achieved. Moreover, Zhang *et al.* (2012) contributed on the impact of potassium ferrate (K_2FeO_4) sludge dewatering and noticed a reduction in the SRF value and moisture content of initial filter sludge cake from 7.08×10^{9}m/kg and 86.13%, to 4.92×10^{9}m/kg and 75.35% when treated with 1200mg K_2FeO_4/l at pH of 3. This claim revealed that SRF value of the raw sample was approximately 1.5 times the SRF of the treated sludge at pH3, indicating that treating with potassium ferrate at pH3 was suitable for bound water release from the sludge floc pores. Literature findings showed investigation on the impact of potassium ferrate (K_2FeO_4) oxidation on sludge dewaterability

(Chen *et al.* 2012). Results of the study revealed SRF reduction from 18.6 x10^{12} to 2.7 x10^{12} m/kg with a maximum reduction of 85% when concentration of K_2FeO_4 dosage increased from 0 to 500mgK_2FeO_4/l sludge. On the contrary, the additional rise in potassium ferrate caused an increased SRF value but lower than that of the control sludge. This elucidate that K_2FeO_4 oxidation accounts for improved sludge dewaterability through a fragmented sludge floc and significant released bound water (Zhang *et al.* 2012). CST reduced from 58.7 to 61.8% and then to 88.8%, within 1 min when the concentration of persulfate ($S_2O^2{}_8$) increased from 0.1 to 0.3 and to 1.2 mmol/gVSS in the presence of 1.5 mmol/gVSS Fe^{2+}(Zhen *et al.* 2012). It was further noticed that the % CST reduction dropped when the concentration of the persulfate was added over 1.2 mmol/gVSS. This showed that Fe^{2+} has potential to stimulate persulfate ($S_2O^2{}_8$) so that production of sulphate radicals can be consistent and optimised sludge dewaterability through sludge CST reduction rate can be sustainable. Sludge conditioning was reported using electrochemical pre-treatment (Yuan *et al.* 2011) and result showed that when the electrolysis time was set as 15 min, the CST and SRF values reduced from 60.8 s and 8.67×10^{11} m/kg for untreated sludge to 45.5 s and $4.56 \times 10^{\ 11}$m/kg for treated sludge with an electrolysis voltage of 20 V. In contrast, When the electrolysis voltage was improved to 50 V, both the CST and SRF values speedily reached 79.4 s and $1.33 \times 10^{\ 12}$m/kg, increases of 30.59% and 53.4%, linked to the unconditioned sludge. This outcome revealed that small electrolysis voltage <20 V will optimise sludge dewaterability, while in excess of 30 V, sludge dewaterability declines. Buyukkamaci and Kucukselek (2007) reported 95% SFR and CST improved dewatering efficiency using optimum dosage of 0.9% mass fraction of initial bulk sludge for a cationic polyelectrolyte treatment while 8% alum dosage and 8-12 % lime dosage obtained 80.5 and 60% CST and SRF improvement. Nevertheless, Hou and Li (2003) initiated an optimum dosing of 15 mg $\mathrm{kg}^{\ -1}$ for another cationic polymer of polyacrylamide at which dewatering efficiency increased with reduction in both CST (20.95 s to 15 s) and SRF (1.33 to 0.13 Tm $\mathrm{kg}^{\ -1}$) respectively. In addition, the divalent cations was reported as an efficient chemical conditioner in activated sludge treatment (Guan *et al.* 2012). The report showed that calcium chloride can enhance the dewaterability of activate sludge by relating with the protein, phenols and hydroxyl functional group in the sludge flocs and neutralising the surface charge of flocs. It was further observed that the calcium ions destroyed the colloids double electrode layers, causing agglomeration of the sludge particles (Pevere *et al.* 2007). Research authors, reported 60 to 80% improvement in sludge dewatering using thermal conditioning in numerous full-scale installations with limitation of odour and corrosion and high strength which has been resolved using combined thermo-chemical pre-treatment with low temperature hydrolysis by acid or alkaline hydrolysis (Neyens and Baeyens 2003; Saha *et al*. 2011). Ayol (2005) and Ayol and Dental (2005) reported polymer conditioned sludge with low doses of (10-15 g/m^3) Enviro-Zyme 216 resulting in an increased sludge dewaterability in terms of CST and final solid content of cakes for two anaerobically digested sludge’s. The role of iron in determining the dewatering properties and floc structure was investigated by Novak *et al.* (2001), and the outcome was that the iron used for conditioning WAS protein was removed from solution and the CST decreased. This shows that the protein component of the biopolymer accounts for the dewatering difficulties and the release of protein into the solution was due to the reduction and solubility of Iron and weak attachment of protein to the bio-sludge floc. Wang *et al.* (2014), research reported that dose of anionic surfactant sodium dodecyl sulphate (SDS) does not just cause a significant release of EPS (protein) from sludge but result confirms an increased SDS dosage from 0.104 to 2.084 g/l leading to CST and SRF value of the control sludge to increase dramatically from 21.1s to 107.8s and 1.83 x 10^{13} m/kg to 1.15 x 10^{14} m/kg respectively. There was also a rise in the water content of sludge cake from 73.1 to 85.3% with increased SDS dose from 0.104 to 2.084 g/l. This shows a declination in the sludge dewaterability efficiency. However, a high positive correlations between the protein level and dewaterability parameters (CST (0.974), SRF (0.981) and moisture content of filter cake (0.903)) was further reported. These results showed that sludge dewaterability was considerably reduced when more proteins were released during the sludge pretreatment process. In this study focus will be on CST and not SRF.

2.3.3 Effects of funnel geometry and stirring on Activated sludge dewaterability

The capillary suction time (CST) device has two vital components namely; 10mm and 18mm diameter reservoir used for a quick and slow filtering of light and heavy sludges. The CST measurements are higher with the 10mm diameter compared to the 18mm diameter. However, a larger 18 mm diameter funnel is suitable for heavy sludges (primary sludges), because it significantly reduces the time taken to conduct the test (Scholz 2005). The CST test times using circular funnels are generally higher than when using rectangular funnels (Lee 1994a) and this was attributed to rectangular device capacity to solve the problem of anisotropic filter paper by making use of the unidirectional flow in only one direction.

The key issue with conventional CST test using a funnel (Figure 2.49) lies on the impact of sedimentation which is noticed with heavy sludges (Scholz 2005). The effect of sedimentation on heavy sludges like primary sludge can be explained through the accumulation of the sludge flocs and suspended matter on top of the test filter paper by gravity sedimentation. In the research study conducted by Lee and Hsu (1992) a rectangular funnel was identified to be a better option to cylindrical funnel for estimating the CST when a heavy sludge (high solid concentration and a high specific resistance to filtration) was used during the dewaterability analysis, but on the contrary cylindrical funnel was reported to be the preferred option when the sludge concentration, sedimentation, and cake resistance was low. The hypothetical explanation by Chen *et al.* (1995) who built upon the dynamic model of Lee (1994b) by including particle sedimentation and affirmed that sedimentation was the key limiting factor on the dynamics of capillary suction device when the wet front was large. Therefore, particle sedimentation may be ignored when the CST device wet front was small during the dewatering process. Subsequently, a small circular funnel is satisfactory for CST tests using secondary sludges with a low cake resistance and low sedimentation, whereas a larger circular or rectangular reservoir is superior for CST tests using primary sludges with an elevated cake resistance due to the impact of sedimentation.

Literature has made it obvious that one of the main issues with testing primary sludges using the CST device was the accumulation of suspended solids and heavy sludge flocs on the top of the filter paper during CST test process (Scholz 2006). The over estimation of the sludge cake resistance becomes an issue since the fundamental theory of the CST test procedure does not accommodate the impact of sedimentation (Bockstal *et al.* 1985; Christiansen and Dick 1985). It was also added that a flow of bubbles could be brought into the CST device to reduce sedimentation (Leu 1981). Scholz (2005) further suggested the introduction of a constant current using a stirrer within the sludge reactor (Figure 2.49) may reduce sedimentation and enhance the CST test result. Scholz (2006), commented that stirring had only a low impact on CST test but in unstirred heavy sludges sedimentation occurred. Scholz (2005; 2006) carried out subsequent studies involving the link between filter papers and stirring and discovered that stirring had higher impact on CST result in Whatman 17 filter paper compared to Fisher 200 chromatography (Chr) paper. On the contrary, it was noticed that the results of CST tests using Fisher 200 Chr papers were not so negatively impacted by sedimentation as the results using Whatman 17 Chr filter papers. This provided a direction and rationale for the current study as the choice of funnel and filter paper and sirring regime was taken into consideration during the dewatering test.

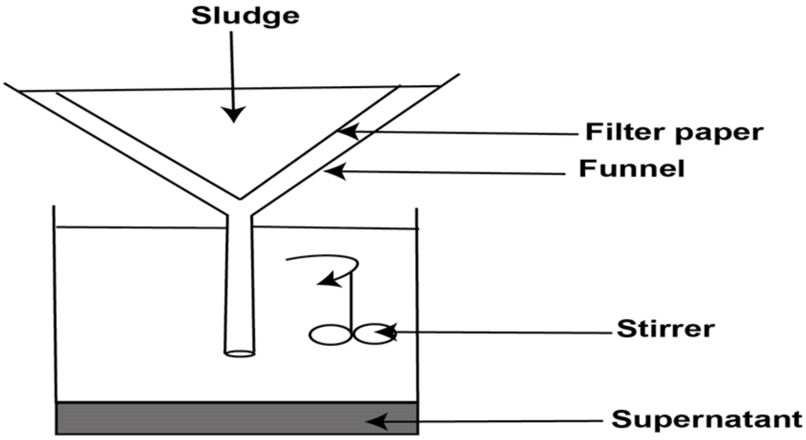

Figure 2.49. Schematic on how funnel geometry and stirring impact activated sludge dewaterability

Chapter Three

Materials and Methods

3.0 Introduction

This chapter presents materials and methods used in the study on optimisation of the design and operation of chemically dosed activated sludge plants and it is categorised into five sections. The first section (3.1) gives a brief description of the research area and unit process under study. The second section (3.2) gives description of the materials used in the research ranging from analytical reagent and glass ware. It also covers accounts of the equipment utilised, preparation of stand stock solution utilised in dosing chemicals during experimentation. The third section (3.3) covers data collection which included mixed liquor suspended solid test (MLSS-test), settleability test, capillary suction test (CST) and anaerobic digestion biogas production test. The fourth section (3.4) discusses statistical data analysis procedure and modelling of experimental and predicted data using solver optimisation tool and Minitab 17 software. In the final section (3.5) health and safety and waste disposal measures are described.

3.1 Activated Sludge Settleability, Digestibility and Dewaterability Sampling

Activated sludge samples (five batch sample with sample number N=40 was collected for aluminium dosed sludge; three batch sample with sample number (N) =24 was collected for ferric dosed sludge and two batch sample with sample number (N) =16 was collected for calcium sludge experimental analysis, (Appendix B)) were collected regularly over a three-year period (2014-2016) from the Minworth Wastewater Treatment Plant (WWTP) (Figure 3.1) in the West Midlands in the United Kingdom. The WWTP unit process is an activated sludge plant with an average design flow of 450 mega litres per day (ML/D) at full flow to treatment (FFT) of 1070 ML/D. It serves the treatment needs of 1.3 million population in 24 Aeration Lane with a capacity of 250,000 cubic metres and 54 circular FST in operation. Figure 3.2 shows half cross-section of a circular tank in Minworth treatment with a stilling well and its dimension while Table 3.1 further provides Minworth site flow data. The mixed liquor samples was collected in 32.5L plastic containers, from the distribution chambers prior to the final sedimentation tank (FST) before the chemical dosing point (Figure 3.1) and transferred to the laboratory-scale plant for analysis. All analysis was completed within 24 hours of sampling. The mixed liquor suspended solids (MLSS) concentration of the samples ranged from 2800 to 3500mg/L, with the pH ranging from 6.5 to 7.5 and a phosphate concentration of 7–12mg/L. All chemicals including aluminium sulphate, ferric chloride and calcium hydroxide used were of analytical grade and purchased from Sigma Aldrich (Gillingham, UK). All experiments were commenced within 24 hours of sampling and aluminium, ferric and calcium (Al^{3+} , Fe^{3+} and Ca^{2+}) salt were used for the CPR processes.

Minworth was chosen for this research because it represented the typical conventional activated sludge, and chemical dosing was carried out upstream of the aeration basin allowing the collection of mixed liquor samples without any chemical dosed.

Figure 3.1. Flow Scheme of Minworth Wastewater Treatment Plant (Everard 2009)

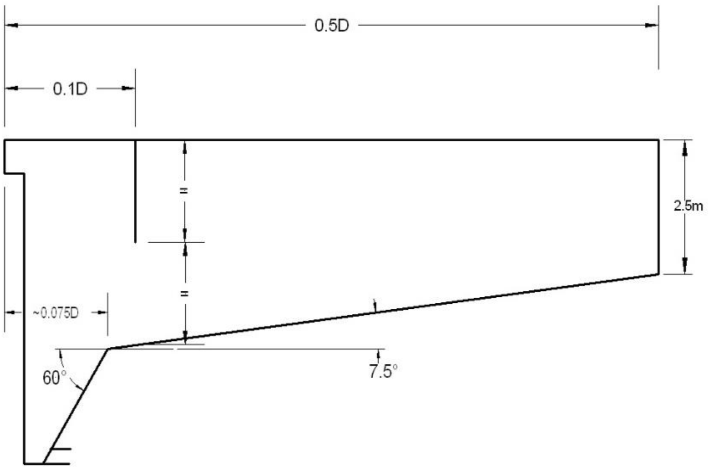

Figure 3.2. ASP-7 Minworth Severn Trent Water (STW) Hypothetical Tank with stilling well

Table 3.1. Site Flow Data of FST at the Minworth sewage works

Parameters and Formulae	Site Flow data
FFT (for 8 tanks)	77120 (m^3/day)
DWF	77120(m^3/day)
Normal = 1.2 x DWF	92544(m^3/day)
RAS = 0.5 x DWF	38560(m^3/day)

Maximum RAS = 1.5 x DWF	115680(m^3/day)
Influent MLSS	3.0g/l
Maximum SSVI	120ml/g

3.2 Materials

The following analytical reagents were used for this current research namely; Ferric chloride hexahydrate ($\mathrm{Fe\,Cl_3\,6H_2O}$); Aluminium sulphate Hexadecahydrate ($\mathrm{Al_2(SO_4)16H_2}$ O), calcium hydroxide (Ca$\mathrm{(OH)_2}$), Distilled water and Trigene disinfectant. The glassware and other wares required included; 20 millilitres (mL) and 50mL pipette, 2L(litres) beakers, 2L Flat round bottom flask, 1L Graduated measuring cylinders, 1000mL Volumetric flasks, Glass funnels, desiccators, spatula, mortar and pestle, wash bottles, filter paper: Whatman Glass Microfibre paper (GF/A), Ceramic crucible, Bio-Hazard Bags, Towels, Disposal Bags, Stop watch, Dropping pipette, Tweezers and Securing clips. The equipment's required included; Settlometer (Triton Electronics Limited 2018b: Type 305 SSVI Triton UK), Overhead stirrer, Desiccator, Oven (Gallenhamp Model OV-440 Registered Trademark), Manual Hand PH Meter, Autoclave Machine, Diaphragm Suction Pump, Buchner funnel, Side-arm conical flask, magnetic stirrer, Dwyer flex-tube series 1222 U-tube manometer containing red gauge fluid, Standard Capillary Suction Time (CST) apparatus (Triton Electronics Limited 2018a: Model 305B Triton UK).

3.2.1 Preparation of Standard Solutions of 1000ppm (part per million) for Aluminium, Ferric and Calcium Salt

The stock solution (1000ppm or mg/L) of Aluminium salt was prepared by completely dissolving 12.16g of hydrated aluminium sulphate with a purity level of 96.06% w/w in distilled water, while same procedure was followed for Fe (5.015g ferric chloride) and Ca (91.95g calcium hydroxide) salt. The procedure used to estimate how many grams of aluminium, ferric and calcium salt required from hydrated aluminium sulphate ($\mathrm{Al_2(SO_4)16H_2}$ O), Iron (III) chloride ($\mathrm{Fe\,Cl_3\,6H_2O}$) powder and calcium hydroxide (Ca$\mathrm{(OH)_2}$), with a purity level of 96.06%, 96.5% and 95.0% w/w, to prepare aluminium (Al), ferric (Fe) and calcium (Ca) standard stock solution in 1 litre with a target concentration of 1000mg/L Al, 1000mg/L Fe and 1000mg/L Ca respectively was explained in **3.2.1.1 to 3.2.1.3**

3.2.1.1 The preparation of stock solution of 1000ppm Fe

The procedure that was used to estimate how many grams Iron (III) chloride ($\mathrm{Fe\,Cl_3\,6H_2O}$) powder with a purity level of 96.5% w/w, will be required to prepare Iron (Fe) standard stock solution in 1 litre with a target concentration of 1000mg/L is explained below:

Fe was based on the proportionality method of mass-mole relationship (Equation 3.1). The mass of a chemical substance is directly proportional to its amount (n) in mole and it can be mathematically represented as follows:

$$\text{Mass (m)} \propto \text{Amount (n)} \tag{3.1}$$

$$\frac{\text{Mass (m)in grams}}{\text{Amount (n)in moles}} = \text{Constant} \tag{3.2}$$

Where,

Constant of proportionality = Molar mass (g/mol)

The molecular weight of $\mathrm{Fe\,Cl_3\,6H_2O}$ = 270.30g/mol

The atomic weight of Fe = 55.85g/mol

But,

1mole of $\mathrm{Fe\,Cl_3\,6H_2O}$ = 270.30g

1 mole of Fe = 55.85g/mol

The concentration (C) of Fe = 1000 ppm = 1000mg/L= 1g/L).

This implies that 1g of Fe in the 1L solution will be required. Also, 96.5 % w/w means 96.5g of $\mathrm{Fe\,Cl_3\,6H_2O}$ is present in 100g of the solution.

Therefore,

$$\mathrm{m(FeCl_3 6H_2O)} = \frac{270.30\mathrm{g}}{55.85\mathrm{g}} \times \frac{100.00\mathrm{g}}{96.50\mathrm{g}} \times 1.00\mathrm{g} \;= 5.0153\mathrm{g \text{ of } FeCl_3 6H_2O}$$

However, after the mass of the $\mathrm{Fe\,Cl_3\,6H_2O}$ was calculated, the lumps of the hexahydrated iron (III) chloride was ground using a mortar and pestle before it was weighed into a weighing boat. The weighing boat was first placed on the weighing balance to zero the equipment and afterwards, 5.0153g of the solid was weighed into the weighing boat which was then transferred into a beaker. It was vital to make sure all the solid are transferred and, to ensure this, the weighing boat was rinsed with distilled water from the wash bottle. More so, to ensure all the solids are dissolved additional distilled water was added and the beaker swirled. Also, for better consistency, a glass stirring rod was used. After satisfaction with the dissolution of all the solids the solution was transferred into the volumetric flask using a glass funnel. Furthermore, the beaker alongside with the glass funnel was rinsed with distilled water two to three times to ensure none of the original solution was left behind. Consequently, immediately the rinsing process was completed, the stopper was placed into the volumetric flask. The flask was then shaken to ensure all the solids are in solution. Following this further, the flask was filled to the line mark using distilled water from the wash bottle and care was taken to ensure when getting close to the line that the addition of water is done drop wise using a dropping pipette. The eye level was also fixed on the point at which the bottom meniscus of the solution touches the line mark of the flask to avoid the error of over shooting the line. Finally, once this was achieved, the flask was stoppered firmly in place and homogeneity of the solution was attained by gently inverting and shaking the flask.

3.2.1.2 The preparation of stock solution of 1000ppm Al

The procedure that was used to estimate how many grams of aluminium salt will be needed from hydrated aluminium sulphate($\mathrm{Al_2(SO_4)\ 16H_2}$O) with a purity level of 96.06% w/w, to prepare alum (Al) standard stock solution in 1 litre with a target concentration of 1000mg/L Al was equally based on the proportionality method of mass-mole relationship (Equation 3.1 and 3.2) used for ferric salt.

The molecular weight of $\mathrm{Al_2(SO_4)16H_2O = 630.14g/mol}$

The atomic weight of Al = 53.964g/mol

But,

1mole of $\mathrm{Al_2(SO_4)16H_2O = 630.14g}$

1 mole of Al = 53.964g/mol

The concentration (C) of Al = 1000 ppm = 1000mg/lL= 1g/l).

This implies that 1g of Al in the 1L solution will be required. Also, 96.06% w/w means 96.06g of $\mathrm{Al_2(SO_4)16H_2O}$ is present in 100g of the solution.

Therefore,

$$\mathrm{m(Al_2(SO_4)16H_2O)} = \frac{630.14\mathrm{g}}{53.964\mathrm{g}} \times \frac{100.00\mathrm{g}}{96.06\mathrm{g}} \times 1.00\mathrm{g}\ = 12.156\mathrm{g\ of\ Al_2(SO_4)16H_2O}$$

However, after the mass of the $\mathrm{Al_2(SO_4)\ 16H_2}$ O was calculated, it was weighed into a weighing boat. The weighing boat was initially placed on the weighing balance to zero the equipment and afterwards, 12.156g of the solid will be weighed into the weighing boat which is then transferred into a beaker. It was vital to make sure all the solids are transferred and to ensure this, the weighing boat was rinsed with distilled water from the wash bottle. More so, to ensure all the solids are dissolved additional distilled water was added and the beaker swirled. Also, for better consistency, a glass stirring rod was used. After satisfaction with the dissolution of all the solids the solution was transferred into the volumetric flask using a glass funnel. Furthermore, the beaker alongside with the glass funnel was rinsed with distilled water two to three times to ensure none of the original solution is left behind. Consequently, immediately the rinsing process was completed, the stopper was placed into the volumetric flask. The flask was then shaken to ensure all the solids are in solution. Following this further, the flask was filled to the line mark using distilled water from the wash bottle and care was taken to ensure when getting close to the line that the addition of water is done in drop wise using a dropping pipette. The eye level was also fixed on the point at which the bottom meniscus of the solution touches the line mark of the flask to avoid error of over shooting the line. Finally, once this was achieved, the flask was stoppered firmly in place and homogeneity of the solution was attained by gently inverting and shaking the flask.

3.2.1.3 The preparation of stock solution of 1000ppm Ca

The procedure used to estimate how many grams will be needed from calcium hydroxide (Ca$(\mathrm{OH})_2$)with a purity level of 95.0% w/w, to prepare calcium (Ca) standard stock solution in 1litre with a target concentration of 1000mg/L Ca will be based on the proportionality method of mass-mole relationship (Equation 3.1 and 3.2)

Hence, from Equation 3.1 the following holds:

The molecular weight of $\mathrm{Ca(OH)_2} = 40.08\mathrm{g/mol}$

The atomic weight of Ca = 74.09 g/mol

But,

1mole of $\mathrm{Ca(OH)_2} = 40.08\mathrm{g}$

(Ca$(\mathrm{OH})_2$) = 40.08g

1 mole of Ca = 74.09 g/mol

The concentration (C) of Ca = 1000 ppm = 1000mg/lL= 1g/L).

This implies that 1g of Ca in the 1L solution will be required. Also, 95.0% w/w means 95.0g of $\mathrm{Ca(OH)_2}$ is present in 100g of the solution.

$$\mathrm{m(Ca(OH)_2)} = \frac{74.09\mathrm{g}}{40.08\mathrm{g}} \times \frac{100.00\mathrm{g}}{95.00\mathrm{g}} \times 1.00\mathrm{g} \; = 1.95\mathrm{g\ of\ Ca(OH)_2}$$

However, after the mass of m ($Ca(OH)_2$) was calculated, it was weighed into a weighing boat and the weighing boat was first being put on the weighing balance to zero the equipment and afterwards, 1.95g of the solid was weighed into the weighing boat which was then transferred into a beaker. It was important to make sure all the solid are transferred and to ensure this, the weighing boat was rinsed with distilled water from the wash bottle. More so, to ensure all the solids are dissolved additional distilled water was added and the beaker swirled. Also, for better consistency, a glass stirring rod was used. After satisfaction with the dissolution of all the solids the solution was transferred into the volumetric flask using a glass funnel. Furthermore, the beaker alongside with the glass funnel was rinsed with distilled water two to three times to ensure none of the original solution is left behind. And again, immediately the rinsing process was completed, the stopper was placed into the volumetric flask. The flask was then shaken to ensure all the solids are in solution. Following this further, the flask was filled to the line mark using distilled water from the wash bottle and care was taken to ensure when getting close to the line that the addition of water is done in drop wise using a dropping pipette. The eye level was also fixed on the point at which the bottom meniscus of the solution touches the line mark of the flask to avoid error of over shooting the line. Finally, once this was achieved, the flask was stoppered firmly in place and homogeneity of the solution was attained by gently inverting and shaking the flask.

3.3 Data Collection

The data collection for activated sludge settleability, digestibility and dewaterability test was conducted through sampling from Minworth WWTP over three years period as earlier mentioned. However, surplus activated sludge (SAS) samples were collected from the aeration zone prior to any chemical dosing. For samples collected for the digestibility test, bioaugmentation was carried out by seeding with digested sludge collected from the anaerobic digestion zone to ensure sufficient volatile fatty acid (VFA) is available for the anaerobic digestion procedure. Also, during the sludge seeding process it was ensured that all the batch tested sludges were inoculated with the same digested sludge to avoid differences in the degradation process of the substrate utilised (Moreno-Andrade and Buitron 2004; Smith 2006). More so, in order to reduce the impact of both related site-specific variables (sludge age, wastewater composition and chemical dosage) and experimental variables (sludge storage, anaerobic digester organic loading and seed sludge) the surplus activated sludge (SAS) was successfully chemically (Ferric and Aluminium) simulated in a laboratory batch scale tests by constantly keeping the experimental condition in place. All analysis (settlometer test, mixed liquor suspended solids (MLSS), digestibility and dewaterability test) was completed within 24 hours of sampling because research findings showed that longer storage times reduces biogas generation due to the degradability of the readily biodegradable carbon (Smith and Carliell-

Marquet 2009). Aluminium (Al^{3+}), Ferric (Fe^{3+}) and Calcium (Ca^{2+}) were used as a sludge coagulant for phosphorus removal. Appendix B shows the sampling schedule (sampling phase and testing) for the impact of Al, Fe and Ca on activated sludge settleability, digestibility and dewaterability. The sample number considered for aluminium dosed sludge was N= 40 over dosing concentration boundary of 0, 10, 20, 30, 40, 50, 100, 150mg/L for five batch sampling, while Ferric (five batch sampling) and calcium (two batch sampling) dosed sludge were N= 24 and N= 16 respectively. Appendix D shows the table of cummulative Biogas Volume Production for Aluminium (Al^{3+}) and Ferric (Fe^{3+}) Dosed and Undosed surplus activated sludge (SAS) for (12days). The settlometer test, morphological analysis with scanning electron microscope (SEM), mixed liquor suspended solids (MLSS), digestibility and dewaterability test will be further explained in sections 3.3.1 to 3.3.5 respectively.

3.3.1 Settlometer test

The mixed liquor samples were mixed gently by swirling the container in an air tight condition, so that the flocs are not broken and no air was entrapped into the sample container. 3250mL of the mixed sample was transferred into a 5L beaker and treated with a varing concentration of aluminium, ferric and calcium salt (0, 10, 20, 30, 40, 50, 100, 150mg/L). The samples were stirred for 10 minutes at 2 revolutions per minute (rev/min) using an overhead stirrer (Figure 3.3) before being used for the settlometer test.

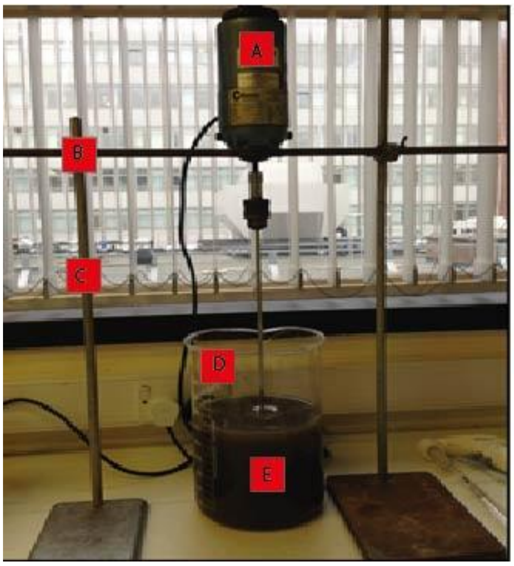

A= Overhead stirrer used for 10minute stirring at 2 revolution per minute
B = Clamp
C= Retort Stand
D = Five (5) lires (L) Beaker
E= Aluminium, Ferric and Calcium dosed sludge stirred in a 5L Beaker

Figure 3.3. The overhead stirrer used to achieve a 10 min mixing effect

The standard Water Research Council (WRc) settling test (Ekama *et al.*1997) was performed in a 3.25L type 305 settlometer equipment (Triton Electronics Limited 2018b: Type 305 SSVI Triton UK) (Figure 3.4) with 100mm diameter and 500mm height , a slow speed stirrer(1rev/min) used to prevent any event of sludge bridging to the wall. The process has been previously described by MCR (2008).

Figure 3.4. Type 305 Settlometer Test (Triton Electronic Limited 2018b)

The settled solid volume (SSV) (mL/L), mixed liquor suspended solids (MLSS) (g/L), SSVI (mL/g) and ZSV (m/h) result was obtained from the following Equation 3.1 to 3.7**;**

$$\mathrm{ZSV\ (m/h)} = \frac{(\mathrm{H_2} - \mathrm{H_1}) \times 0.6}{(\mathrm{T_2} - \mathrm{T_1})} \tag{3.1}$$

$$\mathrm{SSV\ (mL/L)} = \frac{\text{Volume of Settled Sludge after 30 mins,ml} \times 1000\ \mathrm{mL/L}}{\text{Sample Volume,mL}} \tag{3.2}$$

$$\mathrm{SSVI\ (mL/g)} = \frac{\text{Volume of Settled Sludge after 30 mins }, \frac{\mathrm{mL}}{\mathrm{L}}(\frac{1000\mathrm{mg}}{\mathrm{g}})}{\text{MLSS Concentration,mg/L}} \tag{3.3}$$

When the initial height is equal to 50cm SSVI was calculated from Equation 3.4 while when the initial height is not equal to 50cm Equation 3.5 was utilised.

$$\mathrm{SSVI\ (mL/g)} = \frac{\text{Final Height of the blanket (cm)} \times 20000}{\text{MLSS Concentration (mg/L)}} \tag{3.4}$$

$$\mathrm{SSVI\ (mL/g)} = \frac{\%\, volume}{\%\, solid} = \frac{\text{Initial Height of the blanket (cm)} \times 100}{\text{MLSS Concentration } \left(\frac{\mathrm{mg}}{\mathrm{L}}\right) \times 10{,}000} \tag{3.5}$$

$$\%\, Solid = \frac{\text{MLSS (g/L)}}{10{,}000} \tag{3.6}$$

$$\%\, Volume = \frac{\text{Final Height (cm)}}{\text{Initial Height (cm)}} \times 100 = \tag{3.7}$$

where,$\mathrm{H_2}$ is the initial height of the settlometer cylinder (cm), $\mathrm{H_1}$is the height of the final point selected on the gradient (cm), $\mathrm{T_2}$ is the time of the final point selected on the gradient (min), $\mathrm{T_1}$ is the 0 (min) and MLSS is the mixed liquor suspended solids (g/L).

3.3.2 Morphological Analysis with Scanning Electron Microscope(SEM)

The variability in the morphology of the sludge floc quality in tested activated sludge sample in the laboratory-scale plant was examined using the scanning electron microscope (SEM -Joel-6060LV) (Figure 3.5). The sludge morphological investigation was conducted for both the control and aluminium, ferric and calcium treated sludge samples.

Figure 3.5. SEM - Joel JSM-6060LV

3.3.3 Mixed Liquor Suspended Solids test (MLSS-test)

The MLSS test was conducted using a vacuum filter mechanism (Figure 3.6). This consisted of a Buchner funnel connected to a side-arm flask by means of a neoprene adapter with a tube leading to a vacuum pump. The advantage of the vacuum filtration mechanism is that it allows the liquid to drain quickly through the filter medium compared to conducting filtration by force of gravity. The protocol involved first and foremost the use of a tweezers to take a GF/A filter paper and weighed using a weighing balance and the reading was recorded. The vacuum filter mechanism was then set up and the filter paper was weighed and placed into a filter base placed in a 2L filtering flask with a short-side arm connected to a vacuum equipment to achieve filtration under suction. Distilled water was used to wet the edges of the filter paper placed in the filter base to ensure the filer paper covers the voids in the filter base and afterwards the equipment was turned on and 1000mL of the MLSS sample was poured over the filter as close to the centre as possible using a measuring cylinder. The measuring cylinder was rinsed with distilled water onto the filter and then all the liquid was left to drain into the flask before removing the filter paper.

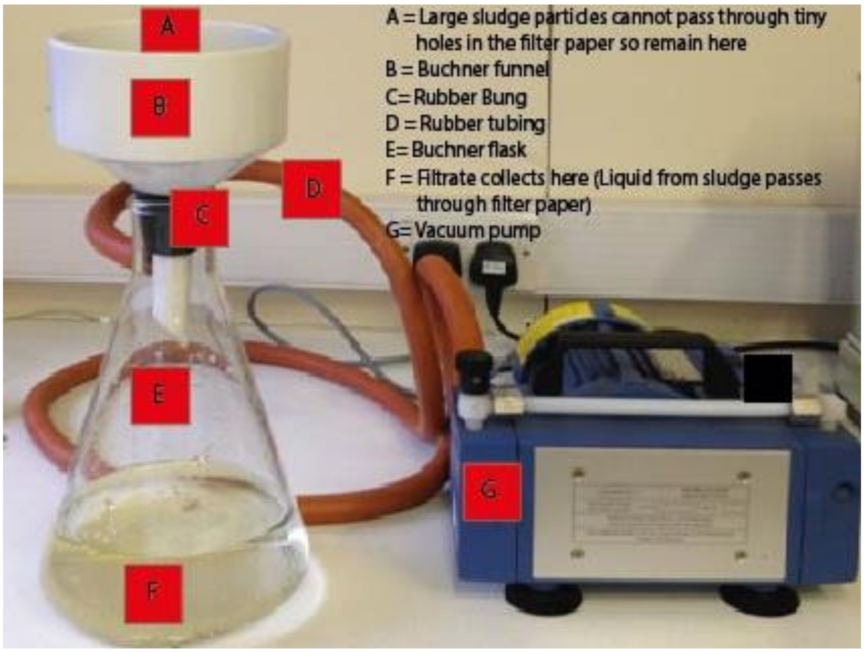

Figure 3.6. Filter Vacuum Mechanism

The wet filter paper with the activated sludge was then be placed on a glass plate using tweezers and this was then oven dried (Gallenhamp Model OV-440 Registered Trademark) at a temperature of 140℃ for 37 min and the oven dried sludge cake with filter paper was removed from the oven using the tweezers and then weighed to obtain the dry weight of filter paper and sludge cake. The MLSS result was obtained from Equation 3.8:

$$(MLSS\ (\mathrm{g/L})\ = (\mathrm{W}_2 - \mathrm{W}_1) \times 1000 \qquad (3.8)$$

Where, W_2 is the Weight of Filter Paper and Dried Sludge Cake and W_1 is the Weight of Empty Filter Paper.

3.3.4 Digestibility test

Two quantities of 2L flat round-bottom flasks were used as the laboratory digester for both the Fe^{3+} and Al^{3+} dosed samples alongside their respective controls. The two bioreactors (digesters) containing the SAS were made up of one as the test (chemical-dosed sludge) and the other as the control (Figure 3.7). As a control, 1500 mL of SAS was measured without chemical and transferred into the first flat round-bottom flask. To give it some organic carbon, 20.5g of sucrose was added, which facilitated readily degradable carbon, and a magnetic stirrer was used to give it slow stirring to promote uniformity of the sample in the digesters. From the anaerobic sludge tank, 40g of sludge was used for bioaugmentation to enhance and speed up the microbial activities. They were also flushed with nitrogen gas to ensure anaerobic conditions. The second flat round-bottom flask containing the same sample was then pretreated with 200 mL of 100mg/L as Fe^{3+} solution. The experiments were also repeated with 100mg/L as Al^{3+} solution. Initial jar tests showed that phosphorus levels were reduced to <0.5mg/L between 50 and 100mg/L doses of the metal salts. The maximum dose of 100mg/L was then chosen for the digestion experiments. The test and control sludge samples were digested at mesophilic temperatures (35°C) for 12 days until the biogas production subsided. The temperature of digestion was maintained at 35°C throughout the experiment as most mesophiles grow best within the temperature range of 30–35°C (Yong *et al.* 2015; Zhu *et al.* 2017; Farooq *et al.* 2017; Gerardi 2003). The experiments were repeated in triplicate, and average data are reported. The digestibility of the test and control sludge was evaluated by measuring the biogas volume using a manometer (Dwyer flex-tube series 1222 U-tube manometer containing red gauge fluid Michigan, USA.). All digestibility experiments were commenced within 24 hours of sampling, as findings have shown that longer storage times reduce biogas generation due to the degradability of the readily biodegradable carbon (Smith and Carliell-Marquet 2008). The result for control and Ferric (Fe) for Batch 1, 2 and 3 are illustrated in Figure 7.2 (Chapter 7). The experiment was repeated using aluminium coagulant (Al) (100mg/L) and the result for un-dosed and aluminium dosed sludge for batches 1, 2 and 3 are also illustrated in Figure 7.1 (Chapter 7).

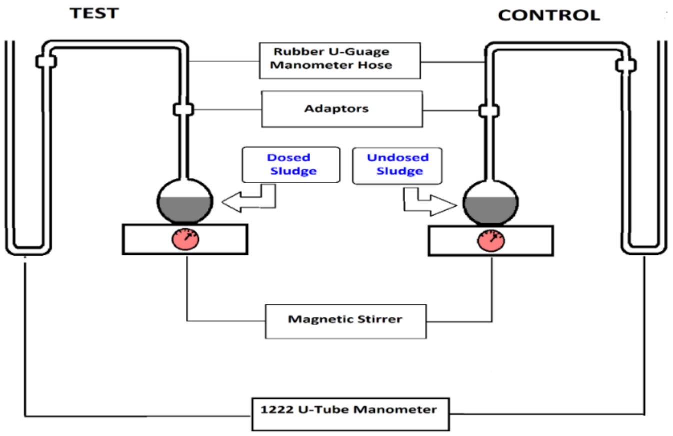

Figure 3.7. Biogas Anaerobic Digestion for Test and Control Set-up

3.3.5 Dewaterability test

A series of laboratory batch scale experiments were conducted in 1000mL beakers with a sludge sample of 500mL. The experimental reaction was initiated immediately by adding volumes of Aluminium (Al^{3+}), Ferric (Fe^{3+}) and Calcium (Ca^{2+}) (0, 10, 20, 25 and 50mls) to each beaker containing 500mls of sludge. The homogeneity of the sludge mixture was ensured throughout the reaction by stirring at 2 revolutions per minute (2rpm) using an overhead stirrer. Then, 25mL of the control and Aluminium, Ferric and Calcium (10, 20, 40, 50mg/L) was collected and analysed using a standard Triton UK-Type 304B capillary suction time (CST) device (Essex, UK) (Triton Electronics Limited 2018a), equipped with a 18mm reservoir resting on a standard Whatman No.17 grade chromatography paper. The dewaterability of the sludge was monitored using the CST dewaterability parameter. Three replicates of each dewaterability condition were performed with the samples analysed in triplicate to ensure the reproducibility of the experimental test results, and the mean values of CST were then recorded and reported. The details of the experimental procedures have been previously described in detail by Scholz (2005) and Sawalha and Scholz (2007; 2010). All the test results reported are the means and standard deviation of three independent samples.

The improvement of sludge dewaterability using sludge conditioners Aluminium, Ferric and Calcium) was evaluated using the Equation 3.9 for reduction percentage of CST ($\mathrm{R}_{\%}$):

$$\mathrm{R}_{\%} = {(\mathrm{CST}_0 - \mathrm{CST}_\mathrm{d})}/{\mathrm{CST}_0} \times 100 \tag{3.9}$$

Where,

CST_0 = Initial Sludge CST(s)

CST_d = Sludge CST after chemical dosing (s)

The CST device components include; CST Meter, Perspex block assembly, stainless steel funnel (18mm and 10mm diameter reservoir) and filter papers (Whatman 17.0 Grade). The CST test was carried out by pouring the primary and secondary test samples into the 18mm and 10mm diameter reservoir placed on Whatman 17.0 filter paper. The filtrate is drained from the reservoir through the capillary suction effect of the filter paper so that a filter cake is formed on the filter paper. This reveals that CST test value is not influenced by the mass of liquid in the reservoirs, provided that the liquid capacity can generate the required suction pressure (Smeulders and Meeten 1995). The fluid soaks the paper and disseminate outwards in a circular shape based on the viscosity of the filtrate and filterability of the sludge. The sludge cake resistance (m/s) is measured based on the distance the filtrate travels along the paper as function of time. The filter resistance is taken as negligible while the CST value is calculated as the time taken for the filtrate to travel between two (2) concentric and adjustable circles on the filter paper (Figure 3.8).

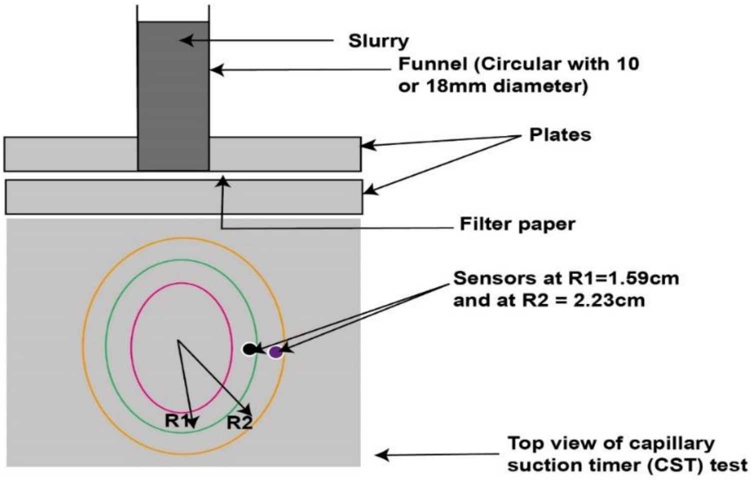

Figure 3.8. Pictorial View of Capillary Suction Time Test Device

Although, CST test suffers from limitations tied to incomparability of test data using different types of sludge and the potential of replicated test producing variable result, but Scholz (2005,2006) has requested more concentration on the precision of CST result and this current research will fill this gap by building it into the CST test assessment. More details on the CST device operation and protocol are reported in Baskerville and Gale (1968). Although there is another dewaterability indicator test called the specific resistance of cake to filtration (SRF) reported in Carman (1938); Gale (1967); Lo *et al.* (2001); Smeulders and Meeten (1995). However, for this current study, CST was utilised.

3.4 Data Analysis and Model Validation

The measured ZSV and SSVI from the three years batch settling tests were used in modelling new Aluminium (Al^{3+}), ferric (Fe^{3+}) and calcium (Ca^{2+}) dosed activated sludge settleability. Typical result of the data set of batch tests was analysed using the Minitab 17 software and solver optimisation tool. The solver optimisation tool allows the solver parameter to be set for the target objective of a reduced sum of square deviation (SSD) value so that the model fits the experimental data while the minitab 17 allows the design of an experimental model for investigation of the impact of input variables on the response variable at the same time. Results were also analysed using the non-linear regression in the minitab 17 software (Minitab Inc. 2016) and the F-test ($F>0.05$), lack of fit test ($P>0.05$), R^2 (coefficient of determination), residual plot, probability plot and interval plot was used to validate how the ZSV model fits the ZSV experimental data.

The non-linear regression was used because the proposed operational curve demonstrated a non-linear correlation. This non-linear regression analysis produces an equation that explains the non-linear relationship between a continuous response variable and one or more predictor variables and predicts new observations. This was utilised since the parameters are not linear and cannot be modelled using the ordinary least squares regression model the correlations with linear parameters. The description of the function that satisfy both the prior knowledge about the shape of the expected response curve (exponential growth or decay curve) and non-linear assumptions for modelling the revised chemically dosed (Aluminium, Ferric and Calcium) activated sludge settleability equation was provided in the solver optimisation tool procedure (section 3.4.1). Figure 3.9, shows a pictorial view of the solver optimisation tool. This mathematical modelling will not just provide representation of real life situation using mathematical equation but will further predict their future behaviour which is key in decision-making. Further analysis was conducted using statistical Minitab time series procedure that uses a simple forecasting and smoothing method. This analyses data collected over time called a time series and decomposes the data into its component parts (impact of Aluminium, Ferric and Calcium on ZSV actual and model) and extends the evaluation of the components into the future to provide forecasts as a decision making tool. The revised activated sludge settleability model realized in Chapter Four, Five and Six was designed to analyse the effects of Aluminium (Al^{3+}), Ferric (Fe^{3+}) and Calcium (Ca^{2+}) dosing concentrations on activated sludge settleability indicators; zone settling velocity (ZSV) and stirred specific volume index (SSVI) using linear transformation of polynomials and exponential functions to achieve replication of a non-linear correlation between the Al^{3+}, Fe^{3+} and Ca^{2+} dosing concentrations and settleability indicators (ZSV and SSVI).

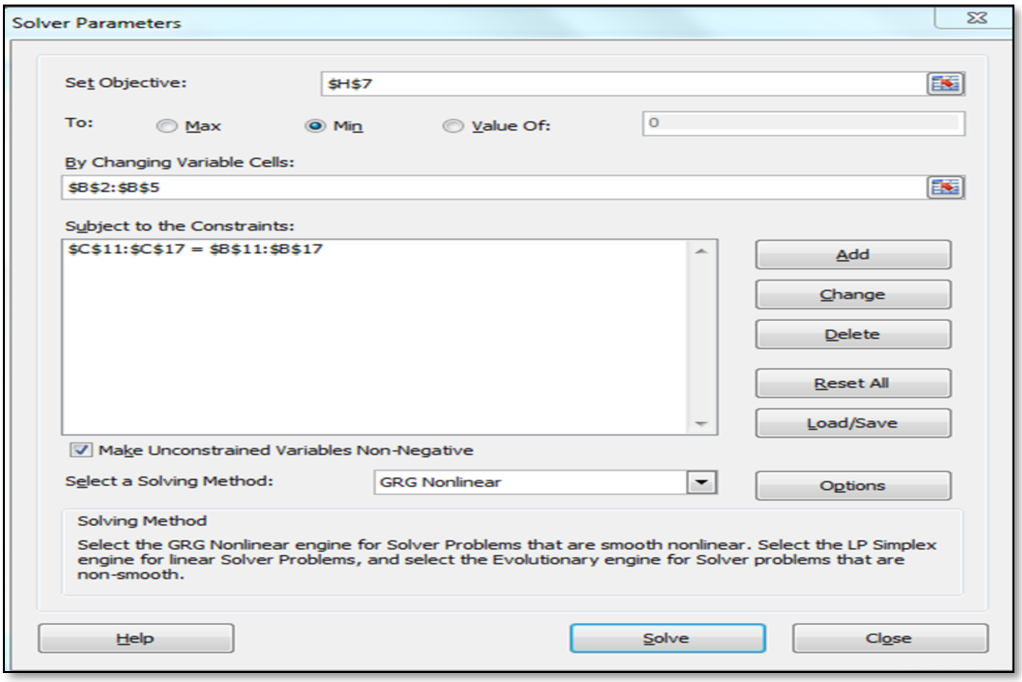

Solver Parameters

Set Objective: $H$7

To: ○ Max ● Min ○ Value Of: 0

By Changing Variable Cells: $B$2:$B$5

Subject to the Constraints: $C$11:$C$17 = $B$11:$B$17

☑ Make Unconstrained Variables Non-Negative

Select a Solving Method: GRG Nonlinear

Solving Method

Select the GRG Nonlinear engine for Solver Problems that are smooth nonlinear. Select the LP Simplex engine for linear Solver Problems, and select the Evolutionary engine for Solver problems that are non-smooth.

Figure 3.9.Solver optimisation tool

3.4.1 Solver optimisation tool procedure

Step1 Experimental Test data

It requires an actual data which in this current research is the ZSV and SSVI experimental data collected during a laboratory batch settling test. A column with time values for settleability after 30 minutes was entered into the cells of an excel spreadsheet and the actual ZSV experimental data collected was inserted into another column.

Step 2 Mathematical Model that fits the ZSV operational curve

Based on the law of exponential decay, the actual data should follow a proposed mathematical model provided in the Equation 4.1, 5.3 and 6.3 (Chapters Four, Five and Six) that fits the zone settling velocity (ZSV) operational curves which was then entered into the excel spreadsheet.

$$\mathrm{ZSV_{Al}} = ((\mathrm{C_0})_{\mathrm{Al}}\,(\mathrm{D_C})_{\mathrm{Al}} + (\mathrm{ZSV_0})_{\mathrm{Al}})\mathrm{e}^{-((\mathrm{K_d})_{\mathrm{Al}}-(\mathrm{C_K})_{\mathrm{Al}}(\mathrm{D_C})_{\mathrm{Al}})\mathrm{X_{Al}}} \qquad (4.11)$$

$$\mathrm{ZSV_{Fe}} = ((\mathrm{C_0})_{\mathrm{Fe}}\,(\mathrm{D_C})_{\mathrm{Fe}} + (\mathrm{ZSV_0})_{\mathrm{Fe}})\mathrm{e}^{-((\mathrm{K_d})_{\mathrm{Fe}}-(\mathrm{C_K})_{\mathrm{Fe}}(\mathrm{D_C})_{\mathrm{Fe}})\mathrm{X_{Fe}}} \qquad (5.3)$$

$$\mathrm{ZSV_{Ca}} = ((\mathrm{C_0})_{\mathrm{Ca}}\,(\mathrm{D_C})_{\mathrm{Ca}} + (\mathrm{ZSV_0})_{\mathrm{Ca}})\mathrm{e}^{-((\mathrm{K_d})_{\mathrm{Ca}}-(\mathrm{C_K})_{\mathrm{Ca}}(\mathrm{D_C})_{\mathrm{Ca}})\mathrm{X_{Ca}}} \qquad (6.3)$$

From this model the known values are the values of actual zone settling velocity (ZSV), activated sludge concentration (X) and dosing concentration protocol (Dc). The unknown parameters ZSVo, $\mathrm{C_O}$, $\mathrm{K_d}$ and $\mathrm{C_K}$ were identified from the model and inserted in various cells within the excel spreadsheet. A non-linear parameter fitting was used to determine the values of the unknown parameters for aluminium, ferric and calcium dosed sludge with sample numbers (N=40; N=24 and N=16).

Step 3 Plot of ZSV Operational Curve and ZSV model Curve

The initial stage of the non-linear parameterisation involved plotting all the data of the ZSV as a function of chemical dosing (Al^{3+}, Fe^{3+} and Ca^{2+}) concentration to check if the data is a linear or non-linear correlation. Also, it was observed that using the built in excel function there are no function that will give us the observed behaviour of a non-linear representation of ZSV and SSVI as a function of aluminium, ferric and calcium dosing concentration as reported in Figure 4.2 and 4.3 (Chapter Four); Figure 5.2 and 5.3 (Chapter Five) and Figure 6.2 and 6.3 (Chapter Six) and hence the non-linear parameterisation was utilised. The actual mean values of ZSV data were plotted against the chemical dosing (aluminium, ferric and calcium) concentration and a non -linear curve was obtained**.** Dummy value of a number 1 was entered for each of the four unknown($(\mathrm{ZSV_0})_{\mathrm{Al}}$; $(\mathrm{K_d})_{\mathrm{Al}}$; $(\mathrm{C_0})_{\mathrm{Al}}$ and $(\mathrm{C_K})_{\mathrm{Al}}$, $(\mathrm{ZSV_0})_{\mathrm{Fe}}$; $(\mathrm{K_d})_{\mathrm{Fe}}$; $(\mathrm{C_0})_{\mathrm{Fe}}$ and $(\mathrm{C_K})_{\mathrm{Fe}}$ and $(\mathrm{ZSV_0})_{\mathrm{Ca}}$; $(\mathrm{K_d})_{\mathrm{Ca}}$; $(\mathrm{C_0})_{\mathrm{Ca}}$ and $(\mathrm{C_K})_{\mathrm{Ca}}$) settleability coeffiicents for aluminium, ferric and calcium dosed sludge. The ZSV model curve was plotted by adding another series of curve to the actual ZSV curve. The dummy values were used to test run the effect of changing the various unknown values. The essence of adding the ZSV model to the existing actual ZSV was to predict the output data of the actual ZSV and use the changing unknown values to obtain a ZSV model value that matches the existing ZSV experimental data.

Step 4 Adjustment of the unknown parameters

The dummy value assigned to the unknown parameters was adjusted because the output data of the ZSV model does not fit the actual ZSV model. Different values were used to predict the ZSV model data that fits the actual ZSV data and the effect of the variation was observed to know the set of values that can be tested.

Step 5 Calculating Deviations

In a linear fitting, deviations are used to check how well model data fits the actual data measured. The same approach applies in a non-linear model and as such measurement of deviation is vital in obtaining a set of ZSV model data that predicts the actual ZSV data. In achieving this, the column was created on an excel spreadsheet to calculate the squared deviation (SD) using Equation 3.10. This gives the squared residual error between the model and the actual (experimental) ZSV measured.

$$\mathrm{SD} = (\mathrm{ZSV\ Experimental} - \mathrm{ZSV\ Model})^2 \qquad (3.10)$$

Step 6 Sum of Square Deviation (SSD)

This allowed the standard deviation (SD) values to be reduced as small as possible so that a better model data that fits the actual data was obtained. This was computed by summing up the data obtained for the various SDs. The value of SSD was reduced by adjusting the values of the four unknown parameters until a reasonable value was obtained.

The evaluation of the solver optimisation tool using typical data of impact of aluminium, ferric and calcium dosing (mg/L) on ZSV (m/h) will be covered in more detail in Chapters Four, Five and Six.

3.4.2 Stirred Sludge Volume Index (SSVI) Expression for Chemically Dosed Sludge (Aluminium, Ferric and Calcium)

The conventional Vesilind (1968) equation (Equation 1.1) was utilised in modifying the conventional Pitman (1980,1984) and White (1975) model.

$$\mathrm{ZSV} = \mathrm{v_O} \mathrm{e}^{-\mathrm{KX}} \qquad (1.1)$$

Equation 4.11, 5.3 and 6.3 (Chapter Four, Five and Six) shows the new proposed settleability model equations for aluminium, ferric and calcium dosed sludge

$$\mathrm{ZSV_{Al}} = ((\mathrm{C_0})_{\mathrm{Al}}\,(\mathrm{D_C})_{\mathrm{Al}} + (\mathrm{ZSV_0})_{\mathrm{Al}})\mathrm{e}^{-((\mathrm{K_d})_{\mathrm{Al}}-(\mathrm{C_K})_{\mathrm{Al}}(\mathrm{D_C})_{\mathrm{Al}})\mathrm{X_{Al}}} \qquad (4.11)$$

Where,

$\mathrm{ZSV_{Al}}$ = Actual settling velocity (m/h) $\mathrm{Al^{3+}}$ dosed sludge

$(\mathrm{ZSV_0})_{\mathrm{Al}}$ = Maximum settling velocity (m/h) for $\mathrm{Al^{3+}}$ dosed sludge

$(\mathrm{K_d})_{\mathrm{Al}}$ = Empirical $\mathrm{Al^{3+}}$ dosed sludge settling parameter relating to sludge compaction

$(\mathrm{C_0})_{\mathrm{Al}}$= Empirical $\mathrm{Al^{3+}}$ dosing constant related to stokes settling velocity

$(\mathrm{C_K})_{\mathrm{Al}}$ = Empirical $\mathrm{Al^{3+}}$ dosing constant related sludge compaction

$(\mathrm{D_C})_{\mathrm{Al}}$ = $\mathrm{Al^{3+}}$ dosing concentration (mg/L)

$\mathrm{X_{Al}}$= $\mathrm{Al^{3+}}$ dosed MLSS concentration (mg/L)

$$\mathrm{ZSV_{Fe}} = ((\mathrm{C_0})_{\mathrm{Fe}}\,(\mathrm{D_C})_{\mathrm{Fe}} + (\mathrm{ZSV_0})_{\mathrm{Fe}})\mathrm{e}^{-((\mathrm{K_d})_{\mathrm{Fe}}-(\mathrm{C_K})_{\mathrm{Fe}}(\mathrm{D_C})_{\mathrm{Fe}})\mathrm{X_{Fe}}} \qquad (5.3)$$

Where,

$\mathrm{ZSV_{Fe}}$ = Actual settling velocity (m/h) $\mathrm{Fe^{3+}}$ dosed sludge

$(\mathrm{ZSV_0})_{\mathrm{Fe}}$ = Maximum settling velocity (m/h) for $\mathrm{Fe^{3+}}$ dosed sludge

$(\mathrm{K_d})_{\mathrm{Fe}}$ = Empirical $\mathrm{Fe^{3+}}$ dosed sludge settling parameter relating to sludge compaction

$(\mathrm{C_0})_{\mathrm{Fe}}$= Empirical $\mathrm{Fe^{3+}}$ dosing constant related to stokes settling velocity

$(\mathrm{C_K})_{\mathrm{Fe}}$ = Empirical $\mathrm{Fe^{3+}}$ dosing constant related sludge compaction

$(\mathrm{D_C})_{\mathrm{Fe}}$ = $\mathrm{Fe^{3+}}$ dosing concentration (mg/L)

$\mathrm{X_{Fe}}$= $\mathrm{Fe^{3+}}$dosed MLSS concentration (mg/L)

$$\mathrm{ZSV_{Ca}} = ((\mathrm{C_0})_{\mathrm{Ca}}\ (\mathrm{D_C})_{\mathrm{Ca}}\ + (\mathrm{ZSV_0})_{\mathrm{Ca}})\mathrm{e}^{-((\mathrm{K_d})_{\mathrm{Ca}} - (\mathrm{C_K})_{\mathrm{Ca}}(\mathrm{D_C})_{\mathrm{Ca}})\mathrm{X_{Ca}}} \qquad (6.3)$$

Where,

$\mathrm{ZSV_{Ca}}$ = Actual settling velocity (m/h) $\mathrm{Ca^{2+}}$ dosed sludge

$(\mathrm{ZSV_0})_{\mathrm{Ca}}$ = Maximum settling velocity (m/h) for $\mathrm{Ca^{2+}}$ dosed sludge

$(\mathrm{K_d})_{\mathrm{Ca}}$ = Empirical $\mathrm{Ca^{2+}}$ dosed sludge settling parameter relating to sludge compaction

$(\mathrm{C_0})_{\mathrm{Ca}}$= Empirical $\mathrm{Ca^{2+}}$ dosing constant related to stokes settling velocity

$(\mathrm{C_K})_{\mathrm{Ca}}$ = Empirical $\mathrm{Ca^{2+}}$ dosing constant related sludge compaction

$(\mathrm{D_C})_{\mathrm{Ca}}$ = $\mathrm{Ca^{2+}}$ dosing concentration (mg/L)

$\mathrm{X_{Ca}}$= $\mathrm{Ca^{2+}}$dosed MLSS concentration (mg/L)

Pitman and white expression (Equation 1.2) provides correlation between settleability constant and SSVI

$$\frac{\mathrm{v_O}}{\mathrm{K}} = 68\mathrm{e}^{-0.016\mathrm{SSVI}} \qquad (1.2)$$

Rearranging Equation 1.2 becomes Equation 3.11

$$\mathrm{v_O} = 68\mathrm{k}\mathrm{e}^{-0.016\mathrm{SSVI}} \qquad (3.11)$$

Equation 3.11 can be re-written in terms of $\mathrm{ZSV_O}$ and Equation (3.11) becomes Equation (3.12)

$$\mathrm{ZSV_O} = 68\mathrm{k}\mathrm{e}^{-0.016\mathrm{SSVI}} \qquad (3.12)$$

Substitute Equation 3.12 into the proposed model Equation (4.11, 5.3 and 6.3) and it becomes Equation (3.13, 3.14 and 3.15)

$$\mathrm{ZSV} = \left((\mathrm{C_0})_{\mathrm{Al}}\ (\mathrm{D_C})_{\mathrm{Al}} + 68(\mathrm{K_d})_{\mathrm{Al}}\mathrm{e}^{-0.016\mathrm{SSVI_{Al}}}\right) \times (\mathrm{e}^{-(\mathrm{K_d})_{\mathrm{Al}}\mathrm{X_{Al}} + (\mathrm{C_K})_{\mathrm{Al}}(\mathrm{D_C})_{\mathrm{Al}}\mathrm{X_{Al}}} \qquad (3.13)$$

$$\mathrm{ZSV} = \left((\mathrm{C_0})_{\mathrm{Fe}}\ (\mathrm{D_C})_{\mathrm{Fe}} + 68(\mathrm{K_d})_{\mathrm{Fe}}\mathrm{e}^{-0.016\mathrm{SSVI_{Fe}}}\right) \times (\mathrm{e}^{-(\mathrm{K_d})_{\mathrm{Fe}}\mathrm{X_{Fe}} + (\mathrm{C_K})_{\mathrm{Fe}}\mathrm{D_C}\mathrm{X_{Fe}}}) \qquad (3.14)$$

$$\mathrm{ZSV} = \left((\mathrm{C_0})_{\mathrm{Ca}}\ (\mathrm{D_C})_{\mathrm{Ca}} + 68(\mathrm{K_d})_{\mathrm{Ca}}\mathrm{e}^{-0.016\mathrm{SSVI_{Ca}}}\right) \times (\mathrm{e}^{-(\mathrm{K_d})_{\mathrm{Ca}}\mathrm{X_{Ca}} + (\mathrm{C_K})_{\mathrm{Ca}}\mathrm{D_C}\mathrm{X_{Ca}}}) \qquad (3.15)$$

Divide both side of Equation (3.13, 3.14 and 3.15) by $(\mathrm{e}^{-(\mathrm{K_d})_{\mathrm{Al}}\mathrm{X_{Al}} + (\mathrm{C_K})_{\mathrm{Al}}(\mathrm{D_C})_{\mathrm{Al}}\mathrm{X_{Al}}})$, $(\mathrm{e}^{-(\mathrm{K_d})_{\mathrm{Fe}}\mathrm{X_{Fe}} + (\mathrm{C_K})_{\mathrm{Fe}}(\mathrm{D_C})_{\mathrm{Fe}}\mathrm{X_{Fe}}})$ and $(\mathrm{e}^{-(\mathrm{K_d})_{\mathrm{Ca}}\mathrm{X_{Ca}} + (\mathrm{C_K})_{\mathrm{Ca}}(\mathrm{D_C})_{\mathrm{Ca}}\mathrm{X_{Ca}}})$ and Equation (3.13, 3.14 and 3.15) becomes Equation (3.16, 3.17 and 3.18) respectively

$$\frac{\mathrm{ZSV_{Al}}}{(\mathrm{e}^{-(K_d)_{Al}X_{Al}+(C_K)_{Al}(D_C)_{Al}X_{Al})})} = ((\mathrm{C_0})_{Al}(\mathrm{D_C})_{Al} + 68(\mathrm{K_d})_{Al}\mathrm{e}^{-0.016\mathrm{SSVI}_{Al}} \tag{3.16}$$

$$\frac{\mathrm{ZSV_{Fe}}}{(\mathrm{e}^{-(K_d)_{Fe}X_{Fe}+(C_K)_{Fe}(D_C)_{Fe}X_{Fe})})} = ((\mathrm{C_0})_{Fe}(\mathrm{D_C})_{Fe} + 68(\mathrm{K_d})_{Fe}\mathrm{e}^{-0.016\mathrm{SSVI}_{Fe}} \tag{3.17}$$

$$\frac{\mathrm{ZSV_{Ca}}}{(\mathrm{e}^{-(K_d)_{Ca}X_{Ca}+(C_K)_{Ca}(D_C)_{Ca}X_{Ca})})} = ((\mathrm{C_0})_{Ca}(\mathrm{D_C})_{Ca} + 68(\mathrm{K_d})_{Ca}\mathrm{e}^{-0.016\mathrm{SSVI}_{Ca}} \tag{3.18}$$

Subtract $(\mathrm{C_0})_{Al}(\mathrm{D_C})_{Al}$, $(\mathrm{C_0})_{Fe}(\mathrm{D_C})_{Fe}$ and $(\mathrm{C_0})_{Ca}(\mathrm{D_C})_{Ca}$ from both side of Equation (3.16, 3.17 and 3.18) and Equation (3.16,3.17 and 3.18) becomes Equation (3.19, 3.20 and 3.21).

$$\frac{\mathrm{ZSV_{Al}}}{(\mathrm{e}^{-(K_d)_{Al}X_{Al}+(C_K)_{Al}(D_C)_{Al}X_{Al}})} - (\mathrm{C_0})_{Al}(\mathrm{D_C})_{Al} = 68(\mathrm{K_d})_{Al}\mathrm{e}^{-0.016\mathrm{SSVI}_{Al}} \tag{3.19}$$

$$\frac{\mathrm{ZSV_{Fe}}}{(\mathrm{e}^{-(K_d)_{Fe}X_{Fe}+(C_K)_{Fe}(D_C)_{Fe}X_{Fe}})} - (\mathrm{C_0})_{Fe}\,(\mathrm{D_C})_{Fe} = 68(\mathrm{K_d})_{Fe}\mathrm{e}^{-0.016\mathrm{SSVI}_{Fe}} \tag{3.20}$$

$$\frac{\mathrm{ZSV_{Ca}}}{(\mathrm{e}^{-(K_d)_{Ca}X_{Ca}+(C_K)_{Ca}(D_C)_{Ca}X_{Ca}})} - (\mathrm{C_0})_{Ca}\,(\mathrm{D_C})_{Ca} = 68(\mathrm{K_d})_{Ca}\mathrm{e}^{-0.016\mathrm{SSVI}_{Ca}} \tag{3.21}$$

Divide both side of Equation (3.19, 3.20 and 3.21) by $68(\mathrm{K_d})_{Al}$, $68(\mathrm{K_d})_{Fe}$ and $68(\mathrm{K_d})_{Ca}$ and Equation (3.19, 3.20 and 3.21) becomes Equation (3.22, 3.23 and 3.24)

$$\frac{\mathrm{ZSV_{Al}}}{68(\mathrm{K_d})_{Al}(\mathrm{e}^{-(K_d)_{Al}X_{Al}+(C_K)_{Al}(D_C)_{Al}X_{Al}})} - \frac{(\mathrm{C_0})_{Al}(\mathrm{D_C})_{Al}}{68(\mathrm{K_d})_{Al}} = \mathrm{e}^{-0.016\mathrm{SSVI}_{Al}} \tag{3.22}$$

$$\frac{\mathrm{ZSV_{Fe}}}{68\mathrm{k}(\mathrm{e}^{-(K_d)_{Fe}X_{Fe}+(C_K)_{Fe}(D_C)_{Fe}X_{Fe}})} - \frac{(\mathrm{C_0})_{Fe}(\mathrm{D_C})_{Fe}}{68(\mathrm{K_d})_{Fe}} = \mathrm{e}^{-0.016\mathrm{SSVI}_{Fe}} \tag{3.23}$$

$$\frac{\mathrm{ZSV_{Ca}}}{68\mathrm{k}(\mathrm{e}^{-(K_d)_{Ca}X_d+(C_K)_{Ca}(D_C)_{Ca}X_{Ca}})} - \frac{(\mathrm{C_0})_{Ca}\,(\mathrm{D_C})_{Ca}}{68(\mathrm{K_d})_{Ca}} = \mathrm{e}^{-0.016\mathrm{SSVI}_{Ca}} \tag{3.24}$$

Take ln of both side of Equation (3.22, 3.23 and 3.24) and Equation (3.22, 3.23 and 3.24) becomes Equation (3.25, 3.26 and 3.27)

$$\ln\left(\frac{\mathrm{ZSV_{Al}}}{68(\mathrm{K_d})_{Al}(\mathrm{e}^{-(K_d)_{Al}X_{Al}+(C_K)_{Al}(D_C)_{Al}X_{Al}})} - \frac{(\mathrm{C_0})_{Al}(\mathrm{D_C})_{Al}}{68(\mathrm{K_d})_{Al}}\right) = \ln\mathrm{e}^{-0.016\mathrm{SSVI}_{Al}} \tag{3.25}$$

$$\ln\left(\frac{\mathrm{ZSV_{Fe}}}{68\mathrm{k}(\mathrm{e}^{-(K_d)_{Fe}X_{Fe}+(C_K)_{Fe}(D_C)_{Fe}X_{Fe}})} - \frac{(\mathrm{C_0})_{Fe}(\mathrm{D_C})_{Fe}}{68(\mathrm{K_d})_{Fe}}\right) = \ln\mathrm{e}^{-0.016\mathrm{SSVI}_{Fe}} \tag{3.26}$$

$$\ln\left(\frac{\mathrm{ZSV_{Ca}}}{68\mathrm{k}(\mathrm{e}^{-(K_d)_{Ca}X_d+(C_K)_{Ca}(D_C)_{Ca}X_{Ca}})} - \frac{(\mathrm{C_0})_{Ca}\,(\mathrm{D_C})_{Ca}}{68(\mathrm{K_d})_{Ca}}\right) = \ln\mathrm{e}^{-0.016\mathrm{SSVI}_{Ca}} \tag{3.27}$$

But, lne =1 and hence Equation (3.25, 3.26 and 3.27) becomes the following expressions below for the new activated sludge settleability model use to analyse the effects of aluminium, ferric and calcium dosing on activated sludge settleability indicators(SSVI):

$$\mathrm{SSVI_{Al}(mL/g)} = -\ln\left[\left(\frac{\mathrm{ZSV_{Al}}}{68((\mathrm{K_d})_{Al}\mathrm{X_{Al}}) + ((\mathrm{C_K})_{Al}(\mathrm{D_C})_{Al}\mathrm{X_{Al}})}\right) - \left(\frac{(\mathrm{C_0})_{Al}(\mathrm{D_C})_{Al}}{68(\mathrm{K_d})_{Al}}\right)\Big/_{0.016}\right]$$

$$\mathrm{SSVI_{Fe}(mL/g)} = -\ln\left[\left(\frac{\mathrm{ZSV_{Fe}}}{68((\mathrm{K_d})_{\mathrm{Fe}}\ \mathrm{X_{Fe}}) + ((\mathrm{C_K})_{\mathrm{Fe}}(\mathrm{D_C})_{\mathrm{Fe}}\,\mathrm{X_{Fe}})}\right) - \left(\frac{(\mathrm{C_0})_{\mathrm{Fe}}\,(\mathrm{D_C})_{\mathrm{Fe}}}{68(\mathrm{K_d})_{\mathrm{Fe}}}\right)\Big/_{0.016}\right]$$

$$\mathrm{SSVI_{Ca}(mL/g)} = -\ln\left[\left(\frac{\mathrm{ZSV_{Ca}}}{68((\mathrm{K_d})_{\mathrm{Ca}}\ \mathrm{X_{Ca}}) + ((\mathrm{C_K})_{\mathrm{Ca}}(\mathrm{D_C})_{\mathrm{Ca}}\,\mathrm{X_{Ca}})}\right) - \left(\frac{(\mathrm{C_0})_{\mathrm{Ca}}\,(\mathrm{D_C})_{\mathrm{Ca}}}{68(\mathrm{K_d})_{\mathrm{Ca}}}\right)\Big/_{0.016}\right]$$

This is reported in the result and discussion section (Chapter Four, Five and Six) as Equation (4.22-$\mathrm{SSVI_{Al}(mL/g)}$, 5.14-$\mathrm{SSVI_{Fe}(mL/g)}$ and 6.14-$\mathrm{SSVI_{Ca}(mL/g)}$) respectively.

3.5 Health & Safety and Waste Disposal Measures

The issues relating to health and safety before and during the PhD research analysis were medium to high risk and the current research passed the Coventry University ethical approval process after completing the ethics form online. However, the following forms and document were uploaded and approved:

- Health and Safety Assessment Form
- PhD Research Project Laboratory Learning Contract.
- COSHH (Control of Substance Hazardous to Health) Form for Treated Wastewater Effluent
- COSHH (Control of Substance Hazardous to Health) Form for the use of Ferric chloride hexahydrate and Hydrated Aluminium sulphate chemicals for Activated Sludge Settleability, Digestibility and Dewaterability Test.

The health and safety precautions as identified in the ethical form completed in meeting the health and safety requirement in the laboratory during the current research includes;

- Stringent conformity with the safety policy in the laboratory during disposal of the dried activated sludge cake and activated sludge effluent
- Familiarisation with the Material Safety Data Sheet (MSDS) of all reagent and activated sludge was ensured before commencement of experiment.

Chapter Four

The Impact of Aluminium Dosing on Activated Sludge Settleability

4.0 The Research Objectives and Activated Sludge Settleability

The Literature review in chapter two has provided information that chemical coagulant Aluminium (Al^{3+}) could optimise activated sludge settleability. However, there is limited information from previous studies on investigating activated sludge settleability process and the impact of aluminium on activated sludge settleability. Therefore, one of the broad objectives of this study is to evaluate the impact of chemical dosing aluminium on activated sludge settleability will be considered in this Chapter. Four of the research objectives namely to evaluate the impact of chemical dosing (Aluminium-Al^{3+}, Ferric -Fe^{3+} and Calcium-Ca^{2+}) on activated sludge settleability parameter (ZSV and SSVI) data, develop models to predict zone settling velocity (ZSV) and stirred sludge volume index (SSVI) as a function of chemical dosing (Al^{3+}, Fe^{3+} and Ca^{2+}) concentration using estimated laboratory ZSV and SSVI data, investigate the impact of chemical dosing (Al^{3+} and Fe^{3+}) on experimental biogas production generation in a laboratory scale anaerobic digester and investigate the impact of chemical dosing (Al^{3+}, Fe^{3+} and Ca^{2+}) concentrations on dewaterability of activated sludge will be explored in Chapters Four, Five, Six, Seven and Eight respectively; the ZSV and SSVI is measured as an indicator of activated sludge settleability in Chapters Four, Five and Six.

4.1 The Impact of Aluminium Dosing on Activated Sludge Settleability

4.1.1 Introduction

The use of metal salts such as aluminium, ferric and calcium (Al^{3+}, Fe^{3+} and Ca^{2+}) in precipitation of phosphorus in activated sludge plants has increased considerably in recent years to achieve tighter discharge consents for phosphorus removal in treated wastewater effluent. The modelling of the settleability of the resultant aluminium, ferric and calcium dosed sludge in current engineering practice for design and optimisation are still based on conventional sludge settleability models. There are limited studies that have reported on the effects of chemical dosing (Al^{3+}, Fe^{3+} and Ca^{2+}) concentrations on activated sludge settleability and no studies have optimised the exponential form of the Vesilind equation and validated the numerical expression to include chemical dosing parameters.

Previous studies have reported that phosphorus removal is achieved by either enhanced biological phosphorus removal (EBPR) or chemical phosphorus removal (CPR). The use of EBPR is limited by the requirement for strong wastewater with high, readily biodegradable biological oxygen demand (BOD) hence CPR is the most widely used for phosphorus removal in wastewater (Section 1.1 and 2.1.7.2 and 2.1.7.3). The factors affecting activated sludge settleability such as extracellular polymeric substances (EPS), particle size and structure, cations, and flocculating capability has been addressed in section1.1 (Chapter One) and section 2.1.6.1, 2.1.6.2 and 2.1.6.3 (Chapter Two). The final settling tank (FST) contributes greatly to the design and operation of the activated sludge process (ASP). The evaluation of zone settling velocity (ZSV) is vital in both the design and modelling of FSTs.

The settling classifications are typically reliant on the nature and concentration of the sludge particulates and the interaction between the activated sludge particulates. The activated sludge process, principle of operation, function, types of FST and classification of settling characteristic of activated sludge have been addressed in section 2.1.1 to 2.1.3 (Chapter Two). The modelling of activated sludge settleability to date is based on Pitman (1980, 1984) and White (1975) settleability model. The Pitman (1980, 1984) and White (1975) model which is based on Vesilind (1968) expression for explaining the activated sludge settling characteristics for municipal and industrial wastewater treatment. The model was developed based on the settling characteristics of conventional sludge. With high aluminium (Al^{3+}) salt dosage in the precipitation of phosphates today, the overall characteristics of sludge are different from the conventional sludges on which the Pitman (1980,1984) and White(1975) model was based. Therefore, there is a need to develop a new model that describes the settling properties of aluminium sludge. The proposed new model equation describing the extra weight of aluminium dosing in ASP will address the limitation of the Pitman (1980,1984) and White(1980) model for conventional activated sludge.

The purpose of this chapter is to evaluate the impact of chemical dosing (Al^{3+}, Fe^{3+} and Ca^{2+}) concentration on activated sludge settleability parameter (ZSV and SSVI) and develop models to predict ZSV and SSVI as a function of chemical dosing (Al^{3+}, Fe^{3+} and Ca^{2+}) concentration using estimated laboratory ZSV and SSVI data using a new type 305 setlometer equipment (Triton Electronic Limited 2018b, UK) (Chapter Three - Figure 3.4). The ZSV and SSVI is measured as an indicator of activated sludge settleability. More information on the settling velocity models are available in section 2.1.4 (Chapter Two). The methodology on settleability test has been addressed in section 3.3.1 (Chapter Three).

4.2 Result and Discussion

The results obtained from the research investigation on the impact of aluminium on activated sludge settleability was presented based on the four categories namely Effects of Aluminium dosing on Activated Sludge Morphology (4.2.1), Effects of Aluminium Dosing on ZSV and SSVI (4.2.2), Data Analysis and Model Validation (4.2.3), Model Development and Model Validity for Aluminium Dosed sludge (4.2.4), New Model Calibration to Include Aluminium Dosing Parameter (4.2.5), Validation of New Model for Impact of Aluminium Dosing on ZSV and SSVI (4.2.6), Summary and perspectives (4.2.7) and Conclusions (4.2.8).

4.2.1 Effects of Aluminium Dosing on Activated Sludge Morphology

Microscopic analysis of sludge flocs for control sample (0mg/L) and aluminium dosed (20, 50,100 and 150mg/L) in the SEM - Joel JSM-6060LV showed initial evidence of interfloc bridging, open floc formation and spindly bulking potential in the control sample (Figure 4.1a) while in the aluminium treated sample (20mg/L) some reduced interfloc bridging was observed with improved sludge compaction (Figure 4.1b). However, a better improvement was noticed at a dosing concentration of 50mg/L with reduction in the interfloc bridging but open floc formation and spindly bulking reduction with better sludge compaction (Figure 4.1c) and treatment with increased aluminium dosing concentration of 100-150mg/L (Figure 4.1d and e) also showed better sludge compaction.

The control sludge floc exhibiting an interfloc bridging indicates interference with bio-aggregation of floc particles leading to slow settling rate and reduced sludge compactibility and overall reduced activated sludge settleability. On the other hand, the aluminium-treated sludge floc showed the impact of aluminium in the reduction of the length of the filament organism into smaller filaments. We can therefore infer that aluminium treated sludge reduced the issues of extending filamentous organisms over floc forming bacteria in the entire sludge particle surface (interfloc bridging), scattering of floc forming bacteria into smaller set along extended filamentous organism (open floc formation) and floc-forming bacteria formed along filament length of filamentous organism (spindly bulking). This result reported in Ojo and Ifelebuegu (2018) agrees with findings of Luo *et al.* (2013); Agridiotis *et al.* (2007); Gerardi (2002); Eikelboom (2000); Richard (2003) and Chambers and Tomlinson (1982) on sludge bio-flocculation and improvements in sludge settleability. This also explains the observation of Ojo and Ifelebuegu (2016) in the improvement of sludge settleability with increasing dose of aluminium in a full-scale activated sludge treatment plant.

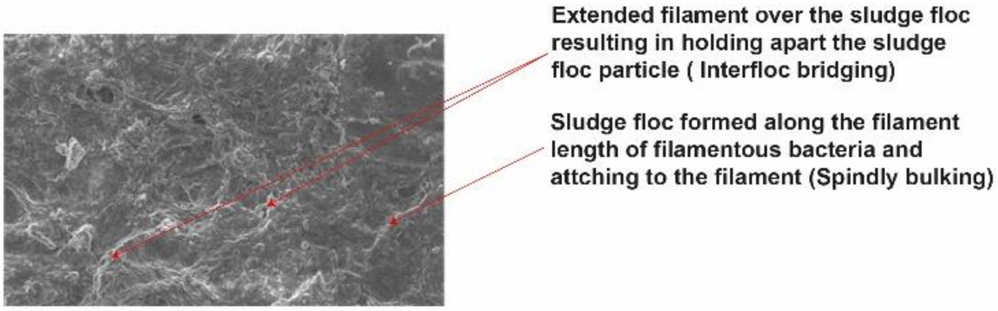

Figure 4.1a. SEM of floc (Control 0mg/L)

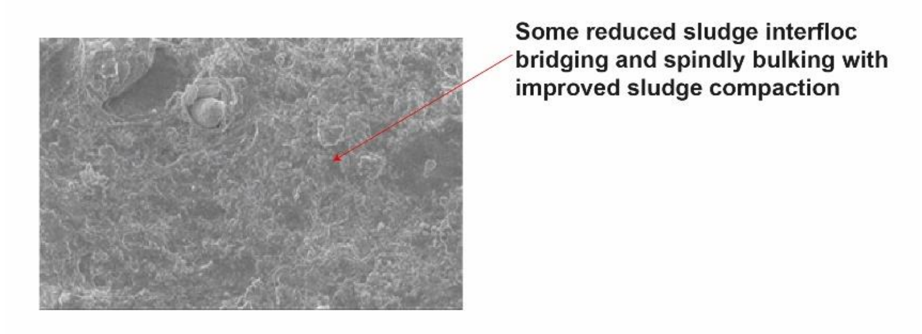

Some reduced sludge interfloc bridging and spindly bulking with improved sludge compaction

Figure 4.1b. SEM of floc (Al-Dosed 20mg/L)

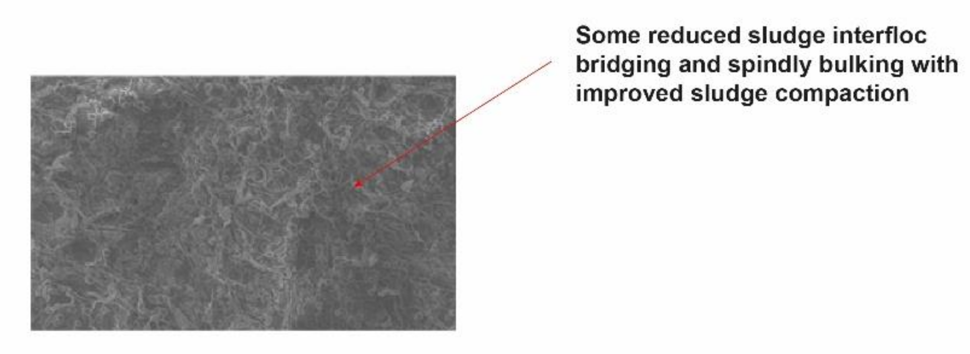

Some reduced sludge interfloc bridging and spindly bulking with improved sludge compaction

Figure 4.1c. SEM of floc (Al-Dosed 50mg/L)

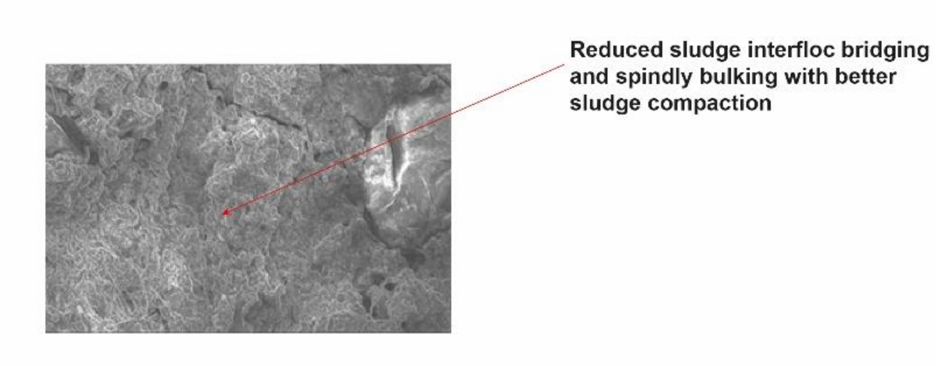

Reduced sludge interfloc bridging and spindly bulking with better sludge compaction

Figure 4.1d. SEM of floc (Al-Dosed 100mg/L)

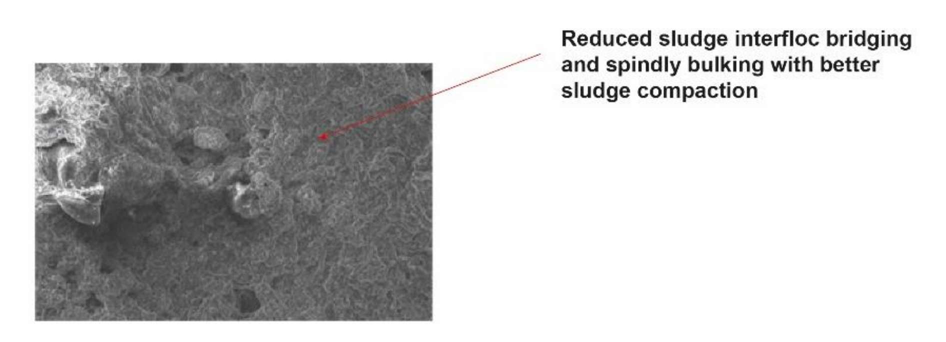

Reduced sludge interfloc bridging and spindly bulking with better sludge compaction

Figure 4.1e. SEM of floc (Al-Dosed 150mg/L)

4.2.2 Effects of Aluminium Dosing on ZSV and SSVI

The ZSV was estimated over a range of un-dosed and aluminium dosed activated sludge concentrations (0, 20, 50,100 and 150mg/L) for 5 batch test regimes (LOT-B and LOF-A) and the results from a typical ZSV test for aluminium (Phase 3) are shown in Figure 4.2 a-e (ZS = zone settling, TS = transition settling, CS = compression settling) and the ZSV's were obtained from the slope of the linear graph. The results from the typical ZSV test for aluminium dosed sludge (Figure 4.2 a-e) indicates that approximately 50% of the original sludge volume within the sludge depth of the settling column settled after 5 to 10 minutes for both the control and aluminium treated sludge. It was observed from the zone settling curve (ZSC) that the initial faster settling is probably due to the absence of spaces between the sludge flocs causing a free settling without interference. However, after the initial first 10 mins of settling, it was noticed that the change in the sludge height with time (ZSV) began to decline. This agrees with the previous work (Vesilind 1968) and can be explained by the floc to floc interaction based on their proximity and slowing down of their settling velocities. Consequently, within this zone settling regime, the agglomeration of floc bacteria tends to settle as a zone of blanket (sludge blanket) accounting for the decrease in the settling velocity (Tchobanoglous and Burton 1991).

In addition, as the settling velocity began to approach the zero axes, there was a possible dehydration of water from the sludge floc pore spaces due to the compressive forces acting on the floc bacteria as the sludge floc enters a compression settling regime. Also, the linear portion of the ZSCs (Figure 4.2 a-e) represents the settling velocity of the sludge flocs as reported in previous work (Vanderhasselt and Vanrolleghem 2000) and as such an increased sludge concentration will result in a decrease in the settling velocity due to increased resistance to water flow through the settling sludge column.

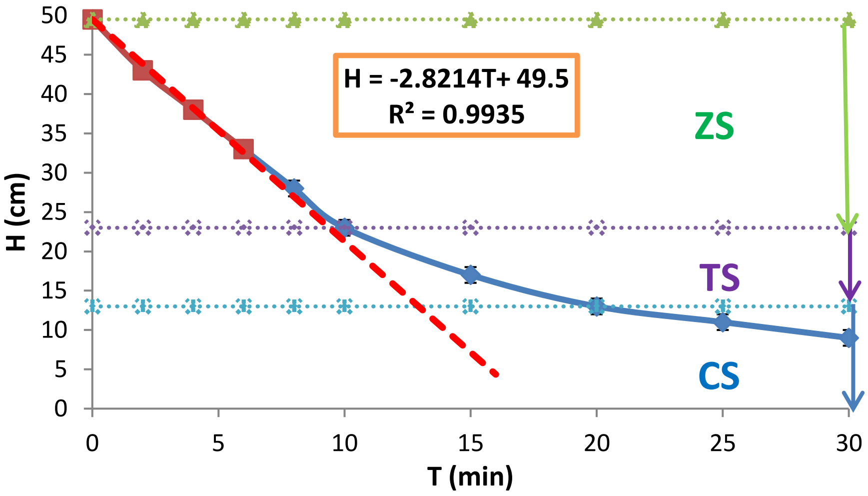

Figure 4.2a. ZSC for Un-dosed sludge (error bars represent the standard deviation of the mean)

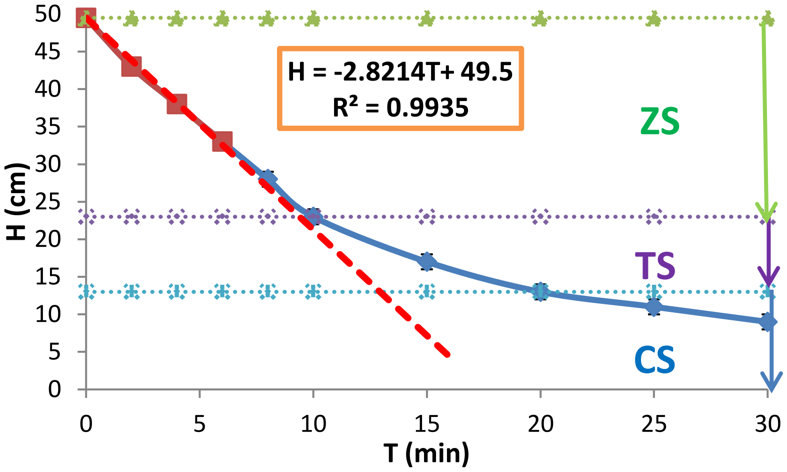

Figure 4.2b. ZSC for 20mg/L Aluminium dosed sludge (error bars represent the standard deviation of the mean)

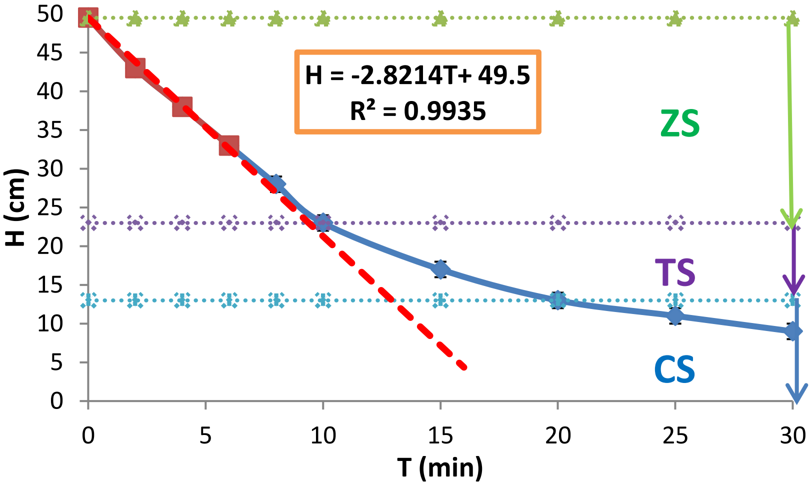

Figure 4.2c. ZSC for 50mg/L Aluminium dosed sludge (error bars represent the standard deviation of the mean)

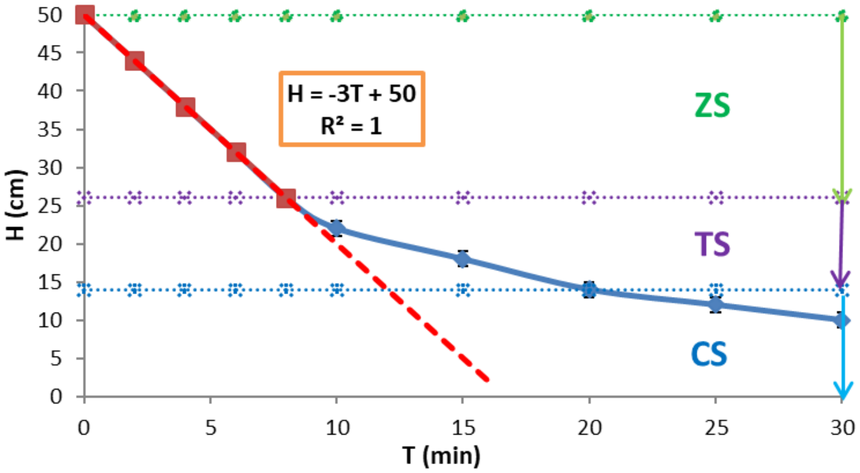

Figure 4.2d. ZSC for 100mg/L Aluminium dosed sludge (error bars represent the standard deviation of the mean)

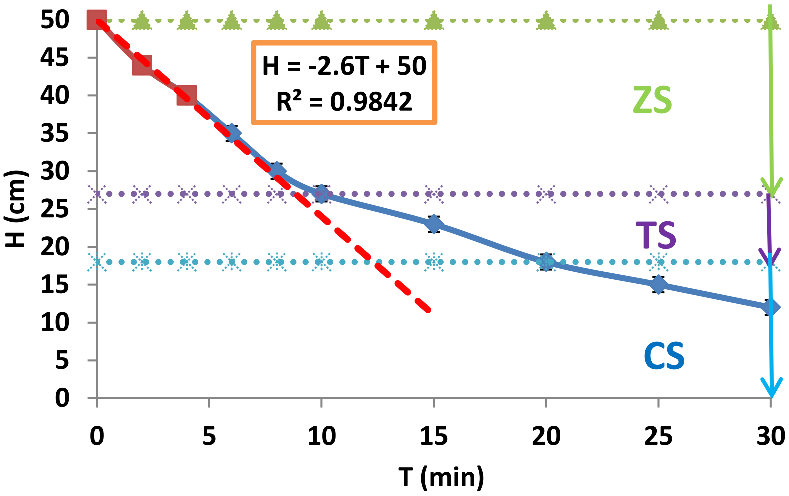

Figure 4.2e. ZSC for 150mg/L Aluminium dosed sludge (error bars represent the standard deviation of the mean)

The results of the impact of aluminium dosing on activated sludge settleability index (ZSV and SSVI) are summarised in Table 4.1. It was observed that the ZSV values increased at the beginning with increasing concentration of aluminium dose (10, 20, 30, 40 and 50mg/L) and started to decrease after 100mg/L dose concentration (100 and 150mg/L). A reversed trend was observed for the SSVI, which decreased with increasing dose of aluminium up to 50mg/L dose rate. At 100mg/L dose rate the SSVI had started to increase. A smaller SSVI value represented a faster settling rate of activated sludge and vice versa. This agrees with the work of Ojo and Ifelebuegu (2016), who reported that increasing concentration of aluminium dose in a full-scale activated sludge plant resulted to improved settleability until an aluminium dose of about 145mg/Lwhen settleability disintegrated and the sludge started to bulk.

Table 4.1 Mean and Standard deviation (SD) of ZSV and SSVI for Aluminium un-dosed and dosed sludge for five batch settling tests (Sample number (N) =40; 2014-2017)

	Dosing concentration (mg/L)							
Parameters	Control	Aluminium dosed						
	0	10	20	30	40	50	100	150
Mean &SD ZSV(m/h)	1.57± 0.06	1.64±0.06	1.73±0.06	1.81±0.08	1.89±0.09	1.96±0.07	1.79±0.06	1.67±0.07
Mean &SD SSVI(mL/g)	64.94±11.23	61.37±10.54	54.82±6.98	52.62±7.78	48.37±5.98	45.53±6.42	52.50±4.27	61.19±13.71
Mean &SD (X) (g/L)	2.67±0.17	2.75±0.15	2.82±0.16	2.88±0.16	2.96±0.19	3.02±0.19	3.17±0.23	3.37±0.23

The improvement noticed in activated sludge settleability (low SSVI and high ZSV) at initial aluminium dosage rates (10 and 50mg/L) observed can be attributed to the surface charge theory of the activated sludge (Gray 1990; Eikelboom *et al.* 1998; Agridiotis *et al.* 2007; Liu *et al.* 2010; Martins *et al.* 2011). Although, Forster (1996) explained that the theory of bulking could be based on filamentous bacteria concept but Urbain *et al.* (1993) reported that filament content in activated sludge is not the only issue contributing to activated sludge settleability, but other serious challenges such as surface chemistry of the sludge contributes to poor settling sludge within the FST. The impact of aluminium dosed sludge can be further explained through charge neutralisation of negatively charged colloids by cationic hydrolysis products (Daun and Gregory 2003). Previous studies by Urbain *et al.* (1993) supported that the overall activated sludge floc structure is negatively charged due to the physical and chemical interactions between floc bacteria, extracellular polymeric substances (EPS) and multivalent cations. It was posited that aluminium dosed salts have the potential to be strongly immersed by the surface of sludge flocs because of the produced positively charged metal hydroxides which account for the charge neutralisation process and charge reversal during periods of aluminium overdosing. In the present study, the observed behaviour of the SSVI that initially decreased at a dose rate of 10 and 50 mg/L and started increasing at 100mg/L dose concentration (100 to 150mg/L) may be due to charge reversal because of overdosed aluminium coagulant. Two competing reactions are involved in the precipitation of phosphorus by aluminium namely formation of metal hydroxide (aluminium hydroxide) and metal phosphate (aluminium phosphate) (De Haas *et al.* 2000a) (Equations 4.1-4.2). The reaction in Equation 4.1 is more thermodynamically and kinetically favoured over the reaction in Equation 4.2. At the lower dosing concentration, the formation of $\mathrm{AlPO_4}$ is predominant. However, at the higher dosing concentrations when the phosphates in the wastewater have been precipitated, the excess aluminium results in the formation of hydroxides as in Equation 4.1. This is responsible for the disintegration of the overall floc structure at higher aluminium concentration resulting to drop in ZSV and increase in the SSVI.

$$\mathrm{Al^{3+} + 3H_2O \rightarrow Al(OH)_3 + 3H^+} \qquad (4.1)$$

$$\mathrm{Al^{3+} + {PO_4}^{3-} \rightarrow AlPO_4} \qquad (4.2)$$

Researchers have reported that EPS could also impact the activated sludge settling processes and physicochemical properties of activated sludge flocs (surface charge) due to the ability of its internal layer to tightly bound and adhere closely with strong stability to the cellular surface (Sheng *et al.* 2010). In support of this claim, Wang *et al.* (2013b) reported similar linear relationship between loosely and tightly bound EPS and SSVI since the activated sludge flocs are reported to be embedded in the EPS structure and the amount of EPS extractable from the activated sludge is positively related to SSVI (Biggs and Lant 2000; Jin *et al.* 2003; Wilén *et al.* 2003). In the current study, the observed trend in the SSVI with increasing chemical dosing could be explained through EPS binding capacity to microbial cells through its bridging nature with aluminium and the overall impact on the EPS content in the activated sludge flocs (Higgins and Sobeck 2002; Sheng *et al.* 2006; Sheng *et al.* 2010). It has also been previously reported that negatively charged mineral and sludge particles can form flocs by cation bridging when multivalent cations (aluminium) are dosed into an ASP (Piirtola 2000).

The improvement in settleability of the activated sludge at lower Al^{3+} concentations can also be attributed to ability of aluminium to neutralise the sludge surface charge (Higgins and Novak 1997b and Subramanian *et al.* 2010), decreased surface charge is related to decrease SSVI values (Mikkelsen *et al.* 1996; Wilén *et al.* 2003; Thompson and Forster 2003) and ability to form larger flocs due to higher valence and low solubility (Li *et al.* 2012). The decrease in ZSV and increase in SSVI and hence decreased settleability at the higher dose concentrations are attributed to surface charge reversal linked to high aluminium dosing rate and high surface charge which is a function of weaker bonding between the various sludge floc fractions resulting to the breakage of the general activated sludge floc structure (Thompson and Forster 2003; Agridiotis *et al.* 2007; Kara *et al.* 2008, Ojo and Ifelbuegu 2016).The reduction in the ZSV values with increasing SSVI also indicates a sludge with a slow settling rate that may hinder the activated sludge compressibility and underflow concentration within the FST (Gerardi 2002).

4.2.3 Data Analysis

The measured ZSV and stirred specific volume index (SSVI) from the three years batch settling tests were used in modelling new aluminium dosed activated sludge settleability. The typical result of the data set of batch tests were analysed using the Minitab 17 software and solver optimisation tool. The solver optimisation tool allows the solver parameter to be set for the target objective of a reduced sum of square deviation (SSD) value so that the model fits the experimental data while the minitab 17 allows the design of an experimental model for investigation of the impact of input variables on the response variable at the same time. Results were also analysed using the non-linear regression in the minitab 17 software and the F-test (F>0.05), lack of fit test (P>0.05), R^2 (coefficient of determination), residual plot, probability plot and interval plot related to the aluminium dosed sludge was used to validate how the ZSV model fits the ZSV experimental data.

4.2.4 Model Development and Model Validity for Aluminium Dosed Sludge

The most familiar approach to evaluating sludge settleability in wastewater treatment processes is using the sludge volume index (SVI) method since it gives a result very quickly in the laboratory. Based on the definition of SVI as the volume occupied per unit mass of sludge particulate (mL/g) after 30 minute of settling; it implies that SVI is a function of settling velocity all through the settling column where the activated sludge varies with respect to time (t) and settling height (H). However, employing SVI as a variable in the evaluation of the real settling in FSTs is contentious since the test relies on the initial sludge concentration before it is being deduced, which contradicts the expectation of a true process parameter for sludge settleability. As FST is known to perform a unique function in the design and operation of the activated sludge process, the evaluation of ZSV in the modelling and design of the FST becomes paramount (Tchobanoglous and Burton 1991 and Ekama *et al.* 1997). Given the limitations of SVI, a more robust approach was introduced called the zone settling velocity test (ZSV). The ZSV approach allows settling velocities to be evaluated over a range of activated sludge concentrations (X) to estimate the rate of zone settling in the settling column where flocs are in proximity to each other. The resultant ZSV values are then used to regulate various models relating the settling velocity and solids concentration. Although, since the mass flux theory was developed by Kynch (1952), various studies have been conducted to examine the relationship between zone settling velocity and activated sludge concentration (Vesilind 1968; Dick and Young 1972; Vearenbergh 1980; Cho *et al.* 1993) but the most acceptable models are those suggested by Vesilind (1968) (Equation 1.1- $ZSV = \mathrm{v_0\ e^{-kX}}$) and Dick and Young (1972) (Equation 4.3). Following previous work by White (1975) and Haandel and Lubbe (2012), it was revealed that these models define the correlation between zone settling velocity and sludge concentration.

$$\mathrm{ZSV} = \mathrm{Vo}\ (\mathrm{X})^{\mathrm{K}} \tag{4.3}$$

The Capital $\mathrm{V_0}$ and K are sludge settleability constants expression for Dick and Young (1972) expression in Equation (4.3). The $\mathrm{V_0}$ explains the effect of sludge settleability on the actual settling velocity while K explains the effect of sludge settleability on sludge compaction (sludge volume index-SVI).

Meanwhile, other researchers have utilised the empirical relationship with the sludge settleability parameters such as SVI, diluted sludge volume index (DSVI) and stirred sludge volume index (SSVI) to obtain the Vesilind Small $\mathrm{v_0}$ and k parameter (Pitman 1984; Ekama and Marias 1986; Wahlberg and Keinath 1988; Giokas *et al.* 2003; and Diagger 1995). The research conducted by Pitman (1980, 1984) involving analysis of six years of full-scale studies resulted in the development of an empirical relationship between the constants of the Vesilind equation and SSVI. The correlation obtained was expressed in Equation 1.2 ($\frac{\mathrm{v_0}}{\mathrm{k}} = 68\mathrm{e}^{(-0.016\times \mathrm{SSVI})}$). The reason for the introduction of SSVI subscript 3.5g/L ($SSVI_{3.5}$) was to resolve the issue of poor settling sludges in the settling column. As earlier mentioned, SVI is the most common sludge settleability indicator used to measure the settling characteristics of suspended growth of activated sludge solids in activated sludge process (ASP). This is because of the simplicity with which the SVI (unstirred) test is performed. However, SVI suffers some major drawbacks since there is no consistent relationship between SVI and suspended solids concentration in mg/L (MLSS) (Dick and Vesilind 1969), but this challenge was addressed in review conducted by Dick and Vesilind (1969) suggesting an inclusion of a slow stirring regime (1 -2 revolution per minute) and this led to proposed stirred specific volume index (SSVI) test using a 4L-settling column instead of the 1L-settling column in unstirred SVI test (White 1976). In the attempt of resolving the issue of poor settling sludge's, White (1975) advised the use of a standard sludge concentration (X) of 3.5g/L thus re-defining it as $SSVI_{3.5}$ against the previous expression of SSVI to achieve a slow stirring regime in the settling column.

Further research by Ekama and Marias (1986) was analysed along with that of other researchers (Rachwall *et al.* 1982; White 1975; Koopman and Cadee 1983) and came up with the findings that Pitman's empirical expression in Equation 1.2 resulted in a good description for all and that a relationship exists between $\frac{V_0}{K}$ and k. This was expressed as in Equation 4.4:

$$K = 0.88 - 0.393 \times \log(v_0 \times k) \tag{4.4}$$

Where,

K, k and v_0 = Sludge settleability constants.

However, since the value of k is known then the value of v_0 can be computed as follows using Equations (4.3 and 4.4).

$$V_0 = (\frac{v_0}{K}) \times k \tag{4.5}$$

However, it is challenging to investigate settling behaviour of activated sludge at low concentrations specifically below 1kg/m³ due to the limit of measurement and because there is no interaction with the sludge particles and settling velocity will be a function of individual floc properties and also, since no clear relationship with the concentration of the activated sludge particle exists at low sludge concentration. This challenge was resolved by other researchers by utilising Vesilind functions in different ways to determine the settling process at low concentration namely; modelling directly the functions (Takacs *et al*. 1991; Dupont and Dahl 1995) and defining particles with different velocities (Dupont and Henze, 1992; Lyn *et al.* 1992; Otterpohl and Freund 1992 and Mazzolani *et al.* 1998). Previous studies also reported the investigation of their own data from unit processes in South Africa (Smollen and Ekama 1984) and numerous activated sludge processes (Pitman 1980, 1984; Tuntoolavest and Grady 1980; Rachwall *et al.* 1982) and concluded that Vesilind's equation gave a better description of the actual settling performance of activated sludge. Following a further result from research conducted by Catunda *et al.* (1989); Catunda and Van-Haandel (1992), rearranging Equations 4.3 to 4.5 will make it possible to express K and Vo as a function of SSVI which can be expressed as follows:

$$k = 0.16 + 2.7 \times 10^{-3} \times SSVI \tag{4.6}$$

$$v_0 = (10.9 + 0.18 \times SSVI) \times e^{(-0.016 \times SSVI)} \tag{4.7}$$

Where,

SSVI= Stirred sludge volume index mL/g

The empirical coefficient v_0 and k are obtained by performing ZSV test over a range of mixed liquor suspended solids (MLSS) concentration for sludge samples. Upon substituting Equations 4.6 and 4.7 into Equation 4.3, Equation 4.8 is obtained;

$$v_0 = (11.2 - 0.06 \times SSVI) \qquad (4.8)$$

It can be concluded that Catunda *et al.* (1989); Catunda and Van –Haandel (1992) findings agree with the earlier mentioned researchers' view and that Equations 4.6-4.7 and Equation 4.8 can be utilised to compute the constants k and v_0 directly from the SSVI values without conducting a ZSV test. Therefore, Vesilind equation has been adopted as the foundation for describing activated sludge settling in an FST. In an earlier study by Ojo and Ifelebuegu (2018), the batch settling test measurements of [zone settling curve (ZSC)] of ZSV reveals ZSV as a linear representation (Figure 4.2d) of sludge height as a function of time (m/h) for 100mg/L Al^{3+} dosed sludge. Also, the results as previously reported Ojo and Ifelebuegu (2018), showed that the ZSV increased, while SSVI decreased with increasing concentrations of Al^{3+} salt up to <100mg/L. Beyond this concentration the sludge settleability disintegrated due mainly to surface charge reversal. Within the full range of concentrations of Al^{3+} used (0 to 150mg/L), a non-linear representation of ZSV and SSVI as a function of Al^{3+} dosing concentrations were observed as presented in Figures 4.3 (Phase 3 result-LOF D3) and 4.4 (Phase 3 result-LOF G3). This provided a basis for the modification of the conventional empirical model of ZSV (Equation (1.1)) to include a new Al^{3+} dosing parameter. It further demonstrated that Al^{3+} dosing concentrations had a non-linear correlation with ZSV and SSVI.

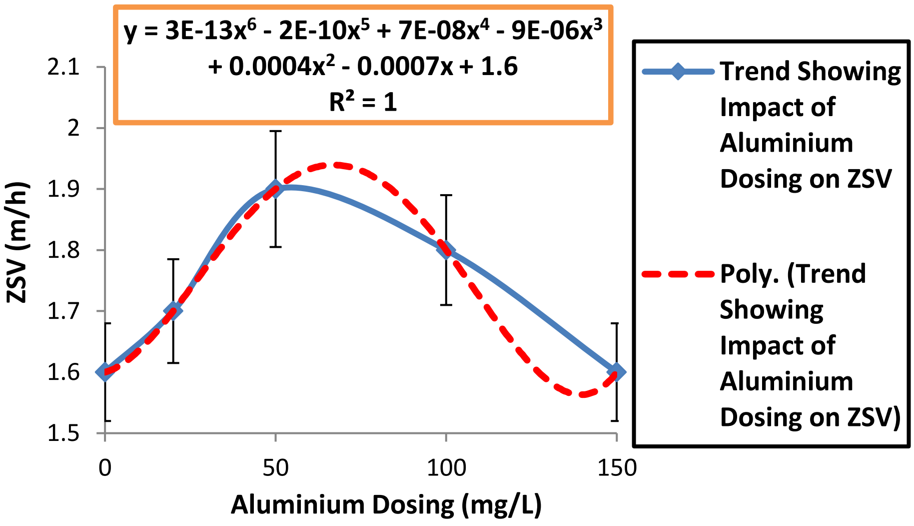

Figure 4.3. The Impact of Aluminium Dosing (mg/L) on ZSV (m/h) (error bars represent standard deviation of the mean)

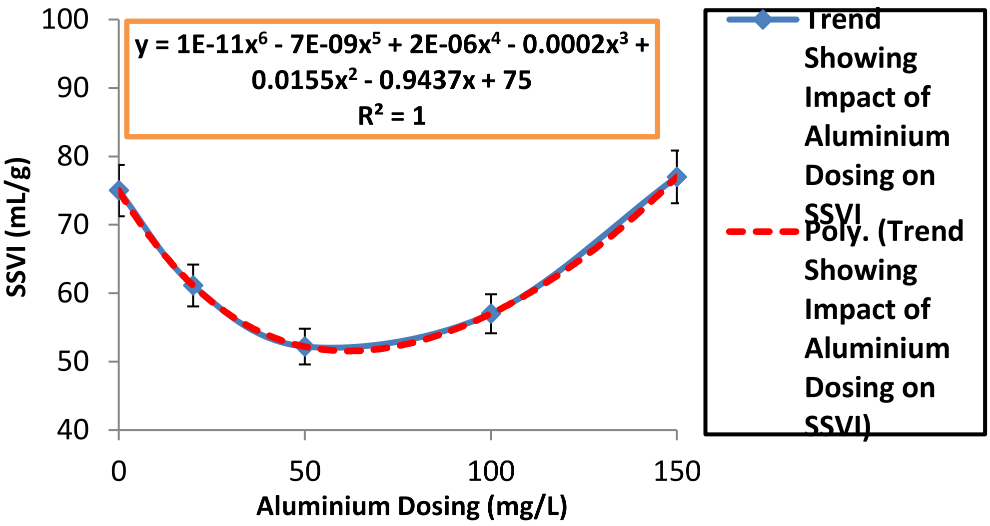

Figure 4.4. The Impact of Aluminium Dosing (mg/L) on SSVI (mL/g) (Error bars represent standard deviation of the mean)

The conventional empirical model for sedimentation in FSTs expressed as a function of solid concentration, termed Vesilind equation is illustrated in Equation 1.1. The empirical coefficient v_0 and k are obtained by performing ZSV test over a range of mixed liquor suspended solids (MLSS) concentration for both un-dosed and Al^{3+} dosed sludge as mentioned earlier and applying linear regression to the linearised form of the Vesilind equation to obtain a new expression in Equation 4.9.

$$\ln \mathrm{ZSV} = -\mathrm{k}\mathrm{X} + \ln \mathrm{v}_0 \qquad (4.9)$$

The plot of natural log of ZSV (m/h) against un-dosed and Al^{3+} dosing concentration for the average data from the various batch test (Table 4.1) is shown in Figure 4.5. The negative of the gradient of each linear regression for the batch test is the Vesilind k value while the intercept is the Vesilind v_0 parameter. However, because we are modelling an Al^{3+} dosed sludge, then Vesilind v_0 and k expression becomes re-defined as ZSV_0 and K_d for Al^{3+} dosed sludge in Equation 4.9. There is a relationship between Al^{3+} dosing concentration and ZSV which was not accounted for in the conventional Vesilind model in Equation 1.1. To express this, it was achieved by the transformation of data in the Vesilind exponential relationship and back tracking to calculate the values of the Vesilind exponential constant parameter. Therefore, the ZSV was plotted against the Al^{3+} dosing concentration up to 150mg/L on a natural log to a linear scale (Figure 4.5). Nevertheless, it was noticed from Figure 4.5, that the relationship between Al^{3+} dose concentrations and the activated sludge settleability can be accurately described for up to 50mg/L dose concentration (Figure 4.6) and the gradient and intercept accounted for the Vesilind coefficients for Al^{3+}($\mathrm{K}_\mathrm{d} = -0.0045$ and $\mathrm{ZSV}_0 = 1.576$ m/h). It can be inferred that the calculated ZSV_0 and $\mathrm{K_d}$ parameter for Al^{3+} dosed sludge from the graph of ln ZSV against Al^{3+} concentrations is a function of the dosing concentrations up to 50mg/L.

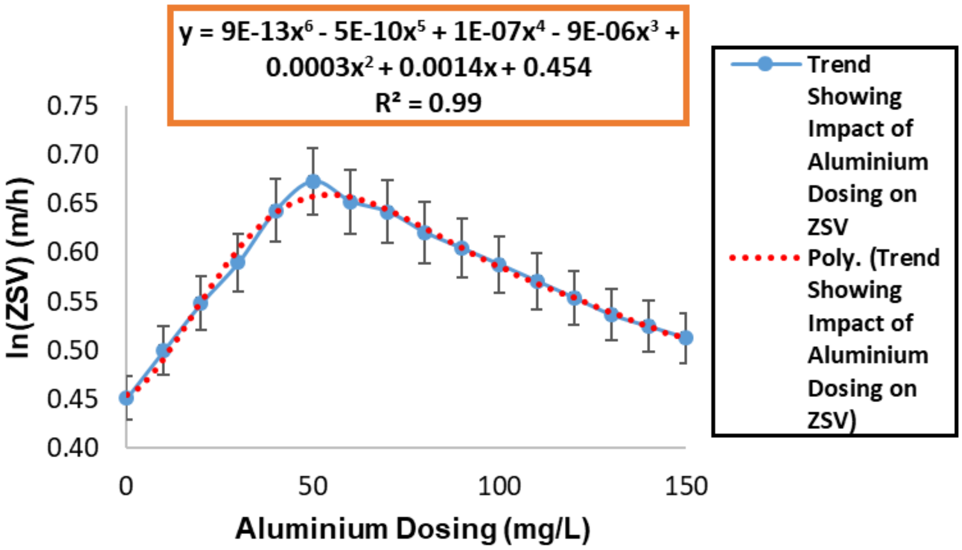

Figure 4.5. Natural log of ZSV against Aluminium Dosing (mg/L) (up to 150mg/L) (the error bars represent the standard deviation of the mean).

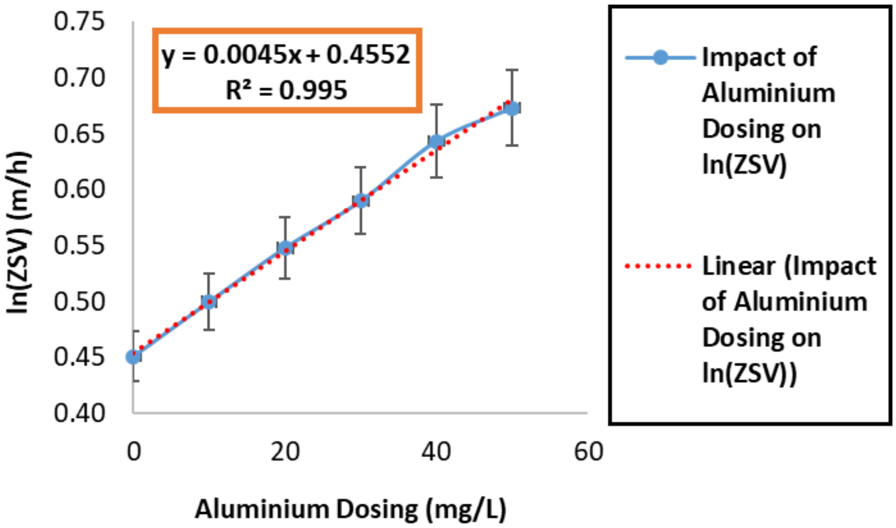

Figure 4.6. Natural log of ZSV against Aluminium Dosing (mg/L) (up to 50mg/L) (the error bars represent the standard deviation of the mean).

The natural logarithm of SSVI was plotted against the Al^{3+} dosing concentration up to 150mg/L (Figure 4.7). However, a linear correlation exist up to 50mg/L (Figure 4.8) and the gradient and intercept of the curves accounted for the coefficient for Al^{3+} $(\mathrm{gradient} =$ 0.0072 and $\mathrm{intercept}$ = 64.78 mL/g).

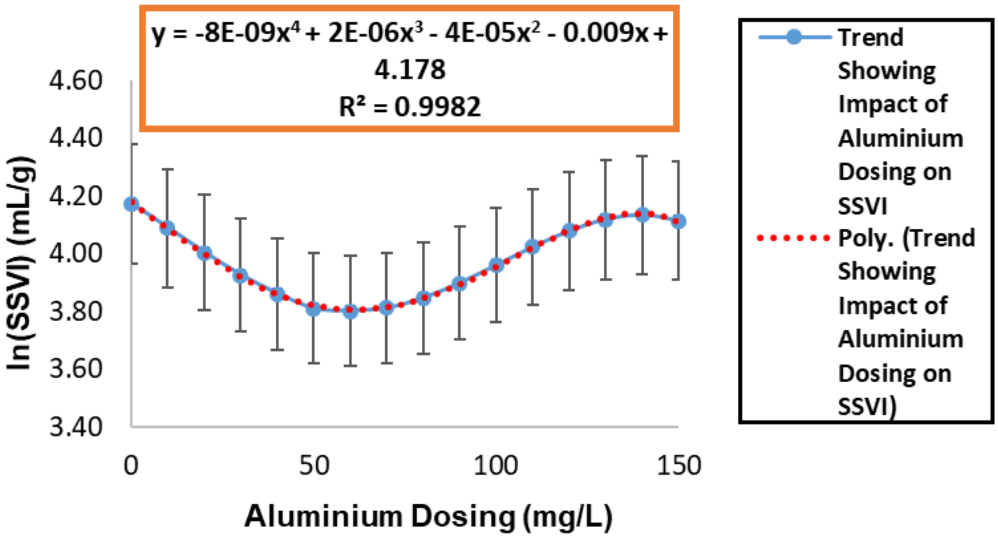

Figure 4.7. ln (SSVI) against Aluminium Dosing (mg/L) (up to 150mg/L) (the error bars represent the standard deviation of the mean).

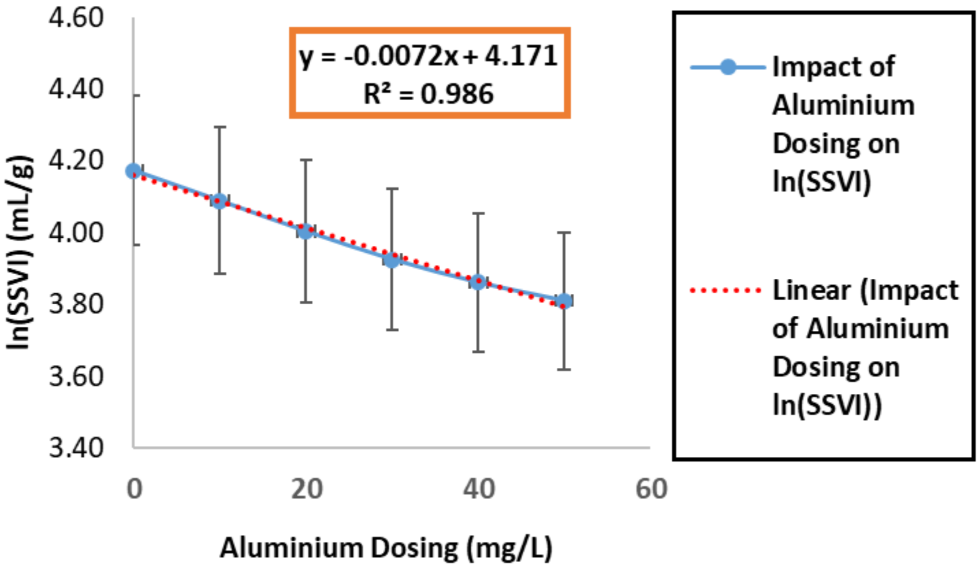

Figure 4.8. ln (SSVI) against Aluminium Dosing (mg/L) (up to 50mg/L) (the error bars represent the standard deviation of the mean)

4.2.5 New Model Calibration to Include Aluminium Dosing Parameter

The simulation and control of settling in final settling tanks (FST) in wastewater treatment depends on calibrated models (Bürger *et al.* 2018). Model validation helps to evaluate whether or not the proposed new mathematical model describes properly the settling characteristics of Al^{3+} sludge. The approach is to check whether the new model fits the experimental batch test results. The exponential form of the Vesilind equation (Equation 1.1) can be optimised to include chemical dosing parameter by investigating a new model equation for settling velocity. The investigated ZSV_0 and K_d parameter for Al^{3+} dosed sludge from the graph of In (ZSV) and In (SSVI) against Al^{3+} dosing concentration (mg/L) shows linearised correlation between ZSV and SSVI with Al^{3+} dosing concentrations (Figures 4.6 and 4.8). The new empirical model for settling velocity for an Al^{3+} dosed activated sludge can take the form of a decay equation ($A = A_0 e^{-\lambda t}$) (Equation 4.10) that obeys the exponential law of decay

$$A = A_0 e^{-\lambda t} \tag{4.10}$$

Where,

A = Activity (the number of unstable nuclei remaining), Bq

A_0 = Original number of unstable nuclei, Bq

e = Constant = 2.718

λ = Decay constant, s^{-1}

t =time, s

The new equation in Equation 4.11 shows the inclusion of a new aluminium dosing concentration (mg/L) $(D_C)_{Al}$ protocol that follows the decay equation.

$$ZSV_{Al} = ((C_0)_{Al}\,(D_C)_{Al} + (ZSV_0)_{Al})e^{-((K_d)_{Al} - (C_K)_{Al}(D_C)_{Al})X_{Al}} \tag{4.11}$$

Where,

ZSV_{Al} = Actual settling velocity (m/h) Al^{3+} dosed sludge

$(ZSV_0)_{Al}$ = Maximum settling velocity (m/h) for Al^{3+} dosed sludge

$(K_d)_{Al}$ = Empirical Al^{3+} dosed sludge settling parameter relating to sludge compaction

$(C_0)_{Al}$= Empirical Al^{3+} dosing constant related to stokes settling velocity

$(C_K)_{Al}$ = Empirical Al^{3+} dosing constant related sludge compaction

$(D_C)_{Al}$ = Al^{3+} dosing concentration (mg/L)

X_{Al}= Al^{3+} dosed MLSS concentration (mg/L)

Equation 4.11 obeys the exponential law of decay and both the additive and the multiplicative rule of exponentials. The empirical coefficients in Equation 4.11 ($((ZSV_0)_{Al}$ and $(K_d)_{Al}$ are typically determined by performing zone settling velocity (ZSV) batch tests over a range of aluminium dosing concentrations (0, 10, 20, 30, 40, 50, 100, 150mg/L) and applying regression analysis and linear approximation to Equation 4.11 by taking the natural log.

For a better understanding of the new empirical heuristic expression for settling velocity for a dosed activated sludge, the comparison of terms in the new Al^{3+} dosed sludge expression (Equation 4.11) and conventional decay equation becomes vital. The version of terms in Equation 4.10 compared with Equation (4.11) is as follows; $\mathrm{A_o} = ((\mathrm{C_0})_{\mathrm{Al}}\ (\mathrm{D_C})_{\mathrm{Al}} + (\mathrm{ZSV_0})_{\mathrm{Al}})$, $\lambda = ((\mathrm{K_d})_{\mathrm{Al}} - (\mathrm{C_K})_{\mathrm{Al}}(\mathrm{D_C})_{\mathrm{Al}})$ and t=$\mathrm{X_{Al}}$. This shows below that applying the additive rule with e as a common factor in Equation 4.11, then Equation 4.12 can be expressed as:

$$((\mathrm{C_0})_{\mathrm{Al}}(\mathrm{D_C})_{\mathrm{Al}}\, e + (ZSV_0)_{Al}\, e) = ((\mathrm{C_0})_{\mathrm{Al}}(\mathrm{D_C})_{\mathrm{Al}} + (ZSV_0)_{Al})e \tag{4.12}$$

On the other hand, applying the multiplicative rule with $\mathrm{X_{Al}}$ as a common factor in Equation (4.11), the expression in Equation 4.13 is obtained

$$-((\mathrm{K_d})_{\mathrm{Al}} - (\mathrm{C_K})_{\mathrm{Al}}(\mathrm{D_C})_{\mathrm{Al}})\mathrm{X_{Al}} = \mathrm{e}^{-(\mathrm{K_d})_{\mathrm{Al}}\mathrm{X_{Al}}} \times \mathrm{e}^{-(\mathrm{C_K})_{\mathrm{Al}}(\mathrm{D_C})_{\mathrm{Al}}\mathrm{X_{Al}}} \tag{4.13}$$

The constants $(\mathrm{ZSV_0})_{\mathrm{Al}}$; $(\mathrm{K_d})_{\mathrm{Al}}$; $(\mathrm{C_0})_{\mathrm{Al}}$ and $(\mathrm{C_K})_{\mathrm{Al}}$, helps in shifting the ZSV model to predict the observed values in aluminium dosed sludge. However, the experimentally estimated ZSV data have been universally used for regulating settling models in the wastewater industry (Vesilind 1968; $\mathrm{ZSV} = \mathrm{v_0}\, e^{-kX}$). Since it is equally common practice to deduce the Vesilind empirical constants ($\mathrm{v_0}$ and k) through conducting batch laboratory ZSV test over a range of concentrations and applying linear regression evaluation to a linearized form of Vesilind's equation ($\ln \mathrm{V} = -\mathrm{kX} + \ln \mathrm{v_0}$), it becomes paramount to apply the same principle to the new Al^{3+} dosed activated sludge model.

We can consider defining F_1 and F_2 from Equation 4.11 as follows: $\mathrm{F_1} = ((\mathrm{ZSV_0})_{\mathrm{Al}} \times (\mathrm{D_C})_{\mathrm{Al}})$ and $\mathrm{F_2} = ((\mathrm{K_d})_{\mathrm{Al}}) - ((\mathrm{C_K})_{\mathrm{Al}}\ (\mathrm{D_C})_{\mathrm{Al}})$ as two functions of ZSV and this gives Equation 4.14.

$$\mathrm{ZSV_{Al}} = \mathrm{F_1}\, \mathrm{e}^{-\mathrm{F_2}\ \mathrm{X_{Al}}} \tag{4.14}$$

As earlier mentioned that there exists an exponential relationship between the ZSV and aluminium dosing (Figures 4.6) but because the relationship is a non-linear relationship, calculating the value of the new empirical coefficient$(\mathrm{ZSV_0})_{\mathrm{Al}}$; $(\mathrm{K_d})_{\mathrm{Al}}$; $(\mathrm{C_0})_{\mathrm{Al}}$ and $(\mathrm{C_K})_{\mathrm{Al}}$ of aluminium dosed activated sludge model can be evaluated by linearising Equation (4.11) to become (4.15). Therefore, the linear approximation (Equation 4.15) was obtained by taking the natural log of Equation 4.11 which can be expressed as:

$$\ln(\mathrm{ZSV_{Al}}) = \ln((\mathrm{C_0})_{\mathrm{Al}}(\mathrm{D_C})_{\mathrm{Al}} + (\mathrm{ZSV_0})_{\mathrm{Al}}) - ((\mathrm{K_d})_{\mathrm{Al}} - (\mathrm{C_K})_{\mathrm{Al}}(\mathrm{D_C})_{\mathrm{Al}})\mathrm{X_{Al}} \tag{4.15}$$

The Equation (4.15) also follows the equation of a straight line (Y = MX + C), M = Slope while C = Intercept and hence Equation 4.15 can be modified as Equation 4.16 by re-defining $\ln\,(\mathrm{ZSV_{Al}}) = \mathrm{Z}$; $(\ln((\mathrm{C_0})_{\mathrm{Al}}(\mathrm{D_C})_{\mathrm{Al}} + (\mathrm{ZSV_0}\,)_{\mathrm{Al}}\,) = \mathrm{P}$ and $((\mathrm{K_d})_{\mathrm{Al}} - (\mathrm{C_K})_{\mathrm{Al}}(\mathrm{D_C})_{\mathrm{Al}}) = Q$ respectively.

$$\mathrm{Z = P - Q\,X} \tag{4.16}$$

The transformation of Equations 4.11 to 4.15 allowed establishing a linear relationship between Z and X (Equation 4.16) and not between ZSV and X since it is already an exponential model. This transformation allows back tracking the constant of the new model for $\mathrm{Al^{3+}}$ dosed sludge $(\mathrm{ZSV_0}\,)_{\mathrm{Al}}$; $(\mathrm{K_d})_{\mathrm{Al}}$; $(\mathrm{C_0})_{\mathrm{Al}}$ and $(\mathrm{C_K})_{\mathrm{Al}}$ to predict the ZSV experimental data. Therefore, once a linear relationship is established between Z and X (Z = P − QX), the value of the $\mathrm{Al^{3+}}$ dosed settleability constants $(\mathrm{ZSV_0}\,)_{\mathrm{Al}}$; $(\mathrm{K_d})_{\mathrm{Al}}$; $(\mathrm{C_0})_{\mathrm{Al}}$ and $(\mathrm{C_K})_{\mathrm{Al}}$ can be evaluated and the experimental value of ZSV and dosing concentrations $(\mathrm{D_C})_{\mathrm{Al}}$ without performing a ZSV batch experiment. A new expression (4.17 and 4.18) was obtained from Equation 4.16 for calculating the value of $(\mathrm{D_C})_{\mathrm{Al}}$ as it relates to aluminium when the four constants $(\mathrm{ZSV_0}\,)_{\mathrm{Al}}$; $(\mathrm{K_d})_{\mathrm{Al}}$; $(\mathrm{C_0})_{\mathrm{Al}}$ and $(\mathrm{C_K})_{\mathrm{Al}}$ for aluminium dosed sludge are known.

$$(\mathrm{D_C})_{\mathrm{Al}} = \frac{\mathrm{e^P} - (\mathrm{ZSV_0}\,)_{\mathrm{Al}}}{(\mathrm{C_0})_{\mathrm{Al}}} \tag{4.17}$$

$$(\mathrm{D_C})_{\mathrm{Al}} = \frac{\mathrm{Q} + (\mathrm{K_d})_{\mathrm{Al}}}{(\mathrm{C_K})_{\mathrm{Al}}} \tag{4.18}$$

The results of the regression analysis using Equation 4.15 showed that the coefficient of determination (R^2) was close to 1 (Figure 4.3). This suggests that the exponential function in Equation (4.11) was suitable to model the $\mathrm{Al^{3+}}$ dosed activated sludge settleability process ($\mathrm{ZSV_{Al}}$). However, the SSVI expression for $\mathrm{Al^{3+}}$ dosed activated sludge can be derived from the new empirical $\mathrm{Al^{3+}}$ dosed activated sludge model for settling velocity in Equation (4.11). The k and $\mathrm{v_0}$ parameter calculated from the expression in Catunda *et al.* (1989) in Equations (4.6) and (4.7) becomes re-written as $(\mathrm{ZSV_0}\,)_{\mathrm{Al}}$ and $(\mathrm{K_d})_{\mathrm{Al}}$ parameter for $\mathrm{Al^{3+}}$ dosed sludge computed in Equations 4.19 and 4.20.

$$(\mathrm{K_d})_{\mathrm{Al}} = 0.16 + 2.7 \times 10^{-3} \times \mathrm{SSVI_{Al}} \tag{4.19}$$

$$(\mathrm{ZSV_0}\,)_{\mathrm{Al}} = (10.9 + 0.18 \times \mathrm{SSVI_{Al}}) \times \mathrm{e}^{(-0.016 \times \mathrm{SSVI_{Al}})} \tag{4.20}$$

Where,

$(\mathrm{K_d})_{\mathrm{Al}}$ = Empirical aluminium dosed activated sludge settling parameter related to sludge compaction (L/g)

$(\mathrm{ZSV_0}\,)_{\mathrm{Al}}$ = Maximum settling velocity for $\mathrm{Al^{3+}}$ dosed activated sludge related to stokes settling velocity (m/h)

$\mathrm{SSVI_{Al}}$ = Stirred sludge volume index (mL/g) Al^{3+} dosed sludge

In deriving a new expression for Al^{3+} dosed SSVI, Equations 4.19 and 4.20, was compared with the existing Pitman (1980) and White (1975) expression in Equation 1.2 and the Equation 1.2 ($\frac{\mathrm{v_0}}{\mathrm{k}} = 68\mathrm{e}^{(-0.016\times\mathrm{SSVI})}$) can be re-written in the form of $(\mathrm{ZSV_0})_{\mathrm{Al}}$ and $(\mathrm{K_d})_{\mathrm{Al}}$ parameter as:

$$(\mathrm{ZSV_0})_{\mathrm{Al}} = 68(\mathrm{K_d})_{\mathrm{Al}}\ \mathrm{e}^{(-0.016\mathrm{SSVI_{Al}})} \tag{4.21}$$

The new SSVI expression (Equation 4.22) was obtained by substituting Equations 4.19–4.21into Equation 4.11. Therefore, the new SSVI expression for aluminium dosed activated sludge (Equation 4.22) was derived from substituting the compared $(\mathrm{K_d})_{\mathrm{Al}}$ and $(\mathrm{ZSV_0})_{\mathrm{Al}}$ parameter calculated from the redefined expression in Catunda et al. (1989) with the Pitman (1980) and White (1975) expression in Equation 1.2 $\{\frac{\mathrm{v_0}}{\mathrm{k}} = 68\mathrm{e}^{(-0.016\times\mathrm{SSVI})}\}$ and substituting into the new aluminium dosed activated sludge model for settling velocity in Equation 4.11.

$$\mathrm{SSVI_{Al}(mL/g)} = -\ln\left[\left.\left(\frac{\mathrm{ZSV_{Al}}}{68((\mathrm{K_d})_{\mathrm{Al}}\mathrm{X_{Al}})+((\mathrm{C_K})_{\mathrm{Al}}(\mathrm{D_C})_{\mathrm{Al}}\mathrm{X_{Al}})}\right) - \left(\frac{(\mathrm{C_0})_{\mathrm{Al}}(\mathrm{D_C})_{\mathrm{Al}}}{68(\mathrm{K_d})_{\mathrm{Al}}}\right)\right/ 0.016\right] \tag{4.22}$$

The results of regression analysis for the impact of Al^{3+} dosing on SSVI using the experimental data in the batch test conducted showed that the coefficient of determination (R^2) was close to 1 (0.986) (Figure 4.6). This suggests that the linearized expression in Equation 4.22 was suitable to model the impact of Al^{3+} dosing on activated sludge settleability (SSVI) process.

4.2.6 Validation of Novel Model for Impact of Aluminium Dosing on ZSV and SSVI

4.2.6.1 Novel ZSV Model

The heuristic expression used for the derivation of the new model for Al^{3+} dosed sludge expressed in Equation 4.11 $(\mathrm{ZSV_{Al}} = ((\mathrm{C_0})_{\mathrm{Al}}(\mathrm{D_C})_{\mathrm{Al}} + (\mathrm{ZSV_0})_{\mathrm{Al}})\mathrm{e}^{-((\mathrm{K_d})_{\mathrm{Al}}-(\mathrm{C_K})_{\mathrm{Al}}(\mathrm{D_C})_{\mathrm{Al}})\mathrm{X_{Al}}})$ and its linear approximation, $(\ln(\mathrm{ZSV_{Al}}) = \ln((\mathrm{C_0})_{\mathrm{Al}}(\mathrm{D_C})_{\mathrm{Al}} + (\mathrm{ZSV_0})_{\mathrm{Al}}) - ((\mathrm{K_d})_{\mathrm{Al}} - (\mathrm{C_K})_{\mathrm{Al}}(\mathrm{D_C})_{\mathrm{Al}})\mathrm{X_{Al}})$. The experimental data of five batch settling velocity test can be classified into two groups. The first group (Figure 4.2d, Figures 4.3-4.8) were used to develop the model while the second group (Tables 4.2 and 4.3 and Figures 4.9 and 4.10) are used to validate the model. The model was validated using two approach namely; Solver optimization tool and Minitab 17. Although, the batch settling test measurements revealed ZSV as a linear representation (sludge height as a function of time) (Figure 4.2d), but on the contrary a non-linear representation was observed in Figures 4.3 and 4.4 showing ZSV and SSVI as a function of Al^{3+} dosing concentration. The transformation of the data of the parameter in the conventional Vesilind equation further allows the inclusion of a new Al^{3+} dosing parameter $(\mathrm{D_C})$ in the existing Pitman (1980) and White (1975) model in

Equation (1.2) and Catunda *et al.* (1989) in Equations (4.6) and (4.7) which are both in agreement with the Vesilind (1968) expression.

The Solver optimisation tool and Minitab 17 were utilised to fit non-linear model data to actual experimental data through non-linear fitting method (Tables 4.2 and 4.3). Table 4.2 and Figures 4.9 and 4.10 shows a comparison of the experimental and predicted zone settling velocities using Equation 4.11. It was observed that the validation results were good enough and valid for aluminium concentration ranging from (0, 10, 20, 30, 40, 50, and 100mg/L). A regression model will exhibit a lack of fit when it fails to adequately describe the functional relationship between the experimental factors and the response variable. The lack of fit test in Minitab indicates that there is no evidence that the model does not fit the data well because the *P* value was greater than the significance level (*P* Value > α) 0.675 > 0.05 (Table 4.2 and Figures 4.9 and 4.10). This means an α of 0.05 shows that the chance of concluding that the model does not fit the experimental data when it does is only 5 per cent. The 95% confidence interval (CI) values for the estimated values of parameter $((\mathrm{ZSV_0})_{\mathrm{Al}}$; $(\mathrm{K_d})_{\mathrm{Al}}$; $(\mathrm{C_0})_{\mathrm{Al}}$ and $(\mathrm{C_K})_{\mathrm{Al}})$ was significantly different from zero and F-value was greater than 0.05 ($\mathrm{F}_{30,6}$ = 0.82, *P* = 0.675) which depicts a good fit. The non-linear fitting, interval plot, residual plot, and probability plot (Figure 4.8) further establishes the validity of the model using Minitab 17.

Table 4.2: Model Validation Minitab 17and Solver Optimisation Tool Result (Aluminium)

Parameters	Estimated values
ZSV_0	1.377
$\mathrm{C_0}$	0.026
$\mathrm{K_d}$	-0.02
$\mathrm{C_K}$	-0.0023
α	0.05
R^2	0.993
CI	95%
SSD	0.334
DF	36
SS	1.14664
MS	0.01559
F	0.82
P-value	0.675
Lack of fit test	30

DF-degree of freedom, SS-sum of squares, MS-mean square, R^2-R Squared, α-significance level, CI-Confidence Interval, F- Fstatistics

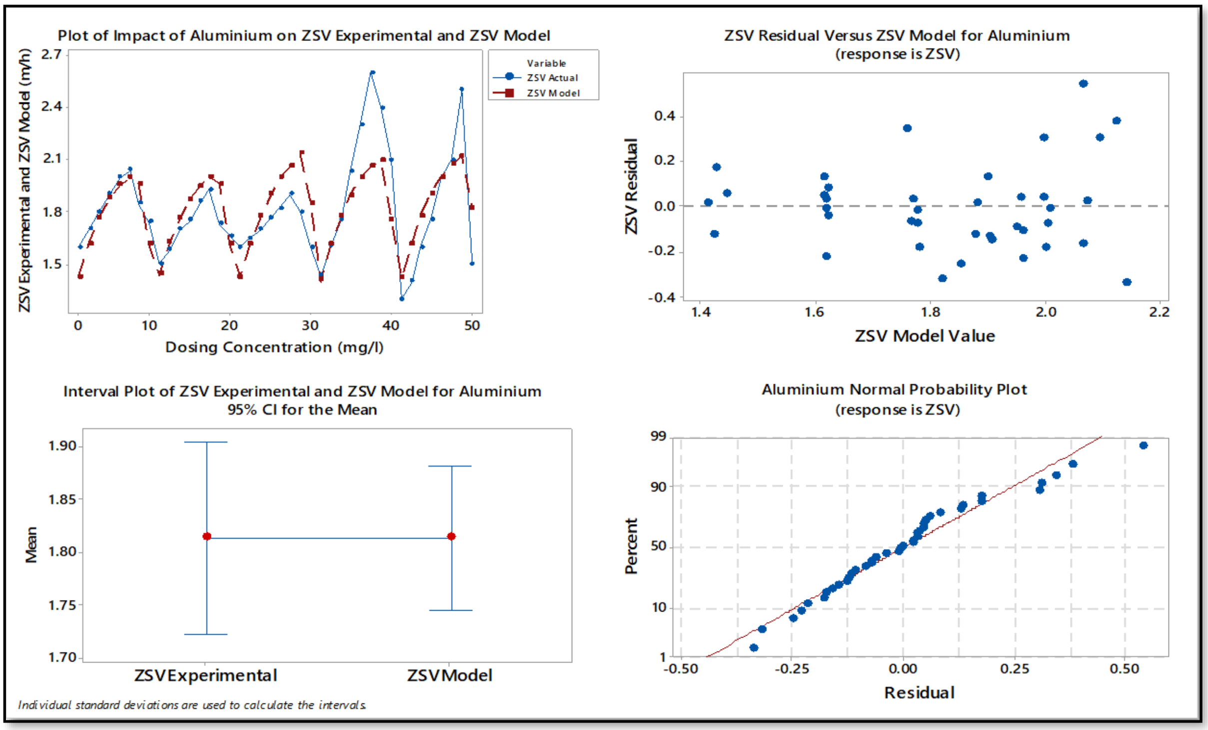

Figure 4.9. Non-linear fitting, interval plot, residual plot, and probability plot

The probability plot creates estimated cumulative distribution function from sample data by plotting the value of each observation against its estimated cumulative probability and a scale transformation allows the fitted distribution to form a straight line. A good distribution fit is one where the observations are near the fitted line. The data in Figure 4.9 are near the fitted line hence it indicates a good distribution fit between model and experimental data. The residual shows how far is the model data from the experimental data and the residual plot in Figure 4.9 shows a good fit. The coefficient of determination (R^2) was 0.993 in Table 4.2, shows that the difference between the observed experimental value and the model predicted values are small and unbiased. The interval plot (Figure 4.9) shows that at 95% CI, the mean value of ZSV model and experimental is significant as the 95% confidence interval bar does not overlap.

The solver optimisation tool allows the solver parameter to be set for the target objective of a reduced sum of square deviation (SSD) value so that the model fits the experimental data. In Table 4.3 and Figure 4.10, a significant SSD value of 0.334 was reported and it indicated the ZSV model fits the actual ZSV value.

Table 4.3- ZSV experimental and ZSV model comparison using Solver optimisation and Minitab 17 for undosed and Aluminium dosed sludge (Sample number (N) =40; 2014-2017)

MLSS (g/l)	ZSV (m/h)	ZSV Model (m/h)	Al-Dosing (mg/L)	Standard deviation	Residual	Squared Residual	Squared ZSV
2.50	0.47	0.37	0.00	9.77×10^{-3}	1.74×10^{-1}	3.02×10^{-2}	0.22
2.76	0.53	0.48	10.00	2.15×10^{-3}	7.95×10^{-2}	6.32×10^{-3}	0.28
2.85	0.59	0.56	20.00	6.88×10^{-4}	3.13×10^{-2}	9.82×10^{-4}	0.35
2.94	0.62	0.62	30.00	2.00×10^{-6}	1.98×10^{-2}	3.91×10^{-4}	0.38
3.04	0.67	0.66	40.00	1.04×10^{-4}	4.41×10^{-2}	1.95×10^{-3}	0.45
3.15	0.71	0.68	50.00	8.20×10^{-4}	4.36×10^{-2}	1.90×10^{-3}	0.50
3.30	0.62	0.68	100.00	4.08×10^{-3}	-1.09×10^{-1}	1.20×10^{-2}	0.38
3.50	0.56	0.52	150.00	1.25×10^{-3}	1.28×10^{-1}	1.63×10^{-3}	0.31
2.84	0.41	0.38	0.00	1.02×10^{-3}	5.77×10^{-2}	3.33×10^{-3}	0.17
2.90	0.46	0.48	10.00	5.43×10^{-4}	-4.23×10^{-2}	1.79×10^{-3}	0.21
2.96	0.52	0.56	20.00	1.68×10^{-3}	-6.53×10^{-2}	4.26×10^{-3}	0.27
3.00	0.56	0.62	30.00	3.42×10^{-3}	-1.25×10^{-1}	1.57×10^{-2}	0.31
3.10	0.62	0.66	40.00	1.26×10^{-3}	-8.79×10^{-2}	7.73×10^{-3}	0.38
3.11	0.67	0.69	50.00	2.28×10^{-4}	-7.38×10^{-2}	5.45×10^{-3}	0.45
3.30	0.55	0.68	100.00	1.79×10^{-2}	-2.29×10^{-1}	5.26×10^{-2}	0.30
3.50	0.51	0.52	150.00	2.15×10^{-4}	4.75×10^{-2}	2.26×10^{-3}	0.26
2.50	0.47	0.37	0.00	9.78×10^{-3}	1.74×10^{-1}	3.02×10^{-2}	0.22
2.60	0.50	0.48	10.00	2.55×10^{-4}	3.16×10^{-2}	9.97×10^{-4}	0.25
2.65	0.53	0.57	20.00	1.51×10^{-3}	-7.48×10^{-2}	5.60×10^{-3}	0.28
2.70	0.57	0.63	30.00	3.95×10^{-3}	-1.30×10^{-1}	1.68×10^{-2}	0.32
2.73	0.60	0.68	40.00	6.68×10^{-3}	-1.77×10^{-1}	3.15×10^{-2}	0.36
2.80	0.64	0.71	50.00	5.50×10^{-3}	-1.62×10^{-1}	2.64×10^{-2}	0.41
2.90	0.59	0.77	100.00	3.13×10^{-2}	-3.39×10^{-1}	1.15×10^{-1}	0.35
3.10	0.47	0.65	150.00	3.36×10^{-2}	-2.51×10^{-1}	6.32×10^{-2}	0.22
2.20	0.36	0.37	0.00	2.50×10^{-5}	1.79×10^{-2}	3.22×10^{-4}	0.13
2.50	0.48	0.48	10.00	1.80×10^{-5}	-7.15×10^{-3}	5.10×10^{-5}	0.23

2.65	0.60	0.57	20.00	9.72×10^{-4}	-1.48×10^{-2}	2.19×10^{-4}	0.36
2.73	0.71	0.63	30.00	6.17×10^{-3}	1.33×10^{-1}	1.77×10^{-2}	0.50
2.74	0.83	0.68	40.00	2.22×10^{-2}	3.04×10^{-1}	9.24×10^{-2}	0.69
2.80	0.96	0.71	50.00	6.05×10^{-2}	5.38×10^{-1}	$2{,}89 \times 10^{-1}$	0.92
3.00	0.88	0.75	100.00	1.79×10^{-2}	3.07×10^{-1}	9.45×10^{-2}	0.77
3.25	0.74	0.61	150.00	1.82×10^{-2}	3.42×10^{-1}	1.17×10^{-1}	0.55
2.40	0.26	0.37	0.00	1.19×10^{-2}	-1.21×10^{-1}	1.48×10^{-2}	0.07
2.50	0.36	0.48	10.00	1.54×10^{-2}	-2.17×10^{-1}	4.72×10^{-2}	0.13
2.55	0.47	0.57	20.00	1.03×10^{-2}	-1.78×10^{-1}	3.16×10^{-2}	0.22
2.62	0.57	0.64	30.00	4.45×10^{-3}	-1.46×10^{-1}	2.13×10^{-2}	0.32
2.68	0.68	0.69	40.00	2.80×10^{-5}	-4.22×10^{-3}	1.80×10^{-5}	0.46
2.75	0.78	0.72	50.00	3.75×10^{-3}	2.79×10^{-2}	7.78×10^{-4}	0.61
2.94	0.91	0.76	100.00	2.29×10^{-2}	3.80×10^{-1}	1.44×10^{-1}	0.83
3.15	0.68	0.64	150.00	1.83×10^{-3}	-3.20×10^{-1}	1.02×10^{-1}	0.46

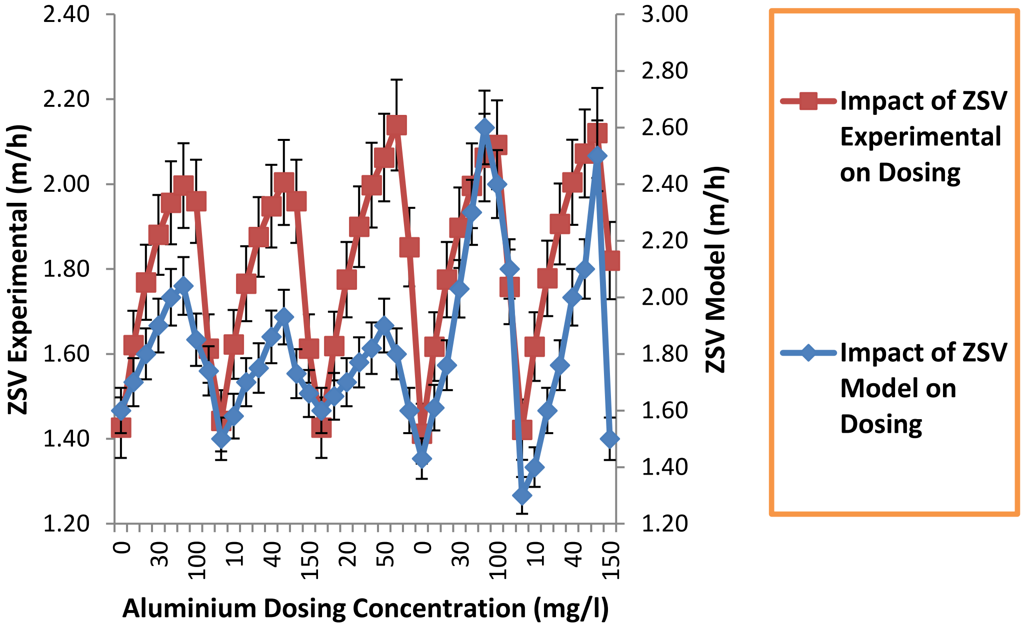

Figure 4.10. Non-linear curve fitting of impact of aluminium on ZSV (the bars represent standard deviation of the mean)

$$ZSV_{Al} = \left((0.026\ (D_C)_{Al}\ + 1.377)e^{-0.020+0.0023(D_C)_{Al}X_{Al}}\right) \qquad (4.23)$$

The values of $(\mathrm{C_0})_{\mathrm{Al}}$; $(\mathrm{ZSV_0})_{\mathrm{Al}}$; $(\mathrm{K_d})_{\mathrm{Al}}$ and $(\mathrm{C_K})_{\mathrm{Al}}$ (Table 4.2) used to validate the numerical model in Equation 4.23 are the same at different dosing concentration (0, 10, 20, 30, 40, 50, and 100mg/L) and approximate to 0.026, 1.377, −0.020, and −0.0023 respectively. Therefore, the new ZSV model for aluminium dosed sludge are expressed as Equation 4.23.

4.2.7 Summary and Perspectives

The results of this work demonstrated that the proposed models developed (Ojo and Ifelebuegu 2019a) as an update of existing models based on conventional activated sludges, can be explicitly used in activated sludge plants to predict the impact of Al^{3+}dosing concentrations on the settleability of activated sludge. The ZSV and SSVI model equations will find applications in the design and optimisation of FSTs for the solids separation of Al^{3+} dosed activated sludge plants. They are valid for Al^{3+}concentrations in the range of 0 to 100mg/L. High surface charges associated with higher concentrations of Al^{3+}, causes a general disintegration of the activated sludge floc structure as previously reported (Ojo and Ifelebuegu 2018). This will result to the Al^{3+} dosed sludge not fitting the proposed equation at concentrations higher than the stated range.

4.2.8 Conclusions

A novel activated sludge settleability model was designed to analyse the effects of Al^{3+} dosing concentrations on activated sludge settleability indicators; zone settling velocity (ZSV) and stirred specific volume index (SSVI) using linear transformation of polynomials and exponential functions to achieve replication of a non-linear correlation between the Al^{3+} dosing concentrations and settleability indicators (ZSV and SSVI). The new empirical model that describes the relationship between Al^{3+} dosing concentrations and the ZSV and SSVI were further validated using non-linear parameterization. The results showed that the settleability indicators of Al^{3+} dosed sludges can be described by the proposed equations which showed a good fit to the experimental data within a dose range of between 0 to <100 mg/L of Al^{3+}. The new model equations will find application in the water industry for the modelling and optimization of Al^{3+} dosed activated plants.

Chapter Five

The Impact of Ferric Dosing on Activated Sludge Settleability

5.0 The Research Objectives and Activated Sludge Settleability

The Literature review in chapter two has provided information that chemical coagulant ferric (Fe^{3+}) could optimise activated sludge settleability. However, there is limited information from previous studies on investigating the impact of ferric on activated sludge settleability. Therefore, one of the broad objectives of this study is to evaluate the impact of chemical dosing (Fe^{3+}) on activated sludge settleability. Four of the research objectives has been stated earlier in section 4.0 (Chapter Four) and section 1.3 (Chapter One). The ZSV and SSVI is measured as an indicator of activated sludge settleability.

5.1 The Impact of Ferric (Fe) Dosing on Activated Sludge Settleability

5.1.1 Introduction

As earlier mentioned in section 4.1.1 , there exist increasingly tighter requirements for effluent quality particulary nutrients (phosphates and nitrates) and the activated sludge process (ASP) have has replaced old biofilters to help meet < 1mg/L phosphorus consents (Ojo and Ifelebuegu 2016). Ferric salts are among the most widely used chemical for the chemical precipitation of phosphorus (Haandel and Lubbe 2012). To achieve effluent phosphorus removal in ASPs, chemical phosphorus removal with ferric salts is predominantly used (Ojo and Ifelebuegu 2016). Ferric salts have merit over other coagulants such as aluminium and calcium used in phosphorus removal and are effective in the removal of phosphorus (P) from wastewater and also are a low-cost product (Luo *et al.* 2017; Kelly and He 2014). The most obvious impact of ferric salt on wastewater treatment plant (WWTP) is the hydrolysis reactions of the ferric salts during P-removal process (Wang *et al.* 2016a,b) and the potential surface charge neutralisation of negatively charged colloids by cationic hydrolysis products (Duan and Gregory 2003; Liu *et al.* 2010). The presence of a high concentration of iron resulting from the CPR process alters the overall sludge characteristics and likely to impact the activated sludge settleability. As mentioned earlier in 4.1.1, that the overall activated sludge floc structure is negatively charged due to the physical and chemical interactions between floc bacteria, EPS and multivalent cations like aluminium and ferric has a great effect on sludge settleability (Urbain *et al.* 1993). This explains why ferric salts (Fe) have the potential to be strongly immersed by the surface of sludge flocs just as aluminium since it produces positively charged metal hydroxides which account for the charge neutralisation process and charge reversal during periods of ferric overdosing rate. Previous studies have also revealed that since the activated sludge flocs are embedded in the EPS structure (Biggs and Lant 2000; Jin *et al.* 2003; Wilén *et al.* 2003) and the amount of EPS extractable from the activated sludge is positively related to stirred sludge volume index (SSVI). The EPS also impacts activated sludge settling processes due to the ability of its internal layer to tightly bound and adhere closely with strong stability to the cellular surface (Laspidou and Rittmann 2002; Sheng *et al.* 2010).

In section 4.1.1, it was stressed that FSTs are important component in the design and operation of activated sludge plants. This makes investigation of zone settling velocity ZSV of great need in designing and modelling activated sludge process. The mentioned settling categories have already been explained in review by Ekama *et al.* 1997 (free, flocculent, zone and compression settling) in section 4.1.1. The modelling of activated sludge settleability to date is based on Pitman (1980) and White (1975) settleability model and this has been covered in section 4.1.1. The model was developed based on the settling characteristics of conventional sludge. However, with high ferric salt dosage required for the precipitation of phosphates today, the overall behaviour of sludge is different from the conventional sludges on which the Pitman and White model was based. Therefore, there is a need to develop a new model that describes the settling properties of ferric dosed sludge. The proposed new model equation describing the extra weight of ferric dosing in ASP will address the restriction of Pitman (1980) and White(1975) model for conventional activated sludge. The purpose of current study is firstly to evaluate the impact of ferric dosing on activated sludge settleability focusing on zone settling velocities (ZSV) and stirred sludge volume index (SSVI), investigate the impact of ferric on activated sludge settling curve and to develop a new model of settleability of ferric dosed activated sludge.

5.2 Result and Discussion

The results obtained from the research investigation on the impact of ferric on activated sludge settleability was presented based on the four categories namely; effects of ferric dosing on activated sludge morphology (5.2.1), effects of ferric dosing on ZSV and SSVI (5.2.2), data afor ferric dosed sludge (5.2.3), model development and model validity for ferric dosed sludge (5.2.4), new model calibration to include ferric dosing parameters (5.2.5), validation of new model for impact of ferric dosing on ZSV and SSVI (5.2.6) and conclusion and practical relevance (5.2.7).

5.2.1 Effects of Ferric Dosing on Activated Sludge Morphology

The microscopic evalaution of sludge flocs for control sample (0mg/L) and ferric dosed (50,100 and 150mg/L) in SEM followed the same pattern and explanation as observed in control sample and aluminium treated sample in chapter four (Figure 4.1a-e). As can be seen in Figure 5.1a, interfloc bridging, open floc formation and spindly bulking also occurred while for ferric treated sample (50mg/L) in Figure 5.1b, some decrease in sludge porosity, interfloc bridging and improved sludge compaction was observed. Furthermore, with increasing dosing concentration of 100mg/L and 150mg/L, the sludge compaction became bettter in Figure 5.1c (100mg/L) and Figure 5.1d (150mg/L) compared to Figure 5.1b (50mg/L). This is an indication that the sludge floc with better compactibility will enhance activated sludge settleability and produce the best effluent quality as reported in Ojo and Ifelebuegu (2019c). This equally agrees with findings of Luo *et al.* (2013); Agridiotis *et al.* (2007); Gerardi (2002); Eikelboom (2000); Richard (2003) and Chambers and Tomlinson (1982) on sludge bio-flocculation and improvements in sludge settleability.

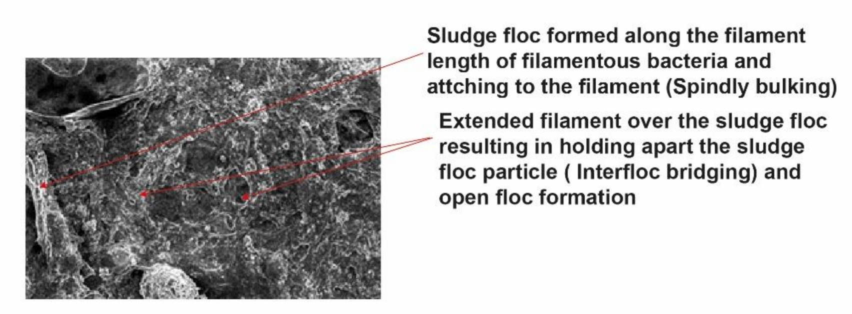
Sludge floc formed along the filament length of filamentous bacteria and attching to the filament (Spindly bulking)

Extended filament over the sludge floc resulting in holding apart the sludge floc particle (Interfloc bridging) and open floc formation

Figure 5.1a. SEM of floc (Control 0mg/L)

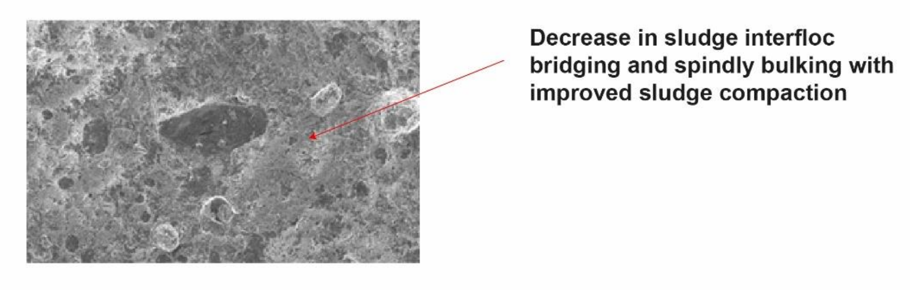
Decrease in sludge interfloc bridging and spindly bulking with improved sludge compaction

Figure 5.1b. SEM of floc (Fe-Dosed 50mg/L)

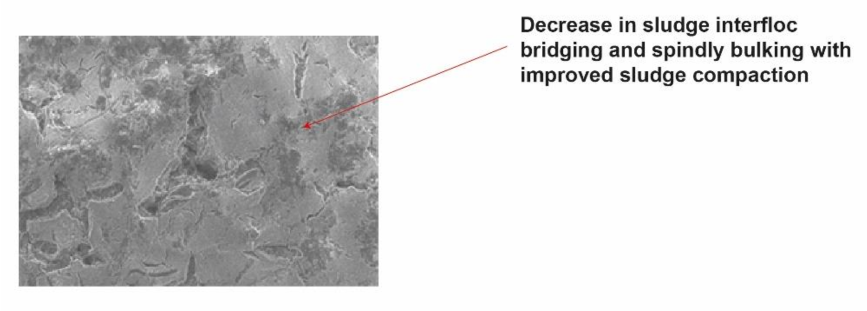
Decrease in sludge interfloc bridging and spindly bulking with improved sludge compaction

Figure 5.1c. SEM floc (Fe-Dosed 100mg/L)

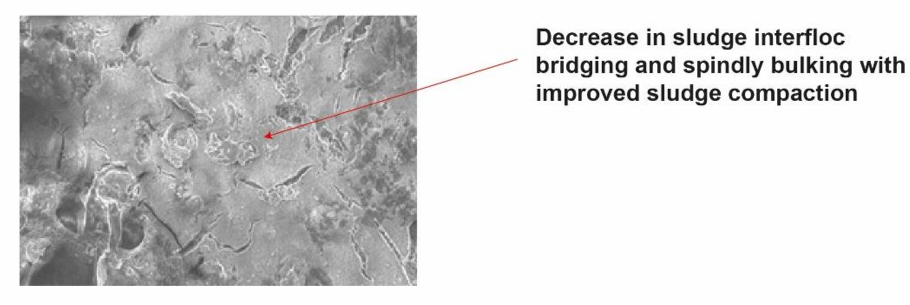
Decrease in sludge interfloc bridging and spindly bulking with improved sludge compaction

Figure 5.1d. SEM floc, (Fe-Dosed 150mg/L)

Besides, wet samples were dosed with 50mg/L ferric and investigation was conducted and comparison was made between the un-dosed wet sludge sample and 50mg/L ferric dosed sludge using a light microscope. It was observed in the control sample (0mg/L) that the filament extended into the bulk solution before treatment with ferric (Figure 5.1e) but when treated with addition of ferric (50mg/L), the length of the filament was reduced to smaller length (Figure 5.1f) and this agreed with result of Agridiotis *et al.* (2006) (Figure 5.1g-h). This is an indication that ferric dosed sludge has the capacity to impact the length of the filament in filamentous organism present in activated sludge (Figure 5.1g) and reducing them to smaller filaments that may be washed away in the settling column (Figure 5.1h).

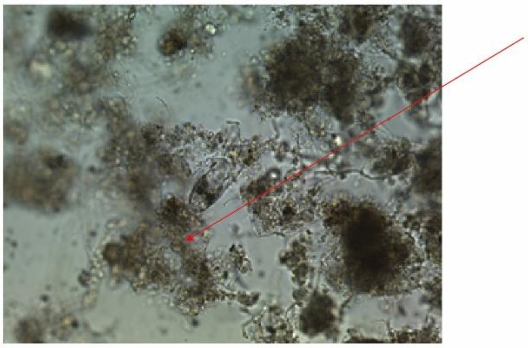

Filament extended into the bulk solution

Figure 5.1e. Control 0mg/L on a wet basis

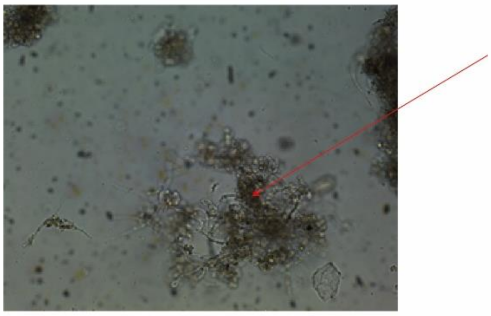

Length of filament reduced into smaller length after ferric treatment

Figure 5.1f. Ferric dosed (50mg/L wet basis)

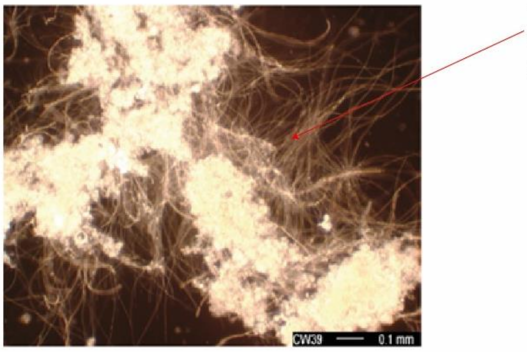

Filament extended into the bulk solution without ferric treatment

Figure 5.1g. Control 0mg/L on a wet basis

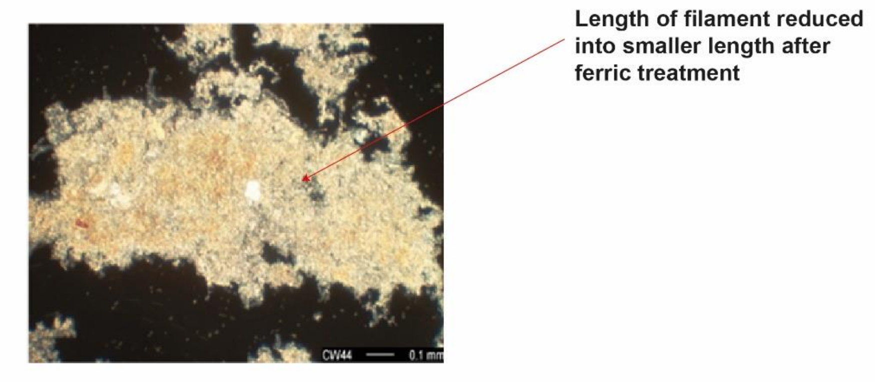

Figure 5.1h. Ferric dosed 30mg/L (wet basis)

5.2.2 Effects of Ferric dosing on ZSV and SSVI

The ZSV were investigated over range of un-dosed and ferric (Fe^{3+}) dosed activated sludge concentrations (0, 20, 50,100 and 150mg/L) for three batch test experiments (LOT- C and LOF-B) and the results from a representative ZSV test for ferric dosed sludge (Phase1) are shown in Figure 5.1 a-e (ZS = zone settling, TS = transition settling, CS = compression settling) and the ZSVs were obtained from the slope of the linear graph.

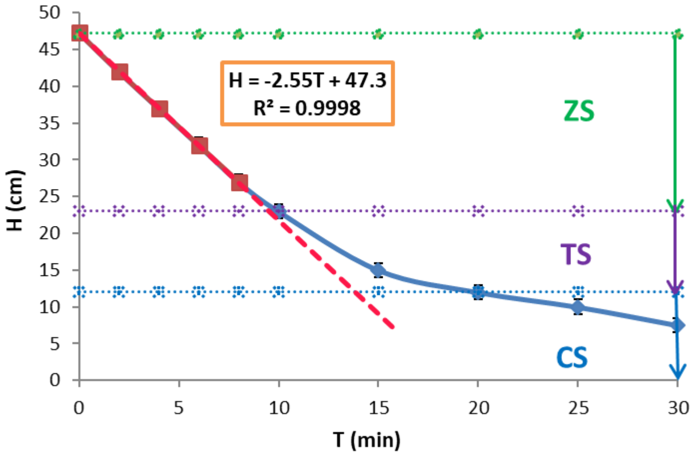

Figure 5.2a. ZSC for Un-dosed sludge (error bars represent the standard deviation of the mean)

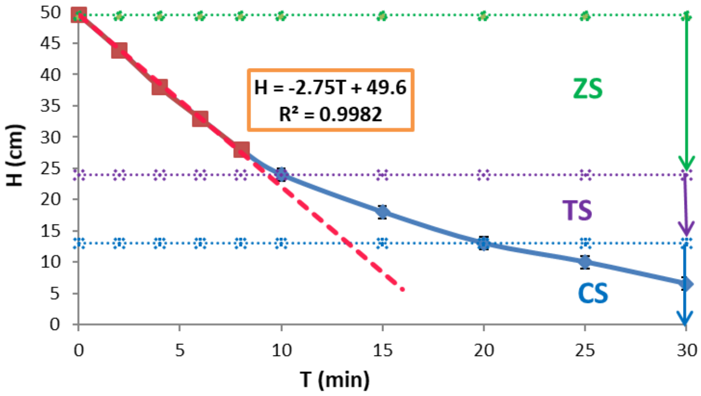

Figure 5.2b. ZSC for 20mg/L ferric dosed sludge (error bars represent the standard deviation of the mean)

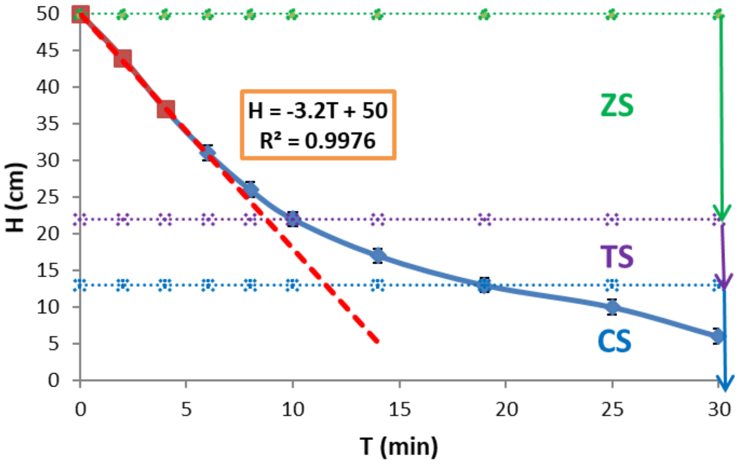

Figure 5.2c. ZSC for 50mg/L ferric dosed sludge (error bars represent the standard deviation of the mean)

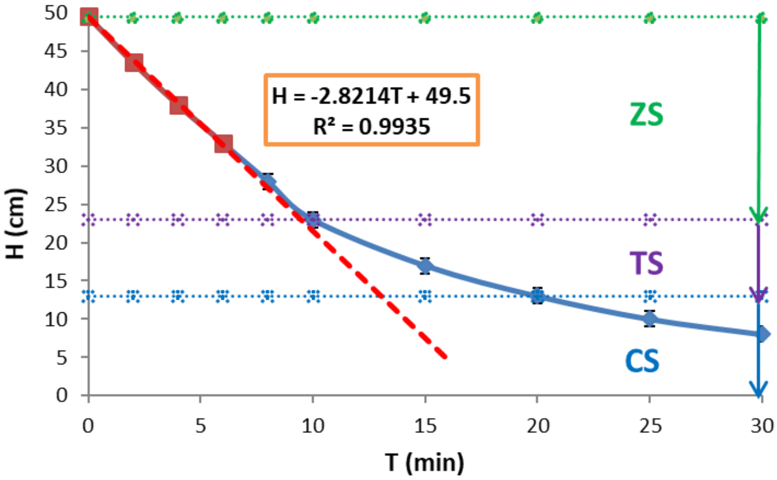

Figure 5.2d. ZSC for 100mg/L ferric dosed sludge (error bars represent the standard deviation of the mean)

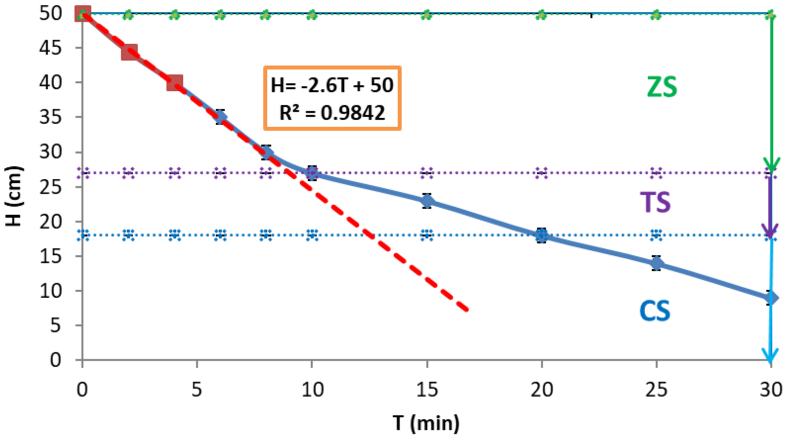

Figure 5.2e. ZSC for 150mg/L ferric dosed sludge (error bars represent the standard deviation of the mean)

The results from the typical ZSV test for ferric dosed sludge (Figure 5.2 a-e) shows that approximately 50% of the initial sludge volume within the sludge depth of the settlometer settled after 5 to 10 minutes for both the control and ferric treated sludge. The same pattern was observed with control and aluminium treated sludge in chapter Four. It was observed from zone settling curve (ZSC) that at first the activated sludge settleability was quicker due to an uninterrupted free settling within the settling column. On the other hand, after the first 10 mins of settling the change in the sludge height with time (ZSV) began to drop. This is in agreement with the observation in previous work (Vesilind 1968), the reason can be attributed to the individual sludge particles slowing down their individual settling velocities and because of the sludge floc to floc collaboration based on their close proximity. Consequently, within the zone settling regime, the observed bioaggregation of sludge flocs tends to settle as a zone of sludge blanket. This explains the decrease in the settling velocity (Tchobanoglous and Burton 1991). Furthermore, as the settling velocity began to approach the zero axes, there was observed dehydration of water from the sludge floc pore spaces and this was attributed to the compressive forces acting on the sludge flocs since the sludge floc has entered a compression settling regime. The linear portion of the ZSCs (Figure 5.2a-e) represents the settling velocity of the sludge flocs and it was further explained in previous work (Vanderhasselt and Vanrolleghem 2000) that there is a relationship between the sludge concentration and settling velocity. It was affirmed that a rise in the sludge concentration will result in a lower settling velocity due to greater resistance to water flow as the sludge passes through the settling sludge column. The results of the impact of ferric dosing on activated sludge settleability index (ZSV and SSVI) are summarised in Table 5.1. It was observed that the ZSV values increased at the beginning with increasing concentration of ferric dose (10, 20, 30, 40 and 50mg/L) and started to decrease after 100mg/L dose concentration (100 and 150mg/L). A reversed trend is observed for the SSVI, which decreased with increasing dose of ferric up to 50mg/L dose rate. At 100mg/L dose rate the SSVI had started to increase. A smaller SSVI value represented a faster settling rate of activated sludge and vice versa. This follows the same pattern with the result obtained for aluminium dosed sludge in Chapter Four (section 4.2.2). The enhancement observed in the activated sludge settleability with a decreasing SSVI and increasing ZSV between ferric dosage rates (10 and 50mg/L) (Table 5.1) can be ascribed to surface charge chemistry of the activated sludge (Liu *et al.* 2010; Martins *et al.* 2011). It was reported that filament content in activated sludge causes sludge bulking (Urbain *et al.*1993) but, it was added that charge neutralisation of negatively charged colloids by cationic hydrolysis products also affects the sludge settleability (Wilfert *et al.* 2015). The further relationship has also been observed between floc bacteria, extracellular polymeric substances (ECPS) and multivalent cations.

Nevertheless, the hypothesis was made that ferric dosed salts have the capacity to be sturdily absorbed by the surface of sludge flocs because of the released positively charged metal hydroxides which explain the charge neutralisation process and charge reversal during periods of ferric overdosing (De Haas *et al.* 2000a). In the current study, the observed characteristics of the SSVI that first reduced at a dose rate of (10 and 50mg/L) and then began to rise at 100mg/L dose concentration (100 to 150mg/L) may be linked to charge reversal as a result of overdosed ferric coagulant. Equations 5.1 and 5.2 show the two competing chemical reactions that take place during precipitation of phosphorus by ferric, namely formation of ferric hydroxide and ferric phosphate. The higher dosing concentrations of ferric when the phosphates in the wastewater have been precipitated, the excess ferric results in the formation of hydroxides as in Equation 5.1. This is accountable for the fragmentation of the overall floc structure at a higher ferric concentration resulting to drop in ZSV and increase in the SSVI.

$$\mathrm{Fe^{3+} + 3H_2O \rightarrow Fe(OH)_3 + 3H^+} \tag{5.1}$$

$$\mathrm{Fe^{3+} + PO_4{}^{3-} \rightarrow FePO_4} \tag{5.2}$$

Table 5.1 Mean and Standard deviation (SD) of ZSV and SSVI for Ferric un-dosed and dosed sludge for three batch settling tests (Sample number (N) =24; 2014-2017)

Dosing concentration (mg/L)								
Parameters	Control	Ferric dosed						
	0	10	20	30	40	50	100	150
Mean&SD ZSV (m/h)	1.54± 0.05	1.63±0.03	1.71±0.03	1.80±0.06	1.90±0.08	1.94±0.11	1.79±0.08	1.66±0.05
Mean&SD SSVI(mL/g)	67.71±8.72	63.45±7.36	59.47±6.53	54.84±5.64	50.89±5.27	48.11±5.05	58.31±3.74	63.27±4.5
Mean &SD (X) (g/L)	2.43±0.08	2.57±0.06	2.66±0.10	2.74±0.11	2.79±0.10	2.82±0.07	2.96±0.22	3.08±0.18

The activated sludge settleability processes and physicochemical properties of activated sludge flocs are affected by another key process parameter called EPS due to the ability of its internal layer that is tightly bound and adhere closely with strong stability to the cellular surface (Sheng *et al.* 2010). In the current study, the pattern observed in the plot of SSVI with increasing ferric dosing (Figure 5.2a-e) may possibly be described by the EPS binding capacity to microbial cells and its bridging nature with ferric and its overall effect on the EPS content in the activated sludge particulate (Sheng *et al.* 2006; Higgins and Sobeck 2002). The enhancement in activated sludge settleability at increasing Fe^{3+} concentrations have been attributed to the ability of ferric to neutralise the sludge surface charge. The reduced surface charge has equally been related to decrease SSVI values and ability to form bigger flocs due to higher valence and low solubility (Subramanian *et al.* 2010). The decrease in ZSV and increase in SSVI and hence decreased activated sludge settleability at the greater ferric dose concentrations are ascribed to surface charge reversal linked to high ferric dosing rate and high surface charge which is a function of weaker bonding between the various sludge floc fractions resulting in the breakage of the general activated sludge floc structure (Thompson and Forster 2003; Agridiotis *et al.* 2007).

5.2.3 Data Analysis

The measured ZSV and stirred specific volume index (SSVI) from the three years batch settling tests were used in modelling new ferric dosed activated sludge settleability. The typical result of the data set of batch tests was analysed using the Minitab 17 software and solver optimisation tool. The solver optimisation tool and the minitab 17 were used and the results were also analysed (as reported in aluminium dosed sludge (section 4.2.3)) using the non-linear regression in the minitab 17 software and the F-test ($F>0.05$), R^2 (coefficient of determination), residual plot, probability plot and interval plot related to ferric dosed sludge was used to validate how the ZSV model fits the ZSV experimental data.

5.2.4 Model development and Model validity for Ferric dosed sludge

The protocol for evaluation of activated sludge settleability and definition of relationship between the zone settling velocity and concentration (Vesilind equation-Equation 1.1) and its justification are reported in section 4.2.4. The Vesilind equation ($\mathrm{ZSV} = \mathrm{v}_0\, \mathrm{e}^{-\mathrm{KX}}$) forms the basis for modelling FSTs in wastewater treatment plants (WWTP).

In a previous study by Ojo and Ifelebuegu (2019c) the batch settling test measurements [zone settling curve (ZSC)] of ZSV reveals ZSV as a linear representation (Figure 5.2d) of sludge height as a function of time (m/h) for 100mg/L Fe^{3+} dosed sludge. Also, the results as earlier reported by Ojo and Ifelebuegu (2019c), showed that the ZSV increased, while SSVI decreased with increasing concentrations of Fe^{3+} salt up to <100mg/L. Fe^{3+} facilitated the agglomeration of the activated sludge flocs, thereby improving settleability. Beyond this concentration there was a slight breakdown in sludge settleability due primarily to surface charge reversal.

In a complete range of concentrations of Fe^{3+} used (0 to 150mg/L), a non-linear representation of ZSV and SSVI as a function of ferric dosing concentration was observed in Figure 5.3 (Phase 1 result -LOF E1) and Figure 5.4 (Phase1 result-LOF H1). This provided an insight into the modification of the conventional empirical model of ZSV (Equation 1.1) to include a new Fe^{3+} dosing parameter. It further reveals Fe^{3+} dosing concentration had a non-linear relationship with ZSV and SSVI.

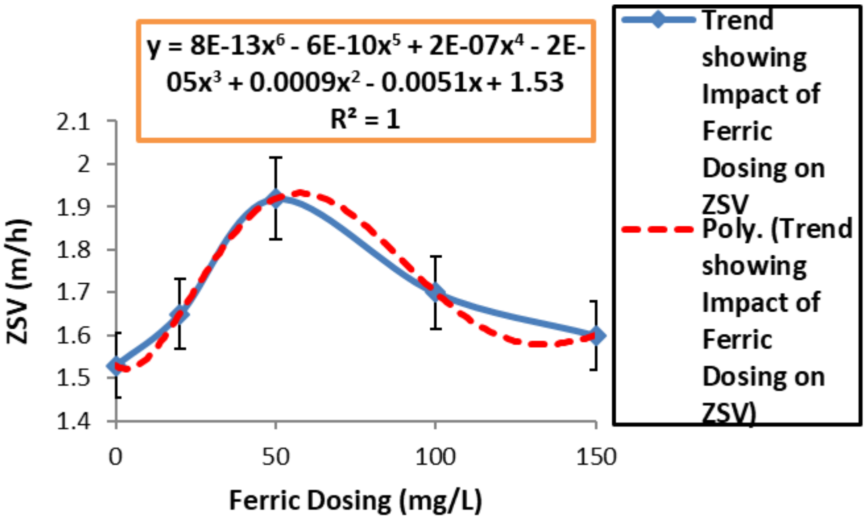

Figure 5.3. The Impact of Ferric Dosing (mg/L) on ZSV (m/h) (error bars represent standard deviation of the mean)

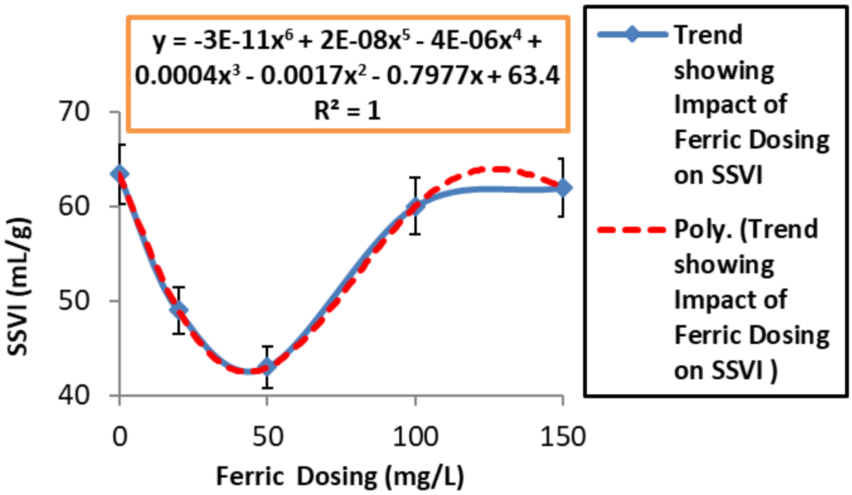

Figure 5.4. The Impact of Ferric Dosing (mg/L) on SSVI (mL/g) (error bars represent standard deviation of the mean)

The conventional empirical model for sedimentation in FSTs expressed as a function of solid concentration, termed Vesilind equation is illustrated in Equation 1.1. It was earlier stated in section 4.2.4 that the empirical coefficient $\mathrm{v_0}$ and k are obtained by performing ZSV test over a range of mixed liquor suspended solids (MLSS) concentration for both un-dosed and Fe^{3+} dosed sludge and applying linear regression to the linearised form of the Vesilind equation to obtain a new expression ($\ln ZSV = -\mathrm{kX} + \mathrm{lnv_0}$) (Equation 4.9 in section 4.2.5).

The plot of natural log of ZSV (m/h) against un-dosed and Fe^{3+} dosing concentration for the average data from the various batch test (Table 5.1) is shown in Figure 5.5. The negative of the gradient of each linear regression for the batch test is the Vesilind k value while the intercept is the Vesilind $\mathrm{v_0}$ parameter. However, because it is a ferric dosed sludge, then Vesilind $\mathrm{v_0}$ and k expression becomes re-defined as ZSV_0 and $\mathrm{K_d}$ for Fe dosed sludge. There is a need to define that there is a relationship between Fe^{3+} dosing concentration and ZSV which was not accounted for in the conventional Vesilind model equation in Equation 1.1. This can be achieved by the transformation of data in the Vesilind exponential relationship and back tracking to calculate the values of the Vesilind exponential constant parameter. Thus, the linearised ZSV was plotted against Fe^{3+}dosing up to 150mg/L (Figure 5.5). However, it was observed from Figure 5.5, that the relationship between Fe^{3+} dose concentrations and the settleability can be accurately described for up to 50mg/L dose concentration (Figure 5.6) and the gradient and intercept accounted for the Vesilind coefficients for Fe ($\mathrm{K_d}$ = -0.0042 and ZSV_0 = 1.534m/h). It can be concluded that the calculated ZSV_0 and $\mathrm{K_d}$ parameter for Ferric dosed sludge from the graph of ln ZSV against Fe dosing concentration is a function of Ferric dose concentrations up to 50mg/L.

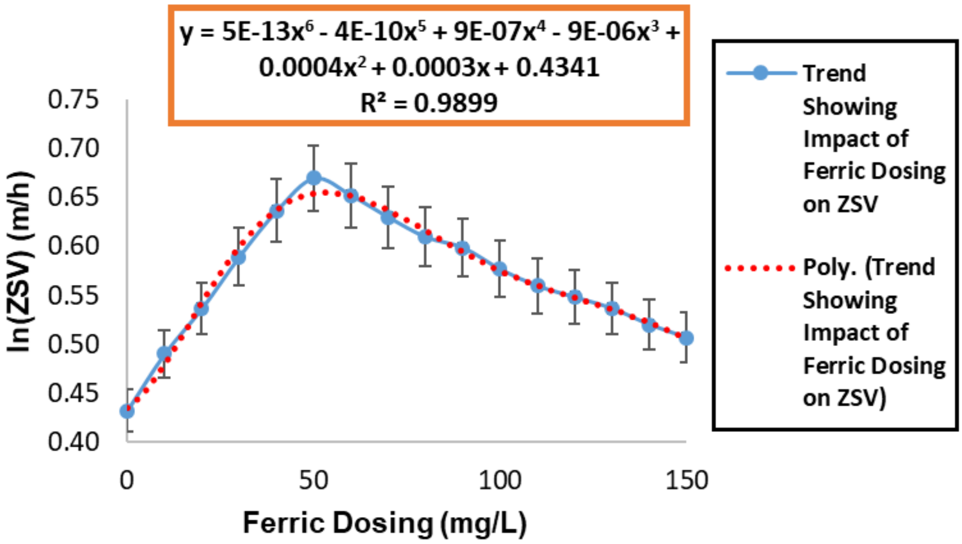

Figure 5.5. Natural log of ZSV against Ferric Dosing (up to 150mg/L) (The error bars represent standard deviation of the mean)

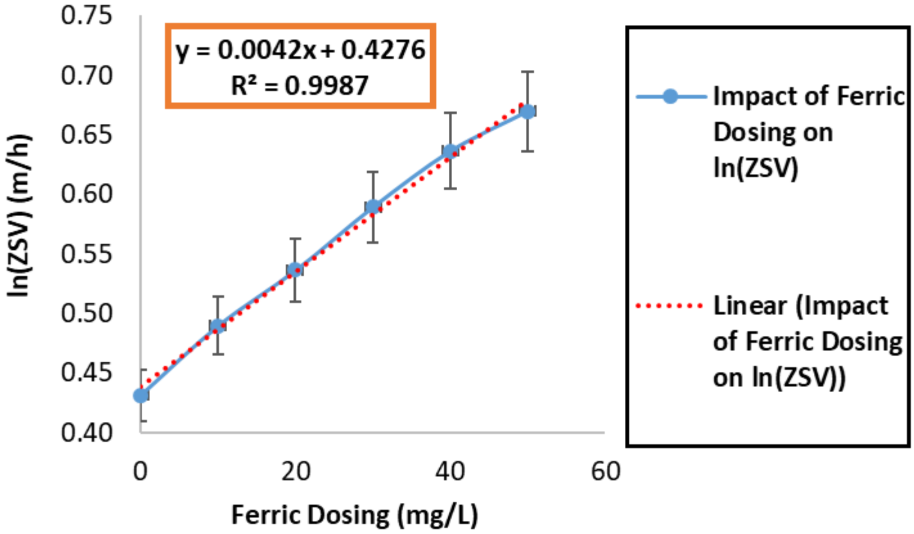

Figure 5.6. Natural log of ZSV against Ferric Dosing (up to 50mg/L) (The error bars represent standard deviation of the mean)

The natural logarithm of SSVI was plotted against the Ferric dosing concentration up to 150mg/L (Figure 5.7). Nevertheless, a linear relation existed up to 50mg/L (Figure 5.8) and the gradient and intercept of the plot accounted for the coefficients for Fe^{3+} ($\text{gradient} = 0.0074$ and $\text{intercept} = 68.10$mL/g).

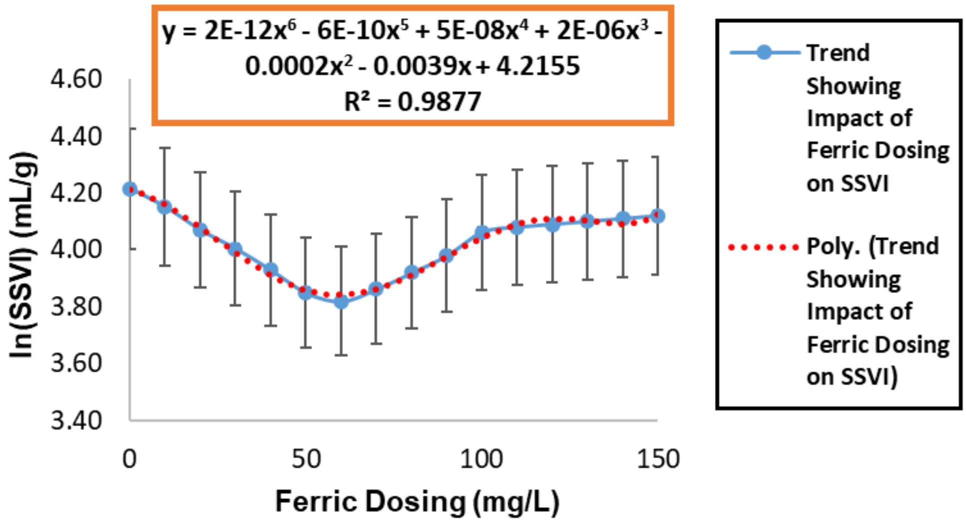

Figure 5.7. Natural log of SSVI against Ferric Dosing (up to 150mg/L) (The error bars represent standard deviation of the mean)

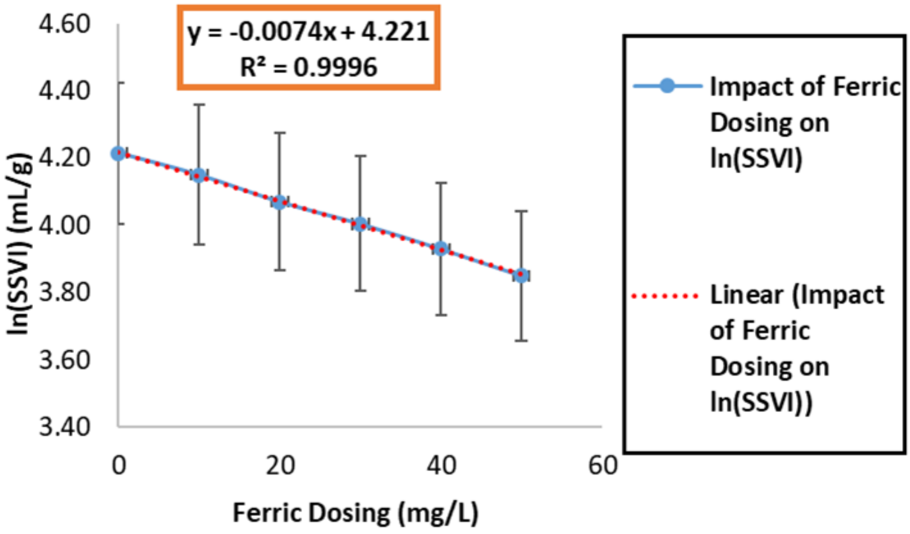

Figure 5.8. Natural log of SSVI against Ferric Dosing (up to 50mg/L)

5.2.5 Novel Model Calibration to Include Ferric Dosing Parameter

The exponential form of the Vesilind equation (Equation 1.1) can be optimised to include ferric dosing parameter by investigating a new model equation for settling velocity. The investigated ZSVo and $\mathrm{K_d}$ parameter for ferric dosed sludge from the graph of ln (ZSV) and ln (SSVI) against ferric dosing concentration (mg/L) (Figures 5.5 - 5.8) shows linearised and exponential correlation between ZSV and SSVI with Ferric dosing concentrations. The new empirical model for settling velocity for a Ferric dosed activated sludge can take the form of a decay equation ($A = A_o e^{-\lambda t}$) (Equation 4.10 - Chapter Four) that obeys the exponential law of decay (the number of unstable nuclei that decay each second in radioactive sample depends on how many unstable nuclei are left in the sample).

The new equation in Equation 5.3 shows the inclusion of a new ferric dosing protocol (Dc) that follows the decay equation.

$$\mathrm{ZSV_{Fe}} = ((\mathrm{C_0})_{\mathrm{Fe}}\ (\mathrm{D_C})_{\mathrm{Fe}}\ + (\mathrm{ZSV_0})_{\mathrm{Fe}})\mathrm{e}^{-((\mathrm{K_d})_{\mathrm{Fe}} - (\mathrm{C_K})_{\mathrm{Fe}}(\mathrm{D_C})_{\mathrm{Fe}})\mathrm{X_{Fe}}} \qquad \textbf{(5.3)}$$

Where,

$\mathrm{ZSV_{Fe}}$ = Actual settling velocity (m/h) $\mathrm{Fe^{3+}}$ dosed sludge

$(\mathrm{ZSV_0})_{\mathrm{Fe}}$ = Maximum settling velocity (m/h) for $\mathrm{Fe^{3+}}$ dosed sludge

$(\mathrm{K_d})_{\mathrm{Fe}}$ = Empirical $\mathrm{Fe^{3+}}$ dosed sludge settling parameter relating to sludge compaction

$(\mathrm{C_0})_{\mathrm{Fe}}$= Empirical $\mathrm{Fe^{3+}}$ dosing constant related to stokes settling velocity

$(\mathrm{C_K})_{\mathrm{Fe}}$ = Empirical Fe^{3+} dosing constant related sludge compaction

$(\mathrm{D_C})_{\mathrm{Fe}}$ = Fe^{3+} dosing concentration (mg/L)

$\mathrm{X_{Fe}}$= Fe^{3+}dosed MLSS concentration (mg/L)

The Equation 4.11 for the new aluminium dosed sludge stated earlier differs from ferric dosed sludge in Equation 5.3, on the account of their different process parameters such as maximum settling velocity, empirical dosing sludge settling parameter relating to sludge compaction, empirical dosing constant related to maximum settling velocity and empirical dosing constant related sludge compaction and dosed MLSS concentration.

Equation 5.3 obeys the exponential law of decay and both the additive and multiplicative rule of exponentials. The empirical coefficients in Equation 5.3 $ZSV_0 \text{ and } \mathrm{k_d}$ are typically determined by performing zone settling velocity (ZSV) batch tests over a range of ferric dosing concentrations (0, 10, 20, 30, 40, 50, 100 and 150mg/L) and applying regression analysis and linear approximation to Equation 5.3 by taking the natural log.

For a clearer comprehension of the new empirical heuristic expression for settling velocity for a dosed activated sludge, the comparison of terms in the new ferric dosed sludge expression and conventional decay equation becomes vital. The version of terms in Equation 4.10 (Chapter Four) compared with Equation 5.3 is as follows; $\mathrm{A_o} = ((\mathrm{C_0})_{\mathrm{Fe}}\ (\mathrm{D_C})_{\mathrm{Fe}} + (\mathrm{ZSV_0})_{\mathrm{Fe}})$, $\lambda = ((\mathrm{K_d})_{\mathrm{Fe}} - (\mathrm{C_K})_{\mathrm{Fe}}\,(\mathrm{D_C})_{\mathrm{Fe}})$ and t=$\mathrm{X_{Fe}}$. This shows below that applying the additive rule with e as a common factor in Equation 5.3 then Equation 5.4 is obtained:

$$((\mathrm{C_0})_{\mathrm{Fe}}(\mathrm{D_C})_{\mathrm{Fe}}\,\mathrm{e} + (\mathrm{ZSV_0})_{\mathrm{Fe}}\,\mathrm{e}) = ((\mathrm{C_0})_{\mathrm{Fe}}\,(\mathrm{D_C})_{\mathrm{Fe}} + (\mathrm{ZSV_0})_{\mathrm{Fe}})\mathrm{e} \qquad 5.4$$

Conversely, applying the multiplicative rule with $\mathrm{X_{Fe}}$ as a common factor in Equation 5.3, the expression in Equation 5.5 was realised.

$$-((\mathrm{K_d})_{\mathrm{Fe}} - (\mathrm{C_K})_{\mathrm{Fe}}(\mathrm{D_C})_{\mathrm{Fe}})\mathrm{X_{Fe}} = \mathrm{e}^{-(\mathrm{K_d})_{\mathrm{Fe}}\,\mathrm{X_{Fe}}} \times \mathrm{e}^{-(\mathrm{C_K})_{\mathrm{Fe}}\,(\mathrm{D_C})_{\mathrm{Fe}}\,\mathrm{X_{Fe}}} \qquad 5.5$$

The constants $(\mathrm{ZSV_0})_{\mathrm{Fe}}$; $(\mathrm{K_d})_{\mathrm{Fe}}$; $(\mathrm{C_0})_{\mathrm{Fe}}$ and $(\mathrm{C_K})_{\mathrm{Fe}}$ helps in shifting the ZSV model to predict the observed values in ferric dosed sludge. However, the experimentally estimated ZSV data have been universally used for regulating settling models in wastewater industry (Vesilind 1968: $\mathrm{ZSV} = \mathrm{v_0 e^{-kX}}$). Since it is common practice to deduce the Vesilind empirical constants ($\mathrm{v_0}$ and k) through conducting batch laboratory ZSV test over a range of concentrations and applying linear regression evaluation to a linearised form of Vesilind equation ($\ln \mathrm{V} = -\mathrm{kX} + \ln \mathrm{v_0}$), it becomes paramount to apply the same principle to the new ferric dosed activated sludge model.

We can consider defining F_1 and F_2 from Equation 5.3 as follows: $\mathrm{F_1} = ((\mathrm{ZSV_0})_{\mathrm{Fe}} \times (\mathrm{D_C})_{\mathrm{Fe}})$ and $\mathrm{F_2} = ((\mathrm{K_d})_{\mathrm{Fe}}) - ((\mathrm{C_K})_{\mathrm{Fe}}\,(\mathrm{D_C})_{\mathrm{Fe}})$ as two functions of ZSV and this gives Equation 5.6

$$\mathrm{ZSV_{Fe}} = \mathrm{F_1}\,\mathrm{e}^{-\mathrm{F_2}\ \mathrm{X_{Fe}}} \tag{5.6}$$

As earlier mentioned that there exists an exponential relationship between the ZSV and Fe dosing (Figure 5.3) but because the relationship is a non-linear relationship, calculating the value of the new empirical coefficient $(\mathrm{ZSV_0})_{\mathrm{Fe}}$; $(\mathrm{K_d})_{\mathrm{Fe}}$; $(\mathrm{C_0})_{\mathrm{Fe}}$ and $(\mathrm{C_K})_{\mathrm{Fe}}$ of ferric dosed activated sludge model can be realised by linearising Equation 5.3 to become Equation 5.7

Therefore, below is the linear approximation (Equation 5.7) obtained by taking the natural log of Equation 5.3:

$$\ln(\mathrm{ZSV_{Fe}}) = \ln((\mathrm{C_0})_{\mathrm{Fe}}\,(\mathrm{D_C})_{\mathrm{Fe}} + (\mathrm{ZSV_0})_{\mathrm{Fe}}) - ((\mathrm{K_d})_{\mathrm{Fe}} - (\mathrm{C_K})_{\mathrm{Fe}}(\mathrm{D_C})_{\mathrm{Fe}})\mathrm{X_{Fe}} \qquad 5.7$$

The Equation 5.7 also follows the equation of a straight line $(\mathrm{Y} = \mathrm{MX} + \mathrm{C})$, M = Slope while C= Intercept and hence Equation 5.7 can be modified as Equation 5.8 by re-defining $\ln(\mathrm{ZSV_{Fe}}) = \mathrm{Z}$; $(\ln((\mathrm{C_0})_{\mathrm{Fe}}\,(\mathrm{D_C})_{\mathrm{Fe}} + (\mathrm{ZSV_0})_{\mathrm{Fe}}) = \mathrm{P}$ and $((\mathrm{K_d})_{\mathrm{Fe}} - (\mathrm{C_K})_{\mathrm{Fe}}\,(\mathrm{D_C})_{\mathrm{Fe}}) = Q$ respectively.

$$\mathrm{Z} = \mathrm{P} - \mathrm{QX} \tag{5.8}$$

The transformation of Equation 5.3 to 5.7 allowed establishing a linear relationship between Z and X (Equation 5.8) and not between ZSV and X since it is already an exponential model. This transformation allows back tracking the constant of the new model for ferric dosed sludge $(\mathrm{ZSV_0})_{\mathrm{Fe}}$; $(\mathrm{K_d})_{\mathrm{Fe}}$; $(\mathrm{C_0})_{\mathrm{Fe}}$ and $(\mathrm{C_K})_{\mathrm{Fe}}$ to predict the ZSV experimental data. Therefore, once a linear relationship is established between Z and X $(\mathrm{Z} = \mathrm{P} - \mathrm{QX})$, the value of the ferric dosed settleability constants $(\mathrm{ZSV_0})_{\mathrm{Fe}}$; $(\mathrm{K_d})_{\mathrm{Fe}}$; $(\mathrm{C_0})_{\mathrm{Fe}}$ and $(\mathrm{C_K})_{\mathrm{Fe}}$ can be evaluated and the experimental value of ZSV and dosing concentrations $(\mathrm{D_C})_{\mathrm{Fe}}$ without performing a ZSV batch experiment. A new expression (5.9 and 5.10) was obtained from Equation 5.8 for calculating the value of $(\mathrm{D_C})_{\mathrm{Fe}}$ as it relates to ferric when the four constants $(\mathrm{ZSV_0})_{\mathrm{Fe}}$; $(\mathrm{K_d})_{\mathrm{Fe}}$; $(\mathrm{C_0})_{\mathrm{Fe}}$ and $(\mathrm{C_K})_{\mathrm{Fe}}$ for ferric dosed sludge are known.

$$(\mathrm{D_C})_{\mathrm{Fe}} = \frac{\mathrm{e}^{\mathrm{P}} - (\mathrm{ZSV_0})_{\mathrm{Fe}}}{(\mathrm{C_0})_{\mathrm{Fe}}} \tag{5.9}$$

$$(\mathrm{D_C})_{\mathrm{Fe}} = \frac{\mathrm{Q} + (\mathrm{K_d})_{\mathrm{Fe}}}{(\mathrm{C_K})_{\mathrm{Fe}}} \tag{5.10}$$

The results of regression analysis using Equation 5.7 showed that all the coefficient of determination (R²) were close to 1 (Figure 5.6). This suggests that the exponential function in Equation 5.3 was suitable to model the ferric dosed activated sludge settleability process (ZSV).

However, the SSVI expression for ferric dosed activated sludge can be derived from the new empirical ferric dosed activated sludge model for settling velocity in Equation 5.3. The k and v_0 parameter calculated from the expression in Catunda *et al.* (1989) in Equation 5.11 and 5.12 becomes re-written as $(ZSV_0)_{Fe}$ and $(K_d)_{Fe}$ parameter for ferric dosed sludge computed in Equations 5.11 and 5.12.

$$(K_d)_{Fe} = 0.16 + 2.7 \times 10^{-3} \times \text{SSVI}_{Fe} \tag{5.11}$$

$$(ZSV_0)_{Fe} = (10.9 + 0.18 \times \text{SSVI}_{Fe}) \times e^{(-0.016 \times \text{SSVI}_{Fe})} \tag{5.12}$$

Where,

$(K_d)_{Fe}$= Empirical ferric dosed activated sludge settling parameter related to sludge compaction (L/g)

$(ZSV_0)_{Fe}$ = Maximum settling velocity for ferric dosed activated sludge related to stokes settling velocity (m/h)

$SSVI_{Fe}$ = Stirred sludge volume index (mL/g) ferric dosed activated sludge

In deriving a new expression for ferric dosed SSVI, Equation 5.11 and Equation 5.12, was compared with the existing Pitman (1980) and White (1975) expression in Equation 1.2 ($\frac{v_0}{k} = 68e^{(-0.016 \times \text{SSVI})}$) and the Equation 1.2 can be re-written in the form of $(ZSV_0)_{Fe}$ and $(K_d)_{Fe}$= parameter as follows:

$$(ZSV_0)_{Fe} = 68(K_d)_{Fe} = e^{(-0.016\ \text{SSVI}_{Fe})} \tag{5.13}$$

The new SSVI expression (Equation 5.14) was obtained by substituting Equations 5.11-5.13 into Equation 5.3. Therefore, the new SSVI expression for ferric dosed activated sludge (Equation 5.14) was derived from substituting the compared $(K_d)_{Fe}$ and $(ZSV_0)_{Fe}$ parameter calculated from the redefined expression in Catunda *et al.* (1989) with the Pitman (1980) and White (1975) expression in Equation 1.2 ($\frac{v_0}{k} = 68e^{(-0.016 \times \text{SSVI})}$) and substituting into the new ferric dosed activated sludge model for settling velocity in Equation 5.3.

$$\mathbf{SSVI_{Fe}(mL/g)} = -\ln\left[\left(\frac{ZSV_{Fe}}{68((K_d)_{Fe}\ X_{Fe}) + ((C_K)_{Fe}(D_C)_{Fe}\ X_{Fe})}\right) - \left(\frac{(C_0)_{Fe}\ (D_C)_{Fe}}{68(K_d)_{Fe}}\right) \Big/ 0.016\right] \tag{5.14}$$

The results of regression analysis for the impact of ferric dosing on SSVI using the experimental data in the batch test conducted showed that all the coefficient of determination (R^2) were close to 1 (Figure 5.8). This suggests that the linearized expression in Equation 5.14 was suitable to model the impact of ferric dosing on activated sludge settleability (SSVI) process.

5.2.6 Validation of Novel Model for Impact of Ferric Dosing on ZSV and SSVI

5.2.6.1 Novel ZSV Model

The heuristic expression used for derivation of the new model for ferric dosed sludge expressed in Equation 5.3 $(ZSV_{\mathrm{Fe}} = ((\mathrm{C}_0)_{\mathrm{Fe}}\,(\mathrm{D}_\mathrm{C})_{\mathrm{Fe}} + (\mathrm{ZSV}_0)_{\mathrm{Fe}})\mathrm{e}^{-((\mathrm{K}_\mathrm{d})_{\mathrm{Fe}}-(\mathrm{C}_\mathrm{K})_{\mathrm{Fe}}\,(\mathrm{D}_\mathrm{C})_{\mathrm{Fe}})\mathrm{X}_{\mathrm{Fe}}})$ and its linear approximation $(\ln(\mathrm{ZSV}_{\mathrm{Fe}}) = \ln((\mathrm{C}_0)_{\mathrm{Fe}}\,(\mathrm{D}_\mathrm{C})_{\mathrm{Fe}} + (\mathrm{ZSV}_0)_{\mathrm{Fe}}) - ((\mathrm{K}_\mathrm{d})_{\mathrm{Fe}} - (\mathrm{C}_\mathrm{K})_{\mathrm{Fe}}\,(\mathrm{D}_\mathrm{C})_{\mathrm{Fe}})\mathrm{X}_{\mathrm{Fe}})$. The experimental data of three batch (ferric) settling velocity test can be classified into two groups. The first group (Figures 5.2 - 5.6) were used to develop the model while the second group (Tables 5.2 - 5.3, Figures 5.9 and Figure 5.10) are used to validate the model.

The model was validated using two approaches namely; solver optimisation tool and minitab 17. Although, the batch settling test measurements revealed ZSV as a linear representation (sludge height as a function of time) (Figure 5.2), but, on the contrary, a non-linear representation was observed in Figures 5.5 - 5.6, showing ZSV and SSVI as a function of ferric dosing concentration. This also allows the inclusion of a new ferric dosing parameter $(\mathrm{D}_\mathrm{C})_{\mathrm{Fe}}$ in the existing Pitman (1980) and White (1975) model reported in Equation 1.2 and Catunda *et al.* (1989) in Equations 4.6 and 4.7 which are both in agreement with the Vesilind (1968) expression.

The solver optimisation tool and Minitab 17 was utilised to fit non-linear model data to actual experimental data for ferric dosed sludge (Table 5.2-5.3). Table 5.3 and Figure 5.9-5.10 shows a comparison of the experimental and predicted zone settling velocities using Equation 5.3. It was observed that the validation result is good enough and valid for ferric concentration ranging from (0, 10, 20, 30, 40, 50, and 100mg/L). The non-linear fitting, interval plot, residual plot and probability plot (Figure 5.9) further establishes the validity of the model using Minitab 17. The probability plot creates estimated cumulative distribution function from ferric dosed sample data by plotting the value of each observation against its estimated cumulative probability and a scale transformation allows the fitted distribution to form a straight line.

A good distribution fit is one where the observations are near the fitted line. The data in Figure 5.9 are near the fitted line hence it indicates a good distribution fit between the model and experimental data. The residual shows how far the model data from the experimental data is and the residual plot in Figure 5.9 shows a good fit. The coefficient of determination (R^2) was 0.998 in Table 5.2, shows that the difference between the observed experimental value and the model predicted values are small and unbiased. The interval plot (Figure 5.9) shows that at 95%

confidence interval (CI), the mean value of ZSV model and experimental is significant as the 95% confidence interval bar does not overlap.

Table 5.2: Model Validation Minitab 17 and Solver Optimisation Tool Result for Ferric

Parameters	Estimated values
ZSV_0	0.740
C_0	0.0089
K_d	-0.290
C_K	-0.0025
α	0.05
R^2	0.998
SSD	0.1410

R²-R Squared, α-significance level, CI-Confidence Interval

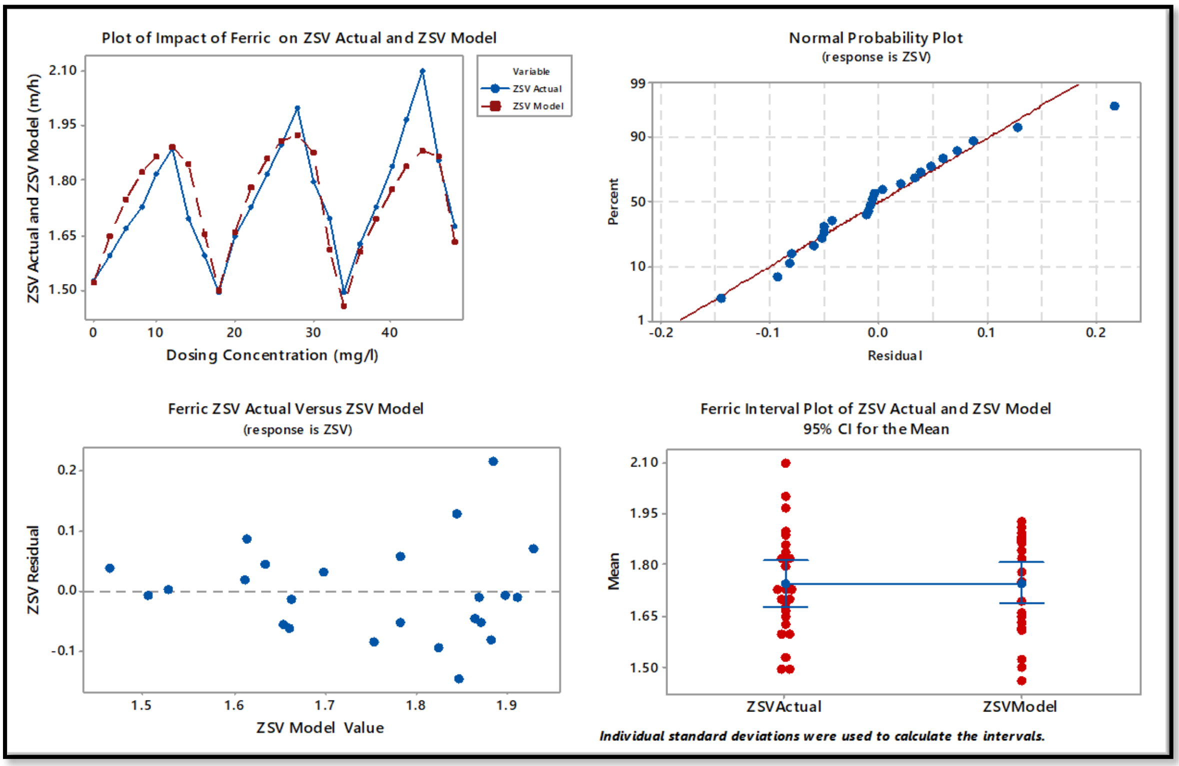

Figure 5.9. Non-Linear Fitting, Interval Plot, Residual Plot and Probability plot (Ferric)

The probability plot creates estimated cumulative distribution function from ferric dosed sample data by plotting the value of each observation against its estimated cumulative probability and a scale transformation allows the fitted distribution to form a straight line.

A good distribution fit is one where the observations are near the fitted line. The data in Figure 5.8 are near the fitted line hence it indicates a good distribution fit between model and experimental data. The residual shows how far the model data from the experimental data is and the residual plot in Figure 5.9 shows a good fit. The coefficient of determination (R^2) was 0.998 in Table 5.2, shows that the difference between the observed experimental value and the model predicted values are small and unbiased. The interval plot (Figure 5.9) shows that at 95% CI, the mean value of ZSV model and experimental is significant as the 95% confidence interval bar do not overlap. The solver optimisation tool allows the solver parameter to be set for the target objective of a reduced sum of square deviation (SSD) value so that the model fits the experimental data. In Table 5.2 and Figure 5.10, a significant SSD value of 0.141 was reported and it indicated the ZSV model fits the actual ZSV value.

Table 5.3. ZSV experimental and ZSV model Comparison using Solver optimisation and Minitab 17 for Ferric Dosed Sludge (Sample number (N) =24; 2014-2017)

MLSS (g/l)	ZSV (m/h)	ZSV Model (m/h)	Fe-Dosing (mg/L)	Standard deviation	Residual	Squared Residual	Squared ZSV
2.50	1.53	1.53	0.00	1.00×10^{-5}	3.44×10^{-3}	1.00×10^{-5}	2.34
2.60	1.60	1.65	10.00	2.79×10^{-3}	-5.29×10^{-2}	2.79×10^{-3}	2.56
2.68	1.67	1.75	20.00	6.65×10^{-3}	-8.16×10^{-2}	6.65×10^{-3}	2.79
2.74	1.73	1.82	30.00	8.73×10^{-3}	-9.34×10^{-2}	8.73×10^{-3}	2.99
2.78	1.82	1.87	40.00	2.55×10^{-3}	-5.05×10^{-2}	2.55×10^{-3}	3.31
2.80	1.89	1.89	50.00	4.00×10^{-5}	-5.93×10^{-3}	4.00×10^{-5}	3.57
2.72	1.70	1.84	100.00	2.1×10^{-2}	-1.45×10^{-1}	2.1×10^{-2}	2.89
2.90	1.60	1.66	150.00	3.47×10^{-3}	-5.90×10^{-2}	3.48×10^{-3}	2.56
2.45	1.50	1.50	0.00	2.00×10^{-5}	-4.64×10^{-3}	2.00×10^{-5}	2.25
2.62	1.65	1.66	10.00	1.40×10^{-4}	-1.16×10^{-2}	1.40×10^{-4}	2.72
2.75	1.73	1.78	20.00	2.63×10^{-3}	-5.13×10^{-2}	2.63×10^{-3}	2.99
2.84	1.82	1.86	30.00	1.87×10^{-3}	-4.31×10^{-2}	1.86×10^{-3}	3.31
2.89	1.90	1.91	40.00	1.10×10^{-4}	-1.02×10^{-2}	1.10×10^{-4}	3.61
2.90	2.00	1.93	50.00	5.21×10^{-3}	7.23×10^{-2}	5.22×10^{-3}	4.00
3.15	1.80	1.88	100.00	6.39×10^{-3}	-7.99×10^{-2}	6.38×10^{-3}	3.24

3.25	1.70	1.61	150.00	7.45×10^{-3}	8.64×10^{-2}	7.46×10^{-3}	2.89
2.35	1.50	1.46	0.00	1.47×10^{-3}	3.83×10^{-2}	1.46×10^{-3}	2.25
2.50	1.63	1.61	10.00	4.20×10^{-4}	2.03×10^{-2}	4.10×10^{-4}	2.67
2.55	1.73	1.70	20.00	1.04×10^{-3}	3.23×10^{-2}	1.04×10^{-3}	2.99
2.63	1.84	1.78	30.00	3.52×10^{-3}	5.93×10^{-2}	3.52×10^{-3}	3.39
2.70	1.97	1.84	40.00	1.64×10^{-2}	1.28×10^{-1}	1.64×10^{-2}	3.88
2.76	2.10	1.88	50.00	4.70×10^{-3}	2.17×10^{-1}	4.70×10^{-3}	4.41
3.00	1.86	1.87	100.00	6.00×10^{-5}	-7.64×10^{-3}	6.00×10^{-5}	3.46
3.10	1.68	1.63	150.00	2.22×10^{-3}	4.71×10^{-2}	2.22×10^{-3}	2.82

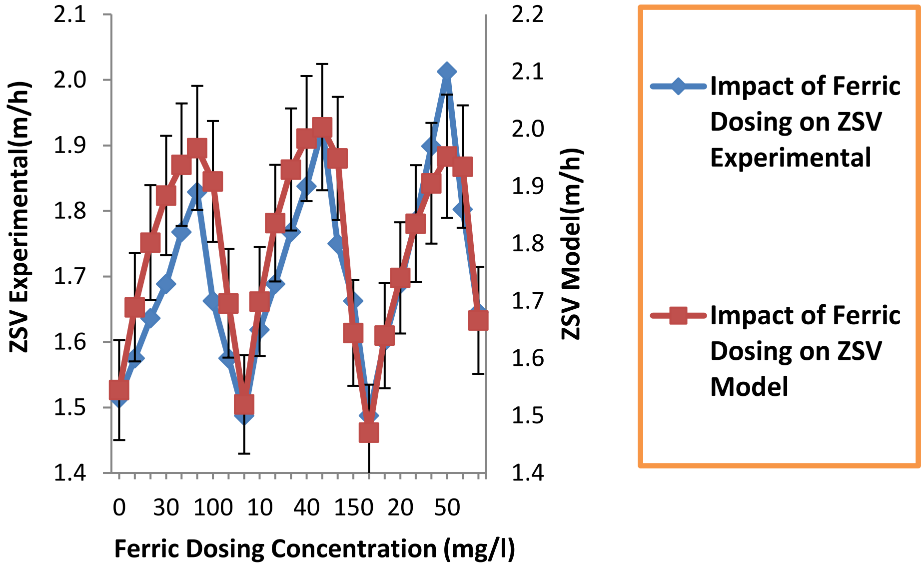

Figure 5.10. Non-Linear Curve Fitting of Impact of Ferric on ZSV (The bars represent standard deviation of the mean)

$$\mathrm{ZSV_{Fe}} = \left((0.0089\ (\mathrm{D_C})_{\mathrm{Fe}}\ +\ 0.740)\mathrm{e}^{-0.290+0.0025\ (\mathrm{D_C})_{\mathrm{Fe}}\,\mathrm{X_{Fe}}}\right) \qquad (5.15)$$

The values of, $(\mathrm{C_0})_{\mathrm{Fe}}$; $(\mathrm{ZSV_0})_{\mathrm{Fe}}$; $(\mathrm{K_d})_{\mathrm{Fe}}$ and $(\mathrm{C_K})_{\mathrm{Fe}}$ for ferric dosed sludge (Table 5.2) used to validate the numerical model in Equation 5.15 are the same at different dosing concentration (0, 10, 20, 30 ,40 ,50 and 100mg/L) and approximate to 0.0089, 0.740, -0.290 and -0.0025 respectively. Therefore, the new ZSV model for ferric dosed sludge is expressed as Equation 5.15.

5.2.7 Conclusion and practical relevance

The impact of ferric dosing on activated sludge settleability (ZSV and SSVI) was studied in batch settling tests over a three years period using a type 305 settlometer. The results showed that ZSV increased while SSVI decreased with increasing dose of Fe^{3+}. The best settleability was achieved at 50mg/L dose of Fe^{3+}. The improved settleability with increasing dose of Fe^{3+} was attributed to the improve bioaggregation of the activated sludge with dosing and through EPS binding capacity to microbial cells through its bridging nature with ferric. The sludge settleability started to decline between >50mg/L to 150mg/L dose concentrations. The decrease in ZSV and increase in SSVI and hence decreased settleability at the higher dose concentrations are attributed surface charge reversal linked to high ferric dosing rate and high surface charge which is a function of weaker bonding between the various sludge floc fractions resulting to the breakage of the general activated sludge floc. A new activated sludge settleability model was proposed to analyse the effects of ferric dosing on activated sludge settleability indicators using the linear transformation of exponential functions to achieve replication of a non-linear correlation between the ferric dosing concentrations and settleability indicators (ZSV and SSVI). The new empirical model that describes the relationship between ferric dosing concentration and the ZSV and SSVI, were further validated using non- linear parameterization. The results showed that the settleability indicators of Fe^{3+} dosed sludges can be described by the equations:

- $\mathrm{ZSV_{Fe}} = \left((0.0089\,(\mathrm{D_C})_{\mathrm{Fe}} + 0.740)\mathrm{e}^{-0.290+0.0025\,(\mathrm{D_C})_{\mathrm{Fe}}\,\mathrm{X_{Fe}}}\right)$
- $\mathrm{SSVI_{Fe}(mL/g)} = -\ln\left[\left(\frac{\mathrm{ZSV_{Fe}}}{68((\mathrm{K_d})_{\mathrm{Fe}}\,\mathrm{X_{Fe}})+((\mathrm{C_K})_{\mathrm{Fe}}(\mathrm{D_C})_{\mathrm{Fe}}\,\mathrm{X_{Fe}})}\right) - \left(\frac{(\mathrm{C_0})_{\mathrm{Fe}}\,(\mathrm{D_C})_{\mathrm{Fe}}}{68(\mathrm{K_d})_{\mathrm{Fe}}}\right)\Big/0.016\right]$

The proposed new models showed a good fit to the experimental data up to a dose range of 50mg/L of Fe^{3+}. The new model equations will find application in the water industry for the modelling and optimization of Fe^{3+} dosed activated plants.

Chapter Six

The Impact of Calcium Dosing on Activated Sludge Settleability

6.0 The Research Objectives and Activated Sludge Settleability

The literature review in Chapter Two has provided information that chemical coagulant calcium (Ca) could improve activated sludge settleability. However, inadequate studies have been made available on investigating activated sludge settleability process and the impact of chemical coagulant calcium on activated sludge settleability. Therefore, among the main key aims of this current research on optimisation of the design and operation of chemically dosed activated sludge plants (ASP) is to evaluate the impact of calcium on activated sludge settleability. Four of the research objectives namely; to evaluate the impact of Ca on activated sludge settling curve, the impact of chemical dosing Ca on estimated experimental activated sludge settleability parameters (ZSV and SSVI) data, and develop models to predict ZSV and SSVI as a function of Ca dosing concentration using estimated laboratory ZSV and SSVI data will be explored in this chapter. The ZSV and SSVI is measured as an indicator of activated sludge settleability.

6.1 The Impact of Calcium (Ca) on Activated Sludge Settleability

6.1.1 Introduction

As mentioned in section 4.1.1 and 5.1.1 that the need to achieve low levels of phosphates in wastewater effluents has resulted to the increased use of metal salts during wastewater treatment. Apart from coagulants like Aluminium (Al) and Ferric (Fe) already explored, calcium (Ca) salts can also be used for precipitation of insoluble metal phosphate from wastewater (Haandel and Lubbe 2012; Ojo and Ifelebuegu 2016). Aluminium salts alongside ferric and calcium salts are the most widely used chemical for the chemical precipitation of phosphorus. The impact of aluminium, ferric, and calcium coagulant on activated sludge have been explained through charge neutralisation of negatively charged colloids by cationic hydrolysis products (Duan and Gregory 2003; Liu *et al.* 2010). Urbain *et al.* (1993) further commented that the overall activated sludge floc structure is negatively charged due to the physical and chemical interactions between floc bacteria and EPS and divalent cations (Ca). This explains why calcium salt salts (Ca) has the potential to be strongly immersed by the surface of sludge flocs since it produces positively charged metal hydroxides which account for the charge neutralisation process and charge reversal during periods of calcium overdosing rate. Ye *et al.* (2016) added that calcium (II) ion (Ca^{2+}) has the capacity to increase the production of EPS and promote the development of microbial aggregates which is key in bio-flocculation and activated sludge settleability. Earlier studies have also shown that since the activated sludge flocs are embedded in the EPS structure (Wilén *et al.* 2003; Jin *et al.* 2003).

In section 4.1.1 and 5.1.1, it was stressed that FSTs are important component in the design and operation of activated sludge plants. This makes investigation of zone settling velocity ZSV of great need in designing and modelling activated sludge process. The mentioned settling categories (free, flocculent, zone and compression settling) has been explained in section 4.1.1. The modelling of activated sludge settleability to date is based on Pitman (1980) and White (1975) settleability model and this has been covered in section 4.1.1. The model was developed based on the settling characteristics of conventional sludge. With high calcium salt dosage in the precipitation of phosphates today the overall behaviour of sludge is different from the conventional sludges on which the Pitman(1980) and White(1975) model was based. Therefore, there is a need to develop a new model that describes the settling properties of calcium dosed sludge. The proposed new model equation describing the extra weight of calcium dosing in ASP will address the restriction of Pitman(1980) and White(1975) model for conventional activated sludge. The purpose of current study is firstly to evaluate the impact of calcium dosing on activated sludge settleability focusing on zone settling velocities (ZSV) and stirred sludge volume index (SSVI), investigate the impact of calcium on activated sludge settling curve and to develop a new model of settleability of calcium dosed activated sludge.

6.2 Result and Discussion

The results obtained from the research investigation on the impact of calcium on activated sludge settleability was presented based on the four categories namely effects of calcium dosing on activated sludge morphology (6.2.1), effects of calcium dosing on ZSV and SSVI (6.2.2), data analysis and model validation for calcium dosed sludge (6.2.3), model development and model validity for calcium dosed sludge (6.2.4), new model calibration to Include calcium dosing parameter (6.2.5), validation of new model for impact of calcium dosing on ZSV and SSVI (6.2.6) and conclusion and practical relevance (6.2.7).

6.2.1 Effects of Calcium dosing on Activated Sludge Morphology

The microscopic evalaution of sludge flocs for control sample (0mg/L) and calcium dosed (20, 50, 100 and 150mg/L) in SEM followed the same pattern and explanation as observed in control sample and aluminium ferric treated sample in Chapters Four and Five respectively (4.2.1 and 5.2.1). As can be seen in Figure 6.1a, interfloc bridging, open floc formation and spindly bulking also happened while for calcium treated sample (20mg/L) in Figure 6.1b, some decrease in sludge porosity, interfloc bridging and improved sludge compaction was noticed. Further more, with increasing dosing concentration of 50mg/L, 100 mg/L and 150mg/l, the sludge compaction became bettter in Figure 6.1c (50mg/L), Figure 6.1d (100mg/L) and Figure 6.1e (150mg/L) compared to Figure 6.1b (20mg/L). This further supports findings of Luo *et al*. (2013); Agridiotis *et al.* (2007); Gerardi (2002); Eikelboom (2000); Richard (2003) and Chambers and Tomlinson (1982) on sludge bio-flocculation and improvements in sludge settleability

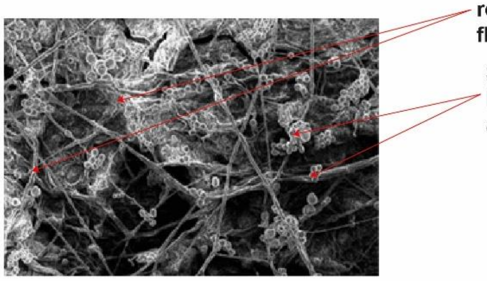

Extended filament over the sludge floc resulting in holding apart the sludge floc particle (Interfloc bridging)

Sludge floc formed along the filament length of filamentous bacteria and attching to the filament (Spindly bulking)

Figure 6.1a. SEM of floc (Control 0mg/L)

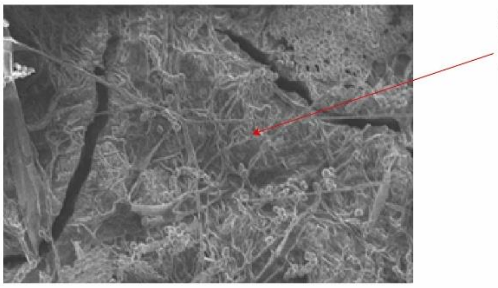

Some reduction in the effect of interfloc bridging and Spindly bulking with some level of sludge compaction

Figure 6.1b.SEM of floc (Ca-Dosed 20mg/L)

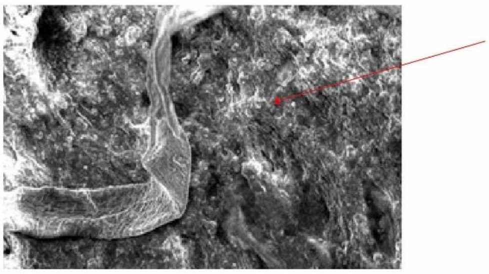

Reduction in the effect of sludge interfloc bridging and spindly bulking with a better sludge compaction

Figure 6.1c. SEM of floc (Ca-Dosed 50mg/L)

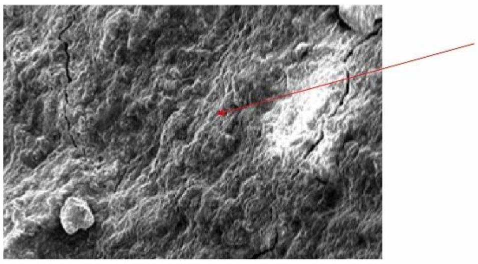

Reduction in the effect of sludge interfloc bridging and spindly bulking with an enhanced sludge compaction

Figure 6.1d. SEM of floc (Ca-Dosed (100mg/L)

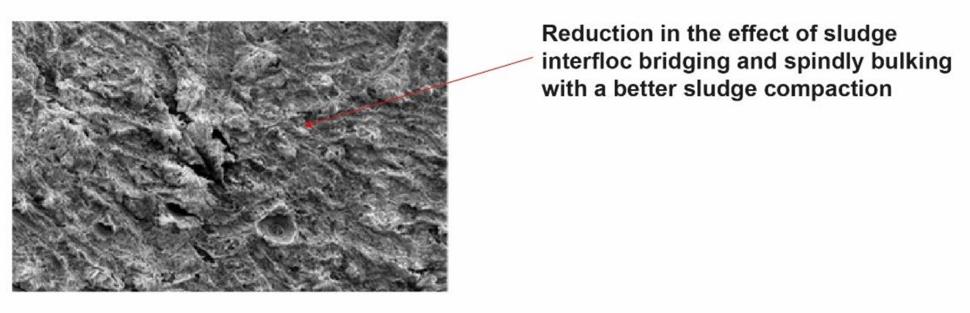

Figure 6.1e. SEM of floc (Ca-Dosed 150mg/L)

6.2.2 Effects of Calcium dosing on ZSV and SSVI

The ZSV were estimated over range of un-dosed and calcium (Ca) dosed activated sludge concentrations (0, 20, 50,100 and 150mg/L) for 2 batch test regimes in calcium (LOT- D and LOF-C) and the results from a typical ZSV test for calcium are shown in Figures 6.2a-e (ZS = zone settling, TS = transition settling, CS = compression settling) and the ZSVs were obtained from the slope of the linear graph.

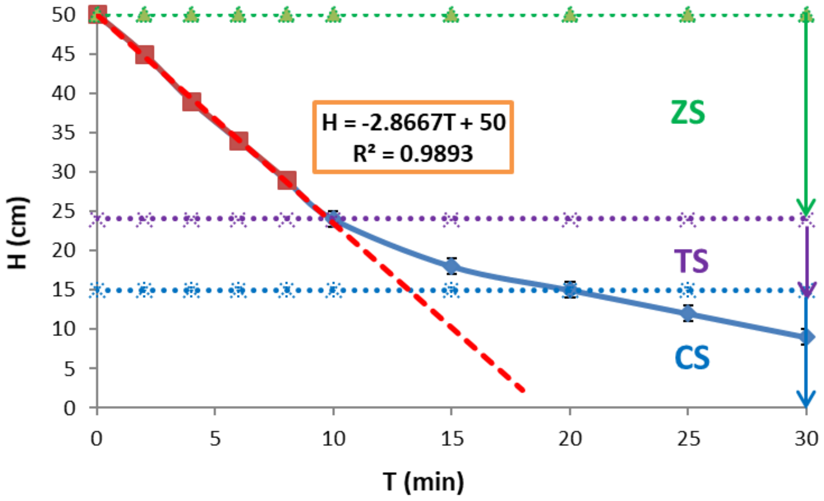

Figure 6.2a. ZSC for Undosed sludge (error bars represent the standard deviation of the mean)

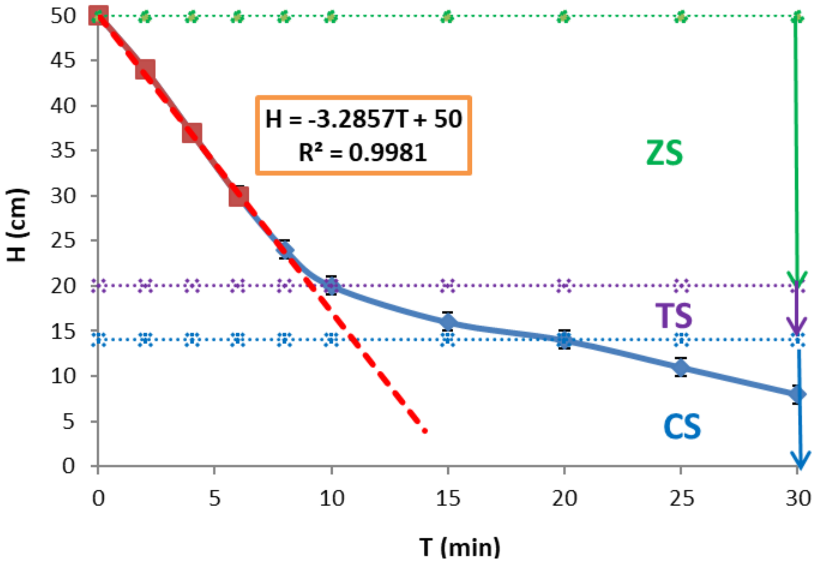

Figure 6.2b. ZSC for 20mg/L Calcium dosed sludge (error bars represent the standard deviation of the mean)

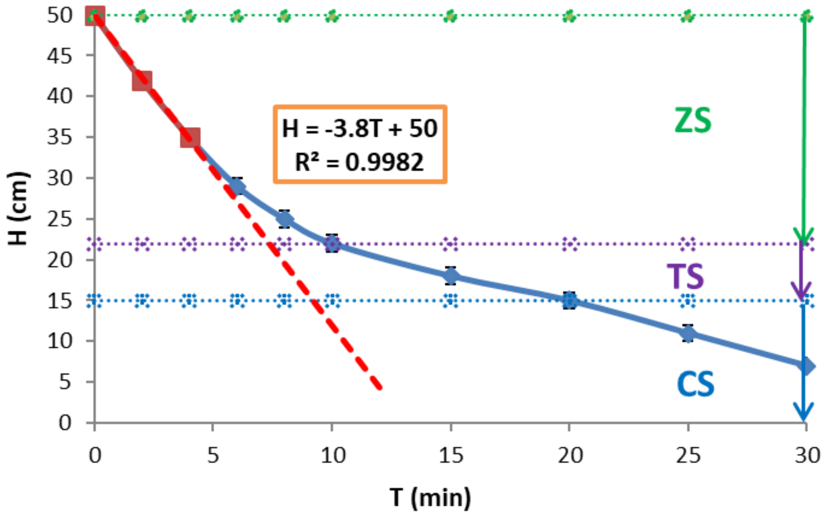

Figure 6.2c. ZSC for 50mg/L Calcium dosed sludge (error bars represent the standard deviation of the mean)

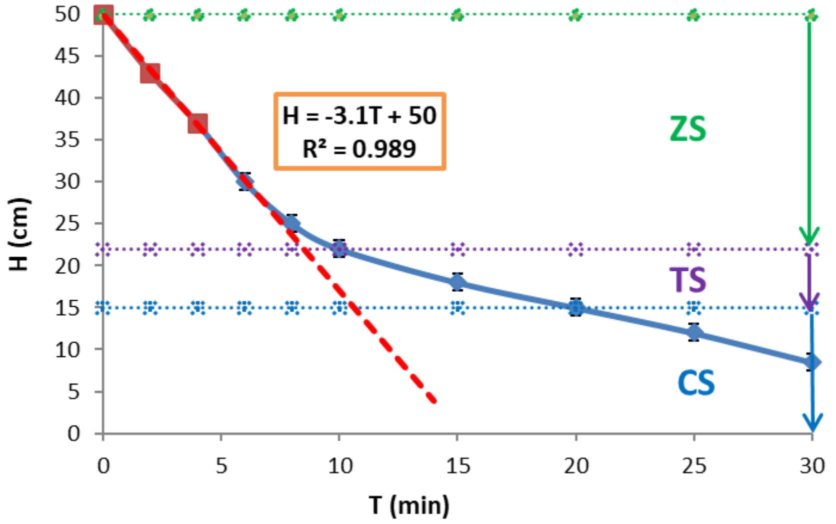

Figure 6.2d. ZSC for 100mg/LCalcium dosed sludge (error bars represent the standard deviation of the mean)

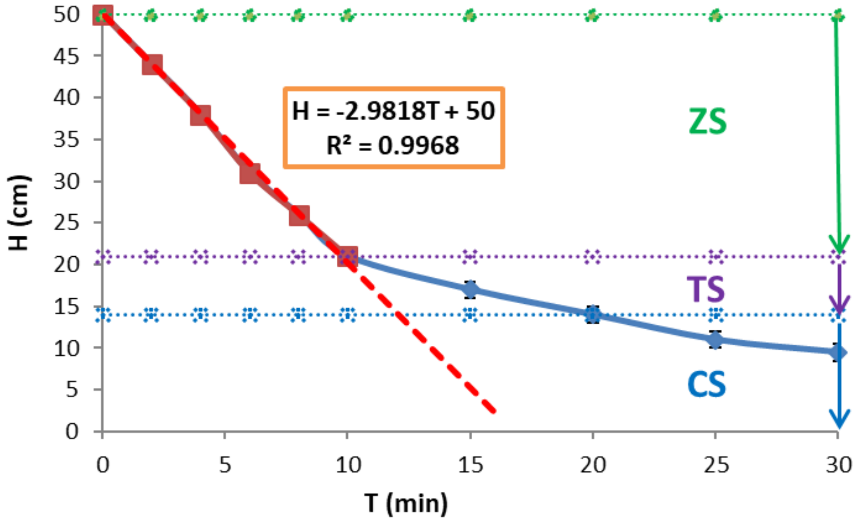

Figure 6.2e. ZSC for 150mg/LCalcium dosed sludge (error bars represent the standard deviation of the mean)

The results from the typical ZSV test for calcium (Figures 6.2a-e) indicates that approximately 50% of the original sludge volume within the sludge depth of the settling column settled after 5 to 10 minutes for both the control and calcium treated sludge. The same pattern was observed with control and aluminium and ferric treated sludge in Chapters Four and Five respectively. It was observed from zone settling curve (ZSC) that the initial faster settling is probably due to the absence of spaces between the sludge flocs causing a free settling without interferences. Nevertheless, after the initial first 10 mins of settling, it was noticed that the change in the sludge height with time (ZSV) began to decline. This agrees with the previous work (Vesilind 1968) and can be explained by the floc to floc interaction based on their proximity and slowing down of their settling velocities.

Consequently, within this zone settling regime, the agglomeration of floc bacteria tends to settle as a zone of blanket (sludge blanket) accounting for the decrease in the settling velocity (Tchobanoglous and Burton 1991). In addition, as the settling velocity began to approach the zero axes, there was a possible dehydration of water from the sludge floc pore spaces due to the compressive forces acting on the floc bacteria as the sludge floc enters a compression settling regime. Also, the linear portion of the ZSCs (Figures 6.2a-e) represents the settling velocity of the sludge flocs as reported in previous work (Vanderhasselt and Vanrolleghem 2000) and as such an increased sludge concentration will result in a decrease in the settling velocity due to increased resistance to water flow through the settling sludge column.

The results of the impact of calcium dosing on activated sludge settleability index (ZSV and SSVI) are summarised in Table 6.1. It was observed that the ZSV values increased at the beginning with increasing concentration of calcium dose (10, 20, 30, 40 and 50mg/L) and started to decrease after 100mg/L dose concentration (100 and150mg/L). A reversed trend is observed for the SSVI, which decreased with increasing dose of calcium up to 50 mg/L dose rate. At 100mg/L dose rate the SSVI had started to increase. A smaller SSVI value represented a faster settling rate of activated sludge and vice versa. This result trend follows the same pattern with the result obtained by Ye *et al.* (2016) only up to calcium dosing concentration of 50mg/L in which the SVI (sludge volume index) decreased. The difference in Ye *et al.* (2016) result on the implication of the microbial community shift to sludge settleability with the addition of Ca^{2+} and current study may be due to the nature of sludge utilised (synthetic wastewater) in the jar test and the feed sludge that was seeded. The seeded feed sludge will make the process of biological decomposition to occur more quickly. Also, the sludge settleability parameter used for measurement of the sludge settleability was the unstirred (SVI). The current study used the stirred specific volume index (SSVI). Although, SVI is the most common sludge settleability indicator used to measure the settling characteristics of activated sludge because of the simplicity with which the SVI (unstirred) test is performed. However, SVI suffers some major draw backs since there is no consistent relationship between SVI and suspended solids concentration in mg/L (MLSS), but this challenge was addressed in a review conducted by Ojo and Ifelebuegu 2018; Dick and Vesilind (1969) suggesting the inclusion of a slow stirring regime (1–2 revolutions per minute). This led to a proposed stirred specific volume index (SSVI) test using a 4 L settling column instead of the 1 L settling column in the unstirred SVI test (White 1976), which was adopted in the jar test experiments in the current study. Furthermore, the result trend follows the same pattern with the result obtained for aluminium and ferric dosed sludge in Chapters Four and Five (sections 4.2.2 and 5.2.2).

The improvement noticed in activated sludge settleability (low SSVI and high ZSV) at initial calcium dosage rates (10 and 50mg/l) observed can be attributed to the surface charge theory of the activated sludge (Gray 1990; Eikelboom *et al.* 1998, Agridiotis *et al.* 2007 Liu *et al.* 2010; Martins *et al.* 2011). Although Forster (1996) explained that the theory of bulking could be based on filamentous bacteria concepts, Agridiotis *et al.* (2007) reported that filament content in activated sludge is not the only issue contributing to activated sludge settleability but other serious challenges such as surface chemistry of the sludge contributes to poor settling sludge within the FST. The impact of calcium dosed sludge can be further explained through charge neutralisation of negatively charged colloids by cationic hydrolysis products (Duan and Gregory 2003). Previous studies by Urbain *et al.* (1993) supported that the overall activated sludge floc structure is negatively charged due to the physical and chemical interactions between floc bacteria, extracellular polymeric substances (EPS) and multivalent cations.

Table 6.1. Mean and Standard deviation of ZSV and SSVI for Calcium un-dosed and dosed sludge for two batch settling tests (Sample number (N) =16; 2016-2017)

	Dosing concentration (mg/L)							
Parameters	Control	Calcium dosed						
	0	10	20	30	40	50	100	150
Mean &SD ZSV(m/h)	1.72 ± 0.02	1.80±0.06	1.88±0.08	1.98 ± 0.11	2.08±0.18	2.16±0.21	1.85±0.07	1.74±0.06
Mean &SD SSVI(mL/g)	75.11±1.40	69.64±3.58	62.74±3.54	57.50±4.95	52.53±4.96	49.00±5.01	59.78±10.22	65.42±13.27
Mean &SD (X) (g/L)	2.85±0.21	2.95±0.21	3.03±0.25	3.11±0.27	3.17±0.24	3.23±0.25	3.43±0.25	3.63±0.25

It was suggested that calcium dosed salts have the potential to be strongly immersed by the surface of sludge flocs because of the produced positively charged metal hydroxides which account for the charge neutralisation process and charge reversal during periods of calcium overdosing. In the present study, the observed behaviour of the SSVI that initially decreased at a dose rate of 10 and 50mg/L and started increasing at 100mg/L dose concentration (100 to 250 mg/L) may be due to charge reversal because of overdosed calcium coagulant. Two competing reactions are predominatly involved in the precipitation of phosphorus by calcium namely formation of metal hydroxide (calcium hydroxide) and metal phosphate (calcium phosphate) (De Haas 2000a) (Equations 6.1 - 6.2). The reaction in Equation 6.1 is more thermodynamically and kinetically favoured over the reaction in Equation 6.2. At the lower dosing concentration, the formation of $\mathrm{CaPO_4}$ is predominant. However, at the higher calcium dosing concentrations when the phosphates in the wastewater have been precipitated, the excess calcium results in the formation of hydroxides as in Equation 6.1. This is responsible for the disintegration of the overall floc structure at higher calcium concentration resulting to drop in ZSV and increase in the SSVI.

$$\mathrm{Ca^{2+} + 2H_2O \rightarrow Ca(OH)_2 + 2H^+} \qquad (6.1)$$

$$\mathrm{Ca^{2+} + {PO_4}^{3-} \rightarrow CaPO_4} \qquad (6.2)$$

Researchers have reported that EPS could also impact the activated sludge settling processes and physicochemical properties of activated sludge flocs (surface charge) due to the ability of its internal layer to tightly bind and adhere closely with strong stability to the cellular surface (Sheng *et al.* 2010). In support of this claim, Wang *et al.* (2013) reported similar linear relationship between loosely and tightly bound EPS and SSVI since the activated sludge flocs are reported to be embedded in the EPS structure and the amount of EPS extractable from the activated sludge is positively related to SSVI (Biggs and Lant 2000; Jin *et al.* 2003; Wilen *et al.* 2003). In the current study, the observed trend in the SSVI with increasing chemical dosing could be explained through EPS binding capacity to microbial cells through its bridging nature with calcium and overall impact on the EPS content in the activated sludge flocs (Higgins and Sobeck 2002; Sheng *et al.* 2006; Sheng *et al.* 2010). This is supported by the observations in Figures 6a-g which showed improved bioaggregation at lower calcium dosing concentrations compared to the undosed sludge. The improvement in settleability of the activated sludge at lower $\mathrm{Ca^{2+}}$ concentrations can also be attributed to ability of calcium to neutralise the sludge surface charge (Higgins and Novak 1997b and Subramanian *et al.* 2010), decreased surface charge is related to decreased SSVI values (Mikkelsen *et al.* 1996 ; Wilen *et al.* 2003; Thompson and Forster 2003). The decrease in ZSV and increase in SSVI and hence decreased settleability at the higher calcium dosing concentrations are attributed to surface charge reversal linked to high calcium dosing rate and high surface charge which is a function of weaker bonding between the various sludge floc fractions resulting in the breakage of the general activated sludge floc structure (Thompson and Forster 2003; Agridiotis *et al.* 2007; Kara *et al.* 2008, Ojo and Ifelbuegu 2016). The reduction in the ZSV values with increasing SSVI also indicates a sludge with a slow settling rate that may hinder the activated sludge compressibility and underflow concentration within the FST (Gerardi 2002).

6.2.3 Data Analysis

The measured ZSV and stirred specific volume index (SSVI) from the three years batch settling tests were used in modelling new calcium dosed activated sludge settleability. The typical result of the data set of batch tests was analysed using the Minitab 17 software and solver optimisation tool. The solver optimisation tool and the Minitab 17 were used and the results were also analysed as reported in aluminium and ferric dosed sludge (section 4.2.3 and 5.2.3) using the non-linear regression in the minitab 17 software and the F-test (F>0.05), R² (coefficient of determination), residual plot, probability plot and interval plot related to ferric dosed sludge was used to validate how the ZSV model fits the ZSV experimental data.

6.2.4 Model development for Calcium dosed sludge

The procedure for evaluation of activated sludge settleability and description of relationship between the zone settling velocity and concentration (Vesilind equation-Equation 1.2) and its justification are reported in section 4.2.3. The Vesilind equation $(ZSV = \mathrm{v}_0 \; \mathrm{e}^{-\mathrm{KX}})$ forms the foundation for modelling FSTs in wastewater treatment plants (WWTP).

In the present study, the batch settling test measurements (zone settling curve (ZSC)) of ZSV (Phase 1 result -LOF C) reveals ZSV as a linear representation (Figure 6.2d) of sludge height as a function of time (m/h) for calcium dosed sludge but a non-linear representation of ZSV and SSVI as a function of calcium dosing concentration was observed in Figure 6.3 (Phase 1 result -LOF F1) and Figure 6.4 (Phase1 result-LOF I1). This provided an insight into the modification of the conventional empirical model of ZSV Equation 1.1 $(ZSV = \mathrm{v}_0 \; \mathrm{e}^{-\mathrm{KX}})$ to include a new calcium (Ca) dosing parameter. It further reveals the impact calcium (Ca) dosing concentration on ZSV and SSVI as a non-linear correlation which is contrary to empirical Vesilind deduction of ZSV.

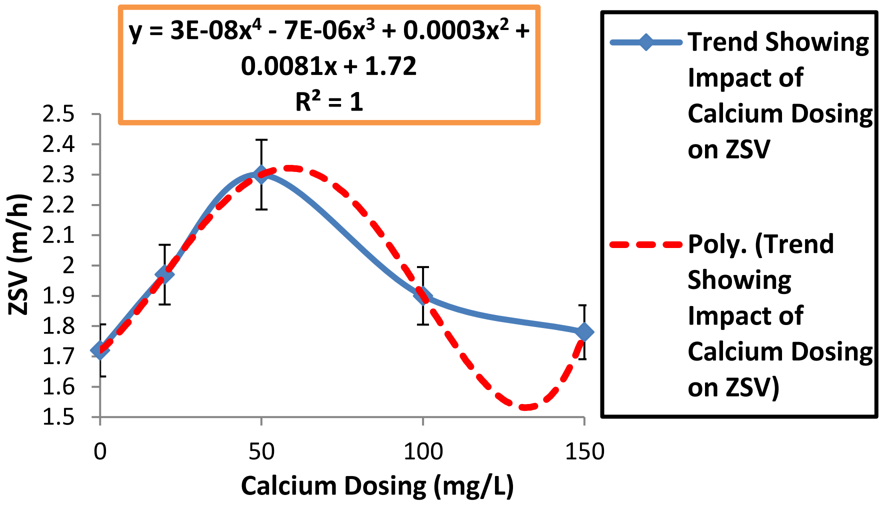

Figure 6.3. The Impact of Calcium Dosing (mg/L) on ZSV (m/h) (error bars represent standard deviation of the mean)

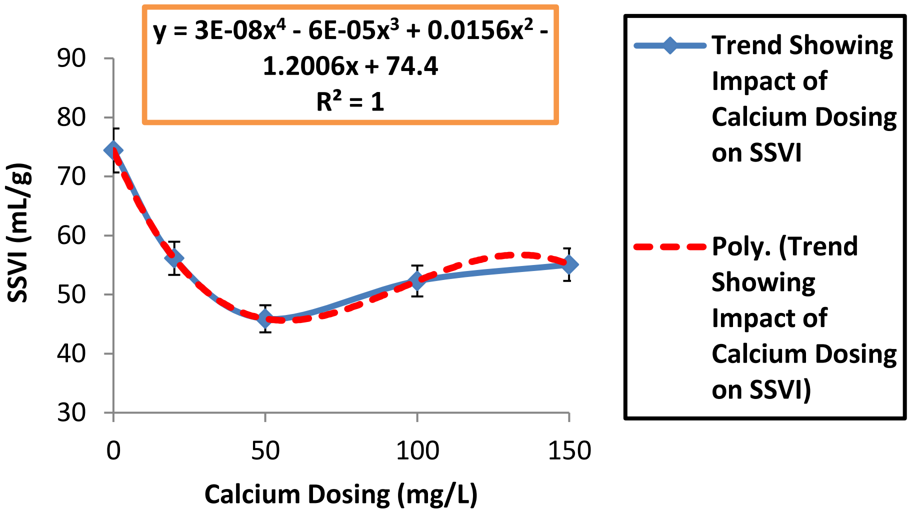

Figure 6.4. The Impact of Calcium Dosing (mg/L) on SSVI (mL/g) (error bars represent standard deviation of the mean)

The conventional empirical model for sedimentation in FSTs expressed as a function of solid concentration, termed Vesilind equation is illustrated in Equation 1.1. The empirical coefficient v_0 and k are obtained by performing ZSV test over a range of mixed liquor suspended solids (MLSS) concentration for both un-dosed and calcium (Ca^{2+}) dosed sludge as mentioned in section 4.2.3 and applying of linear regression to the linearised form of the Vesilind equation to obtain a new expression ($\ln \mathrm{ZSV} = -\mathrm{kX} + \ln v_0$) (Equation 4.11 in section 4.2.5).

The plot of natural log of ZSV (m/h) against un-dosed and Ca^{2+} dosing concentration for the average data from the various batch test (Table 6.2) is shown in Figure 6.5. The negative of the gradient of each linear regression for the batch test is the Vesilind K value while the intercept is the Vesilind $\mathrm{v_0}$ parameter. However, because it is a Ca^{2+} dosed sludge, then Vesilind $\mathrm{v_0}$ and k expression becomes re-defined as ZSV_0 and $\mathrm{K_d}$ for calcium dosed sludge. It is important to define that there is a relationship between calcium sludge dosing concentration and ZSV which was not accounted for in the conventional Vesilind model equation in Equation 1.1. This can be achieved by the transformation of data in the Vesilind exponential correlation and back tracking to calculate the values of the Vesilind exponential constant parameter. Thus, the linearised ZSV was plotted against Ca^{2+}dosing up to 150mg/L (Figure 6.5). Therefore, it was observed from Figure 6.6, that the relationship between Ca^{2+} dose concentrations and the settleability can be accurately described for up to 50mg/L dose concentration and the gradient and intercept accounted for the Vesilind coefficients for calcium ($\mathrm{K_d}$ = -0.0048 and ZSV_0 = 1.712 m/h). It can be inferred that the calculated ZSV_0 and $\mathrm{K_d}$ parameter for calcium dosed sludge from the graph of In (ZSV) against Ca^{2+} dosing concentration (Figure 6.6) are function of calcium dose concentrations up to 50mg/L.

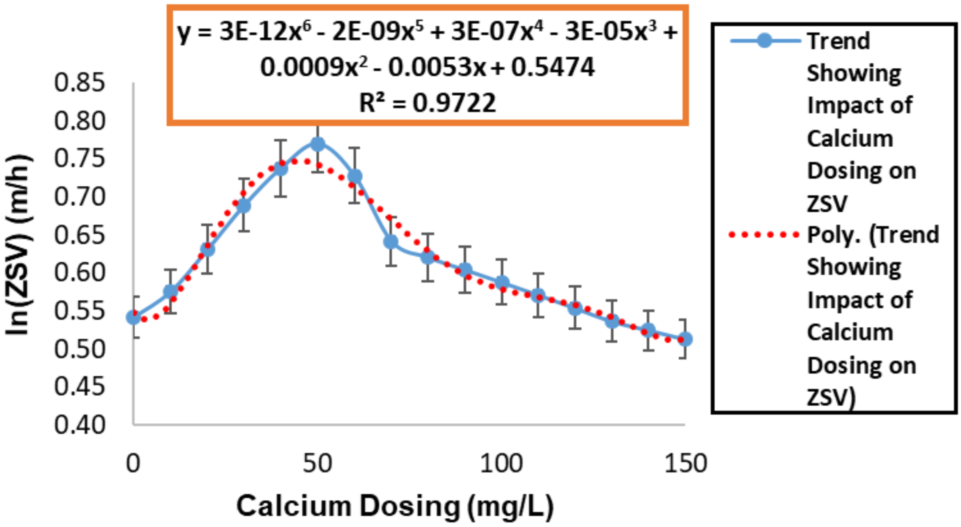

Figure 6.5. Natural log of ZSV against Calcium Dosing (up to 150mg/L) (The error bars represent standard deviation of the mean)

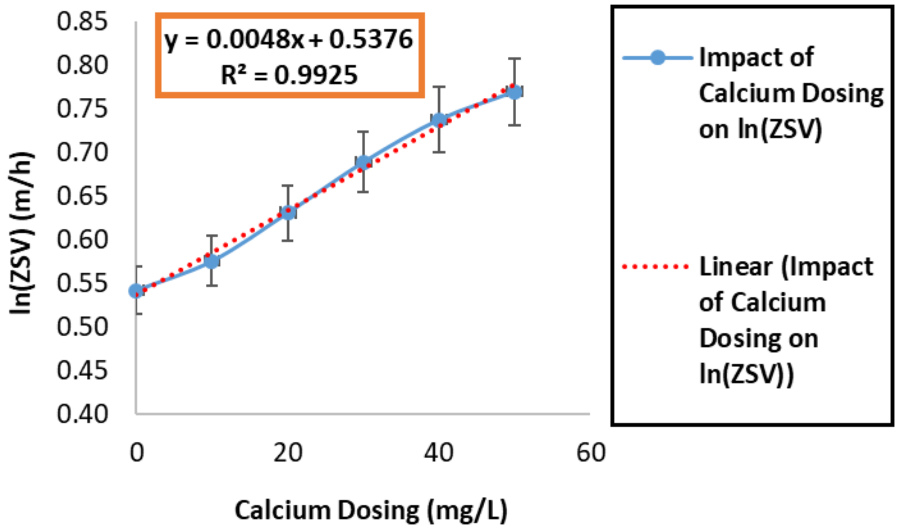

Figure 6.6. Natural log of ZSV against Calcium Dosing (mg/L) (error bars represent the standard deviation of the mean)

The natural logarithm of SSVI was plotted against the calcium dosing concentration up to 150mg/L (Figure 6.7). Nevertheless, a linear relation existed up to 50mg/L (Figure 6.8) and the gradient and intercept of the plot accounted for the coefficients for Ca^{2+} (gradient = 0.0099 and intercept = 76.386 mL/g).

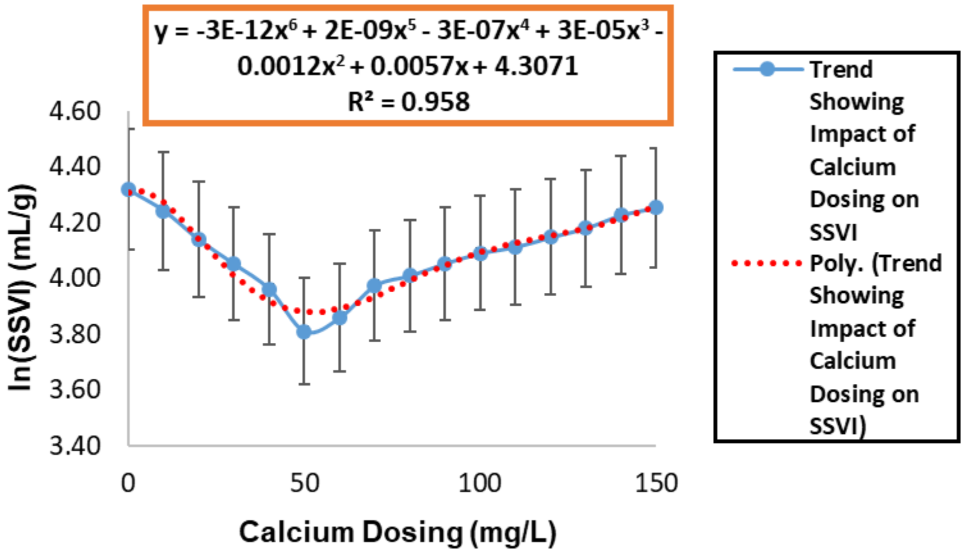

Figure 6.7. Natural log of SSVI against Calcium Dosing (up to 150mg/L) (The error bars represent standard deviation of the mean)

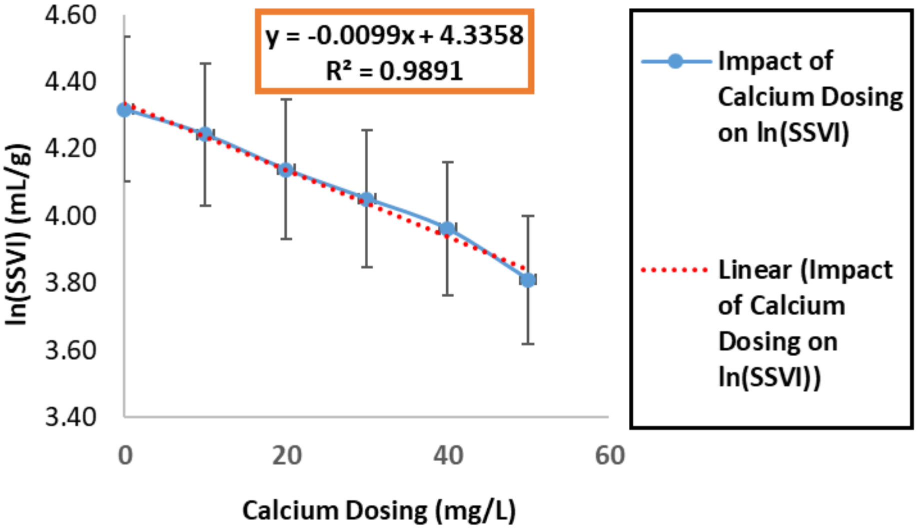

Figure 6.8. ln (SSVI) against Calcium Dosing Concentration (up to 50mg/L) (error bars represent standard deviation of the mean)

6.2.5 Novel Model Calibration to Include Calcium Dosing Parameter

The exponential form of the Vesilind equation (Equation 1.1) can be optimised to include a calcium dosing parameter by investigating a new model equation for settling velocity. The investigated $\mathrm{ZSV_0}$ and $\mathrm{K_d}$ parameter for calcium dosed sludge from the graph of ln (ZSV) and ln (SSVI) against calcium dosing concentration (mg/L) (Figures 6.5-6.8) shows linearised and exponential correlation between ZSV and SSVI with calcium dosing concentrations.

The new empirical model for settling velocity for a calcium dosed activated sludge can take the form of the decay equation ($A = A_o e^{-\lambda t}$) (Equation 4.11-Chapter Four) that obeys the exponential law of decay.

The new equation in Equation 6.3 shows the inclusion of a new calcium dosing protocol (Dc) that follows the decay equation.

$$\mathrm{ZSV_{Ca}} = ((\mathrm{C_0})_{\mathrm{Ca}}\,(\mathrm{D_C})_{\mathrm{Ca}} + (\mathrm{ZSV_0})_{\mathrm{Ca}})\mathrm{e}^{-((\mathrm{K_d})_{\mathrm{Ca}} - (\mathrm{C_K})_{\mathrm{Ca}}(\mathrm{D_C})_{\mathrm{Ca}})\mathrm{X_{Ca}}} \tag{6.3}$$

Where,

$\mathrm{ZSV_{Ca}}$ = Actual settling velocity (m/h) $\mathrm{Ca^{2+}}$ dosed sludge

$(\mathrm{ZSV_0})_{\mathrm{Ca}}$ = Maximum settling velocity (m/h) for $\mathrm{Ca^{2+}}$ dosed sludge

$(\mathrm{K_d})_{\mathrm{Ca}}$ = Empirical $\mathrm{Ca^{2+}}$ dosed sludge settling parameter relating to sludge compaction

$(\mathrm{C_0})_{\mathrm{Ca}}$= Empirical Ca^{2+} dosing constant related to stokes settling velocity

$(\mathrm{C_K})_{\mathrm{Ca}}$ = Empirical Ca^{2+} dosing constant related sludge compaction

$(\mathrm{D_C})_{\mathrm{Ca}}$ = Ca^{2+} dosing concentration (mg/L)

$\mathrm{X_{Ca}}$= Ca^{2+}dosed MLSS concentration (mg/L)

The Equation 4.11 for the new aluminium dosed sludge stated earlier differs from calcium dosed sludge in Equation 6.3, on the account of their different process parameters such as maximum settling velocity, empirical dosing sludge settling parameter relating to sludge compaction, empirical dosing constant related to maximum settling velocity and empirical dosing constant related sludge compaction and dosed MLSS concentration.

Equation 6.3 obeys the exponential law of decay and both the additive and multiplicative rule of exponentials. The empirical coefficients in Equation 6.3 ZSV_0 and $\mathrm{k_d}$ are typically determined by performing zone settling velocity (ZSV) batch tests over a range of calcium dosing concentrations (0, 10, 20, 30, 40, 50,100 and 150mg/L and applying regression analysis and linear approximation to Equation 6.3 by taking the natural log.

For a better knowledge of the new empirical heuristic expression for settling velocity for a dosed activated sludge, the evaluation of terms in the new calcium dosed sludge expression and conventional decay equation becomes important. The version of terms in Equation 4.10 (Chapter Four) compared with Equation 6.3 is as follows:

$\mathrm{A_o} = ((\mathrm{C_0})_{\mathrm{Ca}}\ (\mathrm{D_C})_{\mathrm{Ca}} + (\mathrm{ZSV_0})_{\mathrm{Ca}})$, $\lambda = ((\mathrm{K_d})_{\mathrm{Ca}} - (\mathrm{C_K})_{\mathrm{Ca}}\,(\mathrm{D_C})_{\mathrm{Ca}})$ and t=$\mathrm{X_{Ca}}$.

This shows below that applying the additive rule with e as a common factor in Equation 6.3 then Equation 6.4 is obtained:

$$((\mathrm{C_0})_{\mathrm{Ca}}(\mathrm{D_C})_{\mathrm{Ca}}\,\mathrm{e} + (\mathrm{ZSV_0})_{\mathrm{Ca}}\,\mathrm{e}) = ((\mathrm{C_0})_{\mathrm{Ca}}\,(\mathrm{D_C})_{\mathrm{Ca}} + (\mathrm{ZSV_0})_{\mathrm{Ca}})\mathrm{e} \qquad 6.4$$

Conversely, applying the multiplicative rule with $\mathrm{X_{Ca}}$ as a common factor in Equation 6.3, the expression in Equation 6.5 was realised.

$$-((\mathrm{K_d})_{\mathrm{Ca}} - (\mathrm{C_K})_{\mathrm{Ca}}(\mathrm{D_C})_{\mathrm{Ca}})\mathrm{X_{Ca}} = \mathrm{e}^{-(\mathrm{K_d})_{\mathrm{Ca}}\,\mathrm{X_{Ca}}} \times \mathrm{e}^{-(\mathrm{C_K})_{\mathrm{Ca}}\,(\mathrm{D_C})_{\mathrm{Ca}}\,\mathrm{X_{Ca}}} \qquad 6.5$$

The constants $(\mathrm{ZSV_0})_{\mathrm{Ca}}$; $(\mathrm{K_d})_{\mathrm{Ca}}$; $(\mathrm{C_0})_{\mathrm{Ca}}$ and $(\mathrm{C_K})_{\mathrm{Ca}}$ helps in shifting the ZSV model to predict the observed values in calcium dosed sludge. However, the experimentally estimated ZSV data have been universally used for regulating settling models in wastewater industry (Vesilind 1968: $ZSV = \mathrm{v_0 e^{-kX}}$). Since it is common practice to deduce the Vesilind empirical constants ($\mathrm{v_0}$ and k) through conducting batch laboratory ZSV test over a range of concentrations and applying linear regression evaluation to a linearized form of Vesilind equation $(\ln \mathrm{V} = -\mathrm{kX} + \ln \mathrm{v}_0)$, it becomes paramount to apply the same principle to the new calcium dosed activated sludge model.

We can consider defining F_1 and F_2 from Equation 6.3 as follows: $\mathrm{F}_1 = ((\mathrm{ZSV}_0)_{\mathrm{Ca}} \times (\mathrm{D}_\mathrm{C})_{\mathrm{Ca}})$ and $\mathrm{F}_2 = ((\mathrm{K}_\mathrm{d})_{\mathrm{Ca}}) - ((\mathrm{C}_\mathrm{K})_{\mathrm{Ca}} (\mathrm{D}_\mathrm{C})_{\mathrm{Ca}})$ as two functions of ZSV and this gives Equation 6.6

$$\mathrm{ZSV}_{\mathrm{Ca}} = \mathrm{F}_1 \, \mathrm{e}^{-\mathrm{F}_2 \, \mathrm{X}_{\mathrm{Ca}}} \tag{6.6}$$

As earlier mentioned that there exists an exponential relationship between the ZSV and calcium dosing (Figure 6.3) but because the relationship is a non-linear relationship, calculating the value of the new empirical coefficient $(\mathrm{ZSV}_0)_{\mathrm{Ca}}$; $(\mathrm{K}_\mathrm{d})_{\mathrm{Ca}}$; $(\mathrm{C}_0)_{\mathrm{Ca}}$ and $(\mathrm{C}_\mathrm{K})_{\mathrm{Ca}}$ of calcium dosed activated sludge model can be realised by linearising Equation 6.3 to become Equation 6.7

Therefore, below is the linear approximation (Equation 6.7) obtained by taking the natural log of Equation 6.3:

$$\ln(\mathrm{ZSV}_{\mathrm{Ca}}) = \ln((\mathrm{C}_0)_{\mathrm{Ca}} (\mathrm{D}_\mathrm{C})_{\mathrm{Ca}} + (\mathrm{ZSV}_0)_{\mathrm{Ca}}) - ((\mathrm{K}_\mathrm{d})_{\mathrm{Ca}} - (\mathrm{C}_\mathrm{K})_{\mathrm{Ca}} (\mathrm{D}_\mathrm{C})_{\mathrm{Ca}}) \mathrm{X}_{\mathrm{Ca}} \tag{6.7}$$

The Equation 6.7 also follows the equation of a straight line $(\mathrm{Y} = \mathrm{MX} + \mathrm{C})$, M = Slope while C= Intercept and hence Equation 6.7 can be modified as Equation 6.8 by re-defining $\ln(\mathrm{ZSV}_{\mathrm{Ca}}) = \mathrm{Z}$; $(\ln((\mathrm{C}_0)_{\mathrm{Ca}} (\mathrm{D}_\mathrm{C})_{\mathrm{Ca}} + (\mathrm{ZSV}_0)_{\mathrm{Ca}}) = \mathrm{P}$ and $((\mathrm{K}_\mathrm{d})_{\mathrm{Ca}} - (\mathrm{C}_\mathrm{K})_{\mathrm{Ca}} (\mathrm{D}_\mathrm{C})_{\mathrm{Ca}}) = Q$ respectively.

$$\mathrm{Z} = \mathrm{P} - \mathrm{QX} \tag{6.8}$$

The transformation of Equation 6.3 to 6.7 allowed establishing a linear relationship between Z and X (Equation 6.8) and not between ZSV and X since it is already an exponential model. This transformation allows back tracking the constant of the new model for calcium dosed sludge $(\mathrm{ZSV}_0)_{\mathrm{Ca}}$; $(\mathrm{K}_\mathrm{d})_{\mathrm{Ca}}$; $(\mathrm{C}_0)_{\mathrm{Ca}}$ and $(\mathrm{C}_\mathrm{K})_{\mathrm{Ca}}$ to predict the ZSV experimental data. Therefore, once a linear relationship is established between Z and X $(\mathrm{Z} = \mathrm{P} - \mathrm{QX})$, the value of the calcium dosed settleability constants $(\mathrm{ZSV}_0)_{\mathrm{Ca}}$; $(\mathrm{K}_\mathrm{d})_{\mathrm{Ca}}$; $(\mathrm{C}_0)_{\mathrm{Ca}}$ and $(\mathrm{C}_\mathrm{K})_{\mathrm{Ca}}$ can be evaluated and the experimental value of ZSV and dosing concentrations $(\mathrm{D}_\mathrm{C})_{\mathrm{Ca}}$ without performing a ZSV batch experiment. A new expression (6.9 and 6.10) was obtained from Equation 6.8 for calculating the value of $(\mathrm{D}_\mathrm{C})_{\mathrm{Ca}}$ as it relates to calcium when four constants $(\mathrm{ZSV}_0)_{\mathrm{Ca}}$; $(\mathrm{K}_\mathrm{d})_{\mathrm{Ca}}$; $(\mathrm{C}_0)_{\mathrm{Ca}}$ and $(\mathrm{C}_\mathrm{K})_{\mathrm{Ca}}$ for calcium dosed sludge are known.

$$(\mathrm{D}_\mathrm{C})_{\mathrm{Ca}} = \frac{\mathrm{e}^{\mathrm{P}} - (\mathrm{ZSV}_0)_{\mathrm{Ca}}}{(\mathrm{C}_0)_{\mathrm{Ca}}} \tag{6.9}$$

$$(\mathrm{D}_\mathrm{C})_{\mathrm{Ca}} = \frac{\mathrm{Q} + (\mathrm{K}_\mathrm{d})_{\mathrm{Ca}}}{(\mathrm{C}_\mathrm{K})_{\mathrm{Ca}}} \tag{6.10}$$

The results of regression analysis using Equation 6.7 showed that all the coefficient of determination (R^2) were close to 1 (Figure 6.6). This suggests that the exponential function in Equation 6.3 was suitable to model the calcium dosed activated sludge settleability process (ZSV).

However, the SSVI expression for calcium dosed activated sludge can be derived from the new empirical calcium dosed activated sludge model for settling velocity in Equation 6.3. The k and $\mathrm{v_0}$ parameter calculated from the expression in Catunda et al. (1989) in Equation 6.11 and 6.12 becomes re-written as $(\mathrm{ZSV_0})_{\mathrm{Ca}}$ and $(\mathrm{K_d})_{\mathrm{Ca}}$ parameter for calcium dosed sludge computed in Equation (6.11) and (6.12)

$$(\mathrm{K_d})_{\mathrm{Ca}} = 0.16 + 2.7 \times 10^{-3} \times \mathrm{SSVI_{Ca}} \tag{6.11}$$

$$(\mathrm{ZSV_0})_{\mathrm{Ca}} = (10.9 + 0.18 \times \mathrm{SSVI_{Ca}}) \times \mathrm{e}^{(-0.016 \times \mathrm{SSVI_{Ca}})} \tag{6.12}$$

Where,

$(\mathrm{K_d})_{\mathrm{Ca}}$= Empirical calcium dosed activated sludge settling parameter related to sludge compaction (L/g)

$(\mathrm{ZSV_0})_{\mathrm{Ca}}$ = Maximum settling velocity for calcium dosed activated sludge related to stokes settling velocity (m/h)

$SSVI_{\mathrm{Ca}}$ = Stirred sludge volume index (mL/g) calcium dosed activated sludge

In deriving a new expression for calcium dosed SSVI, Equation 6.11 and Equation 6.12, was compared with the existing Pitman (1980) and White (1975) expression in Equation 1.2 ($\frac{\mathrm{v_0}}{\mathrm{k}} = 68\mathrm{e}^{(-0.016 \times \mathrm{SSVI})}$) and the Equation 1.2 can be re-written in the form of $(\mathrm{ZSV_0})_{\mathrm{Ca}}$ and $(\mathrm{K_d})_{\mathrm{Ca}}$= parameter as follows:

$$(\mathrm{ZSV_0})_{\mathrm{Ca}} = 68(\mathrm{K_d})_{\mathrm{Ca}} = \mathrm{e}^{(-0.016\ \mathrm{SSVI_{Ca}})} \tag{6.13}$$

The new SSVI expression (Equation 6.14) was obtained by substituting Equations 6.11 -6.13 into Equation 6.3. Therefore, the new SSVI expression for calcium dosed activated sludge (Equation 6.14) was derived from substituting the compared $(\mathrm{K_d})_{\mathrm{Ca}}$ and $(\mathrm{ZSV_0})_{\mathrm{Ca}}$ parameter calculated from the redefined expression in Catunda *et al.* (1989) with the Pitman (1980) and White (1975) expression in Equation 1.2 ($\frac{\mathrm{v_0}}{\mathrm{k}} = 68\mathrm{e}^{(-0.016 \times \mathrm{SSVI})}$) and substituting into the new calcium dosed activated sludge model for settling velocity in Equation 6.3.

$$\mathbf{SSVI_{Ca}(mL/g)} = -\ln\left[\left(\frac{\mathrm{ZSV_{Ca}}}{68((\mathrm{K_d})_{\mathrm{Ca}}\ \mathrm{X_{Ca}})+((\mathrm{C_K})_{\mathrm{Ca}}(\mathrm{D_C})_{\mathrm{Ca}}\,\mathrm{X_{Ca}})}\right)-\left(\frac{(\mathrm{C_0})_{\mathrm{Ca}}\,(\mathrm{D_C})_{\mathrm{Ca}}}{68(\mathrm{K_d})_{\mathrm{Ca}}}\right)\Big/_{0.016}\right] \tag{6.14}$$

The results of regression analysis for the impact of calcium dosing on SSVI using the experimental data in the batch test conducted showed that all the coefficient of determination (R^2) were close to 1 (Figure 6.8). This suggests that the linearized expression in Equation 6.14 was suitable to model the impact of calcium dosing on activated sludge settleability (SSVI) process.

6.2.6 Validation of Novel Model for Impact of Calcium Dosing on ZSV and SSVI

6.2.6.1 Novel ZSV Model

The heuristic expression used for derivation of the new model for calcium dosed sludge expressed in Equation 6.3 ($\mathrm{ZSV_{Ca}} = ((\mathrm{C_0})_{\mathrm{Ca}}\,(\mathrm{D_C})_{\mathrm{Ca}} + (\mathrm{ZSV_0})_{\mathrm{Ca}})\mathrm{e}^{-((\mathrm{K_d})_{\mathrm{Ca}}-(\mathrm{C_K})_{\mathrm{Ca}}\,(\mathrm{D_C})_{\mathrm{Ca}})\mathrm{X_{Ca}}}$) and its linear approximation ($\ln(\mathrm{ZSV_{Ca}}) = \ln((\mathrm{C_0})_{\mathrm{Ca}}\,(\mathrm{D_C})_{\mathrm{Ca}} + (\mathrm{ZSV_0})_{\mathrm{Ca}}) - ((\mathrm{K_d})_{\mathrm{Ca}} - (\mathrm{C_K})_{\mathrm{Ca}}\,(\mathrm{D_C})_{\mathrm{Ca}})\mathrm{X_{Ca}}$). The experimental data of two batch (calcium) settling velocity test can be classified into two groups. The first group (Figures 6.1 - 6.5) were used to develop the model while the second group (Tables 6.2 - 6.3, Figure 6.9 and Figure 6.10) are used to validate the model. The model was validated using two approaches namely; solver optimisation tool and Minitab 17. Although the batch settling test measurements revealed ZSV as a linear representation (sludge height as a function of time) (Figure 6.1), on the contrary, a non-linear representation was observed in Figures 6.5-6.6, showing ZSV and SSVI as a function of calcium dosing concentration. This also allows the inclusion of a new calcium dosing parameter $(\mathrm{D_C})_{\mathrm{Ca}}$in the existing Pitman (1980) and White (1975) model reported in Equation 1.2 and Catunda *et al.* (1989) in Equation 4.6 and 4.7 which are both in agreement with the Vesilind (1968) expression.

The solver optimisation tool and Minitab 17 were utilised to fit non-linear model data to actual experimental data for calcium dosed sludge (Tables 6.2 - 6.3). Table 6.3 and Figures 6.9 - 6.10 shows a comparison of the experimental and predicted zone settling velocities using Equation 6.3. It was observed that the validation result is good enough and valid for calcium concentration ranging from (0, 10, 20, 30, 40, 50, and 100mg/L). The non-linear fitting, interval plot, residual plot and probability plot (Figure 6.9) further establishes the validity of the model using Minitab 17. The probability plot creates estimated cumulative distribution function from calcium dosed sample data by plotting the value of each observation against its estimated cumulative probability and a scale transformation allows the fitted distribution to form a straight line.

A good distribution fit is one where the observations are near the fitted line. The data in Figure 6.9 are near the fitted line hence it indicates a good distribution fit between the model and experimental data. The residual shows how far the model data from the experimental data is and the residual plot in Figure 6.9 shows a good fit. The coefficient of determination (R^2) was 0.998 in Table 6.2, shows that the difference between the observed experimental value and the model predicted values are small and unbiased. The interval plot (Figure 6.9) shows that at 95 per cent CI, the mean value of ZSV model and experimental is significant as the 95% confidence interval bar do not overlap.

Table 6.2: Model Validation Minitab 17and Solver Optimisation Tool Result (Calcium)

Parameters	Estimated values
ZSV_0	2.346
C_0	0.0346
K_d	0.112
C_K	-0.002
α	0.05
R^2	0.998
CI	95%
SSD	0.112

R^2-R Squared, α-significance level, CI-Confidence Interval, SSD-sum of squared deviation

The solver optimisation tool allows the solver parameter to be set for the target objective of a reduced sum of square deviation (SSD) value so that the model fits the experimental data. In Table 6.2 and Figure 6.10, a significant SSD value of 0.112 was reported and it indicated the ZSV model fits the actual ZSV value.

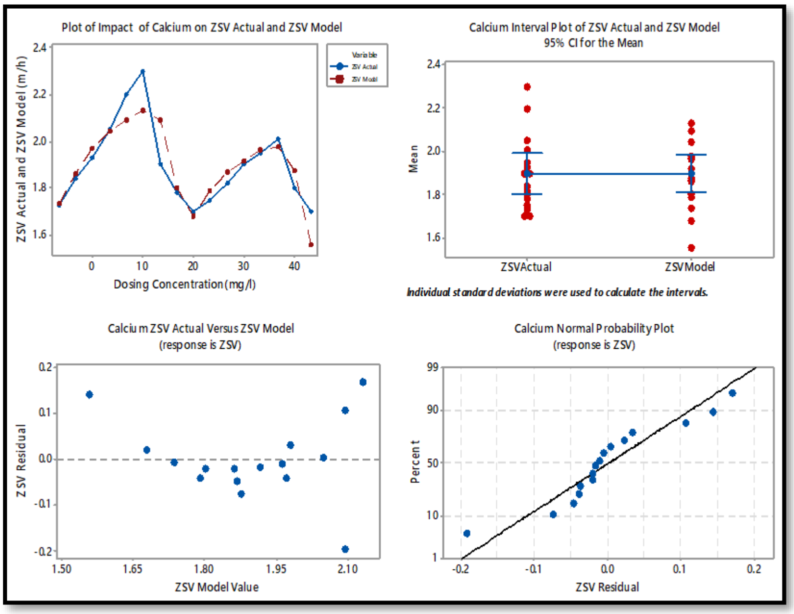

Figure 6.9. Non-Linear Fitting, Interval Plot, Residual Plot and Probability plot (Calcium)

Table 6.3. ZSV experimental and ZSV model Comparison using Solver optimisation and Minitab 17 for Calcium Dosed Sludge (Sample number (N) =16; 2016-2017)

MLSS (g/l)	ZSV (m/h)	ZSV Model (m/h)	Ca-Dosing (mg/L)	Standard deviation	Residual	Squared Residual	Squared ZSV
2.70	1.73	1.74	0.00	3.00×10^{-5}	-5.25×10^{-3}	3.00×10^{-5}	2.99
2.80	1.84	1.86	10.00	4.30×10^{-4}	-2.08×10^{-2}	4.30×10^{-4}	3.39
2.85	1.93	1.97	20.00	1.55×10^{-3}	-3.93×10^{-2}	1.55×10^{-3}	3.72
2.92	2.05	2.05	30.00	2.00×10^{-5}	4.01×10^{-3}	2.00×10^{-5}	4.20
3.00	2.20	2.09	40.00	1.14×10^{-2}	1.07×10^{-1}	1.14×10^{-2}	4.84
3.05	2.30	2.13	50.00	2.88×10^{-5}	1.70×10^{-1}	2.88×10^{-2}	5.29
3.25	1.90	2.09	100.00	3.74×10^{-2}	-1.93×10^{-1}	3.74×10^{-2}	3.61
3.45	1.78	1.80	150.00	4.10×10^{-4}	-2.03×10^{-2}	4.10×10^{-4}	3.17
3.00	1.70	1.68	0.00	4.80×10^{-4}	2.20×10^{-2}	4.80×10^{-4}	2.89
3.10	1.75	1.79	10.00	1.48×10^{-3}	-3.85×10^{-2}	1.48×10^{-3}	3.06
3.20	1.82	1.87	20.00	2.23×10^{-3}	-4.72×10^{-2}	2.23×10^{-3}	3.31
3.30	1.90	1.92	30.00	2.60×10^{-4}	-1.63×10^{-2}	2.60×10^{-4}	3.61
3.34	1.95	1.96	40.00	1.10×10^{-4}	-1.07×10^{-2}	1.10×10^{-4}	3.80
3.40	2.01	1.93	50.00	1.07×10^{-3}	3.28×10^{-2}	1.07×10^{-3}	4.04
3.60	1.80	1.88	100.00	5.71×10^{-3}	-7.56×10^{-2}	5.71×10^{-3}	3.24
3.80	1.70	1.56	150.00	2.05×10^{-2}	1.43×10^{-1}	2.05×10^{-3}	2.89

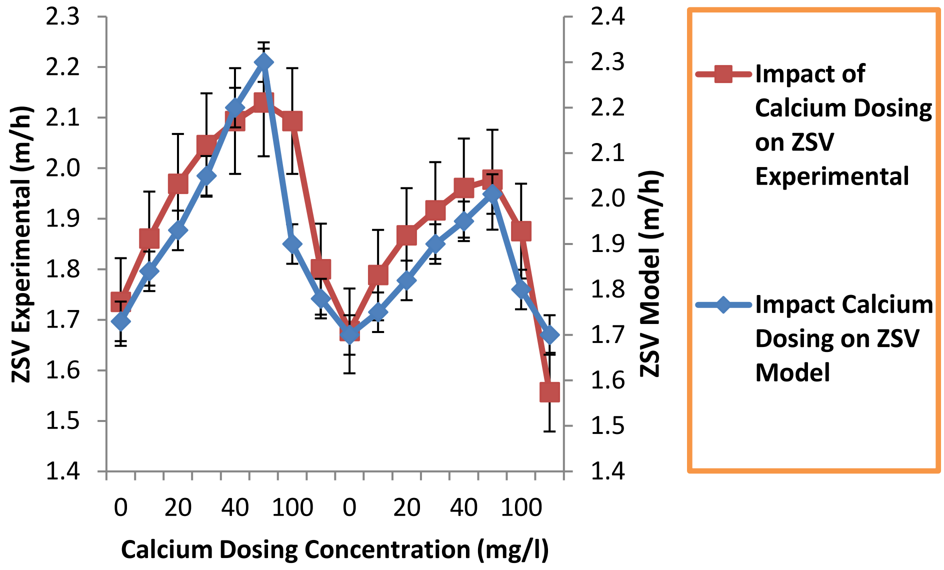

Figure 6.10. Non-Linear Curve Fitting of Impact of Calcium on ZSV (The bars represent standard deviation of the mean)

$$\mathrm{ZSV_{Ca}} = (0.035\ (\mathrm{D_C})_{\mathrm{Ca}}\ +\ 2.346)\mathrm{e}^{-(0.112+0.0020\ (\mathrm{D_C})_{\mathrm{Ca}}\ \mathrm{X_{Ca}})} \qquad (6.15)$$

The values of $(\mathrm{C_0})_{\mathrm{Ca}}$; $(\mathrm{ZSV_0})_{\mathrm{Ca}}$; $(\mathrm{K_d})_{\mathrm{Ca}}$; and $(\mathrm{C_K})_{\mathrm{Ca}}$ for calcium dosed sludge (Table 6.2) used to validate the numerical model in Equation 6.15 are the same at different dosing concentration (0, 10, 20, 30, 40, 50 and 100mg/L) and approximate to 0.035, 2.346, 0.112 and -0.002 respectively. Therefore, the new ZSV model for calcium dosed sludge is expressed as Equation 6.15.

6.2.7 Conclusion and practical relevance

The impact of calcium dosing on activated sludge settleability (ZSV and SSVI) was studied in batch settling tests over a three-year period using a type 305 settlometer. The results showed that ZSV increased while SSVI decreased with increasing dose of $\mathrm{Ca^{2+}}$. The best settleability was achieved at 50mg/L dose of $\mathrm{Ca^{2+}}$. The improved settleability with increasing dose of $\mathrm{Ca^{2+}}$ was attributed to the improve bioaggregation of the activated sludge with dosing and through EPS binding capacity to microbial cells through its bridging nature with calcium salt. The sludge settleability started to decline between >50mg/L to 150mg/L dose concentrations. The decrease in ZSV and increase in SSVI and hence decreased settleability at the higher dose concentrations are attributed surface charge reversal linked to high calcium dosing rate and high surface charge which is a function of weaker bonding between the various sludge floc fractions resulting to the breakage of the general activated sludge floc. A new activated sludge settleability model was proposed to analyse the effects of calcium dosing on activated sludge settleability indicators using the linear transformation of exponential functions to achieve replication of a non-linear correlation between the calcium dosing concentrations and settleability indicators (ZSV and SSVI). The new empirical model that describes the relationship between calcium dosing concentration and the ZSV and SSVI, were further validated using non- linear parameterization. The results showed that the settleability indicators of Ca^{2+} dosed sludges can be described by the equations:

$$\mathrm{ZSV_{Ca}} = (0.035\,(\mathrm{D_C})_{\mathrm{Ca}} + 2.346)\mathrm{e}^{-(0.112+0.0020\,(\mathrm{D_C})_{\mathrm{Ca}})\mathrm{X_{Ca}})}$$

$$\mathrm{SSVI_{Ca}}(\mathrm{mL/g}) = -\ln\left[\left(\frac{\mathrm{ZSV_{Ca}}}{68((\mathrm{K_d})_{\mathrm{Ca}}\,\mathrm{X_{Ca}}) + ((\mathrm{C_K})_{\mathrm{Ca}}(\mathrm{D_C})_{\mathrm{Ca}}\,\mathrm{X_{Ca}})}\right) - \left(\frac{(\mathrm{C_0})_{\mathrm{Ca}}\,(\mathrm{D_C})_{\mathrm{Ca}}}{68(\mathrm{K_d})_{\mathrm{Ca}}}\right)\Big/_{0.016}\right]$$

The proposed new models showed a good fit to the experimental data up to a dose range of 50mg/L of Ca^{2+}. The new model equations will find application in the water industry for the modelling and optimization of Ca^{2+} dosed activated plants.

Chapter Seven

The Impact of Chemical Dosing on Activated Sludge Digestibility

7.0 Research objectives and Activated Sludge Digestibility

Chemical phosphorus removal using salts of aluminium, ferric and calcium impact the physical and chemical characteristics of activated sludge as mentioned in the literature review section 2.2. Whilst numerous studies have been reported on the use of metal salts for the conditioning of sludge and their effects on sludge treatment processes, Smith and Carliell-Marquet (2008, 2009) have reported on the digestibility of Fe dosed sludge, with a reduced biogas production rate as a result of Fe dosing. Also, various studies have reported the impact of calcium on activated sludge digestibility (Section 1.1 and 2.2). Research on the effects of Al^{3+} salt on the digestibility of activated sludge is limited in the literature. Hence, one of the broad objectives of this current study is to evaluate the impact of chemical dosing (Al^{3+} and Fe^{3+}) on experimental biogas production in a laboratory scale anaerobic digester. This current study provides a comparative assessment of the effects of Fe^{3+} and Al^{3+} on the digestibility of surplus activated sludge (SAS). This was carried out in a locally fabricated laboratory anaerobic digester. The biogas volume production measured as an indicator of activated sludge digestibility.

7.1 Impact of chemical dosing (Al^{3+} and Fe^{3+}) on Activated sludge digestibility

7.1.1 Introduction

The generation of huge quantity of surplus activated sludge (SAS) is causing a serious problem for wastewater treatment plant (WWTP) due to increasing SAS treatment and sludge disposal cost which is resulting in serious environmental pollution (Wong *et al.* 2015). With the mandatory effluent discharge consent for phosphate removal becoming tighter under the EU Water Framework Directive, there is a growing demand for treatment plant upgrades to meet P consents in WWTP effluents. Activated sludge process (ASP) is the most universally used technique for municipal wastewater treatment (WWT) and is able to achieve higher P removal to levels of less than 1mg/L (Ojo and Ifelebuegu 2019b). The two main processes for phosphorus removal are biological phosphorus removal (BPR) and chemical phosphorus removal (CPR). Both processes are used independently and, most times, in combination to achieve effluent consents for P. While BPR is considered the most environmentally friendly option, it has its limitations, particularly, the requirement for strong biological oxygen demand (BOD) in the influent wastewater. Consequently, most WWTPs in Europe use CPR to achieve their effluent P consents using mainly ferric (Fe^{3+}) and aluminium (Al^{3+}) salts for precipitation of phosphorus (Ojo and Ifelebuegu 2019b; Wilfert *et al. 2015*).

CPR has been reported to cause an increased volume of sludge between 37 and 97% (Yeoman *et al.* 1988). Thus, the CPR processes are to likely impact downstream processes due to the heavier load of metal salts used in the processes. The anaerobic digestion (AD) is a vital downstream process in activated sludge plants (Sawatdeenarunat *et al.* 2015). The anaerobic digestion process is a well-known technology that biologically treats and degrades organic substrates in the absence of oxygen, the impact of which has been progressively increasing over the last decade (Zhang *et al.* 2016; Romero-Güiza *et al.* 2016). The addition of coagulants (Al^{3+} and Fe^{3+}) can adversely impact the AD process of the resultant sludges due to increased sludge production. Sludge treatment and disposal accounts for nearly 60% of the entire running cost of WWTPs (Zhou *et al.* 2014) and, therefore, there is a need to further comprehend the purpose of process optimisation and cost savings.

There have been various reports on the use of metal salts for the conditioning of sludge and their effects on sludge treatment processes (Zhang *et al.* 2016; Romero-Güiza *et al.* 2016; Niu *et al.* 2013; Zhou *et al.* 2014; Haandel and Lubbe 2012). Also, previous studies by Smith and Carliell-Marquet (2008, 2009) have reported on the digestibility of Fe dosed sludge, with a reduced biogas production rate as a result of Fe dosing. Research on the effects of Al^{3+} salt on the digestibility of activated sludge is limited in the literature. This current study provides a comparative assessment of the effects of Fe^{3+} and Al^{3+} on the digestibility of surplus activated sludge (SAS).

7.2 Results and discussion

The sludge digestibility was investigated in locally assembled laboratory biogas anaerobic digesters (Figure 3.6-Chapter Three). The results obtained from the investigation on the impact of aluminium and ferric on activated sludge digestibility was presented based on the effects of aluminium (Al^{3+}) and ferric (Fe^{3+}) dosing on biogas production (7.2.1) and conclusion and practical relevance (7.2.2).

7.2 Effects of Aluminium and Ferric Dosing on Biogas Production

The sludge digestibility was investigated in a laboratory-scale anaerobic digester (Figure 3.8). All the test results reported in Table 7.1 and Figures 7.1 - 7.2 are the means and standard deviation of three independent samples. The results as earlier reported (Ojo and Ifelebuegu 2019b), showed that the mean cumulative biogas volumes produced for the undosed digested sludges after the first sludge age (12 days) were 31.56 ± 2.3 and 34.91 ± 1.3mL, compared with the Al^{3+}-dosed sludge of 24.85 ± 1.3mL and Fe^{3+}-dosed sludge of 22.46 ± 1.5mL, respectively. This indicates a 21.3% and 35.7% reduction in the biogas volume as a result of CPR using 100mg/L of Al^{3+} and Fe^{3+} respectively.

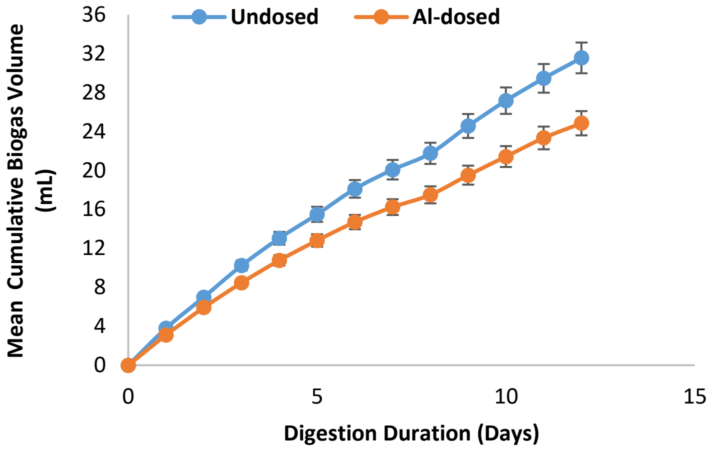

Figure 7.1. The effects of Al^{3+}dosed surplus activated sludge (SAS) for chemical phosphorus removal (CPR) on the cumulative biogas generation in an anaerobic digester. Error bars represent the standard deviation (SD) of three independent replicates.

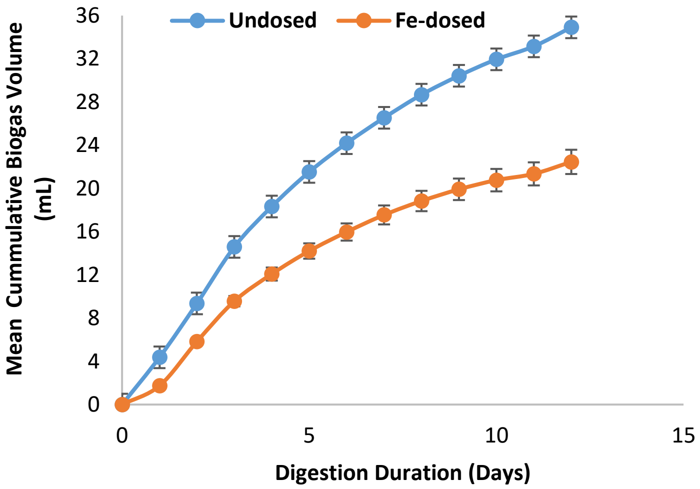

Figure 7.2. The effects of Fe^{3+}dosed surplus activated sludge (SAS) for chemical phosphorus removal (CPR) on the cumulative biogas generation in an anaerobic digester. Error bars represent the standard deviation (SD) of three independent replicates.

Table 7.1. Cumulative biogas volume production for Aluminium and Ferric and Undosed SAS after 12 days.

Cumulative biogas (mL) after 12 days	**Fe^{3+}Dosed SAS (Undosed)**	**Al^{3+}Dosed SAS (Undosed)**
	22.46 ± 1.5 (34.91 ± 1.3)	24.85 ± 1.3 (31.56 ± 2.3)
% Biogas reduction	35.7%	21.3%

Reduced biogas production as a result of chemical phosphorus removal using ferric has been previously reported (Smith and Carliell-Marquet 2009). Biogas reductions of 20% (Kindzierski and Hrudey 1986; Yeoman *et al.,* 1990), 21–32% (Dentel and Gossett 1982) and 32% (Johnson *et al.* 2003) were previously reported for mixed sludges. The current study showed a 19.65% and 35.16% reduction in the biogas volumes after CPR treatment with 100mg/L of Al^{3+} and Fe^{3+} salts respectively. This is in agreement with the range of 20–50% reduction previously reported by Ofverstrom *et al.* (2010). Although the previous studies were on mixed sludge, the current research provides data on SAS and compares the biogas reduction effects of aluminium and ferric salts. There was a clear indication that between the Al^{3+}- and Fe^{3+}-digested sludge, Fe^{3+} caused an estimated 15.51% further reduction in biogas production compared with Al^{3+}. Therefore, for the purpose of CPR, Al^{3+}-dosed sludge yields about 15.51% more biogas than Fe^{3+}-dosed activated sludge.

The reason for this high rate of biogas production in un-dosed sludge compared with the metal (Al^{3+} and Fe^{3+}) dosed sludges may be attributed to the increased availability of the substrate for metabolism and possibly due to the microbial community in the seeded sludge being more susceptible to breaking down un-dosed SAS compared with aluminium- and ferric-dosed SAS. The reduced biogas production for the Al^{3+}- and Fe^{3+} dosed sludges can also be due to the substrates, such as proteins, that form the majority of the components in the sludge (SAS) being tightly bound to the surface of the Al^{3+} dosed sludge precipitate and Fe^{3+} dosed sludge being entangled within the sludge floc (Dentel and Gossett 1982). It has been suggested that the reduction in biogas volume of Al^{3+} dosed sludge compared with un-dosed sludge may be due to the time length of producing and hydrolysing the substrate (Angelidaki *et al.* 1999; Park *et al.* 2006). Further, the strong bond of proteins to aluminium may cause a reduction in the rate of biogas production (Park *et al.* 2006). It has also been inferred that the biogas reduction may be attributed to the reduced availability of microbial population to organics (Kindzierski and Hrudey 1986; Dentel and Gossett 1982).

7.3. Conclusion

The effects of chemical phosphorus removal using Al^{3+} and Fe^{3+} salts on activated sludge digestibility in batch settling tests using a locally designed laboratory anaerobic digester were investigated. The results demonstrated that the use of Al^{3+} and Fe^{3+} salts reduced the digestibility of surplus activated sludge, with Al^{3+} salt having up to 15% less reduction effect compared with Fe^{3+}. Nevertheless, other findings made in current study was that there exist in terms of reduction in the biogas volume, 15.51% savings in the impact of aluminium salt on biogas reduction volume compared to utilising the ferric dosing in the SAS sample.

Chapter Eight

The Impact of Chemical Dosing on Activated Sludge Dewaterability

8.0 Research objectives and Activated Sludge Dewaterability

The use of CPR impacts the rheology of activated sludge as have been reported in the previous chapters. This is expected to also impact on the dewaterability of sludge. While most of these studies focused on the effects of the use of conditioners when used for conditioning during sludge treatment processes (Chapter Two-section 2.3), there has been limited research on the effects of the chemicals used in the upstream activated sludge process for the precipitation of phosphorus on the downstream dewatering process. Therefore, the fourth research objective of this work was to investigate the impact of chemical dosing ferric, aluminium and calcium (Fe^{3+}, Al^{3+} and Ca^{2+}) concentration on laboratory simulated dewaterability (CST) data using a new CST type 304B suction device. The current study aims to investigate the effects of CPR on the dewaterability of WWTP primary sludge and surplus activated sludge (SAS). The capillary suction time (CST) is measured as an indicator of activated sludge dewaterability.

8.1 The Impact of Chemical Dosing Aluminium, Ferric and Calcium on Activated sludge dewaterability

8.1.1 Introduction

Surplus activated sludge (SAS) is constantly been produced in large quantity which is a grave problem for the operation of municipal and industrial wastewater treatment plants (WWTP) due to high SAS treatment and disposal costs. Through, the required effluent discharge consent for phosphate removal becoming stricter under the EU Water Framework Directive, there is a rising demand for treatment works improvements to meet P consents in WWTP effluents. The activated sludge process (ASP) is the most widely used technique for municipal wastewater treatment and is able to achieve higher P removal to levels of less than 1mg/L (Ojo and Ifelebuegu 2019a). The two main processes for phosphorus removal namely biological phosphorus removal (BPR) and chemical phosphorus removal (CPR), and the limitation of BPR compared to CPR have been already mentioned in section 7.1.1. Most WWTPs in Europe use CPR to achieve their effluent P consents using mainly ferric (Fe^{3+}), aluminium (Al^{3+}) salts and calcium (Ca^{2+}) for phosphorus precipitation (Haandel and Lubbe 2012; Ojo and Ifelebuegu 2016).

Dewatering processes is one of the important downstream processes apart from the anaerobic digestion (AD) reported in section 7.1.1. The dewatering of sludge is to reduce the sludge volume by separating the water from the activated sludge (AS) solids (Niu *et al.* 2013). The addition of coagulants (Fe^{3+}, Al^{3+} and Ca^{2+}) can adversely impact the dewaterability of the resulting sludges due to increased sludge production. Also, a huge amount of the excess sludge produced from WWTP contains between 90-95% water which is initiating serious environmental pollution (Wong *et al.* 2015; Liang *et al.* 2015). The treatment and disposal cost of SAS accounts for 60 % of the total operating cost for a WWTP (Zhou *et al.* 2014). Thus, a better understanding of the dewatering of sludge processes is required, for the purpose of process optimisation and cost savings.

Numerous factors have been reported to affect the dewaterability of activated sludge, including surface chemistry (zeta potential) (Lee and Liu 2000); yield stress, which explains the sludge rheological characteristics (Lotito *et al.* 1997); bound water content (Keiding *et al.* 2001) and extracellular polymeric substances (EPS) content (Mowla *et al.* 2013). Some chemicals have been researched as conditioners for the improvement of sludge dewaterability including chemical coagulants such as aluminium sulphate, ferric chloride, calcium hydroxide, polyelectrolyte, surfactants and enzymes (Ruiz-Hernando *et al.* 2013), acids and surfactants (Chen *et al.* 2001), Fenton's reagent pretreatment (Tony *et al.* 2008), calcined aluminium salt and potassium ferrate (Ye *et al.* 2012). While most of these studies focused on the effects of the use of these conditioners when used for conditioning during sludge treatment processes, there has been limited research on the effects of the chemicals used in the upstream activated sludge process for the precipitation of phosphorus on the downstream dewatering process. The aim of this current study is to investigate the effects of CPR (Fe^{3+}, Al^{3+} and Ca^{2+}) on the dewaterability of WWTP primary sludge and secondary sludge (surplus activated sludge(SAS)).

8.2 Results and discussion

The capillary suction time (CST) are globally used dewaterability parameters for monitoring sludge dewaterability. The CST test estimates the filtration rate in terms of time for free water to pass between two electrodes using a filter paper as the medium (Scholz 2005; Sawalha and Scholz 2010). Wong *et al.* (2015); Wakeman (2007) and Feng *et al.* (2009) stated that longer CST indicates poor sludge dewaterability while shorter CST indicates good sludge dewaterability. The sludge digestibility was investigated using a new standard Triton UK-Type 304B capillary suction time (CST) device (Essex, UK) (Triton Limited 2018a), equipped with a 18mm reservoir resting on a standard Whatman No.17 grade chromatography paper (Figure 3.9-Chapter Three). The results obtained from the investigation on the impact of aluminium, ferric and calcium on activated sludge dewaterability was presented based on the effects of ferric (Fe^{3+}), aluminium (Al^{3+}) and calcium (Ca^{2+}) dosing on activated sludge dewaterability using two different sludge namely primary sludge and surplus activated sludge (SAS) (secondary sludge) respectively (8.2.1) and conclusion and practical relevance (8.2.2).

8.2.1 Effects of Aluminium, Ferric and Calcium Dosing on Sludge Dewaterability

The results of the sludge dewaterability (mean CST) for Fe^{3+}, Al^{3+} and Ca^{2+} dosed primary sludge and secondary sludge at concentrations of 0, 20, 30, 40 and 50mg/L for the batch tests (1 and 2) using an 18-mm reservoir are summarised in Tables 8.1 and 8.2. All test results reported in Tables 8.1 and 8.2 are the means and standard deviation of three independent primary and secondary sludge samples. In previous studies by Ojo and Ifelebuegu (2019b), result showed that the mean CST reduced with the increasing concentration of Fe^{3+}, Al^{3+} and Ca^{2+} doses (20, 30, 40 and 50mg/L) in primary sludge, while mean CST increased with the increasing concentration of Fe^{3+}, Al^{3+} and Ca^{2+} doses (20, 30, 40 and 50mg/L) in secondary sludge. Shorter CST indicates good dewaterability, while longer CST signifies poor dewaterability (Wong *et al.* 2015; Feng *et al.* 2009).

The chemically dosed primary sludges showed reduced CST (better dewaterability) compared with the undosed sludge. The CST decreased with increasing doses of Fe^{3+}, Al^{3+} and Ca^{2+}. As can be seen in Table 8.1, there was a 25.1%, 16.2% and 26.77% improvement in the rate of dewaterability of primary sludge at 50mg/L CPR doses of Fe^{3+}, Al^{3+} and Ca^{2+} salts respectively. This indicates that CPR, by a pre-precipitation method where phosphorus is precipitated out in the primary sedimentation tank, would be more beneficial for enhancing sludge dewaterability. The observed CST reduction for the primary sludge following the CPR may be due to the ability of multivalent (Fe^{3+} and Al^{3+} salts) and divalent (Ca^{2+}) coagulants to interact with the microbial clusters and break the EPS structure bound with water (Laspidou and Rittman 2002; Nelson *et al.* 1998). This could also be due to the neutralisation of the negative charge on the sludge floc since the EPS is negatively charged and responsible for an increased surface charge of microbial aggregates which causes decreased settleability and flocculability of microbial clusters (Liu *et al.* 2007; Liu *et al.* 2010).

Table 8.1. Mean and standard deviation data of capillary suction time (CST) and CST reduction efficiency for undosed and Aluminium, Ferric and Calcium coagulant dosed primary sludges

Coagulant Concentration (mg/L)	**CST (s)**			**% CST Reduction**		
	Fe^{3+}	**Al^{3+}**	**Ca^{2+}**	**Fe^{3+}**	**Al^{3+}**	**Ca^{2+}**
0	18.0 ± 3.04	18.0 ± 3.04	18.0 ± 3.04	-	-	-
20	16.26 ± 2.22	16.83 ± 3.95	15.92 ± 1.55	9.67	6.50	11.52
30	15.29 ± 1.77	16.24 ± 4.54	14.93 ± 2.36	15.10	9.75	17.00
40	14.39 ± 1.84	15.66 ± 5.18	14.03 ± 1.36	20.10	13.00	22.10
50	13.49 ± 2.18	15.07 ± 5.86	13.18 ± 1.68	25.10	16.25	26.77

However, the neutralisation effect of increasing chemical dosing (Fe^{3+}, Al^{3+} and Ca^{2+}) on the primary sludge will improve dewaterability with a shorter CST value. This is due to reduced repulsive forces between the sludge flocs and release of bound water to the sludge floc matrix (Vaxelaire and Cezac 2004; Wu *et al.* 1997). It was mentioned that surface charge chemistry and disruption of the EPS structure are responsible for shorter CST (Li *et al.* 2005; Dursun *et al.* 2006). The observed shorter CST reported in the primary sludge could also be due to polymer bridging (Higgins *et al.* 2006) resulting in the destabilisation of colloidal particles present in sludge floc. Therefore, in the current study, it can be concluded that the reduced CST, as a function of the impact of chemical dosing (Fe^{3+}, Al^{3+} and Ca^{2+}) on the primary sludge, improved dewaterability due to the surface charge chemistry and disruption of the sturdy EPS structure bound with water.

Furthermore, the result of CST reduction efficiency for aluminium, ferric and calcium on primary sludge is in agreement with CST reduction of 88 per cent (35s to 15.5s) at an optimum dosing of 2gFe/l (Wong *et al.* 2015), 31.4% to 50.7% at 500mg Zero Valent Iron (ZVI)/L (Zhao and Bache 2014), 47% to 48.6% using classical Fenton oxidation process (Tony *et al.* 2009; Buyukkamaci 2004) 69.88% (8.5s*l/g to 2.56s*l/g) at an optimum dosing of 0.05gAl/gTSS (Cao *et al.* 2016), 25.16% (60.8 to 45.5s) at 20V electrolysis voltage (Yuan *et al.* 2011) and 95% using cationic polyelectrolyte organic additive (Buyukkamaci and Kucukselek 2007) reported by previous researchers. Further support was given to these CST result by other investigators that shorter CST indicates good dewaterability while longer CST depicts poor dewaterability (Feng *et al.* 2009; Wakeman 2007).

In contrast, the results of the sludge dewaterability (mean CST) for Fe^{3+}, Al^{3+} and Ca^{2+} dosed secondary sludge (SAS) at a concentration of 0, 20, 30, 40 and 50mg/L using an 18-mm reservoir are presented in Table 8.2. From the results, it was observed that the mean CST increased with the increasing concentration of ferric, aluminium and calcium (20, 30, 40 and 50 mg/L). At 50 mg/L of Fe^{3+}, Al^{3+} and Ca^{2+} CPR doses, 63.82%, 72.96% and 52.56% reductions in SAS dewaterability (increased CST values) were respectively observed, indicating that if CPR is applied by co-precipitation in activated sludge plants using these salts, there will be a significant reduction in the dewaterability rates of the resultant SAS. The observed behaviour may be due to the interaction between the multivalent coagulants (Fe^{3+}, Al^{3+} and Ca^{2+}) and higher EPS content, which has a tendency to limit the flocculating and settleability ability of microbial clusters (Liu *et al.* 2010).

Table 8.2. Mean and standard deviation data of CST for undosed and dosed sludge surplus activated sludges.

Coagulant Concentration (mg/L)	**CST (s)**			**% CST Increase**		
	Fe^{3+}	**Al^{3+}**	**Ca^{2+}**	**Fe^{3+}**	**Al^{3+}**	**Ca^{2+}**
0	33.17 ± 2.04	33.17 ± 2.04	33.17 ± 2.04	-	-	-
20	43.7 ± 1.76	47.97 ± 1.37	37.13 ± 1.46	31.75	44.62	11.96
30	47.91 ± 2.77	52.49 ± 0.71	41.11 ± 1.61	44.46	58.26	23.95
40	51.23 ± 4.87	55.57 ± 2.56	46.37 ± 2.85	54.47	67.54	39.80
50	54.33 ± 4.87	57.37 ± 5.60	50.60 ± 2.21	63.82	72.96	52.56

This limitation will further cause the water retention capacity and quantity of bound water in the EPS to rise and, hence, restricts the outflow of interstitial water from the sludge floc pore spaces (Chen *et al.* 2001; Houghton *et al.* 2001). Another probable reason may be due to the reduction and solubility of coagulants (Fe^{3+}, Al^{3+} and Ca^{2+}), causing protein to enter into the solution and a fragile connection between the protein structure and the sludge floc, which may limit dewaterability improvement (Novak *et al.* 2001). Also, it may be due to increased resistance and binding from the sludge floc (Neyens and Baeyens 2003).

8.3. Conclusion

The effects of chemical phosphorus removal using Fe^{3+}, Al^{3+} and Ca^{2+} on activated sludge dewaterability in batch settling test using a new CST type 304B suction device were investigated. The results demonstrated that the use of Fe^{3+}, Al^{3+} and Ca^{2+} salts improved the dewaterability of primary sludge by 25%, 16% and 26% but significantly reduced the dewaterability of SAS by 64%, 73% and 53% respectively. The results demonstrated that using Fe^{3+}, Al^{3+} and Ca^{2+} salts in the CPR process will improve the dewaterability of primary sludge but decrease the dewaterability of SAS. It can therefore be inferred that for the purpose of optimising the dewaterability of activated sludge, a pre-precipitation process where phosphorus is removed in the primary tank would be more ideal during the CPR process.

Chapter Nine

Conclusion and Perspective

9.1 General Conclusion

The impact of metal salts (Al^{3+}, Fe^{3+} and Ca^{2+}) dosing on activated sludge settleability (ZSV and SSVI) was studied in batch settling tests using MLSS from a full-scale WWTP over a three year' period using a type 305 settlometer.The effects of the chemical dosing on the dewaterability and digestibility of activated sludge was also investigated. The results showed that ZSV increased while SSVI decreased with increasing dose of Al^{3+}, Fe^{3+} and Ca^{2+}. The best settleability was achieved at 50mg/L dose of Al^{3+}, Fe^{3+} and Ca^{2+}. The improved settleability with increasing dose of Al^{3+}, Fe^{3+} and Ca^{2+} was attributed to the improve bioaggregation of the activated sludge with dosing and through EPS binding capacity to microbial cells through its bridging nature with aluminium, ferric and calcium. The sludge settleability started to decline between > 50mg/L to 150mg/L dose concentration for aluminium, ferric and calcium salts. The decrease in ZSV and increase in SSVI and hence decreased settleability at the higher dose concentrations are attributed to surface charge reversal linked to high aluminium, ferric and calcium dosing rate and high surface charge which is a function of weaker bonding between the various sludge floc fractions resulting to the breakage of the general activated sludge floc.

The experimental data collected over three years from a full-scale activated sludge plant was further used to propose a new activated sludge settleability model to analyse the effects of aluminium, ferric and calcium dosing on activated sludge settleability indicators using the linear transformation of exponential functions to achieve replication of a non-linear relationship between the aluminium, ferric and calcium dosing concentrations and settleability indicators (ZSV and SSVI). The following conclusions were drawn;

- ZSV increased while SSVI decreased with increasing aluminium, ferric and calcium concentration for concentration range of 0 to <100mg/L Al^{3+}, Fe^{3+} and Ca^{2+}. High surface charges associated with higher concentrations of Al^{3+}, Fe^{3+} and Ca^{2+} causes a general disintegration of the activated sludge floc structure.
- This will result to the Al^{3+}, Fe^{3+} and Ca^{2+} dosed sludge not fitting the proposed equation at concentrations higher than the stated range (0 to <100mg/L Al^{3+}, Fe^{3+} and Ca^{2+}).
- The ZSV for an aluminium, ferric and calcium dosed sludge could be described by the expressions taking into account the Al^{3+} , Fe^{3+} and Ca^{2+} dosing concentrations;

$$\mathrm{ZSV}_{\mathrm{Al}} = \left((0.026\,(\mathrm{D_C})_{\mathrm{Al}} + 1.377)\mathrm{e}^{-0.020+0.0023(\mathrm{D_C})_{\mathrm{Al}}\mathrm{X}_{\mathrm{Al}}}\right)$$

$$\mathrm{ZSV_{Fe}} = \left((0.0089\,(\mathrm{D_C})_{\mathrm{Fe}} + 0.740)\mathrm{e}^{-0.290+0.0025\,(\mathrm{D_C})_{\mathrm{Fe}}\,\mathrm{X_{Fe}}}\right)$$

$$\mathrm{ZSV_{Ca}} = (0.035\,(\mathrm{D_C})_{\mathrm{Ca}} + 2.346)\mathrm{e}^{-(0.112+0.0020\,(\mathrm{D_C})_{\mathrm{Ca}}\,\mathrm{X_{Ca}}})$$

Similarly, the results of regression analysis for the impact of Al^{3+}, Fe^{3+} and Ca^{2+} dosing on SSVI using the experimental data in the batch test conducted showed that the coefficient of determination (R^2) was close to 1 (0.986) and could be expressed as:

$$\mathrm{SSVI_{Al}(mL/g)} = -\ln\left[\left(\frac{\mathrm{ZSV_{Al}}}{68((\mathrm{K_d})_{\mathrm{Al}}\mathrm{X_{Al}}) + ((\mathrm{C_K})_{\mathrm{Al}}(\mathrm{D_C})_{\mathrm{Al}}\mathrm{X_{Al}})}\right) - \left(\frac{(\mathrm{C_0})_{\mathrm{Al}}(\mathrm{D_C})_{\mathrm{Al}}}{68(\mathrm{K_d})_{\mathrm{Al}}}\right)\Big/_{0.016}\right]$$

$$\mathrm{SSVI_{Fe}(mL/g)} = -\ln\left[\left(\frac{\mathrm{ZSV_{Fe}}}{68((\mathrm{K_d})_{\mathrm{Fe}}\,\mathrm{X_{Fe}}) + ((\mathrm{C_K})_{\mathrm{Fe}}(\mathrm{D_C})_{\mathrm{Fe}}\,\mathrm{X_{Fe}})}\right) - \left(\frac{(\mathrm{C_0})_{\mathrm{Fe}}\,(\mathrm{D_C})_{\mathrm{Fe}}}{68(\mathrm{K_d})_{\mathrm{Fe}}}\right)\Big/_{0.016}\right]$$

$$\mathrm{SSVI_{Ca}(mL/g)} = -\ln\left[\left(\frac{\mathrm{ZSV_{Ca}}}{68((\mathrm{K_d})_{\mathrm{Ca}}\,\mathrm{X_{Ca}}) + ((\mathrm{C_K})_{\mathrm{Ca}}(\mathrm{D_C})_{\mathrm{Ca}}\,\mathrm{X_{Ca}})}\right) - \left(\frac{(\mathrm{C_0})_{\mathrm{Ca}}\,(\mathrm{D_C})_{\mathrm{Ca}}}{68(\mathrm{K_d})_{\mathrm{Ca}}}\right)\Big/_{0.016}\right]$$

The proposed new models showed a good fit to the experimental data up to a dose range of 50mg/L of Al^{3+}, Fe^{3+} and Ca^{2+}. The new model equations will find application in the water industry for the modelling and optimisation of Al^{3+}, Fe^{3+} and Ca^{2+} dosed activated plants.

The data collected over three years from a full-scale activated sludge plant was further used to investigate the effects of chemical phosphorus removal using Fe^{3+}, Al^{3+} and Ca^{2+} salts on activated sludge digestibility in batch settling tests using a locally designed laboratory anaerobic digester and activated sludge dewaterability using a new CST type 304B suction device were investigated. The following conclusions were drawn;

- ✓ The use of Fe^{3+} and Al^{3+} salts reduced the digestibility of surplus activated sludge, with Al^{3+} salt having up to 15% less reduction effect compared with Fe^{3+}.
- ✓ The high rate of biogas production in un-dosed sludge compared to treatment (Al^{3+} and Fe^{3+}-dosed) may be attributed to increased availability of the substrate for metabolism and possibly due to the microbial community in the seeded sludge been more susceptible to breaking down un-dosed surplus activated sludge (SAS) compared to aluminium and ferric dosed SAS.

- ✓ Also, Fe^{3+}, Al^{3+} and Ca^{2+} salts improved the dewaterability of primary sludge by 25%, 16% and 26% but significantly reduced the dewaterability of SAS by 64%, 73% and 53%, respectively.
- ✓ The reason for CST reduction in primary sludge is due to surface chemistry and disruption of EPS structure causing the release of interstitial water into surrounding sludge matrix through the interaction between multivalent and divalent ions (Al^{3+}, Fe^{3+} and Ca^{2+}) and sludge particles.
- ✓ The CST increase in secondary sludge is due to the interaction of multivalent coagulant (Al^{3+} and Fe^{3+}) and divalent ion (Ca^{2+}) with higher EPS content limiting the outflow of interstitial water from the sludge floc pore spaces.

The results demonstrated that using Fe^{3+}, Al^{3+} and Ca^{2+} salts in the CPR process will improve the dewaterability of primary sludge but decrease the dewaterability of SAS. It can therefore be inferred that for the purpose of optimising the dewaterability of activated sludge, a pre-precipitation process where phosphorus is removed in the primary tank would be more ideal during the CPR process. Nevertheless, other findings made in current study was that there exist in terms of reduction in the biogas volume, a 15.51% saving in the impact of Al^{3+} on biogas reduction volume compared to utilising the Fe^{3+} dosing in the SAS sample.

9.2 Implications of the empirical relationship of Zone Setling Velocity (ZSV) and Stirred Sludge Volume Index (SSVI)

Although, some theoretical and practical implication of the empirical relationship of ZSV and SSVI has been discussed in section 2.1.4 and 2.1.5 and also in section 4.2.3. However, it was reported that activated sludge process (ASP) is the most widely used process for wastewater treatment (François *et al.* 2016). It was also added that the effluent quality is largely affected by the solid-liquid separation in the ASP (Wilfert *et al.* 2015). The solid-liquid separation depends on both sludge biological flocculation (Bio-flocculation) and activated sludge settleability. Liao *et al.* (2001) already affirmed that 70-90% of final sedimentation tanks (FST) have faced solid-liquid separation problem. Jin *et al.* (2003) have also reported two main causes of poorly activated sludge settleability namely; filamentous bulking sludge (proliferation of filamentous bacteria) and bulking sludge due to poor flocculation properties such as small or light floc formation. Large and strong flocs are desirable for good settleability and compactibility of activated sludge. Wen *et al.* (2015) reported that one of the most common solutions to the poor biological flocculation performance of ASP is the dosing of flocculants and coagulants. This will not just enhance the agglomeration of active sludge flocs but will also impact on chemical phosphorus removal (CPR). The phosphorus (P) removal will reduce the effect of eutrophication in ASPs. The solid components of an activated sludge is made up of small sludge particles with large number of negative surface charges (Jin *et al.* 2003). The presence of electrical double layer (EDL) will further cause repulsion of these negatve adjacent sludge particles in the activated sludge system which hinders bioflocculation in FSTs (Lui *et al.* 2017). Sedimentation has been reported to be one of the most vital process that determines the performance of ASP (Li and Strenstrom 2014a). The driving force that will enhance the activated sludge sedimentation processes are the trivalent and divalent cations (aluminium, ferric and calcium). These metal ions have the ability to destroy the EDL and improve bio-flocculation by agglomeration of dispersed sludge particles in the ASP (Higgins and Sobeck 2004,2002). The multivalent cations bind different entities in the sludge flocs by bridging of the negatively charged functional group present on the biopolymers (extracellular polymeric substances-EPS) that make up the microorganism used in the ASP.

Dick and Vesilind (1969) have reported the shortcomings of sludge volume index (SVI) as it failed to relate the initial settling velocity of activated sludge. Therefore, the SVI will vary with both the sludge volume and concentration. However, White (1975) reported that the limitations of SVI were addressed when the water research council (WRc) proposed the stirred sludge volume index (SSVI) to replicate an ideal situation in the FST. Whilst the SVI is measured under complete quiescence, the SSVI was evaluated using a test device fitted with a low speed stirrer rotating at one revolution per minute (1rpm). The evaluation of zone settling velocity (ZSV) is vital in both the design and modelling of FSTs (Ojo and Ifelebuegu 2019a). The ZSV is a key sludge settleability parameter to evaluate the sludge settling properties, since it determines the extent to which a FST can be loaded during wastewater treatment. The ZSV approach allows settling velocities to be evaluated over a range of activated sludge concentrations (X) to estimate the rate of zone settling in the settling column where flocs are in proximity to each other. The resultant ZSV values are then used to regulate various models relating the settling velocity and solids concentration. The simulation and control of settling in final settling tanks (FST) in wastewater treatment depends on calibrated models (Bürger *et al.* 2018). Model validation in this current study will help to evaluate whether or not the proposed new mathematical model describes properly the settling characteristics of Al^{3+},Fe^{3+} and Ca^{2+} sludge. The approach is to check whether the new model fits the experimental batch test results.

The effect of aluminium (Al^{3+}), ferric (Fe^{3+}) and calcium (Ca^{2+}), dosing on activated sludge settleability indicators; zone settling velocity (ZSV) and stirred specific volume index (SSVI) were examined in laboratory-based batch settleability tests over a three year period using a type 305 settlometer. The experimental data revealed that ZSV increased with increasing dose of aluminium, ferric and calcium salts as SSVI decreased with the highest changes obtained at a dose rate of 50mg/L dose of aluminium (Al^{3+}), ferric (Fe^{3+}) and calcium (Ca^{2+}). The improved settleability with increasing dose of Al^{3+}, Fe^{3+} and Ca^{2+} was attributed to the improved bioaggregation of the activated sludge with dosing and through EPS binding ability to aggregates cells through its bridging nature with aluminium, ferric and calcium salts. The sludge settleability started to decline between >50mg/L to 150mg/L dose concentrations (aluminium, ferric and calcium). The decrease in ZSV and increase in SSVI and hence decreased settleability at the higher dose concentrations (Al^{3+},Fe^{3+} and Ca^{2+}) are attributed to surface charge reversal linked to high aluminium, ferric and calcium dosing rate and high surface charge which is a function of weaker bonding between the various sludge floc fractions resulting to the breakage of the general activated sludge floc. The implication is that the wastewater sample was from a facility that treats both municipal and industrial wastewater. The wastewater treatment plant (WWTP) is not a chemically dosed plant and therefore the chemical dosing was done on a laboratory-scale basis. Grady *et al.* (1999) and Park *et al.* (2006) have reported that activated sludge from industrial origins exhibits poor bio-flocculation compared to domestic origin because of the absence of wastewater EPS. Based on the result in this current study, the sampled WWTP with no influent aluminium, ferric and calcium dosing concentration, with addition of a dose rate of 50mg/L dose of aluminium (Al^{3+}), ferric (Fe^{3+}) and calcium (Ca^{2+}) should improve bio-flocculation characteristics and overall should lead to substantial optimisation of the WWTP operation. Nevertheless, the proposed new activated sludge settleability models for aluminium, ferric and calcium dosed activated sludge showed a good fit to the experimental data up to 50mg/L dose of Al^{3+}, Fe^{3+} and Ca^{2+}. The new model equations will find application in the water and wastewater industry for the modelling and optimisation of Al^{3+}, Fe^{3+} and Ca^{2+}dosed activated sludge plants.

9.3 Further Research

The current study has shown that the external factors of final sedimentation tank (FST) affects the efficiency of the activated sludge plant. The role of inorganic coagulant (Aluminium, Ferric and Calcium salt) in activated sludge settleability has been covered. Further investigation will be required to evaluate how the internal hydrodynamic behaviour of FST impacts chemically dosed (Al^{3+}, Fe^{3+} and Ca^{2+}) activated sludge settleability using Computational Fluid Dynamics (CFD) software. Further still, investigation on the impact of other chemicals like the inorganic coagulants (Poly-Aluminium-Chloride; PAC), and organic polymers (Polyacrylamide-PAM) on activated sludge settleability using CFD can be explored.

References

Abbott, T., and Eskicioglu, C. (2015) ‘Effects of metal salt addition on odor and process stability during the anaerobic digestion of municipal waste sludge’. *Waste Management*, 46 (449-458)

Abdelsalam, E., Samer, M., Attia, Y.A., Abdel-Hadi, M.A., Hassan, H.E., Badr, Y. (2016) ‘Comparison of nanoparticles effects on biogas and methane production from anaerobic digestion of cattle dung slurry’. *Renew. Energy* 87, 592-598

Abu-Orf, M., Dental, S., Dursun D., and Turkmen, M. (2007) Pilot-scale evaluation of enzyme pre-treatment to enhance dewatering: effects of shear and polymer. *In: WEF/AWWA joint residuals and biosolids management conference,* Denver, CO, USA: Water Environment Federation; 1180-1195

Abu-Orf, M., Laquidara, M., Muller, C., Park, C., and Novak, J. (2004) ‘Adjusting floc cations to improve effluent quality: The case of aluminium addition at Sioux City wastewater treatment facility. In Proceedings of the Water Environment Federation: Session 41–50, New Orleans, LA, USA

Agarwal, S., Abu-Orf, M., and Novak, J. T. (2005) ‘Sequential polymer dosing for effective dewatering of ATAD sludges’. *Water Research* 39(7), 1301-1310

Agridiotis, V., Forster, C.F. and Carliell-Marquet, C. (2007) ‘Addition of Al and Fe salts during treatment of paper mill effluents to improve activated sludge settlement characteristics’. *Journal of Bio-resource Technology*, *98* (15), 2926-2934

Ahn, J.-H., and Forster, C.F. (2002) ‘A comparison of mesophilic and thermophilic anaerobic upflow filters treating paper-pulp-liquors’. *Process Biochemistry* 38, 257-262

Ahn, J.-H., Do, T. H., Kim, S.D., and Hwang, S. (2006) ‘The effect of calcium on the anaerobic digestion treating swine wastewater’. *Biochemical Engineering* 30, 33-38

Ahring, B. K. (2003). Perspectives for anaerobic digestion. *In: Advances in Biochemical Engineering/Biotechnology*, T. Scheper (ed.), 81, Springer-Verlag, Berlin Heidelberg

Aisami, A., Yasid, N.A., Wan Johari, W.L., and Shukor, M.Y. (2017) ‘Estimate of the Q value the temperature coefficient for the Growth of Pseudomonas sp. AQ5-04 on Phenol’. *Journal of Bioremediation Science and Technology Research (BSTR)* 55(1), 24-26

Alrawi, R. A., Ahmadb, A., Ismail, N. and Kadir, M. O. Ab. (2011) 'Effect of Aluminium Sulphate Dosage and Mixing Ratio on Organic Loading Removal and Settling Velocity of Palm Oil Mill Effluent Particles'. *Journal of Industrial Research & Technology* 1 (2), 103-109

Al-Diwamy, L.J., and Cross, T. (1978) 'Ecological studies of *Nocardia* foams and other actinomycetes in aquatic habitats'. In *Nocardia and Streptomyces* (eds.M. Modarski, W. Kurytowicz and J. Jeljaszewiz) 153-74, Fischer V, Stuttgart, Germany

American Public Health Association (APHA), American Water Works Association and Water Pollution Control Federation, (1998) *Standard Methods for the Examination of Water and Wastewater.* 20th edn. Washington, DC, USA

Andreadakis, A.D. (1993) 'Physical and chemical properties of activated sludge floc'. *Journal of Water Research* 27 (12), 1707–1714

Anderson, N.E. (1945) 'Design of Settling Tanks for Activated Sludge'. Sewage Works Journal, 17(1), 50-63

Anderson, D.T. and Hammer, M.J. (1973) Effects of alum on activated sludge biota. *Water and Sewage Works*, **120**, 63–67

Angelidaki, I., Ellegaard, L., and Ahring, B. (1999) 'A comprehensive model of anaerobic bio-conversion of complex substrates to biogas'. *Biotechnology and Bioengineering* 63 (3), 363-372

Angelidaki, I., and Ahring, B. (1994) 'Anaerobic thermophilic digestion of manure at different ammonia loads: effect of temperature'. *Water Research* 28, 727–731

Angelidaki, I., and Ahring, B. (1993) 'Thermophilic anaerobic digestion of livestock waste: the effect of ammonia'. *Applied Microbiology and Bio-technology* 38, 560–564.

Angelidaki, I., and Ahring, B.K. (1992) 'Effects of free long-chain fatty acids on thermophilic anaerobic digestion'. *Applied Microbiology Bio-technology* 37,808–812

Anon (1979) 'Filamentous Micro-Organisms in Activated Sludge'. *New Quarterly of the Sanitary Engineering Research Laboratory* 29 (2), 1-2. University of California, Berkeley

Appels, L., Baeyens, J., Degrève, J., Dewil, R. (2008) 'Principles and potential of the anaerobic digestion of waste-activated sludge'. *Progress in Energy and Combustion Science* 34, 755-781

Ardern, E. and Lockett, W. T. (1914) 'Experiments on the oxidation of sewage without the aid of filters'. *Journal of the Society of Chemical Industry*, 33(10), 523–539

Ardern, E. and Lockett, W.T. (1923) ‘The Activated Sludge Process Withington Works’. *Chemistry and Industry* 225T-230T

Arimieari, L.W., and Ademiluyi, J.O. (2018) ‘Modelling the Relationship between Sludge Filtration Resistance and Capillary Suction Time’. *Journal of Environmental Protection*, 9, 91-99

Ariunbaatar, J., Panico, A., Esposito, G., Pirozzi, F., and Lens, P.N.L. (2014) ‘Pre-treatment methods to enhance anaerobic digestion of organic solid waste’. *Applied Energy Journal* 123,143–156

Armbruster,M., (2003) Untersuchung der moglichen leistugssteigerung von Nachklarbeken mit Hilife numerischer Rechungen’ PhD Thesis, University of Karlesruche

Arsova, L. (2010) *Anaerobic Digestion of Food Waste: Current Status, Problems and an Alternative Product*, Dissertation, Columbia University, Berlin, 2010

Ayol, A. (2005) ‘Enzymatic treatment effects on dewaterability of anaerobically digested biosolids-I: performance evaluations’. *Process Biochemistry* 40, 2427-2434

Ayol, A., and Dentel, S.K. (2005) ‘Enzymatic treatment effects on dewaterability of anaerobically digested biosolids: laboratory characterizations of drainability and filterability’. *Process Biochemistry*, 40, 2435-2442

Azam, H.M., and Finneran, K.T. (2014) ‘Fe (III) reduction-mediated phosphate removal as vi-vianite (Fe3 (PO4)2·8H2O) in septic system wastewater’. *Chemosphere* 97 (2014) 1–9

Bache, D.H., Papavasilopoulos, E.N., Rasool, E., and Zhao, Y.Q. (2003) ‘Polymers in alum sludge dewatering: development and control’. *Water Environment Journal* 17(2), 106-110

Baetzold, R.C., and Somorjai, G.A. (1976) ‘Pre-exponential factors in surface reactions’. *Journal of catalysis* 45(1), 94-105

Baeyens J, Hosten L, and Van Vaerenbergh E. (1997) Afvalwaterzuivering (Wastewater treatment). 2nd edn. The Netherlands: Kluwer Academic Publishers [in Dutch]

Bajcar, T., Steinman, F., Sirok, B., and Preseren, T. (2011) ‘Sedimentation efficiency of two continuously operating circular settling tanks with different inlet- and outlet arrangements’. *Journal of Chemical Engineering* 178, 217–224

Banks, C.J., Zhang, Y., Jiang, Y., and Heaven, S. (2012) ‘Trace element requirements for stable food waste digestion at elevated ammonia concentrations’. *Bioresource Technology* 104, 127-135

Barnard, J.L. (1975) ‘Nutrient Removal in Biological Systems’. *Water pollution control* 74,143-154

Barnard, J.L. (1976) ‘A Review of Biological Phosphorus Removal in the Activated Sludge Process’. *Water Research* 2, 136-144 South Africa

Baskerville, R.C., and Gale, R.S. (1968) ‘A simple automated instrument for determining the filterability of sewage sludges’. *Water Pollution Control* 67, 233-241.

Batstone, D.J., and Jensen, P.D. (2011) ‘Anaerobic processes’. *In: Wilderer, P., editor. Treatise water science*, Oxford: Elsevier, 615–39

Bayané, A., and Guiot, S.R. (2010) Animal digestive strategies versus anaerobic digestion bioprocesses for biogas production from lignocellulosic biomass’. *Reviews in Environmental Science and Biotechnology* 10, 43–62

Bender, J., Rodriguez-Eaton, S., Ekanemesang U.M. and Phillips P. (1994) ‘Characterization of metal-binding bio-flocculants produced by the cyanobacterial component of mixed microbial mats’. *Journal of Applied and Environmental Microbiology 60*, 2311

Bien, J.B. (1991) ‘The application of ultrasound in the preparation of sludge for its mechanical dewatering’. *Acustica Journal* 74, 279–283.

Bien, J.B., and Wolny, L. (1997) ‘Changes of some sewage sludge parameters prepared with an ultrasonic field’. *Water Science and Technology* 36, 101–106.

Biggs, C. (2000) *Activated sludge flocculation: investigating the effect of shear rate and cation concentration on flocculation dynamics*. Ph.D. thesis. Australia: University of Queensland

Biggs, C., and Lant, P. (2000) ‘Activated sludge flocculation: on-line determination of floc size and the effect of shear’. *Water Research Journal* 34 (9), 2542-2550

Bitton, G. (2005) *Wastewater Microbiology.* 3rd edn.USA: Wiley-Liss

Bjornsson, L., Murto, M., and Mattiasson, B. (2000) ‘Evaluation of parameters for monitoring an anaerobic co-digestion process’. *Appl. Microbiol. Biotechnol.* 54, 844–849

Bockstal, F., Fourarge, J.H., and Rahier, G. (1985) ‘Constant pressure cake filtration with simultaneous sedimentation’. *Filtration and Separation* 22, 255

Bohm, N., and Kulicke, W.M. (1997) ‘Optimization of the use of polyelectrolytes for dewatering industrial sludges of various origins’. *Colloid Polymer Science* 275, 73-81

Bokil, S.D. and Bewtra, J.K. (1972) ‘Influence Of Mechanical Blending On Aerobic Digestion of Waste Activated Sludge’. Proc.,6th int. *Association on water pollution research and control (IAWPRC)*, London: 421-438

Bolzonella, D., Pavan, P., Battistoni, P., and Cecchi, F. (2005) ‘Mesophilic anaerobic digestion of waste activated sludge: influence of the solid retention time in the wastewater treatment processes’. *Journal of Process Biochemistry* 40, 1453-1460

Boon, A.G. (1995) ‘Septicity in sewers: causes, consequences and containment’. *Water Science and Technology* 31 (7), 237-253

Bowen, R.B., Dempsey, B.A. (1992) ‘Improved performance of activated sludge without addition of inorganic solids’. *Water Science Technology* 26 (9-11), 2511-2514

BP (2014) ‘Statistical Review of World Energy’ [online] available from <http://www.bp.com/en/global/ corporate/about-bp/energy-economics/statistical-review-of-world-energy.html> [10 March 2015]

Bretscher, U., Krebs, P., and Hager, W.H. (1992) ‘Improvement of Flow in Final Settling Tanks’. *Journal of Environmental Engineering* 118 (3), 307-321

Bruus, J.H., Nielsen, P.H., and Keiding, K. (1992) ‘On the Stability of Activated Sludge Flocs with implication to Dewatering’. *Water Research Journal* 26, 1597

Buhr, H., and Andrews, J. (1977) ‘The thermophilic anaerobic digestion process. *Water Research* 11,129-143

Bürger, R. (2000) ‘Phenomenological foundation and mathematical theory of sedimentation consolidation processes’. *Chem. Eng. J.* 80 (1-3), 177-188

Bürger, R., Diehl, S., and Nopens, I. (2011) ‘A consistent modelling methodology for secondary settling tanks in wastewater treatment’. *Water Research Journal* 45 (6), 2247-2260

Bürger, R., Diehl, S., Faras, S., Nopens, I., and Torfs, E. A (2013) 'Consistent modelling methodology for secondary settling tanks: A reliable numerical method'. *Water Sci. Technol.* 68, 192–208

Bürger, R.; Careaga, J.; Diehl, S.; Ryan, M.; Zambrano, J. (2018) 'Estimating the hindered-settling flux function from a btch test in a cone'. *Chem. Eng. Sci. 192*, 244–253

Burt, D. J., and Ganeshalingam, J. (2005) *Design and Optimisation of Final Clarifier Performance with CFD Modelling: The CIWEM / Aqua Enviro joint conference on Design and Operation of Activated Sludge Plants* [online] available from <http://74.125.155.132/scholar?q=cache:8e3dfP6BukIJ:scholar.google.com/&hl=en&as_sdt=0,5 > [20 February 2014]

Burt, D. J., Ganeshalingam, J., Hammond, C., and Egarr, D. (2013) *Modelling the Dynamic Response of a Secondary Clarifier to a Sea Water Incursion at the Radford STW: 7TH European Waste Water management conference* [online] available from < https://www.researchgate.net/publication/313088584_Modelling_the_Dynamic_Response_of_a_Secondary_Clarifier_to_a_Sea_Water_Incursion_at_the_Radford_STW> [20 May 2015]

Busch, P., and Stumm, W. (1968) Chemical interactions in the aggregation of bacteria: bioflocculation in wastewater. *Environmental Science and Technology* 2, 49-53

Bustos, M.C. (1999) 'Sedimentation and Thickening, Phenomenological Foundation and Mathematical Theory'. (8), (Ed.), Springer

Buyukkamaci, N. (2004) 'Biological sludge conditioning by Fenton's reagent'. *Process Biochemistry* 39 (11), 1503–1506

Buyukkamaci, N., and Kucukselek, E. (2007) 'Improvement of dewatering capacity of a petrochemical sludge'. *Journal of Hazardous Materials* 144, 323-327

Caccavo, Jr., F., Frflund, B., Kloeke, F.V.O., and Nielsen, P.H. (1996) 'Deflocculation of Activated Sludge by the Dissimilatory Fe (III)-Reducing Bacterium Shewanella Alga Br Y'. *Applied and Environmental Microbiology* 62, 1487

Canales, A., Pareilleux, A., Rols, J., Goma, G., and Huyard, A. (1994) 'Decreased sludge production strategy for domestic wastewater treatment'. *Water Science Technology* 30 (8), 97–106

Cao, B., Zhang, W., Wang, Q., Huang, Y., Meng, C., and Wang, D. (2016) 'Wastewater sludge dewaterability enhancement using hydroxyl aluminium conditioning: Role of aluminium speciation'. *Water Research* 105, 615-624

Carlsson, M., Lagerkvist, A., Morgan-Sagastume, F. (2012) 'The effects of substrate pre-treatment on anaerobic digestion systems: a review'. *Waste Management* 32, 1634-1650

Carlsson (1998) *Introduction to Sedimentation Theory in Waste Water Treatment: System and Control Group Uppsala University* [online] available from <http://www.it.uu.se/edu/course/homepage/h2orentek/WWT98/sett98.pdf > [7 February 2014]

Carman, P.C. (1938) 'A study of the mechanism filtration'. *Transactions of the Institution of Chemical Engineers* 16, 168

Carrèrea, H., Rafrafi, Y., Battimelli, A., Torrijos, M., Delgenes, J.P., Ruysschaert, G. (2010) 'Methane potential of activated sludge and fatty residue: Impact of Co-digestion and alkaline pre-treatments'. *Open Environmental Engineering Journal* 3, 71–76

Cassey, T.D. (1992) *water and waste water hydraulics*. New Delhi: Oxford University Press

Catunda P.F.C., and Van Haandel A.C. (1992) Activated sludge settling-part I: experimental determination of settling characteristics. Water SA, 18(3), 165-172

Catunda P.F.C., Van Haandel A.C., Araujo L.S and Vilar A. (1989) 'Determination of the settleability of activated sludge'. *Presented At the 15th Congress of the Brazilian Sanitary Engineering Organisation*: Belem

Chambers, B., and Tomlinson, E. (1982) *Bulking of Activated Sludge*, 1st ed. Ellis Horwood for the Water Research Centre: Chichester, UK

Chambers, B. and Tomlinson, E.J. (1981) *Control Strategies for Bulking Sludge*: *Operator's Manual*. Proceedings of the Regional Meeting of the Water Research Centre, Stevenage

Chang, M.C., Chuang, S.H., and Lin, H.L. (1997) 'Effects of calcium ion on sludge conditioning'. *Water Science and Technology* 35, 217-222

Chen, Y.G., Yang, H.Z., and Gu, G.W. (2001) 'Effect of acid and surfactant treatment on activated sludge dewatering and settling'. *Water Res*earch 35, 2615–2620

Chen, G., Yue, P.L., and Mujumdar, A.S. (2007) Dewatering and drying of wastewater treatment sludge'. In A.S. Mujumdar, Ed., *Handbook of Industrial Drying*. Florida: Taylor & Francis

Chen, H., Mujumdar, A.S., and Raghavan, G.S.V. (1996) ‘Laboratory experiments on electroosmotic dewatering of vegetable sludge and mine tailings’. *Drying Technology* 14 (10), 435–445

Chen, C. h., Zhang, P., Zeng, G., Deng, J., Zhou, Y., and Lu, H. (2010) ‘Sewage sludge conditioning with coal fly ash modified by sulphuric acid. *Chem. Eng. Journal* 158, 616-622

Chen, W., Lingyun, J., Panyue, Z., and Guangming, Z. (2012) ‘Effect of potassium ferrate oxidation on sludge disintegration, dewaterability and anaerobic biodegradation’. *International biodeterioration and biodegradation* 1-6

Chen, Y.G., Chen, Y.S., and Gu, G.W. (2004) ‘Influence of pretreating activated sludge with acid and surfactant prior to conventional conditioning on filtration dewatering’. *Chemical Engineering Journal* 99, 137–143

Chen, G.W., Lin, W.W., and Lee, D.J. (1995) ‘Effects of particle sedimentation on capillary suction time CST’. *Journal of the Chinese Institute of Chemical Engineering*, 29, 375-377

Chen, H.H., and Lee, A.H.I. (2014) ‘Comprehensive overview of renewable energy development in Taiwan’. *Renewable Sustainable Energy Reviews* 37, 215–28

Cho, S., Colin, F., Sardin, M., and Prost, C. (1993) ‘Settling velocity model of activated sludge’. *Water Research Journal* 27 (7), 1237-1242

Choong, Y.Y., Norli, I., Abdullah, A.Z., and Yhaya, M.F. (2016) ‘Impacts of trace element supplementation on the performance of anaerobic digestion process: A critical review’. *Bioresource Technology* 209, 369-379

Chong, S., Sen, T.K., Kayaalp, A., and, Ang, H.M. (2012) ‘The performance enhancements of up-flow anaerobic sludge blanket (UASB) reactors for domestic sludge treatment-a state-of-the-art review’. *Water Research*, 46:3434-3470

Christiansen, G. L, and Dick, R.I. (1985) ‘Specific resistance measurements: non parabolic Data’. *Journal of Environmental Engineering* 111, 243-257.

Christensen, G. L. (1983) Units for specific resistance. *Journal of Water Pollution Control Federation*, 417-419

Chu, C.P., and Lee, D.J. (1999) ‘Three stages of consolidation dewatering of sludge’. *Journal of Environmental Engineering* 125, 959-965

Christensen, J.R., Sorensen, P.B., Christensen, G.L. and Hansen, J.A. (1993) Mechanisms for Overdosing in Sludge Conditioning. *Journal of Environmental Engineering*, 119, 158-171

Christy, P.M., Gopinath, L.R., and Divya, D. (2014) 'A review on anaerobic decomposition and enhancement of biogas production through enzymes and microorganisms'. *Renewable and Sustainable Energy Reviews* 34,167–173

Chun, J., Kang, S.O., Hah, Y. and Goodfellow, M. (1996) 'Phylogeny of My- Colic Acid-Containing Actinomycetes'. *Journal of Industrial Microbiology* 17, 205-213

Chynoweth, D.P., Owens, J.M., and Legrand, R. (2001) 'Renewable methane from anaerobic digestion of biomass'. *Renewable Energy* 22, 1–8

Chynoweth, D.P., Owens, J.M., and Legrand, R. (2011) 'Renewable methane from anaerobic digestion of biomass'. *Renewable energy* 22, 1-8

Cirne, D.G., Lehtomaki, A., Bjornsson, L., and Blackall, L. L. (2007) 'Hydrolysis and microbial community analyses in two-stage anaerobic digestion of energy crops'. *J. Appl Microbiol.* 103, 516–527

Clark, T., Burgess, J.E., T. Stephenson, T., and Arnold-Smith, A.K (2000) 'The influence of iron-based co-precipitants on activated sludge biomass'. *Journal of Transactions of the Institution of Chemical Engineers* 78

Colin, F., and Gazbar, S. (1995) 'Distribution of water in sludges in relation to their mechanical dewatering'. *Water Research Journal* 29(8), 2000-2005

Comeau, Y., Hall, K.J. and Oldham, W.K (1985) 'A Biochemical Model for Biological Enhanced Phosphorus Removal'. *Journal of Water research* 20 (12), 1511-1521

Comte, S., Guibaud, G., and Bandu, M. (2007) 'Effect of extraction method on EPS from activated sludge: an HPSEC investigation'. *Journal of Hazardous Materials* 140, 129-137

Conn, E.E., Stumpf, P.K., Bruening, G., Doi R.H. (1987) *Outlines of Biochemistry*. Singapore: John Wiley & Sons Inc.

Coumans, W.J, and Kerkhof, P.J.A.M. (1992). The solid-water bound strength in sewage sludge. *In: AIChE annual meeting, Miami Beach*, Fla, 1073-1078

Cousin, C., and Ganczarczyk, J. J. (1999) ‘The Effect of Cationic Salt Addition on the Settling and Dewatering Properties of an Industrial Activated Sludge’. *Water Environment Research*, 71(2)251-254

Crozes, G., White, P., and Marshall, M. (1995) ‘Enhance coagulation-Its effect on NOM removal and chemical costs’. *Journal of American Water Works Association* 87 (1), 78-89

Cuéllar, A.D., Webber, M.E. (2008) Cow power: the energy and emissions benefits of converting manure to biogas. *Environmental Research Letters* 3, 034002

Culp, R. L., Wesner, G. M., and Culp, G. L. (1978). *Handbook of Advanced Wastewater Treatment.* 2nd ed. Van Nostrand Reinhold Co., NY

Curvers, D., Usher, S.P., Kilcullen, A.R., Scales, P.J., Saveyn, H., and Van der Meeren, P. (2009) ‘The influence of ionic strength and osmotic pressure on the dewatering behaviour of sewage sludge’. *Chem. Eng. Sci.* 64, 2448–2454

D’Abzac, P., Bordas, F., Van Hullebusch, E., Lens, P.N.L., and Guibaud, G. (2010) ‘Extraction of extracellular polymeric substances (EPS) from anaerobic granular sludges: comparison of chemical and physical extraction protocols’. *Applied Microbiology and Biotechnology* 46,197-201

Dahl, C.P., Larsen, T. and Peterson, O. (1994) ‘Numerical Modelling and Measurement in a Test Secondary Settling Tank’. *Journal of Water Science and Technology* 30(2), 219-228

Daigger, G.T. (1995) ‘Development of refined clarifier operating diagrams using an updated settling characteristics database’. *Journal of Water Environment Research* 67 (1), 95-100.

Diagger, G.T., and Roper, R.E. (1985). ‘The relationship between SVI and activated sludge settling characteristics’. *Journal of Water Pollution Control Federation* 57,859 - 866

Das, D., Keinath, T. M., Parker, D., and Wahlberg, E. J. (1993) ‘Floc breakup in activated sludge plants’. *Water Environment Research* 65(2)138-145

Davis L.M., Cornwell, A.D. (1998) Introduction to environmental engineering. 3rd edition New York

De Clercq, B. (2003) ‘*Computational fluid dynamics of settling tanks: development of experiments and rheological, settling, and scraper sub models’*. Unpublished PhD thesis. Ghent: University of Ghent

De Clercq, J. G. U., Nopens, I. G. U., Defrancq, J., and Vanrolleghem, P. (2008). 'Extending and calibrating a mechanistic hindered and compression settling model for activated sludge using in-depth batch experiments'. *Water research Journal* 42(3):781-91

De Clercq, J., Jacobs, F., Kinnear, D.J., Nopens, I., Dierckx, R.A., Defrancq, J., and Vanrolleghem, P.A. (2005) 'Detailed spatio-temporal solids concentration profiling during batch settling of activated sludge using a radiotracer'. *Water Research Journal* 39 (10), 2125-2135

De Haas, D., Wentzel, M., and Ekama, G. (2000a) 'The use of simultaneous chemical precipitation in modified activated sludge systems exhibiting biological excess phosphate removal Part 1: literature review'. *Water SA* 26 (4), 439-452

De Jong, P., Voors, E.H. and Vander Pluijm J.L.P.M. (1993) 'Manual on Chemical Phosphorus Removal'. *STOWA Report No.* 93-06

Demirel, B., and Scherer, P. (2011) Trace element requirements of agricultural biogas digesters during biological conversion of renewable biomass to methane. *Biomass Bioenergy* 35, 992–998

Demirel, B., and Yenigun, O. (2002) 'Two-phase anaerobic digestion processes: a Review. J Chem. Technol.Biotechnol. 77, 743–55

Dentel S.K., and Gosset J.M. (1982) 'Effect of chemical coagulation on anaerobic digestibility of organic materials'. *Journal of water research* 16, 707-718

Devlin, D.C., Esteves, S.R.R., Dinsdale, R.M., and Guwy, A.J. (2011) 'The effect of acid pre-treatment on the anaerobic digestion and dewatering of waste activated sludge, *Bioresource Technology*. 102, 4076–4082

Dhaliwal, B.S. (1979) '*Nocardia Amarae* And Activated Sludge Foaming'. *Journal of the Water Pollution Control Federation* 57, 344-50

Dick, R.I., and Young, K.W. (1972) *'Analysis of thickening performance of final settling tanks: Proceedings of the 27th Industrial Waste Conference'.* Purdue University, Lafayette, Indiana, USA

Dick, R.I and Ewing, B., (1967) 'The Rheology of Activated Sludge'. *Journal of Water Pollution Control Federation* 39(4), 543-560

Dentel, S.K. (2001) 'Conditioning, thickening, and dewatering: research update/research needs'. *Water Science and Technology*, 44, 9-18

Dick, R.I., and Vesilind, P.A. (1969) ‘Sludge volume index-what is it?’. *J. Water Pollut. Control Fed.* 41, 1285–1291

Dieude-Fauvel, E., and Dental, S.K. (2011) ‘Sludge conditioning: impact of polymers on floc structure’. *Journal of Residual Science Technology* 8(3):101-108

Dignac, M.F., Urbain, V., Rybacki, D., Bruchet, A., Snidaro, D., and Scribe, P., (1998) ‘Chemical description of extracellular polymers: implication on activated sludge floc structure’. *Water Science and Technology* 38, 45–53

Dong, X., Plugge, C.M., and Stams, A.J.M. (1994) ‘Anaerobic degradation of propionate by a mesophilic acetogenic bacterium in coculture and triculture with different methanogens’. *Applied Environmental Microbiology* 60, 2834-2838

Duan, J., and Gregory, J. (2003) ‘Coagulation by hydrolysing metal salts’. *Journal Advances in Colloid Interface Science* 100–102, 475–502

Dupont, R., and Dahl, C. (1995) ‘A one-dimensional model for a secondary settling tank including density current and short-circuiting’. *Water Science and Technology* 31 (2), 215-224

Dupont, R., and Henze, M. (1992) ‘Modelling of the secondary clarifier combined with the activated sludge model no. 1.’ Water Science and Technology 25(6), 285–300

Dursun, D., Turkmen, M., Abu-Orf, M., and Dental, S.K., (2006) ‘Enhanced sludge conditioning by enzyme pre-treatment: comparison of laboratory and pilot scale dewatering results’. *Water Science and Technology* 54(5), 33-41

Eastman, J.A., Ferguson, J.F. (1981) ‘Solubilization of particulate organic carbon during the acid phase of AD’. *Journal of the Water Pollution Control Federation* 53, 352-366

Eikelboom, D.E., Andreadakis, A., and Andreasen, K. (1998) ‘Survey of filamentous populations in nutrient removal plants in four European countries’. *Journal of Water Science Technology* 37, 281–289

Eikelboom, D.H. and Van Buijsen, H.J.J. (1981) ‘*Microscopic Sludge Investigation Manual’.* TNO Research Institute for Environmental Hygiene, Delft

Eikelboom, D.H. (2000) ‘Process Control of Activated Sludge Plants by Microscopic Investigation: IWA Publishing’. London *Engineering Journal* 192, 219–225

Ekama, G.A., Barnard, J.L., Gunthert, F.W., Krebs, P., McCorquadale, J.A., Parker, D.S., and Wahlberg, E.J. (1997) "*Secondary Settling Tanks, Theory, Modelling, Design and Operation", International association of water quality, Scientific Report No 6, (IAWQ)*

Ekama, G.A., and Marais, P. (2002) *'Hydrodynamic Modelling of Secondary Settling Tanks, WRC Report No. 835/1/02 Part 1. Water Resources Group, Department of Civil Engineering, University of Cape Town*' South Africa.

Ekama, G.A., Wentzel, M.C. (2008) 'Organic material removal'. B*iology of Wastewater Treatment: Principle, Modelling Design* 53

Ekama, G.A., and Marais, G.V.R. (1986) 'Sludge Settleability and Secondary Settling and Design Procedures'. *Journal of Water Pollution Control* 87, 101-113

Eriksson, L., and Alm, B. (1991) 'Study of flocculation mechanisms by observing effects of a complexing agent on activated sludge properties'. *Water Science and Technology* 24, 21

Emara, M.M., Ahmed, F.A., Abd El-Aziz, F.M., and Abd El –Razek, A.M.A. (2014) 'Biological Nutrient Removal in Bardenpho Process'. *Journal of American Science* 10(5s)

European Commission, (2000) 'Directive 2000/60/EC of the European parliament and of the council of establishing a framework for Community action in the field of water policy'. [Online] availablefrom<http://europa.eu.int/comm/environment/water/water-framework/index_en.html [16 June 2014]

European Commission, (1991) 'Directive 91/271/EEC of 21 May 1991 Concerning Urban Waste Water Treatment. European Community – Environmental Legislation: Water 398–417 Official Journal L135/40' [Online] available from <http:// europa-eu.int/comm/environment/water/water-urbanwaste/directiv.html> [May 2013]

European Commission (EC), (2016) 'Sewage Sludge Directive 86/278/EEC' [Online] available from < http://ec.europa.eu/environment/waste/sludge/index.htm> [22 July 2016]

European Commission (EC), (1986) 'Council Directive 86/278/EEC of 12th June 1986 on the protection of the environment, and in particular of the soil, when sludge sewage is used in agricultural'. *Journal of European Communities* 4(7), 181/6-12.

Everard, P. (2016) 'Minworth Sewage Treatment Works' [Online] Available from < https://www.pickeverard.co.uk/case-study/minworth/> [12 July 2016]

Fang, H.H., and Liu, H. (2002) ‘Effect of pH on hydrogen production from glucose by a mixed culture. *Bioresour. Technol*. 82, 87–93

Farooq, M., Bell, H.A., Almustapha, M.N., and Andresen, M.J. (2017) ‘Bio-methane from anaerobic digestion using activated carbon adsorption’. *Anaerobe Journal* 46, 33-40

Farquhar, G.J. and Boyle, W.C. (1971a) ‘Identification of Filamentous Micro- Organisms in Activated Sludge’. *Journal of the Water Pollution Control Federation* 43,603–620

Fehrenbach, H., Giegrich, J., Reinhardt, G., Schmitz, J., Sayer, U., Gretz, M. (2008) ‘Criteria for a sustainable use of bioenergy on a global scale’. Germany: *Report on behalf of the German Federal Environmental Agency*

Feng, X., Deng, J., Lei, H., Bai, T., Fan, Q., and Li, Z. (2009) ‘Dewatering of waste activated sludge with ultrasonic conditioning’. *Journal of Bio-resource Technology* 100, 1074–1081

Feng, Y., Zhang, Y., Quan, X., and Chen, S. (2014) ‘Enhanced anaerobic digestion of waste activated sludge digestion by the addition of zero valent iron’. *Water Research* 50, 242-250

Fenxia, Y., Liu, X. and Li, Y. (2014) ‘Extracellular polymeric substances and dewaterability of waste activated sludge during anaerobic digestion’. *Water Science and Technology* 70 (9), 1555-1560

Fermoso, F.G., Bartacek, J., Jansen, S., and Lens, P.N.L. (2009) ‘Metal supplementation to UASB bioreactors: from cell-metal interactions to full-scale application’. *Science of Total Environment* 407, 3652-3667

Filipe, C.D.M., Diagger, G.T., and Grady Jr, C.P.L. (2001a) ‘A metabolic model for acetate uptake under anaerobic conditions by glycogen-accumulating organisms: stoichiometry, kinetics and effects of pH. *Biotech.Bioeng*. 76(1), 17-31

Foladori, P., Andreottola, G., and Ziglio, G. (2010) ‘*Sludge Reduction Technologies in Wastewater Treatment Plants*’. IWA Publishing

Forster, C. F., and Christopher F. (2003) *Wastewater treatment and technology*. London Thomas Telford

Forster, C.F. (1982). ‘A further examination of mass flux theory as applied to activated sludge settlement’*.* *Biotechnology letters* 4, 381-386.

Forster, C.F. (1971) Activated Sludge Surfaces In Relation to the Sludge Volume Index. *Journal of Water Research* 5, 861-70

Forster, C.F., (1996) ‘Aspects of the behaviour of filamentous microbes in activated sludge’. *Journal of CIWEM* 10, 290–294

Forster C.F. (1983) ‘Bound water in sewage sludges and its relationship to sludge surfaces and sludge viscosities’. *Journal of Chemical Technology and Biotechnology 33B*, 76

Fowler, D., Coyle, M., Skiba, U., Sutton, M.A., Cape, J.N., Reis, S., Sheppard, L.J., Jenkins, A., Grizzetti, B., Galloway, J.N., Vitousek, P., Leach, A., Bouwman, A.F., Butterbach-Bahl, K., Dentener, F., Stevenson, D., Amann, M., and Voss, M. (2013). ‘The global nitrogen cycle in the twenty-first century’. *Philosophical Transactions Royal Society B* 368 (1621)

Franceschini O. (2010). Dewatering of sludge by freezing. Master thesis. Civil and Mining Engineering, Lulea University of Technology

François, P., Locatelli, F., Laurent, J., and Bekkour, K. (2016) ‘Experimental study of activated sludge batch settling velocity profile’. Flow Measurement and Instrumentation Journal 48, 112–117

Frolund, B., Palmgren, R., Keiding, K., and Nielson, P.H. (1996) ‘Extraction of extracellular polymers from activated sludge using a cation exchange resin’. *Water Research* 30, 1749-1758

Gale, R.S., and Baskerville, R.C. (1967) ‘Capillary suction method for determination of the filtration properties of a solid/liquid suspension’. *Chemistry and Industry Journal* 9, 355-356.

Gale, R.S. (1967) ‘Filtration theory with special references to sewage sludges’. *Water Pollution Control* 66, 622-631

Gallipoli, A., Gianico, A., Gagliano, M.C., and Braguglia, C.M. (2014) ‘Potential of high frequency ultrasounds to improve sludge anaerobic conversion and surfactants removal at different food/inoculum ratio, *Bioresource Technology* 159, 207–214

Gas Technology, Inc. (2003) *HIMET-A two-stage anaerobic digestion process for converting waste to energy*

Ge, H.Q., Batstone, D.J., Keller, J. (2013) ‘Operating aerobic wastewater treatment at very short sludge ages enables treatment and energy recovery through anaerobic sludge digestion’. *Water Research* 47, 6546-6557

Ge, J.; Meng, X.; Song, Y.; Terracciano, A. (2018) 'Effect of phosphate releasing in activated sludge on phosphorus removal from municipal wastewater'. *Environ. Sci. 67*, 216–223

Gerardi, M.H. (2002) *Settleability Problems and Loss of Solids in the Activated Sludge Process*. New Jersey: Wiley & Sons

Gerardi, M.H. (2003) *The Microbiology of Anaerobic Digesters*. New Jersey, 51-57: Wiley-Interscience

Gharibi, H., Sowlat, M.H., Mahvi, A.H., Keshavarz, M., Safari, M.H., and Lotfi, S. (2013) 'Performance evaluation of a bipolar electrolysis/electrocoagulation (EL/EC) reactor to enhance the sludge dewaterability'. *Chemosphere* 90 (4), 1487–1494

Ghawi, A.G., and Kris, J. (2011) 'Improvement Performance of Secondary Clarifiers by a Computational Fluid Dynamics Model'. *Slovak Journal of Civil Engineering* 19 (4), 1 – 11

Ghawi, A.G., and Kris, J. (2012) 'A Computational Fluid Dynamics Model of Flow and Settling in Sedimentation Tanks' *Applied Computational Fluid Dynamics Journal* (2), 19-34

Ghosh, S., and Pohland, F.G. (1974) 'Kinetics of substrate assimilation and product formation in anaerobic digestion'. *Journal of Water Pollution Control Federation* 46 (4), 748-759

Gianico, A., Braguglia, C.M., Mescia, D., and Mininni, G. (2013) 'Ultrasonic and thermal pretreatments to enhance the anaerobic bioconversion of olive husks'. *Bioresource Technology* 147, 623–626

Giokas, D., Diagger G.T., Sperling M.V., Kim Y., and Paraskevas A. (2003) 'Comparison and evaluation of empirical zone settling velocity parameters based on sludge volume index using unified settling characteristics database'. *Journal of Water Research* 37, 3821-3836

Girault, R., Bridoux, G., Nauleau, F., Poullain, C., Buffet, J., Peu, P., et al. (2012) 'Anaerobic co-digestion of waste activated sludge and greasy sludge from flotation process: batch versus CSTR experiments to investigate optimal design'. *Bioresour. Technol.* 105, 1–8

Goel, R., Tokutomi, T., and Yasui, H. (2003) 'Anaerobic digestion of excess activated sludge with ozone pretreatment'. *Water Sci. Technol.* 47, 207–214

Gogate, P.R., and Kabadi, A. M. (2009) 'A review of application of cavitation in biochemical engineering/biotechnology'. *Biochem. Eng.* 44, 60-72

Gonzalez-Gil, G., Lopes, S.I.C., Saikaly, P.E., and Lens, P.N.L. (2012) ‘Leaching and accumulation of trace elements in sulfate reducing granular sludge under concomitant thermophilic and low pH conditions’. *Bioresour. Technol.* 126, 238–246

Gosset J., and McCary P., Wilson J., and Evans D. (1978) ‘Anaerobic digestion of sludge from chemical treatment’. *Journal of the Water Pollution Control Federation* 50, 533-542

Gou, C., Yang, Z., Huang, J., Wang, H., Xu, H., and Wang, L. (2014) ‘Effects of temperature and organic loading rate on the performance and microbial community of anaerobic co-digestion of waste activated sludge and food waste’. *Chemosphere*, 105,146-151

Goula, A. M., Kostoglou, M., Karapantsios, T. D., and Zouboulis, A. I. (2008) ‘The Effect of Influent Temperature Variations in a Sedimentation Tank for Potable Water Treatment: A Computational Fluid Dynamics Study’. *Water Research* 42, 3405 – 3414

Govoreanu, R. G., Saveyn, H., Van der Meeren, P., and Vanrolleghem, P. (2004) ‘Simultaneous determination of activated sludge floc size distribution by different techniques’. *Water science and technology*, 50(12), 16-39

Grady, L, Diagger, G. and Lim. (1999). Biological Wastewater Treatment., 2nd Edition. Marcel Dekker, Inc., New York, NY

Graham, T. M. (1999) *Predicting the performance of belt filter presses using the Crown Press for laboratory simulation, DTIC Document, College of Engineering and Science.* South Carolina: Clemson University

Gray, N.F. (1990) Activated Sludge Theory and Practice. London: Oxford Science Publications

Gray, N.F. (2010) Water *Technology-An Introduction for Environmental Scientists and Engineers*. 3rd edn. London: Elsevier

Gray, N.F. (2004) *Biology of Waste Water Treatment: Series on Environmental Volume 4 Science and Management*. 2nd edn. London: Imperial College Press

Gregory, J. (1997) ‘The density of particle aggregates’. *Water Science Technology Journal* 36 (4), 1-13

Griborio, A. (2004) *Secondary Clarifier Modeling: A Multi-Process Approach*. Unpublished Ph.D. thesis. University of New Orleans

Guan, B., Yu, J., Fu, H., Guo, M., and Xu, X. (2012) 'Improvement of activated sludge dewaterability by mild thermal treatment in $CaCl_2$ solution'. *Water research* 46 (2), 425-432

Gujer, W., and Zehnder, A.J.B. (1983) 'Conversion processes in anaerobic digestion. *Water Sci. Technol*.15, 127–167

Gustavsson, J., Shakeri Yekta, S., Sundberg, C., Karlsson, A., Ejlertsson, J., Skyllberg, U., and Svensson, B.H. (2013a) 'Bioavailability of cobalt and nickel during anaerobic digestion of sulphur-rich stillage for biogas formation'. *Applied Energy* 112, 473-477

Guyonvarch, E., Ramin, E., Kulahci, M., and Plosz, B.G. (2015) 'ICFD: Interpreted Computational Fluid Dynamics—Degeneration of CFD to one-dimensional advection-dispersion models using statistical experimental design—The secondary clarifier'. *Water Res.* 83, 396–411

Haandel, A.C.V. and Lubbe, J.G.M.V. (2012) *Handbook of Biological Wastewater Treatment: Design and Optimisation of Activated Sludge System*. *2nd edn.* London: IWA Publishing.

Haberl, H., Sprinz, D., Bonazountas, M., Cocco, P., Desaubies, Y., Henze, M., (2012) 'Correcting a fundamental error in greenhouse gas accounting related to bioenergy*'. Energy Policy* 45-222, 18-23

Hammer J.M., and Hammer, J.M.JR. (2008) *Water and Waste Water Technology*. 6th edn. New jersey-Ohio: Pearson Hall

Haschemeyer, A.E.V., Guschlbauer, W., and Devries, A.L. (1977) 'Water binding by antifreeze glycoproteins from Antarctic fish'. *Nature* 269, 87-88

Heikal, H.A.M., El Baz, A.R., El-Hafiz, A.A., and Farghaly, S.M. (2017) '*Study the Performance of Circular Clarifier in Existing Potable Water Treatment Plant by Computational Fluid Dynamics*; International Water Resources Association: Paris, France

Hendriks, A.T.W.M., and Zeeman, G. (2009) 'Pre-treatments to enhance the digestibility of lignocellulosic biomass'. *Bio-resource Technology* 100, 10-18

Herwijn, A. J., Heij, E. J. L., IJzermans, J. J., Coumans, W. J. & Kerkhof, P. J. (1995) 'Determination of specific cake resistance with a new capillary suction time apparatus'. *Industrial and Engineering Chemistry Research* 34 (4), 1310-1319

Higgins, M.J., and Novak, J.T. (1997b) 'The effect of cations on the settling and dewatering of activated sludges: laboratory results'. *Water Environment Research* 69, 215-224.

Higgins, M.J., and Novak, J.T. (1997a) ‘Characterization of exocellular protein and its role in bioflocculation’. *Journal of Environmental Engineering* 123, 479-485

Higgins, M.J., and Novak, J.T. (1997c) ‘Dewatering and settling of activated sludges: the case for using cation analysis’. *Water Environment Federation* 69, 225-232.

Higgins M.J. (1995) *The roles and interactions of metal salts, proteins, and polysaccharides in the settling and dewatering of activated sludge.* Unpublished Ph.D. thesis. Blacksburg, Virginia: Virginia Polytechnic Institute and State University

Higgins, M.J., Tom, L.A., and Sobeck, D.C. (2004a) ‘Case Study I: Application of the Divalent Cation Bridging Theory to improve biofloc properties and industrial activated sludge system performance: Direct addition of divalent cations’. *Water Environment Research* 76,344-352

Higgins, M.J. and Sobeck, D.C. (2002) ‘Examination of Three Theories for Mechanisms of Cation-Induced Bioflocculation’. *Water Research* 36, 527

Higgins, M.J., Sobeck, D.C., Owens, S.J., and Szabo, L.M. (2004b) ‘Case Study II: Application of the Divalent Cation Bridging Theory to improve biofloc properties and industrial activated sludge system performance: Using alternatives to sodium based chemicals’. *Water Environment Research* 76, 353-359

Higgins, M.J., Chen, Y., and Murthy, S.N. (2006) *Understanding factors affecting polymer demand for conditioning and dewatering*. IWA Publishing, ISBN: 1-84339-726-9.

Hiemenz, P., and Rajagopalan, R. (1997) *Principles of colloid and surface chemistry*. Marcel Dekker, New York, USA.

Hii, K., Baroutian, S., Parthasarathy, R., Gapes, D.J., Eshtiaghi, N. (2014) ‘A review of wet air oxidation and thermal hydrolysis technologies in sludge treatment’. *Bio-resource Technology* 155, 289–99

Hirota, M., Okada, H., Misaka, Y., and Kato, K. (1975) ‘Dewatering of organic sludge by pulverized coal’. *Water Pollution Control Federation* 47(12), 2774-2782

Hou, C.H., and Li, K.C. (2003) ‘Assessment of sludge dewatering using rheological properties’. *Journal of Chinese Institute of Engineers* 26(2), 221-226

Houghton, J. I. and Stephenson, T. (2002) ‘Effect of Influent Organic Content on Digested Sludge Extracellular Polymer Content and Dewaterability’. *Water Research* 36 (14), 3620-3628

Houghton, J., Quarmby, J., and Stephenson, T. (2001) ‘Municipal wastewater sludge dewatering and the presence of microbial extracellular polymer’. *Water Science and Technology* 44(2), 373-379

Hsu, Y.H. and Lee, D.J. (1995) ‘Measurement of bound water in sludges: a comparative study’. *Water Environ Res* 67(3), 310-317

Huan, L., Yiying, J., Mahar, R.B., Zhiyu, W., and Yongfeng, N. (2009) ‘Effects of ultrasonic disintegration on sludge microbial activity and dewaterability’. *Journal Hazard Materials* 161, 1421-1426

Huang, H.N., Zheng, X., Chen, Y.G., Liu, H., Wan, R., and Su, Y.L. (2017) ‘Alkaline fermentation of waste sludge causes a significant reduction of antibiotic resistance genes in anaerobic reactors’. *Science Total Environment* 580, 380-387.

Huggins, D.L., Piedrahita, R.H., and Rumsey T. (2005) ‘Use of computational fluid dynamics (CFD) for aquaculture raceway design to increase settling effectiveness’. *Aqua-cultural Engineering* 33, 167–180

Hvitved-Jacobsen, T. (2002) ‘Sewer systems and processes’. *In Sewer Processes: Microbial and Chemical Process Engineering of Sewer Networks*. 2ed. CRC Press

Hwang, K.Y., Shin, E.B., and Choi, H.B. (1997) ‘A mechanical pre-treatment of waste activated sludge for improvement of anaerobic digestion system’. *Water Science Technology* 36, 111–116

Jameel, P. (1989) ‘The use of ferrous chloride to control dissolved sulphides in interceptor sewers’. *Journal of Water Pollution Control Federation* 61 (2), 230-236

Jang, H.M., Cho, H.W., Park, S.K., Ha, J.H., and Park, J.M. (2014) ‘Influence of thermophilic aerobic digestion as a sludge pre-treatment and solids retention time of mesophilic anaerobic digestion on the methane production, sludge digestion and microbial communities in a sequential digestion process, *Water Res.* 48, 1–14

Jarrell, K.F., and Kalmokoff, M.L. (1988) ‘Nutritional Requirements of the Methanogenic Archaebacteria’. *Canadian Journal of Microbiology NRC Research Press*, 557–576

Jenkins, D., Richard, M.D., and Daigger, G.T. (1993) *Manual on the Causes and control of Activated Sludge Bulking and Foaming*. New York Lewis Publishers.

Jenkins, D., Richard, M. G., and Daigger, G. T. (2003) *Manual on the Causes and Control of Activated Sludge Bulking and Foaming and Other Solids Separation Problems*. 3rd ed. London: IWA Publishing

Jenkins, D., Richards, M.G. and Daigger, G.T. (1984) *Manual on the Causes and Control of Activated Sludge Bulking and Foaming*. Water Research Commission, Pretoria, South Africa

Jeyanayagam, S. (2006) 'Design and operation of final clarifiers'. *Florida water resources journal*, (35) available from < http://www.fwrj.com/techarticle06/0106%20tech2.pdf> [June 5 2014]

Jeyanayagam, S. (n.d.) Design and operations of final clarifiers [online] available from < http://www.fwrj.com/techarticle06/0106%20tech2.pdf > [20 May 2016]

Jeyanayagam, S. (2005) '*True Confessions of the Biological Nutrient Removal Process.' Florida Water Resources Journal* [online] available from < http://www.fwrj.com/TechArticle05/0105%20tech2.pdf > [20 June 2011]

Jiang, X., Sommer, S.G., and Christensen, K.V. (2011) A review of the biogas industry in China. *Energy Policy* 39, 6073-6081

Ji, J., Zhang, J., Yang, L., He, Y. Zhang, R., Liu, G., and Chen, C. (2017) 'Impact of co-pretreatment of calcium hydroxide and steam explosion on anaerobic digestion efficiency with corn stover'. *Environmental Technology* 38 (12), 1465-1473

Jin, B., Wilen, B., and Lant, P. (2003) 'A comprehensive insight into floc characteristics and their impact on compressibility and settleability of activated sludge'. *Chemical Engineering Journal*, 95(1-3), 221-234

Jin, B., Wilén, B.-M., and Lant, P. (2004) 'Impacts of morphological, physical and chemical properties of sludge flocs on dewaterability of activated sludge'. *Chemical Engineering Journal* 98(1), 115-126

Johnson, D. K., Carliell-Marquet, C. M., and Forster, C. F. (2003) 'An examination of the treatment of iron-dosed waste activated sludge by anaerobic digestion'. *Journal of Environmental Technology* 24(8), 937-945

Jorand, F., Zartarian, F., Thomas, F., Block, J., Bottero, J., Villemin, G., Urbain, V., and Manem, J. (1995) 'Chemical and structural (2d) linkage between bacteria within activated sludge flocs'. *Water Research Journal* 29 (7), 1639-1647

Jung, K.W., Hwang, M.J., Ahn, K.H., and Ok, Y.S. (2015) 'Kinetic study on phosphate removal from aqueous solution by biochar derived from peanut shell as renewable adsorptive media. *Int. J. Environ. Sci. Technol*. 12, 3363–3372.

Junoh, H., Yip, C.H., and Kumaran, P. (2016) 'Effect on $Ca(OH)_2$ pretreatment to enhance biogas production of organic food waste'. *Journal of Earth Environ. Sci.* 32.

Kadlec, R.H., and Wallace, S. (2008) *'Treatment wetlands'.* Boca Raton, Florida: CRC Press

Kakii, K., Kitamura, S., and Shirakashi, T. (1985) 'Effect of Calcium Ion on Sludge Characteristics'. *Journal of Fermentation Technology* 63, 263

Kalyuzhnyi, S., Veeken, A., and Hamelers, B. (2000) 'Two-particle model of anaerobic solid- state fermentation'. *Water Sci.Technol.* 41, 43–50

Kappeler, J., and Gujer W. (1994) 'Verification and applications of a mathematical model for aerobic bulking'. *Water Resource Journal* 28(2), 311–322

Kara, F., Gurakan, G.C., and Sanin, F.D. (2008) 'Monovalent cations and their influence on activated sludge floc chemistry, structure, and physical characteristics'. *Journal of Biotechnology and Bioengineering* 100 (2), 231-239

Kartashevsky, M., Semiat, R., and Dosoretz, C.G. (2015) 'Phosphate adsorption on granular ferric hydroxide to increase product water recovery in reverse osmosis-desalination of secondary effluents'. *Desalination* 364, 53–61

Kaseng, K., Ibrahim, K., Paneerselvam, S. V. and Hassan, R. S. (1992) 'Extracellular enzyme and acidogen profiles of a laboratory-scale two-phase anaerobic digestion system'. *Process Biochemistry* 27, 43-47

Katsiris, N., and Kouzeli-Katsiri, A. (1987) 'Bound water content of biological sludges in relation to filtration and dewatering'. *Water Res* 21, 1319-1327

Kayser, R. (2005). 'Activated Sludge Process'. *In: Environmental Biotechnology*: *Concept and Applications*, 79-119.

Keiding, K., Wybrandt, L., and Nielson, P.H., (2001) 'Remember the water: comment on EPS colligative properties'. *Water Science Technology Journal* 43, 17-23

Keiding, K., and Nielsen, P.H. (1997) 'Desorption of organic macromolecules from activated sludge: effect of ionic composition'. *Water Research* 31, 1665-1672

Kelley, P.T., and He, Z. (2014) ‘Nitrogen removal and recovery in biochemical systems: A review’. *Bio resource Technology* 153, 351-360

Kempa, E.S., and Fukas-Plonka, L. (1982) ‘Determination of the specific resistance: A critical review. *Flemish Chapter of the Filtration Society*, London

Khanal, S.K., Isik, H., Sung, S., and van Leeuwen, J. (2006). Ultrasonic conditioning of waste activated sludge for enhanced aerobic digestion. *In: Proceeding of IWA specialized conference-sustainable sludge management: state of the art, challenges and perspectives* Moscow, Russia

Kida, K., Shigematsu, T., Kijima, J., Numaguchi, M., Mochinaga, Y., Abe, N., et al. (2001) ‘Influence of Ni^{2+} and Co^{2+} on methanogenic activity and the amounts of coenzymes involved in methanogenesis’. *J. Biosci. Bioeng.* 91, 590–595

Kim, J., Park, C., Kim, T.H., Lee, M., Kim, S., Kim, S.W., and Lee, J. (2003) ‘Effects of various pretreatments for enhanced anaerobic digestion with waste activated sludge’. *Journal of Bioscience and Bioengineering* 95, 271–275

Kim, J.K., Oh, B.R., Chun, Y.N., and Kim, S.W. (2006) ‘Effects of temperature and hydraulic retention time on anaerobic digestion of food waste’. *Bioscience and Bio-engineering* 102, 328-332

Kim, D.S., Jung, N.S., and Park, Y.S. (2008) ‘Characteristics of nitrogen and phosphorus removal in SBR and SBBR with different ammonium loading rates’. *Korean Journal of Chemical Engineering* 25, 793-800

Kindzierski, W., and Hrudey, S. (1986) ‘Effects of phosphorus removal chemicals upon methane production during anaerobic sludge digestion’. *Canadian Journal of Civil Engineering* 13, 33-38

Kinnear, D. (2002) *Biological solids sedimentation: a model incorporating fundamental settling parameters*. Unpublished Ph.D. thesis. USA: Department of Civil and Environmental Engineering, University of Utah

Knowles, R. (1982) ‘Denitrification’. *Microbiology Reviews* 46, 43-70

Kolda, B.C. (1995) *Impact of polymer type, dosage, and mixing regime and sludge type on sludge floc properties*. Unpublished Masters Thesis. Blacksburg, Virginia: Virginia Polytechnic Institute and State University

Kondusamy, D., and Kalamdhad, A.S. (2014) ‘Pre-treatment and anaerobic digestion of food waste for high rate methane production – A review’. *Journal of Environmental Chemical Engineering* 2, 1821-1830

Koopman B and Cadee K. (1983) ‘Prediction of thickening capacity using diluted sludge volume index’. *Journal of Water research* 17 (10), 1427-1431

Kougias, P.G., Boe, K., Angelidaki, I. (2013) ‘Effect of organic loading rate and feedstock composition on foaming in manure-based biogas reactors. *Bio-resources and Technology* 144, 1-7

Komisar, S.J., Weinert, C.G., Hickey, R.F., Veltman, S., and Switzenbaum, M.S. (1998) ‘Complete on-site treatment of aircraft deicing wastewater using sequencing anaerobic fluidized bed-slow sand filter system’. *Process Water Environment Federation 71st Annual Technical Conference USA.*

Krebs, P., Vischer, D., and Gujer, W. (1995) ‘Inlet-structure design for final clarifiers’. *Journal of environmental engineering* 121(8), 558-564

Krebs, P. (1995) ‘Success and shortcomings of clarifier modelling’. *Water Science and Technology* 31 (2), 181-191

Krebs, P., Armbruster, M., and Rodi, W. (1998) ‘Laboratory experiments of buoyancy influenced flow in clarifiers Laboratory experiments of buoyancy-influenced flow in clarifiers’. *Journal of Hydraulic Research* 36 (5), 831-851

Krebs, P. (1991) ‘The hydraulics of final settling tanks’. *Water Science and Technology* 23, (1966), 1037-1046

Kroiss, H., Rechberger H., and Egle, L. (2011). ‘Phosphorus in Water Quality and Waste Management, Integrated Waste Management: Volume II’. Available from<https://www.intechopen.com/books/integrated-waste-management-volume-ii/phosphorus-in-water-quality-and-waste-management > [10 May 2014]

Kwietniewska, E., and Tys, J. (2014) ‘Process characteristics, inhibition factors and methane yields of anaerobic digestion process, with particular focus on micro-algal biomass fermentation’. *Renewable Sustainable Energy Reviews* 34, 491-500

Kynch, G.J. (1952) ‘A theory of sedimentation’. *Transactions of the Faraday Society* 48 (1952), 166-176

Kumar, S., Das, A., Srinivas, G.L.K., Dhar, H., Ojha, V.K., and Wong, J. (2016) ‘Effect of calcium chloride on abating inhibition due to volatile fatty acids during the start-up period in anaerobic digestion of municipal solid waste’. *Environmental Technology* 37(12), 1501-1509

Labatut, R.A., Angenent, L.T., and Scott, N.R. (2011) ‘Biochemical methane potential and biodegradability of complex organic substrates’. *Bioresource Technology* 102, 2255-2264

Lakehal, D., Krebs, P., Krijgsman, J., and Rodi, W. (1999) ‘Computing shear flow and sludge blanket in secondary clarifiers’. *Journal of Hydraulic Engineering* 125 (3), 253-262

Lakehal, D. (2002) ‘On the modelling of multiphase turbulent flows for environmental and hydrodynamic applications’. *International Journal of Multiphase Flow* 28(5), 823-863

Lai, T.E., Nopharatana, A., Pullammanappallil, P.C., and Clarke, W.P. (2001) ‘Cellulolytic activity in leachate during leach-bed anaerobic digestion of municipal solid waste’. *Bioresour. Technol.* 80, 205–210

Langenhoff, A.A.M., Brouwers-Ceiler, D.L., Engelberting, J.H.L., Quist, J.J., Wolkenfelt, J.G.P.N., Zehnder, A.J.B., et al. (1997) ‘Microbial reduction of manganese coupled to toluene oxidation’. *Federation of European Microbiological Societies (FEMS) Microbiology Ecology* 22, 119–127

Larsen, P. (1977) ‘On the hydraulics of rectangular settling basins’. *Report No. 1001. Technical report, Department of Water Resources Engineering*. Lund, Sweden: Lund Institute of Technology

Lar, S.J., Li, R. and Li, X. (2010) ‘The Influence of Calcium and Iron Supplementation on the Methane Yield of Biogas Treating Dairy Manure’, *Energy Sources, Part A: Recovery, Utilization, and Environmental Effects*, 32(17), 1651-1658

Laspidou, C.S., and Rittmann, B.E. (2002) ‘A unified theory for extracellular polymeric substances, soluble microbial products, and active and inert biomass’. *Water Resources* 36 (11), 2711-2720

Lau, A. O., Strom, P. F., and Jenkins, D. (1984) ‘The competitive growth of floc-forming and filamentous bacteria: a model for activated sludge bulking’. *Journal Water Pollution Control Fed*eration 56

Lechevalier, H. A. (1975) *Actinomycetes of Sewage Treatment Plants*. EPA-600/2-75-031. U.S. EPA, Cincinnati, OH.

Le-Clech, P., Chen, V., and Fane, T.A.G. (2006) ‘Fouling in membrane bioreactors used in wastewater treatment’. *Journal of Membrane Science* 284, 17-53

Ledezma, P., Kuntke, P., Buisman, C.J.N., Keller, J., and Freguia, S. (2015) 'Source-separated urine opens golden opportunities for microbial electrochemical technologies'. *Trends Biotechnology* 33, 214-220

Lee, C.H., and Liu, J.C. (2000) 'Enhanced sludge dewatering by dual polyelectrolytes conditioning'. *Water Res.* 34(18), 4430–4436

Lee, D. and Hsu, Y. (1994) 'Use of capillary suction apparatus for estimating the averaged specific resistance of filtration cake'. *Journal of Chemical Technology and Biotechnology* 59 (1), 45-51

Lee, D.J., and Hsu, Y.H. (1995) 'Measurement of bound water in sludges: a comparative study'. *Water Environ Res* 67(3), 310-317.

Lee, D.J., and Lee, S.F. (1995) 'Measurement of bound water content in sludge: use of differential scanning calorimetry (DSC)'. *J Chem Tech Biotechnol* 62, 359-3565

Lee, D.J. (1994a) 'Measurement of bound water in waste activated sludge: use of the centrifugal settling method'. *J. Chem. Tech. Biotechnol.* 63,139-144

Lee, D.J. (1994b) 'A dynamic model of capillary suction apparatus'. *Journal of Chemical Engineering Japan* 27, 216-221.

Lee D.J., and Hsu, Y.H. (1992) 'Fluid flow in capillary suction apparatus'. *Industrial and Engineering Chemistry Research,* 31, 2379-2385.

Lee, D.Y., Lin, Y.F., Jing, Z., and Xu, J. (2001) 'Effects of agricultural waste on the sludge conditioning'. *Journal of China Inst. Environ. Eng.*11, 209-214

Lee, H.B., Jhon, M.S., and Anderson, J.D. (1975) 'Nature of water in synthetic hydrogels'. *J Colloid Interface Sci.* 51, 225

Lee, M., Hidaka, T., Hagiwara, W., and Tsuno, H. (2009) 'Comparative performance and microbial diversity of hyper thermophilic and thermophilic co-digestion of kitchen garbage and excess sludge'. *Bioresour. Technol*. 100, 578–585

Lee, T. T., Wang, F.Y., and Newell, R. B. (1999) 'Distributed parameter approach to the dynamics of complex biological processes'. *American Institute of Chemical Engineers* Journal 45, (10) 2245-2268

Lees, E.J., Noble, B., Hewitt, R., and Parsons, S.A. (2001) 'The impact of residual coagulant on downstream treatment processes'. *Environmental Technology* 22, 113-122

Lefebvre, E., and Legube, B. (1990) ‘Coagulation par Fe (III) de substances humiques extremites deaux de surface: effect in pH de la concentration en substances humiques’. *Water Research* 24, 591-606

Letterman, R.D., A. Amirtharajah and C. R. O’ Melia. (1999). Coagulation and Flocculation. *In Water Quality and Treatment, Handbook for Community Water Supplies*. Chapter 6. 5th ed. New York, NY: McGraw-Hill Inc

Lettinga G. (2014) *My anaerobic sustainability story,1st ed*: Amsterdam: LeAf

Leu, W. (1981) Cake filtration. PhD. Dissertation, University of Houston, Houston

Leven, L., Wijnbladh, E., Tuvesson, M., Kragelund CHalin, S. (2016) ‘Control of Microthrix Parvicella and Sludge Bulking by Zone in a Full-Scale WWTP’. *Water Sci. Technol. 73*, 866–872

Lewicki, P.P., Busk, G.C., and Labuza, T.P. (1978) ‘Measurement of gel-water binding capacity of gelatin, potato starch and carrageenan gels by suction pressure’. *J. Colloid Interface Sci.* 64, 501-509.

Li, B., Stenstrom, M.K. (2014a) ‘Dynamic one-dimensional modelling of secondary settling tanks and design impacts of sizing decisions’. *Water Research Journal* 50, 160-170

Li, B., and Stenstrom, M.K. (2014b) ‘Research advances and challenges in one-dimensional modelling of secondary settling Tanks: A critical review’. *Water Research Journal* 65, 40-63

Li, C.W., Lin, J.L., Kang, S.F., and Liang, C.L. (2005) ‘Acidification and alkalization of textile chemical sludge: volume/solid reduction, dewaterability, and Al (III) recovery’. *Separation and Purification Technology* 42, 31–37

Li, D., and Ganczarczyk, J. (1990) ‘Structure of activated sludge flocs’. *Biotechnology and Bioengineering* 35, 57-65

Li, D. H., and Ganczarczyk, J. J. (1991) ‘Size distribution of activated sludge flocs’. *Research Journal of the water pollution control federation* 63(5), 806-814

Li, G., Gao, S., Zhang, G., and Zhang, X. (2014a) ‘Enhanced absorption of phosphate from aqueous solution by manufactured iron (III) –copper (II) binary oxides’. *Chemical Engineering* 235, 124-131

Li, H.S., Wen, Y., Cao, A.S., Huang, J.S., Zhou, Q., and Somasundaran, P. (2012) ‘The influence of additives ($\mathrm{Ca^{2+}}$,$\mathrm{Al^{3+}}$ and $\mathrm{Fe^{3+}}$) on the interaction energy and loosely bound extracellular polymeric substances (EPS) of activated sludge and their flocculation mechanisms.' *Journal of Bio-resource Technology* 114, 188-194.

Li, T., Wang, H., Dong, W., Lui, T., Ouyang, F., Zhang, Q. (2014b) 'Phosphate removal during Fe (II) oxidation in the presence of Cu (II): characteristics and application for electro-plating wastewater treatment'. *Sep. Purif. Technol.* 132, 388-395.

Li, X.Y., and Yang, S.F. (2007) 'Influence of loosely bound extracellular polymeric substances (EPS) on the flocculation, sedimentation and dewaterability of activated sludge'. *Water Research* 41 (5), 1022-1030

Li, Y., He, X., Hu, H., Zhang, T., Qu, J., and Zhang, Q. (2018) 'Enhanced phosphate removal from wastewater by using in situ generated fresh trivalent Fe composition through the interaction of Fe (II) on $CaCO_3$'. *Environmental Management* 221, 38-44

Liang, P., Huang, X., Qian, Y., Wei, Y.S., Ding, G.J. (2006) 'Determination and comparison of sludge reduction rates caused by microfaunas' predation'. *Bio-resource Technology 97, 854-861*

Liang, J., Huang, S., Dai, Y., Li, L., and Sun, S. (2015) 'Dewaterability of five sewage sludges in Guangzhou conditioned with Fenton's reagent/lime and pilot -scale experiments using ultrahigh pressure filtration system'. *Water research* 84, 243-254

Liao, B., Allen, D., Droppo, I., Leppard, G., and Liss, S. (2000) 'Bound water content of activated sludge and its relationship to solids retention time, floc structure and surface properties'. *Water Environment Research* 72 (6), 722-730

Liao, B.Q., Allen, D.G., Leppard, G.G., Droppo, I.G., and Liss, S.N. (2002) 'Interparticle interactions affecting the stability of sludge flocs'. *Colloid Interface Science* 249, 372-380

Liao, B.Q, Allen, D.G., Droppo, I.G., Leppard, G.G., and Liss, S.N. (2001) 'Surface properties of sludge and their role in bioflocculation and settleability'. *Water Research* 35, 339-350

Liao, B.Q., Droppo, I.G., Leppard, G.G., and Liss, S.N. (2006) 'Effect of solids retention time on structure and characteristics of sludge flocs in sequencing batch reactors'. *Water Res. 40*, 2583–2591

Liss, S., Droppo, I., Flannigan, D., and Leppard, G. (1996) 'Floc architecture in wastewater and natural riverine systems'. *Environment Science Technology* 30, 680-686

Liu, X.M., Sheng, G.P., and Yu, H.Q. (2007) ‘DLVO approach to the flocculability of a photosynthetic H2-producing bacterium, Rhodopseudomonas acidophila’. *Environmental Science and Technology* 41, 4620-4625

Liu, Y., and Sun D. (2011) ‘Calcium augmentation for enhanced denitrifying granulation in sequencing batch reactors’. *Journal of Process Biochemistry* 46 987-992

Liu, X.M., Sheng, G.P., Yu, H.Q., Luo, H.W., Zhang, F., and Yuan, S.J. (2010) ‘Contribution of extracellular polymeric substances (EPS) to the sludge aggregation’. *Environmental Science and Technology* 44, 4355-4360

Liu, L., Yan, H., Tan, W., and Zhu, G. (2017) ‘Influence of $\mathrm{Na}^{+}, \mathrm{K}^{+}, \mathrm{Mg}^{2+}, \mathrm{Ca}^{2+}$ and Fe^{3+} on filterability and Settleability of drilling sludge.’ Chinese *Journal of Chemical Engineering* 25, 658-664

Liu, C.F. (2008) ‘Prediction of methane yield at optimum pH for anaerobic digestion of organic fraction of municipal solid waste’. *Bioresour. Technol.* 99, 882–888

Liu, Y., Zhang, Y., Quan, X., Li, Y., Zhao, Z., Meng, X., and Chen, S., (2012) ‘Optimization of anaerobic acidogenesis by adding Fe^{o} powder to enhance anaerobic wastewater treatment’. *Chemical Engineering Journal* 192, 179-185

Lo, I.M.C., Lai, K.C.K., and Chen, G.H. (2001) ‘Salinity effect on mechanical dewatering of sludge with and without chemical conditioning’. *Environmental Science and Technology* 35, 4691–4696.

Lo, H.M., Chiang, C.F., Tsao, H.C., Pai, T.Y., Liu, M.H., and Kurniawan, T.A. (2012) ‘Effects of spiked metals on the MSW anaerobic digestion. *Waste Management Research* 30,32–48

Lotito, V., Spinosa, L., Mininni, G., and Antonacci, R. (1997) ‘The rheology of sewage sludge at different steps of treatment’. *Water Science and Technology* 36 (11), 79–85

Lu, C., and Spielman, L. (1985) ‘Kinetics of floc breakage and aggregation in agitated liquid suspensions. *Journal of Colloid and Interface Science* 103(1), 95-105

Lu, M.-C., Lin, C.-J., Liao, C.-H., Huang, R.-Y., and Ting, W.-P. (2003) ‘Dewatering of activated sludge by Fenton’s reagent’. Advances in Environmental Research 7 (3), 667–670

Luedecke, D., Hermanowiz, S.W. and Jenkins, D. (1989) ‘Precipitation of ferric phosphate in activated sludge: a chemical model and it verification’. *Journal of Water science technology* 21, 325-337

Lyberatos, G., and Skiadas, I.V. (1999) 'Modelling of anaerobic digestion - a review'. Global Nest International Journal 1, 63-76

Lyn, D.A., Stamou, A.I., and Rodi, W. (1992) 'Density currents and shear induced flocculation in sedimentation tanks'. *Hydraulic Engineering* 118 (6), 849-867

Luo, D., Yuan, L., Liu, L., Wang, Y., and Fan, W. (2017) 'The Mechanism of biological phosphorus removal under Anoxic-aeration alternation condition with starch as sole carbon source and its biochemical pathway'. *Biochemical Journal* 132

Luo,G., Liang,W., Tan,H., Yao,C., Zhang,N., Lu, L. (2013) 'Effects of calcium and magnesium addition on the start-up of sequencing batch reactor using bio-floc technology treating solid aquaculture waste'. *Journal of Aqua-cultural Engineering* 57 32- 37

Luostarinen, S., Luste, S., and Sillanpää, M. (2009) 'Increased biogas production at wastewater treatment plants through co-digestion of sewage sludge with grease trap sludge from a meat processing plant' *Bioresource Technology* 100, 79–85

Mancell-Egala, W.A.S.K., Kinnear, D.J., Jones, K.L., Clippeleir, H.D., Takacs, I., and Murthy, S.N. (2016) 'Limit of stokesian settling concentration characterizes sludge settling velocity'. *Water Res.* 90, 100–110

Mahdavi Mazdeh, F. (2014) *Investigating flocculation and discrete settling behaviour of activated sludge by means of particle size analysis*. Unpublished PhD thesis. Ghent, Belgium: Ghent University

Mahmoud, N., Zeeman, G., Gijzen, H., and Lettinga, G. (2003) 'Solids removal in upflow anaerobic reactors, a review'. *Bioresour. Technol.* 90, 1–9.

Mao, C., Feng, Y., Wang, X., and Ren, G. (2015) 'Review on research achievements of biogas from anaerobic digestion'. Renewable and Sustainable *Energy Reviews* 45, 540–555

Martel, C.J. (1993) 'Fundamentals of sludge dewatering in freezing beds'. *Water Science Technology* 28(1), 29-35

Martins, R.C., Lopes, D.V., Quina, M.J., and Quinta-Ferreira, R.M. (2012) 'Treatment improvement of urban landfill leachates by Fenton-like process using ZVI'. *Chemical Engineering Journal* 192, 219–225

Martins, A.M.P., Karahan, O., and Van Loosdrecht, M.C.M. (2011) 'Effect of polymeric substrate on sludge settleability'. *Journal of Water Research* 45 (1), 263-273

Martins, A.M.P., Pagilla, K.R., Heijnen, J.J., and van Loosdrecht, M.C.M. (2004) ‘Bulking filamentous sludge: A Critical Review.’ *Journal of Water Research* 38 (4), 793–817

Mata-Alvarez, J., Mace, S., and Llabres, P. (2000) ‘Anaerobic digestion of organic solid wastes: an overview of research achievements and perspectives’. *Bioresource Technol* 74, 3–16

Mata-Alvarez, L. (2003) *Biomethanization of Organic Fraction of Municipal Solid Waste, ISBN: 1-900222-14-0.* London: IWA Publishing

Mata-Alvarez, J., Dosta, J., Romero-Güiza, M.S., Fonoll, X., Peces, M., Astals, S.A. (2014) ‘Critical review on anaerobic co-digestion achievements between 2010 and 2013’. *Renewable and Sustainability Energy Review* 36, 412–27

Matko, T., Fawcett, N., Sharp, A., and Stephenson, T. (1996) ‘Recent Progress In The Numerical Modelling Of Wastewater Sedimentation Tanks’. *Transactions of the institution of chemical engineers* 74, 197-204

Marinetti, M., Malpei, F. and Bonomo, L. (2009) ‘Relevance of expression phase in dewatering of sludge with chamber filter presses’. *Journal of Environmental Engineering* 135(12), 1380-1387

Mazzolani, G., Pirozzi, F., and d’Antonoi, G. (1998) ‘A generalized settling approach in the numerical modelling of sedimentation tanks’. *Water Science and Technology* 38 (3), 95-102

MCR-Process &Technology (2008) Stiro-Settlometer [online] available from < http://www.mcrpt.com/english/pdf/manuel_stiro.pdf > [10 February 2014)

McCorquodale, J. A., La Motta, E. J., Griborio, A., Homes, I., and Georgiou, D. (2004) ‘*Development of software for modelling activated sludge clarifier systems. Technical report, Department of civil and environmental engineering’.* University of New Orleans, New Orleans

Merchant, S.S., and Helmann, J.D. (2012). Chapter 2- Elemental Economy: Microbial Strategies for Optimizing Growth in the Face of Nutrient Limitation. In: Robert, K.P. (Ed.), *Advances in Microbial Physiology*. Academic Press, 91–210

Metcalf and Eddy, Inc. (2014) *Wastewater Engineering: Treatment and Reuse. 4th edn.* New York: McGraw-Hill

Metcalf and Eddy, Inc. (2004) *Wastewater Engineering: Treatment and Reuse*. 4th edn. New York: McGraw-Hill.

Metcalf and Eddy, (2003) *Wastewater engineering treatment and reuse*. McGraw-Hill

Metcalf & Eddy, Inc. (1991) *Wastewater Engineering Treatment, Disposal and Reuse*. 3rd edn; Tchobanoglous, G., Burton, F. L., Eds.; McGraw-Hill: New York

Mikkelsen, L. H. (2001) 'The shear sensitivity of activated sludge: relations to filterability,rheology and surface chemistry'. *Journal of Colloid and Interface Science* 182, 1-14

Mikkelsen, L. H., Gotfredsen, A., Agerbak, M., Nielsen, P., and Keiding, K. (1996) 'Effects of colloidal stability on clarification and dewatering of activated sludge'. *Water Science and Technology* 34(3-4), 449-457

Mikkelsen, L. H. and Nielsen, P. H. (2001) 'Quantification of the bond energy of bacteria attached to activated sludge floc surfaces'. *Water science and technology*, 43(6), 67-75

Mikkelsen, L., and Keiding, K. (2002) 'Physico-chemical characteristics of full scale sewage sludges with implication to dewatering'. *Water Research* 36 (10), 2451-2462

Mikkelsen, L.H. (2003) 'Applications and limitations of the colloid titration method for measuring activated sludge surface charges'. *Water Research* 37, 2458-2466

Minitab Inc. (2016) Minitab 17: Getting Started with Minitab 17. [Online] Available from < http://www.dec.ny.gov/docs/water_pdf/drrichard1.pdf> [20 May 2016]

Montalvo, S., Guerrero, L., Borja, R., Sánchez, E., Milán, Z., CortésI, I. (2012) 'Application of natural zeolites in anaerobic digestion processes: a review'. *Applied Clay Science* 58,125–133

Moreno-Andrade, I., and Buitron, G. (2004) 'Influence of the origin of the inoculum on the anaerobic biodegradability test'. *Water Science and Technology* 49 (1), 53–59

Morgan, J.W., Forster, C.F., and Evison, L. (1990) 'A comparative study of the nature of biopolymers extracted from anaerobic and activated sludges'. *Water Research* 24, 743-753

Mosey, F.E., and Fernandes, X.A. (1989) 'Patterns of hydrogen in biogas from the anaerobic digestion of milk sugars'. *Water Sci.Technol.* 21, 187–196

Mowla, D., Tran, H.N., and Allen, G.D. (2013) 'A Review of the properties of biosludge and its relevance to enhanced dewatering processes'. *Biomass and Bioenergy* 58, 365-378.

Mowla D. (1996) Simulation of fluidized bed driers. In: *Proceeding of CHISA96 conference* Prague, Czech Republic

Muller, C.D. (2001) *High-Intensity Shear as a Wet Sludge Disintegration Technology and a Mechanism for Floc Structure Analysis*. Unpublished Masters Thesis. Blacksburg, Virginia: Virginia Polytechnic Institute and State University

Murthy, S.N., Novak, J.T., and Holbrook, R.D. (2000) 'Optimizing Dewatering of Bio solids from Auto thermal Thermophilic Aerobic Digesters (ATAD) Using Inorganic Conditioners'.*Water Environment Research* 72, 714

Murthy, S.N., Novak, J.T., and De Haas, R.D. (1998) 'Monitoring cations to predict and improve activated sludge settling and dewatering properties of industrial wastewaters'. *Journal of Water Science and Technology* 38, 119-126

Murthy, S.N. (1998) *Bio-flocculation: Implications for Activated Sludge Properties and Wastewater Treatment*. Unpublished Ph.D. Thesis. Blacksburg, Virginia: Virginia Polytechnic Institute and State University

Na, S., Kim, Y.U., and Khim, J. (2007) 'Physiochemical properties of digested sewage sludge with ultrasonic treatment'. *Ultrasonics Sonochemistry journal* 14, 281–285

Nagao, N., Tajima, N., Kawai, M., Niwa, C., Kurosawa, N., Matsuyama, T., Yusoff, F.M., and Toda, T. (2012) 'Maximum organic loading rate for the single-stage wet anaerobic digestion of food waste'. *Journal of Bio-resource Technology* 118, 210–218

Nancharaiah, Y.V., Mohan, S.V., and Lens, P.N.L. (2016) 'Recent advances in nutrient removal and recovery in biological and bioelectrochemical systems'. *Bioresour. Technol.* 215,173–185

Neis, U. (2000) 'Ultrasound in water, wastewater and sludge treatment'. *Journal of Water* 21, 36–39

Nelson, T.C., Huang, J.Y.C., and Ramaswami, D. (1998) 'Decomposition of exopolysaccharide slim by a bacteriophage enzyme'. *Water Research* 22(9), 1185-1188.

Nelson, T.C., Huang, J.Y.C., and Ramaswami, D. (1998) 'Decomposition of exopolysaccharide slim by a bacteriophage enzyme'. *Water Research Journal* 22(9), 1185-1188

Neyens, E., Baeyens, J., Dewil, R., and De heyder, B. (2004) 'Advanced sludge treatment affects extracellular polymeric substances to improve activated sludge dewatering'. *Journal of Hazardous Material* 106, 83–92

Neyens, E., and Baeyens, J. (2003) 'A review of thermal sludge pre-treatment processes to improve dewaterability'. *Journal of Hazardous Materials* 98, 51-67

Nges, I.A., and Liu, J. (2010) ‘Effects of solid retention time on anaerobic digestion of dewatered-sewage sludge in mesophilic and thermophilic conditions’. *Renewable Energy* 35, 2200–6.

Nges, I. A., and Björnsson, L. (2012) ‘High methane yields and stable operation during anaerobic digestion of nutrient-supplemented energy crop mixtures’. *Bio- mass Bioenergy* 47, 62–70

Nguyen, T.P., Hilal, N., Hankins, N.P., and Novak, J.T. (2008b) ‘The relationship between cation ions and polysaccharide on the floc formation of synthetic and activated sludge’. *Journal of Desalination* 227 (1-3), 94-102

Nguyen, T.P., Hilal, N., Hankins, N.P., and Novak, J.T. (2008a) ‘Characterization of synthetic and activated sludge and conditioning with cationic polyelectrolytes’. *Desalination* 227, 103-110

Nielson, P.H, and Jahn A. (1999) ‘Extraction of EPS’. *In: Microbial extracellular substances: characterization, structure and function.* ed. by Wingender, J., Neu, T.R., and Flemmin, H.C. Berlin Heidelberg: Springer-Verlag, 49-72

Nielsen, P.H and Keiding, K. (1998) ‘Disintegration of Activated Sludge Flocs in Presence of Sulphide’. *Water Research* 32, 313

Nielsen, A.H., Lens, P., Vollertsen, J., and Hvitved-Jacobsen, T. (2005) ‘Sulphide-iron interactions in domestic wastewater from a gravity sewer’. *Water Research* 39 (12), 2747-2755

Ning, X., Wen, W., Zhang, Y., Li, R., Sun, J., Wang, Y., (2015) ‘Enhanced dewaterability of textile dyeing sludge using micro- electrolysis pretreatment’. *J. Environ. Manag.* 161, 181–187

Niu, M., Zhang, W., Wanga, D., Chen, Y., and Chen, R. (2013) ‘Correlation of physicochemical properties and sludge dewaterability under chemical conditioning using inorganic coagulants’. *Bio-resource technology* 144,337-343

Noike, T., Endo, G., Chang, J.E., Yaguchi, J., Matsumoto, J. (1985) ‘Characteristics of carbohydrate degradation and the rate-limiting step in anaerobic digestion’. *Biotechnol. Bioeng.* 28, 1482–1489

Nopens, I., Koegst, T., Mahieu, K., Vanrolleghem, P.A. (2005) ‘PBM and activated sludge flocculation: From experimental data to calibrated model’. *American institute of Chemical Engineers Journal* 51 (5), 1548-1557

Nopens, I. (2005) *Modelling the activated sludge flocculation process: a population balance approach*. Unpublished PhD thesis. Belgium: University of Ghent

Notebaert, F., Wilms, D., and Van Haute, A. (1975) ‘A new deduction with a larger application of the specific resistance to filtration of sludges’. *Water Research* 9(7), 667-673

Novak, J.T., Muller, C.D., and Murthy, S.N. (2001) ‘Floc structure and the role of cations’. *Water Science and Technology* 44 (10), 209–213

Novak, J.T., and Park, C. (2004) ‘Chemical conditioning of sludges’. *Water Science Technology* 49, 73-80

Novak, J.T (2010) *Effects of Aluminium and Iron on Odors, Digestion Efficiency and Dewatering Properties.* Unpublished Ph.D. thesis. Virginia-USA: Virginia Polytechnic Institute & State University

Novak, J. T., and Haugan, B. E. (1980) ‘Mechanisms and methods for polymer conditioning of activated sludge’. *Journal of Water Pollution Control Federation* 52**,** 2571

Novak, J. T., and Haugan, B. E. (1979) Chemical conditioning of activated sludge. *Journal of Environmental Engineering* 105, 993

Novak, J.T., Love, N.G., Smith, M.L., and Wheeler, E.R. (1998) ‘The effect of cationic salt addition on the settling and dewatering properties of an industrial activated sludge’. *Water Environment Research* 70, 984-996

Novak, J.T., Sadler, M.E., and Murthy, S.N. (2003) ‘Mechanisms of Floc Destruction during Anaerobic and Aerobic Digestion and the Effect on Conditioning and Dewatering of Biosolids’. *Water Research* 37, 3136 - 3144.

Novak, J. T. (2006) ‘Dewatering of sewage sludge’. *Drying Technology* 24(10), 1257-1262.

Oehmen, A., Lemos, P.C., Carvalho, G., Yuan, Z., Keller, J., Blackhall, L.L., and Ries, M.A.M. (2007) ‘Advances in enhanced biological phosphorus removal: from micro to macro scale’. *Water research* 41(11), 2271-2300

Ofverstrom, S., Jansen, J.L., and Dauknys, R. (2011b) ‘Impact of iron salts dosing on anaerobic digestion process and struvite/vivianite formation: review’. *Proceedings of the 12th international conference on environmental science and technology, Rhodes, Greece*

Ofverstrom, S., Dauknys, R., and Sapkaite, I. (2011a) ‘The effect of iron salt on anaerobic digestion and phosphate release to sludge liquor’. *Environmental Protection Engineering* 3(5), 123-126

OFGEM (2014) *'Non-Domestic Renewable Heat Incentive (RHI)'* [online] available from< https:// www.ofgem.gov.uk/environmental-programmes/non-domestic-renewable-heatincentive-rhi> [22 March 2014]

Ofverstrom, S., Sapkaite, I., and Dauknys, R. (2010) 'An investigation of impact of iron and aluminium addition on the anaerobic digestion process'. *Proceedings from the Linnaeus Eco-Tech 10, Kalmar, Sweden*

Ohm, T.I., Chae, J.S., Kim, J.E., Kim, H.K., and Moon, S.H. (2009) 'A study on the dewatering of industrial waste sludge by fry-drying technology'. *Journal of Hazardous Material* 168, 445– 450

Ojo, P. and Ifelebuegu, A.O (2015) 'Optimising final clarifier design and performance of an activated sludge plant using mathematical modelling'. *International journal of environmental engineering*, 2(1) 2374-1724

Ojo, P. and Ifelebuegu, A.O. (2016) 'The Impact of Alum on the Bulking of a Full scale Activated Sludge Plant '. *Environmental Engineering* 3(2374-1724), 6-10

Ojo, P., and Ifelebuegu, A.O. (2018) 'The Impact of Aluminium Salt for Chemical Phosphorus Removal on the Settleability of Activated Sludge'. *Environments 5*, 1–13

Ojo, P., and Ifelebuegu, A.O. (2019a) 'Effect of Aluminium Salt Dosing on Activated Sludge Settleability Indicators: A New Settleability Model Development'. *Water* 11, 179

Ojo, P., and Ifelebuegu, A.O. (2019b) 'The Effects of Aluminium- and Ferric Based Chemical Phosphorus Removal on Activated Sludge Digestibility and Dewaterability'. *Journal of Processes* 7, 228

Ojo, P., and Ifelebuegu, A.O. (2019c) 'Modelling the effects of ferric salt dosing on the Settleability of activated sludge'. *Journal of Environmental Chemical Engineering* 7(5), 103256

Oleszkiewicz, J.A., and Sharma, V.K. (1990) 'Stimulation and inhibition of anaerobic processes by heavy metals – a review'. *Biol. Wastes* 31, 45–67

Olivier, J., Vaxelaire, J. and Vorobiev, E. (2007) 'Modelling of cake filtration: An overview'. *Separation Science and Technology* 42, 1667-1700

Olivier, J., Ginisty, P., and Vaxelaire, J. (2018) 'Sludge conditioning prior to dewatering: Introducing drainage index as a new parameter'. *Environmental Technology & Innovation* 11, 286-298

Ormeci, B. (2004) ‘Freeze-thaw conditioning of activated sludge: effect of monovalent, divalent and trivalent cations’. *Journal of Residuals Sci. Technol*. 1(3), 143-150

Osborn, D.W., and Nicholls, H.A. (1978) ‘optimisation of the activated sludge process for the biological removal of phosphorus’. *Prog. Wat.Tech.* 10(12), 261-277

Ostrem, K. (2004) *Greening waste: anaerobic digestion for treating the organic fraction of Municipal solid wastes*. Earth Engineering Center Columbia University 286-298

Otterpohl, R., and Freund, M. (1992) ‘Dynamic models for clarifiers of activated sludge plants with dry and wet weather flows’. *Water Science and Technology* 26 (5/6), 1391-1400

Ozinsky, A.E., and Ekama, G.A. (1995) ‘*Secondary Settling Tank Modelling and Design Part 1: Review of Theoretical and Practical Development’* [online] 21(4) 325-332, available from < http://www.wrc.org.za/Knowledge%20Hub%20Documents/Water%20SA%20Journals/Manuscripts/1995/04/WaterSA_1995_04_0946.PDF> [24May 2014]

Padival, N.A., Kimbell, W.A., and Redner, J.A. (1995) ‘Use of iron salts to control dissolved sulphide in trunk sewers’. *Journal of Environmental Engineering* 121 (11), 824

Palm, J.C., Jenkins, D., and Parker, D.S. (1980) ‘Relationship between organic loading, dissolved-oxygen concentration and sludge settleability in the completely- mixed activated-sludge process’. *Journal of Water Pollution Control Federation* 52 (10), 2484–2506

Parawira, W. (2004) *Anaerobic treatment of agricultural residues and wastewater application of high-rate reactors*. Doctoral Dissertation. Sweden: Department of Biotechnology, Lund University

Park, B., Ahn, J., Kim, J., and Hwang, S. (2004) ‘Use of microwave pre-treatment for enhanced anaerobiosis of secondary sludge’. *Water Science Technology* 50, 17-23

Park, C.M., and Novak, J.T. (2013) ‘The effect of direct addition of iron (III) on anaerobic digestion efficiency and odour causing compounds’. *Water Science and Technology* 68, 2391-2396

Park, C., Fang, Y., Murthy, S.N., and Novak, J.T., (2010) ‘Effects of floc aluminum on activated sludge characteristics and removal of 17-alpha-ethinylestradiol in wastewater systems’. *Water Res.* 44, 1335–1340.

Park, C., Muller, C.D., Abu-Orf, M.M., and Novak, J.T. (2006) ‘The effect of wastewater cations on activated sludge characteristics: Effects of Aluminium and Iron in Floc’. *Water Environment Research* 79, 31-40.

Parker, D., Kaufman, W., and Jenkins, D. (1970). *Characteristics of Biological Flocs in Turbulent Regimes.* Berkeley, California: University of California, Sanitary Engineering Research Laboratory.

Parker, D.S., Jenkins, D., and Kaufman, W.J. (1971) 'Physical Conditioning of the Activated Sludge Floc'. *Journal of the Water Pollution Control Federation* 43, 1817-1824

Parker, D.S., Jenkins, D., and Kaufman, W.J. (1972) 'Floc Breakup in Turbulent flocculation Processes'. *Journal of the Sanitary Engineering Division American Society of Civil Engineers* 98, 79-99

Parker, P.J., and Collins, A.G. (1999) 'Ultra-rapid freezing of water treatment residuals'. *Water Research* 33, 2239–2246.

Parker, D., Appleton, R., Bratby, J. and Melcer, H. (2004) 'North American performance experience with anoxic and anaerobic selectors for activated sludge bulking control'. *Water Science and Technology*, 50 (7), 221-228.

Parmer, N., Singh, A., and Ward, O.P. (2001) 'Enzyme treatment to reduce solids and improve settling of sewage sludge'. *Journal of Industrial Microbiology and Biotechnology* 26:383-386

Peavy, S.H., Rowe, R.D., and Tchobanoglous, G. (1985) *Environmental Engineering*. New York: McGraw-hill, Inc

Peeters, B., Herman, S. (2007) 'Monitor cations in CPI wastewater for better performance'. *Chemical Engineering Journal* 114, 56-62

Peeters, B., Dewil, R., Lechat, D., and Smets, I.J. (2011) 'Quantification of the exchangeable calcium in activated sludge flocs and its implication to sludge settleability'. J*ournal of separation and purification Technology* 83, 1-8

Peng, G., Ye, F. and Li, Y. (2011) 'Comparative investigation of parameters for determining the dewaterability of activated sludge'. *Water Environment Research* 83(7), 667-671

Pevere, A., Guibaud, G., van Hullebusch, E.D., Boughzala, W., and Lens, P.N.L. (2007) 'Effect of Na^+ and Ca^{2+} on the aggregation properties of sieved anaerobic granular sludge'. *Colloids and Surfaces A: Physicochemical and Engineering Aspects* 306 (1-3), 142-149

Philips, S., Rabaey, K., and Verstraete, W. (2003) 'Impact of iron salts on activated sludge and interaction with nitrite or nitrate'. *Journal of Bioresource Technology* 88, 229-239

Pipes, W. O. (1979) ‘Bulking, deflocculation, and pin-point floc’. *Journal of Water Pollution Control Federation 51*

Pipes, W.O. (1978b) ‘Actinomycetes Scum Formation in Activated Sludge Processes’. *Journal of the Water Pollution Control Federation* 5, 628-634

Pipes, W.O. (1967) ‘Bulking of Activated Sludge’. *Advances in Applied Micro- biology* 9,185-234

Pitman, A. R., (1980) ‘Settling properties of extended aeration sludge’. *Water pollution control federation* 52 (3), 524-536

Pitman, A.R. (1984) *Operation of biological nutrient removal plants: In Theory, Design and Operation of Nutrient Removal Activated Sludge Processes Edited by Wiechers H.N.S. et al.* Water Research Commission, Pretoria

Pobeheim, H., Munk, B., Lindorfer, H., and Guebitz, G.M. (2011) ‘Impact of nickel and cobalt on biogas production and process stability during semi-continuous anaerobic fermentation of a model substrate for maize silage’. *Water Research* 45, 781–787

Ponsa, S., Ferrer, I., Vazquez, F., and Font, X. (2008) ‘Optimization of the hydrolytic acidogenic anaerobic digestion stage (55℃) of sewage sludge: influence of pH and solid content’. *Water Research* 42, 3972–3980

Probstein, R.F. (2003) *Physicochemical Hydrodynamics: An Introduction*. Hoboken, New Jersey: John Wiley & Sons

Punal, A., Trevisan, M., Rozzi, A., and Lema, J. (2000) ‘Influence of C: N ratio on the start-up of up-flow anaerobic filter reactors’. *Water Research* 34, 2614–2619

Piirtola, L., Uusitalo, R., and Vesilind, A. (2000) ‘Effect of mineral materials and cations on activated and alum sludge settling’. *Water Research* 34(1), 191-195

Qi, X., Zhang, S., Wang, Y., and Wang, R. (2005) ‘Advantages of the integrated pig-biogas-vegetable greenhouse system in North China’. *Ecological Engineering* 24,175-83

Rabinowitz, B. and Marias, G.v.R. (1980) Chemical and biological phosphorus removal in the activated sludge process. M.A.SC. Thesis Univ.Capetown S.A., Res.Rep.No. W32

Rachwal, A. J., Johstone, D.W.M., Hanbury, M.J., and Critchard, D.J. (1982). ‘The Application of Settleability Tests for the Control of Activated Sludge Plants’. In *Bulking of Activated Sludge,* Eds. Chambers, B., and Tomlinson, E.J. 13, 224-44. Chichester: Ellis Horwood Ltd. England

Rai CL, Struenkmann, G., Muller, J., and Rao, P.G. (2001) 'Influence of ultrasonic disintegration on sludge growth and its estimation by respirometry'. *Environ Sci. Technol.* 38, 5779-5785

Ramin, E., Wagner, D.S., Yde, L., Binning, P.J., Rasmussen, M.R., Mikkelsen, P.S., and Plosz, B.G. (2014) 'A new settling velocity model to describe secondary sedimentation'. *Water Res.* 55, 447–458

Raposo, F., Fernández-Cegrí, V., De La Rubia, M.A., Borja, R., Béline, F., Cavinato, C., Demirer, G., Fernández, B., Fernández-Polanco, M., Frigon, J.C., Ganesh, R., Kaparaju, P., Koubova, J., Méndez, R., Menin, G., Peene, A., Scherer, P. Torrijos, M., Uellendahl, H., Wierinck, I. and. de Wilde, V. (2011) 'Biochemical methane potential (BMP) of solid organic substrates: evaluation of anaerobic biodegradability using data from an international interlaboratory study'. *Journal of Chemical Technology and Biotechnology* 86(8), 1088-1098

Raszka, A., Chorvatova, M., and Wanner, J. (2006) 'The role and significance of extracellular polymers in activated sludge-Part I: literature review'. *Journal of Acta Hydrochimica et Hydrobiologica* 34, 411-424

Rasmussen, H., Bruus, J.H., Keiding, K. and Nielsen, P.H. (1994) 'Observation on dewaterability and physical, chemical and microbiogical changes in anaerobically stored activated sludge from a nutrient removal plant'. *Water Research* 28, 417-425

Rasmussen, M., and Larsen, T. (1996) 'A method for measuring sludge settling characteristics in turbulent flows'. *Water Research* 30 (10), 2363-2370

Rasmussen, H. and Nielsen, P.H. (1996) 'Iron Reduction in Activated Sludge Measured with Different Extraction Techniques'. *Water Research* 30, 551

Reardon, R. (2005) 'Clarification concepts for treating peak wet weather wastewater flows'. *Journal of Florida Water Resources*, 25-30

Rehl, T., and Müller, J. (2011) 'Life cycle assessment of biogas digestate processing technologies'. *Resource Conservation Recycling* 56, 92–104

Rensing, C., and Maier, R.M. (2003) 'Issues underlying use of biosensors to measure metal Bioavailability'. *Ecotoxicology and Environmental Safety* 56, 140–147

Richard M. (1989) 'Activated Sludge Microbiology'. *The Water Pollution Control Federation* USA, 350

Richard, M. (2003) ‘*Activated Sludge Microbiology Problems and Their Control’* [Online] Available from < http://www.dec.ny.gov/docs/water_pdf/drrichard1.pdf> [10 July 2015]

Riffat, R. (2012) ‘*Fundamentals of wastewater treatment and engineering’*. Boca Raton, Florida: CRC Press

Rincón, B., Borja, R., González, J.M., Portillo, M.C., Sáiz-Jiménez, C. (2008) ‘Influence of organic loading rate and hydraulic retention time on the performance, stability and microbial communities of one-stage anaerobic digestion of two-phase olive mill solid residue’. *Bio-chemical Engineering Journal* 40, 253–261

Rittmann, B.E., and McCarty, P.L. (2001) *Environmental Biotechnology*: New York, NY, USA: McGraw-Hill

Rittmann, B.E., and Laspidou, C.S. (2002) ‘A unified theory for extracellular polymeric substances, soluble microbial products, and active and inert biomass’. *Water Res. 36*, 2711–2720

Robinson, J., and Knocke, W.R. (1992) ‘Use of dilatometric and drying techniques for assessing sludge dewatering characteristics’. *Water Environ Res.* 64(1), 60-68.

Rosen, M.J. (2004). Surfactant and Interfacial Phenomena. John Wiley & Sons, New York.

Romero-Güiza, M.S., Vila, J., Mata-Alvarez, J., Chimenos, J.M., and Astals, S. (2016) ‘The role of additives on anaerobic digestion: A review’. *Journal of Renewable and Sustainable Energy Reviews* 58, 1486-1499

Romero-Güiza, M.S., Vila, J., Mata-Alvarez, J., Chimenos, J.M., and Astals, S. (2016) ‘The role of additives on anaerobic digestion: A review’. *Journal of Renewable and Sustainable Energy Reviews* 58, 1486-1499.

Rudolfs, W., and Setter, L. (1931) ‘After-effect of ferric chloride on sludge digestion’. *Sewage Works Journal* 3 (3), 352-361

Rudolfs, W., Baumgartner, W., and Setter, L. (1932) ‘Effect of coagulants on sludge digestion’. *Sewage Works Journal*

Ruiz-Hernando, M., Martinez-Elorza, G., Labanda, J., and Llorens, J. (2013) ‘Dewaterability of sewage sludge by ultrasonic, thermal and chemical treatments’. *Journal of Chemical Engineering* 230, 102–110

Sanin, F.D., and Vesilind, P.A. (2000) ‘Bio-flocculation of activated sludge: the role of calcium ions and extracellular polymers’. *Environmental Science and Technology* 21, 1405-1412

Sanin, F.D., Vatansever, A., Turtin, I., Kara, F., Durmaz, B., and Sesay, M.L. (2006) ‘Operational conditions of activated sludge: influence on flocculation and dewaterability’.*Drying Technology Journal* 24, 1297-1306

Sanin, F.D., Clarkson, W.W., Vesilind, P.A. (2011) *Sludge engineering: the treatment and disposal of wastewater sludges*. 1st ed. Pennsylvania: DEStech Publications Inc

Sakai, Y., Fukase, T., Yasui, H., and Shibata, M. (1997) ‘An activated sludge process without excess sludge production’. *Water Science Technology* 36, 163-170.

Salminen, E., Rintala, J., Lokshima, L.Y., and Vavilin, V.A. (2000) ‘Anaerobic batch degradation of solid poultry slaughterhouse waste. *Water. Sci.Technol.* 41, 33–41

Sanchez, E., Borja, R., Travieso, L., Martın, A., Colmenarejo, M. (2005) ‘Effect of organic loading rate on the stability, operational parameters and performance of a secondary up flow anaerobic sludge bed reactor treating piggery waste’. *Bio-resource Technology* 96,335-344

Sarkar J, Shah J, Ramesh M. (2004). Method of dewatering sludge using enzymes, United State Patent, US 6733673B2

Sawalha, O., and Scholz, M. (2007) ‘Assessment of capillary suction time (CST) test methodologies’. *Environmental Technology* 28(12), 1377-1386.

Sawalha, O., and Scholz, M. (2010) ‘Modeling the relationship between capillary suction time and specific resistance to filtration’. *Journal of Environmental Engineering* 136(9), 983-991.

Sawalha, O. (2010) *Capillary Suction Time (CST): developments in testing methodology and reliability of results*. Unpublished Ph.D. thesis. United Kingdom: University of Edinburgh

Sawatdeenarunat, C., Surendra, K.C., Takara, D., Oechsner, H., and Khanal, S.K. (2015) ‘Anaerobic digestion of lignocellulosic biomass: challenges and opportunities’. *Bioresour.Technol.* 178, 178–186

Sauer, K., and Thauer, R.K. (2000) ‘Methyl-coenzyme M formation in methanogenic archaea. Involvement of zinc in coenzyme M activation’. *European Journal of Biochemistry* 267, 2498–2504

Schattauer, A., Abdoun, E., Weiland, P., Plöchl, M., Heiermann, M. (2011) ‘Abundance of trace elements in demonstration biogas plants. *Bio-system Engineering* 108, 57–65

Schönheit, P., Moll, J., and Thauer, R.K. (1979) ‘Nickel, cobalt, and molybdenum requirement for growth of Methanobacterium thermoautotrophicum’*. Archives Microbiology* 123, 105-107

Schamber, D.R., Larock, B., Siegert, I., and Banks, C. (2005) ‘The effect of VFA additions on the anaerobic digestion of cellulose and glucose in batch reactors’. *Process Biochemistry* 40, 3412-3418

Schink, B. (1997) ‘Energetics of syntrophic cooperation in methanogenic degradation. *Microbiol Mol. Biol. Rev.* 61:262–280

Scholz, M. (2005) ‘Review of recent trends in capillary suction time CST dewaterability testing research’. *Industrial and Engineering Chemistry* Research 44, 8157-8163

Scholz, M. (2006) ‘Revised capillary suction CST test to reduce consumable costs and improve dewaterability interpretation’. *Journal of chemical technology and biotechnology* 81, 336-344

Schuler, A.J., and Jang, H. (2007a) ‘Causes of variable biomass density and its effects on settleability in full-scale biological wastewater treatment systems’. *Environmental Science and Technology* 41 (5), 1675-1681

Schuler, A.J., and Jang, H. (2007b) ‘Density effects on activated sludge zone settling velocities’. *Water Research Journal* 41 (8), 1814-1822

Schuler, A.J., and Jang, H. (2007c) ‘Microsphere addition for the study of biomass properties and density effects on settleability in biological wastewater treatment systems’. *Water Research* 41 (10), 2163-2170.

Scott, D.S. (1973) ‘Use and production of iron salts for phosphorus removal’. *Research Report No. 5, Environment Canada*

Seo, K.W., Choi, Y., Gu, B.M., Kwon, E.E., Tsang, Y.F., Rinklebe, J., and Park, C. (2017) ‘Pilot-scale investigation of sludge reduction in aerobic digestion system with endospore-forming bacteria’. *Chemosphere Journal* 186, 202-208

Sezgin, M., Jenkins, D. and Parker, D.S. (1978) ‘A Unified Theory of Filamentous Activated Sludge Bulking’. *Journal of the Pollution Control Federation* 50,352-358

Sezgin, M., Palm, J. H., and Jenkins, D. (1980) 'The role of filamentous microorganisms in activated-sludge settling'. *Journal of Progress Water Technology* 12 (6), 97–107.

Sheng, G.P, Yu, H.Q, and Li, X.Y. (2010) 'Extracellular polymeric substances (EPS) of microbial aggregates in biological wastewater treatment systems: a review'. *Biotechnology Advances Journal* 28, 882-894

Sheng, G, P., Yu, H.Q., and Li, X, Y. (2006) 'Stability of sludge flocs under shear conditions: roles of extracellular polymeric substances (eps)'. *Biotechnol. Bioeng.* 93 (6), 1095-1102.

Shi, C.H., Zhu, N.W., Wu, P.X., Li, P., and Wu, J.H. (2013) 'Heavy metals removal from sewage sludge and dewaterability improvement by bioleaching'. *China Environmental Science* 33, 474–479

Shin, H.-S., Kang, S.T., and Nam, S.Y. (2000) 'Effect of carbohydrates to protein ratio in EPS on sludge settling characteristics'. *Biotechnology and Bioprocess Engineering* 5, 460-464

Siebritz I.P., Ekama G. A., and Marias G. V.R. (1982) 'A Parametric Model for Biological Excess Phosphorus Removal'. *Journal of Water Science and Technology* 15 (3-4), 127-152

Siegert, I., and Banks, C. (2005) 'The effect of VFA additions on the anaerobic digestion of cellulose and glucose in batch reactors'. *Process Biochemistry* 40 (2005), 3412-3418

Singer, P. (1972) 'Anaerobic control of phosphate by ferrous iron'. *Journal of Water Pollution Control Federation* 44 (4), 663-669

Smeulders, J.B.A.F., and Meeten, G.H. (1995) 'Interpretation of filterability measured by the capillary suction time method'. *Chemical Engineering Science* 50, 1273-1279

Smollen, M. (1986a) 'Dewaterability of municipal sludges 1: A comparative study of specific resistance to filtration and capillary suction time as dewaterability parameters'. *Water SA* 12, 277-132.

Smollen, M. (1986b) 'Dewaterability of municipal sludges 2: Sludge characterization and behaviour in terms of SRF and CST parameters'. *Water SA* 12, 133-138.

Smith, J. A., and Carliell-Marquet, C. M. (2009) 'A novel laboratory method to determine the biogas potential of iron-dosed activated sludge'. *Journal of Bio-Resource Technology*, 100(5), 1767-1774

Smith, J. A., and Carliell-Marquet, C. M. (2008) ‘The digestibility of iron-dosed activated sludge’. *Journal of Bio-Resource Technology*, 99(18), 8585-8592

Smith, J. (2006) *An Investigation into the Anaerobic Digestibility of Iron-dosed Activated Sludge*. Ph.D. Thesis, University of Birmingham

Smith, K.J., and Vesilind, P.A. (1995) ‘Dilatometric measurement of bound water in wastewater sludge’. *Water Res.* 29(12), 2621-2626

Smollen, M., and Ekama, G.A. (1984) ‘Comparison of empirical settling velocity equations in flux theory for secondary settling tanks: South Africa’. *Water Sci. Technol.* 10, 175–184

Sobeck, D.C., and Higgins, M.J. (2002) ‘Examination of Three Theories for Mechanisms of Cation-Induced Bioflocculation’. *Water Research* 36, 527

Song, X.W., and Zhou, L.X. (2008) ‘The influence of bioleaching on dewaterability of municipal sewage sludge’. *Acta Scienctiarum Circumiectus Journal* 28, 2012–2017

Song, L.J., Zhu, N.W., Yuan, H.P., Hong, Y., and Ding, J. (2010) ‘Enhancement of waste activated sludge aerobic digestion by electrochemical pre-treatment’. Water Research 44, 4371–4378

Sorensen, B.L., and Wakeman, R.J. (1996) ‘Filtration characterisation and specific surface area measurement of activated sludge by Rhodamine B adsorption’. *Water Research Journal 30*, 115

Sorensen, B. L. and Sorensen, P. B. (1997) ‘Structure compression in cake filtration’. *Journal of Environmental Engineering* 123(4), 345-353.

Sponza, D.T. (2002) ‘Extracellular polymer substances and physicochemical properties of flocs in steady and unsteady state activated sludge systems’. *Process Biochemistry* 37, 983-998

Sponza, D.T. (2003) ‘Investigation of extracellular polymer substance (EPS) and Physicochemical properties of different activated sludge flocs under steady-state conditions’. *Enzyme and Microbial Technology* 32, 375-385

Speece, R.E. (1996) *Anaerobic Biotechnology for Industrial Wastewaters*, Archae Press, Nashville, TE, USA 394-400

Spicer, P., Keller, W., and Pratsinis, S. (1996) ‘The Effect of Impeller Type on Floc Size and Structure during Shear-Induced Flocculation’. *Journal of Colloid and Interface Science* 184(1), 112-122

Steiner, A.E., McLaren, D.A., and Foster C.F. (1976) 'The nature of activated sludge flocs'. *Water Research Journal 10*, 25.

Stratton, H., Seviour, B. and Brooks, P. (1998) 'Activated Sludge Foaming: What Causes Hydrophobicity and Can It Be Manipulated To Control Foaming'. *Journal of Water Science and Technology* 37(4-5), 503-509

Stobe C.T. (1964) 'About the behaviour of the upflow activated sludge process' *publication of sanitary engineering institute of the university of Hannover Germany* (18)

Stofkoper J.A. and Trentelman C.C.M. (1982) 'Guidelines For Design Of Circular Final Settling Tanks For Activated Sludge System'. *Journal of Water*, 15(14), 344-354

Standard methods for examination of water and wastewater -SMEW (1995) *Method 2710C settled sludge volume.* 19th edn.

Stypka, A. (1998) *Factors Influencing Sludge Settling Parameters and Solids Flux In the Activated Sludge Process. Report No 4*. [Online] available from < http://www2.lwr.kth.se/forskningsprojekt/Polishproject/JPS4.pdf> [16 September 2014]

Styles, D., Mesa Dominguez E., and Chadwick, D. (2016) 'Environmental balance of the UK biogas sector: An evaluation by consequential life cycle assessment'. *Science of the Total Environment* 50-561, 241-253

Sun, Y., Zheng, H., Zhai, J., Teng, H., Zhao, C., Zhao C., and Liao (2014) 'Effects of surfactants on the improvement of sludge dewaterability using cationic flocculants'. *Public Library of Science Journal* 9(10), 111036

Sun, Y., Fan, W., Zheng, H., Zhang, Y., Li, F., and Chen, W. (2015) 'Evaluation of dewatering performance and fractal characteristics of alum sludge'. *Public Library of Science (PLOS) One* 10 (6)

Smolders, G.J.F., Van der Meij, J., Van loosdrecht, M.C.M., and Heijnen, J.J. (1994a) 'Model of the anaerobic metabolism of the biological phosphorus removal process: stoichiometry and pH influence. *Biotech.Bioeng.* 43,461-470

Sosnowski, P.A., Wieczorek, S., and Ledakowicz, S. (2002) 'Anaerobic co-digestion of sewage sludge and organic fraction of MSWs'. *Advances in Environmental Research* 7, 609–616

Stickland, A.D., Burgess, C., Dixon, D.R., Harbour, P.J., Scales, P.J., Studer, L.J., and Usher, S.P. (2008) 'Fundamental dewatering properties of wastewater treatment sludges from filtration and sedimentation testing'. *Chem. Eng. Sci.* 63, 5283–5290

Saha, M., Eskicioglu, C., and Marin, J. (2011) 'Microwave, ultrasonic and chemo-mechanical pre-treatment for enhancing methane potential of pulp mill wastewater treatment sludge'. *Bioresource Technology* 102, 7815-7826

Snidaro, D., Zartarian, F., Jorand, F., Bottero, J.C., Block, J.C., and Manem, J. (2006) 'Characterization of Activated Sludge Flocs Structure'. *Water Science Technology* 36 (4), 313-320

Subramanian, S.B., Yan, S., Tyagi, R.D., and Surampalli, R.Y. (2010) 'Extracellular polymeric substances (EPS) producing bacterial strains of municipal wastewater sludge: isolation, molecular identification, EPS characterization and performance for sludge settling and dewatering.' *Journal of Water Research* 44 (7), 2253-2266

Tada, C., Yang, Y., Hanaoka, T., Sonoda, A., Ooi, K., and Sawayama, S. (2005) 'Effect of natural zeolite on methane production for anaerobic digestion of ammonium rich organic sludge'. *Bio-Resource Technology* 96,459-464

Takács, I., Patry, G. G., and Nolasco, D. (1991) 'A dynamic model of the clarification-thickening process'. *Water Research Journal* 25(10):1263-1271

Takeda, M., Ishigami, M., Shimada, A., Matsuoka, H., and Nakamura, I. (1994) 'Separation and preliminary characterization of acidic polysaccharides produced by Enterobacter sp'. *Journal of Fermentation and Bioengineering* 78, 140

Tarpagkou, R., and Pantokratoras, A. (2014) 'The influence of lamellar settler in sedimentation tanks for potable water treatment: A computational fluid dynamic study'. *Powder Technology Journal* 268, 139-149

Tchobanoglous, G., Stensel, H.D., Tsuchihashi, R., Burton, F., Abu-Orf, M., Bowden, G., and Pfrang, W. (2014) '*Metcalf & Eddy/Aecom: Wastewater Engineering Treatment and Resource Recovery, Fifth. ed.* McGraw e Hill Education, New York

Tchobanoglous, G., and Burton, F. (1991) Wastewater Engineering: Treatment, Disposal, Reuse. Metcalf and Eddy, INC; Newyork: McGraw-Hill

Tchobanoglous, G., Burton, F. L., and Stensel, H. D. (2003). *Wastewater Engineering: Treatment and Reuse*, 4th Edition. Metcalf and Eddy. McGraw-Hill Science

Tebbutt, T.H.Y. (1998) *Principles of Water Quality Control*. 5th edn. Oxford: Butterworth-Heinemann

Tezuka, Y. (1969) 'Cation-Dependent flocculation in a *Flavobacterium* species predominant in activated sludge'. *Applied Microbiology Journal 17*, 222

Thapa, K.B., Qi, Y., Clayton, S.A., and Hoadley, A.F.A. (2009) 'Lignite aided dewatering of digested sewage sludge'. *Water Research* 43, 623-634

Thistlethwayte, D.K.B. (1972). *The Control of Sulphides in Sewerage Systems*. Sydney

Thomas, D., Judd, S., and Fawcett, N. (1999) 'Flocculation modelling: a review'. *Water Research* 33(7)1579-1592

Thomas, L., Jungschaffer, G., and Sprossler, B. (1993) 'Improved sludge dewatering by enzymatic treatment'. *Water Science Technology* 28(1), 189-192

Thompson, G., and Forster, C.F. (2003) 'Bulking in activated sludge plants treating paper mill wastewaters'. *Journal of Water Research* 37, 2636–2644

Timmerman, M.W. (1979) 'Biological phosphate removal from domestic wastewater using anaerobic /aerobic treatment'. *Develop. Ind. Microbiol.* 20, 285

Tiwari, M. K., Saumyen, G., Harendranath, C. S., and Shweta, T. (2006) 'Influence of extrinsic factor on granulation in UASB reactor'. *Appl. Microbiol. & Biotech.* 71, 145–154

To, V.H.P., Nguyen, T.V., Vigneswaran, S., and Ngo, H.H. (2016a) 'A review on sludge dewatering indices'. *Water Sci. Technol.* 74 (1), 1–16.

To, V.H.P., Nguyen, T.V., Vigneswaran, S., Nghiem, L.D., Murthy, S., Bustamante, H., and Higgins, M. (2016b) 'Modified centrifugal technique for determining polymer demand and achievable dry solids content in dewatering'. *Desalin. Water Treat.* 57 (53), 1–11

To, V. H. P., Nguyen, T. V., Vigneswaran, S., Nghiem, L., Murthy, S., Bustamante, H. and Higgins, M. J. (2014) *Modified centrifugal index and sludge characteristics in assessing sludge dewatering.* In: IWA International Young Water Professional Conference, Taipei, Taiwan

Tony, M.A., Zhao, Y.Q., Fu, J.F., and Tayeb, M. (2008) ‘Conditioning of aluminum-based water treatment sludge with Fenton’s reagent: Effectiveness and optimising study to improve dewaterability’. *Chemosphere Journal* 72, 673-677

Tony, M.A., Zhao, Y., and Tayeb, A.M., (2009) ‘Exploitation of Fenton and Fenton-like reagents as alternative conditioners for alum sludge conditioning’. *Journal of Environmental Science* 21 (1), 101–105.

Tomlinson, E. J., and Chambers, B. (1979) ‘Methods for prevention of bulking in activated sludge’. *Journal of Water Pollution Control Federation* 78

Tomar, M., and Abdullah, T.H.A. (1994) ‘Evaluation of chemicals to control the generation of malodorous hydrogen-sulphide in wastewater’. *Water Research* 28 (12), 2545-2552

Torfs, E., Balemans, S., Locatelli, F., Diehl, S., Bürger, R., Laurent, J., François, P., and Nopens, I. (2017) ‘on constitutive functions for hindered settling velocity in 1-D settler models: Selection of appropriate model structure’. *Water Research* 110, 38-47

Torfs, E., Vlasschaert, P., Amerlinck, Y., Diehl, S., and Raimund, B. (2013b) ‘*Towards improved 1-D settler modelling: calibration of the Bu¨rger model and case study. In Proceedings of 86th Annual Water Environment Federation Technical Exhibition and Conference (WEFTEC 2013), number 2011, page 17*’ Mc Cormick Place South, Chicago, IL, and USA.

Torfs, E., Nopens, I., Winkler, M.K.H., Vanrolleghem, P.A., Balemans, S. and Smets, I.Y. (2016) ‘Settling tests’ [Online] available from < https://experimentalmethods.org/wp-content/uploads/2017/12/Chapter-6.pdf> [20 May 2017]

Triton Electronics Limited (2018a) ‘Type 304 CST’ [online] available from < http://tritonel.com/product/type-304-cst/ > [20 December 2018]

Triton Electronics Limited (2018b) ‘Type 305 SSVI’ [online] available from < http://tritonel.com/product/type-305-ssvi/ > [20 December 2018]

Tuncal, T. (2011) ‘Improving thermal dewatering characteristics of mechanically dewatered sludge: response surface analysis of combined lime-heat treatment’. *Water Environ Research* 83(5), 405-410

Tuntoolavest, M., and Grady, C.P.L.J. (1980) ‘Effect of activated sludge operational conditions on sludge thickening characteristics’. *Water Pollut. Control Fed.* 54, 1112–1117

Turakhia, M.H., Cooksey, K.E., Characklis, W.G. (1983) ‘Influence of calcium-specific chelant on biofilm removal’. *Applied and Environmental Microbiology* 46, 1236-1238

Turchiuli, C., and Fargues, C. (2004) ‘Influence of structural properties of alum and ferric flocs on sludge dewaterability’. *Chem. Eng. J.* 204 (1-3) 123-131

Tyagi, V.K., and Lo, S.L. (2011) ‘Application of physico-chemical pre-treatment methods to enhance the sludge disintegration and subsequent anaerobic digestion: an up to date review’. *Reviews in Environmental Science and Biotechnology* 10, 215–242

Urbain, V., Block, J.C., and Manem, J. (1993) ‘Bio-flocculation in activated sludge: An analytical approach’. *Journal of Water Research* 27, 829–838.

USEPA (1974) *Process design manual for sulphide control in sanitary sewerage systems*. Washington, D.C., s.n.

Van der Roest, H.F., Roeleveld, P., and Stamperius, P. (1999) ‘Optimising sludge treatment in the Netherlands’. *Water* 21, 23–25.

Vaerenbergh, E.V. (1980) ‘Numerical computation of secondary settler area using batch settling data’. *Tribune Cebedeau* 33, 369–374

Van Fleet, G., Barr, J., and Harris, A. (1974) ‘Treatment and disposal of chemical phosphate sludge in Ontario’. *Journal of the Water Pollution Control Federation* 46 (3), 582-587

Vanderhasselt, A., and Vanrolleghem, P.A. (2000) ‘Estimation of sludge sedimentation parameters from single batch settling curves’. *Water Research Journal* 34 (2), 395-406

Van Haandel, A.C., Lettinga, G. (1994) *Anaerobic Sewage Treatment -a Practical Guide for Regions with a Hot Climate*, Wiley, New York

VanLoon, G.W., and Duffy, S.J. (2011) ‘Environmental Chemistry’. *A global perspective.* 3rd ed. New York: Oxford University Press Inc.

Vanrolleghem, P., Van der Schueren, D., Krikilion, G., Grijspeerdt, K., Willems, P., and Verstraete, W. (1996) ‘On-line quantification of settling properties with in-sensor-experiments in an automated settlometer’. *Water Science and Technology* 33 (1), 37-51

Vaxelaire, J., and Cezac, P. (2004) ‘Moisture distribution in activated sludges: a review’, *Water Research* 38, 2215–2230

Vega-Rodriguez, B.A. (1983) ‘Quantitative evaluation of *Nocardia* spp. presence in activated sludge’. M.Sc. Thesis, Department of Civil Engineering, University of California, Berkeley

Velegol, D., Feick, J.D., and Collins, R.L. (2000) ‘Electrophoresis of spherical particles with a random distribution of zeta potential or surface charge’. *J. Colloid Interface Sci*. 230, 114-121

Verwey, E., and Overbeek, J. (1948) *Theory of the stability of lyophobic colloids*. The Netherlands: Elsevier

Vesilind, P. (1988) ‘Capillary suction time as a fundamental measure of sludge dewaterability’. *Journal of Water Pollution Control Federation*, 215-220

Vesilind, P.A. (2000) ‘Sludge disposal: ethics and expediency’. *Water Science and Tech*nology 42 (9) 1-5

Vesilind, P. A. (2003) ‘Wastewater treatment plant design’. *Water Environment Federation and International Water Association (IWA) publishing*

Vesilind, P.A. (1968) ‘Theoretical considerations: design of prototype thickeners from batch settling tests’. *Journal of Water Sewage Works* 115 (7), 302–307

Vesilind, P.A., and Hsu, C.C. (1997) ‘Limits of sludge dewatering’. *Water Sci. Technol.* 36(11), 87-91

Vesilind, P.A., Wallinmaa, S., and Martel, C.J. (1991) ‘Freeze-thaw sludge conditioning and double layer compression’. *Canadian Journal of Civil Engineering* 18, 1078-1083

Vesilind, P.A., and Martel, C.J. (1990) ‘Freezing of water and wastewater sludges’. *Environmental Engineering American Society Civil Engineers* 116 (5), 854-862

Vijayaraghavan, K., Sudharsan Varma, V., and Kamala Nalini, S.P. (2012) ‘Hydrogen generation from biological solid waste of milk processing effluent treatment plan’. *International Journal of Current Trends in Research* 1, 17-23

Vintiloiu, A., Boxriker, M., Lemmer, A., Oechsner, H., Jungbluth, T., Mathies, E., and Ramhold, D. (2013). ‘Effect of ethylenediaminetetraacetic acid (EDTA) on the bioavailability of trace elements during anaerobic digestion’. *Chemical Engineering Journal* 223, 436-441

Vorkamp, K., Herrmann, R., and Hvitved-Jacobsen, T. (2001) ‘Characterisation of organic matter from anaerobic digestion of organic waste by aerobic microbial activity’. Bio-resource Technology 78, 257-265.

Vrieze, J.D., Lathouwer, L.D., Verstraete, W., and Boon, N. (2013) ‘High-rate iron-rich activated sludge as stabilizing agent for the anaerobic digestion of kitchen waste’. *Water Research* 47, 3732-3741

Wang, W., Lud, Y., and Qiao, W. (2010). ‘Possible solutions for sludge dewatering in China’. *Frontiers of Environmental Science and Engineering* 4(1), 102-107

Wang, Z.W., Liu, Y., and Tay, J.Y., (2005a) ‘Distribution of EPS and cell surface hydrophobicity in aerobic granules’. *Applied Microbiology and Biotechnology* 69, 469-473

Wakeman, R.J. (2007) ‘Separation technologies for sludge dewatering’. *Journal of Hazardous Materials* 144, 614–619

Wahlberg, E.J. (1992). Activated sludge bioflocculation: measurement, influencing factors, and physical enhancement. Ph.D. thesis, Clemson University, Clemson, USA

Wahlberg, E.J., and Keinath, T.H. (1968) ‘Development of Settling Curves Using SVI’ *Journal of Water Pollution Control Federation* 60(12) 2095-2100

Wahlberg, E.J., and Keinath, T.M. (1988) ‘Development of settling flux curves using SVI’. *Journal of Water Pollution Control Federation* 60 (12), 2095–2100

Wan, J., Gu, J., Zhao, Q., and Liu, Y. (2016) ‘COD capture: a feasible option towards energy self-sufficient domestic wastewater treatment’. *Science Reports* 6, 250-254

Wanner, J. (1994) Activated Sludge Bulking and Foaming Control. Technomic Publishing, Lancaster, USA

Wang, Z., Gao, M., Wang, Z., She, Z., Chang, Q., Sun, C., Zhang, J., Ren, Y., and Yang, N. (2013b) ‘Effect of salinity on extracellular polymeric substances of activated sludge from an anoxic-anaerobic sequencing batch reactor.’ *Journal of Chemosphere* 93 (11), 2789-2795

Wang, Y., Yu, Y., Li, H., and Shen, C. (2016a) ‘Comparison study of phosphorus adsorption on different waste solids: fly ash, red mud and ferric–alum water treatment residues’. *Journal of Environ. Sci. China.* 50, 79–86.

Wang, Z., Fan, Y., Li, Y., Qu, F., Wu, D., and Kong, H. (2016b) ‘Synthesis of zeolite/hydrous lanthanum oxide composite from coal fly ash for efficient phosphate removal from lake water’. *Micropor. Mesopor. Mat*. 222, 226–234

Wang, H.F., Hu, H., Wang, H.J. and Zeng, J. (2019) 'Combined use of inorganic coagulants and cationic polyacrylamide for enhancing dewaterability of sewage sludge'. *Journal of Cleaner Production* 211, 387-395

Wang, F., Wang, Y., and Ji, M. (2005b) 'Mechanisms and kinetics models for ultrasonic waste activated sludge disintegration'. *Journal of Hazardous Material* 123, 145-150

Wang, J.P., Yuan, S.J., Wang, Y., and Yu, H.Q. (2013a) 'Synthesis, characterization and application of a novel starch-based flocculant with high flocculation and dewatering properties'. *Water Res.* 47, 2643–2648

Wang, S., and Viraraghavan, T. (1997) 'Wastewater sludge conditioning by fly ash'. *Waste Manag Journal* 17(7), 443-450

Wang, L.F., Wang, L.L., Li, W.W, He, D.Q, Jiang, H., Ye, X.D., Yuan, H.P., Zhu, N.W., and Yu, H.Q. (2014) 'Surfactant- mediated settleability and dewaterability of activated sludge'. *Chemical Engineering Science Journal* 116, 228-234

Wang, X., Yang, G., Feng, Y. Ren, G. Han, X. (2012) 'Optimizing feeding composition and carbon–nitrogen ratios for improved methane yield during anaerobic codigestion of dairy, chicken manure and wheat straw'. *Bio-resource Technology* 120, 78-83

Watts, W.R., Sypros, A., and Koopan, B. (1996) 'One-dimensional modeling of secondary clarifiers using a concentration and feed velocity dependent dispersion coefficient'. *Water Research Journal* 30 (9), 2112-2124

Wawrzynczk, J., Szewczyk, E., Norrlow, O., and Szwajcer Dey, E. (2007) 'Application of enzymes, sodium tripolyphosphate and cation exchange resin for the release of extracellular polymeric substances from sewage sludge. Characterization of the extracted polysaccharides/ glycoconjugates by a panel of lectins'. *Journal of Biotechnology* 130, 274-281

WEF-Water Environment Federation (2005) *Clarifier Design WEF Manual of Practice No.FD-8,* 2nd Edn., McGraw-Hill, New York [online] available from < http://www.assettler.com/COKTURME%20TANKLARI%20TASARIMI.pdf> [20 May 2015]

Wentzel, M.C., Marias, G.v.R., Loewenthal, R.E., and Ekama, G.A. (1988) 'Enhanced polyphosphate organism cultures in activated sludge systems-1; Enhanced culture development'. *Water SA* 14(2), 81-92.

Wentzel, M.C., Lotter, L.H., Loewenthal, R.E., Dold, P.L., and Marias, G.v.R. (1986) ‘Metabolic behaviour of Acinetobacter spp in enhanced biological phosphorus removal-A biochemical model’. *Water SA* 12, 209-224

Westerholm, M., Hansson, M., and Schnürer, A. (2012) ‘Improved biogas production from whole stillage by co-digestion with cattle manure’. *Bio-resource Technology* 114, 314-319

White, M.J.D. (1976) ‘Design and control of secondary settlement tanks’. *Water Pollut. Control* 75, 459-467

White (1975) settling of activated sludge, technical report TR11, WRC, Stevenage, UK

Wicklein, E. and Samstag, R. (2009) ‘Comparing Commercial and Transport CFD Models for Secondary Sedimentation’. *Water Environment Federation* (1977), 1-16

Wilén, B., and Nielsen, J. L. (2000) ‘Influence of microbial activity on the stability of activated sludge flocs’. *Journal of colloid and interface science* 18,145-156

Wilfert, P., Kumar, P.S., Korving, L., Witkamp, G.J., and Van Loosdrecht, M.C.M. (2015) ‘The relevance of phosphorus and iron chemistry to the recovery of phosphorus’. *Journal of Environmental Science Technology*, 49(16), 9400-9414

Williams, R.J.P., and Fraústo da Silva, J.J.R. (2000) ‘The distribution of elements in cells’. *Coordination Chemistry Review* 200–202, 247–348

Wilén, B.M., Jin, B., and Lant, P. (2003) ‘The influence of the key chemical constituents in activated sludge on surface and flocculation properties’. *Water Research* 37, 2127-30

Wilén, B.-M., Lumley, D., Mattsson, A., and Mino, T. (2008) ‘Relationship between floc composition and flocculation and settling properties studied at a full scale activated sludge plant’. *Water Research Journal* 42 (16), 4404-4418.

Wilén, B.-M., Lumley, D., Mattsson, A., and Mino, T. (2010) ‘Dynamics in Flocculation and Settling Properties Studied at a Full-Scale Activated Sludge Plant’. *Water Environment Research* 82 (2), 155-168

Wingender, J., Neu, T., and Flemming, H.C. (1999) *What are bacterial extracellular polymeric substances? In: Microbial extracellular substances: characterization, structure and function*. Berlin Heidelberg: Springer-Verlag 1, 1-18

Wojciechowska, E. (2005) ‘Application of microwaves for sewage sludge conditioning’. *Water Research* 39, 4749–4754

Wong, J.W.C., and Gu, X.Y. (2004) ‘Enhanced heavy metal bioleaching efficiencies from anaerobically digested sewage sludge with coinoculation of Acidithiobacillus ferrooxidans ANYL-1 and Blastoschizomyces capitatus Y5’. *Water Science and Technology* 50, 83–89

Wong, J.W.C., Zhou, J., Zhou, L.X., Kurade, M.B., Selvam, A. (2014) ‘Influence of sludge solids content on sludge dewaterability using bioleaching’. *Advances in Environmental Research* 3, 199–206

Wong, J.W.C., Zhou, J., Kurade, M.B., and Murugesan, K. (2015) ‘Influence of ferrous ions on extracellular polymeric substances content and sludge dewaterability during bioleaching’. *Bioresource Technology* 179, 78–83

Wood, H.G., and Ljungdahl, L. (1991) ‘Autotrophic character of acetogenic bacteria. In: In Shively J.M, Barton, L.L, editors. Variations in autotrophic life. San Diego, Calif.: Academic Press; 201–250

Wu, C.C., Huang, C.P., and Lee, D.J. (1997) ‘Effect of polymer dosage on alum sludge dewatering characteristics and physical properties’. *Journal of Colloids and Surfaces A: Physicochemical and engineering aspects* 122, 89-96

Wu, J., and He, C. (2010) ‘Experimental and modelling investigation of sewage solids sedimentation based on particle size distribution and fractal dimension’. *International Journal of Environment Science and Technology* 7(1), 37-46

Wu, C.C., Huang, C.P., and Lee, D.J. (1998) ‘Bound water content and water binding strength on sludge flocs’. *Water Res.* 32, 900–904

Wu, C.C., Lee, D.J., and Huang, C. (2000) ‘Determination of optimal dose of polyelectrolyte sludge conditioner considering particle sedimentation effects’. *Advances in Environmental Research* 4, 245-249

Wu, C. (2013) Optimization of sludge dewatering through pretreatment equipment selection, and testing’. *Dry. Technol.* 31, 193-201.

Xiao, K., Deng, J., Zeng, L., Guo, T., Gong, Y., Yang, B., Zhao, X., and Duan, H. (2019) ‘Enhancement of municipal sludge dewaterability by electrochemical pretreatment’. *Journal of Environmental Sciences* 75, 98-104

Xing, J., Criddle, C., and Hickey, R. (1997) Effects of a long-term periodic substrate perturbation on an anaerobic community. *Water Research* 31, 2195–2204.

Xu, G., Yin, F., Xu, Y., and Yu, H. (2017) ‘A force-based mechanistic model for describing activated sludge settling process’. *Water Res.* 127, 118–126

Yang, S.F., and Li, X.Y. (2009) ‘Influence of extracellular polymeric substances (EPS) on the characteristics of activated sludge under non-steady state conditions’. *Process Biochemistry* 44, 91-96

Yang, S.S., Guo, W.Q., Chen, Y.D., Wu, Q.L., Luo, H.C., Peng, S.M., Zheng, H.S., Feng, X.C., Zhou, X., and Ren, N.Q. (2015) ‘Economical evaluation of sludge reduction and characterization of effluent organic matter in an alternating aeration activated sludge system combining ozone/ultrasound pre-treatment’. *Bio-resource Technology* 177, 194-203.

Ye, C., Yang, X., Zhao, F., and Ren, L. (2016) ‘The shift of the microbial community in activated sludge with calcium treatment and its implication to sludge settleability’. *Bioresource Technology* 207, 11-18

Ye, F., Liu, X., and Li, Y. (2012) ‘Effects of potassium ferrate on extracellular polymeric substances (EPS) and physicochemical properties of excess activated sludge’. *Journal of Hazardous Materials* 199–200, 158–163

Yen, H.W., and Brune, D.E. (2007) ‘Anaerobic co-digestion of algal sludge and waste paper to produce methane’. *Bioresour. Technol* 98, 130–134.

Yeoman, S., Stephenson, T., Lester, J. and Perry, R. (1988) ‘The removal of phosphate during wastewater treatment; a review’. *Environmental Pollution* 49, 183-255

Yeoman, S., Lester, J., and Perry, R. (1990) ‘The effects of chemical phosphorus precipitation on anaerobic digestion’. *Environmental Technology* 11, 709–720

Yong, Z.H., Dong, Y.L., Zhang, X., and Tan, T.W. (2015) ‘Anaerobic co-digestion of food waste and straw for biogas production’. *Renew. Energy* 78, 527-530

Yuan, Z., Pratt, S., and Batstone, D.J. (2012) ‘Phosphorus recovery from wastewater through microbial processes’. Journal of *Current Opinion in Biotechnology,* 23(6), 878-883

Yuan, H., Yan, X., Yang, C., and Zhu, N. (2011) ‘Enhancement of waste activated sludge dewaterability by electro-chemical pre-treatment’. *Journal of Hazardous Materials* 187, 82-85

Yukseler, H., Tosun, I., and Yetis, U. (2007) ‘A new approach in assessing slurry filterability’. *Journal of Membrane Science* 303, 72-79

Yu, G.H., He, P.J., Shao, L.M., and He, P.P. (2008) ‘Stratification structure of sludge flocs with implications to dewaterability’. *Environmental Science and Technology* 42 (21), 7944-7949

Yu, H. Q., Tay, J. H., and Herbert, H. P. F. (2001) ‘The role of calcium in sludge granulation during UASB reactor start up’. *Water Res.* 35, 1052-1060

Zandvoort M.H., Geerts, R., Lettinga, G., Lens, P.N. L. (2003) ‘Methanol degradation in granular sludge reactors at sub-optimal metal concentrations: role of iron, nickel and cobalt’. *Enzyme and Microbial Technology* 33,190–198

Zandvoort, M.H., van Hullebusch, E.D., Peerbolte, A., Golubnic, S., Lettinga, G., and Lens, P.N. (2005) ‘Influence of pH shocks on trace metal dynamics and performance of methanol fed granular sludge bioreactors’. *Biodegradation* 16, 549–567

Zeidan, A., Rohani, S., and Bassi, A. (2004) ‘Dynamic and steady-state sedimentation of polydisperse suspension and prediction of outlets particle-size distribution’. *Chemical Engineering Science* 59 (13), 2619-2632

Zhang, D., Chen, Y.G., Zhao, Y.X., and Zhu, X.Y. (2010b) ‘New sludge pre-treatment method to improve methane production in waste activated sludge digestion’. *Environ. Sci. Technol.* 44, 4802–4808

Zhang, D.J., Li, Z.L., Lu, P.L., Zhang, T., and Xua, D.Y. (2006) ‘A method for characterizing the complete settling process of activated sludge’. *Water Research* 40 (14), 2637–2644

Zhang, G., Yang, J., Liu, H., and Zhang, J. (2009) ‘Sludge ozonation: disintegration, supernatant changes and mechanisms’. *Bio-resource Technology* 100, 1505-1509

Zhang, L., De Schryver, P., De Gusseme, B., De Muynck, W., Boon, N., and Verstraete, W. (2008) ‘Chemical and biological technologies for hydrogen sulphide emission control in sewer systems: a review’. *Water Research* 42 (1-2), 1-12

Zhang, L., Lee, Y., Jahng, D. (2011) ‘Anaerobic co-digestion of food waste and piggery wastewater: focusing on the role of trace elements’. *Bio-resource Technology102*, 5048–5059

Zhang, T., Liu, L., Song, Z., Ren, G., Feng, Y., and Han, X., et al. (2013) ‘Biogas production by co- digestion of goat manure with three crop residues’. *Public library of science (PLOS ONE)* 8, 66845

Zhang, W., Zou, Z., and Sui, J. (2010a) 'Numerical simulation of a horizontal sedimentation tank considering sludge recirculation'. *Journal of Environmental Sciences* 22(10) 1534-1538

Zhang, Y., Feng, Y., and Quan, X. (2015b) 'Zero-valent iron enhanced methanogenic activity in anaerobic digestion of waste activated sludge after heat and alkali pre-treatment'. *Journal of Waste Management 38, 297-302*

Zhang, Y., Feng, Y., Yu,Q., Xu,Z., and Quan, X. (2014) 'Enhanced high-solids anaerobic digestion of waste activated sludge by the addition of scrap iron'. *Journal of Bio-resource Technology* 159, 297-304

Zhang, Y. Q., Deng, Y., Chen, R.Y., Cui, Z.L., Chen, X. P., Yost, R., Zhang, F.S., and Zou, C.Q. (2012) 'The reduction in zinc concentration of wheat grain upon increased phosphorus-fertilization and its mitigation by foliar zinc application'. *Plant Soil* 361, 143–152.

Zhang, X.H., Lei, H.Y., Chen, K., Liu, Z., Wu, H., and Liang, H.Y. (2012) 'Effect of potassium ferrate (K_2FeO_4) on sludge dewaterability under different pH conditions'. Chem. Eng. J. 210, 467-474

Zhang, Y., Grassia, P., Martin, A., Usher, S.P., and Scales, P.J. (2015a) 'Designing thickeners by matching hindered settling and gelled suspension zones in the presence of aggregate densification'. *Chem. Eng. Sci.* 134, 297–307

Zhang, Q., Hu, J., and Jahng, D. (2016) 'Biogas from anaerobic digestion processes: research updates'. *Renewable Energy*, 98, 108–119.

Zhao, Y.Q., and Bache, D.H. (2014) 'Integrated effects of applied pressure, time and polymer doses on alum sludge dewatering behaviour'. *Waste Management Journal* 22, 813-819

Zhao, Y.Q., Papavasilopoulos, E.N., Bache, D.H., and Mackinnon, P.A. (2002) 'Polymer conditioning of alum sludge and discrepancies between estimates of the optimum dosage'. *Water Science and Technology* 46, 115-121.

Zhao, Y.Q. (2006) 'Involvement of gypsum (Ca SO4.2H2O) in water treatment sludge dewatering: a potential benefit in disposal and reuse'. *Separation Sci. Technol.* 41(12), 2785-2794.

Zhao, Y.Q. (2002) 'Enhancement of alum sludge dewatering capacity by using gypsum as skeleton builder'. *Colloids Surf A* 211, 205-212.

Zhen, G., Yan, X., Zhou, H., Chen, H., Zhao, T., and Zhao, Y. (2011) ‘Effects of calcined aluminium salts on the advanced dewatering and solidification/stabilization of sewage sludge’. *Journal of Environmental Science* 23(7), 1225– 1232.

Zhen, G., Lu, X., Li, Y.Y., Liu, Y., and Zhao. (2015) ‘Influence of zero valent scrap iron (ZVSI) supply on methane production from waste activated sludge’. *Chemical Engineering Journal* 263, 461–470

Zhen, G., Lu, X., Niu, J., Su, L., Chai, X., Zhao, Y., Li, Y.Y., Song, Y., and Niu, D.J. (2013) ‘Inhibitory effects of a shock load of Fe(II)-mediated persulphate oxidation on waste activated sludge anaerobic digestion. *Chemical Engineering Journal* 233, 274–281.

Zhen, G., Lu, X., Li, Y.Y., and Zhao, Y. (2014a) ‘Combined electrical-alkali pre-treatment to increase the anaerobic hydrolysis rate of waste activated sludge during anaerobic digestion’. *Applied Energy* 128, 93–102.

Zhen, G.Y., Lu, X.Q, Li, Y.Y., and Zhao, Y.C (2014b) ‘Enhanced dewaterability of sewage sludge in the presence of Fe (II)-activated persulfate oxidation’. *Bioresource Technology* 116, 259-265.

Zhen, G., Lu, X., Zhao, Y., Chai, X., and Niu, D. (2012) ‘Enhanced dewaterability of sewage sludge in the presence of Fe(II)-activated persulfate oxidation’. *Bioresource Technology* 116, 259-265.

Zheng, Y.D., Xing, M.Y., Cai, L.Z.Y., Xiao, T., Lu, Y.F., and Jiang, J.Z. (2017) ‘Interaction of earthworms -microbe facilitating biofilm dewaterability performance during wasted activated sludge reduction and stabilization’. *Science of the Total Environment* 581, 573-581

Zhou, S. and McCorquodale, J. A. (1992) ‘Influence of skirt radius on performance of circular clarifier with density stratification’. *International Journal for Numerical Methods in Fluids* 14(8), 919-934

Zhao, Q., and Kugel, G. (1996) ‘Thermophilic/mesophilic digestion of sewage sludge and organic wastes’. *Journal Environment Science Health Part A* 31, 2211-2231

Zhou, S., McCorquodale, J.A., and Zhong J. (1993) ‘Semi-implicit skew upwind method for problems in environmental hydraulics’. *International Journal of Numerical Methods in Fluids* 17, 803-823

Zhou, S., and McCorquodale, J.A., and Godo, A.M. (1994) ‘Short circuiting and density interface in primary clarifiers’. *Journal of Hydraulic Engineering* 120, 1060– 1080.

Zhou, Q. (2009) *Investigation on improving efficiency of pre-precipitation process at Sjölunda wastewater treatment plant.* Unpublished Master thesis. Sweden: Lund University

Zhou, X., Wang, Q., Jiang, G., Zhang, X., and Yuan, Z. (2014) ‘Improving dewaterability of waste activated sludge by combined conditioning with zero-valent iron and hydrogen peroxide’. *Bioresource Technology Journal* 174, 103-107.

Zhu, X., Treu, L., Kougias, P.G., Campanaro, S., and Angelidaki, I. (2017) ‘Characterization of the planktonic microbiome in upflow anaerobic sludge blanket reactors during adaptation of mesophilic methanogenic granules to thermophilic operational conditions’. *Journal of Anaerobe* 46,69-77

Zikanov, O. (2010) *Essential computational fluid dynamics*. New Jersey: Wiley, Hoboken

Zita, A., and Hermansson, M., (1994) ‘Effects of ionic strength on bacterial adhesion and stability of flocs in a wastewater activated sludge system’. *Applied and Environmental Microbiology* 60 (9), 3041-3048

Zou, J., Zhang, L., Wang, L., and Li, Y. (2017) ‘Enhancing phosphorus release from waste activated sludge containing ferric or aluminium phosphates by EDTA addition during anaerobic fermentation process’. *Chemosphere* 171, 601–608

Appendices

Appendix A- Determination of discrete settling velocity for a spherical discrete particle

The settling velocity of discrete particles (V_s) obeys stokes law and it is used to determine the settling velocity of discrete particles (Tebutt 1998 and Cassey 1992). The settling velocity (V_s) is evaluated as follows:

Step 1

If a particle was suspended in water, it will initially have two forces acting upon it namely; force of gravity and buoyant force. This is expressed in Equation (1.0 and 2.0) respectively.

$$F_G \; = \rho_{p\, g\, V_P} \qquad (1.0)$$

Where,

g = Gravitational constant (m/s²)

V_P = Volume of particle (m³)

ρ_P = Density of particle (kg/m³)

(F_G) = Force of gravity

$$F_B \; = \rho_{w\, g\, V_p} \qquad (2.0)$$

Where,

ρ_w = density of water (kg/m³)

V_P = volume of Particle (m³)

(F_B) = Buoyant force

Step2

Since these forces (i.e. F_G and F_B) are in opposite direction there will be no net force when $\rho_p = \rho_w$ and no acceleration of the Particle in the relation to the water will occur. However, if the density of the Particle (ρ_p) differs from that of the water (ρ_w), a net force (F_{Net}) will be exerted and the Particle will accelerate in the direction of the force (Peavy 1985).

Thus,

$F_{Net} = F_G - F_B$

$$F_{NET} = (\rho_{P-} \rho_W) V_{P\,g} \tag{3.0}$$

Hence,

The net force (F_{NET}) becomes the driving force for acceleration. However, since motion has been initiated by F_{NET},then a third force will result due to viscous friction. This force is called the Drag force (F_D), which is quantified by dimensional analysis (Equation 4.0)

$$F_{D\,=}\ C_D\ A_P\ \rho_W\ {V_S}^2/_2 \tag{4.0}$$

Where,

C_D = Newton's Drag coefficient

A_P= Cross-sectional area of Particle Perpendicular to the direction of movement (m²)

V_S = Settling Velocity of Particle (m/s)

However, because the Drag force (F_D) acts in the opposite direction to the driving force (F_{NET}) and increases as the square of the velocity, acceleration occur at a decreasing rate until a steady velocity (terminal velocity) is reached at the point where F_D equals F_{NET} (Equation 5.0).

Hence,

$F_{NET} = F_D$

$$(\ \rho_P\ - \rho_W)\ \mathrm{g} V_P = C_D\ A_P\ \rho_W\ {V_S}^2/_2 \tag{5.0}$$

But from Eqn 5.0,

$$ {V_S}^2 = 2g\ V_P\ (\ \rho_{P\,-}\ \rho_W\ )\ \backslash\ C_D\ A_P\ \rho_W \tag{6.0}$$

But,

For spherical particle,

$$V_p = \frac{4}{3}\pi r^3 \tag{7.0}$$

$$A = \pi r^2 \tag{8.0}$$

$$r = d/2 \tag{9.0}$$

Where

Ø= diameter of Particle

r = radius of particle

Substitute Equation 7.0, 8.0 and 9.0 into Equation 6.0 then Equation 10.0 holds as follows:

$$V_S{}^2 = \frac{4}{3}\, g\, (\, \rho_{P\,-}\, \rho_W\,)\; d\backslash\; C_D\;\; \rho_W \qquad (10.0)$$

However, C_D changes with the characteristics of different flow regimes' (Peavy 1985). Hence for laminar flow, transitional, and turbulent flow, the values of C_D are expressed in Equation 11.0, 12.0 and 13.0 respectively.

Laminar flow: $C_D = {}^{24}\!/_{Re}$ (11.0)

Transitional flow: $C_D = \; {}^{24}\!/_{Re} + {}^{3}\!/_{\sqrt{Re}}$ + 0.34 (12.0)

Turbulent flow: CD = 0.4 (13.0)

Where,

Re = Reynolds number

But,

Laminar flow: Re ≤ 1

Transitional flow: Re $> 10^4$

Turbulent flow: Re $\leq 1 \;\leq\; 10^4$

However, According to Tebbutt (1998) in sedimentation, the reynoulds number (Re) can be expressed in Equation 14.0

$$Re \;=\; V_S\;Ø\backslash\vartheta \qquad (14.0)$$

Where,

ϑ = coefficient of Kinematic Velocity (kg/m/s)

Substitute Equation 11.0 and Equation 14.0 into Equation 10.0 and Equation 15.0 is realised.

$$V_S = \;(\;\rho_{P\,-}\,\rho_W\,)\; gØ^2\backslash\; 18\;\rho_{w\,\vartheta} \qquad (15.0)$$

But,

Specific gravity of Particle $(S_P) = {}^{\rho_P}/_{\rho_W}$ (16.0)

Substitute Equation 16.0 into Equation 15.0 and Equation 17.0 is obtained.

$$V_S = (S_P - 1)\, g\emptyset^2 \backslash\ 18\, \vartheta \quad (17.0)$$

Equationn 17.0 known as stokes law for laminar flow. Therefore type-1 settlement analysis is based on the classic laws of sedimentation formed by Newton and stokes.

Equation 17.0 can be re-written in relation to dynamic viscosity (μ) since kinematic viscosity is dynamic viscosity divided by density of water (μ/ρ).

$$V_S = (\rho_P - \rho_W)\, g\emptyset^2 \backslash\ 18\mu$$

But,

Stokes law for turbulent flow holds by substituting Equation 13.0 and Equation 16.0 into Equation 10.0 and Equation 18.0 is realised as the *stokes law for turbulent flow*.

$$V_S = \sqrt{3.3\, g\, (S_P - 1)} = \sqrt{3.3\mathrm{g}\, (\rho_P - \rho_W)/\, \rho_w} \quad (18.0)$$

However, under quiescent conditions discrete Particle settles out at their terminal velocity, which will remain constant provided the fluid temperature does not alter. The knowledge of this velocity is fundamental in the design of sedimentation tanks and in evaluation of their performance. *Therefore a sedimentation tank is designed to remove all particles that have a terminal velocity (Vs) equal to or greater than (>) Vs*. The selection of V_S depends on the specific function of the tank and on the Physical characteristics of the Particle to be removed (Gray 2010). The rate at which clarified wastewater is produced $(Q^/)$ in sedimentation tank can be expressed as Equation 19.0:

$$Q^/ = V_S\ \mathrm{A} \quad (19.0)$$

Where,

Vs = the terminal Velocity or settling velocity of Particle (m/s)

A = the surface area of the settling chamber (m^2)

Therefore, in theory, the rate of clarification by type1 settlement is independent of depth (h). The Surface overflow rate (SOR) or surface loading (SL) which is the average daily flow in cubic meters per day (m^3/d) divided by the total surface area of the sedimentation tank in square meters(m²), (i.e.$Q/ /A$). This in equivalent to the terminal settling velocity (Vs) is the basis of sedimentation tank design. However, the modern sedimentation tanks are operated in a continuous – flow basis. Therefore the hydraulic Retention Time (HRT) of the tank should be long enough to ensure that all Particles with the desired velocity (Vs) would settle to the bottom of tank (Gray 2010) and the relation for HRT is provided in Equation 20.0.

HRT = (tank volume/influent flow) = $^{24V}/_{Q}$ (20.0)

Where,

V = Tank Volume (m³)

Q = Influent (m³/day)

In this case, the depth of sedimentation tank was taken as the water depth at the side wall measured from the tank bottom to the top of the overflow weir. However, this excludes the additional depth resulting from the slightly sloping bottom in both rectangular and circular sedimentation tanks. The relation between the terminal velocity (Vs) and the HRT can be expressed as Equation 21.0:

$$V_s = \frac{D}{HRT} \tag{21.0}$$

Where,

D= Depth (m)

Nonetheless, according to Cassey (1992), stokes law suffers from certain limitations which includes; shapes of particle not always spherical in real practice, liquid may not be at rest , All particles may not be discrete, stokes law is valid only often Re≤ 1.0 and fluid temperature may not be consistent.

Appendix B- Activated Sludge Sampling Schedule for Settleability, Digestibility and Dewaterability test (Sampling Location: Minworth Wastewater treatment plant (WWTP)

Appendix B1: Activated Sludge Settleability Batch Test Schedule

Batch test (Date) for Activated sludge settleability		
Aluminium	Ferric	Calcium
Batch 1 (7th November 2014)	Batch 1 (7th November 2014)	Batch 1 (5th December 2014)
Batch 2 (4th December 2014)	Batch 2 (15th November 2014)	Batch 2 (2nd June 2016)
Batch 3 (9th December 2014)	Batch 3 (1st March 2016)	
Batch 4 (1st March 2016)	Sampling Location: Minworth Wastewater treatment plant (WWTP)	
Batch 5 (2nd June 2016)		

Appendix B2: Activated Sludge Digestibility Batch Test Schedule

Batch test (Date) for Activated sludge digestibility (12days)	
Aluminium	Ferric
Batch 1 (1st June 2016 to 16th June 2016)	Batch 1 (11th April 2016 to 26th April 2016)
Batch 2 (17th June 2016 to 4th July 2016)	Batch 2 (27th April 2016 to 12th May 2016)
Batch 3 (5th July 2016 to 21st July 2016)	Batch 3 (13th May 2016 to 30th May 2016)

Appendix B3: Activated Sludge Dewaterability Batch Test Schedule

Batch test (Date) for Activated sludge dewaterability		
Aluminium	Ferric	Calcium
Batch1 (16th February 2016) (Primary sludge)	Batch1 (16th February 2016) (Primary sludge)	Batch1 (16th February 2016) (Primary sludge)
Batch 2 (17th February 2016) (Secondary sludge)	Batch 2(17th February 2016) (Secondary sludge)	Batch 2 (17th February 2016) (Secondary sludge)

Appendix C-Tables of the factors that influence precision of laboratory Iron dosed sludge and its past research Evaluation

Table C1: The Factors that influence precision of laboratory Iron dosed sludge (Smith and Carliell-Marquet 2009)

S/N	Factor	Evaluation	Control procedures
1	Solids concentration	Typical total solid concentration in an activated sludge basin was 3.5g/l. The total solid concentration of return activated sludge (RAS) is greater.	Mix RAS with Settled Sewage in the correct proportion to produce a TS concentration of 3.5 g/l.
2	Activity of biomass	In co-precipitation Fe is dosed directly into the activated sludge basin where the biomass is 'active' due to the input of fresh settled sludge. The activated sludge collected and stored for use in a laboratory has reduced activity and thus reactions that occur are not representative of those during full-scale operation.	The addition of Settled Sewage to the RAS in a ratio of 70:30 approximately would produce an 'active' biomass for the duration of the experiment.
3	Quantity of Fe needed	Dosing ratios of Fe: P is typically between 1.5:1 and 3:1. P-concentrations in Fe- dosed activated sludge are approximately 40 mg/g total solid (TS).	Use a Fe: P molar ratio of 2:1. Aim for a total P concentration (afterdosing) of 40 mg/gTS and use this value to back-calculate amount of Fe and P required.
4	Type of Fe	Ferrous (Fe(II)) is cheaper and more efficient at removing P if pH and DO levels are favourable (Thistleton et al., 2001).	Use FeSO4.7H2O. Keep pH > 7 and aerate well
5	P availability	P bound in the RAS solids is unavailable for reaction with Fe. However, P in the Settled sewage is available for reaction.	Add additional P to the RAS: Settled Sewage (SS) mixture to increase the P available to Fe, bearing in mind the desired 40 mg P/g TS in the final mixture.
6	Balance of pH	The addition FeSO4 7H2O will reduce the pH. A pH of between 7 and 8 is required for Fe(II) to oxidise to Fe(III) and react with the available P (Thistleton et al., 2001).	During Fe addition, add drops 6 N NaOH to the mixture to maintain pH > 7.

7	Oxygen availability	In order for the Fe (II) to oxidise to ferric (Fe (III)), oxygen is needed. Typical DO levels in an activated sludge plant (ASP) are between 0.1 and 2.5 mg/g. Excessive oxygen will destroy the floc structure, while Inadequate oxygen and the RAS:Settled Sewage(SS) will become anoxic and the Fe will not oxidise or react with the P.	Aerate the system with diffused air (stones) and monitor DO. Increase or decrease air flow accordingly
8	Fe:P reaction speed	P and Fe need to be drip-fed to best simulate concentrations at full-scale ASP.	Add 1 ml of Fe and P every 15 min for 7.5 h.
9	Maturation time	Reactions will continue to occur after the final addition of Fe and P.	Leave the mixture to mature overnight.

Table C2: Past research Evaluation of the Impact of CPR on AD (Smith and Carliell-Marquet 2009)

CPR Sludge	AD Approach	Feedback	Analysis	References
Primary dosed in lab with Fe	Lab-scale Batch Test	50% of volatile solid looks indigestible	Poor digestion	Rudolfs and Setter (1931)
Primary dosed in lab with Fe and Al	Lab-scale Batch Test	Volatile solid (VS) destruction was slower than control	Slower AD	Ruldolfs et al. (1932)
Wastewater dosed in lab with Ca, Fe or Al	Full-scale digester	Lime-dosage too high, high pH Increase, Al-dosed = decrease biogas volume and Fe-dosed = lower biogas volume.	Less biogas	Van Fleet et al. (1974)
Wastewater dosed in lab with Al and Fe	Lab-scale, semi-continuous bench scale.	Failure due to low pH	Impaired AD (67% less efficient)	Gossett et al. (1978)
Primary dosed at WWTP with Al	Full-scale digester	Overdose of Al (400 mg/l) Stable AD with 250 mg/l dosage.	Impaired AD at high dosage	Emig (1979)
Raw sewage dosed in lab with Al and Fe	Lab-scale Batch Test and semi-continuous bench-scale	Decrease CH_4/VS fed. Decrease biogas/COD fed Coagulation resulted in organics being less available to microorganism	CPR sludge is less biodegradable	Dentel and Gossett (1982)
Activated sludge dosed in Lab with Al and Fe	Lab-scale Batch Test	Decrease CH_4/VS fed. Reduced accessibility of organics	Impaired AD	Kindzierski and Hrudey (1986)

Primary dosed at lab with Al and Fe	Lab-scale semi-continuous bench-scale		Impaired AD	Yeoman et al. (1990)
Activated sludge dosed at WWTP with Fe	Lab-scale semi-continuous bench-scale	Vol. of biogas decreases with increased amounts of bound Fe	Decreased vol. of biogas	Johnson et al. (2003)
Activated sludge dosed at WWTP with Fe	Lab-scale semi-continuous bench-scale	Lower vol. of biogas and CH_4	Impaired AD	Smith (2006)
Activated sludge dosed in Lab with Fe	Lab –Scale Batch Test	Lower vol. of biogas and CH_4	Impaired AD	Smith (2006)
Direct dose to digester Al, Fe and $CaCl_2$	Lab-scale semi-continuous bench-scale	Soluble P limitation (Good AD needs soluble P < 50–60 mg/l) and Poor substrate contact	Small dose Fe = enhances AD Large dose Fe = impairs AD	Pfeffer and White (1964)
AS dosed in Lab with Al	Lab-scale Digester	Al is not toxic to microorganisms	No detrimental effect	Grigoropoulos et al. (1971)
Primary and MLSS dosed in lab with Fe	Lab-scale semi-continuous bench-scale		No detrimental effect	Malhrota and Parrillo (1971)
Secondary sludge dosed at WWTP with Al	Full-scale Digester	Gas volumes were similar before and after dosing	No detrimental effect	O'Shaughnessy et al. (1974)
Primary dosed WWTP with Fe	Lab-scale, semi-continuous bench-scale	Fe-dosed sludge required longer to degrade	CPR sludge digests successfully if diluted 60%	Jack et al. (1976)
Primary dosed at pilot plant with Fe	Pilot Plant	Decrease CH_4/VS destroyed Decrease CH_4/VS fed CPR sludge contained more proteins and hence made less CH4	CPR sludge digested normally	Ghyoot and Verstraete (1997)

Appendix D- Cummulative Biogas Volume Production for Aluminium (Al^{3+}) and Ferric (Fe^{3+}) Dosed and Undosed surplus activated sludge (SAS) for (12days)

D1: Cummulative Biogas Volume Production for Aluminium (Al^{3+}) Dosed and Undosed surplus activated sludge (SAS) for (12days) sludge age (Batch 1, 2 and 3)

Digestion duration (days)	**Cummulative Biogas (mL)**	
	Undosed SAS	**Al^{3+}Dosed SAS**
0.00	0.00	0.00
1.00	3.80	3.10
2.00	7.00	5.92
3.00	10.24	8.47
4.00	13.04	10.77
5.00	15.50	12.81
6.00	18.11	14.70
7.00	20.08	16.24
8.00	21.76	17.50
9.00	24.57	19.52
10.00	27.17	21.43
11.00	29.46	23.34
12.00	31.56	24.85

D2: Cummulative Biogas Volume Production for Ferric (Fe^{3+}) Dosed and Undosed surplus activated sludge (SAS) for (12days) sludge age (Batch 1, 2 and 3)

Digestion duration (days)	**Cummulative Biogas (mL)**	
	Undosed SAS	**Fe^{3+}Dosed SAS**
0.00	0.00	0.00
1.00	4.37	1.74
2.00	9.36	5.83
3.00	14.59	9.57
4.00	18.33	12.08
5.00	21.53	14.21
6.00	24.19	15.97
7.00	26.54	17.55
8.00	28.68	18.84
9.00	30.43	19.92
10.00	31.95	20.77
11.00	33.15	21.35
12.00	34.91	22.46

List of Tables (LOT)

LOT A- Tables of the urban wastewater treatment directive, Main component of and Unit processes of Activated sludge plant

LOT A1: The Urban Wastewater Treatment Directive (91/271/EEC)

Parameter	Minimum concentration (mg/l)	Minimum percentage reduction
Biological oxygen demand (BOD)	25	70-90
Chemical oxygen demand (COD)	125	75
Suspended solids (SS)	35	90
Total phosphorus (TP)	1 (10000 to 100000 Population Equivalent-PE) and 2 (>100000PE)	80
Total nitrogen (TN)	10 (10000 to 100000PE) and 15 (>100000PE)	70-80

LOT A2: Main Component of an Activated Sludge Process (ASP) (Gray 2004)

Component	Role
Reactor	Adequate mixing and aeration and the reactor is called aeration basin.
Activated sludge	Microbial biomass within the aeration reactor which comprise of bacteria and other microfauna and flora.
Aeration/Mixing	Dual process and the incoming wastewater is vital and the aeration and mixing is achieved either by surface or diffused aeration.
Sedimentation Tank	Microbial biomass is separated from the treated effluent
Returned sludge	Settled activated sludge in the sedimentation tank is recycled back to the reactor to maintain the microbial population at a required concentration in order to ensure continuation of treatment.

LOT A3: Descriptive unit processes in activated Sludge treatment (Tchobanoglous et al. 2003)

Unit Processes	Explanation of Unit processes
Preliminary	Removal of wastewater constituents like floatables, grits, grease, rags that can cause potential operational and maintenance problems

Primary	Removal of some level of suspended solids (SS) and organic matter (OM) from the wastewater
Secondary	Removal of biodegradable OM in suspension and SS in wastewater. This unit process may also include options for nutrient removal
Tertiary	Removal of residual SS after completion of secondary treatment process.
Advanced	Removal of dissolved solids (DS) and SS for re-use application after secondary treatment

LOT B-Tables of Settling batch test results for Un-dosed/Aluminium dosed sludge (Phase 1-5)

LOT B1: Table 1 to 7 for Un-dosed and Aluminium Dosed Sludge (Phase 1)

Table 1. Un-dosed 0mg/L for ZSV and SSVI (7/11/2014) (EXP=Experimental time, CAL Time = Calculated time)

Height (cm)	EXPTime (min)	CALTime (min)	SV (mL)	MLSS (g/L)	SSV (mL/L)	SSVI (mL/g)	ZSV (m/h)
50.00	30.00	0.00	3250.00	2.68	180.00	67.2	1.60
43.00	28.00	2.00	2795.00	2.68			
39.00	26.00	4.00	2535.00	2.68			
34.00	24.00	6.00	2210.00	2.68			
29.00	22.00	8.00	1885.00	2.68			
24.00	20.00	10.00	1560.00	2.68			
18.00	15.00	15.00	1170.00	2.68			
13.00	10.00	20.00	845.00	2.68			
10.00	5.00	25.00	650.00	2.68			
9.00	0.00	30.00	585.00	2.68			

Table 2. Aluminium dosed 20 mg/L for ZSV and SSVI (7/11/2014)

Height (cm)	EXPTime (min)	CALTime (min)	SV (mL)	MLSS (g/L)	SSV (mL/L)	SSVI (mL/g)	ZSV (m/h)
50.00	30.00	0.00	3250.00	2.85	160.00	56.10	1.80
45.00	28.00	2.00	2925.00	2.85			
38.00	26.00	4.00	2470.00	2.85			
32.00	24.00	6.00	2080.00	2.85			
26.00	22.00	8.00	1690.00	2.85			
22.00	20.00	10.00	1430.00	2.85			
19.00	15.00	15.00	1235.00	2.85			
15.00	10.00	20.00	975.00	2.85			
11.00	5.00	25.00	715.00	2.85			
8.00	0.00	30.00	520.00	2.85			

Table 3. Aluminium dosed 50 mg/L for ZSV and SSVI (7/11/2014)

Height (cm)	EXPTime (min)	CALTime (min)	SV (mL)	MLSS (g/L)	SSV (mL/L)	SSVI (mL/g)	ZSV (m/h)
50.00	30.00	0.00	3250	3.15	140.00	45.20	2.04
42.00	28.00	2.00	2730	3.15			
37.00	26.00	4.00	2405	3.15			
32.00	24.00	6.00	2080	3.15			
27.00	22.00	8.00	1755	3.15			
23.00	20.00	10.00	1495	3.15			
18.00	15.00	15.00	1170	3.15			
14.00	10.00	20.00	910	3.15			
10.00	5.00	25.00	650	3.15			
7.00	0.00	30.00	455	3.15			

Table 4. Aluminium dosed 100 mg/L for ZSV and SSVI (7/11/2014)

Height (cm)	EXP Time (min)	CALTime (min)	SV (mL)	MLSS (g/L)	SSV (mL/L)	SSVI (mL/g)	ZSV (m/h)
50.00	30.00	0.00	3250.00	3.30	170.00	51.50	1.85
44.00	28.00	2.00	2860.00	3.30			
37.00	26.00	4.00	2405.00	3.30			
31.00	24.00	6.00	2015.00	3.30			
25.00	22.00	8.00	1625.00	3.30			
20.00	20.00	10.00	1300.00	3.30			
17.00	15.00	15.00	1105.00	3.30			
14.00	10.00	20.00	910.00	3.30			
12.00	5.00	25.00	780.00	3.30			
8.50	0.00	30.00	553.00	3.30			

Table 5. Aluminium dosed 150 mg/L for ZSV and SSVI (7/11/2014)

Height (cm)	EXPTime (min)	CALTime (min)	SV (mL)	MLSS (g/L)	SSV (mL/L)	SSVI (mL/g)	ZSV (m/h)
50.00	30.00	0.00	3250.00	3.50	190.00	54.30	1.74
43.00	28.00	2.00	2795.00	3.50			
39.00	26.00	4.00	2535.00	3.50			
34.00	24.00	6.00	2210.00	3.50			
30.00	22.00	8.00	1950.00	3.50			
27.00	20.00	10.00	1755.00	3.50			
22.00	15.00	15.00	1430.00	3.50			
19.00	10.00	20.00	1235.00	3.50			
15.00	5.00	25.00	975.00	3.50			
9.50	0.00	30.00	618.00	3.50			

Table 6. Aluminium dosed 200 mg/L for ZSV and SSVI (7/11/2014)

Height (cm)	EXPTime (min)	CALTime (min)	SV (ml)	MLSS (g/L)	SSV (mL/L)	SSVI (mL/g)	ZSV (m/h)
50.00	30.00	0.00	3250.00	3.70	220.00	59.00	1.60
44.00	28.00	2.00	2860.00	3.70			
39.00	26.00	4.00	2535.00	3.70			
34.00	24.00	6.00	2210.00	3.70			

29.00	22.00	8.00	1885.00	3.70			
25.00	20.00	10.00	1625.00	3.70			
21.00	15.00	15.00	1365.00	3.70			
17.00	10.00	20.00	1105.00	3.70			
13.00	5.00	25.00	845.00	3.70			
11.00	0.00	30.00	715.00	3.70			

Table 7. Aluminium dosed 250 mg/L for ZSV and SSVI (7/11/2014)

Height (cm)	EXPTime (min)	CALTime (min)	SV (mL)	MLSS (g/L)	SSV (mL/L)	SSVI (mL/g)	ZSV (m/h)
50.00	30.00	0.00	3250.00	3.95	260.00	65.82	1.50
45.00	28.00	2.00	2925.00	3.95			
40.00	26.00	4.00	2600.00	3.95			
35.00	24.00	6.00	2275.00	3.95			
30.00	22.00	8.00	1950.00	3.95			
25.00	20.00	10.00	1625.00	3.95			
20.00	15.00	15.00	1300.00	3.95			
17.00	10.00	20.00	1105.00	3.95			
15.00	5.00	25.00	975.00	3.95			
13.00	0.00	30.00	845.00	3.95			

LOT B2: Table 8 to 14 for Un-dosed and Aluminium Dosed Sludge (Phase 2)(EXP=Experimental time, CAL Time = Calculated time)

Table 8. Un-dosed 0mg/L for ZSV and SSVI (4/12/2014)

Height (cm)	EXPTime (min)	CALTime (min)	SV (mL)	MLSS (g/L)	SSV (mL/L)	SSVI (mL/g)	ZSV (m/h)
50.00	30.00	0.00	3250.00	2.84	150.00	52.82	1.50
45.00	28.00	2.00	2925.00	2.84			
40.00	26.00	4.00	2600.00	2.84			
35.00	24.00	6.00	2275.00	2.84			
30.00	22.00	8.00	1950.00	2.84			
25.00	20.00	10.00	1625.00	2.84			
20.00	15.00	15.00	1300.00	2.84			
15.00	10.00	20.00	975.00	2.84			
10.00	5.00	25.00	650.00	2.84			
7.5.00	0.00	30.00	487.50	2.84			

Table 9. Aluminium dosed 20 mg/L for ZSV and SSVI (4/12/2014)

Height (cm)	EXPTime (min)	CALTime (min)	SV (mL)	MLSS (g/L)	SSV (mL/L)	SSVI (mL/g)	ZSV (m/h)
50.00	30.00	0.00	3250.00	2.96	140.00	47.30	1.70
44.00	28.00	2.00	2860.00	2.96			
39.00	26.00	4.00	2535.00	2.96			
33.00	24.00	6.00	2145.00	2.96			
27.00	22.00	8.00	1755.00	2.96			
23.00	20.00	10.00	1495.00	2.96			
19.00	15.00	15.00	1235.00	2.96			
14.00	10.00	20.00	910.00	2.96			

10.00	5.00	25.00	650.00	2.96			
7.00	0.00	30.00	455.00	2.96			

Table 10. Aluminium dosed 50 mg/L for ZSV and SSVI (4/12/2014)

Height (cm)	EXPTime (min)	CALTime (min)	SV (mL)	MLSS (g/L)	SSV (mL/L)	SSVI (mL/g)	ZSV (m/h)
49.00	30.00	0.00	3250.00	3.11	122.50	39.40	1.93
43.00	28.00	2.00	2852.00	3.11			
37.00	26.00	4.00	2454.00	3.11			
31.00	24.00	6.00	2056,00	3.11			
26.00	22.00	8.00	1724.00	3.11			
22.00	20.00	10.00	1459.00	3.11			
17.00	15.00	15.00	1127.00	3.11			
14.00	10.00	20.00	928.00	3.11			
10.00	5.00	25.00	663.00	3.11			
6.00	0.00	30.00	398.00	3.11			

Table 11. Aluminium dosed 100 mg/L for ZSV and SSVI (4/12/2014)

Height (cm)	EXPTime (min)	CALTime (min)	SV (mL)	MLSS (g/L)	SSV (mL/L)	SSVI (mL/g)	ZSV (m/h)
50.00	30.00	0.00	3250.00	3.30	160.00	48.50	1.73
44.00	28.00	2.00	2860.00	3.30			
37.00	26.00	4.00	2405.00	3.30			
32.00	24.00	6.00	2080.00	3.30			
27.00	22.00	8.00	1755.00	3.30			
22.00	20.00	10.00	1430.00	3.30			
17.00	15.00	15.00	1105.00	3.30			
13.00	10.00	20.00	845.00	3.30			
10.00	5.00	25.00	650.00	3.30			
8.00	0.00	30.00	520.00	3.30			

Table 12. Aluminium dosed 150 mg/L for ZSV and SSVI (4/12/2014)

Height (cm)	EXP Time (min)	CALTime (min)	SV (mL)	MLSS (g/L)	SSV (mL/L)	SSVI (mL/g)	ZSV (m/h)
49.00	30.00	0.00	3250.00	3.50	184.00	52.57	1.66
43.00	28.00	2.00	2852.00	3.50			
37.00	26.00	4.00	2454.00	3.50			
32.00	24.00	6.00	2122.00	3.50			
27.00	22.00	8.00	1791.00	3.50			
22.00	20.00	10.00	1459.00	3.50			
17.00	15.00	15.00	1128.00	3.50			
13.00	10.00	20.00	862.00	3.50			
10.00	5.00	25.00	663.00	3.50			
9.00	0.00	30.00	597.00	3.50			

Table 13. Aluminium dosed 200 mg/L for ZSV and SSVI (4/12/2014)

Height	EXPTime	CALTime	SV	MLSS	SSV	SSVI	ZSV

(cm)	(min)	(min)	(mL)	(g/L)	(mL/L)	(mL/g)	(m/h)
49.00	30.00	0.00	3250.00	3.60	204.00	58.30	1.50
44.00	28.00	2.00	2918.00	3.60			
39.00	26.00	4.00	2587.00	3.60			
34.00	24.00	6.00	2255.00	3.60			
29.00	22.00	8.00	1923.00	3.60			
24.00	20.00	10.00	1592.00	3.60			
20.00	15.00	15.00	1327.00	3.60			
16.00	10.00	20.00	1061.00	3.60			
12.00	5.00	25.00	796.00	3.60			
10.00	0.00	30.00	663.00	3.60			

Table 14. Aluminium dosed 250 mg/L for ZSV and SSVI (4/12/2014)

Height (cm)	EXPTime (min)	CALTime (min)	SV (mL)	MLSS (g/L)	SSV (mL/L)	SSVI (mL/g)	ZSV (m/h)
50.00	30.00	0.00	3250	3.70	220.00	59.50	1.20
46.00	28.00	2.00	2990	3.70			
42.00	26.00	4.00	2730	3.70			
38.00	24.00	6.00	2470	3.70			
34.00	22.00	8.00	2210	3.70			
30.00	20.00	10.00	1950	3.70			
24.00	15.00	15.00	1560	3.70			
18.00	10.00	20.00	1170	3.70			
13.00	5.00	25.00	845	3.70			
11.00	0.00	30.00	715	3.70			

LOT B3: Table 15 to 21 for Un-dosed and Aluminium Dosed Sludge (Phase 3) (EXP=Experimental time, CAL Time = Calculated time)

Table 15. Un-dosed 0mg/L for ZSV and SSVI (9/12/2014)

Height (cm)	EXPTime (min)	CALTime (min)	SV (mL)	MLSS (g/L)	SSV (mL/L)	SSVI (mL/g)	ZSV (m/h)
48.00	30.00	0.00	3250.00	2.50	188.00	75.00	1.60
42.00	28.00	2.00	2844.00	2.50			
37.00	26.00	4.00	2505.00	2.50			
32.00	24.00	6.00	2167.00	2.50			
27.00	22.00	8.00	1828.00	2.50			
23.00	20.00	10.00	1557.00	2.50			
15.00	15.00	15.00	1016.00	2.50			
12.00	10.00	20.00	813.00	2.50			
10.00	5.00	25.00	678.00	2.50			
9.00	0.00	30.00	610.00	2.50			

Table 16. Aluminium dosed 20mg/L for ZSV and SSVI (9/12/2014)

Height (cm)	EXPTime (min)	CALTime (min)	SV (mL)	MLSS (g/L)	SSV (mL/L)	SSVI (mL/g)	ZSV (m/h)
49.50	30.00	0.00	3250.00	2.65	162.00	61.13	1.70
43.00	28.00	2.00	2823.00	2.65			
38.00	26.00	4.00	2495.00	2.65			

33.00	24.00	6.00	2167.00	2.65
28.00	22.00	8.00	1838.00	2.65
23.00	20.00	10.00	1510.00	2.65
17.00	15.00	15.00	1116.00	2.65
13.00	10.00	20.00	854.00	2.65
11.00	5.00	25.00	723.00	2.65
8.00	0.00	30.00	526.00	2.65

Table 17. Aluminium dosed 50mg/L for ZSV and SSVI (9/12/2014)

Height (cm)	EXPTime (min)	CALTime (min)	SV (mL)	MLSS (g/L)	SSV (mL/L)	SSVI (mL/g)	ZSV (m/h)
50.00	30.00	0.00	3250.00	2.80	140.00	52.20	1.90
44.00	28.00	2.00	2860.00	2.80			
37.00	26.00	4.00	2405.00	2.80			
31.00	24.00	6.00	2015.00	2.80			
26.00	22.00	8.00	1690.00	2.80			
22.00	20.00	10.00	1430.00	2.80			
17.00	13.00	15.00	1105.00	2.80			
12.00	9.00	20.00	780.00	2.80			
9.00	6.00	25.00	585.00	2.80			
7.00	0.00	30.00	455.00	2.80			

Table 18. Aluminium dosed 100mg/L for ZSV and SSVI (9/12/2014)

Height (cm)	EXPTime (min)	CALTime (min)	SV (mL)	MLSS (g/L)	SSV (mL/L)	SSVI (mL/g)	ZSV (m/h)
50.00	30.00	0.00	3250.00	2.90	164.00	57.00	1.80
44.00	28.00	2.00	2860.00	2.90			
38.00	26.00	4.00	2470.00	2.90			
32.00	24.00	6.00	2080.00	2.90			
26.00	22.00	8.00	1690.00	2.90			
22.00	20.00	10.00	1430.00	2.90			
18.00	15.00	15.00	957.00	2.90			
14.00	10.00	20.00	745.00	2.90			
12.00	5.00	25.00	639.00	2.90			
10.00	0.00	30.00	534.00	2.90			

Table 19. Aluminium dosed 150mg/L for ZSV and SSVI (9/12/2014)

Height (cm)	EXPTime (min)	CALTime (min)	SV (mL)	MLSS (g/L)	SSV (mL/L)	SSVI (mL/g)	ZSV (m/h)
50.00	30.00	0.00	3250.00	3.10	240.00	77.00	1.60
44.00	28.00	2.00	2860.00	3.10			
40.00	26.00	4.00	2600.00	3.10			
35.00	24.00	6.00	2275.00	3.10			
30.00	22.00	8.00	1950.00	3.10			
27.00	20.00	10.00	1755.00	3.10			
23.00	15.00	15.00	1495.00	3.10			
18.00	10.00	20.00	1170.00	3.10			
15.00	5.00	25.00	975.00	3.10			

12.00	0.00	30.00	780.00	3.10			

Table 20. Aluminium dosed 200mg/L for ZSV and SSVI (9/12/2014)

Height (cm)	EXP Time (min)	CALTime (min)	SV (mL)	MLSS (g/L)	SSV (mL/L)	SSVI (mL/g)	ZSV (m/h)
50.00	30.00	0.00	3250.00	3.35	260.00	84.00	1.50
45.00	28.00	2.00	2925.00	3.35			
40.00	26.00	4.00	2600.00	3.35			
35.00	24.00	6.00	2275.00	3.35			
30.00	22.00	8.00	1950.00	3.35			
25.00	20.00	10.00	1625.00	3.35			
23.00	15.00	15.00	1495.00	3.35			
19.00	10.00	20.00	1235.00	3.35			
16.00	5.00	25.00	1040.00	3.35			
14.00	0.00	30.00	910.00	3.35			

Table 21. Aluminium dosed 250mg/L for ZSV and SSVI (9/12/2014)

Height (cm)	EXP Time (min)	CALTime (min)	SV (mL)	MLSS (g/L)	SSV (mL/L)	SSVI (mL/g)	ZSV (m/h)
49.50	30.00	0.00	3250.00	3.64	323.00	89.00	1.30
46.00	28.00	2.00	3020.00	3.64			
42.00	26.00	4.00	2758.00	3.64			
36.00	24.00	6.00	2364.00	3.64			
32.00	22.00	8.00	2101.00	3.64			
28.00	20.00	10.00	1838.00	3.64			
24.00	15.00	15.00	1575.00	3.64			
21.00	10.00	20.00	1379.00	3.64			
19.00	5.00	25.00	1247.00	3.64			
16.00	0.00	30.00	1051.00	3.64			

LOT B4: Table 22 to 26 for Un-dosed and Aluminium Dosed Sludge (Phase 4) (EXP=Experimental time, CAL Time = Calculated time)

Table 22. Un-dosed 0mg/L for ZSV and SSVI (1/03/2016)

Height (cm)	EXPTime (min)	CALTime (min)	SV (mL)	MLSS (g/L)	SSV (mL/L)	SSVI (mL/g)	ZSV (m/h)
50.00	30.00	0.00	3250.00	2.20	240.00	109.00	1.46
45.00	28.00	2.00	2925.00	2.20			
41.00	26.00	4.00	2665.00	2.20			
35.00	24.00	6.00	2275.00	2.20			
30.00	22.00	8.00	1950.00	2.20			
26.00	20.00	10.00	1690.00	2.20			
22.00	15.00	15.00	1430.00	2.20			
18.00	10.00	20.00	1170.00	2.20			
14.00	5.00	25.00	910.00	2.20			
12.00	0.00	30.00	780.00	2.20			

Table 23. Aluminium dosed 20mg/L for ZSV and SSVI (1/03/2016)

Height (cm)	EXPTime (min)	CALTime (min)	SV (mL)	MLSS (g/L)	SSV (mL/L)	SSVI (mL/g)	ZSV (m/h)

50.00	30.00	0.00	3250.00	2.65	220.00	90.43	1.76
46.00	28.00	2.00	2990.00	2.65			
38.00	26.00	4.00	2470.00	2.65			
32.00	24.00	6.00	2080.00	2.65			
28.00	22.00	8.00	1820.00	2.65			
26.00	20.00	10.00	1690.00	2.65			
22.00	15.00	15.00	1430.00	2.65			
19.00	10.00	20.00	1235.00	2.65			
15.00	5.00	25.00	975.00	2.65			
11.00	0.00	30.00	715.00	2.65			

Table 24. Aluminium dosed 50mg/L for ZSV and SSVI (1/03/2016)

Height (cm)	EXPTime (min)	CALTime (min)	SV (mL)	MLSS (g/L)	SSV (mL/L)	SSVI (mL/g)	ZSV (m/h)
50.00	30.00	0.00	3250.00	2.80	200.00	71.43	2.60
41.00	28.00	2.00	2665.00	2.80			
33.00	26.00	4.00	2145.00	2.80			
29.00	24.00	6.00	1885.00	2.80			
25.00	22.00	8.00	1625.00	2.80			
22.00	20.00	10.00	1430.00	2.80			
19.00	15.00	15.00	1235.00	2.80			
16.00	10.00	20.00	1040.00	2.80			
13.00	5.00	25.00	845.00	2.80			
10.00	0.00	30.00	650.00	2.80			

Table 25. Aluminium dosed 100mg/L for ZSV and SSVI (1/03/2016)

Height (cm)	EXPTime (min)	CALTime (min)	SV (mL)	MLSS (g/L)	SSV (mL/L)	SSVI (mL/g)	ZSV (m/h)
50.00	30.00	0.00	3250.00	3.00	260.00	86.70	2.40
40.00	28.00	2.00	2600.00	3.00			
35.00	26.00	4.00	2275.00	3.00			
30.00	24.00	6.00	1950.00	3.00			
27.00	22.00	8.00	1755.00	3.00			
24.00	20.00	10.00	1560.00	3.00			
21.00	15.00	15.00	1365.00	3.00			
18.00	10.00	20.00	1170.00	3.00			
15.00	5.00	25.00	975.00	3.00			
13.00	0.00	30.00	845.00	3.00			

Table 26. Aluminium dosed 150mg/L for ZSV and SSVI (1/03/2016)

Height (cm)	EXPTime (min)	CALTime (min)	SV (mL)	MLSS (g/L)	SSV (mL/L)	SSVI (mL/g)	ZSV (m/h)
50.00	30.00	0.00	3250.00	3.25	300.00	92.31	2.10
42.00	28.00	2.00	2730.00	3.25			
36.00	26.00	4.00	2340.00	3.25			
30.00	24.00	6.00	1950.00	3.25			
27.00	22.00	8.00	1755.00	3.25			

24.00	20.00	10.00	1560.00	3.25
21.00	15.00	15.00	1365.00	3.25
19.00	10.00	20.00	1235.00	3.25
17.00	5.00	25.00	1105.00	3.25
15.00	0.00	30.00	975.00	3.25

LOT B5: Table 27 to 31 for Un-dosed and Aluminium Dosed Sludge (Phase 5) (EXP=Experimental time, CAL Time = Calculated time)

Table 27. Un-dosed 0mg/L for ZSV and SSVI (2/06/2016)

Height (cm)	EXPTime (min)	CALTime (min)	SV (mL)	MLSS (g/L)	SSV (mL/L)	SSVI (mL/g)	ZSV (m/h)
50.00	30.00	0.00	3250	2.40	320	133.33	1.30
46.00	28.00	2.00	2990	2.40			
41.00	26.00	4.00	2665	2.40			
37.00	24.00	6.00	2405	2.40			
32.00	22.00	8.00	2080	2.40			
28.00	20.00	10.00	1820	2.40			
25.00	15.00	15.00	1625	2.40			
22.00	10.00	20.00	1430	2.40			
19.00	5.00	25.00	1235	2.40			
16.00	0.00	30.00	1040	2.40			

Table 28. Aluminium dosed 20mg/L for ZSV and SSVI (2/06/2016)

Height (cm)	EXPTime (min)	CALTime (min)	SV (mL)	MLSS (g/L)	SSV (mL/L)	SSVI (mL/g)	ZSV (m/h)
50.00	30.00	0.00	3250.00	2.55	280.00	109.80	1.60
46.00	28.00	2.00	2990.00	2.55			
38.00	26.00	4.00	2470.00	2.55			
32.00	24.00	6.00	2080.00	2.55			
28.00	22.00	8.00	1820.00	2.55			
26.00	20.00	10.00	1690.00	2.55			
23.00	15.00	15.00	1495.00	2.55			
20.00	10.00	20.00	1300.00	2.55			
17.00	5.00	25.00	1105.00	2.55			
14.00	0.00	30.00	910.00	2.55			

Table 29. Aluminium dosed 50mg/L for ZSV and SSVI (2/06/2016)

Height (cm)	EXP Time (min)	CALTime (min)	SV (mL)	MLSS (g/L)	SSV (mL/L)	SSVI (mL/g)	ZSV (m/h)
50.00	30.00	0.00	3250.00	2.75	240.00	87.30	2.10
43.00	28.00	2.00	2795.00	2.75			
35.00	26.00	4.00	2275.00	2.75			
29.00	24.00	6.00	1885.00	2.75			
25.00	22.00	8.00	1625.00	2.75			
22.00	20.00	10.00	1430.00	2.75			
19.00	15.00	15.00	1235.00	2.75			
17.00	10.00	20.00	1105.00	2.75			
15.00	5.00	25.00	975.00	2.75			

12.00	0.00	30.00	780.00	2.75

Table 30. Aluminium dosed 100mg/L for ZSV and SSVI (2/06/2016)

Height (cm)	EXPTime (min)	CALTime (min)	SV (mL)	MLSS (g/L)	SSV (mL/L)	SSVI (mL/g)	ZSV (m/h)
50.00	30.00	0.00	3250.00	2.94	300.00	102.00	2.50
41.00	28.00	2.00	2665.00	2.94			
34.00	26.00	4.00	2210.00	2.94			
29.00	24.00	6.00	1885.00	2.94			
26.00	22.00	8.00	1690.00	2.94			
23.00	20.00	10.00	1495.00	2.94			
21.00	15.00	15.00	1365.00	2.94			
19.00	10.00	20.00	1235.00	2.94			
17.00	5.00	25.00	1105.00	2.94			
15.00	0.00	30.00	975.00	2.94			

Table 31. Aluminium dosed 150mg/L for ZSV and SSVI (2/06/2016)

Height (cm)	EXPTime (min)	CALTime (min)	SV (mL)	MLSS (g/L)	SSV (mL/L)	SSVI (mL/g)	ZSV (m/h)
50.00	30.00	0.00	3250.00	3.15	340.00	108.00	1.50
45.00	28.00	2.00	2925.00	3.15			
40.00	26.00	4.00	2600.00	3.15			
35.00	24.00	6.00	2275.00	3.15			
30.00	22.00	8.00	1950.00	3.15			
27.00	20.00	10.00	1755.00	3.15			
24.00	15.00	15.00	1560.00	3.15			
21.00	10.00	20.00	1365.00	3.15			
19.00	5.00	25.00	1235.00	3.15			
17.00	0.00	30.00	1105.00	3.15			

LOT C- Tables of Settling batch test results for un-dosed and Ferric dosed sludge (Phase 1 -3)

LOT C1: Table 1 to 7 for Un-dosed and Ferric Dosed Sludge (Phase 1) (EXP=Experimental time, CAL Time = Calculated time)

Table 1. Un-dosed 0mg/L for ZSV and SSVI (7/11/2014)

Height (cm)	EXPTime (min)	CALTime (min)	SV (mL)	MLSS (g/L)	SSV (mL/L)	SSVI (mL/g)	ZSV (m/h)
47.30	30.00	0.00	3250.00	2.50	158.50	60.24	1.53
42.00	28.00	2.00	2886.00	2.50			
37.00	26.00	4.00	2542.00	2.50			
32.00	24.00	6.00	2199.00	2.50			
27.00	22.00	8.00	1855.00	2.50			
23.00	20.00	10.00	1580.00	2.50			
15.00	15.00	15.00	1031.00	2.50			
12.00	10.00	20.00	825.00	2.50			
10.00	5.00	25.00	687.00	2.50			
7.5.00	0.00	30.00	515.00	2.50			

Table 2. Ferric dosed 20mg/L for ZSV and SSVI (7/11/2014)

Height (cm)	EXP Time (min)	CALTime (min)	SV (mL)	MLSS (g/L)	SSV (mL/L)	SSVI (mL/g)	ZSV (m/h)
49.60	30.00	0.00	3250.00	2.68	131.00	53.30	1.67
44.00	28.00	2.00	2883.00	2.68			
38.00	26.00	4.00	2490.00	2.68			
33.00	24.00	6.00	2162.00	2.68			
28.00	22.00	8.00	1835.00	2.68			
24.00	20.00	10.00	1573.00	2.68			
18.00	15.00	15.00	1179.00	2.68			
13.00	10.00	20.00	852.00	2.68			
10.00	5.00	25.00	655.00	2.68			
6.50	0.00	30.00	426.00	2.68			

Table 3. Ferric dosed 50mg/L for ZSV and SSVI (7/11/2014)

Height (cm)	EXPTime (min)	CALTime (min)	SV (mL)	MLSS (g/L)	SSV (mL/L)	SSVI (mL/g)	ZSV (m/h)
50.00	30.00	0.00	3250.00	2.80	120.00	41.80	1.89
44.00	28.00	2.00	2860.00	2.80			
37.00	26.00	4.00	2405.00	2.80			
31.00	24.00	6.00	2015.00	2.80			
26.00	22.00	8.00	1690.00	2.80			
22.00	20.00	10.00	1430.00	2.80			
17.00	13.00	14.00	1105.00	2.80			
13.00	9.00	19.00	845.00	2.80			
10.00	6.00	25.00	650.00	2.80			
6.00	0.00	30.00	390.00	2.80			

Table 4. Ferric dosed 100mg/L for ZSV and SSVI (7/11/2014)

Height (cm)	EXPTime (min)	CALTime (min)	SV (mL)	MLSS (g/L)	SSV (mL/L)	SSVI (mL/g)	ZSV (m/h)
49.50	30.00	0.00	3250.00	2.72	162.00	60.00	1.70
43.00	28.00	2.00	2823.00	2.72			
38.00	26.00	4.00	2495.00	2.72			
33.00	24.00	6.00	2167.00	2.72			
28.00	22.00	8.00	1838.00	2.72			
23.00	20.00	10.00	1510.00	2.72			
17.00	15.00	15.00	1116.00	2.72			
13.00	10.00	20.00	854.00	2.72			
10.00	5.00	25.00	657.00	2.72			
8.00	0.00	30.00	526.00	2.72			

Table 5. Ferric dosed 150mg/L for ZSV and SSVI (7/11/2014)

Height (cm)	EXPTime (min)	CALTime (min)	SV (mL)	MLSS (g/L)	SSV (mL/L)	SSVI (mL/g)	ZSV (m/h)
50.00	30.00	0.00	3250.00	2.90	180.00	62.91	1.60
44.00	28.00	2.00	2860.00	2.90			

40.00	26.00	4.00	2600.00	2.90
35.00	24.00	6.00	2275.00	2.90
30.00	22.00	8.00	1950.00	2.90
27.00	20.00	10.00	1755.00	2.90
23.00	15.00	15.00	1495.00	2.90
18.00	10.00	20.00	1170.00	2.90
14.00	5.00	25.00	910.00	2.90
9.00	0.00	30.00	585.00	2.90

Table 6. Ferric dosed 200mg/L for ZSV and SSVI (7/11/2014)

Height (cm)	EXP Time (min)	CALTime (min)	SV (mL)	MLSS (g/L)	SSV (mL/L)	SSVI (mL/g)	ZSV (m/h)
50.00	30.00	0.00	3250.00	3.10	200.00	65.34	1.50
45.00	28.00	2.00	2925.00	3.10			
40.00	26.00	4.00	2600.00	3.10			
35.00	24.00	6.00	2275.00	3.10			
30.00	22.00	8.00	1950.00	3.10			
25.00	20.00	10.00	1625.00	3.10			
20.00	15.00	15.00	1300.00	3.10			
15.00	10.00	20.00	975.00	3.10			
13.00	5.00	25.00	845.00	3.10			
10.00	0.00	30.00	650.00	3.10			

Table 7. Ferric dosed 250mg/L for ZSV and SSVI (7/11/2014)

Height (cm)	EXPTime (min)	CALTime (min)	SV (mL)	MLSS (g/L)	SSV (mL/L)	SSVI (mL/g)	ZSV (m/h)
49.50	30.00	0.00	3250.00	3.30	222.00	67.11	1.30
46.00	28.00	2.00	3020.00	3.30			
42.00	26.00	4.00	2758.00	3.30			
36.00	24.00	6.00	2364.00	3.30			
32.00	22.00	8.00	2101.00	3.30			
28.00	20.00	10.00	1838.00	3.30			
23.00	15.00	15.00	1510.00	3.30			
19.00	10.00	20.00	1247.00	3.30			
14.00	5.00	25.00	919.00	3.30			
11.00	0.00	30.00	722.00	3.30			

LOT C2: Table 8 to 14 for Un-dosed and Ferric Dosed Sludge (Phase 2) (EXP=Experimental time, CAL Time = Calculated time)

Table 8. Un-dosed 0mg/L for ZSV and SSVI (15/12/2014)

Height (cm)	EXPTime (min)	CALTime (min)	SV (mL)	MLSS (g/L)	SSV (mL/L)	SSVI (mL/g)	ZSV (m/h)
50.00	30.00	0.00	3250.00	2.45	160.00	65.60	1.60
45.00	28.00	2.00	2925.00	2.45			
40.00	26.00	4.00	2600.00	2.45			
35.00	24.00	6.00	2275.00	2.45			
30.00	22.00	8.00	1950.00	2.45			
25.00	20.00	10.00	1625.00	2.45			

20.00	15.00	15.00	1300.00	2.45
15.00	10.00	20.00	975.00	2.45
10.00	5.00	25.00	650.00	2.45
8.00	0.00	30.00	520.00	2.45

Table 9. Ferric dosed 20mg/L for ZSV and SSVI (15/12/2014)

Height (cm)	EXPTime (min)	CALTime (min)	SV (mL)	MLSS (g/L)	SSV (mL/L)	SSVI (mL/g)	ZSV (m/h)
50.00	30.00	0.00	3250.00	2.75	150.00	58.80	1.73
44.00	28.00	2.00	2860.00	2.75			
38.00	26.00	4.00	2470.00	2.75			
32.00	24.00	6.00	2080.00	2.75			
27.00	22.00	8.00	1755.00	2.75			
22.00	20.00	10.00	1430.00	2.75			
18.00	15.00	15.00	1170.00	2.75			
15.00	10.00	20.00	975.00	2.75			
13.00	5.00	25.00	845.00	2.75			
7.50	0.00	30.00	488.00	2.75			

Table 10. Ferric dosed 50mg/L for ZSV and SSVI (15/12/2014)

Height (cm)	EXPTime (min)	CALTime (min)	SV (mL)	MLSS (g/L)	SSV (mL/L)	SSVI (mL/g)	ZSV (m/h)
50.00	30.00	0.00	3250.00	2.90	140.00	48.00	2.00
44.00	28.00	2.00	2860.00	2.90			
37.00	26.00	4.00	2405.00	2.90			
31.00	24.00	6.00	2015.00	2.90			
26.00	22.00	8.00	1690.00	2.90			
22.00	20.00	10.00	1430.00	2.90			
17.00	13.00	14.00	1105.00	2.90			
13.00	9.00	19.00	845.00	2.90			
10.00	6.00	25.00	650.00	2.90			
7.00	0.00	30.00	455.00	2.90			

Table 11. Ferric dosed 100mg/L for ZSV and SSVI (15/12/2014)

Height (cm)	EXPTime (min)	CALTime (min)	SV (ml)	MLSS (g/l)	SSV (ml/l)	SSVI (ml/g)	ZSV (m/h)
50.00	30.00	0.00	3250.00	3.15	170.00	54.00	1.80
44.00	28.00	2.00	2795.00	3.15			
38.00	26.00	4.00	2535.00	3.15			
32.00	24.00	6.00	2145.00	3.15			
28.00	22.00	8.00	1820.00	3.15			
23.00	20.00	10.00	1495.00	3.15			
17.00	15.00	15.00	1105.00	3.15			
13.00	10.00	20.00	845.00	3.15			
11.00	5.00	25.00	715.00	3.15			
8.50	0.00	30.00	553.00	3.15			

Table 12. Ferric dosed 150mg/L for ZSV and SSVI (15/12/2014)

Height (cm)	EXPTime (min)	CALTime (min)	SV (mL)	MLSS (g/L)	SSV (mL/L)	SSVI (mL/g)	ZSV (m/h)
50.00	30.00	0.00	3250.00	3.25	190.00	58.50	1.70
45.00	28.00	2.00	2925.00	3.25			
38.00	26.00	4.00	2470.00	3.25			
31.00	24.00	6.00	2015.00	3.25			
27.00	22.00	8.00	1755.00	3.25			
23.00	20.00	10.00	1495.00	3.25			
18.00	15.00	15.00	1170.00	3.25			
14.00	10.00	20.00	910.00	3.25			
12.00	5.00	25.00	780.00	3.25			
9.50	0.00	30.00	618.00	3.25			

Table 13. Ferric dosed 200mg/L for ZSV and SSVI (15/12/2014)

Height (cm)	EXPTime (min)	CALTime (min)	SV (mL)	MLSS (g/L)	SSV (mL/L)	SSVI (mL/g)	ZSV (m/h)
50.00	30.00	0.00	3250.00	3.45	220.00	63.70	1.60
46.00	28.00	2.00	2990.00	3.45			
40.00	26.00	4.00	2600.00	3.45			
34.00	24.00	6.00	2210.00	3.45			
28.00	22.00	8.00	1820.00	3.45			
24.00	20.00	10.00	1560.00	3.45			
19.00	15.00	15.00	1235.00	3.45			
15.00	10.00	20.00	975.00	3.45			
13.00	5.00	25.00	845.00	3.45			
11.00	0.00	30.00	715.00	3.45			

Table 14. Ferric dosed 250mg/L for ZSV and SSVI (15/12/2014)

Height (cm)	EXPTime (min)	CALTime (min)	SV (mL)	MLSS (g/L)	SSV (mL/L)	SSVI (mL/g)	ZSV (m/h)
50.00	30.00	0.00	3250.00	3.75	260.00	69.30	1.50
46.00	28.00	2.00	2990.00	3.75			
40.00	26.00	4.00	2600.00	3.75			
35.00	24.00	6.00	2275.00	3.75			
30.00	22.00	8.00	1950.00	3.75			
24.00	20.00	10.00	1560.00	3.75			
21.00	15.00	15.00	1365.00	3.75			
18.00	10.00	20.00	1170.00	3.75			
15.00	5.00	25.00	975.00	3.75			
13.00	0.00	30.00	845.00	3.75			

LOT C3: Table 15 to 19 for Un-dosed and Ferric Dosed Sludge (Phase 3) (EXP=Experimental time, CAL Time = Calculated time)

Table 15. Un-dosed 0mg/L for ZSV and SSVI (1/03/2016)

Height (cm)	EXP Time (min)	CAL Time (min)	SV (mL)	MLSS (g/L)	SSV (mL/L)	SSVI (mL/g)	ZSV (m/h)

50.00	30.00	0.00	3250.00	2.35	180.00	77.30	1.50
45.00	28.00	2.00	2925.00	2.35			
40.00	26.00	4.00	2600.00	2.35			
35.00	24.00	6.00	2275.00	2.35			
30.00	22.00	8.00	1950.00	2.35			
25.00	20.00	10.00	1625.00	2.35			
20.00	15.00	15.00	1300.00	2.35			
15.00	10.00	20.00	975.00	2.35			
12.00	5.00	25.00	780.00	2.35			
9.00	0.00	30.00	585.00	2.35			

Table 16. Ferric dosed 20mg/L for ZSV and SSVI (1/03/2016)

Height (cm)	EXPTime (min)	CALTime (min)	SV (mL)	MLSS (g/L)	SSV (mL/L)	SSVI (mL/g)	ZSV (m/h)
50.00	30.00	0.00	3250.00	2.55	160.00	66.30	1.73
44.00	28.00	2.00	2860.00	2.55			
38.00	26.00	4.00	2470.00	2.55			
32.00	24.00	6.00	2080.00	2.55			
27.00	22.00	8.00	1755.00	2.55			
23.00	20.00	10.00	1495.00	2.55			
19.00	15.00	15.00	1235.00	2.55			
15.00	10.00	20.00	975.00	2.55			
11.00	5.00	25.00	715.00	2.55			
8.00	0.00	30.00	520.00	2.55			

Table 17. Ferric dosed 50mg/L for ZSV and SSVI (1/03/2016)

Height (cm)	EXPTime (min)	CALTime (min)	SV (mL)	MLSS (g/L)	SSV (mL/L)	SSVI (mL/g)	ZSV (m/h)
50.00	30.00	0.00	3250.00	2.76	140.00	51.84	2.10
43.00	28.00	2.00	2795.00	2.76			
36.00	26.00	4.00	2340.00	2.76			
29.00	24.00	6.00	1885.00	2.76			
22.00	22.00	8.00	1430.00	2.76			
18.00	20.00	10.00	1170.00	2.76			
15.00	15.00	15.00	975.00	2.76			
12.00	10.00	20.00	780.00	2.76			
10.00	5.00	25.00	650.00	2.76			
7.00	0.00	30.00	455.00	2.76			

Table 18. Ferric dosed 100mg/L for ZSV and SSVI (1/03/2016)

Height (cm)	EXPTime (min)	CALTime (min)	SV (mL)	MLSS (g/L)	SSV (mL/L)	SSVI (mL/g)	ZSV (m/h)
50.00	30.00	0.00	3250.00	3.00	190.00	63.70	1.86
43.00	28.00	2.00	2795.00	3.00			
38.00	26.00	4.00	2470.00	3.00			
31.00	24.00	6.00	2015.00	3.00			
27.00	22.00	8.00	1755.00	3.00			
23.00	20.00	10.00	1495.00	3.00			

18.00	15.00	15.00	1170.00	3.00
14.00	10.00	20.00	845.00	3.00
11.00	5.00	25.00	715.00	3.00
9.50	0.00	30.00	618.00	3.00

Table 19. Ferric dosed 150mg/L for ZSV and SSVI (1/03/2016)

Height (cm)	EXPTime (min)	CALTime (min)	SV (mL)	MLSS (g/L)	SSV (mL/L)	SSVI (mL/g)	ZSV (m/h)
50.00	30.00	0.00	3250.00	3.10	210.00	67.91	1.68
44.00	28.00	2.00	2860.00	3.10			
39.00	26.00	4.00	2535.00	3.10			
34.00	24.00	6.00	2210.00	3.10			
28.00	22.00	8.00	1820.00	3.10			
23.00	20.00	10.00	1495.00	3.10			
18.00	15.00	15.00	1170.00	3.10			
15.00	10.00	20.00	975.00	3.10			
12.00	5.00	25.00	780.00	3.10			
10.50	0.00	30.00	683.00	3.10			

LOT D- Tables of Settling test results for un-dosed and Calcium dosed sludge (Phase 1 -2)

LOT D1: Table 1 to 7 for Un-dosed and Calcium Dosed Sludge (Phase 1) (EXP=Experimental time, CAL Time = Calculated time)

Table 1. Un-dosed 0mg/L for ZSV and SSVI (5/12/2014)

Height (cm)	EXP Time (min)	CALTime (min)	SV (mL)	MLSS (g/L)	SSV (mL/L)	SSVI (mL/g)	ZSV (m/h)
50.00	30.00	0.00	3250.00	2.70	201.00	73.10	1.73
46.00	28.00	2.00	2990.00	2.70			
39.00	26.00	4.00	2535.00	2.70			
32.00	24.00	6.00	2318.00	2.70			
27.00	22.00	8.00	1956.00	2.70			
22.00	20.00	10.00	1594.00	2.70			
18.00	15.00	15.00	1304.00	2.70			
15.00	10.00	20.00	1087.00	2.70			
12.00	5.00	25.00	869.00	2.70			
9.00	0.00	30.00	652.00	2.70			

Table 2. Calcium dosed 20mg/L for ZSV and SSVI (5/12/2014)

Height (cm)	EXPTime (min)	CALTime (min)	SV (mL)	MLSS (g/L)	SSV (mL/L)	SSVI (mL/g)	ZSV (m/h)
50.00	30.00	0.00	3250.00	2.85	160.00	60.23	1.93
44.00	28.00	2.00	2860.00	2.85			
37.00	26.00	4.00	2405.00	2.85			
30.00	24.00	6.00	1950.00	2.85			
24.00	22.00	8.00	1560.00	2.85			
20.00	20.00	10.00	1300.00	2.85			
16.00	15.00	15.00	1040.00	2.85			
14.00	10.00	20.00	910.00	2.85			
12.00	5.00	25.00	780.00	2.85			
8.00	0.00	30.00	520.00	2.85			

Table 3. Calcium dosed 50mg/L for ZSV and SSVI (5/12/2014)

Height (cm)	EXPTime (min)	CALTime (min)	SV (mL)	MLSS (g/L)	SSV (mL/L)	SSVI (mL/g)	ZSV (m/h)
50.00	30.00	0.00	3250.00	3.05	140.00	45.46	2.30
42.00	28.00	2.00	2730.00	3.05			
35.00	26.00	4.00	2275.00	3.05			
29.00	24.00	6.00	1885.00	3.05			
25.00	22.00	8.00	1625.00	3.05			
22.00	20.00	10.00	1430.00	3.05			
19.00	15.00	15.00	1235.00	3.05			
15.00	10.00	20.00	975.00	3.05			
11.00	5.00	25.00	715.00	3.05			
7.00	0.00	30.00	455.00	3.05			

Table 4. Calcium dosed 100mg/L for ZSV and SSVI (5/12/2014)

Height (cm)	EXPTime (min)	CAL Time (min)	SV (mL)	MLSS (g/L)	SSV (mL/L)	SSVI (mL/g)	ZSV (m/h)
50.00	30.00	0.00	3250.00	3.25	170.00	52.55	1.90
43.00	28.00	2.00	2795.00	3.25			
38.00	26.00	4.00	2470.00	3.25			
31.00	24.00	6.00	2015.00	3.25			
26.00	22.00	8.00	1690.00	3.25			
22.00	20.00	10.00	1430.00	3.25			
18.00	15.00	15.00	1170.00	3.25			
15.00	10.00	20.00	975.00	3.25			
13.00	5.00	25.00	845.00	3.25			
8.50	0.00	30.00	553.00	3.25			

Table 5. Calcium dosed 150mg/L for ZSV and SSVI (5/12/2014)

Height (cm)	EXPTime (min)	CAL Time (min)	SV (mL)	MLSS (g/L)	SSV (mL/L)	SSVI (mL/g)	ZSV (m/h)
50.00	30.00	0.00	3250.00	3.45	190.00	56.04	1.78
45.00	28.00	2.00	2925.00	3.45			
38.00	26.00	4.00	2470.00	3.45			
31.00	24.00	6.00	2015.00	3.45			
26.00	22.00	8.00	1690.00	3.45			
21.00	20.00	10.00	1365.00	3.45			
17.00	15.00	15.00	1105.00	3.45			
14.00	10.00	20.00	910.00	3.45			
11.00	5.00	25.00	715.00	3.45			
9.50	0.00	30.00	618.00	3.45			

Table 6. Calcium dosed 200mg/L for ZSV and SSVI (5/12/2014)

Height (cm)	EXPTime (min)	CALTime (min)	SV (mL)	MLSS (g/L)	SSV (mL/L)	SSVI (mL/g)	ZSV (m/h)
50.00	30.00	0.00	3250.00	3.65	220.00	60.23	1.67
44.00	28.00	2.00	2860.00	3.65			
38.00	26.00	4.00	2470.00	3.65			

34.00	24.00	6.00	2210.00	3.65
28.00	22.00	8.00	1820.00	3.65
25.00	20.00	10.00	1625.00	3.65
21.00	15.00	15.00	1365.00	3.65
17.00	10.00	20.00	1105.00	3.65
14.00	5.00	25.00	910.00	3.65
11.00	0.00	30.00	715.00	3.65

Table 7. Calcium dosed 250mg/L for ZSV and SSVI (5/12/2014)

Height (cm)	EXP Time (min)	CAL Time (min)	SV (mL)	MLSS (g/L)	SSV (mL/L)	SSVI (mL/g)	ZSV (m/h)
50.00	30.00	0.00	3250.00	3.86	260.00	67.40	1.50
46.00	28.00	2.00	2990.00	3.86			
39.00	26.00	4.00	2535.00	3.86			
35.00	24.00	6.00	2275.00	3.86			
30.00	22.00	8.00	1950.00	3.86			
25.00	20.00	10.00	1625.00	3.86			
20.00	15.00	15.00	1300.00	3.86			
17.00	10.00	20.00	1105.00	3.86			
15.00	5.00	25.00	975.00	3.86			
13.00	0.00	30.00	845.00	3.86			

LOT D2: Table 8 to 12 for Un-dosed and Calcium Dosed Sludge (Phase 2) (EXP=Experimental time, CAL Time = Calculated time)

Table 8. Un-dosed 0mg/L for ZSV and SSVI (2/06/2016)

Height (cm)	EXPTime (min)	CALTime (min)	SV (mL)	MLSS (g/L)	SSV (mL/L)	SSVI (mL/g)	ZSV (m/h)
50.00	30.00	0.00	3250.00	3.00	240.00	69.12	1.70
45.00	28.00	2.00	2925.00	3.00			
38.00	26.00	4.00	2470.00	3.00			
32.00	24.00	6.00	2080.00	3.00			
26.00	22.00	8.00	1690.00	3.00			
23.00	20.00	10.00	1495.00	3.00			
20.00	15.00	15.00	1300.00	3.00			
17.00	10.00	20.00	1105.00	3.00			
14.00	5.00	25.00	910.00	3.00			
12.00	0.00	30.00	780.00	3.00			

Table 9. Calcium dosed 20mg/L for ZSV and SSVI (2/06/2016)

Height (cm)	EXPTime (min)	CALTime (min)	SV (mL)	MLSS (g/L)	SSV (mL/L)	SSVI (mL/g)	ZSV (m/h)
50.00	30.00	0.00	3250.00	3.20	200.00	65.24	1.82
47.00	28.00	2.00	3055.00	3.20			
37.00	26.00	4.00	2405.00	3.20			
30.00	24.00	6.00	1950.00	3.20			

27.00	22.00	8.00	1755.00	3.20			
24.00	20.00	10.00	1560.00	3.20			
19.00	15.00	15.00	1235.00	3.20			
16.00	10.00	20.00	1040.00	3.20			
13.00	5.00	25.00	845.00	3.20			
10.00	0.00	30.00	650.00	3.20			

Table 10. Calcium dosed 50mg/l for ZSV and SSVI (2/06/2016)

Height (cm)	EXPTime (min)	CALTime (min)	SV (mL)	MLSS (g/L)	SSV (mL/L)	SSVI (mL/g)	ZSV (m/h)
50.00	30.00	0.00	3250.00	3.40	180.00	52.54	2.01
43.00	28.00	2.00	2795.00	3.40			
37.00	26.00	4.00	2405.00	3.40			
29.00	24.00	6.00	1885.00	3.40			
26.00	22.00	8.00	1690.00	3.40			
23.00	20.00	10.00	1495.00	3.40			
19.00	15.00	15.00	1235.00	3.40			
15.00	10.00	20.00	975.00	3.40			
11.00	5.00	25.00	715.00	3.40			
9.00	0.00	30.00	585.00	3.40			

Table 11. Calcium dosed 100mg/l for ZSV and SSVI (2/06/2016)

Height (cm)	EXP Time (min)	CALTime (min)	SV (mL)	MLSS (g/L)	SSV (mL/L)	SSVI (mL/g)	ZSV (m/h)
50.00	30.00	0.00	3250.00	3.60	260.00	67.00	1.80
44.00	28.00	2.00	2730.00	3.60			
38.00	26.00	4.00	2210.00	3.60			
32.00	24.00	6.00	1820.00	3.60			
25.00	22.00	8.00	1625.00	3.60			
23.00	20.00	10.00	1495.00	3.60			
20.00	15.00	15.00	1300.00	3.60			
17.00	10.00	20.00	1105.00	3.60			
15.00	5.00	25.00	910.00	3.60			
13.00	0.00	30.00	845.00	3.60			

Table 12. Calcium dosed 150mg/l for ZSV and SSVI (2/06/2016)

Height (cm)	EXP Time (min)	CALTime (min)	SV (mL)	MLSS (g/L)	SSV (mL/L)	SSVI (mL/g)	ZSV (m/h)
50.00	30.00	0.00	3250.00	3.80	280.00	74.80	1.70
46.00	28.00	2.00	2990.00	3.80			
39.00	26.00	4.00	2535.00	3.80			
33.00	24.00	6.00	2145.00	3.80			
28.00	22.00	8.00	1820.00	3.80			
24.00	20.00	10.00	1560.00	3.80			
18.00	15.00	15.00	1365.00	3.80			
16.00	10.00	20.00	1170.00	3.80			
14.00	5.00	25.00	1040.00	3.80			
13.00	0.00	30.00	910.00	3.60			

List of Figures (LOF)

LOF A- Figures of Zone settling curves for un-dosed and Aluminium phase 1 -5

LOF A1: Figure 1 to 6 for Zone Settling Curve for un-dosed and Aluminium Dosed Sludge (Phase 1)

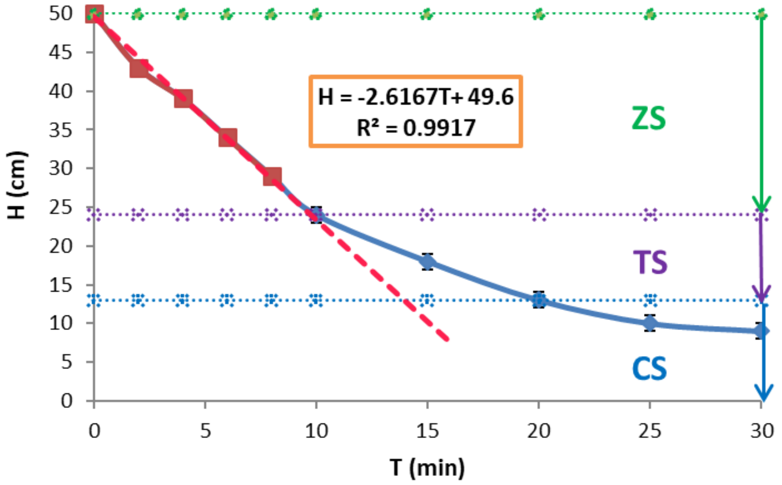

Figure 1. un-dosed 0mg/L for Zone Settling Curve (7/11/2014)

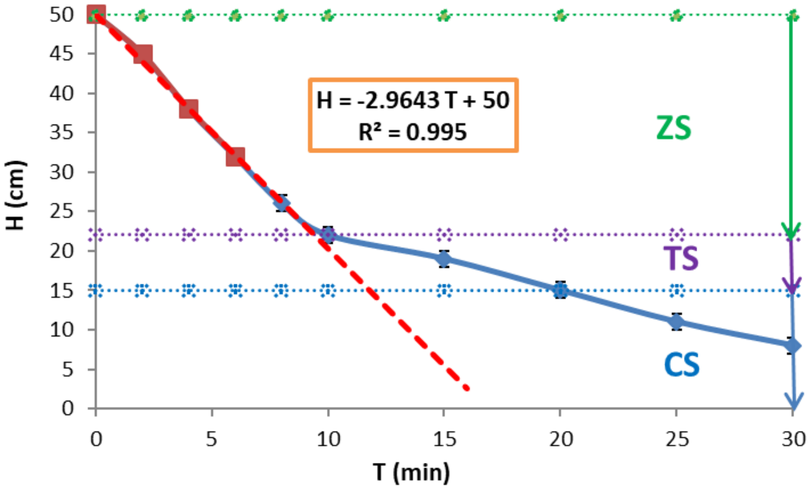

Figure 2. Aluminium dosed 20 mg/L for Zone Settling Curve (7/11/2014)

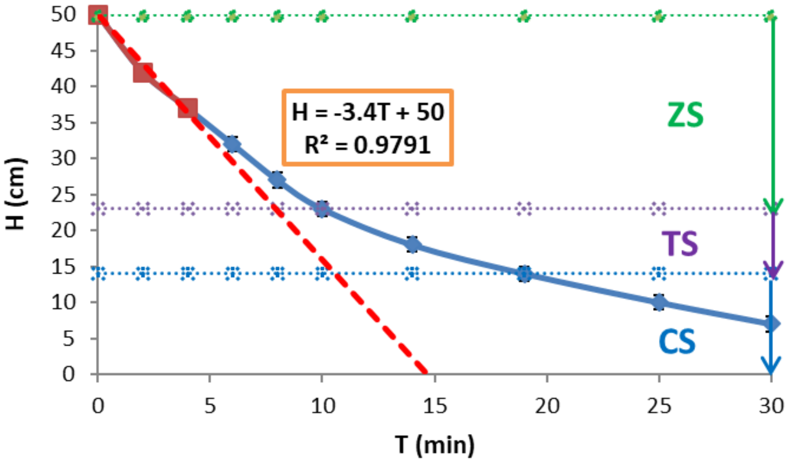

Figure 3. Aluminium dosed 50 mg/L for Zone Settling Curve (7/11/2014)

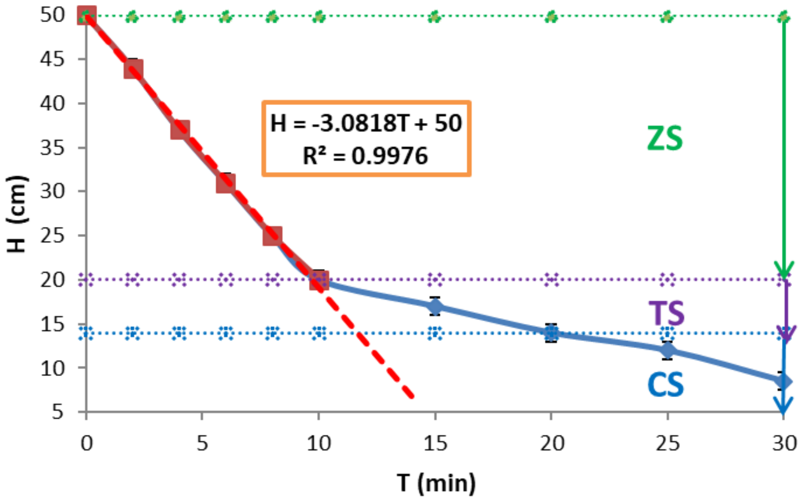

Figure 4. Aluminium dosed 100 mg/l for Zone Settling Curve (7/11/2014)

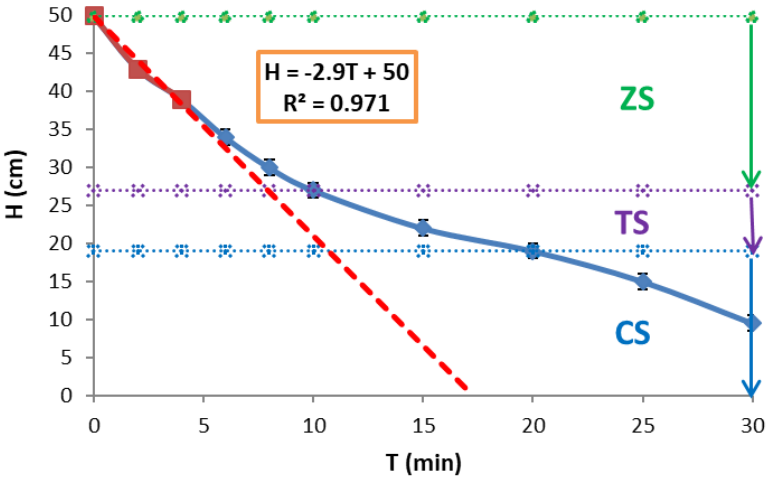

Figure 5. Aluminium dosed 150 mg/L for Zone Settling Curve (7/11/2014)

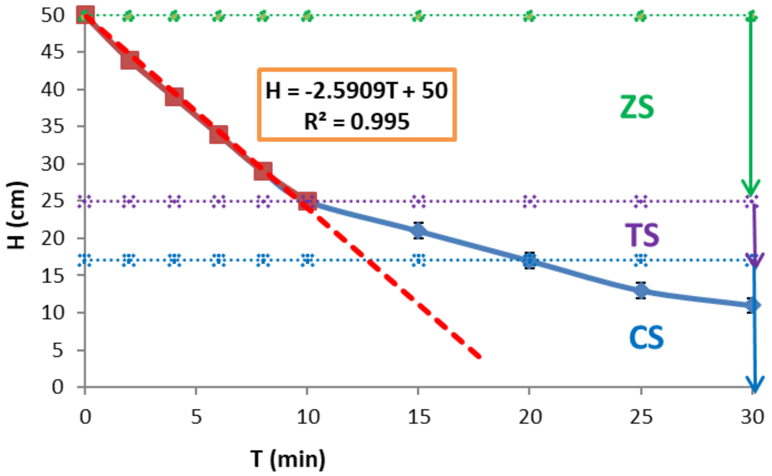

Figure 6. Aluminium dosed 200 mg/L for Zone Settling Curve (7/11/2014)

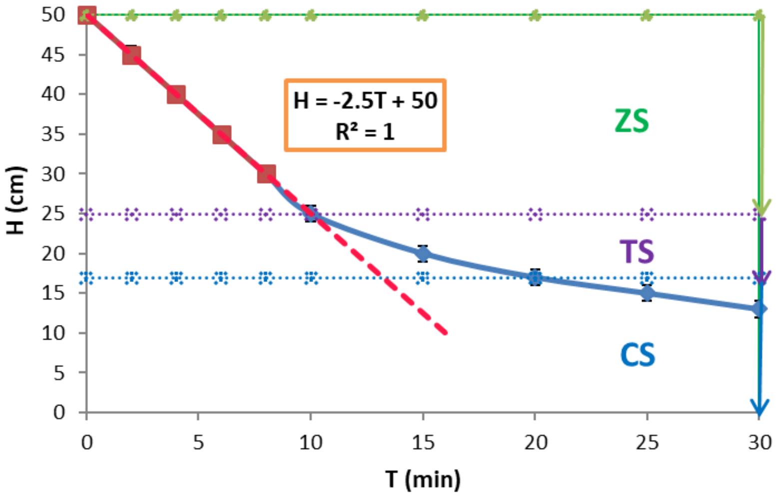

Figure 7. Aluminium dosed 250 mg/L for Zone Settling Curve (7/11/2014)

LOF A2: Figure 8 to 14 for Un-dosed and Aluminium Dosed Sludge (Phase 2)

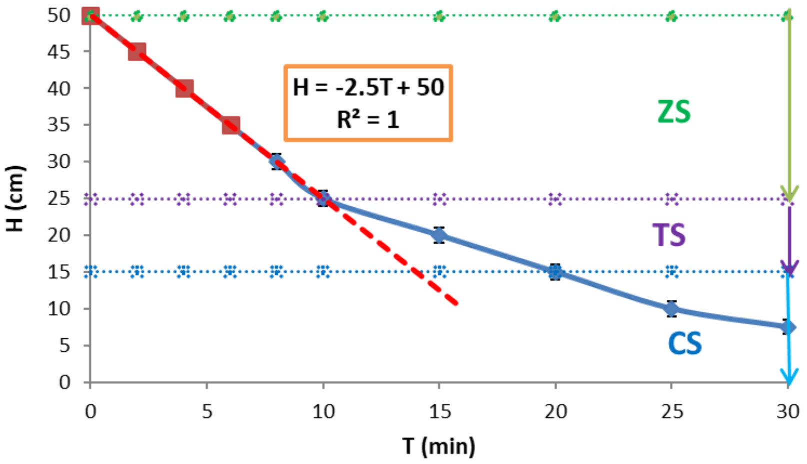

Figure 8. un-dosed 0mg/L for Zone Settling Curve (4/12/2014)

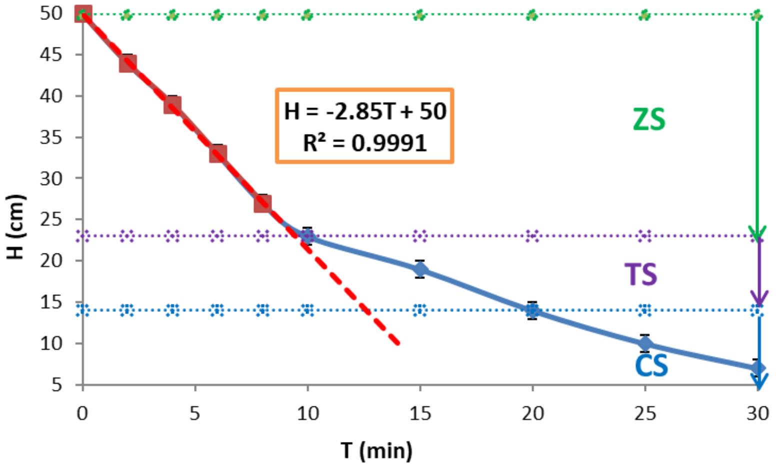

Figure 9. Aluminium dosed 20 mg/L for Zone Settling Curve (4/12/2014)

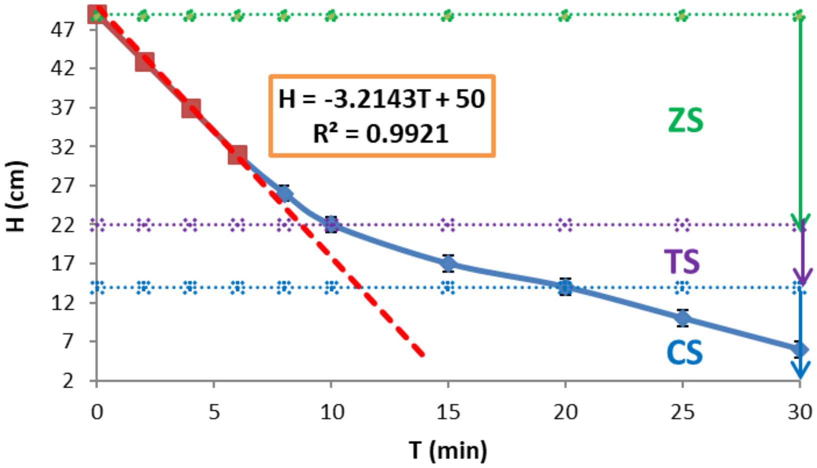

Figure 10. Aluminium dosed Dosed 50 mg/L for Zone Settling Curve (4/12/2014)

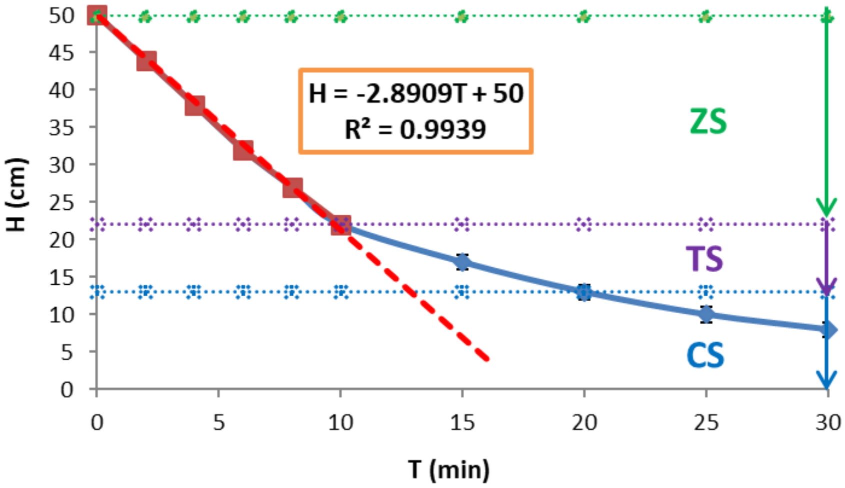

Figure 11. Aluminium dosed 100 mg/L for Zone Settling Curve (4/12/2014)

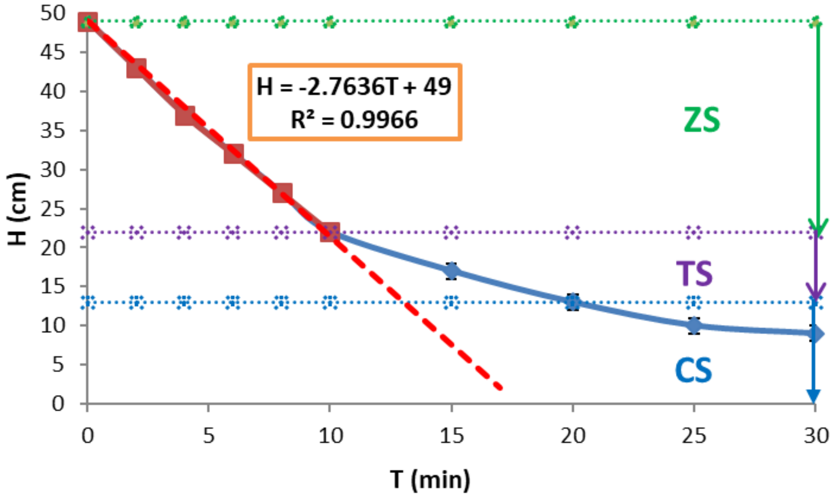

Figure 12. Aluminium dosed 150 mg/L for Zone Settling Curve (4/12/2014)

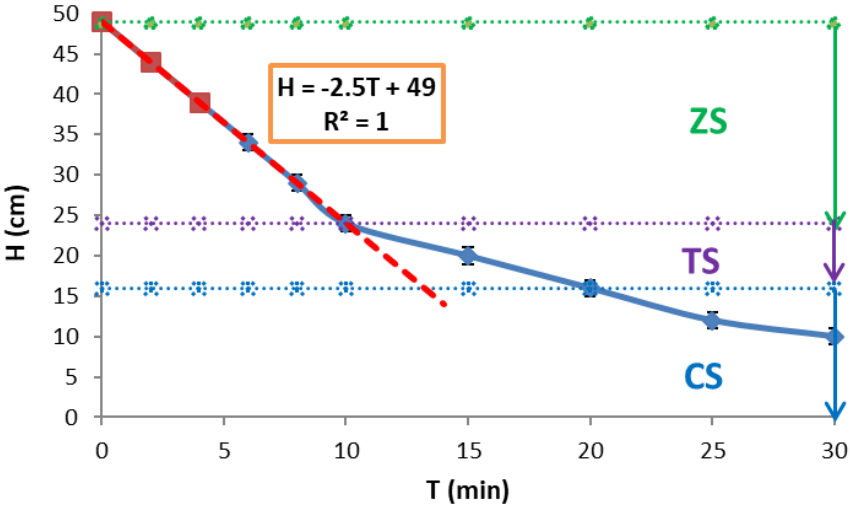

Figure 13. Aluminium dosed 200 mg/L for Zone Settling Curve (4/12/2014)

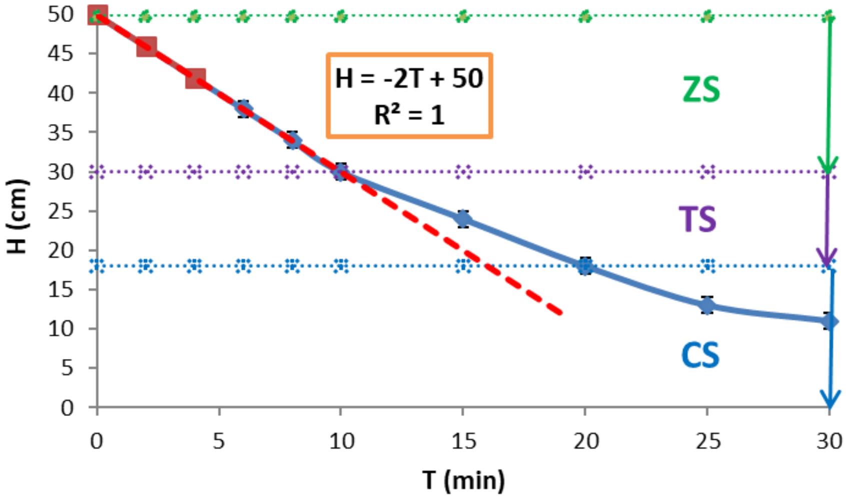

Figure 14. Aluminium dosed 250 mg/L for Zone Settling Curve (4/12/2014)

LOF A3: Figure 15 to 21 for Un-dosed and Aluminium Dosed Sludge (Phase 3)

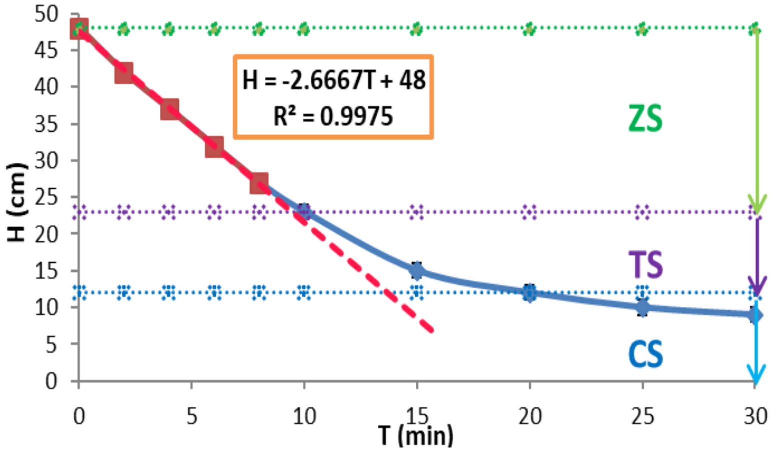

Figure 15. un-dosed 0mg/L for Zone Settling Curve (9/12/2014)

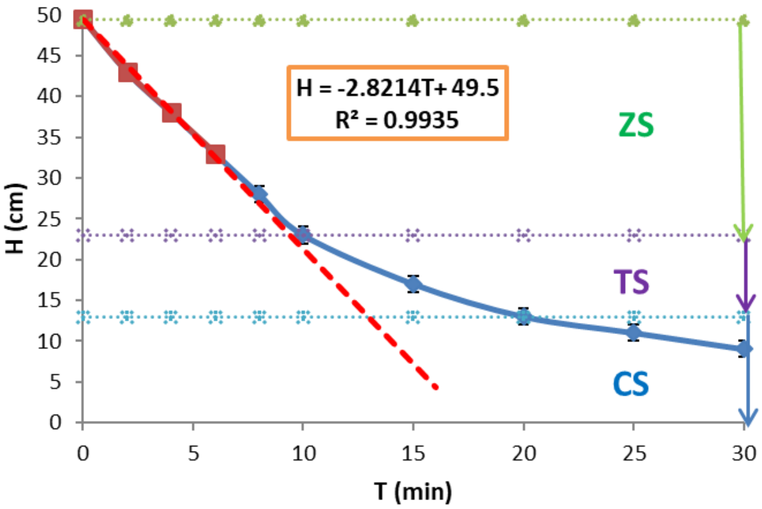

Figure 16. Aluminium dosed 20 mg/L for Zone Settling Curve (9/12/2014)

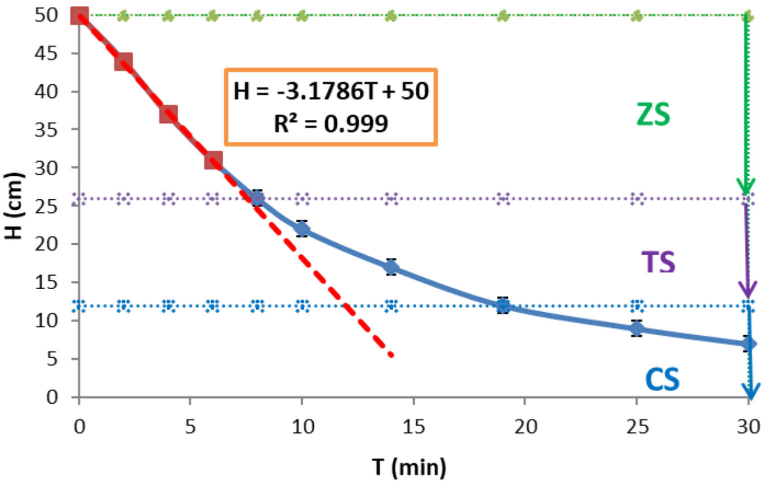

Figure 17. Aluminium dosed 50 mg/L for Zone Settling Curve (9/12/2014)

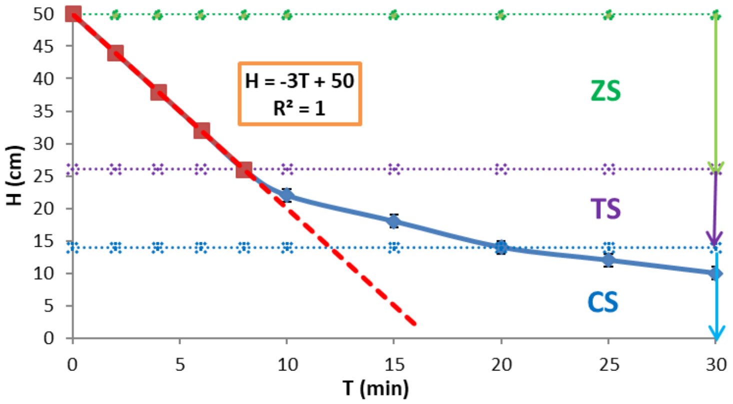

Figure 18. Aluminium dosed 100 mg/L for Zone Settling Curve (9/12/2014)

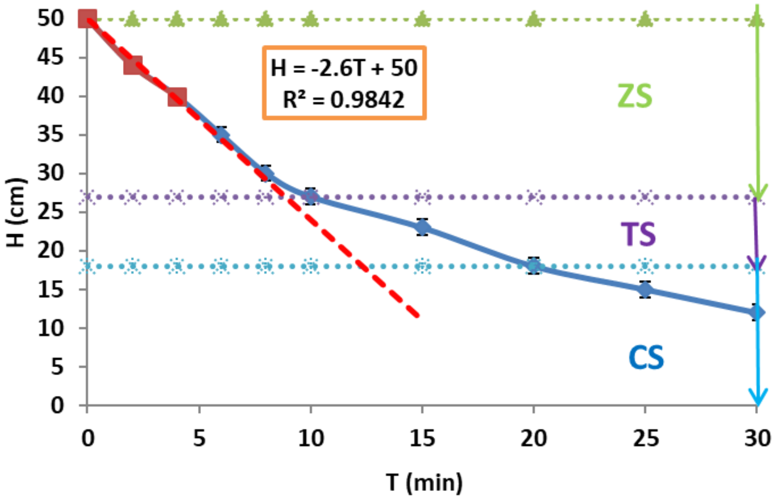

Figure 19. Aluminium dosed 150 mg/L for Zone Settling Curve (9/12/2014)

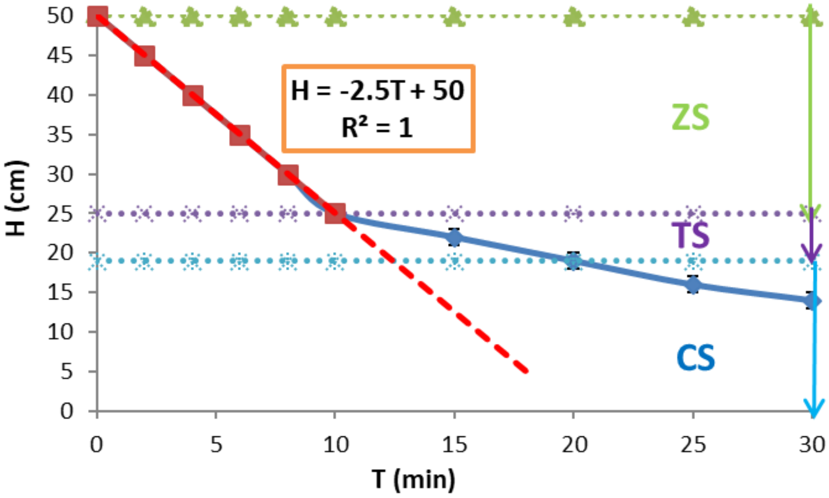

Figure 20. Aluminium dosed 200 mg/L for Zone Settling Curve (9/12/2014)

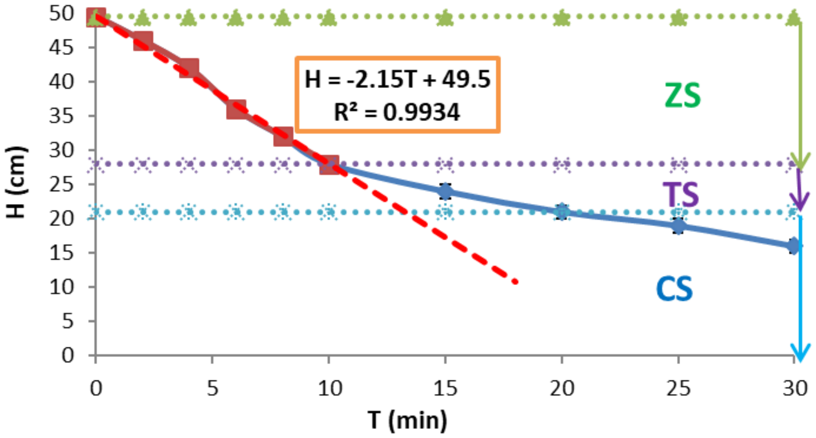

Figure 21. Aluminium dosed 250 mg/L for Zone Settling Curve (9/12/2014)

LOF A4: Figure 22 to 26 for Un-dosed and Aluminium Dosed Sludge (Phase 4)

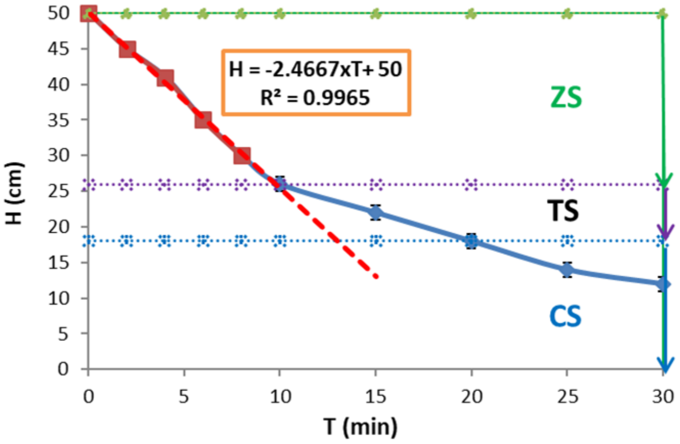

Figure 22. un-dosed 0mg/L for Zone Settling Curve (1/03/2014)

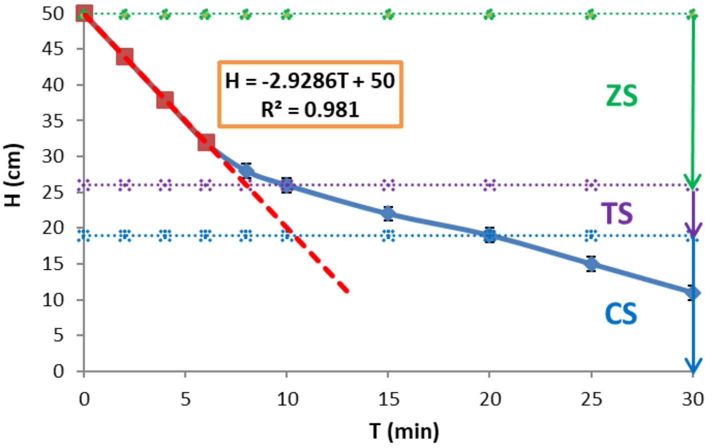

Figure 23. Aluminium dosed 20 mg/L for Zone Settling Curve (1/03/2014)

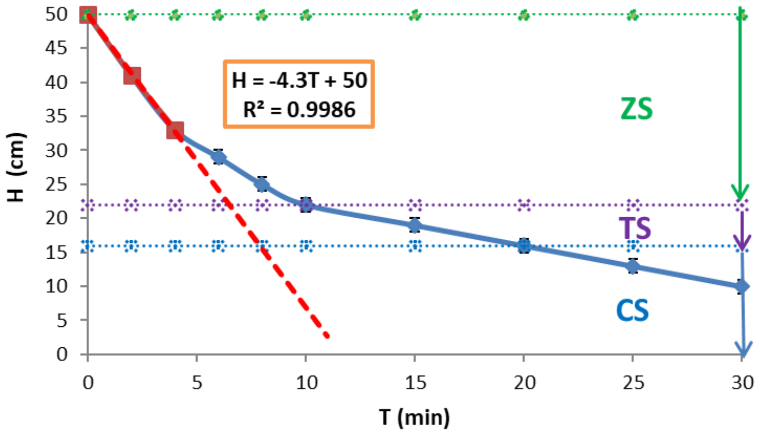

Figure 24. Aluminium dosed 50 mg/L for Zone Settling Curve (1/03/2014)

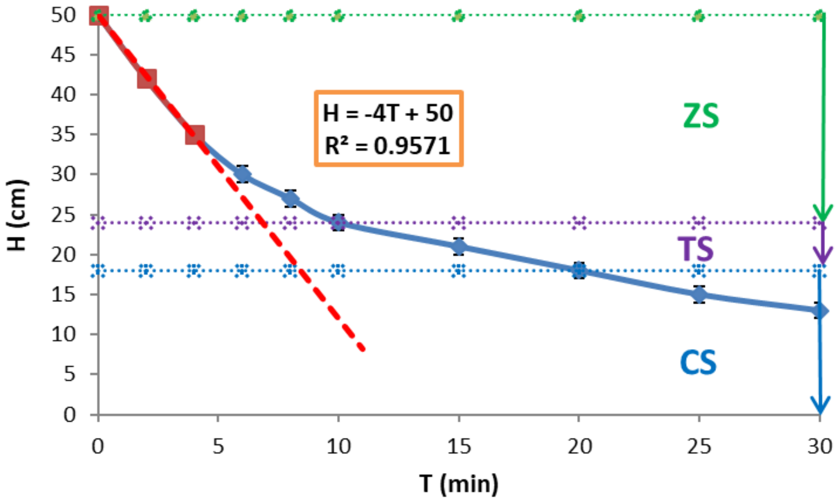

Figure 25. Aluminium dosed 100 mg/L for Zone Settling Curve (1/03/2014)

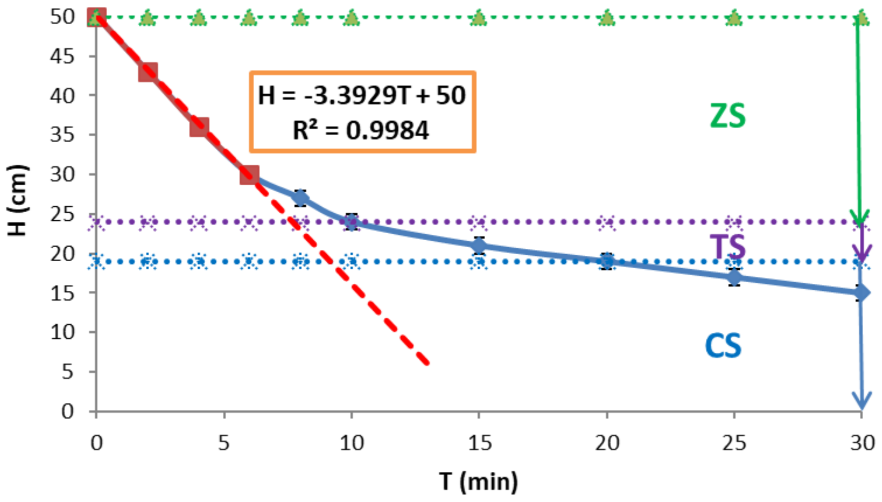

Figure 26. Aluminium dosed 150 mg/L for Zone Settling Curve (1/03/2014)

LOF A5: Figure 27 to 31 for Un-dosed and Aluminium Dosed Sludge (Phase 5)

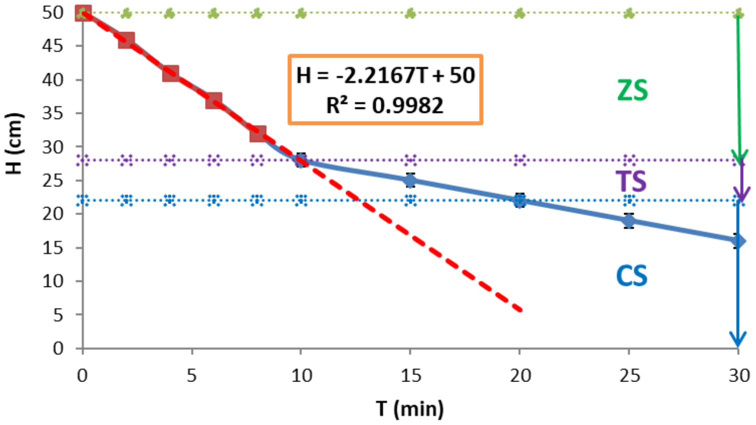

Figure 27. un-dosed 0mg/L for Zone Settling Curve (2/06/2014)

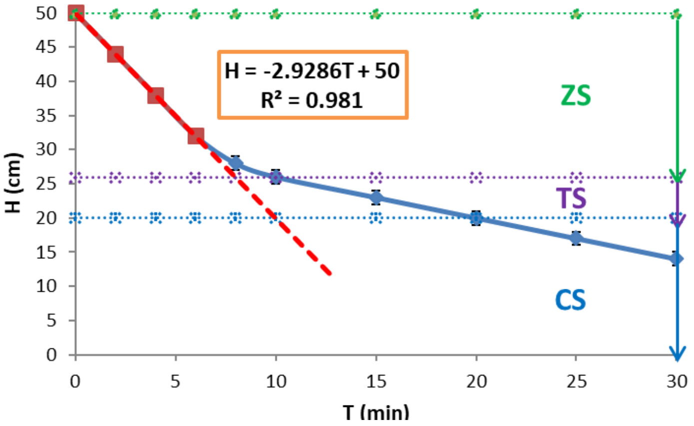

Figure 28. Aluminium dosed 20 mg/L for Zone Settling Curve (2/06/2014)

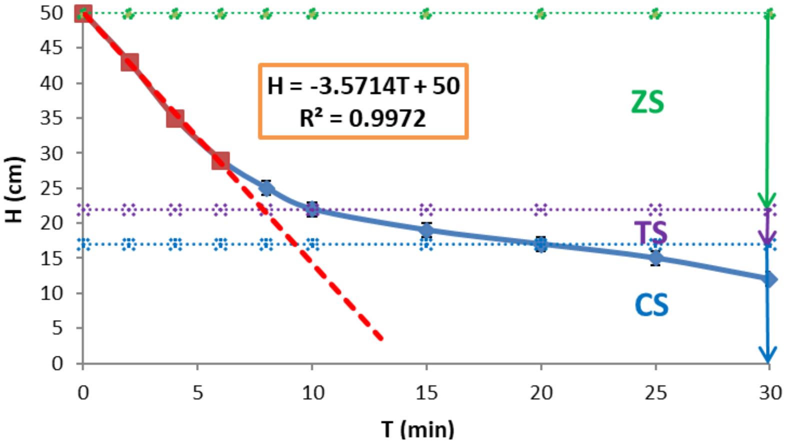

Figure 29. Aluminium dosed 50 mg/L for Zone Settling Curve (2/06/2014)

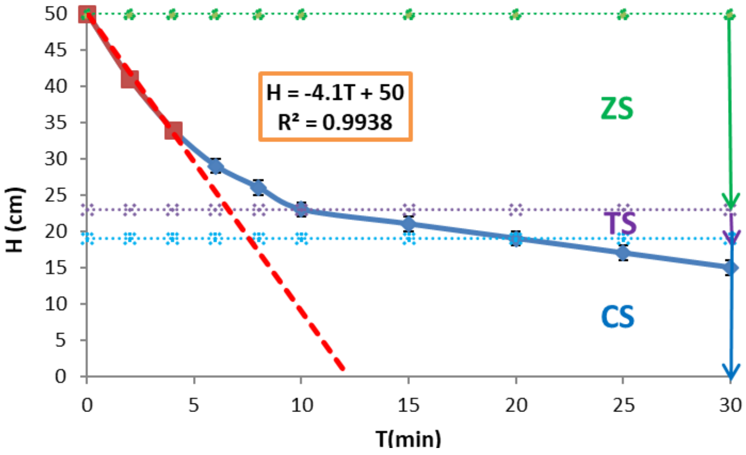

Figure 30. Aluminium dosed 100 mg/L for Zone Settling Curve (2/06/2014)

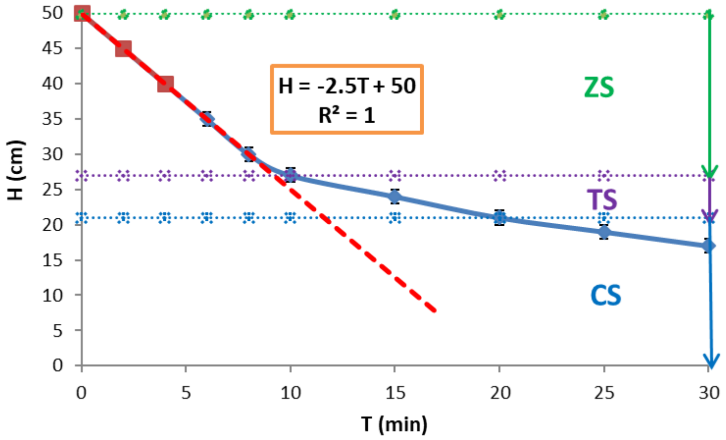

Figure 31. Aluminium dosed 150 mg/L for Zone Settling Curve (2/06/2014)

LOF B- Figures of Zone settling curves for un-dosed and Ferric phase 1 -3

LOF B1: Figure 1 to 7 for Un-dosed and Ferric Dosed Sludge (Phase 1)

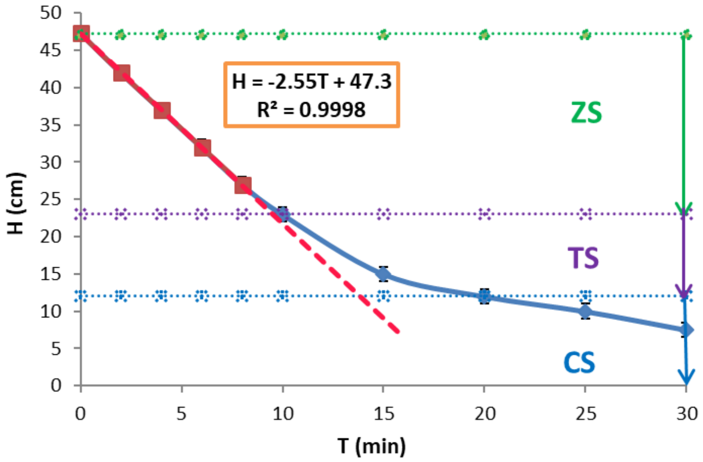

Figure 1. un-dosed 0mg/L for Zone Settling Curve (7/11/2014)

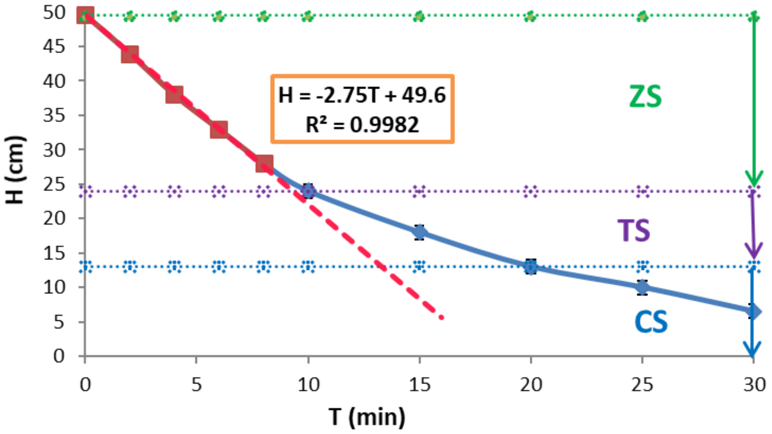

Figure 2. Ferric dosed 20 mg/L for Zone Settling Curve (7/11/2014)

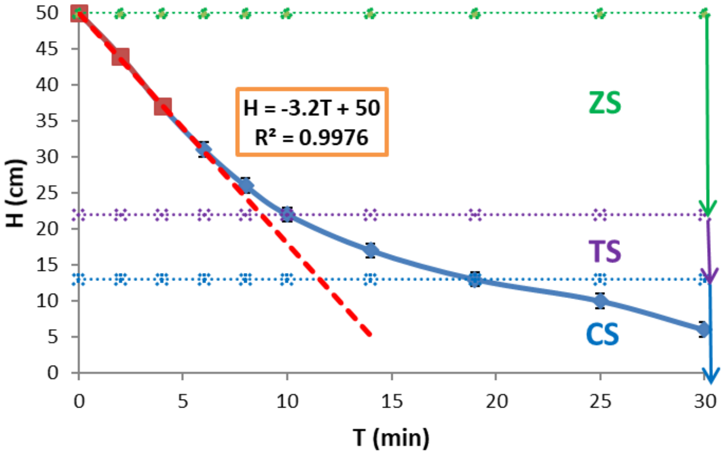

Figure 3. Ferric dosed 50 mg/L for Zone Settling Curve (7/11/2014)

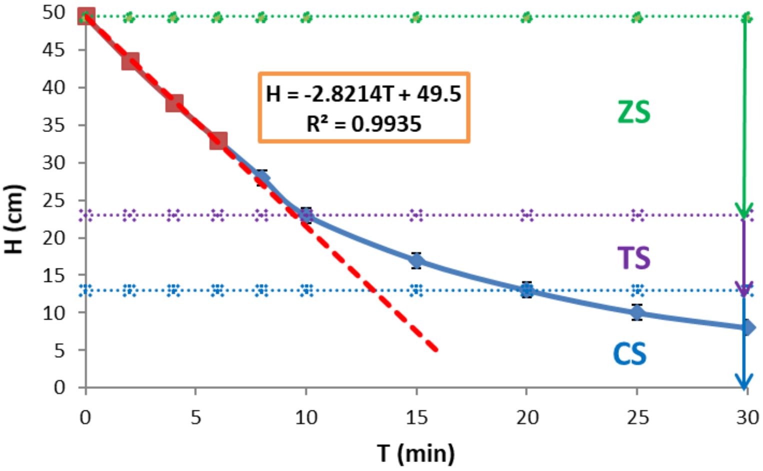

Figure 4. Ferric dosed 100 mg/L for Zone Settling Curve (7/11/2014)

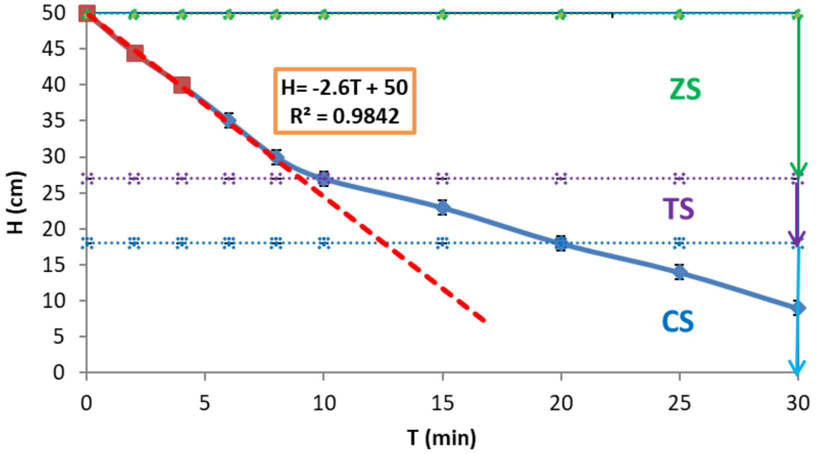

Figure 5. Ferric dosed 150 mg/L for Zone Settling Curve (7/11/2014)

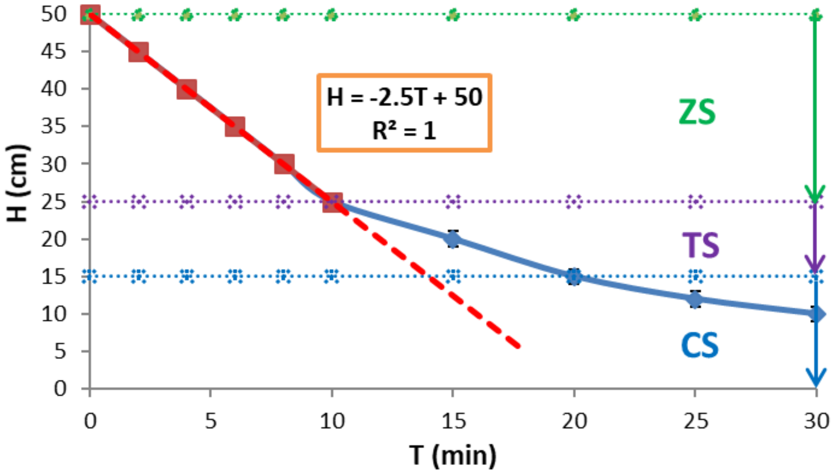

Figure 6. Ferric dosed 200 mg/L for Zone Settling Curve (7/11/2014)

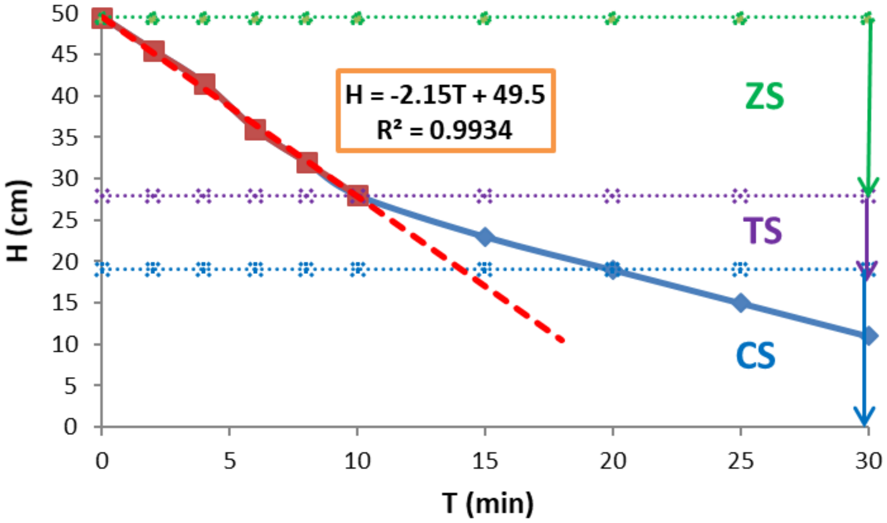

Figure 7. Ferric dosed 250 mg/L for Zone Settling Curve (7/11/2014)

LOF B2: Figure 8 to 14 for Un-dosed and Ferric Dosed Sludge (Phase 2)

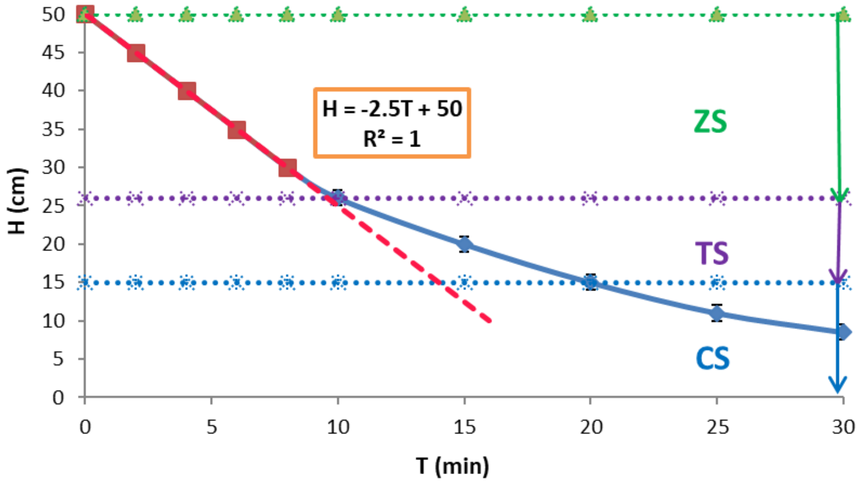

Figure 8. un-dosed 0mg/L for Zone Settling Curve (15/12/2014)

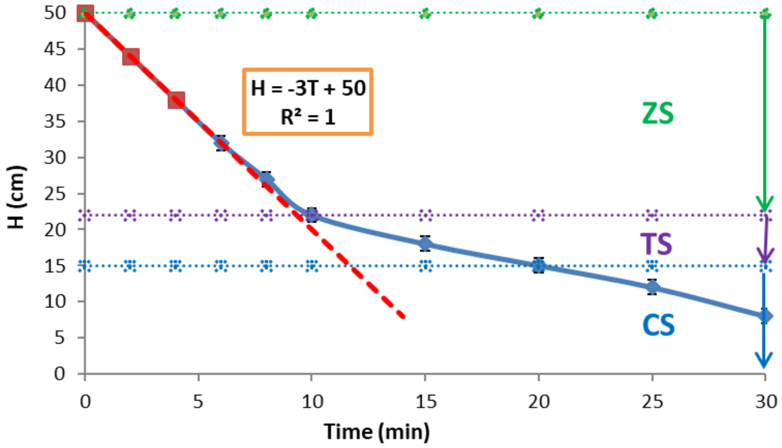

Figure 9. Ferric dosed 20 mg/L for Zone Settling Curve (15/12/2014)

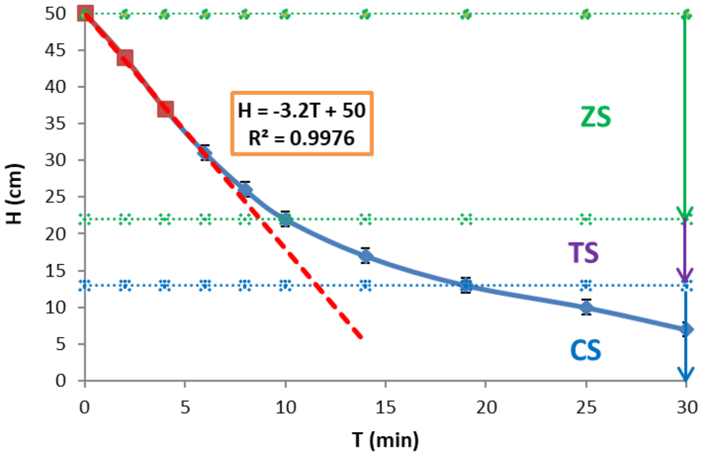

Figure 10. Ferric dosed 50 mg/L for Zone Settling Curve (15/12/2014)

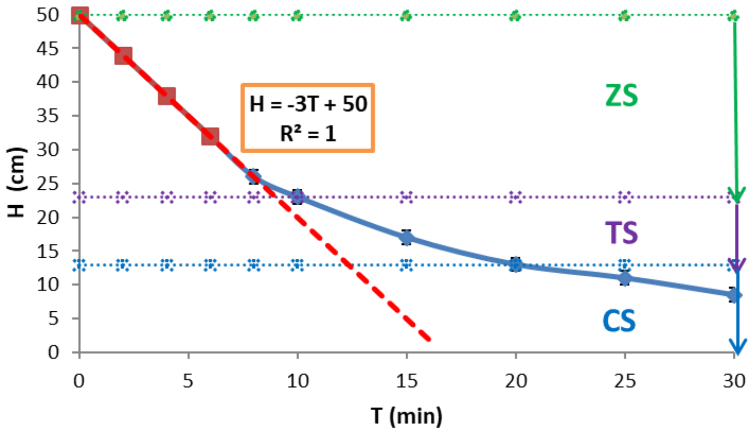

Figure 11. Ferric dosed 100 mg/L for Zone Settling Curve (15/12/2014)

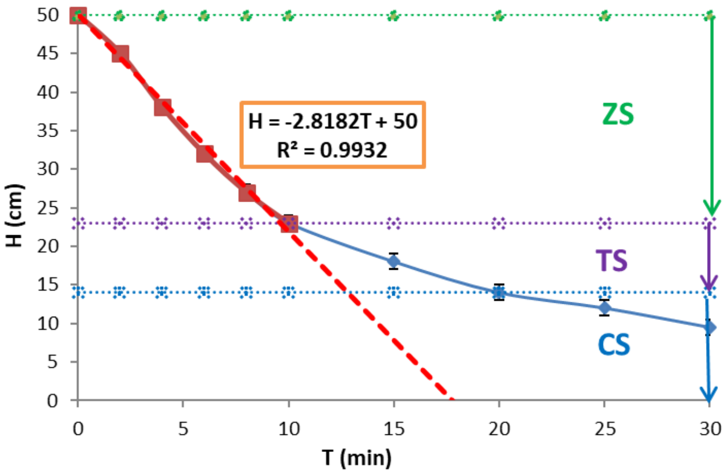

Figure 12. Ferric dosed 150 mg/L for Zone Settling Curve (15/12/2014)

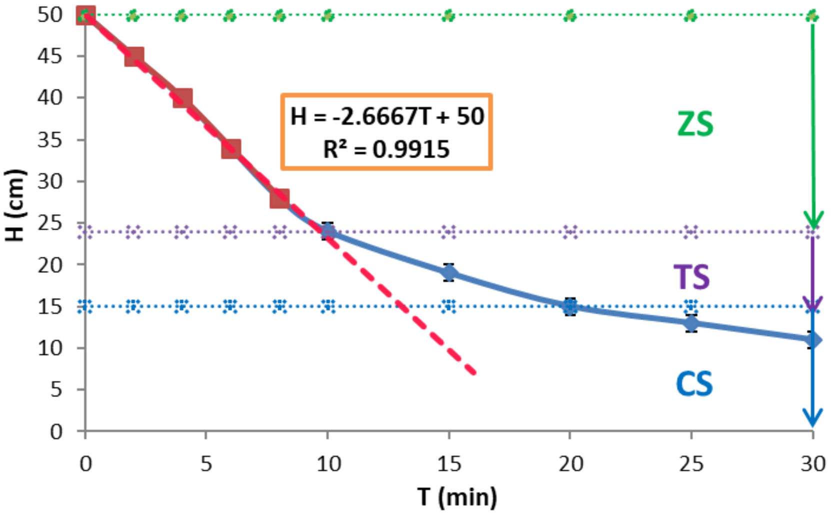

Figure 13. Ferric dosed 200 mg/L for Zone Settling Curve (15/12/2014)

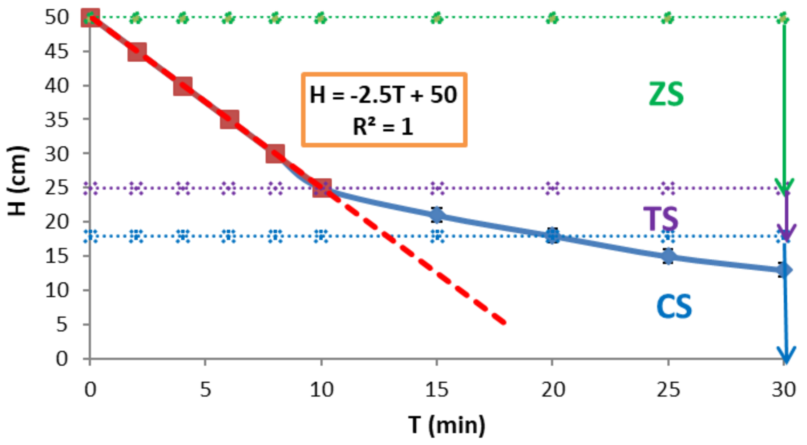

Figure 14. Ferric dosed 250 mg/L for Zone Settling Curve (15/12/2014)

LOF B3: Figure 15 to 19 for Un-dosed and Ferric Dosed Sludge (Phase 3)

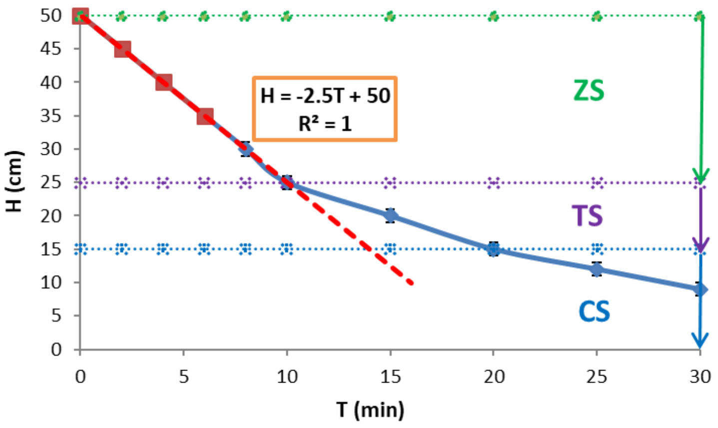

Figure 15. un-dosed 0mg/L for Zone Settling Curve (1/03/2016)

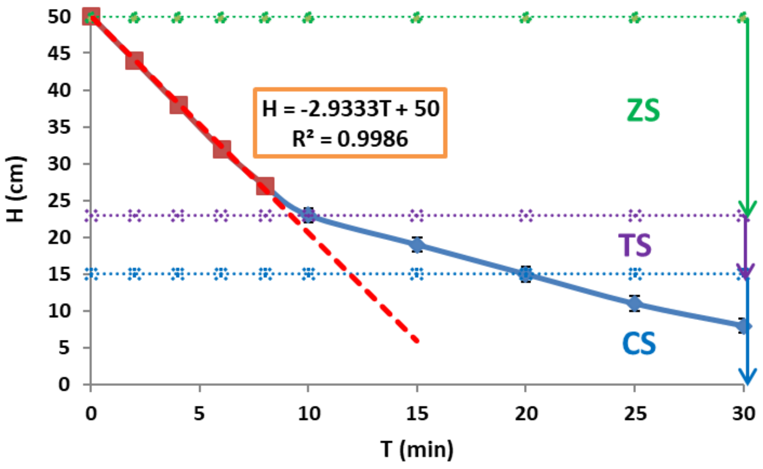

Figure 16. Ferric dosed 20 mg/L for Zone Settling Curve (1/03/201)

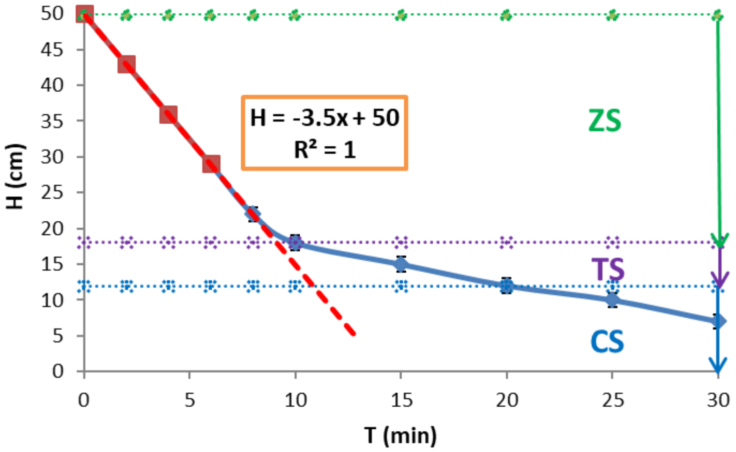

Figure 17. Ferric dosed 50 mg/L for Zone Settling Curve (1/03/2016)

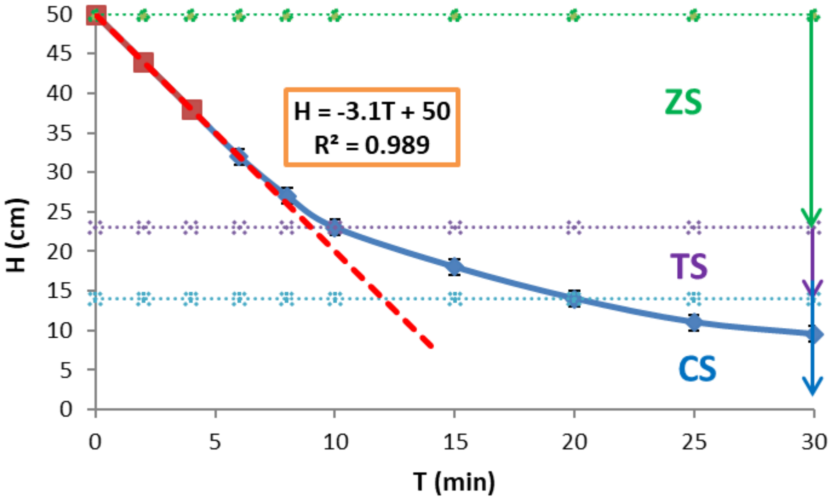

Figure 18. Ferric dosed 100 mg/L for Zone Settling Curve (1/03/2016)

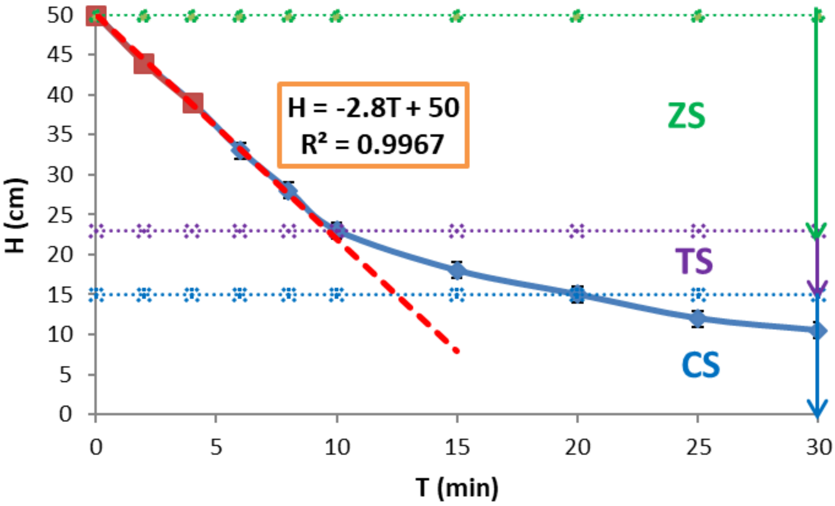

Figure 19. Ferric dosed 150 mg/L for Zone Settling Curve (1/03/2016)

LOF C- Figures of Zone settling curves for un-dosed and Calcium phase 1-2

LOF C1: Figure 1 to 7 for Un-dosed and Calcium Dosed Sludge (Phase 1)

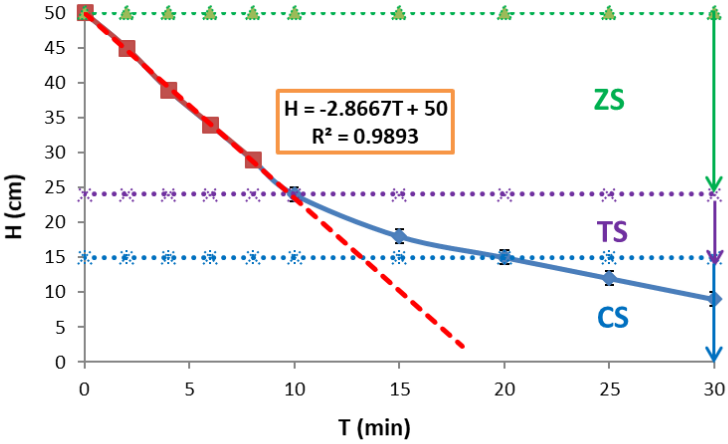

Figure1. un-dosed 0mg/L for Zone Settling Curve (5/12/2014)

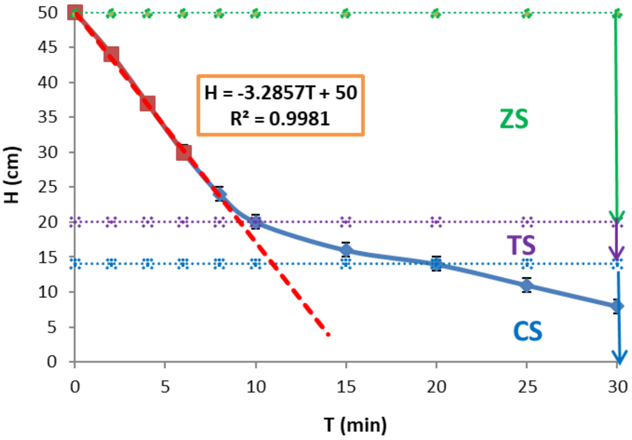

Figure 2. Calcium dosed 20 mg/L for Zone Settling Curve (5/12/2014)

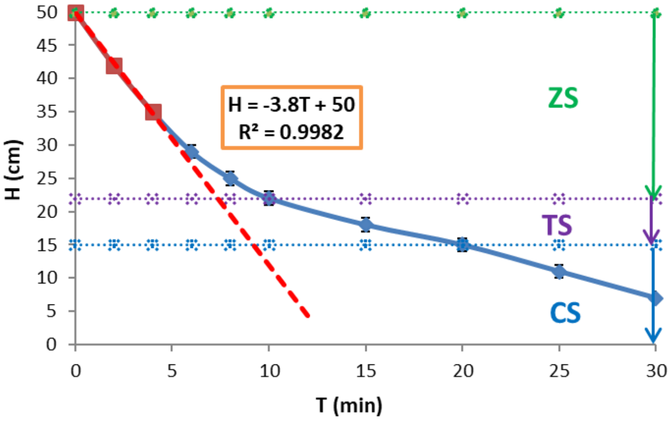

Figure 3. Calcium dosed 50 mg/L for Zone Settling Curve (5/12/2014)

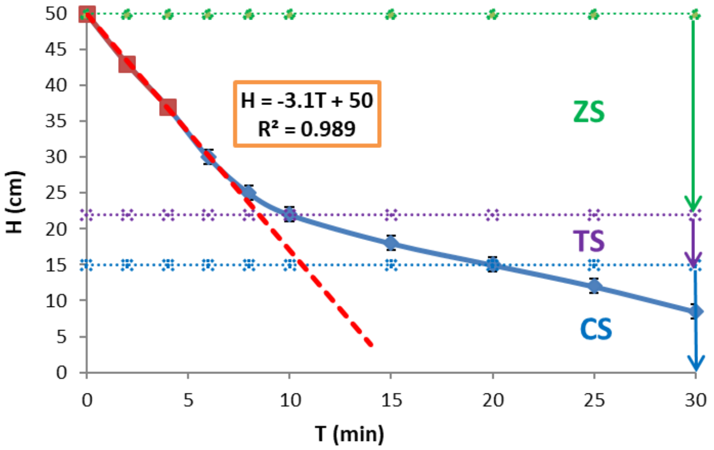

Figure 4. Calcium dosed 100 mg/L for Zone Settling Curve (5/12/2014)

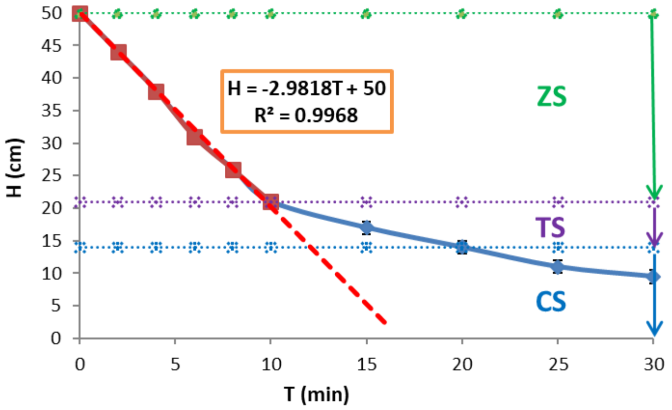

Figure 5. Calcium dosed 150 mg/L for Zone Settling Curve (5/12/2014)

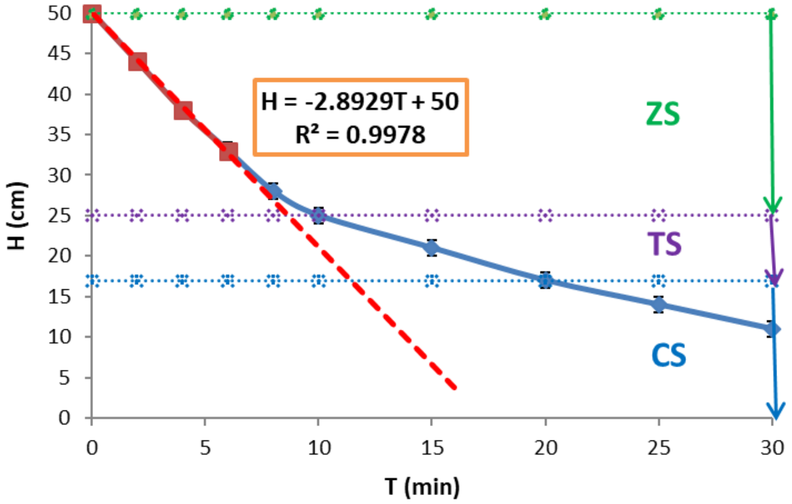

Figure 6. Calcium dosed 200 mg/L for Zone Settling Curve (5/12/2014)

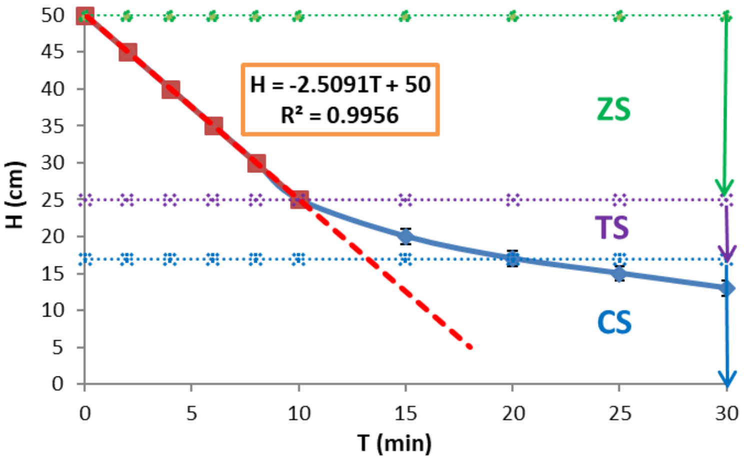

Figure 7. Calcium dosed 250 mg/L for Zone Settling Curve (5/12/2014)

LOF C2: Figure 8 to 12 for Un-dosed and Calcium Dosed Sludge (Phase 2)

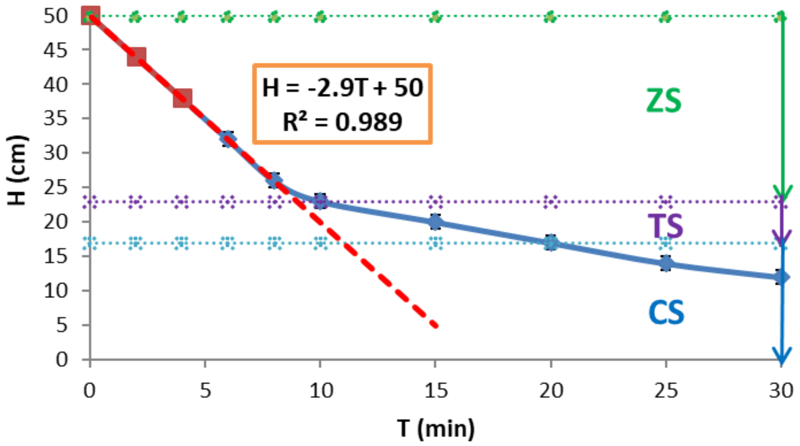

Figure 8. Un-dosed 0mg/L for Zone Settling Curve **(2/06/2016)**

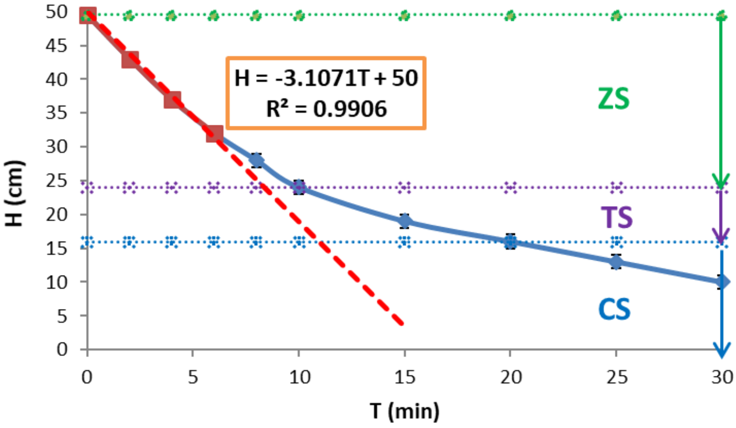

Figure 9. Calcium dosed 20 mg/L for Zone Settling Curve (2/06/2016)

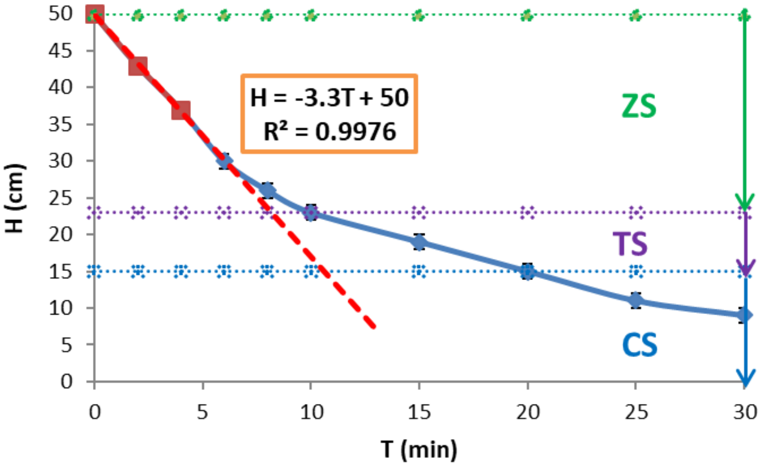

Figure 10. Calcium dosed 50 mg/L for Zone Settling Curve (2/06/2016)

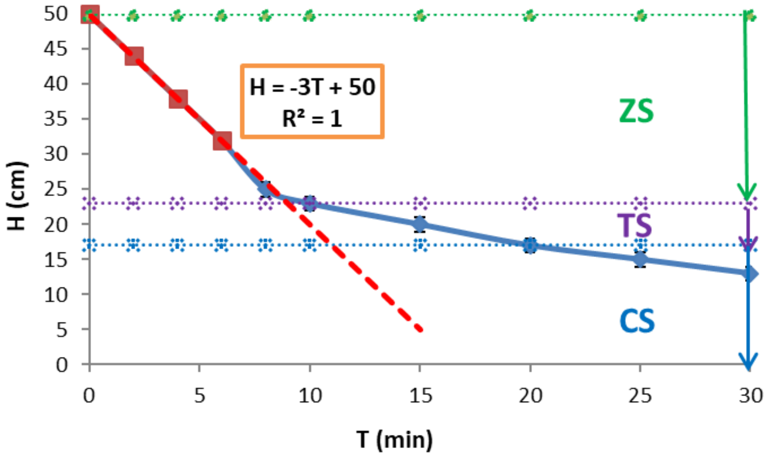

Figure 11. Calcium dosed 100 mg/L for Zone Settling Curve (2/06/2016)

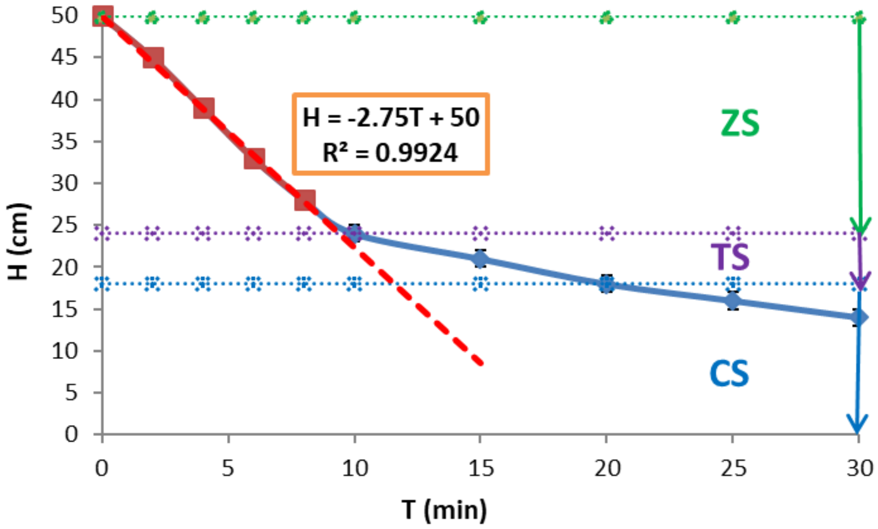

Figure 12. Calcium dosed 150 mg/L for Zone Settling Curve (2/06/2016)

LOF D- Figures of the Impact of Aluminium dosing on ZSV phase 1-5

LOF D1: Figure 1- Impact of Aluminium dosing on ZSV (Phase 1)

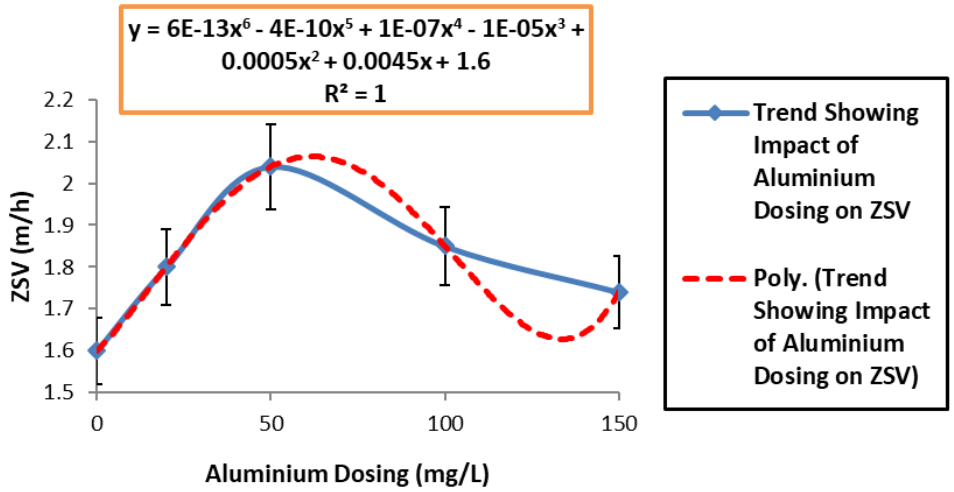

Figure 1. Impact of Aluminium Dosing (mg/L) on ZSV (m/h) (Error bars represent standard deviation of the mean)

LOF D2: Figure 2- Impact of Aluminium dosing on ZSV (Phase 2)

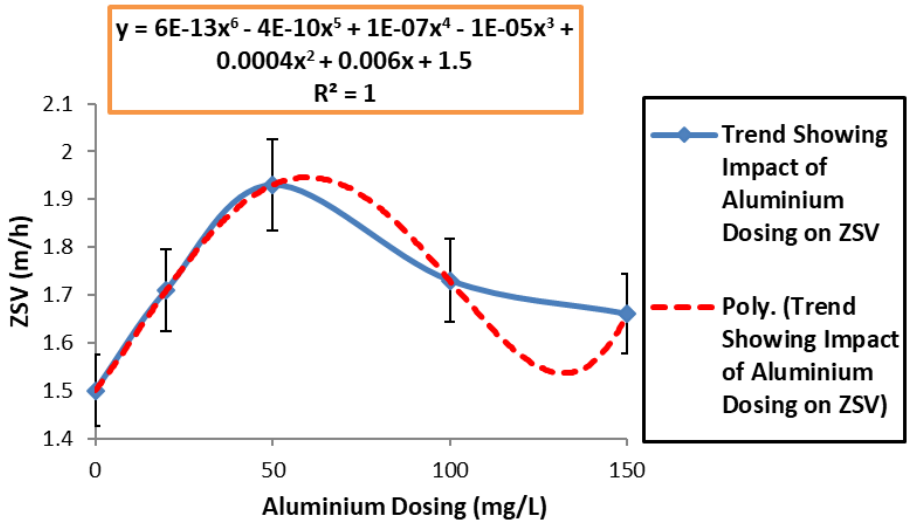

Figure 2. The Impact of Aluminium Dosing (mg/L) on ZSV (m/h) (Error bars represent standard deviation of the mean)

LOF D3: Figure 3- Impact of Aluminium dosing on ZSV (Phase 3)

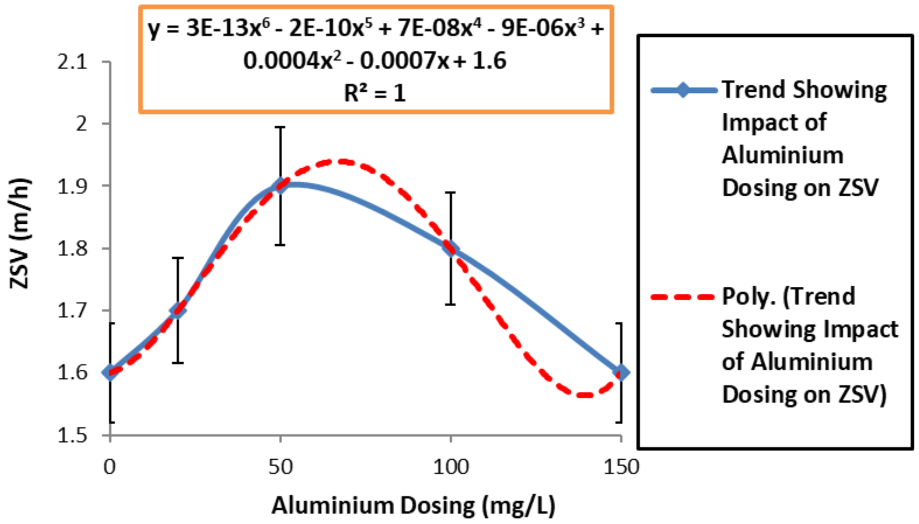

Figure 3. The Impact of Aluminium Dosing (mg/L) on ZSV (m/h) (Error bars represent standard deviation of the mean)

LOF D4: Figure 4- Impact of Aluminium dosing on ZSV (Phase 4)

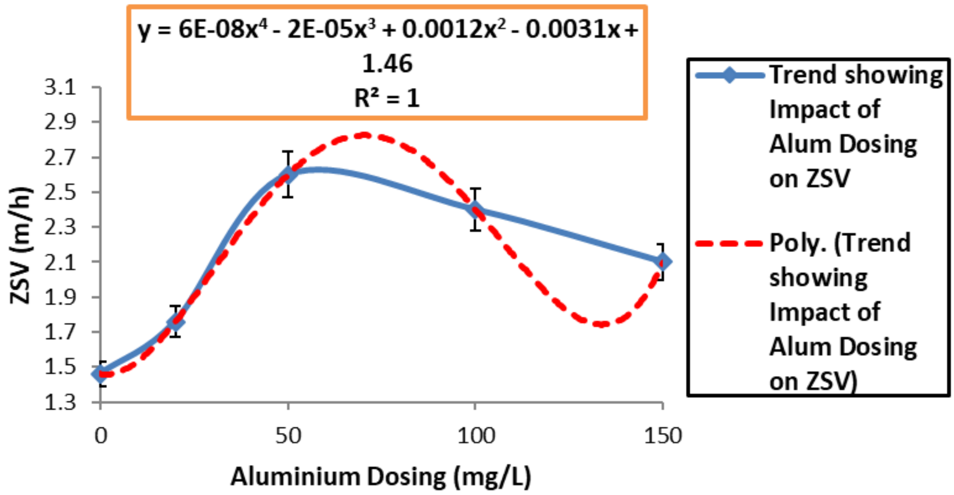

Figure 4. The Impact of Aluminium Dosing (mg/L) on ZSV (m/h) (Error bars represent standard deviation of the mean)

LOF D5: Figure 5- Impact of Al dosing on ZSV (Phase 5)

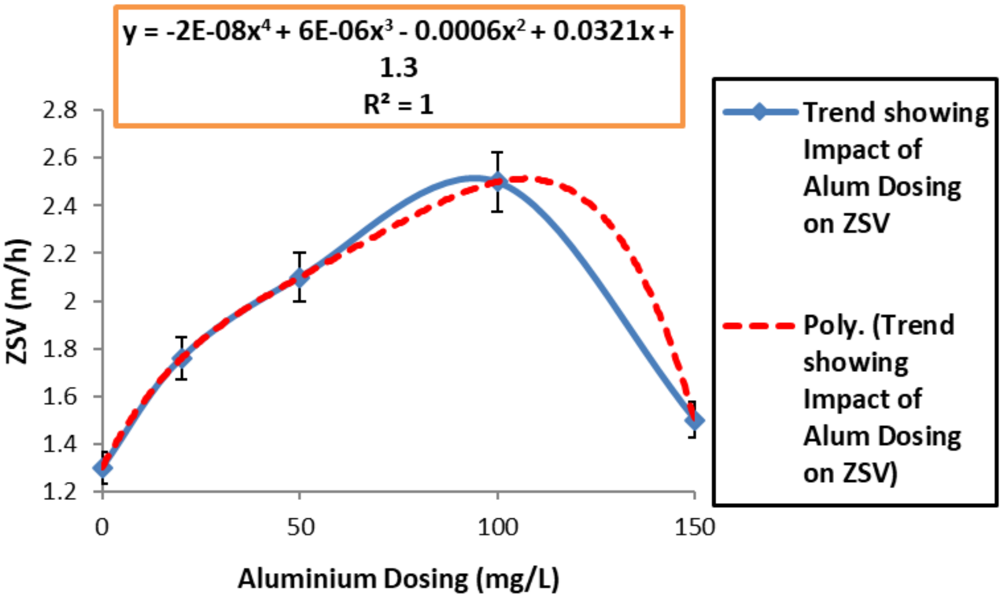

Figure 5. The Impact of Aluminium Dosing (mg/L) on ZSV (m/h) (Error bars represent standard deviation of the mean)

LOF E- Figures of the Impact of Ferric dosing on ZSV phase 1-3

LOF E1: Figure 1- Impact of Ferric dosing on ZSV (Phase 1)

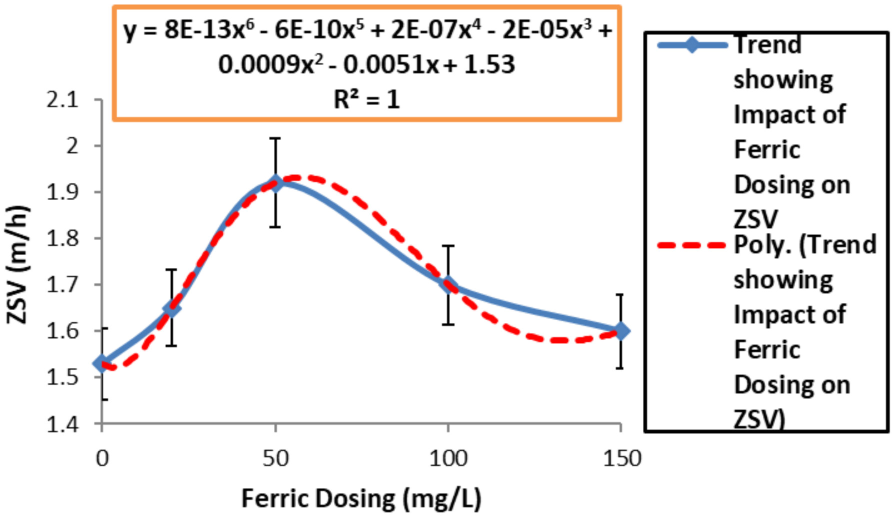

Figure 1. The Impact of Ferric Dosing (mg/L) on ZSV (m/h) (Error bars represent standard deviation of the mean)

LOF E2: Figure 2- Impact of Ferric dosing on ZSV (Phase 2)

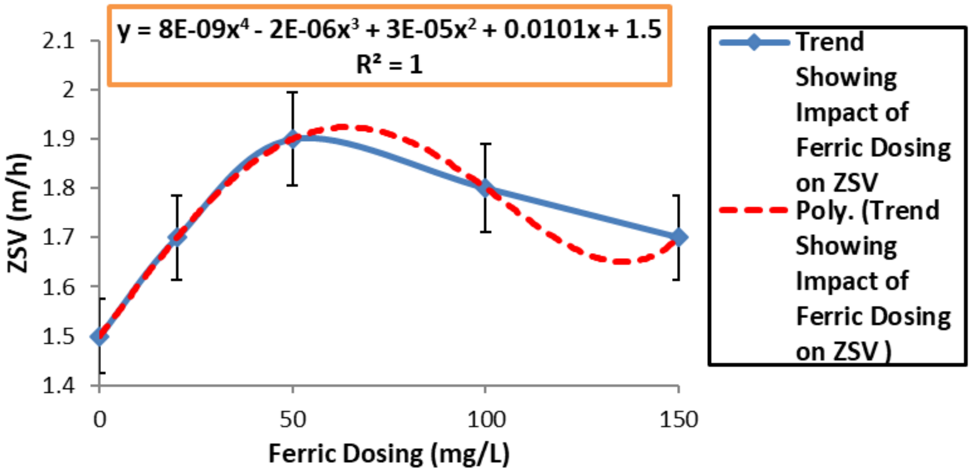

Figure 2. The Impact of Ferric Dosing (mg/L) on ZSV (m/h) (Error bars represent standard deviation of the mean)

LOF E3: Figure 3 - Impact of Ferric dosing on ZSV (Phase 3)

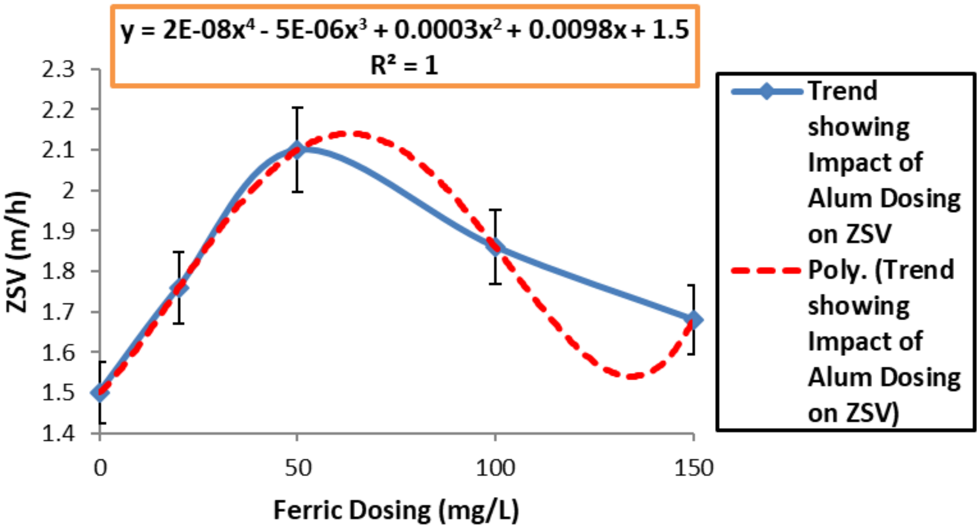

Figure 3. The Impact of Ferric Dosing (mg/L) on ZSV (m/h) (Error bars represent standard deviation of the mean)

LOF F- Figures of the Impact of Calcium dosing on ZSV phase 1-2

LOF F1: Figure 1- Impact of Calcium dosing on ZSV (Phase 1)

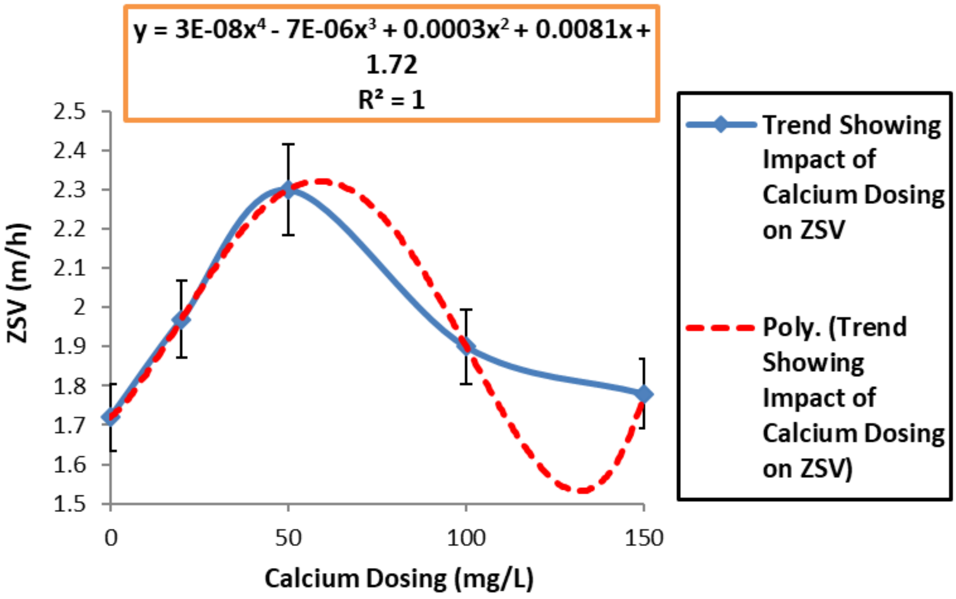

Figure 1. The Impact of Calcium Dosing (mg/L) on ZSV (m/h) (Error bars represent standard deviation of the mean)

LOF F2: Figure 2 - Impact of Calcium dosing on ZSV (Phase 2)

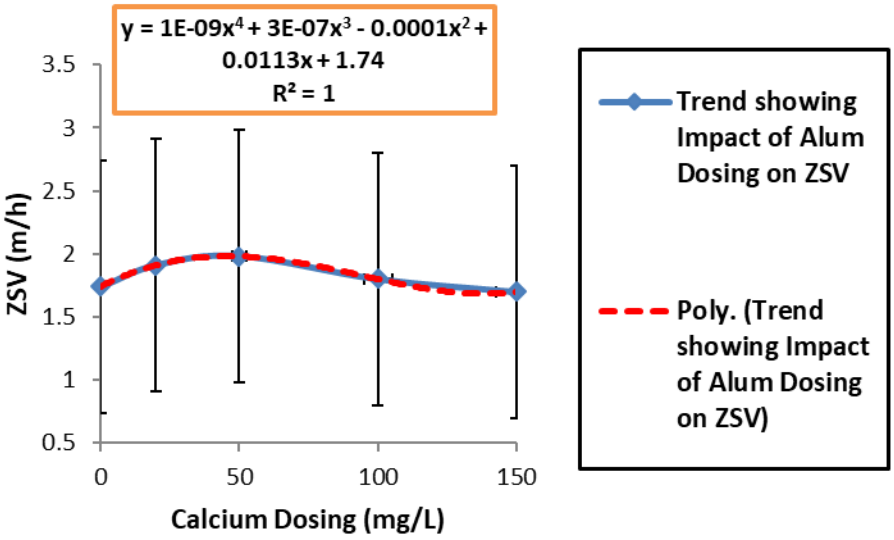

Figure 2. The Impact of Calcium Dosing (mg/L) on ZSV (m/h) (Error bars represent standard deviation of the mean)

LOF G- Figures of the Impact of Aluminium dosing on SSVI phase 1-5

LOF G1: Figure 1- Impact of Aluminium dosing on SSVI (Phase 1)

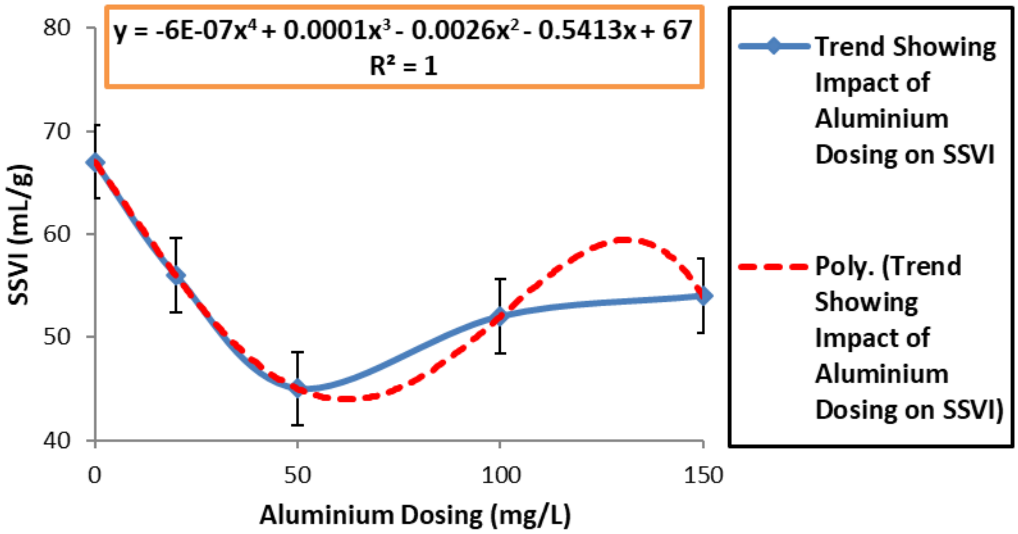

Figure 1. The Impact of Aluminium Dosing (mg/L) on SSVI (mL/g) (Error bars represent standard deviation of the mean)

LOF G2: Figure 2- Impact of Aluminium dosing on SSVI (Phase 2)

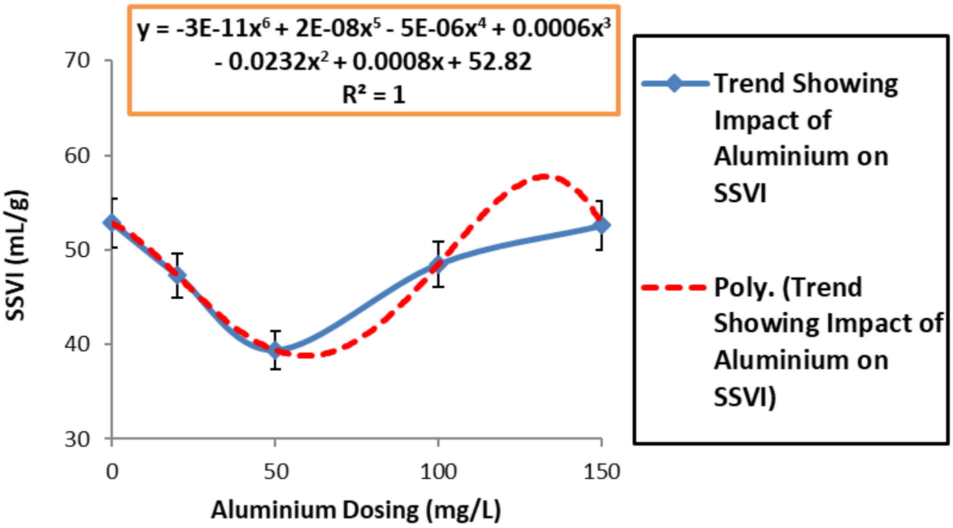

Figure 2. The Impact of Aluminium Dosing (mg/L) on SSVI (mL/g) (Error bars represent standard deviation of the mean)

LOF G3: Figure 3 - Impact of Aluminium dosing on SSVI (Phase 3)

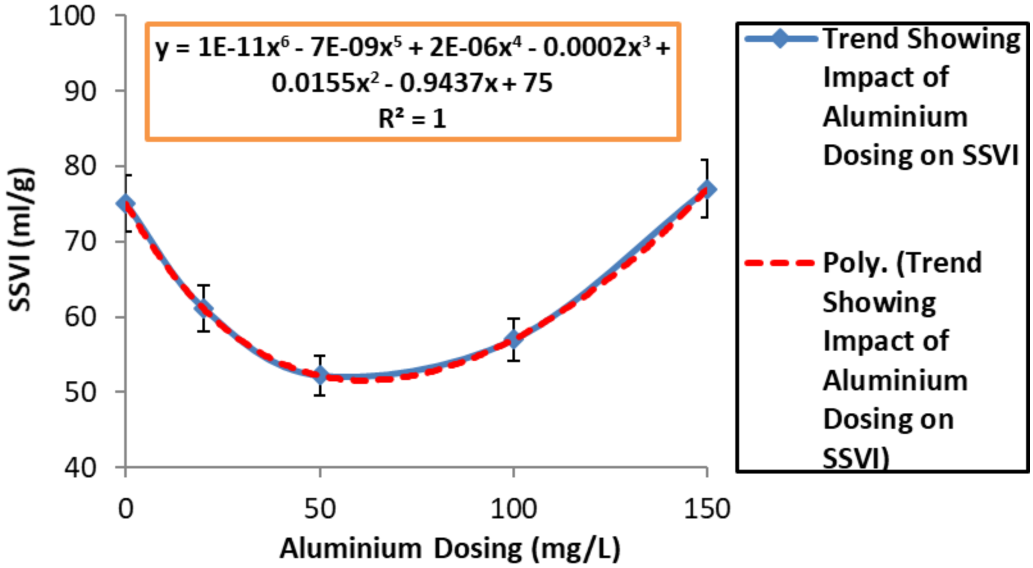

Figure 3. The Impact of Aluminium Dosing (mg/L) on SSVI (mL/g) (Error bars represent standard deviation of the mean)

LOF G4: Figure 4- Impact of Aluminium dosing on SSVI (Phase 4)

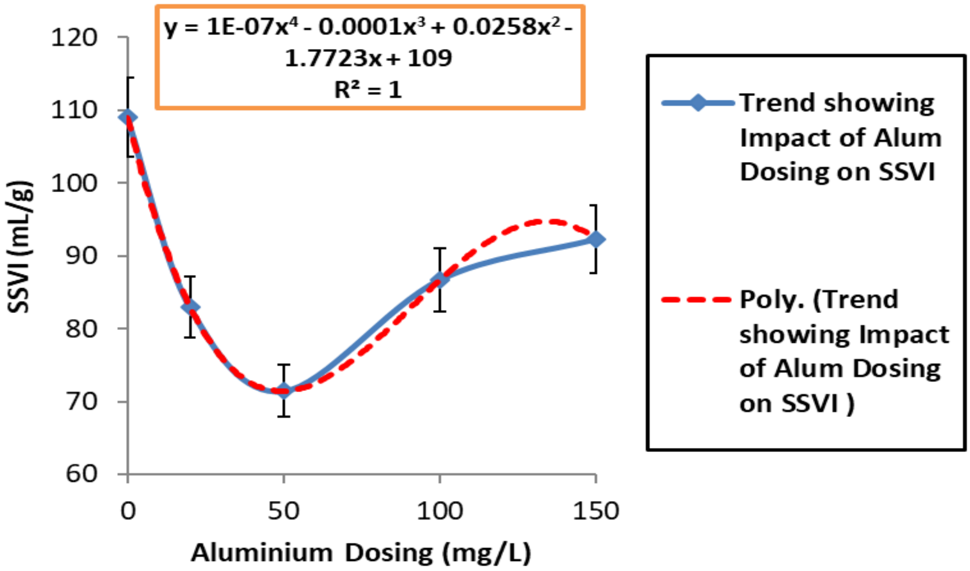

Figure 4. The Impact of Aluminium Dosing (mg/L) on SSVI (mL/g) (Error bars represent standard deviation of the mean)

LOF G5: Figure 5 for of Impact of Aluminium dosing on SSVI (Phase 5)

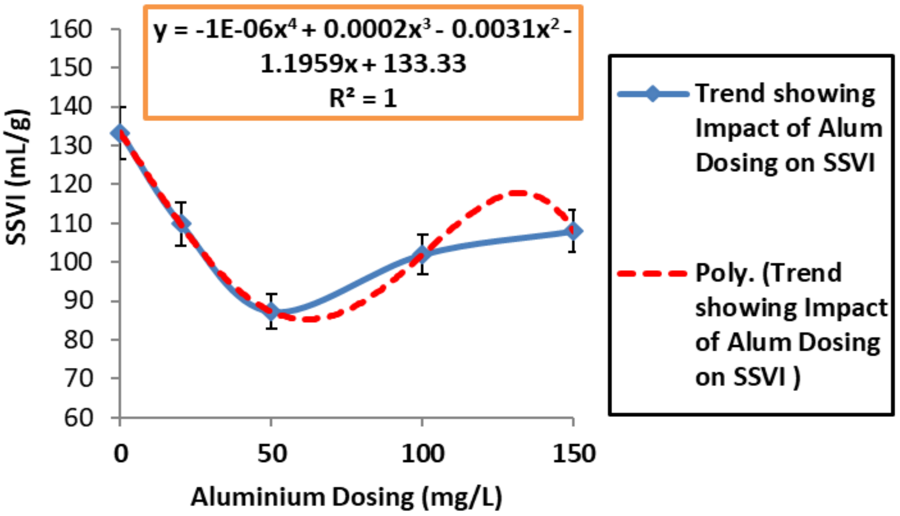

Figure 5. The Impact of Aluminium Dosing (mg/L) on SSVI (mL/g) (Error bars represent standard deviation of the mean)

LOF H- Figures of the Impact of Ferric dosing on SSVI phase 1-3

LOF H1: Figure 1- Impact of Ferric dosing on SSVI (Phase 1)

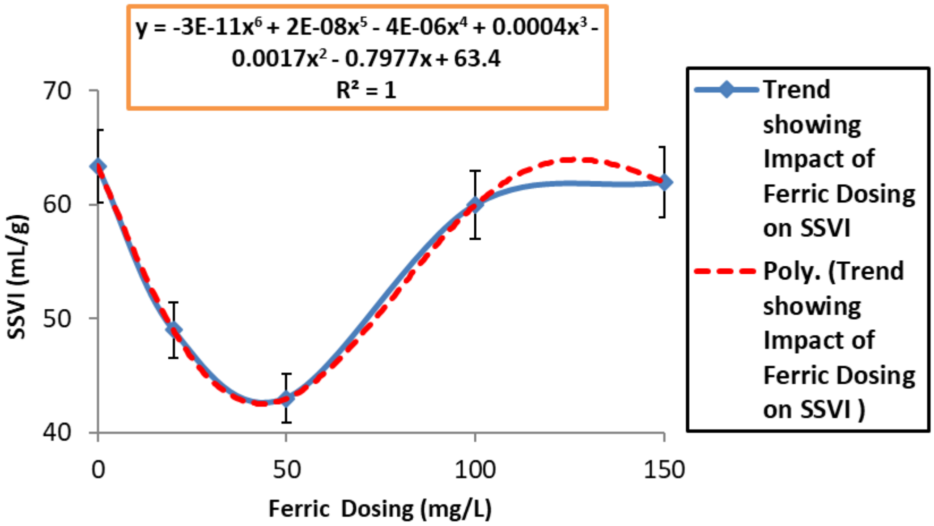

Figure 1. The Impact of Ferric Dosing (mg/L) on SSVI (mL/g) (Error bars represent standard deviation of the mean)

LOF H 2: Figure 2- Impact of Ferric dosing on SSVI (Phase 2)

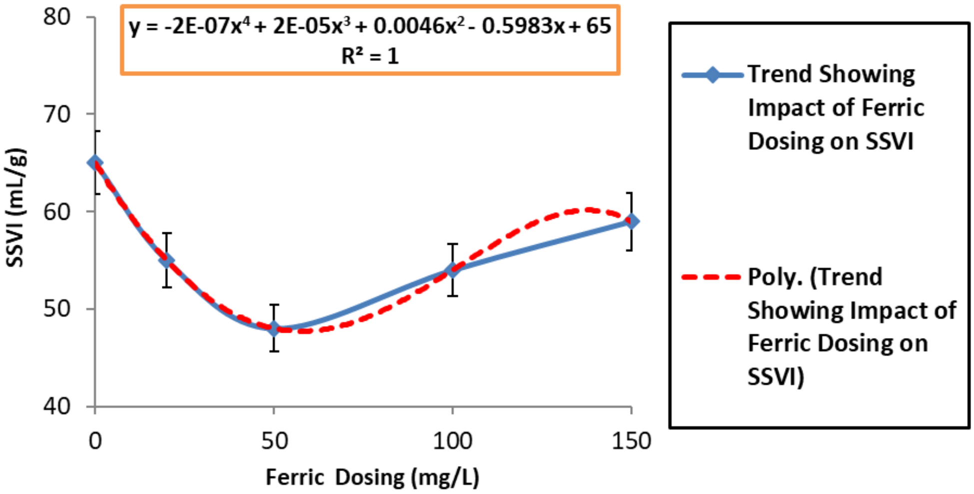

Figure 2. The Impact of Ferric Dosing (mg/L) on SSVI (mL/g) (Error bars represent standard deviation of the mean)

LOF H 3: Figure 3- Impact of Ferric dosing on SSVI (Phase 3)

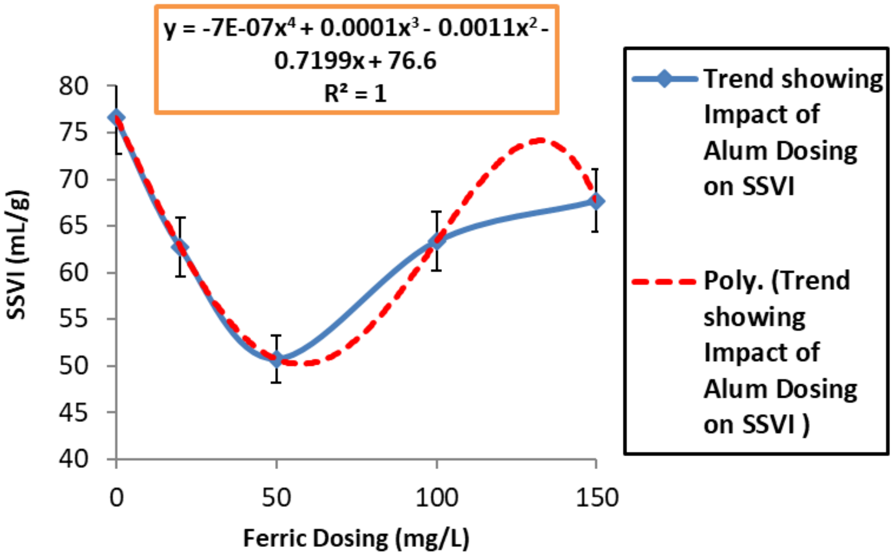

Figure 3. The Impact of Ferric Dosing (mg/L) on SSVI (mL/g) (Error bars represent standard deviation of the mean)

LOF I- Figures of the Impact of Calcium dosing on SSVI phase 1-2

LOF I1: Figure 1- Impact of Calcium dosing on SSVI (Phase 1)

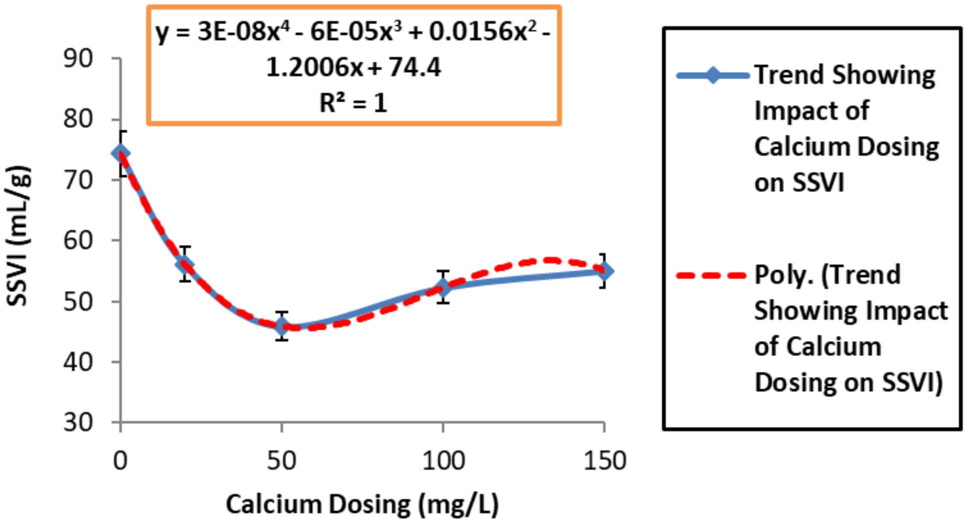

Figure 1. The Impact of Calcium Dosing (mg/L) on SSVI (mL/g) (Error bars represent standard deviation of the mean)

LOF I2: Figure 2- Impact of Calcium dosing on SSVI (Phase 2)

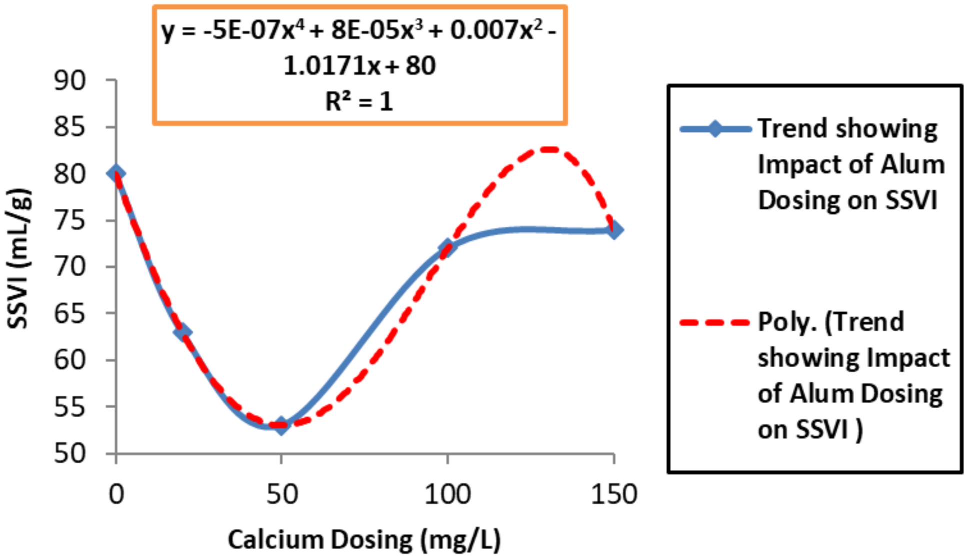

Figure 2. The Impact of Calcium Dosing (mg/L) on SSVI (mL/g) (error bars represent standard deviation of the mean)